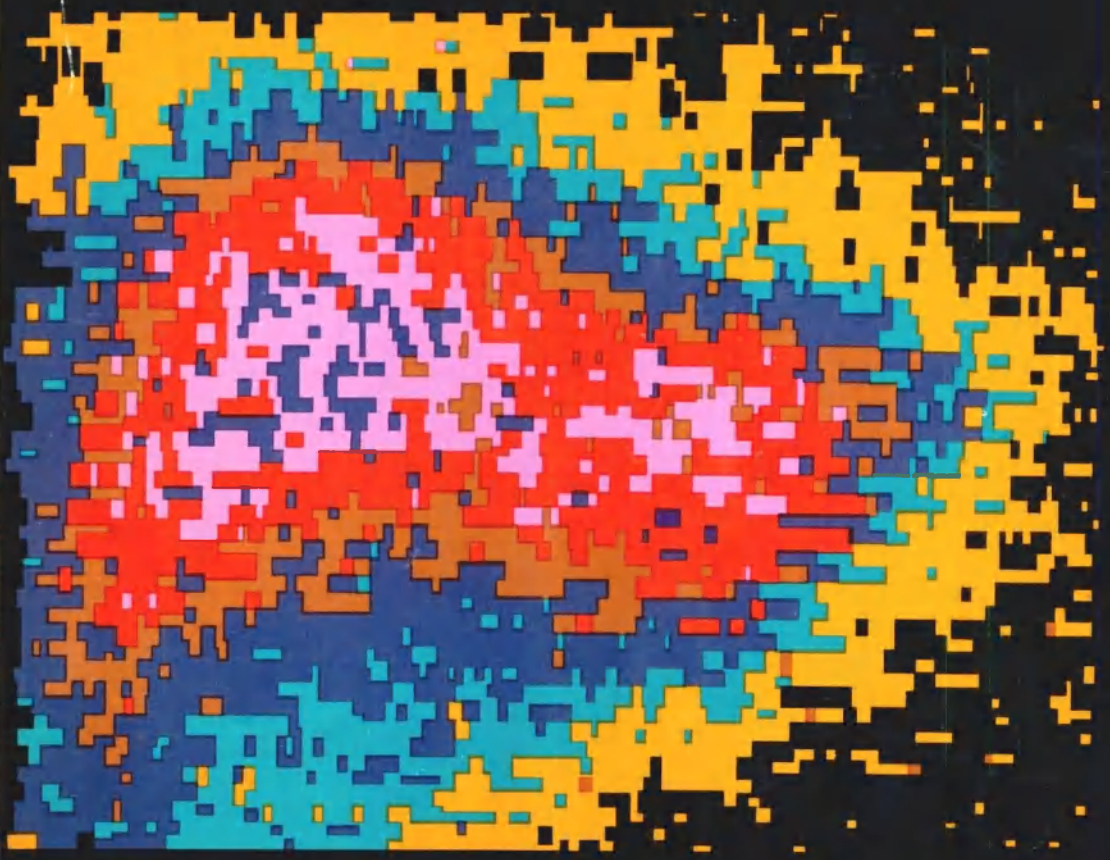

Proceedings of a Symposium, Athens, 20-24 April 1964

MEDICAL RADIOISOTOPE SCANNING

VOL. II

INTERNATIONAL ATOMIC ENERGY AGENCY, VIENNA, 1964

MEDICAL RADIOISOTOPE SCANNING

VOL. II

The following States are Members of the International Atomic Energy Agency:

AFGHANISTAN
ALBANIA
ALGERIA
ARGENTINA
AUSTRALIA
AUSTRIA
BELGIUM
BOLIVIA
BRAZIL
BULGARIA
BURMA
BYELORUSSIAN SOVIET SOCIALIST REPUBLIC
CAMBODIA
CAMEROUN
CANADA
CEYLON
CHILE
CHINA
COLOMBIA
CONGO (LÉOPOLDVILLE)
CUBA
CZECHOSLOVAK SOCIALIST REPUBLIC
DENMARK
DOMINICAN REPUBLIC
ECUADOR
EL SALVADOR
ETHIOPIA
FINLAND
FRANCE
FEDERAL REPUBLIC OF GERMANY
GABON
GHANA
GREECE
GUATEMALA
HAITI
HOLY SEE
HONDURAS
HUNGARY
ICELAND
INDIA
INDONESIA
IRAN
IRAQ
ISRAEL
ITALY
IVORY COAST
JAPAN
REPUBLIC OF KOREA
LEBANON
LIBERIA
LIBYA
LUXEMBOURG
MALI
MEXICO
MONACO
MOROCCO
NETHERLANDS
NEW ZEALAND
NICARAGUA
NIGERIA
NORWAY
PAKISTAN
PARAGUAY
PERU
PHILIPPINES
POLAND
PORTUGAL
ROMANIA
SAUDI ARABIA
SENEGAL
SOUTH AFRICA
SPAIN
SUDAN
SWEDEN
SWITZERLAND
SYRIA
THAILAND
TUNISIA
TURKEY
UKRAINIAN SOVIET SOCIALIST REPUBLIC
UNION OF SOVIET SOCIALIST REPUBLICS
UNITED ARAB REPUBLIC
UNITED KINGDOM OF GREAT BRITAIN AND NORTHERN IRELAND
UNITED STATES OF AMERICA
URUGUAY
VENEZUELA
VIET-NAM
YUGOSLAVIA

The Agency's Statute was approved on 23 October 1956 by the Conference on the Statute of the IAEA held at United Nations Headquarters, New York; it entered into force on 29 July 1957. The Headquarters of the Agency are situated in Vienna. Its principal objective is "to accelerate and enlarge the contribution of atomic energy to peace, health and prosperity throughout the world".

Printed by the IAEA in Austria
October 1964

PROCEEDINGS SERIES

MEDICAL RADIOISOTOPE SCANNING

PROCEEDINGS OF THE SYMPOSIUM ON
MEDICAL RADIOISOTOPE SCANNING
HELD BY THE
INTERNATIONAL ATOMIC ENERGY AGENCY
IN ATHENS, 20-24 APRIL 1964

In two volumes

VOL. II

INTERNATIONAL ATOMIC ENERGY AGENCY
VIENNA, 1964

Symposium on Medical Radioisotope Scanning, Athens, 20 - 26 April 1964.
Proceedings ... held by the International Atomic Energy Agency ... Vienna, the Agency, 1964.
2 vols. (IAEA, Proceedings series)

616.073.75
612.014.483
621.039.85

MEDICAL RADIOISOTOPE SCANNING,
IAEA, VIENNA, 1964
STI/PUB/82

FOREWORD

Medical applications of radioisotopes continue to grow in number and importance and medical centres in almost all countries of the world are now using radioactive materials both in the diagnosis and treatment of disease. An increasing proportion of these applications involves studies of the spatial distribution of radioactive material within the human body, for which purpose highly specialized scanning methods have been elaborated. By these methods it is possible to study the position, size and functional state of different organs, to detect tumours, cysts and other abnormalities and to obtain much useful information about regions of the body that are otherwise inaccessible, except by surgery.

Progress in scanning methods in recent years has been very rapid and there have been many important advances in instrumentation and technique. The development of new forms of the gamma camera and of colour-scanning techniques are but two examples of recent improvements. The production of new radioisotopes and new labelled compounds has further extended the scope of these methods.

To survey these new advances the International Atomic Energy Agency held a Symposium on Medical Radioisotope Scanning in Athens from 20 - 24 April 1964. The scientific programme of the meeting covered all aspects of scanning methods including theoretical principles, instrumentation, techniques and clinical applications. The World Health Organization assisted in the selection of papers by providing a consultant to the selection committee.

The meeting followed the earlier IAEA/WHO Seminar on Medical Radioisotope Scanning in Vienna in 1959, which was attended by 36 participants and at which 14 papers were presented. Some idea of the growth of interest in the subject may be gained from the fact that the Symposium was attended by 160 participants from 26 countries and 4 international organizations, and that 58 papers were presented.

The published proceedings, comprising two volumes, contain all the scientific papers presented at the Symposium together with the subsequent discussions. Volume I covers the sessions devoted to theoretical principles, instrumentation and techniques, whilst Volume II deals with choice of radioisotopes and labelled compounds, clinical applications and interpretation of results. It is hoped that together they will provide a valuable guide to the present status and likely future development of medical radioisotope scanning and its applications.

The Agency gratefully acknowledges the co-operation of the staff of the Greek Atomic Energy Commission.

EDITORIAL NOTE

The papers and discussions incorporated in the proceedings published by the International Atomic Energy Agency are edited by the Agency's editorial staff to the extent considered necessary for the reader's assistance. The views expressed and the general style adopted remain, however, the responsibility of the named authors or participants.

For the sake of speed of publication the present Proceedings have been printed by composition typing and photo-offset lithography. Within the limitations imposed by this method, every effort has been made to maintain a high editorial standard; in particular, the units and symbols employed are to the fullest practicable extent those standardized or recommended by the competent international scientific bodies.

The affiliations of authors are those given at the time of nomination.

The use in these Proceedings of particular designations of countries or territories does not imply any judgement by the Agency as to the legal status of such countries or territories, of their authorities and institutions or of the delimitation of their boundaries.

The mention of specific companies or of their products or brand-names does not imply any endorsement or recommendation on the part of the International Atomic Energy Agency.

CONTENTS OF VOL. II

VII. CHOICE OF ISOTOPES AND LABELLED COMPOUNDS

Organ visualization by photoscanning using micro- and macro-aggregates of radioalbumin (SM-51/32) 3
G. V. Taplin, D. E. Johnson, E. K. Dore and H. S. Kaplan
Discussion 28
The use of technetium-99m as a clinical scanning agent for thyroid, liver and brain (SM-51/50) 33
P. V. Harper, K. A. Lathrop, R. J. McCardle and G. Andros
Discussion 44
Compounds labelled with low-energy gamma-ray emitters for medical isotope scanning (SM-51/38) 47
K. E. Scheer, K. Zum Winkel and M. Georgi
Discussion 67
Scanning with iodine-125 (SM-51/26) 71
M. Ben-Porath, A. Hochman and J. Gross

VIII. CLINICAL APPLICATIONS: BRAIN

Design and function of a brain scanner for clinical use (SM-51/44) ... 81
W. Paul and T. P. Morley
Results of positron scanning in 1200 cases for diagnosis of intracranial lesions (SM-51/35) 95
O. Wilcke
Discussion 104
Evaluation of fluorine-18 as a scanning agent for intracranial tumours (SM-51/41) 109
W. Entzian, S. Aronow, A. H. Soloway and W. H. Sweet
Discussion 120
Scanning techniques for brain-tumour localization (SM-51/99) 121
M. H. Duggan, J. Brice, E. Jones, J. R. Mallard and M. J. Myers
Discussion 144
Selective neoplasm localization with mercury-197 Neohydrin (SM-51/74) 147
D. B. Sodee
Discussion 156
Radioiodinated (I^{131} and I^{125}) fibrinogen for the detection of malignant tumours in man (SM-51/91) 159
G. Monasterio, M. F. Becchini and N. Riccioni
Discussion 171

IX. CLINICAL APPLICATIONS: STOMACH, BONE MARROW, LYMPH NODES, KIDNEYS

Study on the localization of iodine in the stomach (SM-51/14) 175
W. H. Clode, M. Simão Rodrigues, M. A. Perez Fernandez, M. A. Murteira and A. M. Baptista
Discussion 191
Bone-marrow scanning after intravenous injection of colloidal Au^{198} (SM-51/46) 193
L.-G. Larsson and L. Jonsson
Scanning of bone marrow in haematopoietic disorders (SM-51/55) ... 207
R. M. Kniseley, G. A. Andrews, C. L. Edwards and R. Tanida
Discussion 220
La lymphographie indirecte et son intérêt en oncologie (SM-51/5) ... 227
B. Delaloye et P. Magnenat
Discussion 236
Diagnosis of intraspinal neurological syndromes by myeloscintigram (SM-51/103) 237
G. Pantazis, J. Taptas, H. Mikropoulos, N. Kordiolis, V. Samaras, E. Paraschou, C. Savvas and F. Dermentzoglou
Discussion 254
Renal scintiscanning with Hg^{203}-Neohydrin in urologic diseases (SM-51/95) 257
V. Bollini and G. Tori
Discussion 271

X. CLINICAL APPLICATIONS: PANCREAS, LUNGS, SPLEEN

Pancreas scanning with Se^{75}-selenomethionine (SM-51/68) 275
M. Blau
Radioisotope photoscanning of the pancreas with selenomethionine-Se^{75} (SM-51/76) 289
D. B. Sodee
Discussion 300
Diagnosis of massive pulmonary embolism in man by radioisotope scanning (SM-51/73) 303
H. N. Wagner, Jr., D. C. Sabiston, Jr., M. Iio and J. K. Langan
Discussion 323
Photoscanning of the spleen by heat-treated Cr^{51}-labelled erythrocytes in congenital haemolytic anaemias (SM-51/16) 325
H. Gyftaki, C. Proukakis, D. Binopoulos, C. Elias and V. Alevizou
Résultats de l'application clinique de la scintigraphie de la rate dans 500 cas: possibilités et limites (SM-51/34) 337
J. Fischer et R. Wolf
Scintillation scanning of the spleen with red cells labelled with chromium-51 (SM-51/90) 355
F. Spinelli-Ressi
Discussion 367

XI. CLINICAL APPLICATIONS: LIVER

Application de la méthode scintigraphique à l'exploration morphologique du foie au cours de l'amibiase (SM-51/84) 373
R. Gongora et H. Jammet
The value of liver scanning in the diagnosis of echinococcus disease of the liver (SM-51/24) 389
T. Doxiades, P. Gatsou, D. Ikkos, G. Merikas and A. Nastou
Scanning study of 700 livers. Evaluation of the existing diagnostic procedures (SM-51/11) 401
P. Czerniak
Discussion 424
Liver scanning with radiomolybdenum (SM-51/61) 431
L. B. Sorensen
Discussion 445
Profile counting studies of hepatic uptake of labelled materials in man (SM-51/100) 447
E. E. Pochin
Discussion 454

List of Chairmen of Sessions and Secretariat of the Symposium 457
List of Participants 459
Author Index 467

VII

CHOICE OF ISOTOPES AND LABELLED COMPOUNDS

ORGAN VISUALIZATION BY PHOTOSCANNING USING MICRO- AND MACRO-AGGREGATES OF RADIOALBUMIN

G.V. TAPLIN, D.E. JOHNSON, E.K. DORE AND H.S. KAPLAN
SCHOOL OF MEDICINE, UNIVERSITY OF CALIFORNIA, LOS ANGELES, AND THE LOS ALAMOS COUNTY HARBOR GENERAL HOSPITAL, TORRANCE, CALIF., UNITED STATES OF AMERICA

Abstract — Résumé — Аннотация — Resumen

ORGAN VISUALIZATION BY PHOTOSCANNING USING MICRO AND MACRO AGGREGATES OF RADIOALBUMIN . Micro aggregates (10-20 nm) of human serum albumin I^{131} are shown to be superior to other agents for liver-spleen photoscanning. Radiation exposure to these organs is minimized and the test agent can be prepared with relative ease and simplicity. Also the heart, stomach and salivary glands may be clearly visualized with the same material. The techniques and physiological basis for performing and interpreting scans of these organs are described. Their diagnostic value is illustrated. The physiological basis for using macro albumin aggregates (1-10 μm) for visualization of the lungs is presented, along with typical scans in dogs. Toxicity studies and related pathophysiological investigations in animals demonstrate a wide margin of safety for using the large-particle test agents in man. Preliminary experiments in dogs indicate the feasibility of performing lung scans following the inhalation of an aerosol of the same material. This technique is simple, painless and entirely safe. Photoscans are presented from patients with a wide variety of pulmonary disorders.

EXAMEN D'ORGANES PAR PHOTOSCINTIGRAPHIE (AVEC DES MICRO-AGGLOMÉRATS ET DES MACRO-AGGLOMÉRATS DE RADIOALBUMINE). On a constaté que les micro-agglomérats (10 à 20 nm) d'albumine de sérum humain marquée avec ^{131}I sont supérieurs à toutes les autres substances pour la photoscintigraphie de la rate et du foie. Ils permettent de réduire au minimum la radioexposition de ces organes; en outre, leur préparation est relativement facile et simple. La même substance permet d'explorer aussi bien le cœur, l'estomac et les glandes salivaires. Les auteurs exposent les méthodes et les bases physiologiques d'exécution et d'interprétation des scintigrammes de ces organes. Ils donnent des exemples de leur valeur pour le diagnostic. Les auteurs indiquent ensuite les arguments d'ordre physiologique qui militent en faveur de l'utilisation de macro-agglomérats (1 à 10 μ) de radioalbumine pour explorer les poumons et présentent des scintigrammes typiques faits sur des chiens. Les études de toxicité et les recherches pathophysiologiques connexes sur des animaux montrent que l'utilisation de grandes particules dans le cas de l'homme laissent une bonne marge de sécurité. Des expériences préliminaires sur des chiens ont permis de constater qu'il est possible de faire des scintigrammes des poumons après inhalation d'un aérosol contenant la substance indicatrice. Cette méthode est simple, indolore et sans danger. Les auteurs présentent des photoscintigrammes de sujets atteints d'une grande diversité d'affections pulmonaires.

ВИЗУАЛИЗАЦИЯ ОРГАНОВ ПУТЕМ ФОТОСКЕННИРОВАНИЯ. Показано, что микрочастицы (10—20 ммк) альбумина сыворотки человеческой крови, меченого йодом-131, является наилучшим индикатором для фотосканирования печени и селезенки. Доза облучения этих органов минимальна, а приготовление индикатора относительно легко и просто. С помощью этого же вещества можно получить отчетливое визуальное представление о сердце, желудке и слюнных железах. Описываются методы и физиологические основы получения и толкования сканограмм этих органов. Иллюстрируется их значение для постановки диагноза. Физиологические основы применения альбумина в виде макрочастиц (1 — 10 мк) для визуализации легких показаны на примере типичных сканограмм собак. Токсикологическое изучение и соответствующие патофизиологические исследования на животных показывают наличие широких границ безопасности, позволяющих применять индикаторы, состоящие из крупных частиц, для сканирования у людей. Предварительные эксперименты на собаках показали возможность сканирования легких после вдыхания аэрозолей этого же вещества. Этот метод яв-

ляется простым, безболезненным и совершенно безопасным. Будут представлены фотоскенограммы больных с разнообразными легочными заболеваниями.

VISUALIZACIÓN DE ÓRGANOS POR FOTOEXPLORACIÓN (EMPLEO DE MICRO Y MACROAGREGADOS DE RADIOALBÚMINA). Los autores demuestran que los microagregados (10-20 mμ) de seroalbúmina humana marcada con ^{131}I ofrecen para la fotoexploración del hígado y del bazo ventajas señaladas sobre otros productos. La radioexposición de dichos órganos queda reducida a un mínimo y la preparación de la sustancia de ensayo es relativamente fácil. Esa misma sustancia permite visualizar el corazón, el estómago y las glándulas salivales. En la memoria se describen las técnicas y los principios fisiológicos en que se basan la fotoexploración de dichos órganos y la interpretación de los resultados obtenidos, y se subraya el valor diagnóstico de esas técnicas. Se exponen los principios fisiológicos del empleo de macroagregados de albúmina (1-10 μ) para la visualización de los pulmones, y se presentan centelleogramas típicos obtenidos con perros. Estudios de la toxicidad e investigaciones fisiopatológicas realizadas en animales demuestran la existencia de un amplio margen de seguridad para el empleo de los macroagregados con fines médicos. Algunos experimentos preliminares realizados con perros indican que es posible la exploración centelleográfica de los pulmones después de la inhalación de un aerosol de macroagregados. Esa técnica es sencilla y no ocasiona peligro ni dolor alguno. Los autores presentarán fotocentelleogramas de una gran variedad de casos de enfermedades pulmonares.

INTRODUCTION

Human serum radioalbumin is easily converted to particles of any desired size in the range of 10 nm to 100 μm or larger by combinations of heat treatment and pH adjustment [1]. The molecular aggregates so formed retain the radioiodide label more avidly than the untreated material [1]. Micro-aggregates (10 - 20 nm) are stable electronegative colloids and do not require added coating or dispersing agents to remain permanently suspended in normal physiological saline solutions [2].

The micro-aggregated radioalbumin colloids behave much like their inorganic counterparts when injected intravenously. They are rapidly and efficiently removed from the blood by the reticulo-endothelial cells of the body, mainly by those of the liver and spleen [3, 4, 5, 6]. However, unlike inorganic colloids, such as those of gold and thorium, which are retained permanently in the phagocytic cells of the liver and spleen the albumin particles presumably are metabolized by these cells [1]. The radioiodide label is rapidly released to the circulation and excreted in the urine along with albumin degradation products (large and small peptides and tyrosine)[7]. During the iodide excretion period ($T_{\frac{1}{2}}$ 10 h) the unbound iodide behaves exactly as inorganic iodide. It concentrates in the thyroid, salivary glands and stomach [1]. On this basis the liver and spleen may be scanned soon after colloidal radioalbumin injection and, if the thyroid is previously blocked by excess iodide, the salivary glands and stomach may be visualized 3 - 5 h later.

Particles larger than 1.0 μm are known to be trapped temporarily in the lung capillaries as first noted in 1946 by DOBSON [8] during experiments to determine the optimal size of colloidal chromic radiophosphate for estimating liver blood flow from the blood disappearance rate of the tracer. Recently, larger radioactive ceramic microspheres (60 μm) have been used for radiation therapy [9, 10] and for lung scanning [11] because they block pulmonary arterioles. In 1963 a procedure for preparing macro-radioalbumin

aggregates (5-50 μm) which are more suitable for lung scanning was described by us in a scientific exhibit [12]. Typical lung photoscans in rabbits and dogs were displayed and toxicity studies in animals with this agent demonstrated a wide margin of safety for future human use. However, clinical trials were deferred pending further evidence from more complete animal investigations. Additional information was accumulated by Nov. 1963. We were further encouraged by WAGNER [13] who had confirmed and extended our animal toxicity data and had already safely performed 40-50 scans in patients using the same techniques and methods for preparing the test material.

This paper presents further modification and simplification of the preparation of micro- (10-20 nm) and macro-(5-25 μm) radioalbumin aggregates (RAA) in the laboratory. It discusses the physiological mechanisms and technical aspects of their use for multiple organ scanning and illustrates the diagnostic value of liver-spleen, stomach and salivary gland scans from selected problem cases. Experimental data are presented which show the feasibility and extremely low toxicity of macro-RAA for lung scanning. Finally, current clinical experience with lung scans is described from studies in patients with pulmonary emboli, pneumonia, atelectasis, and certain tumours, cysts and abscesses which cause localized areas of relative pulmonary ischemia.

MATERIALS

Solutions of sterile pyrogen-free human serum albumin I^{131} and I^{125}* , carrier-free Cr^{51}-labelled chromic chloride**; normal human serum albumin†; 0.2 normal hydrochloric acid; 0.2 normal sodium hydroxide and normal (0.9%) physiological saline are employed. The saline solutions are preserved with 0.9% decyl alcohol and are obtained from the pharmacy at UCLA in multiple-injection-type rubber-stoppered bottles.

EQUIPMENT

The main items of equipment are:

1. A precision water bath with a suitable attachment for continuous gentle agitation of 30 to 100-ml samples of multiple-injection-type bottles at a constant temperature of 79°C (Fig. 1).
2. A well-type scintillation counter facility for measuring radioactivity levels in samples of test agents and body fluids.
3. An electron microscope with magnification to ~70 000.
4. An electrophoresis apparatus.
5. Photoscanning equipment with 19- and 31-hole focusing collimators††
6. Two scintillation detector-ratemeter-recorder systems.

---

* "Albumatope" obtained from E.R. Squibb and Sons, radiopharmaceutical division.

** 25% human albumin solution ("Albumisol") containing 0.02 molar sodium caprylate and 0.02 molar sodium acetyl tryptophanate, obtained from Merck-Sharpe and Dohme and Co.

† Obtained from E.R. Squibb and Sons, radiopharmaceutical division

†† Picker Magnascanner, Model I

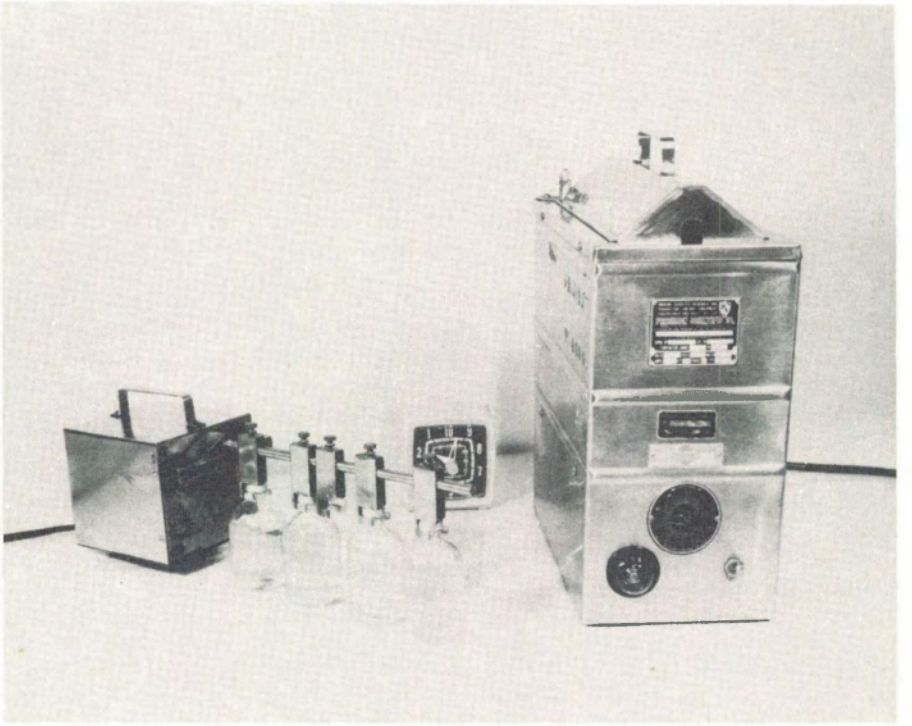

Fig. 1

Motor-driven sample shaker and precision water bath

Current methods of preparing micro- and macro-radioalbumin suspensions

Current procedures originate from BENACERRAF [14] and from abbreviated methods previously reported from this laboratory in 1961 [15] and 1963 [1].

Micro-radioalbumin aggregates (10-20 nm):

1. A 1% radioalbumin solution is prepared by dilution of 5% Albumatope with physiological saline in a sterile multiple-injection-type rubber-stoppered bottle.
2. The pH is adjusted to 10 ± 0.5 by adding 0.8 ml sterile 0.2 normal NaOH per 10 ml of solution.
3. The solution is heated in a water bath at 79°C for 20 min and agitated continuously. It is then cooled below room temperature by immersion in cold water.
4. The pH is reduced to 7.5 ± 0.5 by adding 0.2 normal HCl (0.8 ml/10 ml of solution).
5. Test for sterility and store at 5°C.

Macro-radioalbumin aggregates (5-25 μm)

Steps 1, 2 and 3 are the same as for the small colloidal suspensions.

4. The pH is reduced from 10 to 5.2 by adding 0.2 normal HCl (1.3 ml/10 ml solution). As the pH approaches 5.0 (the isoelectric point of albumin) the clear opalescent colloid is converted to micron-sized particles and takes on a skimmed-milk appearance (particle-size range = 1-10 μm).
5. The suspension is heated at 79°C for another 5 min as in step 1 to increase the size range to 5-25 μm. The material then has the appearance of homogenized whole milk.
6. Particle size is measured by examining the stained particles in a haemocytometer as described later.
7. Test for sterility and store at 5°C.

Note:

(1) I^{125}-labelled albumin can be converted to macro-aggregates in the same manner.

(2) An efficient process for tagging the macro-aggregates with Cr^{51} chloride is yet to be developed. Merely adding the labelled chromic chloride to either the small or large albumin aggregates is only about 50% efficient.

Precautions

1. Sterile equipment, supplies, techniques and pyrogen-free solutions are employed throughout.
2. With macro-aggregates albumin suspensions, the bottle should be shaken vigorously just prior to use to re-suspend the large particles.

Particle-size measurement by electron microscopy

Samples of colloidal aggregates of albumin and of gold-198 are diluted 100 000 times in pure distilled water and then examined by electron microscopy, employing shadow-casting techniques [16]. Figure 2, a composite, permits size comparison of colloidal albumin I^{131} and gold-198 aggregates. Single particles of aggregated albumin molecules measure 10-20 nm and occasional clumps of aggregates rarely exceed 200 nm. The gold suspension is composed of particles of two main sizes. The larger ones measure 10-20 nm and the smaller are probably in the range of 1-3 nm or less (sizes below the maximum resolving power of the scope).

Distilled water and normal human serum albumin are shown at the same magnification (total = 72 000 ×) to help distinguish the colloidal particles from the finely granular appearance of the collodion film and the normal albumin molecules. The colloidal albumin aggregates (10-20 nm) have an average molecular weight of ~550 000 based on ultracentrifuge studies and are thus composed of ~8 albumin molecules, since the molecular weight of albumin is 67 000.

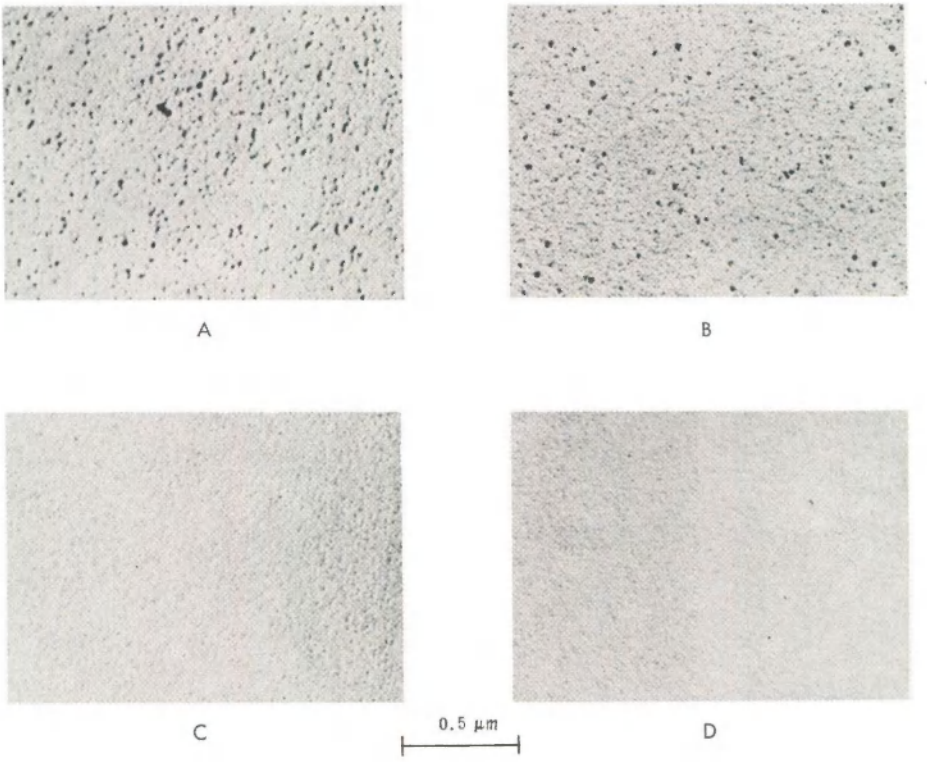

Fig. 2

Electronmicrographs

(total magnification 72 000 x)

A. Small albumin aggregates
B. Colloidal gold-198
C. Normal human serum albumin
D. Distilled water

Particle-size measurement and counting of macro-radioalbumin aggregates

The suspended aggregates are stained with Rose Bengal (pH 6.0) and viewed microscopically (430 ×) in a standard haemocytometer. The particle size of the aggregates is estimated with a filar micrometer. The number of aggregates larger than 5 $\mu m/mm^3$ is determined in the same manner as in counting white blood cells, using Rose Bengal in place of Turk's solution for staining and dilution purposes (Fig. 3).

Stability of human serum albumin I^{131} solutions and micro-RAA

Repeated tests for free I^{131} (collodion dialysis) in unheated and heated radioalbumin samples during storage at 5°C show that the I^{131} label remains

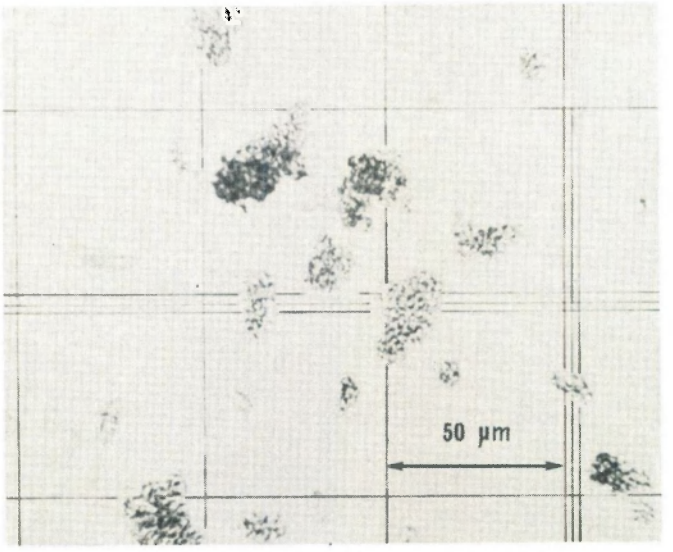

Fig.3

Photomicrograph of macro-radioalbumin aggregates viewed in a haemocytometer

more firmly bound to micro-RAA (heated samples) than to the radioalbumin solutions (unheated samples) from which the RAA were prepared (Table I).

PHYSIOLOGICAL FACTORS IN PHOTOSCANNING

Photoscanning with micro-radioalbumin aggregates

The heart, liver and spleen, stomach and salivary glands may all be scanned in this sequence after intravenous injection of 200-300 µc doses of colloidal RAA [1]. During the first 10-20 min, tracer remains largely within the vascular system and the heart is readily visualized. After 20 min, high levels are attained in the liver and spleen. However, because of the rapid liver release of I^{131}, a loading dose (4 mg/kg) of unlabelled micro-albumin aggregates is required to slow the I^{131} turnover in the liver. With such a loading dose given immediately prior to tracer injection, liver radio-activity levels usually remain sufficiently constant from 15-75 min post injection to permit accurate scanning. If these organs are re-scanned 3-5 h later the entire stomach becomes visible because sufficient I^{131} re-enters the circulation and concentrates in the stomach. A continuing I^{131} cycling process takes place with maintenance of relatively high gastric I^{131} levels for at least 10 h or until the I^{131} tracer is largely excreted in the urine. The stomach I^{131} levels remain high because of the concentrating capacity of the gastric epithelial cells and the inability of the stomach to absorb iodide [17]. The cycling process is maintained by rapid I^{131} absorption from the duodenum.

TABLE I

DIALYZABLE I^{131} IN HEATED VERSUS UNHEATED RADIOALBUMIN SAMPLES DURING STORAGE AT 5°C

Storage time when tested	Batch No.	% Dialyzable I^{131}	
		Unheated samples*	Heated samples**
1 d	147	1.85	2.20
2 weeks	146	1.50	1.60
4 weeks	145	1.49	2.10
6 weeks	144	9.40	2.97
10 weeks	142	----	2.96

* Normal human serum albumin I^{131}, obtained from E.R. Squibb and Sons.
** Heated samples of same batches (20 min. 79°C) at pH 10.0.

In our experience the stomach is better visualized 3-5 h after albumin I^{131} aggregates than after equal doses of inorganic iodide. A possible explanation is that albumin I^{131} is known to be concentrated in the stomach and slowly excreted into the gastric juice [17]. The I^{131} label is then released rapidly by digestive action. Thus, with the colloidal radioalbumin test agent, I^{131} concentrates in gastric mucosa both in the free and protein bound forms. However, the free form is dominant. Only about 4% of normal albumin is catabolized per day in the stomach [18].

Particle size and pulmonary retention of macro-radioalbumin aggregates

Investigations in dogs with RAA of increasing mean size from 1.0 to 20.0 μm show immediate retention in the lungs following intravenous injection and subsequent appearance in the liver and spleen. The larger the mean size, the longer the lung clearance half time [1]. With particles less than 1.0 μm only a few per cent are initially trapped but as the mean size is increased to 2.5 μm approximately 75% are initially deposited with half-time lung-clearance values of 30-60 min. Suspensions exceeding 10 μm mean size are nearly completely retained in the lungs initially and clear more slowly ($T_{\frac{1}{2}}$ = 1-2 h) [1]. Their transposition to the liver and spleen is likewise proportionately slower.

Lung clearance of macro-radioalbumin aggregates

The large aggregates are composed of innumerable minute ones in loosely knit masses of irregular shapes and sizes. These fragile particles are probably fragmented into their submicron-sized components within the capillaries and re-enter the general circulation. This mechanical theory is supported by the relation of particle size to lung deposition and clearance phenomena just described and by other anatomic and physiologic considerations. The mechanical theory is supported by right-heart blood-

pressure measurements made following increasing doses of large particles, given intravenously. No change occurs until large doses are given (50-150 mg/kg), then an immediate but transitory rise occurs. Likewise, similar large doses are required to induce disturbances in the radiocardiogram or to cause observable signs of respiratory distress. Furthermore, by external monitoring of the general circulation (head or extremities) following intravenous injection, complete lung retention can be demonstrated for the first few minutes when the particles exceed 10-15 μm (mean size) and the radiocardiogram shows a single right-heart curve, indicating little or no return from the lungs. Similar mechanical interpretation of the lung retention mechanism has been made by HAMLIN et al. [19] using inorganic radioactive ceramic microspheres (60 μm) for determining functional distribution of right ventricular output in the lungs of dogs and by HAYNIE [11] for experimental lung scanning and by YA et al. [10], PERRY et al. [20], ARIEL [21] and KIM et al. [22] for the radiation treatment of lung cancer. Finally, it is most unlikely that phagocytosis plays any role in clearance because lung macrophages do not line the pulmonary capillary beds as do the Kupffer cells in the liver's sinusoids [23].

PHOTOSCANNING RESULTS IN MAN WITH RADIOALBUMIN AGGREGATES

Human phantom studies

The advantage of photo versus dot scanning of large organs is demonstrated with the Alderson human abdominal phantom. The liver and spleen are filled with I^{131} solutions containing 150 μc in the liver and 7.5 μc in the spleen. Sixteen μc are added to the body of the phantom to simulate the background activity of surrounding organs and tissues. Radionegative tumours are much more difficult to localize than radiopositive ones unless they exceed 2.5 cm in diam. and are located close to the liver surface. Liver photo and dot scans presented in Fig.4 demonstrate that radionegative tumours located directly beneath the surface, measuring 5.0 and 2.5 cm diam. are readily visualized by photoscanning, but may be difficult to identify by dot scanning. The photoscan was made with high contrast to accent differences between maximum and minimum liver radioactivity levels. The dot scan was made to show the liver outline accurately plus surrounding tissue background. Simultaneous use of photo and dot scanning techniques in this manner provides optimal data for diagnostic interpretation.

Results with micro-RAA

Normal liver photoscans

The normal position, shape and size of the liver, all of which vary considerably from person to person, are illustrated in Fig. 5. The outline of the inside of the heart also may be demonstrated during the first 20 min post injection because sufficient tracer remains in the vascular system during this period.

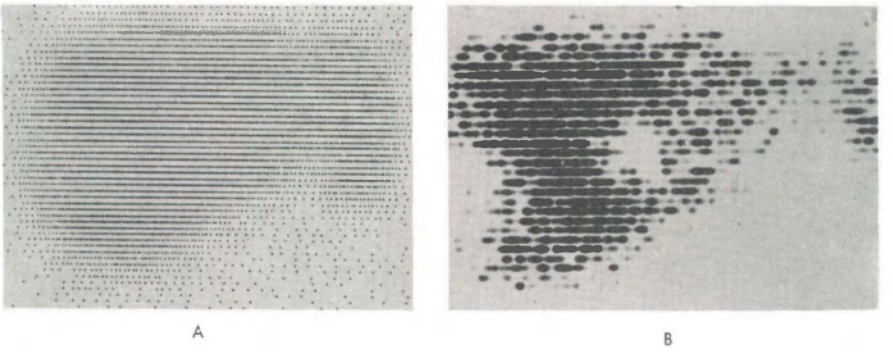

Fig. 4

Alderson human phantom study

(5.0 and 2.5 cm tumours)

A. Dot scan
B. Photo scan

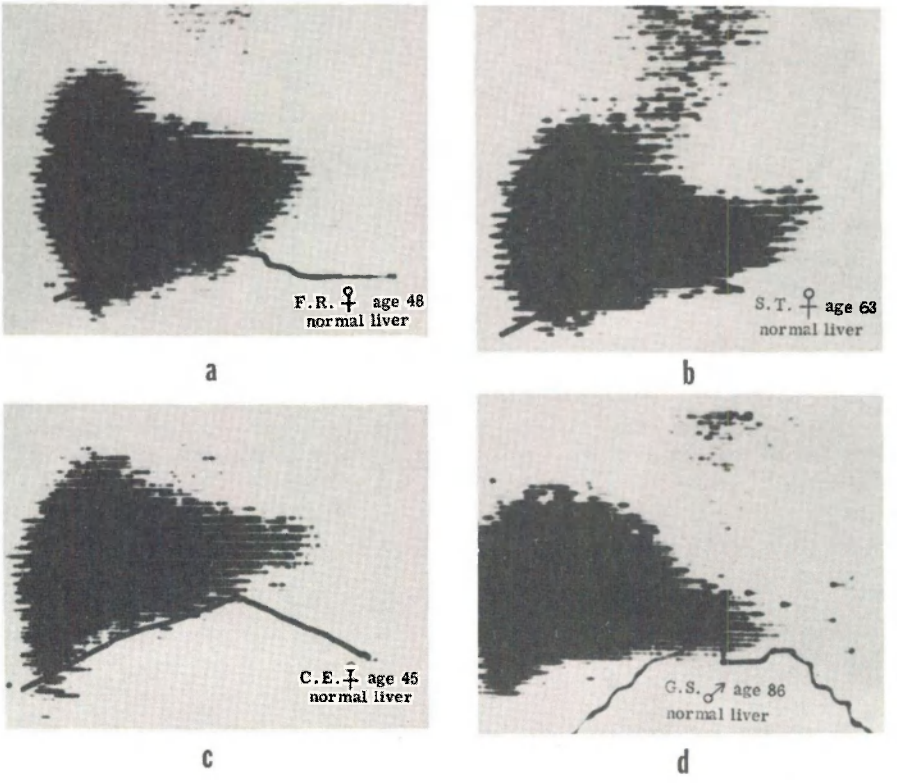

Fig. 5

Normal liver photoscans

Identification of upper abdominal lesions

The photoscan in Fig. 6 is from a patient with acute severe upper intestinal bleeding. It was performed just after he was relieved of shock. A palpable epigastric mass was believed to be spleen by most examiners.

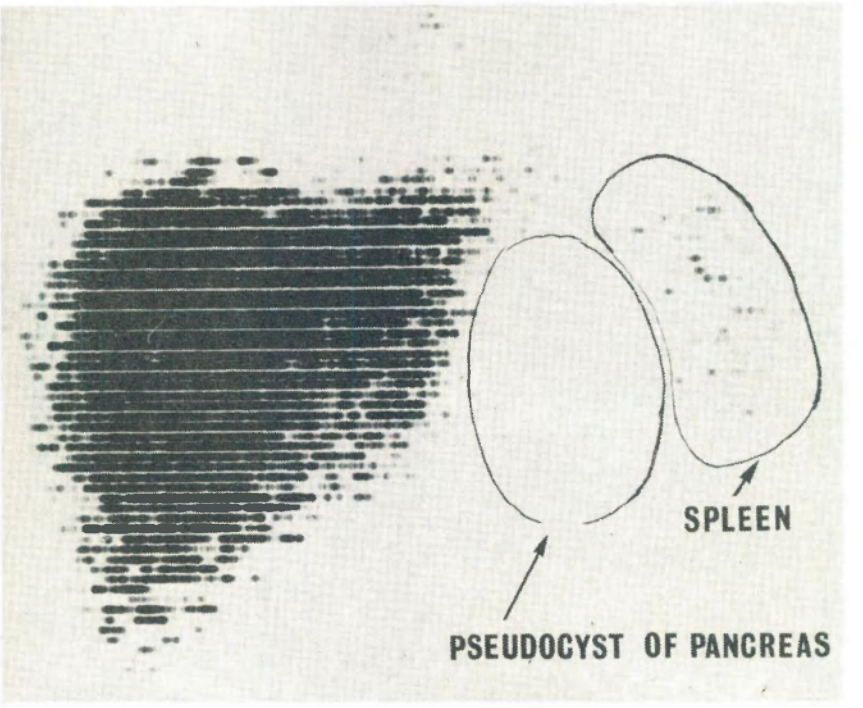

Fig. 6

Photoscan showing spleen and a pseudocyst of the pancreas

However, no radioactivity accumulated in the region of the palpable tumour. Both the spleen* and the liver are shown to be displaced laterally. At operation a pseudocyst of the pancreas was found to have eroded the stomach and caused the gastric bleeding. This is an example of how a photoscan provides useful diagnostic information in a clinical condition where routine radiographic examination is hazardous.

Demonstration of metastatic liver lesions

The composite of three liver photoscans in Fig. 7 demonstrates the capacity of the scanning procedure to identify areas of abnormal tissue in the liver. The first is from a patient with proved liver abscesses. The

* The outline of the spleen was drawn from the dot scan made simultaneously. It was faintly recorded in the photoscan but lost during reproduction.

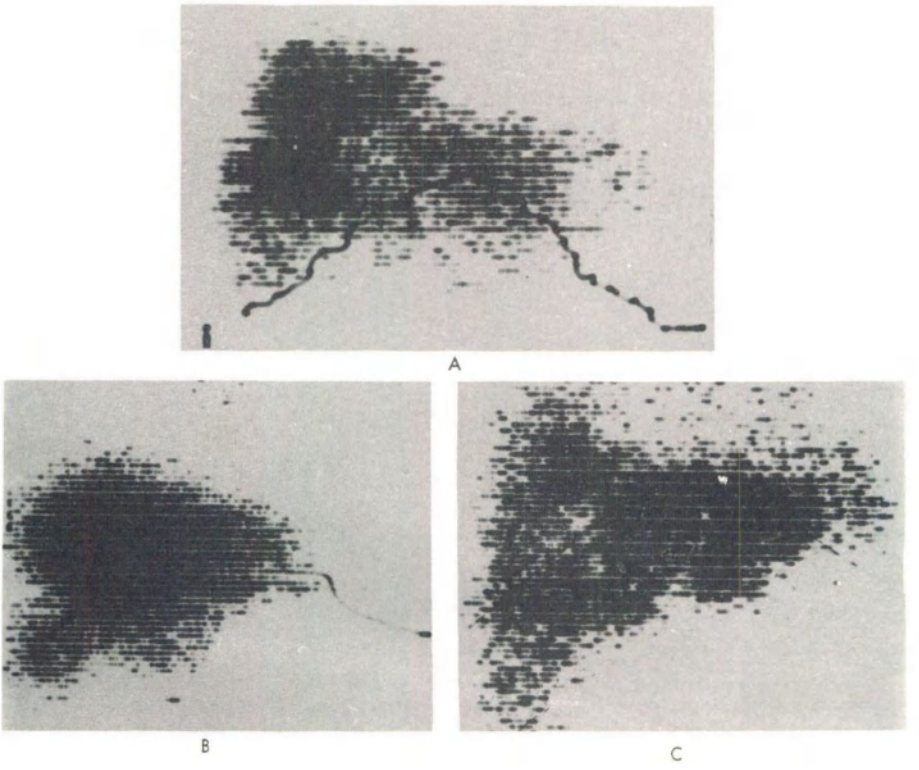

Fig. 7

Abnormal liver photoscans

A. Liver abscesses
B. and C. Metastatic liver malignancy

other two are from individuals with metastatic liver malignancy. The scan helps to select the site where liver biopsy should be taken for histological examination and exact diagnosis.

Serial abdominal scans in Hodgkin's disease

The three photoscans in Fig. 8 are from the same patient, a 14-yr-old boy with Hodgkin's disease. The initial scan performed 15-75 min following injection of albumin I^{131} aggregates shows an enlarged liver and spleen. In the second scan, 4 h later, the stomach appears superimposed upon the liver and spleen. The third scan after 7 h demonstrates more radioactivity in the stomach and less in the liver and spleen. These serial scans display the transposition of free I^{131} from the liver and spleen to the stomach, and demonstrate the proteolytic capacity of the RE cells.

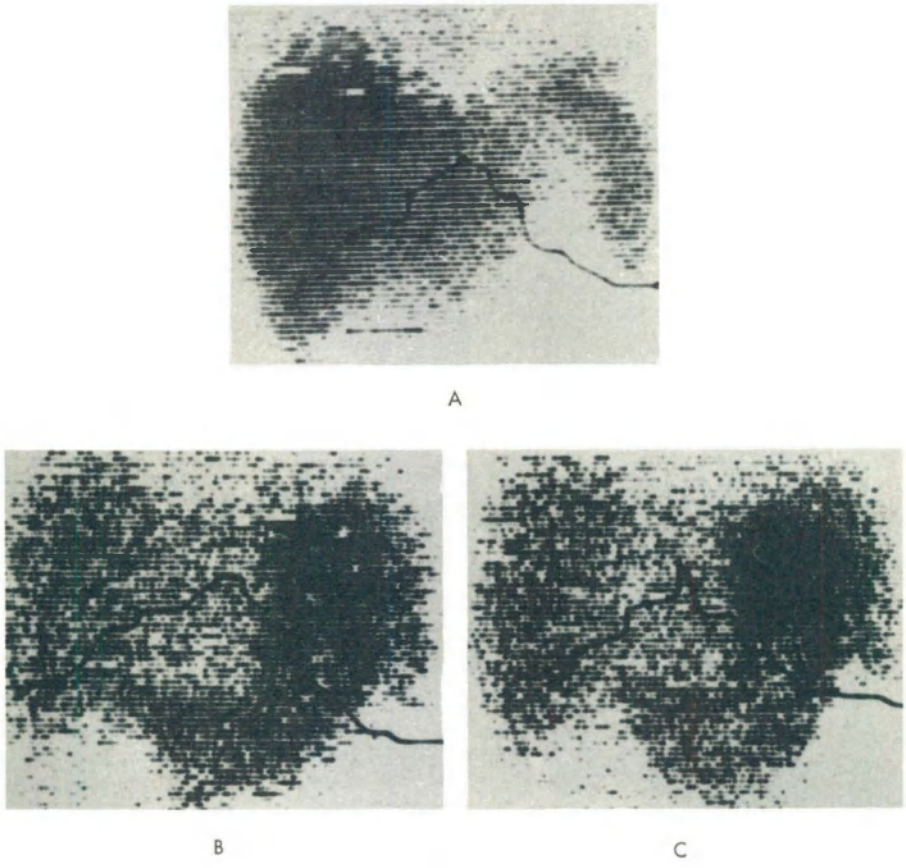

Fig. 8

Serial abdominal scans with albumin I^{131} aggregates

A. Initial scan
B. 4 h
C. 7 h

Stomach and salivary gland scans

Stomach scans of nearly equal quality with the same dose (250 μc) of inorganic radioiodide and radioalbumin are demonstrated in Fig. 9. In addition, the salivary glands may be visualized either immediately after sodium I^{131} injection or 3 - 4 h following the same dose of colloidal radioalbumin aggregates. The parotid, the sublinguals and the thyroid glands are shown in Fig. 10. The thyroid was previously blocked with excess iodide but is still visible. The salivary glands can and must be distinguished from thyroid metastases by their location. size and shape.

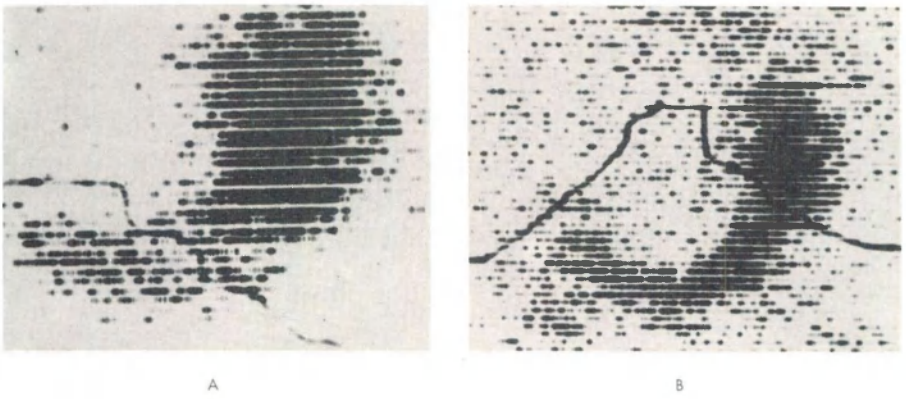

Fig. 9

Gastric photoscans

A. 250 μc albumin I^{131} aggregates 4 h after injection
B. 250 μc sodium I^{131} 15 min after injection

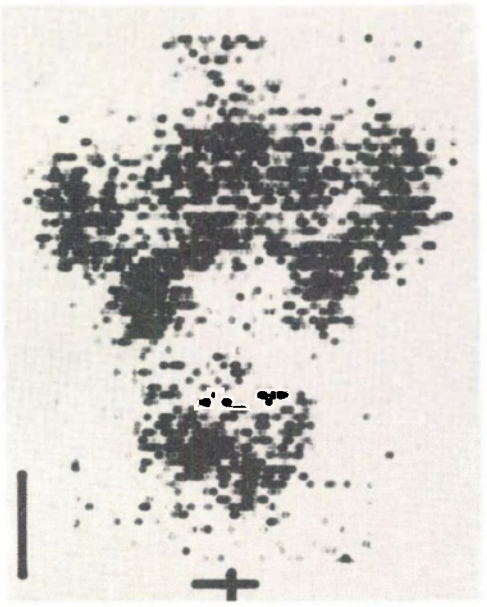

Fig. 10

Photoscan of salivary glands and thyroid 3 h after 25 μc NaI^{131} intravenous injection. Thyroid blocked previously with excess iodide.

LUNG SCANNING WITH MACRO-RADIOALBUMIN AGGREGATES

Technique, dose requirements and calculated radiation exposure

The photoscanning procedure may be started immediately following intravenous injection of macro-RAA (5-25 μm). Doses of 150-300 μc of I^{131}-labelled particles are adequate and the amount of albumin carrier need not exceed 30 μg/kg. Radiation exposure to the lungs from I^{131} is calculated as about 100-200 mr and is at least 20 times less from I^{125}. With scan speeds of 40-50 cm/min the procedure requires about 1 h. Moderately high contrast enhancement is used for photoscanning to accent differences in radioactivity levels within the lung field. In most of our I^{131} studies patients were scanned in the supine position (anterior view of the chest).

Preliminary results

In the few normal subjects (scanned most recently) the entire lung fields are visible posteriorly. In anterior views of the left lower lung, the costophrenic region is partly obscured by the heart. The clavicles cause some interference with viewing the apical regions even with I^{131} scans. They nearly obliterate underlying lung tissue when the scan is made with I^{125}. Normally, there is nearly uniform distribution of radioactivity throughout both lungs, except at the costophrenic angles. In these areas, radioactivity levels are decreased in anterior scans for technical reasons (geometry factors).

Normal I^{131} and I^{125} lung scans are presented in Figs. 11 and 12. In the latter, the rib shadows are distinctly visible. If desired, rib markings may be avoided by adjusting the focusing collimator to view the lung surface just beneath the rib level. Figure 13 illustrates the inability of the scanning procedure to detect multiple small lung tumours (< 2 cm diam.) which are visible by X-ray examination, but the scan demonstrates the larger metastatic lesions in the liver. In massive atelectasis from obstructive bronchogenic carcinoma (Fig. 14) the scan verifies the fact that non-aerated lung tissue becomes ischemic. Regional ischemia is likewise found in areas of lung consolidation and abscess formation (Figs. 15, 16 and 17).

Pulmonary emboli with and without haemorrhagic infarction (venous congestion) produce areas of relative ischemia (bronchial blood supply only) in the regions of the lung supplied by the obstructed artery (Figs. 18 and 19). The lung tissue supplied by the embolized artery presents a wedge-shaped area of decreased radioactivity in the scan. Radiographically a similar wedge-shaped area of relative radiodensity is found when there is associated haemorrhagic infarction. A unique diagnostic feature of the lung scan is its capacity to display the ischemic areas produced by small pulmonary emboli before radiographic signs of infarction or ischemia appear in standard chest X-rays. The scan findings are identical whether or not infarction develops, whereas radiographic changes are far more dependent on infarction which produces the relative radiodensity needed for visualization.

Lung tumours which compress or obstruct pulmonary arteries cause regional ischemia without infarction unless there is pre-existing pulmonary venous congestion [24]. Routine chest films seldom disclose this infor-

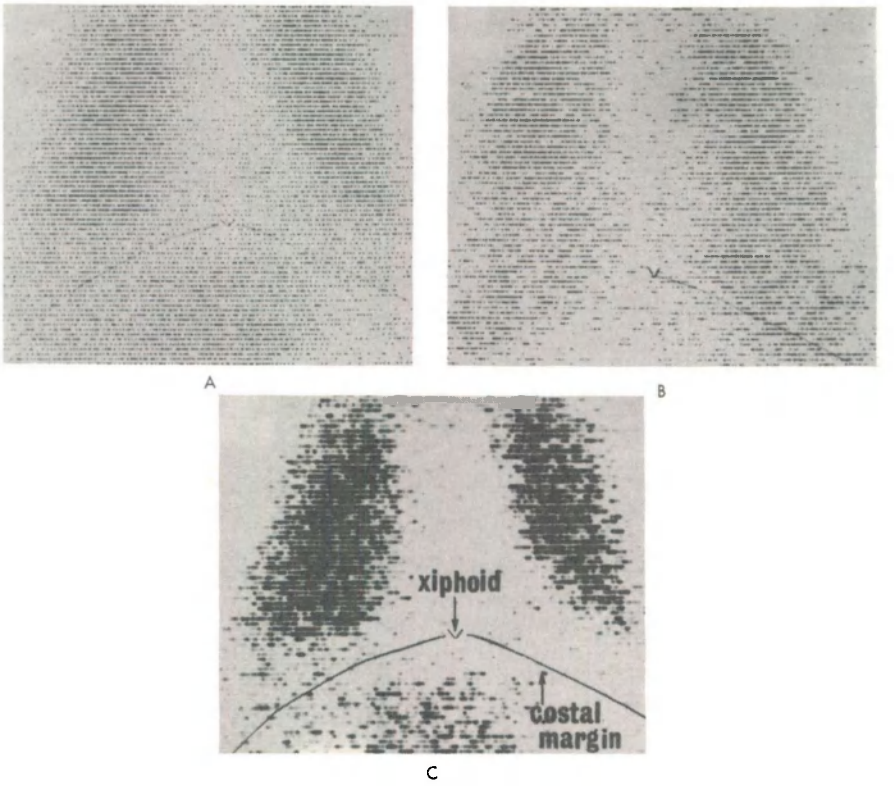

Fig.11

Normal I^{131} lung dot and photoscans

A. AP view
B. PA view
C. AP view

mation (Fig. 13). The lung scan thus aids X-ray interpretation and indicates when pulmonary angiography should be performed. An example of complete left-pulmonary artery obstruction without infarction caused by lung cancer with hilar involvement is presented in Fig. 20. Ischemia of the entire left lung was first detected by scanning. It was later confirmed by angiography. A repeated scan one month following radiation therapy indicates improved pulmonary arterial blood flow, presumably by shrinkage of the obstructive tumour tissue.

Lung scans have been performed in more than 100 patients with macro-RAA entirely without reactions. Emboli first detected by scanning have been confirmed at autopsy in several instances. Lung consolidation from pneumonia, infarction, tumours, atelectasis and large abscesses found by radiography has been associated consistently with regional ischemia in the scan in more than 50 cases.

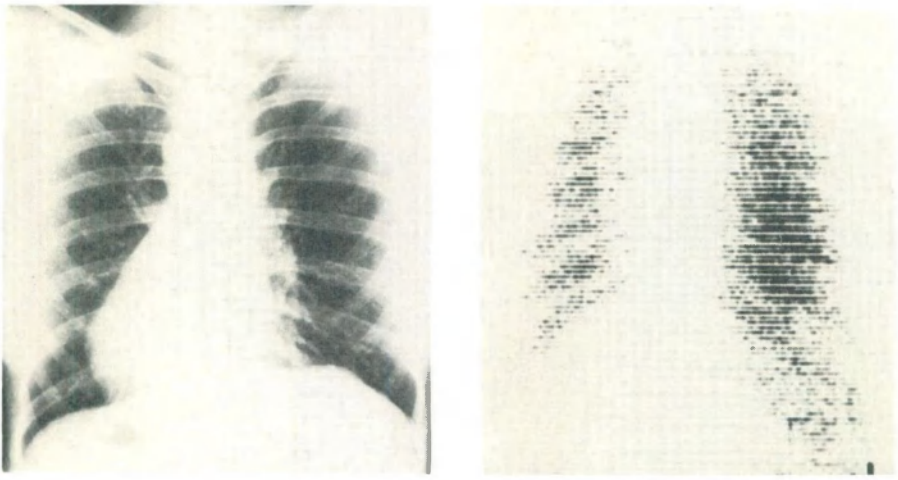

Fig.12

Normal I^{125} lung scan and chest X-ray (PA views)

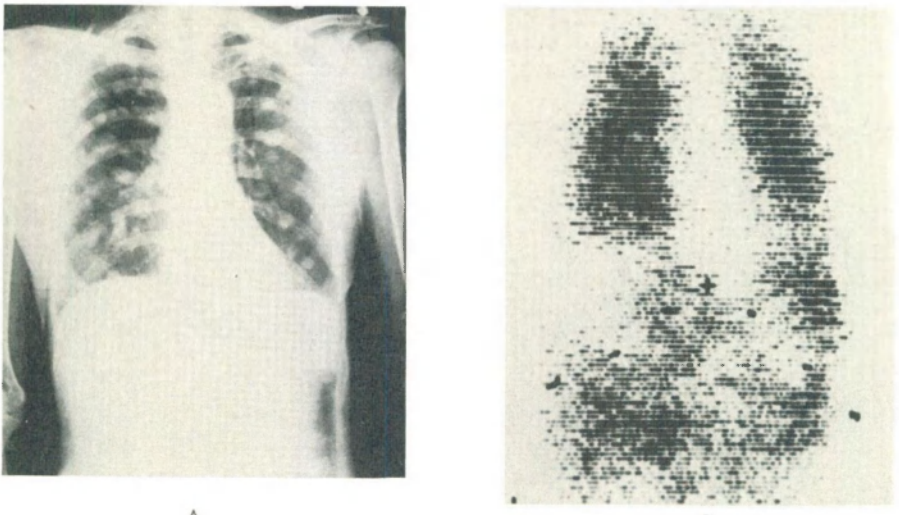

A B

Fig.13

Multiple metastatic lesions of the lungs and liver

A. Chest X-ray; lung lesions
B. Lung-liver scan

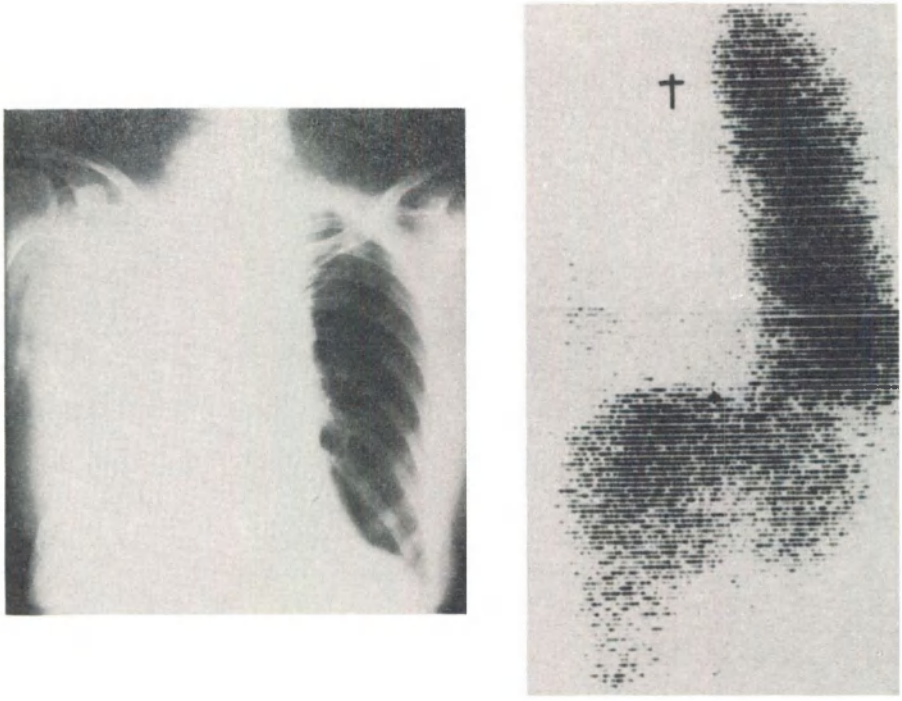

Fig.14

Bronchogenic carcinoma: massive atelectasis and liver metastases

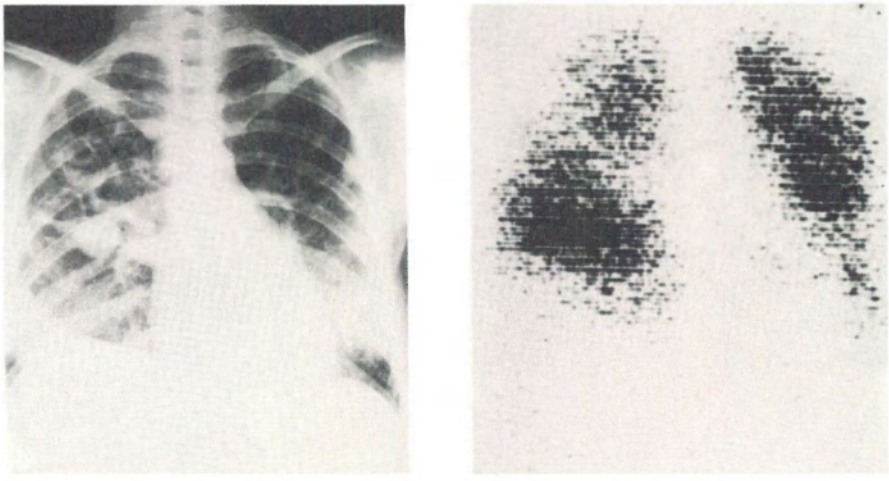

Fig.15

Staphylococcal pneumonia, multiple abscesses

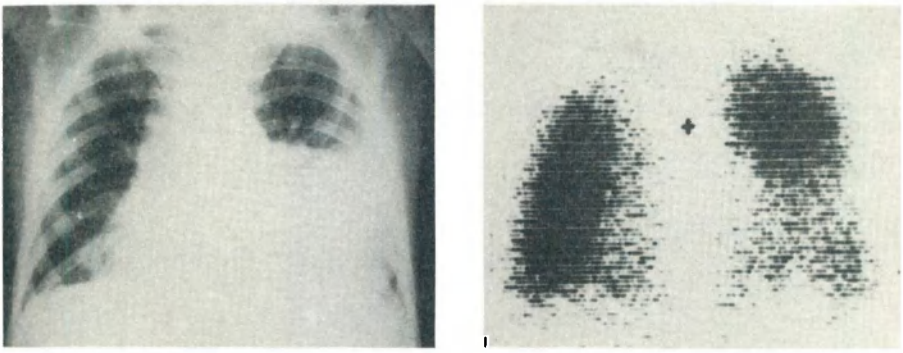

Fig.16

Pneumonia, left lower lobe

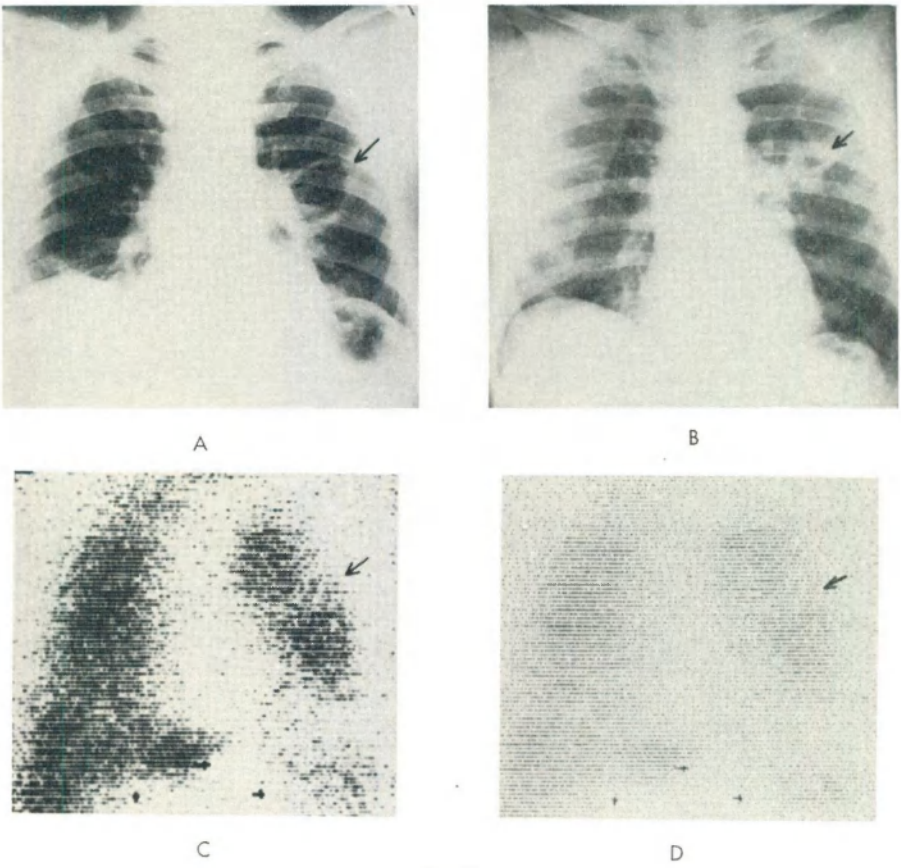

Fig.17

Pulmonary infarct, left upper lobe

A. Chest X-ray, 13/11/63
B. Chest X-ray, 6/12/63
C. Lung and liver photoscan, 13/12/63
D. Lung and liver dot scan, 13/12/63

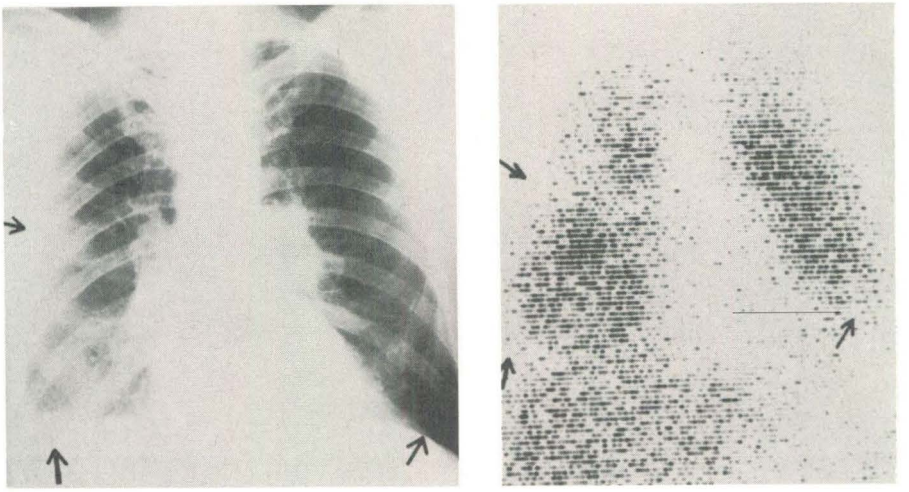

Fig.18

Multiple pulmonary emboli with and without infarction

DISCUSSION

Advantages and limitations of micro-radioalbumin aggregates for organ scanning

Micro-RAA have important advantages over colloidal gold-198 and Rose Bengal I^{131} for scanning the liver, because of their rapid degradation in the liver's Kupffer cells and subsequent urinary excretion of the iodide label within 72 h. Hepatic radiation exposure is at least 100 times less than that from equal doses of gold and about three times less than Rose Bengal I^{131} [1]. For spleen scanning the RAA are preferred over heated homologous Cr^{51} erythrocyte labelling and heating procedures. Furthermore, multiple organs may be visualized sequentially with this agent, namely the heart, liver, spleen, stomach and salivary glands.

The rapid liver turnover of the radioalbumin is also one of its limitations in scanning because strictly constant levels of radioactivity are not maintained during the scanning period. This disadvantage may be partially overcome by simultaneous administration of a loading dose (4 mg/kg) of unlabelled micro-aggregates, which slows the tracer turnover rate in the liver ($T_{\frac{1}{2}}$ = 20 min) by a factor of 3 and thereby provides relatively constant radioactivity levels in the liver for about 1 h.

Potential hazards from large particle injections

The possibility that large particles might enter the cerebral circulation following intravenous injection and produce irreparable brain damage from micro-emboli poses the greatest potential hazard. Fortunately, in the dog,

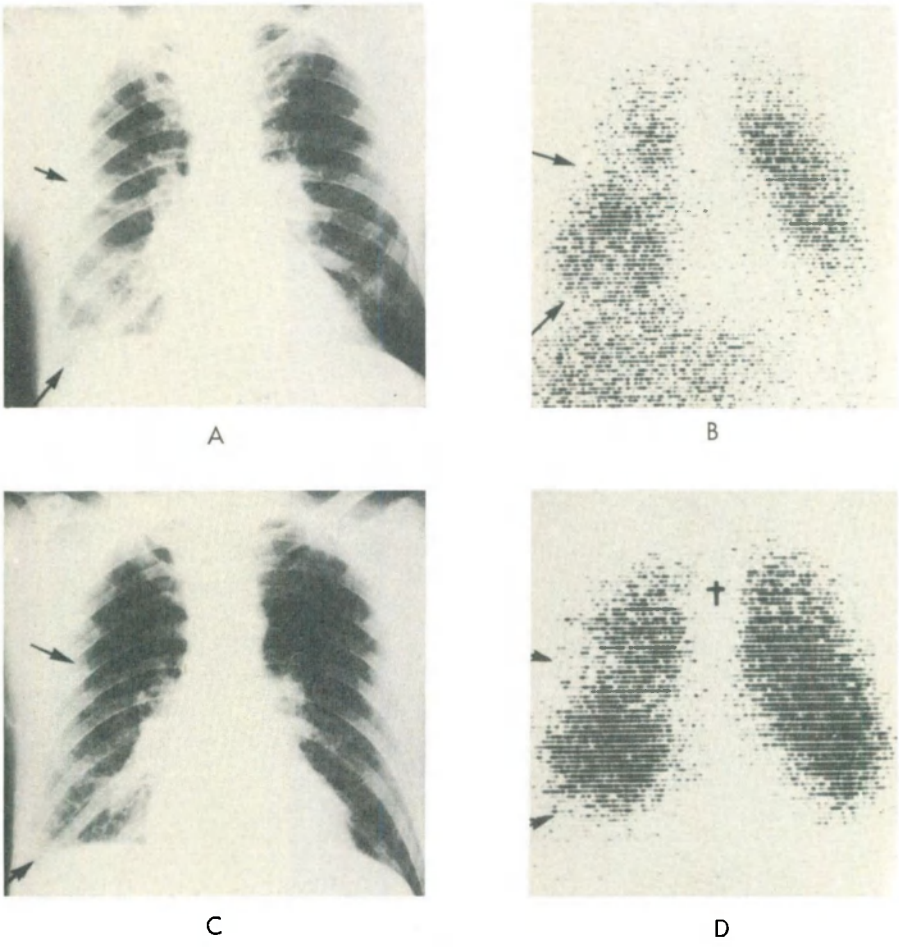

Fig. 19

Pulmonary emboli

A. Chest X-ray, 2/1/64
B. Photoscan, 2/1/64
C. Chest X-ray, 23/1/64
D. Photoscan, 23/1/64

monkey and in man particles in the 5 to 25-μm size range are practically completely retained in the pulmonary capillary bed. More importantly, radioalbumin aggregates of this size are readily demonstrated to pass freely through the capillaries of the brain and lower extremities in both of these animal species following internal carotid or femoral artery injection [25]. To purposely cause temporary capillary retention in the extremities and/or brain the mean particle size must be increased at least threefold (from 15 to 45 μm or more) [25]. Injection of 5 - 25 μm RAA directly into the femoral or internal carotid arteries causes little or no retention in the ex-

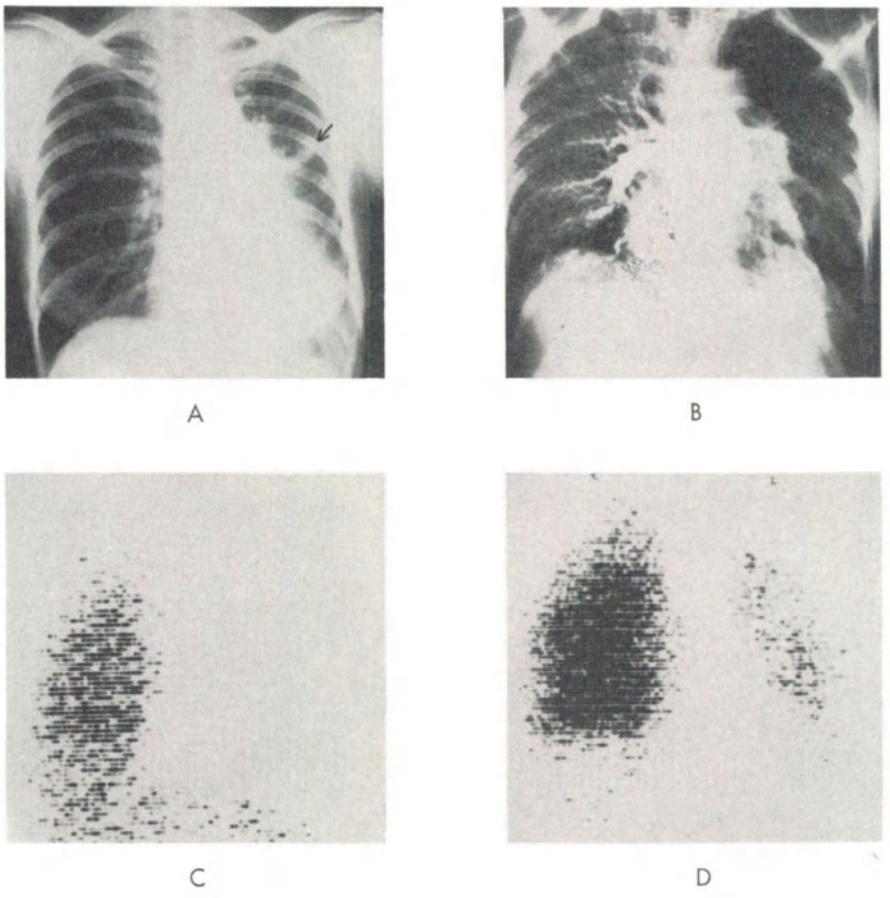

Fig. 20

Left pulmonary artery obstruction without infarction

A. Chest X-ray, 27/11/63
B. Pulmonary arteriogram, 29/11/63
C. Lung photoscan before X-ray therapy, 26/11/63
D. Lung photoscan after X-ray therapy, 8/1/64

tremities or brain initially or later, and the bulk of the material rapidly accumulates in the lung. More importantly, internal carotid artery injections of 1 to 10-mg doses of carrier albumin in 30 to 45-μm radioalbumin aggregates (mean size), have not produced neurological damage detectable by electroencephalography or by behavioural disturbances in either dogs or monkeys [25]. On this basis plus clinical experience, the possibility of central nervous system complications in man from lung scanning is extremely remote even in patients with cardiac shunts. However, as a precautionary measure, lung scans should be performed with the minimum number of particles required and individual particles should not exceed 25 μm.

Direction of future studies with macro-radioalbumin aggregates

Lung scanning. Now that the lung scanning procedure is shown to be safe [13], extensive studies should be made in patients with normal lungs to obtain the control data needed to interpret scans with minor abnormalities. Optimal scanning techniques should be established for I^{131}, Cr^{51} and I^{125} RAA. I^{125} RAA are theoretically superior to higher energy Cr^{51} and I^{131} preparations for visualizing areas of reduced blood flow at the lung surface as produced by pulmonary emboli.

Instrument modifications. A considerable reduction in scanning time is possible by modification of the scanner's collimator, detector-crystal-photomultiplier-tube assembly, scan motor-speed regulator, and light source. Substitution of a thin window, wafer-thin crystal and a collimator with a shorter depth of focus should increase counting efficiency 5 to 10-fold. Thus, with the larger doses of I^{125} permissible because of no beta ray emission, lung and/or liver scans now requiring 60 min should be possible to accomplish in 6-12 min.

Larger albumin I^{125} aggregates for experimental brain and kidney scanning

As mentioned in the discussion, one hemisphere of the brain may be scanned following internal carotid artery injection of I^{125} macro-RAA provided the mean particle size exceeds 15 μm. The optimal size is probably between 30 and 45 μm. Preliminary toxicity studies in 12 dogs, 4 monkeys and 2 baboons indicate a safety factor of about 100. So far the amount of test material needed for scanning (0.05 - 0.10 mg) may be exceeded by at least 100× without causing detectable brain damage. However, extensive data are needed in primates with longer observation periods before initiating clinical trials in patients with metastatic brain tumours.

Similar animal studies are needed to determine optimal particle size, minimal dose requirements and safety factors for instituting clinical investigations of renal scanning with macro-RAA. It is known that arterial injection of 60-μm-sized ceramic microspheres can cause severe cortical necrosis, depending on the number of particles injected [19]. However, in both brain and kidney scanning the likelihood of producing tissue damage is far less with the fragile RAA than with the inert solid spheres which are not metabolized or broken down within the capillaries. If the minute doses needed for scanning can be shown to be non-injurious with a wide margin of safety, brain and kidney scans with this agent should have important advantages over radiomercury compounds now in use [26].

SUMMARY

Current methods of preparing micro- (10-20 nm) and macro- (5-25 μm) radioalbumin aggregates by heat treatment and pH adjustment are described. The small colloidal size suspensions can replace colloidal radiogold and Rose Bengal for liver scanning and Cr^{51}-labelled red blood cells for spleen scans, because of their rapid accumulation in the liver and spleen and subsequent metabolism of the albumin by proteolytic action of the phagocytic cells.

Following release of the I^{131} label to the circulation, the stomach, thyroid and salivary glands may also be scanned. Radiation exposure to these organs is minimal and the test agent can be prepared in any clinical laboratory from commercially available radioalbumin in less than 1 h. The basis and techniques for performing and interpreting scans of these organs are described. Their diagnostic value is illustrated from selected case reports.

Extensive studies in rabbits and dogs demonstrate the feasibility, low toxicity and wide margin of safety for performing human lung scans with macro- (5-25 μm) radioalbumin aggregates. The dose which produces only occasional transient alteration in pulmonary haemodynamics in dogs (50-150 mg/kg) is at least 3000 times larger than that (15-30 μg/kg) needed to perform lung scans in man.

Pulmonary emboli, pneumonia, atelectasis, tumours and other lesions which cause regional pulmonary ischemia, are detectable in the scan as areas of decreased radioactivity. On this basis the lung scan is unique and has diagnostic value by itself. It also helps in the interpretation of chest films and may indicate when pulmonary arteriograms should be performed. Probably its most important application is in the early diagnosis of pulmonary emboli where it can point to the location and size of the lesions before radiologic signs of infarction or ischemia develop.

ACKNOWLEDGEMENTS

The authors are grateful to Mary Lee Griswold for preparation of the aggregated radioalbumin test material and for technical assistance in the basic aspects of this work; to Mitsue Yamaguchi, Robert DiVeroly and Marilyn Rawlings for technical assistance; to Frances Nickles for preparation of the illustrations; to Peter Kalian and Hector Pimental for photographic assistance; to Ruth McCandless for preparing the electronmicrographs, all of the Laboratory of Nuclear Medicine and Radiation Biology of the Department of Biophysics-Nuclear Medicine, University of California at Los Angeles; and to Glen Meloy and Donalee Tabern of the Nuclear Instruments Division of Picker X-ray Corporation for the loan of the Magnascanner used in the clinical studies, and to Tualua Tofili of Harbor General Hospital for technical assistance in the clinical scanning studies.

The clinical work was performed in the Nuclear Medicine Division of the Department of Radiology at the Los Angeles County Harbor General Hospital, Torrance, Calif.

REFERENCES

[1] TAPLIN, G.V., DORE, E.K. and JOHNSON, D.E., "Suspensions of Radioalbumin Aggregates for Photoscanning the Liver, Spleen, Lung and Other Organs", USAEC Report UCLA-519 (1963) and in Press, J. nucl. Med. (1964).

[2] TAPLIN, G.V., DORE, E.K. and JOHNSON, D.E., in Radioaktive Isotope in Klinik und Forschung 5 (FELLINGER, K., HOFER, R., Eds.) Urban and Schwarzenberg, Munich (1963) 346-358.

[3] BIOZZI, G., BENACERRAF, B., HALPERN, B.N., STIFFEL, C. and HILLEMAND, G., Exploration of the Phagocytic Function of the RES with Heat Denatured Human Serum Albumin I^{131} and Application to the Measurement of Liver Blood Flow in Normal Man and in some Pathological Conditions, J. Laborat. Clin. M. 51 (1958) 230.

[4] SHALDON, S., CHIANDUSSI, L., GUEVARA, L., CAESAR, J. and SHERLOCK, S., The Estimation of Hepatic Blood Flow and Intra Hepatic Shunted Blood Flow by Colloidal Heat Denatured Human Serum Albumin, Labelled with I^{131}, J. clin. Invest. 40 (1961) 1346.

[5] IIO, M. and WAGNER, H.N., Jr., Studies of the Reticuloendothelial System (RES) in Man and Dog, J. clin. Invest. 42 (1963) 417.

[6] WAGNER, H., IIO, M. and HORNICK, R., Studies of the Reticuloendothelial System (RES) II. Changes in the Phagocytic Capacity of the RES in Patients with Certain Infections, J. clin. Invest. 42 (1963) 427.

[7] TAPLIN, G.V., DORE, E.K., GARCIA, E.J. and JOHNSON, D.E., Reticuloendothelial System Studies with Radiocolloids, Proc. IX Cong. Intemat. Soc. Hemat., Mexico City (1963) in Press.

[8] DOBSON, E.L. and JONES, H.B., The Behavior of Intravenously Injected Particulate Material: Its Rate of Disappearance from the Blood Stream as a Measure of Liver Blood Flow, Acta med. scand. 144 Suppl. (1952) 273.

[9] RING, G.C., BLUM, A.S., KURBATOV, T., MOSS, W.G. and SMITH, W., Size of Microspheres Passing Through Pulmonary Circuit in the Dog, Amer. J. Physiol. 200 (1961) 1191.

[10] YA, P., GUZMAN, T., LOKEN, M. and PERRY, J., Isotope Localization with Tagged Microspheres, Surgery 49 (1961) 644.

[11] HAYNIE, T., CALHOUN, J.H., NASJLETI, C.E., NOFAL, M.M. and BEIERWALTES, W.H., Visualization of Pulmonary Artery Occlusion by Photoscanning, J. Amer. med. Ass. 185 (1963) 306-8.

[12] TAPLIN, G.V., DORE, E.K., JOHNSON, D.E. and KAPLAN, H.S., Colloidal Radioalbumin Aggregates for Organ Scanning, Scientific Exhibit, 10th Ann. Meet. Nucl. Med. Soc., Montreal, Canada, June 1963.

[13] WAGNER, H.N., Jr., Personal communication.

[13a] WAGNER, H.N., Jr., SABISTON, D.C., Jr., MASAHIRO, I., McAFEE, J.G., MEYER, J.K. and LANGAN, J.K., Pulmonary Blood Flow by Radioisotope Scanning, J. Amer. med. Ass. 187 8 (1964) 601-4.

[14] BENACERRAF, B., BIOZZI, G., HALPERN, B.N. and STIFFEL, C., A Study of the Phagocytic Activity of the Reticuloendothelial System Toward Heat Denatured Human Serum Albumin Tagged with I^{131}, RES Bull 2 (1956) 19.

[15] TAPLIN, G.V., GRISWOLD, M.L. and DORE, E.K., Preparation of Colloidal Suspensions of Human Serum Albumin I^{131} for Estimating Liver Blood Flow and Reticuloendothelial System Functions in Man, USAEC Report UCLA-481 (1961).

[16] PEASE, D.C., Histological Technique for Electron Microscopy, Academic Press, New York (1960).

[17] BROWN-GRANT, K., Extrathyroidal Iodide Concentrating Mechanisms, Physiol. Rev. 41 (1961) 189.

[18] WETTERFORS, J., GULLBERG, R., LILHEDAHL, S.O., PLANTIN, L.O., BIRKE, G. and OLHAGEN, B., Role of the Stomach in Albumin Breakdown, Acta med. scand. 168 (1960) 347.

[19] HAMLIN, R.L., MARSLAND, W.P., SMITH, C.R. and SAPIRSTEIN, L.A., Fractional Distribution of Right Ventricular Output in the Lungs of Dogs, Circul. Res. 5 (1962) 763-6.

[20] PERRY, J., LOKEN, M., RYAN, J. and MAC LEAN, L., Microspheres for Radiation Therapy, Nucleonics 20 (1962) 70.

[21] ARIEL, I.M., Organ Irradiation by Means of Radiation Microspheres, J. nucl. Med. 3 (1962) 195.

[22] KIM, Y.S., LA FAVE, J.W. and MAC LEAN, L.D., Use of Radiating Microspheres in Treatment of Experimental and Human Malignancy, Surgery 59 (1962) 220.

[23] Pulmonary Structure and Function, Ciba Foundation Symposium, Little-Brown and Co., Boston, Mass. (1962).

[24] WESTERMARK, N., On the Roentgen Diagnosis of Lung Embolism, Acta radiol., Stockh. 19 (1938) 357-72.

[25] TAPLIN, G.V., KENNADY, J.C., GRISWOLD, M.L., AKCAY, M.M. and JOHNSON, D.E., Albumin I^{125} Macroaggregates for Brain Scanning (Experimental Basis and Safety), in preparation for presentation at the 11th Ann. Meet. Nucl. Med. Soc., Berkeley, California, June 1964.

[26] McAFEE, J.G. and WAGNER, H.N., Jr., Visualization of Renal Parenchyma by Scintiscanning with Hg^{203} Neohydrin, Radiology 75 (1960) 820.

DISCUSSION

C.M.E. MATTHEWS: With regard to Dr. Taplin's very interesting paper, I should like to mention a different isotope which we have used at Hammersmith Hospital* for studies of lung function. This is Xe^{133} which can be used to measure both regional blood flow and ventilation. For measuring regional blood flow a solution of Xe^{133} in saline is injected intravenously; the amount of radioactivity which arrives in different regions of the lung is proportional to blood flow. For measuring ventilation, gaseous Xe^{133} is inhaled. In Fig. 1, on the left-hand side, records made after injection of Xe^{133} in a normal subject are shown; the count rate in this situation is proportional to perfusion. The middle records were made after a single inhalation of Xe^{133}, so that the count rate is proportional to ventilation. The records on the right-hand side were made after rebreathing Xe^{133} for two minutes; in these the count rate is proportional to lung volume. Figure 2 shows measurements of blood flow per unit volume, ventilation per unit volume and ventilation/perfusion ratio in different parts of the lung. These measurements were made with the subject in a sitting position.

Finally I should like to ask Dr. Taplin whether it is necessary to heat the albumin first at pH 10 as well as at pH 5.2 when preparing the macro aggregates, and also what is the radiation dose to the lungs in his studies?

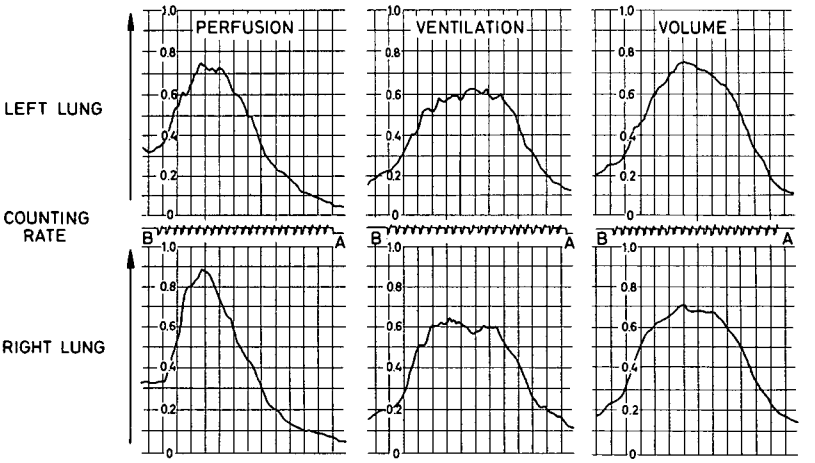

Fig. 1

Scans in a normal subject after Xe^{133} injection (perfusion), a tidal breath of Xe^{133} (ventilation), and after rebreathing the isotope on a closed circuit until equilibrated (volume)
The centre marker indicates displacement every half inch from base (B) to apex (A). Note the peak is much lower down the chest after the injection than after either the tidal breath or equilibration.

* DOLLERY, C.T., HUGH-JONES, P. and MATTHEWS, C.M.E., Use of radioactive xenon for studies of regional lung function, Brit. Med. J. 5311 (20 Oct. 1962) 1006 - 16; DOLLERY, C.T. and GILLAM, P.M.S., The distribution of blood and gas within the lungs measured by scanning after administration of Xe^{133}, Thorax 18 (1963) 316.

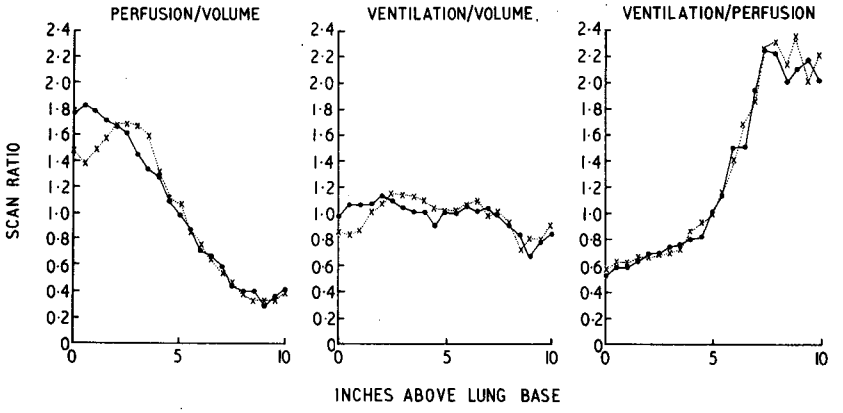

Fig. 2

Distribution of perfusion/volume, ventilation/volume, and ventilation/perfusion calculated from the scans of a normal subject in Fig. 1

The perfusion per unit volume is five to six times higher at the base than at the apex. The ventilation per unit volume is only slightly higher at the base than at the apex: in consequence the ventilation/perfusion ratio is four to five times higher at the apex than at the base.

● left lung
X right lung

G.V. TAPLIN: We first heat the albumin at pH 10 for 20 min at 79°C. This converts the molecular albumin into small aggregates of about 8 - 10 albumin molecules, without displacing the I^{131} label. The yield of aggregates is better than 95%. Reducing the pH to 5.2 produces macro aggregates in the size range of about 1 - 10 μm. Reheating at pH 5.2 for 3 - 5 min at 79°C increases the size range to about 5 - 25 μm.

As to your second question, the radiation dose to the lungs from 300 μc of I^{131}-labelled macro aggregates is about 250 mrads. With I^{125}-labelled particles it would be much less.

H. WAGNER: I should like to show three slides illustrating a method of spleen scanning that we have used successfully in over 200 examinations of patients during the past three years. The method will be described in the May 1964 issue of the "Archives of Internal Medicine" and uses Hg^{197}-labelled or Hg^{203}-labelled 1-bromomercuri-2-hydroxypropane (BMHP), which we synthesized by the method described by Sand and Hofmann in 1903. The method is outlined in Fig. 3; the synthesis is shown in Fig. 4, and a typical spleen scan is seen in Fig. 5. The material both labels red blood cells and damages them to the extent that they are accumulated by the spleen. The high concentration of radioactivity permits clear delineation of the spleen. The main advantages of the method are that it is easy to use and there is no accumulation of radioactivity in the liver, where it might cause confusion in interpretation.

W. PAUL: I should like to ask Dr. Taplin whether he can distinguish between regions of high and low perfusion by the density of deposition of the aggregates.

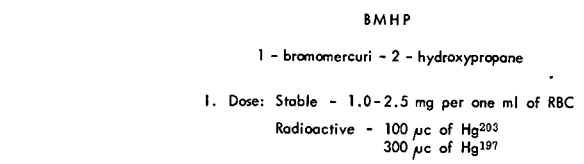

Fig. 3

Spleen scanning with 1-bromomercuri-2-hydroxypropane

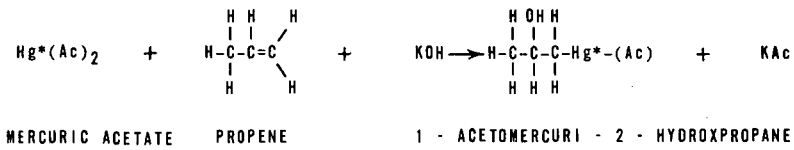

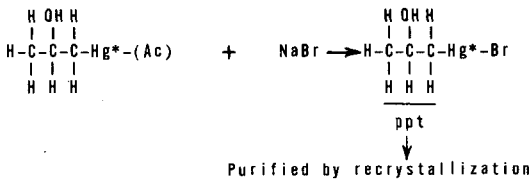

Fig. 4

Synthesis of 1-bromomercuri-2-hydroxypropane

G.V. TAPLIN: Yes. The radiodensity in the scan image of the lungs is linearly related to pulmonary arterial blood flow.

H. GLASS: I was impressed by your right heart clearance curve of the radioactive aggregates. Would you consider that this might permit a more accurate estimation of right heart output to be made, since there would be no distortion of the curve by the left heart peak?

G.V. TAPLIN: The large particles can be used for selective radiocardiography but there is still some distortion due to their accumulation in the lung, which is also in the field of the precordial detector. We believe that their use can be helpful in estimating right heart output.

P. CZERNIAK: I should like to ask Dr. Taplin three questions. First, what is the half-time of retention in the lungs for I^{131}-labelled albumin particles? Secondly, if the half-time is long enough, is it possible to inject enough radioactivity for the local treatment of lung metastases, e.g. metastases of thyroid carcinoma? Thirdly, what quantity of particles of the size described may be injected intravenously into a patient without hazard?

G.V. TAPLIN: The half-time of retention of radio-albumin particles (5 - 25 μm) in the lungs is about 2 h. The time of lung retention can be increased by using somewhat larger particles (10 - 50 μm). With regard to your second question, it is possible to make radio-albumin particles with a

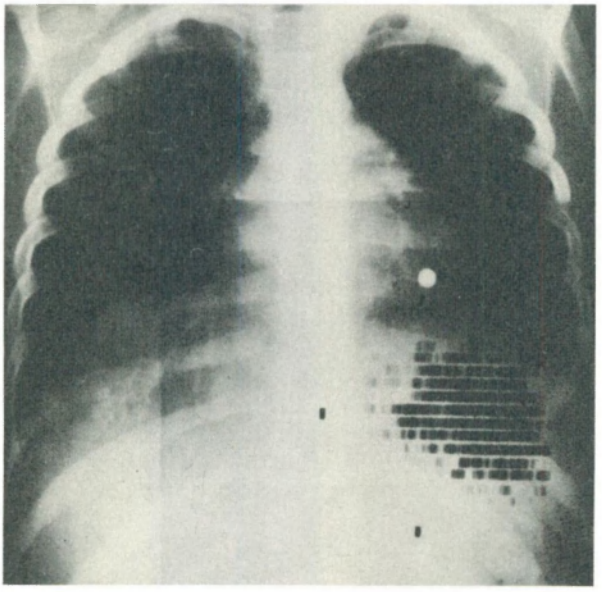

Fig. 5

Scan of spleen obtained with 1-bromomercuri-2-hydroxypropane

specific activity of the order of mc/mg which would be sufficiently high for therapeutic purposes. As to your third question, it is probably safe to inject as much as 10 - 20 mg/kg of high specific activity radio-albumin aggregates in the 5 - 50 μm size range.

P. HARPER: Would you care to comment on the behaviour of macro-aggregated albumin after injection into peripheral arteries?

G.V. TAPLIN: The injection of 5 - 25 μm of macro-aggregated albumin into the femoral arteries of dogs and monkeys results in very little retention in the leg - the particles appear immediately in the lung. This is also true with internal carotid artery injection. To obtain cerebral or peripheral capillary trapping in the dog or monkey, particles of larger mean size, between 25 and 50 μm, are needed. We have not yet done similar studies in man.

THE USE OF TECHNETIUM-99m AS A CLINICAL SCANNING AGENT FOR THYROID, LIVER AND BRAIN

P. V. HARPER, K. A. LATHROP, R. J. McCARDLE AND G. ANDROS
ARGONNE CANCER RESEARCH HOSPITAL*
AND THE DEPARTMENT OF SURGERY,
UNIVERSITY OF CHICAGO HOSPITALS AND CLINICS,
CHICAGO, ILL., UNITED STATES OF AMERICA

Abstract — Résumé — Аннотация — Resumen

THE USE OF Tc^{99m} AS A CLINICAL SCANNING AGENT FOR THYROID, LIVER AND BRAIN. In the search for an isotope that will be "ideal" for scanning, Tc^{99m} appears to offer many advantages. This substance emits a clean 140-keV γ-ray (9% converted) with no particle radiation, has a 6-h physical half-life, and is readily available at reasonable cost as the daughter of 2.7-d Mo^{99}, from which it is readily separated on an alumina column. In its usual form ($Tc^{99m}O_4^-$) it is distributed in the body in a manner very similar to ClO_4^- and I^-, being rapidly distributed in the extracellular space and specifically trapped by the thyroid, stomach and salivary glands. Excretion data indicate a biological half-life of about 2 d. Thyroid scans of a superior quality, with an estimated radiation dosage of 100 mrad to the gland and 5 mrad total-body radiation, may be made between one-half and one hour after a 1-mc dose of this material – a very great improvement over I^{131}. TcO_4 does not cross the blood-brain barrier freely, so that spectacular brain scans have been obtained with 2 to 5 min scanning time by making use of the high count-rate available from 5 to 10-mc doses of Tc^{99m}. As the pentavalent thiocyanate dissolved in fat emulsion, Tc^{99m} localizes in the liver to a large extent; the high count-rate available again permits rapid scans of this gland with improved resolution. It is anticipated that further gains with this isotope may be made possible by the use of probes of increased efficiency and by further manipulation of biological and chemical parameters.

UTILISATION DU ^{99m}Tc COMME AGENT D'EXPLORATION CLINIQUE DE LA THYROÏDE, DU FOIE ET DU CERVEAU. Dans la recherche du radioisotope «idéal» pour la gammagraphie, ^{99m}Tc semble offrir de nombreux avantages. C'est un émetteur gamma pur de 140 keV (converti à 9%), sans rayonnement particulaire, ayant une période de 6 h; on peut l'obtenir facilement et à peu de frais comme produit de filiation de ^{99}Mo, qui a une période de 67 h, dont on le sépare aisément sur une colonne d'alumine. Sous sa forme habituelle ($^{99m}TcO_4^-$), il se répartit dans le corps d'une façon très semblable à ClO_4^- et I^-, c'est-à-dire qu'il est rapidement dispersé dans l'espace extra-cellulaire et accumulé sélectivement par la thyroïde, l'estomac et les glandes salivaires. Les données fournies par les excreta indiquent que la période biologique est d'environ deux jours. On peut faire d'excellents scintigrammes de la thyroïde, avec une irradiation évaluée à 100 mrad pour la thyroïde et à 5 mrad pour l'ensemble du corps, une demi-heure à une heure après administration de 1 mc de ^{99m}Tc, ce qui représente un très grand progrès par rapport à l'utilisation de ^{131}I. TcO_4 ne traverse pas librement la barrière sang-cerveau, de sorte que l'on a obtenu des scintigrammes spectaculaires du cerveau avec un temps de balayage de 2 à 5 min grâce au taux de comptage élevé fourni par des doses de 5 à 10 mc de ^{99m}Tc. Comme le thiocyanate pentavalent se dissout dans une émulsion de corps gras, ^{99m}Tc se localise en grande partie dans le foie; là aussi, le taux de comptage élevé permet des explorations rapides avec une meilleure résolution. On espère qu'il sera possible de faire de nouveaux progrès avec ce radioisotope grâce à l'utilisation de sondes plus efficaces et à une manipulation plus poussée des paramètres biologiques et chimiques.

ИСПОЛЬЗОВАНИЕ Tc^{99m} КАК КЛИНИЧЕСКОГО АГЕНТА ПРИ СКЕННИРОВАНИИ ЩИТОВИДНОЙ ЖЕЛЕЗЫ, ПЕЧЕНИ И МОЗГА. При поисках "идеального" изотопа для сканирования технеций-99 m, повидимому, имеет много преимуществ. Это вещество является чистым гамма-излучателем с энергией 140 кэв (9% конверсия) при отсутствии из-

* Operated by the University of Chicago for the United States Atomic Energy Commission.

лучения частиц, имеет шестичасовой физический период полураспада, умеренную стоимость, является доступным дочерним продуктом молибдена-99 с периодом полураспада 2,7 дня, от которого он легко отделяется на колонке с окисью алюминия. В обычной форме ($Tc^{99m}O_4^-$) он распределяется в организме так же как ClO_4^- и J^-, быстро распространяясь во внеклеточном пространстве, избирательно захватывается щитовидной железой, желудком и слюнными железами. В соответствии с данными выделения период полувыведения составляет приблизительно два дня. Четкие сценнограммы щитовидной железы с расчетной дозой облучения 100 млрд. на железу и 5 млрд. на весь организм могут быть сняты в период от получаса до 1 часа после введения 1 мкюри этого материала — это большое преимущество по сравнению с йодом-131. TcO_4^- не проникает через гемато-энцефалический барьер, поэтому эффектные сценнограммы мозга были получены в течение 2—5 минут при высокой скорости счета в результате использования 5—10 мкюри технеция-99 m. Поскольку пятивалентный тиоцианат растворен в жировой эмульсии, технеций-99m в значительной степени локализуется в печени; при большой скорости счета снова можно получить сценнограммы этого органа с лучшим разрешением. Предполагается, что при использовании этого изотопа можно получить лучшие результаты при применении более эффективных проб и подбора биологических и химических параметров.

EMPLEO DEL ^{99m}Tc COMO AGENTE PARA LA EXPLORACIÓN CLINICA DE LA TIROIDES, EL HÍGADO Y EL CEREBRO. El ^{99m}Tc es uno de los isótopos que más ventajas ofrecen para la exploración centelleográfica. Emite rayos gamma limpios de 140 keV (9% de conversión) sin radiación corpuscular, tiene un período físico de 6 h y puede obtenerse fácilmente a un precio razonalbe como descendiente del ^{99}Mo, (período: 2,7 d) del que se separa sin dificultad en una columna de alúmina. En su forma usual ($^{99m}TcO_4^-$) se distribuye por el cuerpo de manera muy parecida al ClO_4^- y al I^-, penetra rápidamente en el espacio extracelular y es captado selectivamente por la tiroides, el estómago y las glándulas salivales. Los datos facilitados por la excreción indican que su período biológico es de unos 2 d. Con una dosis de irradiación calculada en 100 mrad para la glándula y en 5 mrad para el cuerpo entero, se pueden efectuar exploraciones tiroideas de muy buena calidad entre media hora y una hora después de administrar 1 mc de esta sustancia lo que representa una gran ventaja sobre el ^{131}I. El TcO_4^- no atraviesa libremente la barrera hematoencefálica, lo que ha permitido obtener excelentes imágenes del cerebro con un tiempo de exploración de 2 a 5 min aprovechando el elevado índice de recuento correspondiente a dosis de 5 a 10 mc de ^{99m}Tc. Como el tiocianato pentavalente se disuelve en una emulsión de grasa, gran parte del ^{99m}Tc se localiza en el hígado; en este caso el elevado índice de recuento permite también proceder a una rápida exploración de esta glándula con un mayor poder de resolución. Es muy probable que este tipo de mejores resultados aún utilizando sondas más eficaces y adaptando los parámetros biológicos y químicos a condiciones óptimas.

The objective in any clinical tracer study is to obtain as much useful information as possible consistent with reasonable radiation dosage to the patient, and without undue cost or inconvenience. In order to achieve the greatest possible effectiveness a number of factors must be considered, among them the characteristics of the particular radioactive tracer material chosen. The physical parameters of technetium-99m appear even on casual perusal to be so favourable from this point of view that an extended study of its chemical and biological characteristics was undertaken to explore its possibilities as an agent for clinical use.

Technetium-99m decays [1] with a 6-h physical half-life emitting a clean 0.140 MeV gamma-ray and dissipating only 0.014 MeV/disintegration as low energy beta-like radiation (conversion electrons, Auger electrons, and soft fluorescent photons). Thus the effective half-life is very short, and the energy deposited in the tissues is very small compared to most particle-emitting radionuclides. Even the gamma-ray dose-rate constant is very low (0.61 r/mc-h at 1 cm). It thus would appear feasible to administer substantial millicurie quantities to an individual without intolerable radiation dosage.

The 140-keV gamma may be scanned with conventional equipment, but specially designed detectors provide further substantial advantages. Optimally designed collimators will increase counting efficiency by at least a factor of two over collimators of equal resolution designed for I^{131}, and since 6 mm of lead give complete shielding, a shielded detector weighing 2 or 3 kg is quite feasible [2]. A 1-cm-thick NaI crystal gives maximal counting efficiency and resolution with low background, and the compactness and lightness of the shield and collimator facilitate the use of multiple detector heads (Fig. 1).

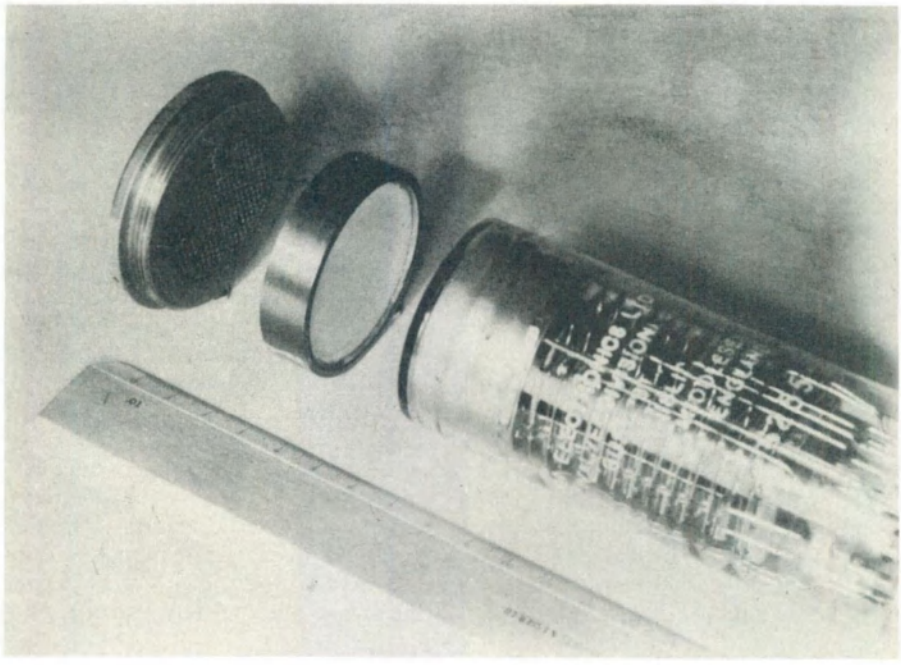

Fig. 1

Exploded view of low-energy collimator-detector. Lead collimator has 253 holes, 6.25-cm focal length, 1.59-cm diam. of view at focus. Efficiency 4.12×10^{-3} counts/disintegration/cm^2. Septum thickness at front end 0.019 cm. NaI crystal 2 in × ½ in with 0.025 cm beryllium jacket. This detector-collimator is satisfactory in the range 27 to 140 keV. At the latter energy 6.3 mm of lead gives complete lateral shielding.

The 6-h half-life of Tc^{99m} that would ordinarily preclude its use poses no problem because this isotope is available as the daughter of 2.8-d molybdenum-99, one of the most abundant of the fission products. This latter material is available at reasonable cost adsorbed on an alumina column from which the daughter technetium-99m may be eluted with dilute (0.1 N) hydrochloric acid as needed [3].

The technetium-99m decays to technetium-99 which in turn decays to stable ruthenium-99. Since the Tc^{99} has a half-life of 2.1×10^5 yr there is no significant residual radioactivity from the decay of Tc^{99m}. One mc of

Tc^{99m} decays to 3×10^{-6} μc of Tc^{99}, and 1 mc of Mo^{99} decays to 3×10^{-5} μc of Tc^{99}.

The chemical form of Tc^{99m} as it is eluted from the generator is that of the stable pertechnetate ion. In strong acid solution this forms the volatile pertechnic acid. The eluate contains traces of other fission products in submicrocurie amounts, consisting largely of I^{131}, Ru^{103} and Ru^{106}. The ruthenium may be removed easily by extraction of the TcO_4^- from 5 N NaOH into methyl ethyl ketone [4]. The ketone then is removed by evaporation and the pertechnetate may be made up to any desired specific activity in sterile solution.

Pertechnetate is reduced by ascorbic acid in 2.5 N HCl. In the presence of Fe^{+++}, which acts as a redox buffer, the technetium is reduced to the +5 state [5] in which it is very reactive. It forms a fat-soluble thiocyanate and makes firm complexes with simple organic compounds such as glycine as well as with proteins. In acid pertechnetate solution (1 N HCl), on the addition of H_2S the technetium activity is precipitated along with elemental sulphur, possibly as the sulphide Tc_2S_7. In the presence of a protective colloid such as 1% gelatin, this remains as a sulphur colloid [6].

Biological studies have been carried out on a number of these compounds of Tc^{99m} and will be reported in detail elsewhere. To summarize these results: pertechnetate belongs to a group of ions (TcO_4^-, ReO_4^-, ClO_4^-, BO_3F^-, I^-, At^-) which have a symmetrical spherical or tetrahedral configuration and which are handled in a similar manner in the organism [7]. The resemblance of TcO_4^- to I^- is particularly close. As judged by the thyroid/serum ratios and by the salivary/serum and gastric-juice/serum ratios [8], pertechnetate is trapped in the stomach, salivary glands and thyroid to nearly the same degree as iodide. Excretion is largely by way of the urine during the first day, although here the resemblance to iodide becomes less marked since increasingly more of the pertechnetate appears in the stools, 10 to 15% being excreted by this route on the third day. The over-all average excretion in 10 subjects was 50% in 1.8 days. Pertechnetate thus appears to be somewhat labile chemically in the body. SORENSEN and ARCHAMBAULT [9] have shown that Tc^{99m} formed from Mo^{99} that has been taken up by the liver remains in the liver, further suggesting that technetium can exist in the body in forms other then pertechnetate, since injected pertechnetate is not localized in the liver.

The blood disappearance curve [9] shows a rapid component with a half-time of 10 min, and a second component of approximately equal magnitude with a half-life of about 6 h. These same components have been observed in gastrectomized-nephrectomized dogs, and in animals pre-treated with ClO_4^- (which abolishes localization), and the curves are quite similar to those for iodide in subjects with blocked thyroids. This would indicate that TcO_4^- is distributed initially in the extracellular space, as is iodide.

Up to 2% of the injected dose of pertechnetate is localized in the thyroid gland in experimental animals (mice) and in euthyroid humans at 30 to 60 min after injection. In uptake measurements in human thyroids the high neck background made it necessary either to measure the change in count-rate after administration of perchlorate, which displaces the TcO_4^- from the gland, or to quantitate the dot scan by scanning an injection standard and subtracting the background count measured on an appropriate adjacent area

of the neck. The use of the thigh background count is not practical. Agreement between these methods was excellent and the TcO_4^- trapping thus measured is practically the same as the trapping of iodide in the propylthiouracil-blocked thyroid. Administration of thyroid hormone decreases this uptake to zero. Administration of thyroid-stimulating hormone does not increase the uptake above normal. In hyperthyroid individuals the localization is increased to between 6 and 30% of the injected dose, and in both Basedow's disease and Plummer's disease the increased trapping of TcO_4^- by the thyroid is clearly independent of TSH.

The usefulness of $Tc^{99m}O_4^-$ as a clinical tracer material in thyroid disease is evident. It allows observation of the ion trapping mechanism without perturbing the gland with blocking or discharging agents, and scans of comparable and sometimes of superior quality to those obtained with radioiodine are obtainable 30 min after intravenous administration of 1 mc of TcO_4^-, the radiation dosage to the thyroid gland being about 100 mrad, i.e. about 1/1000 of that produced by the usual scanning dose of I^{131} (Figs. 2 and 3).

Since it has been shown that materials distributed in the extracellular space may be used profitably for brain scanning [10] this possible use of $Tc^{99m}O_4^-$ was explored. We administered 5 - 10 mc of $Tc^{99m}O_4^-$ intravenously along with 1 g of NaI to minimize localization in the thyroid. Brain scans of excellent quality demonstrating midline as well as lateral lesions were obtained in 10 to 15 min. The localization appears to be almost immediate

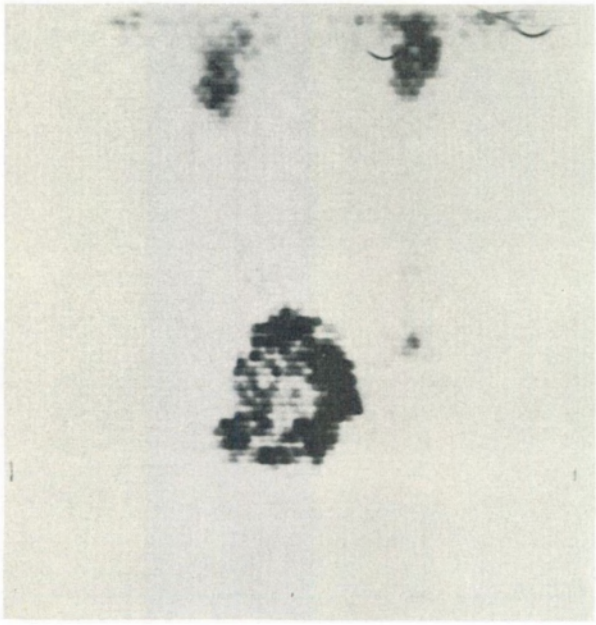

Fig. 2

Thyroid scan 30 min after intravenous administration of 1 mc of Tc^{99m} as TcO_4^-. Note the markedly increased trapping of TcO_4^- in a cystic hyperactive nodule and suppression of uptake in the remainder of the gland. Salivary glands are well visualized.

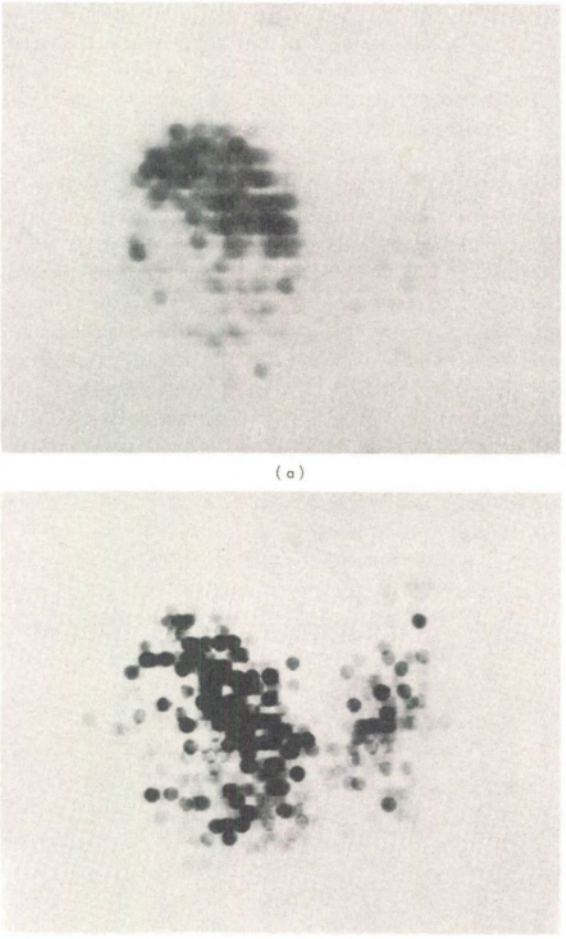

(a)

(b)

Fig. 3

(a) TcO_4^- scan of thyroid similar to Fig. 2
(b) I^{131} scan of same patient
The radiation dosage to the gland with 1 mc of $Tc^{99m}O_4^-$ is about 100 mrad or 1/1000 of the dose from 50 μc of I^{131}.

and has been followed for as long as 3 h. Experience with 100 patients indicates diagnostic accuracy comparable to that of other scanning agents (Figs. 4, 5 and 6).

Localization of Tc^{99m} in the liver as the thiocyanate was achieved by injecting this material dissolved in a commercial fat emulsion prepared for intravenous use (Lipomul). The thiocyanate was prepared as described above, extracted into butyl acetate from the acid solution, the butyl acetate removed by evaporation, and the thiocyanate taken up in the fat emulsion under sterile conditions. Residual technetium activity was removed from

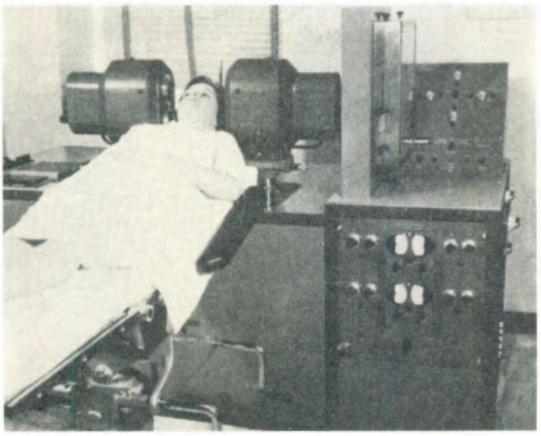

Fig. 4

Argonne Cancer Research Hospital brain scanner. To shorten the scanning time, two detectors are used simultaneously on each side of the head. Optimal collimators, contour limitation, and rapid scanning (2.5 cm/μc) with small index (1.6 mm) give a smoother picture with little line structure in minimal time. Photo readout with diffused spots with Gaussian density profile reduce statistical structure.

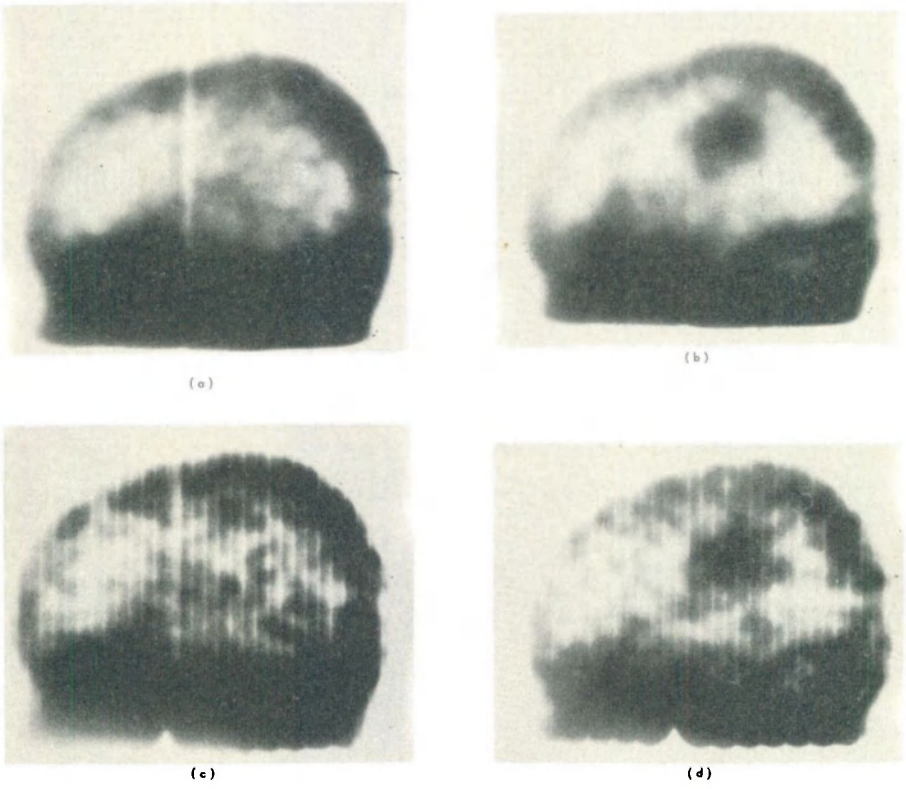

Fig. 5

(a and b) Right and left lateral scans of patient with superficial glioma. Note that tumour is faintly visible from opposite side of head. Duration of scan 15 min; started immediately after intravenous injection of 5 mc of TcO_4^- in 1 g of NaI solution. Total body radiation dosage approximately 60 mrad.

(c and d) Same patient, scanned using 6.3-mm index. Duration of scan 90 s; started 17 min after injection.

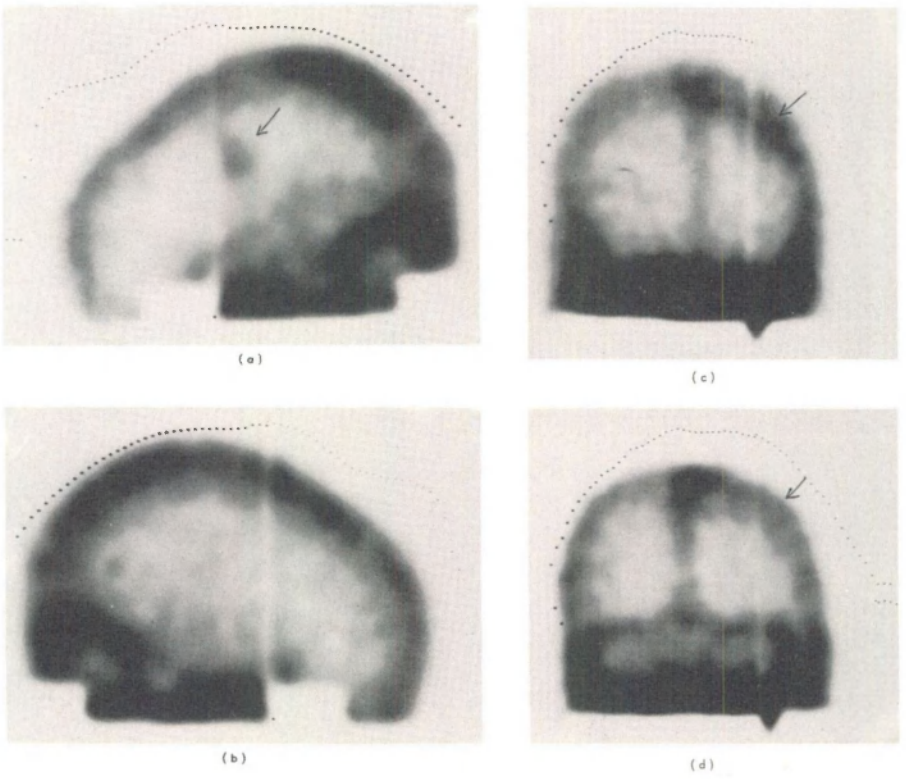

Fig. 6

(a) Left lateral, (b) right lateral, (c) anterior,
(d) posterior scans of patient with oligodendroglioma.
Duration of scans 7-8 min, time for entire examination 45 min.
5 mc TcO_4^- injected intravenously with 1 g of NaI
to reduce thyroid and gastric localization.

the aqueous phase by an ion exchange resin (IR-4B). This material disappears from the blood with a half-time of 40 to 60 min and reaches optimal scanning concentration in the liver in 4 to 6 h, with 50% of the injected dose in the organ. The uptake is apparently parenchymal, being greatly reduced in liver disease (Figs.7 and 8). Good uptake was obtained in one case of primary hepatoma.

Tc^{99m} bound to colloidal sulphur has been used to produce liver and spleen scans. This material disappears from the blood stream with a half-life of 2 to 5 min, and in experimental animals (mice and dogs) 70 to 90% of the injected material is recoverable in the liver, and about 5% in the spleen. With 5 mc of this material, scans are obtainable with count-rates of 20 000 to 50 000/min using collimators designed for thyroid scanning. Under these circumstances, with fine resolution and good statistics, some difficulties arise from the motion of the liver and spleen with respiration.

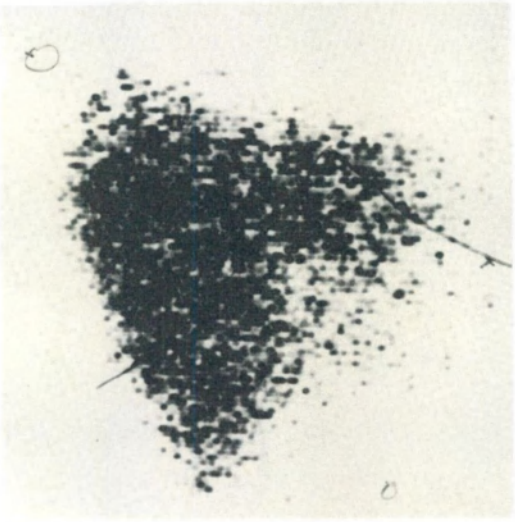

Fig. 7

Normal liver scan using 1 mc of $Tc^{99m}(SCN)_5$ in fat emulsion. Scan started 5 h after injection. Equipment: Picker Magnascanner with thyroid collimator. Note sharp borders of organ.

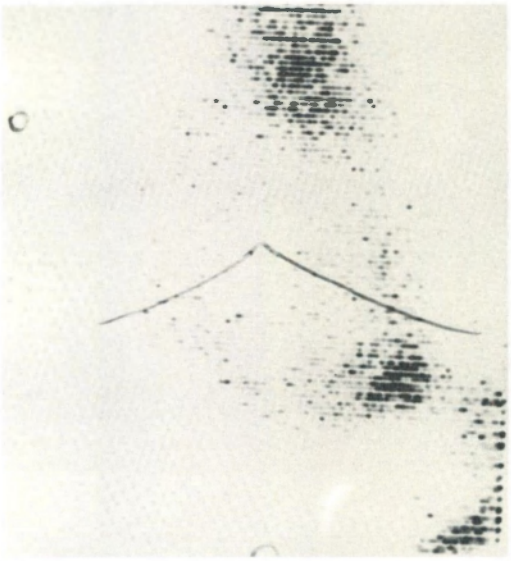

Fig. 8

Liver scan using same technique as in Fig. 7, in patient with severe hepatic damage following prolonged obstructive jaundice. Note greatly reduced uptake, continued presence of circulatory activity in cardiac silhouette, as well as some degradation of $Tc(SCN)_5$ back to TcO_4^- with gastric localization.

Great improvement is obtained by temporary paralysis of the appropriate phrenic nerve with local anaesthetic (Figs. 9 - 12).

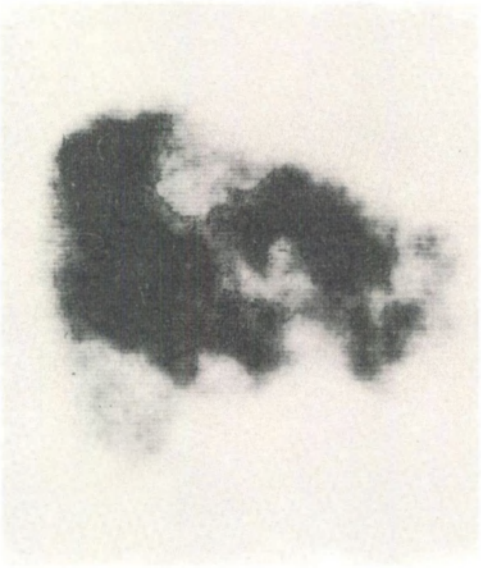

Fig. 9

Metastatic carcinoma of the colon in liver demonstrated with Tc_2S_7 in sulphur emulsion. Scan performed 5 min after intravenous injection of 2 mc of Tc^{99m}. Probe (Fig. 1) used with readout similar to brain scanner. Serrated appearance of superior margin of organ is due to respiratory motion.

Fig. 10

Liver scan showing metastases from carcinoma of breast. Technique same as in Fig. 9. Maximum count-rates 40 000/min. The right phrenic nerve was blocked to prevent motion; however, the motion artifact of the left lobe is evident.

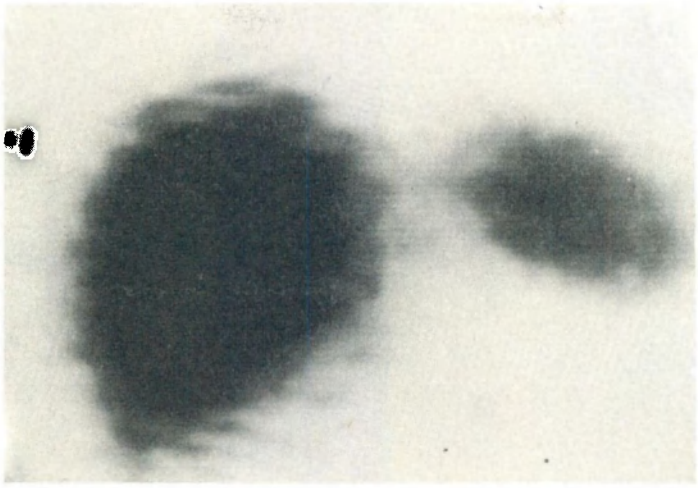

Fig. 11

Posterior scan of liver and spleen using the Tc^{99m} sulphur colloid.
The left phrenic nerve has been blocked. Note motion artifacts in liver scan.

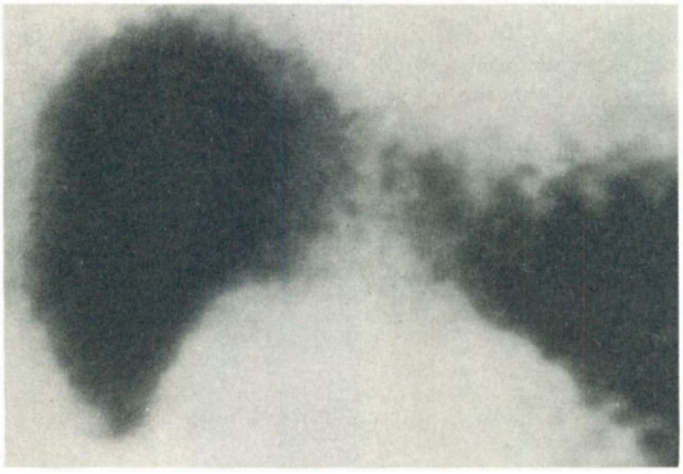

Fig. 12

Similar to Fig. 11 but with right phrenic nerve paralyzed.
Again note the motion artifact in the spleen scan.

The complex of pentavalent technetium with glycine is rapidly excreted in the urine following intravenous administration. Over 90% of the radioactivity may be recovered in the urine after one hour in the mouse, and 60% after 3 h in human subjects. Renal scans are possible with this material (Fig. 13).

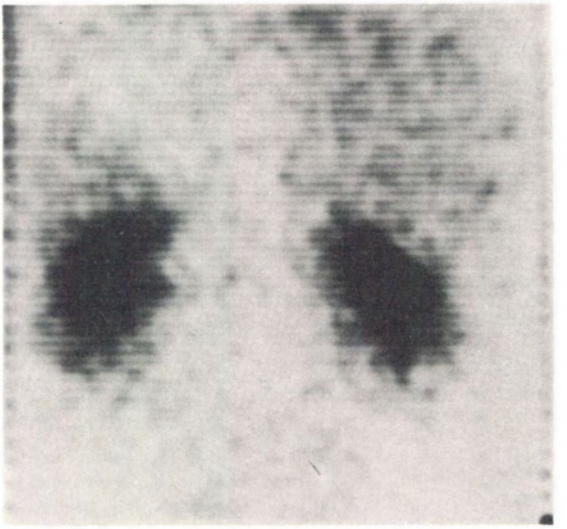

Fig. 13

Renal scan started immediately after intravenous injection of 2 mc Tc^{99m}-glycine preparation showing kidney contours. Duration of scan: 20 min.

To summarize, Tc^{99m} has ideal physical characteristics for a variety of tracer studies in patients, and has versatile chemical characteristics, not yet fully explored, that make it a satisfactory agent for thyroid, liver, brain and kidney scanning, studies of ion trapping by the thyroid, and possibly other uses. It is of especial interest for use in children where radiation dosage is much more critical than in adults.

REFERENCES

[1] STROMINGER, D., HOLLANDER, J.M. and SEABORG, G.T., Rev. mod. Phys. 30 (1958) 673.
[2] HARPER, P.V., BECK, R., CHARLESTON, D. and LATHROP, K.A., Nucleonics 22 (1964) 50 - 4.
[3] TUCKER, W.D., GREENE, M.W., WEISS, A.J. and MURRENHOFF, A., Brookhaven National Laboratory Report No. 3746 (1958).
[4] GERLIT, J.B., Proc. UN Int. Conf. PUAE 7 (1956) 145 - 51.
[5] HOWARD, O.H. and WEBER, C.W., Anal. Chem. 34 (1962) 530 - 3.
[6] STANG, L.G. and RICHARDS, P., Nucleonics 22 (1964) 46 - 9.
[7] WOLFF, J. and MAUREY, J.R., Biochem. biophys. Acta 69 (1963) 58 - 67.
[8] HARPER, P.V., ANDROS, G. and LATHROP, K., Argonne Cancer Research Hospital Semiannual Report to the Atomic Energy Commission 18 (1962) 76 - 88.
[9] SORENSEN, L.B. and ARCHAMBAULT, M., J. Lab. clin. Med. 62 (1963) 330 - 40.
[10] ANGER, H.O. and GOTTSCHALK, A., J. nucl. Med. 4 (1963) 326 - 30.

DISCUSSION

C.M.E. MATTHEWS: I should like to ask Dr. Harper three questions. First, what is the minimum size of brain tumour he can detect using his method? I am thinking of the size as measured at operation, not the ap-

parent size deduced from the scan. Secondly, what is the tumour/brain concentration ratio? Thirdly, is the albumin denatured when labelled with Tc^{99m}?

P. HARPER: The minimum size of brain tumour detected so far was a 2-cm spherical melanoma metastasis measured at autopsy. The tumour/brain ratios measured during operation were in the range of 2 to 3. As to your last question, the albumin was denatured to some extent when labelled with Tc^{99m}.

A. BAPTISTA: What is the clearance coefficient of the liver when you use the colloidal material you mentioned for liver scanning?

P. HARPER: The half-time in the serum is 2 - 3 min for 90% of the activity.

A. BAPTISTA: Does this material stay in the liver like colloidal gold?

P. HARPER: Yes. In 72 h 3% is excreted.

M. TUBIANA: How much time elapses after you administer Tc^{99m} before you make the thyroid scan?

P. HARPER: We start to make the scan about 30 min after intravenous administration of Tc^{99m}.

M. TUBIANA: Is not the interpretation of the pictures made difficult by the presence of a high level of radioactivity in the circulating blood?

P. HARPER: The higher count rates available permit suppression of the background without loss of information.

M. TUBIANA: What dose is received by the thyroid?

P. HARPER: About 100 mrad.

D. SODEE: I should like to know why the brain scans you showed appeared to be out of focus. Is there not a consequent reduction in accuracy in the diagnosis of vascular lesions or tumours?

P. HARPER: The out-of-focus appearance is due to the fact that counts are recorded as diffuse spots, which is how the detector actually sees them. It takes some time to get used to this phenomenon; I would stress, however, that it does not conceal the information.

C. KELLERSHOHN: In connection with the decay scheme of Tc^{99m}, to what extent is the 0.140-MeV gamma radiation converted?

P. HARPER: The 140-keV gamma radiation is 8% converted.

C. KELLERSHOHN: According to the decay scheme you showed, the 0.140-MeV gamma ray follows a 0.002-MeV gamma ray in cascade. To what extent is the latter converted? If the conversion were small, Tc^{99m} would constitute an intense source of 2-keV photons. This would be useful for certain applications.

P. HARPER: I believe that the 0.002-MeV gamma radiation is largely converted. The conversion involves valence electrons so that the half-life of Tc^{99m} is slightly dependent on its chemical state.

COMPOUNDS LABELLED WITH LOW-ENERGY GAMMA-RAY EMITTERS FOR MEDICAL ISOTOPE SCANNING

K.E. SCHEER, K. ZUM WINKEL AND M. GEORGI
CZERNY-KRANKENHAUS DER UNIVERSITÄT HEIDELBERG,
FEDERAL REPUBLIC OF GERMANY

Abstract — Résumé — Аннотация — Resumen

COMPOUNDS LABELLED WITH LOW-ENERGY GAMMA-RAY EMITTERS FOR MEDICAL ISOTOPE SCANNING. Low-energy gamma emitters have a special merit for medical scintillation scanning for the following reasons:

(1) The lead shielding of the collimators is much more effective. Multiple focusing thin-walled hole collimators can therefore be used, making a higher geometrical resolution possible and, therefore, the detection of smaller lesions.

(2) The absorption of the radiation within the body tissue limits the depth of visibility of lesions. In extended organs like the liver, the superposition of radiation originating from the back of the organ is avoided. This allows a better detection of more superficial lesions.

The most important low-energy gamma-emitting nuclide is I^{125}. For thyroid scanning, it is used in the form of iodide. A suitable compound for liver scanning is I^{125}-labelled Rose Bengal. An alternative compound is I^{125}-CAI (heat denatured albumin). For kidney scanning I^{125}-Hippuran was found to be suitable when injected intramuscularly with hyaluronidase to ensure a uniform level of radioactivity in the kidneys.

Another useful low-energy gamma-emitting nuclide for medical scanning is Hg^{197} which may be used as chloride for kidney and spleen scanning. Special precautions must be taken to avoid overlying of kidney and spleen. A higher quality scan is obtained with Hg^{197}-labelled Neohydrin. This compound is also useful for brain-tumour localization.

Typical scans of thyroid, liver, spleen, kidney and brain tumours obtained with low-energy gamma emitters and conventional nuclides and compounds are presented and the merits of the former are discussed.

GAMMAGRAPHIE AU MOYEN DE COMPOSÉS MARQUÉS AVEC DES ÉMETTEURS GAMMA DE FAIBLE ÉNERGIE. Les émetteurs gamma de faible énergie présentent un intérêt particulier en gammagraphie, pour les raisons suivantes:

1. L'écran en plomb des collimateurs est beaucoup plus efficace. On peut donc utiliser des collimateurs à focalisation à canaux multiples, et à parois minces, qui permettent d'avoir un excellent pouvoir de résolution et, par conséquent, de détecter de petites lésions.

2. L'absorption du rayonnement par les tissues limite la profondeur à laquelle les lésions sont «visibles». Dans de grands organes comme le foie, on évite la superposition des rayonnements provenant de la partie postérieure de l'organe, d'où une meilleure détection des lésions superficielles.

Le plus important émetteur gamma de faible énergie est l'iode-125. Pour l'exploration de la thyroïde on l'utilise sous forme d'iodure. Pour le foie, le rose bengale marqué avec ^{125}I convient parfaitement, mais on peut aussi utiliser de l'albumine altérée par la chaleur et marquée avec ^{125}I. Pour le rein, on a constaté que l'hippuran marqué avec ^{125}I donne de bons résultats en injection intra-musculaire, si on le mélange à de l'hyaluronidase pour assurer un niveau uniforme de radioactivité dans cet organe.

Un autre émetteur gamma de faible énergie très utile en gammagraphie est le mercure-197, qui peut être utilisé sous forme de chlorure pour l'exploration du rein et de la rate. On doit prendre des précautions spéciales pour éviter la superposition de ces organes. On obtient un meilleur scintigramme avec de la néohydrine marquée avec ^{197}Hg; ce produit peut servir aussi à localiser les tumeurs du cerveau.

Les auteurs donnent des détails sur des cas typiques d'exploration de tumeurs de la thyroïde, du foie, de la rate, du rein et du cerveau, d'une part avec des émetteurs gamma de faible énergie et d'autre part avec des nucléides et des composés classiques; ils comparent les résultats obtenus.

СОЕДИНЕНИЯ, ИСПОЛЬЗУЕМЫЕ ПРИ МЕДИЦИНСКОМ ИЗОТОПНОМ СКЕННИРОВАНИИ, МЕЧЕННЫЕ С ПОМОЩЬЮ ГАММА-ИЗЛУЧАТЕЛЕЙ НИЗКОЙ ЭНЕРГИИ. Гамма-

излучатели низкой энергии имеют особые преимущества при использовании их для медицинского сцинтилляционного сканнирования по двум причинам:

1. Свинцовая защита коллиматоров значительно эффективнее. Поэтому можно применять тонкостенные коллиматоры с многократной фокусировкой, добиваясь при этом наибольшего геометрического разрешения, и в связи с этим – возможности обнаружения небольших поражений.
2. Поглощение излучения в тканях организма ограничивает глубину обнаружения повреждений. В крупных органах, например в печени, устраняется наложение излучения от заднего отдела органа. Это позволяет лучше обнаруживать более поверхностные поражения.

Наиболее важным гамма-излучающим радиоизотопом низкой энергии является йод-125. При сканнировании щитовидной железы он используется в форме иодида. Соответствующим соединением для сканнирования печени является меченная йодом-125 бенгальская роза. Другим соединением является йод-125 – CAI (денатурированный при высокой температуре альбумин). Установлено, что при сканнировании почек наиболее подходящим соединением для внутримышечного введения вместе с гиалуронидазой с целью обеспечения равномерного уровня радиоактивности в почках является йод-125 – гиппуран.

Другим полезным гамма-излучающим радиоизотопом низкой энергии, который применяется при медицинском сканнировании, является ртуть-197, который можно использовать в виде хлорида при сканнировании почек и селезенки. Необходимо предпринимать особые меры предосторожности, чтобы избежать перекрывания почек и селезенки. При использовании неогидрина, меченного ртутью-197, получают более высококачественные сканнограммы. Это соединение применяется также для установления локализации мозговых опухолей.

Обсуждаются типичные сканнограммы щитовидной железы, печени, селезенки, почек и мозговых опухолей, полученные с помощью гамма-излучателей низкой энергии, и обычных радиоизотопов и соединений, а также достоинства первых.

COMPUESTOS MARCADOS CON EMISORES GAMMA DE BAJA ENERGÍA PARA LA EXPLORACIÓN MÉDICA MEDIANTE ISÓTOPOS. Los emisores gamma de baja energía presentan ventajas especiales para la exploración médica por centelleografía. He aquí las razones:

1. El blindaje de plomo de los colimadores es mucho más eficaz. Por tanto, pueden utilizarse colimadores enfocados con canales de tabiques delgados, lo que da un mayor grado de resolución geométrica y permite, por consiguiente, detectar lesiones más pequeñas.
2. La absorción de la radiación por los tejidos del cuerpo limita la profundidad a que las lesiones pueden ser visualizadas. En órganos de grandes dimensiones, como el hígado, se evita la superposición de las radiaciones procedentes de la parte posterior del órgano, lo que permite detectar mejor las lesiones superficiales.

El emisor gamma de baja energía más importante es el ^{125}I. Para la exploración de la tiroides se utiliza en forma de yoduro. El Rosa Bengala marcada con ^{125}I es un compuesto adecuado para la exploración del hígado. También puede utilizarse albúmina desnaturalizada por el calor, marcada con ^{125}I. Para la exploración del riñón se ha comprobado que el hipurán marcado con ^{125}I da buenos resultados cuando se inyecta por vía intramuscular con hialuronidasa a fin de lograr un nivel uniforme de radiactividad en este órgano.

Otro emisor gamma de baja energía muy útil para la exploración médica es el ^{197}Hg que puede utilizarse en forma de cloruro para la exploración de los riñones y el bazo. Deben tomarse precauciones especiales para evitar la superposición del riñón y el bazo. La exploración da mejores resultados si se utiliza ^{197}Hg marcado con neohidrina. Este compuesto puede emplearse también para la localización de tumores del cerebro.

Los autores presentan centelleogramas típicos de tumores de la tiroides, del hígado, del bazo, del riñón y del cerebro obtenidos con emisores gamma de baja energía y con núclidos y compuestos tradicionales, y examinan las ventajas que ofrecen los primeros.

Low-energy gamma emitters in the field of medical diagnostic procedures or more distinctly in the field of in vivo counting methods are those with a quantum energy below 150 keV. They are not very much in use for in vivo measurements because the tissue absorption below 150 keV is considerable. Corrections for losses in counts are dubious and depend upon variations in organ and body sizes of the patients.

For medical scanning, however, these disadvantages are of minor importance since scanning has to be considered as a semi-quantitative mea-

surement. Differences in count-rates over different regions of the same organ are generally of much more interest than absolute values.

On the other hand, collimation problems and detector sensitivity in scanning are much more important than is usual with in vivo counting methods. Here, however, low-energy gamma-rays offer a distinct advantage.

As far as collimation is concerned the dimensions of the shield may be reduced. This leads to a reduction in the weight of the detector and permits shorter detector skin distances. In multi-hole collimators the walls of the separators may be reduced which leads to a higher aperture. For the same geometry the zone of penumbra is also reduced because of the more distinct limit between absorption in the shield and transparency in the openings of the collimator.

All these factors lead to a better resolution of collimators in the case of low-energy gamma-ray emitters. In addition to this the efficiency of the NaI crystal is more satisfactory for low-energy radiation. The thickness of the crystals, and therefore the background, can be reduced and so a higher signal-to-background ratio results. In the case of extremely low-energy gamma emitters like I^{125} an additional factor arises which influences the scanning conditions. For the 27-keV characteristic X-rays of I^{125} the tissue absorption is so important that only such radiation is recorded which originates near the body surface.

This is especially true in cases of very extended organs such as the liver as will be shown later.

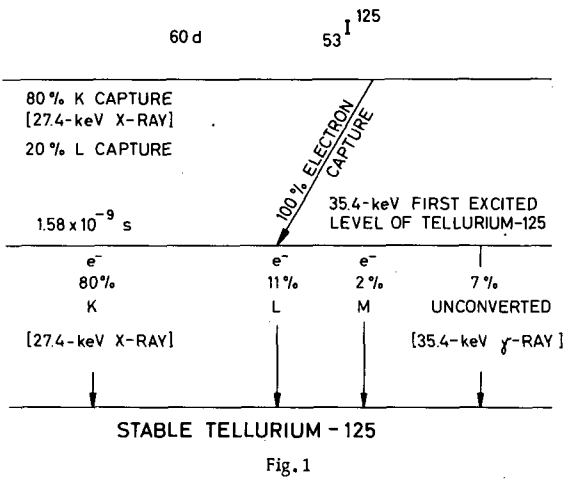

Fig. 1

Decay scheme of I^{125} according to W.G. Myers

Figure 1 shows the simplified decay scheme of I^{125} designed from data compiled by MYERS [1] who was the first to emphasize the value of this isotope for medical purposes. The main energy is between 27.2-35.4 keV. There is a rather high gamma- and X-ray output of 144 ± 6 per 100 disintegrations. This is nearly twice as much as for I^{131}. As compared with this latter isotope the electron energy of I^{125} resulting from conversion and Auger electrons is much lower and therefore there is much less radiation dose to the tissue per disintegration.

Table I gives a comparison of factors important for scanning of I^{125} and I^{131}. Even for a layer of 6.3 cm of water placed between the source and the detector, the ratio of "useless" radiation per detectable photon is much better for I^{125} than for I^{131}. It seems worthwhile to consider that a crystal only 1 mm thick will give nearly 100% detecting efficiency and that such a small crystal volume shows an extremely low background.

For clinical thyroid scans I^{125} is administered to the patient as iodide in the usual peroral way. Regarding the higher number of photons per disintegration 15 μc is the standard dose as compared with 25 μc for I^{131}. Figure 2 shows a scan of a toxic adenoma of the thyroid in a 62-yr-old woman 24 h after the injection of 25 μc of I^{131}. Figure 3 shows a scan of the same patient taken 24 h earlier after the administration of 15 μc of I^{125}. One can see that the outlines of the hot nodule are much clearer in the second pic-

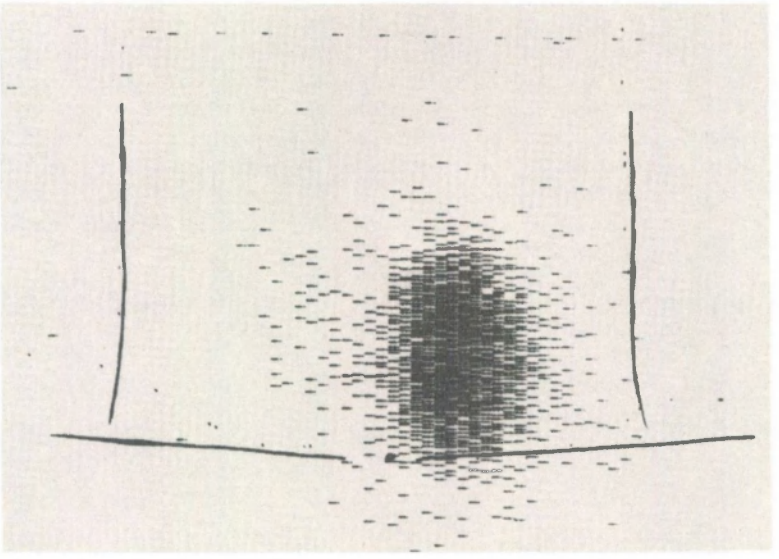

Fig. 2

Scintiscan of the thyroid of a 62-yr-old woman with toxic adenoma after injection of 25 μc of I^{131}

ture than in the first one. In order to allow a comparison care was taken to register the same number of counts in both scans. The same collimator was used, a 7-hole focusing collimator of the "Siemens Nukleograph". In the case of I^{131} a $1\frac{3}{4}$-in to $1\frac{1}{4}$-in crystal and in the case of I^{125} a $1\frac{3}{4}$-in to $\frac{1}{4}$-in crystal was placed in the shield.

Scintiscanning with I^{125} is not limited to small thyroids or toxic adenomata. HÖFER [2] reported that it is equally useful for fairly large goitres.

Figure 4A shows a scan of a fairly extended intrathoracic goitre made with I^{131}. One can see that there is a hot nodule in the left side within the intrathoracic thyroid mass. Fig. 4B shows the scan of the same patient made with I^{125} which was recorded one day earlier. In spite of the relatively deep position of the iodine-accumulating nodule it is fairly well outlined. In ad-

TABLE I

FACTORS FOR COMPARISON OF I^{125} WITH I^{131} ACCORDING TO W. G. MYERS

	Iodine-125	Iodine-131
Photon energy	27400 eV	364 000 eV
Photon "signals" per 100 disintegrations	136	81
Half-thickness in water	2.3 cm	6.3 cm
% transmitted through 6.3 cm of water	14%	50%
"Useless" radiation absorbed/disintegration	16000 eV	200 000 eV
"Useless" radiation per photon "signal" emitted through 6.3 cm of water	254000 eV	943000 eV
Assumed quantum efficiency of detector	100%	50%
Assumed background of detector	9.3 counts/min	250 counts/min

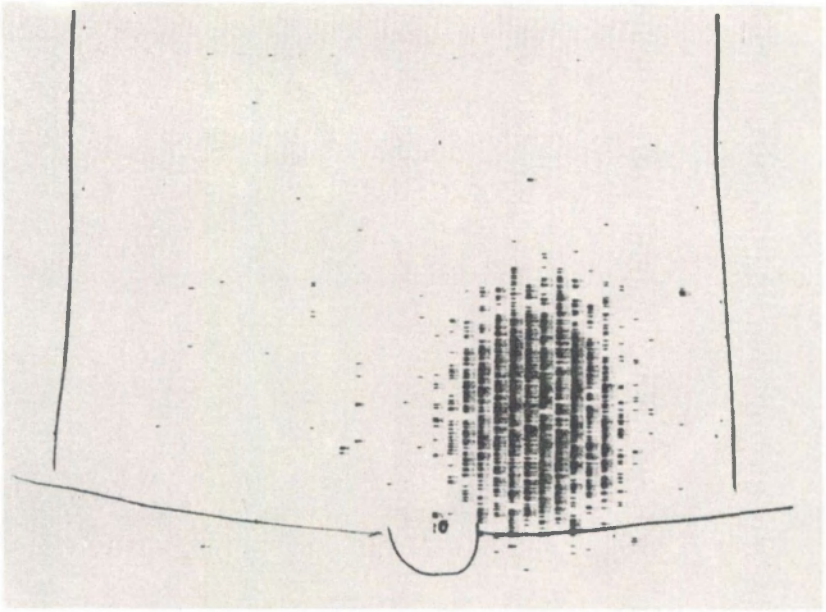

Fig.3

Scintiscan of the thyroid of the same patient as in Fig.2 after injection of 15 μc of I^{125}

dition to this the enlarged thyroid mass on the neck is much more easily distinguished than on the previous scan made with I^{131}.

The very excellent results that we obtained in our thyroid scans with I^{125} encouraged us to use this isotope in routine thyroid examination. The normal dose is 15 μc, delivering sufficient gamma-and X-ray quanta for scanning as well as for the determination of PBI in a well-type crystal. To avoid the only disadvantage of the low-energy gamma-emitting I^{125}, e.g. the inaccuracy of determining the thyroid uptake, we add 1 μc of I^{131} to the 15 μc I^{125} and we measure the uptake by means of a spectrometer set on the 364-keV line whereas scans and PBI are measured by using the I^{125} radiation.

Because of the much longer half-life of I^{125} (60 d as opposed to 8 d of I^{131}), the high ratio of useful photons per tissue-dose delivered is lowered considerably since iodide has a long biologic thyroid half-life. The reduction in thyroid dose calculated for the same counting accuracy is, however, still interesting. On an average the thyroid dose is between one-third and one-half of that delivered with the corresponding amount of I^{131}.

The long half-life of I^{125} is not important for body dose or organ dose when iodide-labelled compounds with a short biologic half-life are used. This is the case in liver scanning. Apart from colloidal gold, I^{131}-labelled Rose Bengal is the most commonly used radioactive compound for liver scans. Instead of I^{131}, I^{125} may be used for labelling.

Regarding the considerable extension in the depth of the liver, the external measurement in case of I^{125} is restricted to a rather superficial part

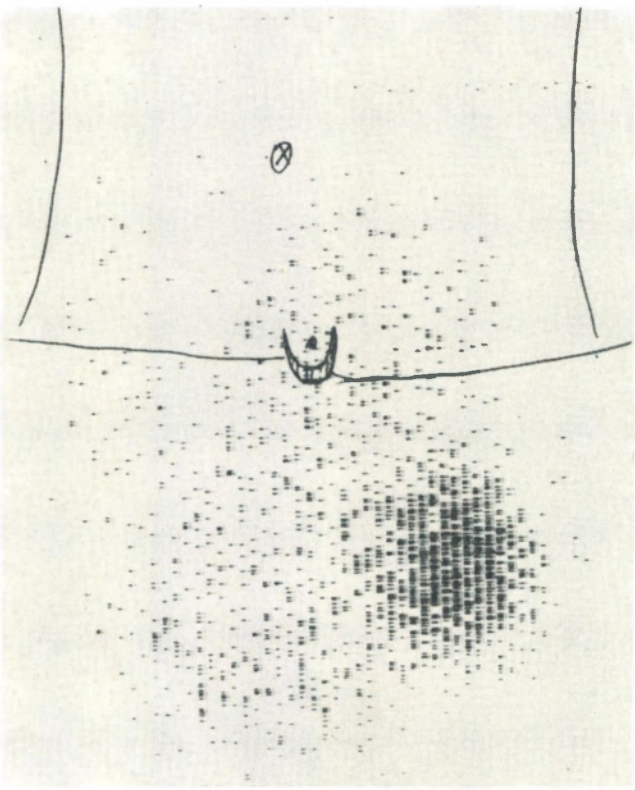

Fig. 4 A

Scintiscan of an intrathoracic goitre after injection of 50 μc of I^{131}

of the liver. This shows some advantages because one of the most limiting factors in liver scanning is the superimposition of non-affected tissue volumes to cold nodules. In the case of liver scans we have only cold nodules to detect and cold nodules have a smaller tissue-nodule activity ratio than, for example, hot nodules in the thyroid. So the chances of detecting cold nodules are much less in a thick organ than in a thin organ, as is shown in a schema ic drawing in Fig. 5.

For a thick organ the limited penetration of low-energy gamma-rays effectively reduces the thickness of the organ and therefore improves the count ratio between the area over the nodule and the area of non-affected tissue.

We tried to demonstrate this by using two equal phantoms made of 1-cm Plexiglas and filled with I^{125} and I^{131} respectively (Fig. 6). The phantoms show a depth on the inside rising from 3 cm to 10 cm on a length of 24 cm. On the inside of the upper wall of the phantom cold nodules in form of Plexiglas cylinders are fixed varying in diameter and height from 1 to 2, 3 and 4 cm. One row of the nodules is arranged in such a way that the largest nodule is on the side of the thinnest layer of activity and the other row is

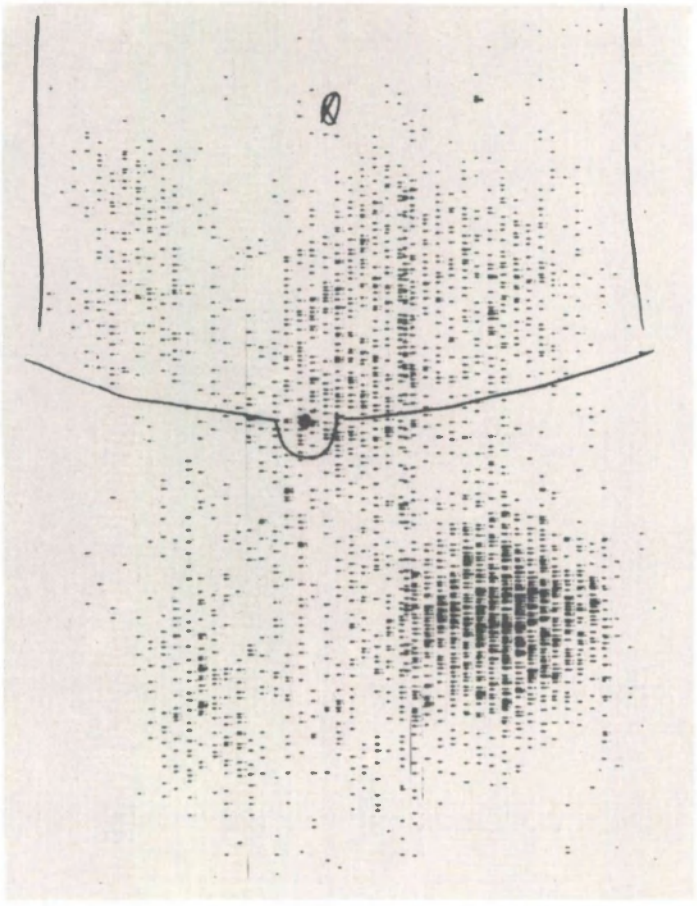

Fig.4B

Scintiscan of the goitre in the same patient as in Fig.4A after injection of 30 μc of I^{125}

fixed inversely so that the largest nodule is inside the thickest layer of radioactivity.

Figure 7 shows in (a) the scan of the I^{131}-filled phantom and in (b) the scan of the I^{125}- filled phantom. On this latter the cold nodules are much better outlined and the 2-cm-diam. nodules are easily distinguished whereas the 2-cm nodules on the I^{131} phantom are not detectable. Figure 8 shows the count-rates for I^{131} and I^{125} measured with a stationary detector over the nodules and the surrounding areas. The count-rate difference for I^{125} (uninterrupted line) is greater for all nodule dimensions and thicknesses of the radioactive layer than for I^{131} (dotted line). These more favourable conditions for scanning are still present when the layer of inactive overlying tissue is increased from 1-cm Plexiglas to 4-cm Plexiglas, simulating a considerable obesity of the patient. Figure 9 shows the scans of the two phantoms. On the I^{131} phantom the 4-cm and 3-cm nodules are only faintly vi-

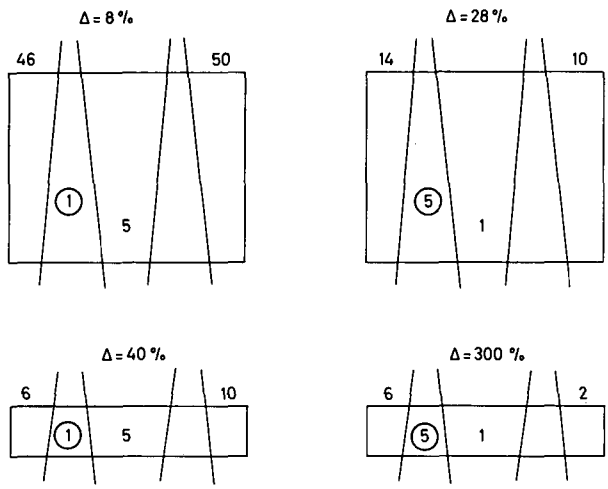

Fig. 5

Differences in the pulse-rates of centres of the same size in organs of different thicknesses at the same geometry

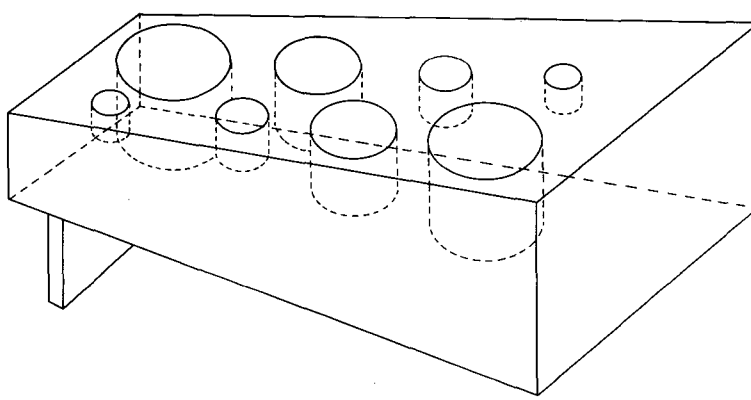

Fig. 6

Schematic drawing of a liver phantom made of Plexiglas

sible. On the I^{125} scan the 4-cm and 3-cm nodules are clearly distinguished and there is still a faint appearance of the 2-cm nodule. On this phantom, however, one sees the much lower pulse-rate of I^{125} as compared with I^{131}, which is caused by the tissue absorption. There is much more statistical inaccuracy therefore on the I^{125} phantom under 4-cm Plexiglas, which, however, can be overcome by applying a larger amount of the labelled compound. Because of the short biologic half-life of Rose Bengal even with a 10 times higher activity administered to the patient the liver dose will still be lower than with I^{131}.

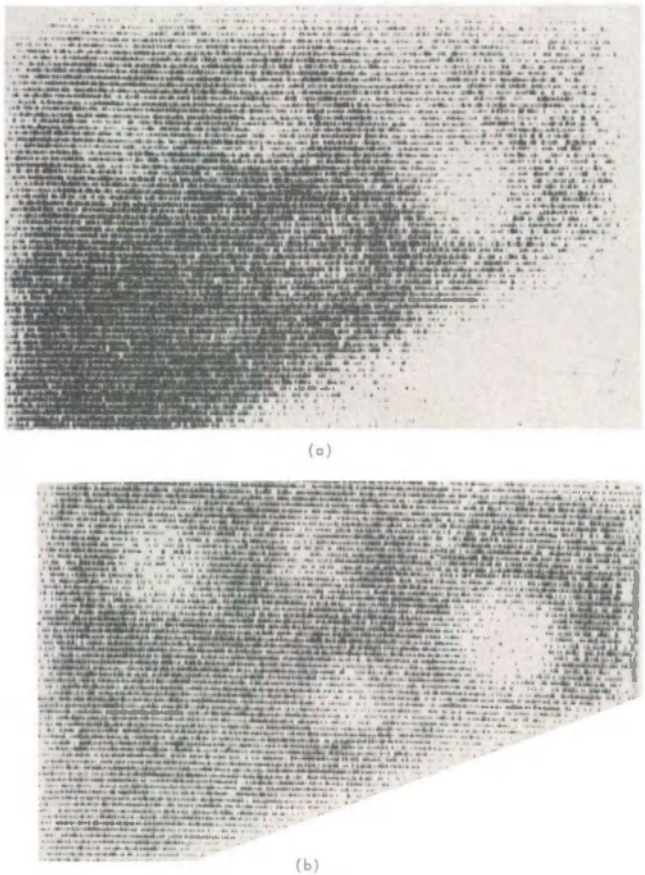

Fig. 7

Phantom scintiscans with 1-cm Plexiglas between activity and detector

(a) Phantom filled with 150 μc of I^{131}
(b) Phantom filled with 150 μc of I^{125}

One may object to liver scans made with I^{125} because they represent only the liver surface or, more accurately, the surface lying on the abdominal wall. There is much evidence, however, that in this case liver metastases will still be detected. OZARDA and PICKREN [3] have shown that in large amounts of autoptic material, in 89% liver metastases were present also on the liver surface. Only 11% showed metastases in the depth of the liver without evidence on the surface. Surface in this case means the actual outside of the liver which can be inspected by the eye. Surface in the case of low-energy gamma scanning, however, means a superficial tissue layer of a few centimeters. Therefore one can expect the number of non-detected liver metastases, because of their situation in the deeper parts of the liver, to be in fact much lower than 11%. So far we do not have enough experience for a statistical evaluation of our own material but there

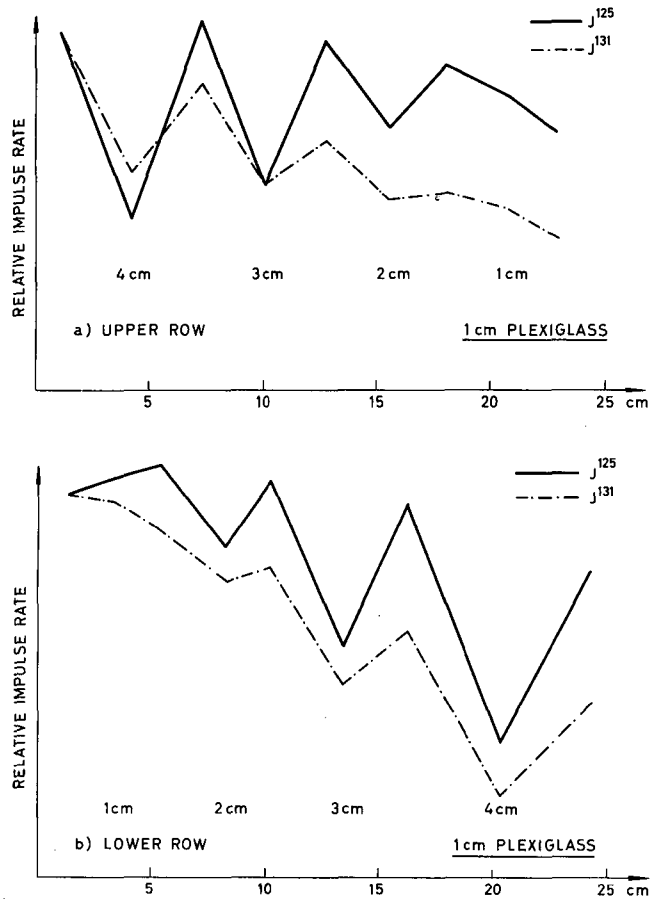

Fig. 8

Differences in the pulse rates of I^{125} and I^{131} with 1-cm Plexiglas between activity and detector

is much evidence that the ability to see smaller nodules will increase the number of detected liver metastases by scanning much more than a non-superficial spread of such metastases will decrease it.

Figure 10 shows a liver scan made with I^{131} Rose Bengal of a patient with a retothelial sarcoma of the stomach penetrating into the liver. One sees a zone of decreased activity extending from the port of the liver to about one-third of the right lobe. The same patient was examined with I^{125} Rose Bengal two days earlier, as shown in Fig. 11. Because the tumour was penetrating the liver from the ventral side the tumour area is well outlined and shows hardly any activity.

Figure 12 shows a liver scan made with colloidal gold on a patient with a rectum carcinoma. Au^{198} has nearly the same gamma energy as I^{131}. The presence of a large metastasis on the lower margin of the liver had already

Fig. 9

Phantom scintiscans with 4-cm Plexiglas between activity and detector

(a) Phantom filled with 150 μc of I^{131}
(b) Phantom filled with 150 μc of I^{125}

been found during the operation. It is easily visible through a defect of fixation of activity on the scan. Furthermore, there is a suspicion of a metastasis on the upper part of the liver. The I^{125} Rose Bengal scan of the same patient performed one day earlier shows this metastasis much more distinctly. On the extended metastasis on the lower margin one sees that a small zone of functioning liver tissue is still surrounding the metastasis (Fig. 13).

A disadvantage of Rose Bengal is its relatively short time of fixation within the liver. This requires a fairly rapid scanning speed to perform the scan in about 20 min. Colloidal heat denaturated albumin labelled with I^{125} stays longer in the reticulo-endothelial system of the liver and permits

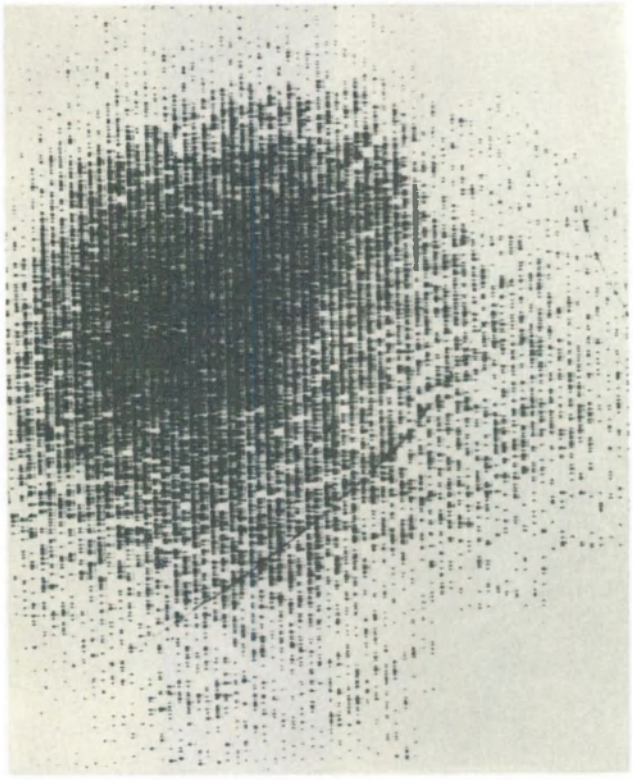

Fig. 10

Liver scintiscan of a 42-yr-old man with a retothelial sarcoma of the stomach; intravenous injection of 250 μc of I^{131} Rose Bengal

scanning at a normal speed within 40-60 min. This compound proved to be very suitable for hepatic scanning.

We have also tried to use I^{125} in form of labelled Hippuran for renal scans but we were not successful. The kidneys in most patients are beyond the depth limiting the useful application of the low-energy gamma-emitting I^{125}.

Another low-energy gamma emitter of medical interest is Hg^{197}. The decay scheme is presented in Fig. 14. Of the 78-keV gamma radiation, 29% is emitted. The main radiation, however, is a K-radiation of 68 keV. The half-value layer in water is 3.8 cm. Hg^{197} therefore is useful for scanning even such deep organs as the kidneys. We made our first attempts with mercuric chloride. Figure 15 shows the scintiscan of a patient who was nephrectomized on the right side. A considerable amount of activity is visible on the right side but this activity is accumulated in the liver. The slightly enlarged left kidney is visible in normal position but there is an additional fixation of activity in the upper lateral region of the kidney, due to a fixation of mercuric chloride in the spleen. The activity fixed in the

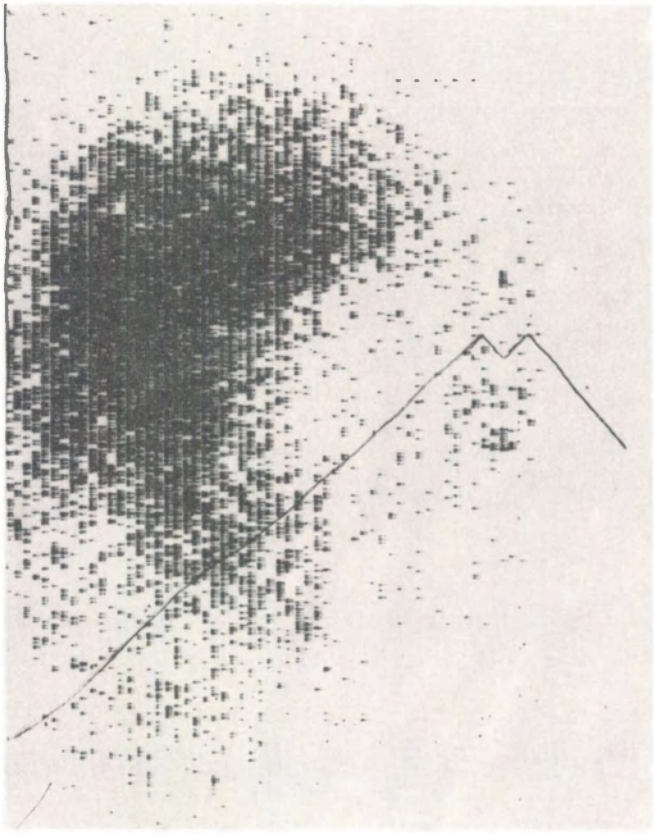

Fig. 11

Liver scintiscan of the same patient as in Fig. 10 after intravenous injection of 250 μc of I^{125} Rose Bengal

kidney is predominant 24 h later, and the liver and spleen are only faintly visible.

Mercuric chloride therefore might be used for kidney scanning but 24 h must elapse before the scanning is begun. A much higher percentage of kidney fixation of mercury is obtained with Neohydrin and hardly any accumulation outside the kidney is observed when using this compound. When we started our first experiments Hg^{197} Neohydrin was not available and we were forced to use mercuric chloride. For several months Hg^{197} Neohydrin has been commercially produced and there is no longer any reason to use Hg^{197} chloride. Hg^{197} Neohydrin gives very excellent kidney scans as shown on Fig. 16. The radiation dose delivered to the kidney with Hg^{197} Neohydrin is about 5% of the dose delivered with Hg^{203} Neohydrin for the same counting accuracy. The problem of the radiation dose is important when Neohydrin is used for scanning of brain tumours. There is much evidence that Neohydrin is more efficient for this purpose than RISA. The amounts of activity that have to be administered for brain-tumour scanning are about five

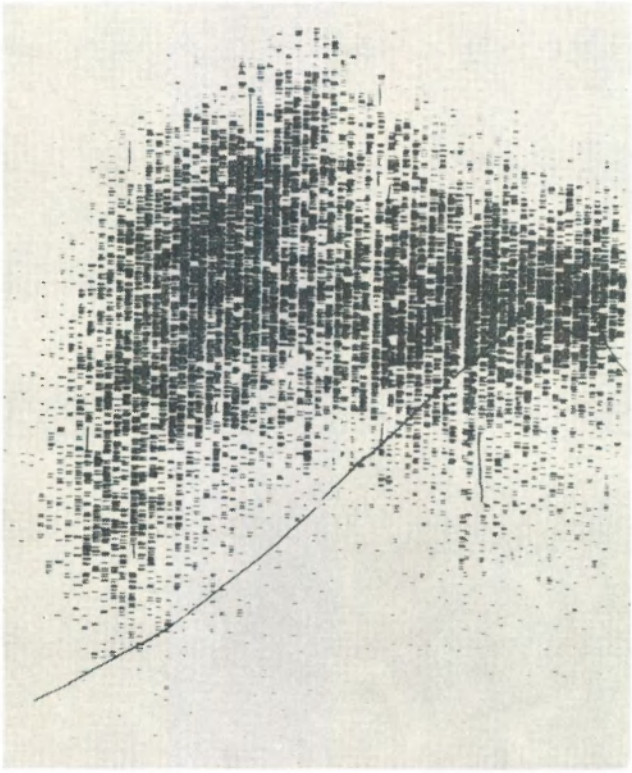

Fig. 12

Liver scintiscan of a 66-yr-old man with an inoperable rectum carcinoma; intravenous injection of 120 μc of Au^{198} colloid

to seven times higher than those required for kidney scanning. The radiation exposure of the kidneys therefore is considerable in brain-tumour scanning and the advantage of Hg^{197} is evident. Figure 17A shows a scintiscan of an ependymoma made with Hg^{203} Neohydrin. There is an accumulation of activity in the left hemisphere and in the frontal lobe. Figure 17B shows a scan of the same patient made with Hg^{197} Neohydrin. The tumour area is much better outlined now and the size and position of the tumour are clearly revealed.

We feel that Hg^{197} Neohydrin is preferable to Hg^{203} Neohydrin for kidney and for brain-tumour scanning because it allows one to obtain better quality scans and because it reduces the radiation exposure of the patient considerably. It is still relatively expensive because of its short half-life but we hope that an increasing demand will improve the supply conditions and lower the price.

Another low-energy gamma-emitting isotope of special medical interest is Tc^{99m}, which has already been mentioned in this Symposium. The 140-keV gamma-energy is still in the range of good quality collimation and

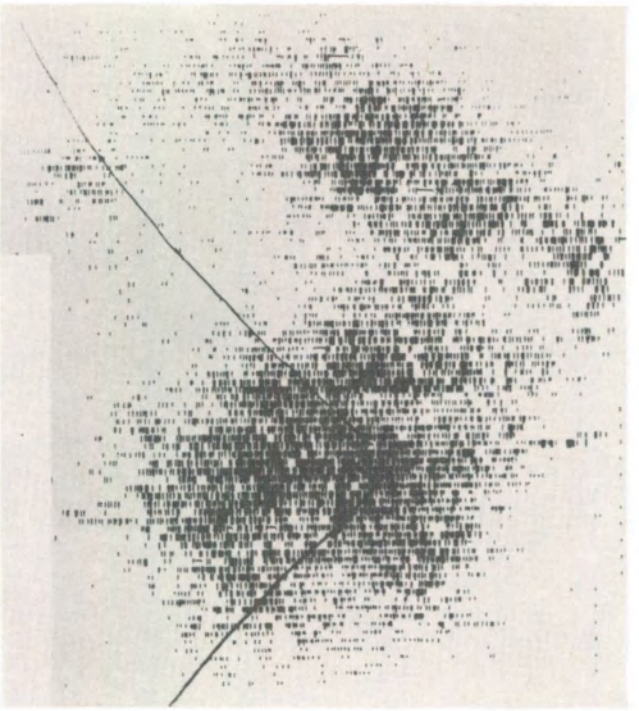

Fig. 13

Liver scintiscan of the same patient as in Fig. 12 after intravenous injection of 120 μc of I^{125} Rose Bengal

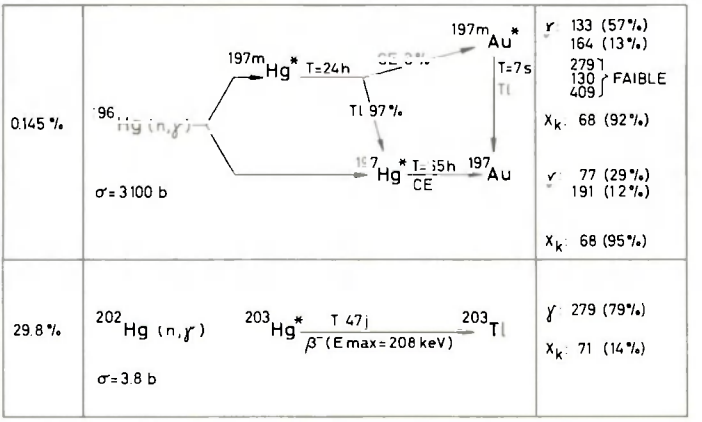

Fig. 14

Decay scheme of Hg^{197} and Hg^{203}

is not much affected by tissue absorption. The very short half-life of 6 h and the absence of beta radiation keep the radiation dose to organs very low.

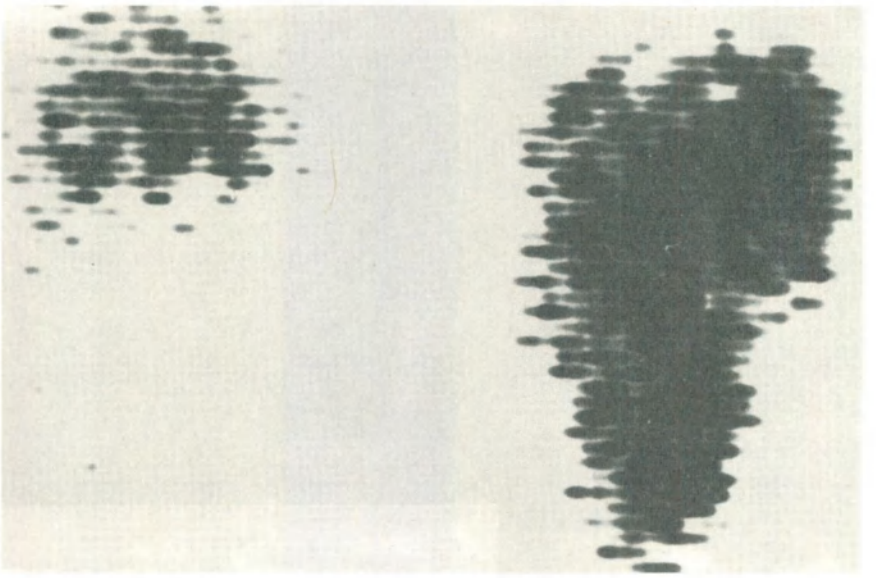

Fig. 15A

Scintiscan of 48-yr-old woman who was nephrectomized because of a hypernephroma, made 2 h after injection of 170 μc $Hg^{197}Cl_2$. Good concentration in the left kidney but also high concentration in liver and spleen

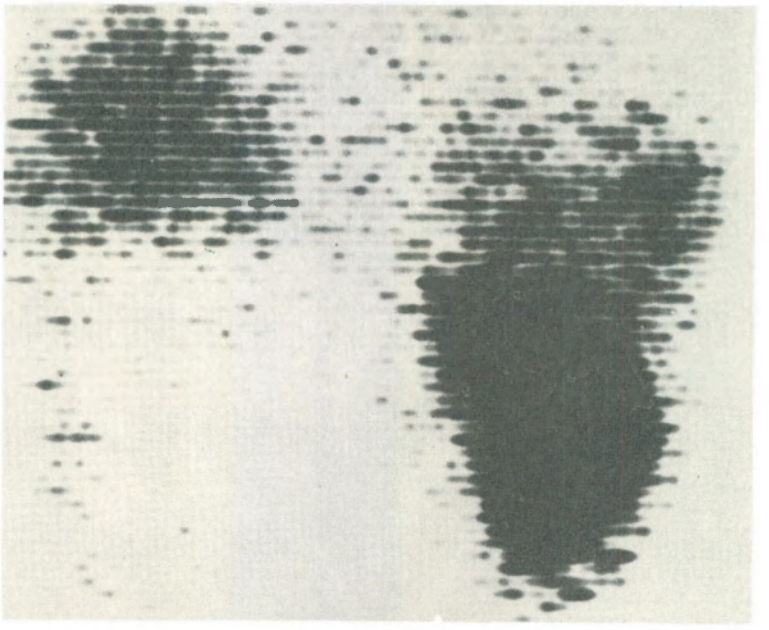

Fig. 15B

Same patient as in Fig. 15A, 24 h after injection, showing better differentiation of activity in kidney, spleen and liver due to higher renal concentration

Fig. 16

Scintiscan of normal kidneys made with Hg^{197} Neohydrin

The physical properties of Tc^{99m} are ideal for medical diagnostic work but there has not been much experience with the chemical and metabolic behaviour of Tc^{99m} compounds. HARPER et al. [4] have shown some iodine-like behaviour of pertechnetate and they could obtain thyroid scans of a fairly good quality. They have found also that technetium may be co-precipitated with sulphur to a colloid showing a typical liver uptake and permitting liver scans.

We have tried to obtain cardiac scans with Tc^{99m} and have found this isotope very useful because the extremely low radiation dose delivered to the body allows the administration of considerable amounts of activity.

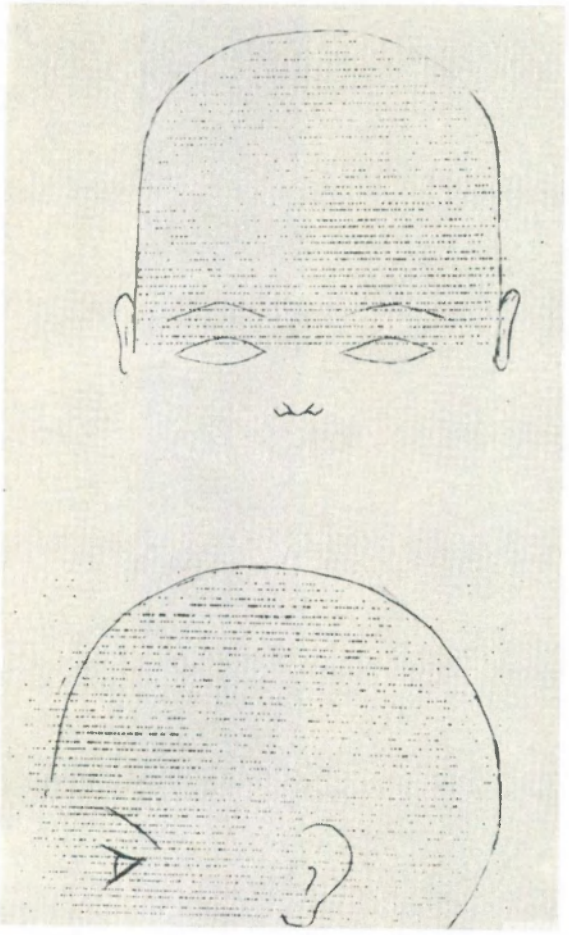

Fig. 17A

Brain scintiscan of a 22-yr-old woman with ependymoma in the left frontal lobe, after the injection of 700 μc of Hg^{203} Neohydrin

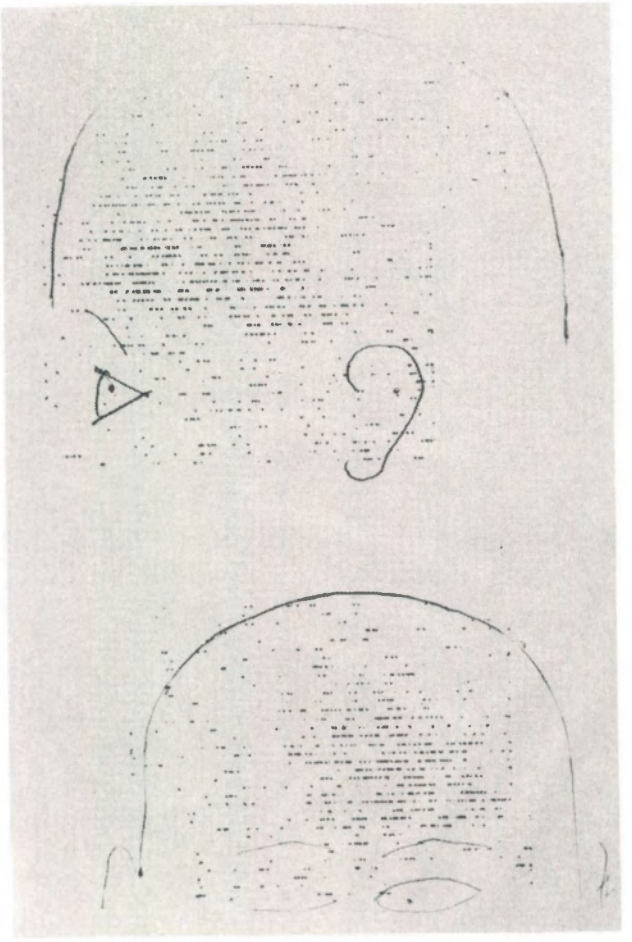

Fig. 17B

Brain scintiscan of the same patient as in Fig. 17A after injection of 700 μc of Hg^{197} Neohydrin

REFERENCES

[1] MYERS, W.G. and VANDERLEEDEN, J.C., Radioiodine-125, J. nucl. Med. 1 (1960) 149.
[2] FELLINGER, K., HÖFER, R. and VETTER, H., Scintigraphie der Schilddrüse mit I^{125}, Nucl.-Med. 3 1 (1962) 20.
[3] OZARDA, A. and PICKREN, J., The topographic distribution of liver metastasis, its relation to surgical and isotope diagnosis, J. nucl. Med. 3 (1962) 149.
[4] HARPER, P.V., ANDROS, G., McCARDLE, R.J. and LATHROP, K., The use of 6-h Tc^{99m} as a clinical tracer material, Sixth International Symposium, Bad Gastein, Radioaktive Isotope in Klinik u. Forschung, 8-11 Jan. 1964.

DISCUSSION

P. HARPER: I think this is an appropriate time to mention the work done by Dr. Schindler of the Department of Physiology, Baylor University, Texas, who has been studying the effects of therapeutic doses of I^{125} in mice. The uptake in the thyroid was about 20% and biological half-time about $3\frac{1}{2}$ d. Doses of 200 μc per animal produced a calculated radiation dosage to the thyroid of about 100 000 rad without appreciable alteration of the physiological function, whilst histological examination after many months showed that the glands were normal. Since most of the radiation dosage is produced by very low-energy short-range conversion electrons and Auger electrons, it seems reasonable to suppose that almost all of this energy is dissipated in the colloid where the isotope is localized. The gland is thus self-shielded. If experiments in progress with hyperthyroid animals with no colloid in the follicles confirm this hypothesis, we shall have to alter substantially our view regarding I^{125} thyroid dosimetry.

I should also like to point out that, with a specially designed collimator and beryllium window crystal, a further gain of 5 or 6 in sensitivity is possible for I^{125} as compared with the sensitivity of conventional detectors for this isotope.

M. BEN-PORATH: We cannot confirm Dr. Schindler's findings with mice. Preliminary results of a series of experiments we are carrying out on rats show that I^{125} radiation doses of 5000 rad to the thyroid do affect its function. The animals have not yet been sacrificed. I do not believe that the mouse is a suitable animal for thyroid investigations. The early work of Goldberg and Chaikoff with I^{131} shows that radiation delivered to the thyroid of the mouse mainly affects the pituitary gland.

I agree with Dr. Harper that specially designed equipment for I^{125} detection would improve sensitivity, but as long as I^{131} has to be used as well as I^{125} for diagnostic purposes, I think most institutions will find it difficult to provide different equipment for I^{125} and I^{131} detection.

C. KELLERSHOHN: Have you done autoradiography with Tc^{99m}?

P. HARPER: Only with electrophoresis strips.

D. KUHL: We have used I^{125}-Rose Bengal for cylindrical liver scanning on the assumption that the low-energy emission, combined with the semi-circular path, would permit a high efficiency examination of the entire outer surface layer of the liver. We found prominent images of the rib cage, however, which confused the liver image to a significant extent, and we have ceased to use this agent. As you would expect, the lateral rib cage was the

more prominent. I should like to ask Dr. Scheer if he has seen rib images on his scans.

K. SCHEER: We did not find that the ribs confused the liver image. This might be partly due to our collimator, which is only 1.5 cm thick, The collimator was only a short distance from the skin, and a rib would not cover more than one third of the openings. In anterior scans there is almost no bone from the thoracic cage lying over the liver.

D. FOLLETT: I should like to ask how you calculated the tissue dose when using I^{125} compared with I^{131}. We have made similar calculations for the two systems, optimized for 2-cm resolution diameter and the same count rate using a method similar to that used by Dewey and Sinclair. We obtained the same result as you, i.e. about one half the radiation dose with I^{125} compared with that with I^{131}. This would seem to indicate the usefulness of the method used by Dewey and Sinclair, presuming your method was different.

K. SCHEER: Our dose calculation was a fairly rough one based on the electron energy and the effective half-life calculated from the data published by the International Commission on Radiological Protection. Our values are probably too high.

J.M. McALISTER: I should like to ask Dr. Ben-Porath what the estimated percentage uptake was in the lung metastases that he showed.

M. BEN-PORATH: The uptake measured was 12-13%. We measured it with a wide-angle collimator at a distance of 50 cm, using a proper standard.

H. VETTER: Speaking on behalf of Dr. Höfer, who is absent at present, I should like to question seriously the validity of Dr. Ben-Porath's method of measuring thyroid uptake of I^{125}. I know that Dr. Höfer has tried to use this isotope for thyroid uptake measurements and that he did not succeed. Thyroid uptake measurements are subject to a number of sources of error and I do not think it desirable to introduce unnecessarily a further one due to the very much increased gamma-ray absorption within the neck. The argument that the use of I^{125} would reduce the radiation dose to the patient is not convincing. If one wants to make full use of the acknowledged advantages of I^{125} for sample measurements in vitro without, at the same time, losing accuracy in measurements in vivo, the best course appears to be to administer a mixture of, say, 3 μc of I^{131} for uptake measurement and 15 μc of I^{125} for the measurement of protein-bound I^{125} in serum. Dr. Höfer and others have shown that this is a fairly satisfactory method.

TABLE I

RESULTS OF UPTAKE MEASUREMENTS WITH I^{125} AND I^{131}

Clinical diagnosis	24-h uptake		24-h excretion		24-h PBI-conversion ratio	
	I^{131}	I^{125}	I^{131}	I^{125}	I^{131}	I^{125}
Hypothyroid	17 ± 7	16 ± 9	57 ± 15	59 ± 11	7 ± 6	8 ± 4
Euthyroid	36 ± 8	32 ± 7	47 ± 10	49 ± 8	27 ± 12	28 ± 11
Hyperthyroid	65 ± 13	64 ± 11	22 ± 14	25 ± 13	74 ± 18	76 ± 17

M. BEN-PORATH: It is possible to make uptake measurements with I^{125}, using a proper phantom and standard. We use a 15-cm diam. neck phantom and a 30-ml standard (a plastic container 2.5 cm in diameter and 6 cm high). We have compared the results of 229 thyroid uptake measurements carried out with I^{125} and with I^{131} (see Table I). From this table it is clear that there is no significant difference between the I^{125} and the I^{131} results. In addition, 20 patients were given "cocktails" of I^{125} and I^{131}, and the results were almost identical. Thyroids larger than 60 g could not be measured accurately with I^{125}, and these cases are measured with I^{131}. Another parameter which shows the accuracy of the results is the 24-h recovery (uptake plus urinary excretion). Normally the recovery is 80 - 90% for euthyroid and hyperthyroid patients. If we see a recovery much lower than the one mentioned, and there is no medical reason for it (as, for instance, renal disease), the uptake is repeated with I^{131}.

SCANNING WITH IODINE-125*

M. BEN-PORATH, A. HOCHMAN AND J. GROSS
THE MEDICAL PHYSICS SECTION, THE ONCOLOGICAL DEPARTMENT OF THE HADASSAH UNIVERSITY HOSPITAL, AND THE DEPARTMENT OF EXPERIMENTAL MEDICINE AND CANCER RESEARCH OF THE HEBREW UNIVERSITY, HADASSAH MEDICAL SCHOOL, JERUSALEM, ISRAEL

Abstract — Résumé — Аннотация — Resumen

SCANNING WITH IODINE-125. The use of I^{125} as I^{125}-iodide for scanning of the thyroid and of thyroid carcinoma metastases and as I^{125}-labelled Rose Bengal for scanning of the liver has been investigated in our laboratories.

In some patients, the thyroid scans and the scans of thyroid carcinoma metastases were repeated with I^{131}. The liver scans were repeated with colloidal Au^{198}. Cold nodules in the thyroid which could not be detected with I^{131} were clearly seen with I^{125}. Anterior metastases in the lungs could be differentiated from posterior metastases with I^{125}, while with I^{131} this was not possible.

Using the same doses of radioactivity the background with I^{131} was much higher and could not be eliminated, as this would have reduced the counting rate over the lesions to levels which could not be detected.

Some of the photoscans and mechanical scans of livers carried out with colloidal Au^{198} could not be interpreted. However, "cold" lesions were clearly seen on the scans of the same livers with I^{125}-labelled Rose Bengal.

GAMMAGRAPHIE AU MOYEN DE L'IODE-125. Les auteurs ont étudié dans leur aboratoire l'emploi de ^{125}I sous forme d'iodure pour la gammagraphie de la thyroïde et des métastases de carcinomes thyroïdiens, ainsi que l'utilisation du rose bengale marqué avec ^{125}I pour la gammagraphie du foie.

Chez certains sujets, les scintigrammes de la thyroïde et des métastases de carcinomes thyroïdiens ont été refaits avec ^{131}I. De leur côté, les scintigrammes du foie ont été refaits avec de l'or-198 colloïdal. Les abcès froids thyroïdiens qui n'étaient pas détectés avec ^{131}I devenaient nettement visibles avec ^{125}I; de même, ^{125}I permettait de distinguer les métastases antérieures des métastases postérieures des poumons, alors que cette distinction n'était pas possible avec ^{131}I.

Pour les mêmes doses de radioactivité, le bruit de fond était beaucoup plus élevé avec ^{131}I et ne pouvait pas être éliminé, car cela eût ramené l'intensité au-dessus des lésions à des niveaux impossibles à detecter.

Plusieurs photo-scintigrammes et mécanogrammes obtenus au moyen de l'or-198 colloïdal n'ont pas pu être interprétés. En revanche, les scintigrammes des mêmes foies au moyen de rose bengale marqué avec ^{125}I faisaient nettement apparaître les lésions «froides».

СКЕННИРОВАНИЕ С ПОМОЩЬЮ ЙОДА-125. Изучалось использование йода-125 в форме иодида, меченного йодом-125, для сканнирования щитовидной железы и метастазов рака щитовидной железы и в виде меченной йодом-125 бенгальской розы для сканнирования печени.

У некоторых больных сканнирование щитовидной железы и сканнирование метастозов рака щитовидной железы было повторено с использованием йода-131. Сканнирование печени было повторено с использованием коллоидного золота-198. "Холодные" узелки в щитовидной железе, которые нельзя обнаружить с помощью йода-131, были отчетливо видны при сканнировании с помощью йода-125. С помощью йода-125 можно было отличить ранние метастазы в легких от поздних, тогда как с помощью йода-131 сделать это не удавалось.

При использовании одинаковых доз, в случае с йодом-131 фон был значительно выше и не мог быть веделен, так как это снизило бы скорость счета над пораженными местами до уровней, которые нельзя обнаружить.

*/The presentation of this paper was made possible by a travelling grant from the Israel Cancer Association.

Некоторые фотоскенннограммы и механические скенннограммы печени, выполненные с помощью коллоидного золота-198 нельзя объяснить. Однако "холодные" участки поражения отчетливо видны на скенннограммах печени тех же больных, если они сделаны с помощью меченной йодом-125 бенгальской розы.

EXPLORACIÓN CON YODO-125. Los autores han estudiado en sus laboratorios el empleo de yoduro marcado con ^{125}I, para explorar la tiroides y las metástasis del cáncer de este órgano, y de Rosa Bengala, marcado también con ^{125}I, para explorar el hígado.

En algunos pacientes, la exploración de la tiroides y de las metástasis del cáncer tiroideo se repitió con ^{131}I. Las exploraciones del hígado se volvieron a efectuar con ^{198}Au coloidal. Los nódulos fríos de la tiroides que no se detectaron con ^{131}I pudieron en cambio observarse claramente con ^{125}I. Las metástasis pulmonares anteriores pudieron diferenciarse de las posteriores con ^{125}I, lo que no fue posible con ^{131}I.

Para iguales dosis de radiactividad, el ^{131}I dio una actividad de fondo mucho más elevada que no fue posible eliminar, ya que ello habría reducido a valores indetectables il índice de recuento en la zona de las lesiones.

Los autores no pudieron interpretar los resultados de algunas de las fotoexploraciones y de las exploraciones hepáticas con impresión mecánica efectuadas mediante ^{198}Au coloidal. Sin embargo, utilizando Rosa Bengala marcado con ^{125}I pudieron observar claramente lesiones « frías » en centelleogramas de hígados ya explorados con otros productos.

One of the most widely used radioisotopes in medical diagnosis is undoubtedly iodine-131. Its availability, low cost, convenient half-life and detectability contribute much to this fact. On the other hand, its beta rays are of little use for tracer purposes, but contribute about 90% of the total radiation dose to small organs (like thyroid) and about 65% to the total body irradiation dose from internally administered I^{131}. Therefore, a quanta-emitting radioisotope of iodine with a minimal beta emission should be preferred for diagnostic work. Such an isotope is iodine-125, which has been suggested for medical radioisotope diagnosis by MYERS and VANDERLEEDEN [1].

For the past 14 months we have been routinely using I^{125} for iodine uptake studies, thyroid scans, localization of thyroid carcinoma metastases, and I^{125}-labelled Rose Bengal for liver scans. Some of the scans were repeated with I^{131} or colloidal Au^{198}.

MATERIAL AND METHODS

The scans were performed with an FH96-Frieseke-Hoepfner Scinti-scanner, with a 2-in × 2-in NaI(Tl) crystal. Mechanical, optical and magnetic recordings, and profiles were obtained simultaneously.

For thyroid scans 25 μc of I^{125} or 75 μc of I^{131} were administered orally. The thyroid was scanned 24 h later, with a 31-hole focusing collimator, at a 2.5-mm/s scanning speed. The distance between scanning rows was 3 mm. Replay speed (when necessary) was 10-20 mm/s.

For lung scans, or for the exploration of iodine-concentrating metastases, doses of 300 μc-500 μc of I^{125}, or 500 μc of I^{131} were used. After 24 h, anterior and posterior scans of the lungs were performed at a 2.5-mm/s speed, distance between rows 4-6 mm.

An X-ray picture of the patient's chest was taken while the patient was lying on the scanner stretcher. The photoscanning device is located directly

underneath the scanned area of the patient, so that the resulting photoscannogram is obtained on the X-ray picture without moving the patient or the film from the X-ray exposure to the end of the scanning.

For liver scans, a dose of 3 μc/kg I^{125}-labelled Rose Bengal was injected intravenously. Scanning was started 20 min later, at a 5-mm/s speed, from down upwards. The distance between rows was 6 mm. Colloidal Au^{198} was injected at the same concentration, the scan was started 60 min later, at a 2.5 mm/s speed. The lungs and liver were scanned with a 5-mm diam., 80-mm long, straight-bore collimator.

RESULTS AND DISCUSSION

The improved resolution, after both scannings, of I^{125} as compared to I^{131} has been reported by several workers [2, 3, 4]. We show this effect in Fig. 1. A patient with an enlarged thyroid and with 3 palpable nodules (Fig. 1 a) was given a tracer dose of 25 μc of I^{125}. The scanning of the thyroid was performed 24 h after administration of the dose when the thyroid uptake was 40%. The photoscan, recorded on Kodak industrial film type M, is shown in Fig. 1b. All three nodules are visualized as "cold" lesions. The scanning was repeated 24 h after the administration of another tracer dose of 75 μc

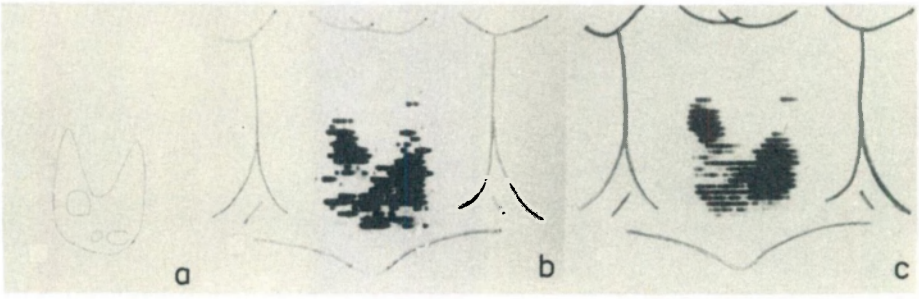

Fig. 1

Thyroid scans
(a) Outline of thyroid and nodules
(b) Photoscan with I^{125}
(c) Photoscan with I^{131}

I^{131}. The thyroid uptake was 42%. The photorecording is shown in Fig. 1c. With I^{131} only the two larger "cold" nodules are seen. These results were expected as the palpable diameter of the smallest nodule was 5 mm, while the point source resolution* of the 31-hole collimator used for the scanning was 5.1 mm for I^{125} and 8.2 mm for I^{131}.

The use of I^{125} for localization of iodine-concentrating metastases of cancers of the thyroid shows an even greater advantage over I^{131}. Figure 2a shows an X-ray of the lungs of a patient suffering from follicular adenocarcinoma of the thyroid. This roentgenogram was defined by the roentgeno-

* As defined by DEWEY and SINCLAIR [5].

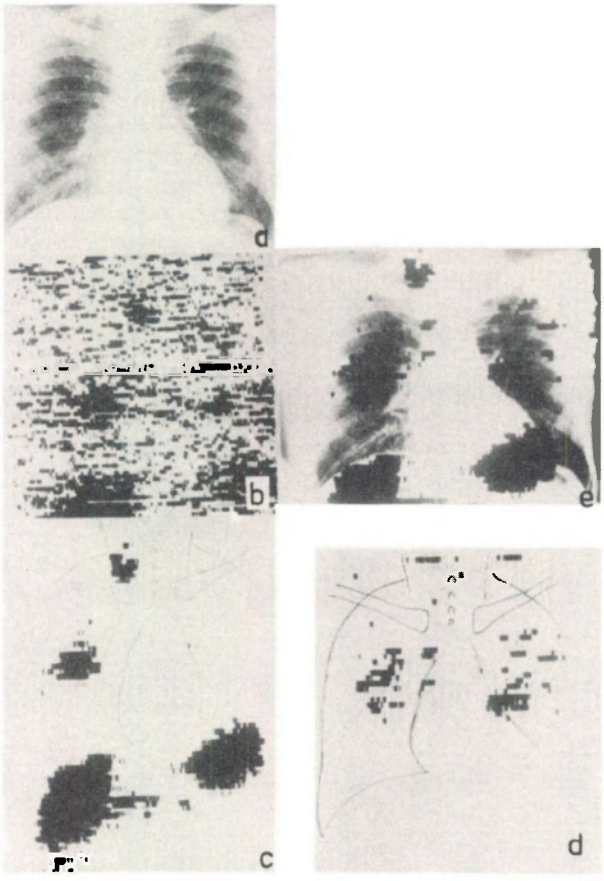

Fig. 2

Scans of thyroid carcinoma metastases
(a) Chest X-ray of patient
(b) Anterior scan with I^{131}
(c) Anterior scan with I^{125}
(d) Posterior scan with I^{125}
(e) Superimposed picture of a, c, d

logists as "without pathological findings". The patient was given a tracer dose of 500 μc I^{131}, and a scannogram of his neck and chest was obtained. The photorecording is shown in Fig. 2b. A substernal nodule is seen, and two foci in the lungs. In addition the liver and the stomach are also clearly seen, but the background is diffuse and complicates the localization. Attempts to eliminate the background by replays from the magnetic memory did not improve the contrast. Eight weeks later scanning was repeated after a dose of 500 μc of I^{125}. The neck and chest photoscans are shown in Fig. 2c. The localization is similar to that obtained with I^{131}, with the difference that only the metastases in the right lobe are visualized and the background is virtually eliminated. A posterior scan of the patient shows foci of concentration

in both lobes (Fig. 2d). Superimposing the chest and back scans we see the same lesions as with I^{131}, with the exception that no background interfered on the I^{125} photoscans. Figure 2e is a superimposed picture of a, c and d. The possibility of differentiating between anterior and posterior metastases is illustrated in another patient (Fig. 3). This patient showed a miliary

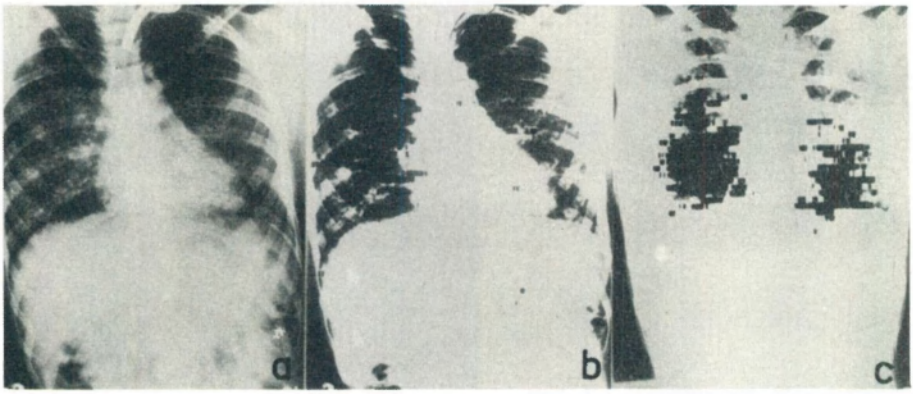

Fig. 3

Scans of thyroid carcinoma metastases
(a) Chest X-ray in scanning position
(b) Anterior scan
(c) Posterior scan

spread of metastases through the lungs (Fig. 3a). Figures 3b and 3c are the chest and back photoscans after 500 μc of I^{125}. In this case the scans were recorded directly on the exposed roentgenogram of the patient, in the actual scanning position. In this case Ilford medical X-ray films were used. Here again we see the anterior and posterior lesions differentiated.

For the determination of the existence of iodine-concentrating lesions in the lungs it is sufficient to perform integral anterior and posterior uptake measurements. For accurate localization of the lesions, a chest- and back-scan with I^{125} gives a more detailed picture.

Fig. 4a is photoscannogram of a normal liver, with I^{125}-labelled Rose Bengal. Immediately after the scanning with Rose Bengal, a dose of colloidal Au^{198} was injected into the patient. Figure 4b is the photoscannogram with colloidal Au^{198}, which was carried out 60 min after the injection. The general picture is the same, the differences in the outlines are due to different scanning speeds.

The photoscan of the liver of a patient with surgically proved cyst, in the extreme right edge on the upper surface of the liver, carried out with I^{125}-labelled Rose Bengal, is shown in Fig. 5a. The cyst can be visualized in this picture. Scanning the same liver with colloidal Au^{198} the picture in Fig. 5b was obtained. This picture would pass as "normal", although with the fore-knowledge of the location of the cyst the density is less in this region than in the rest of the liver. This effect is obviously due to the fact that the cyst absorbed only a small fraction of the 410-keV γ-rays from

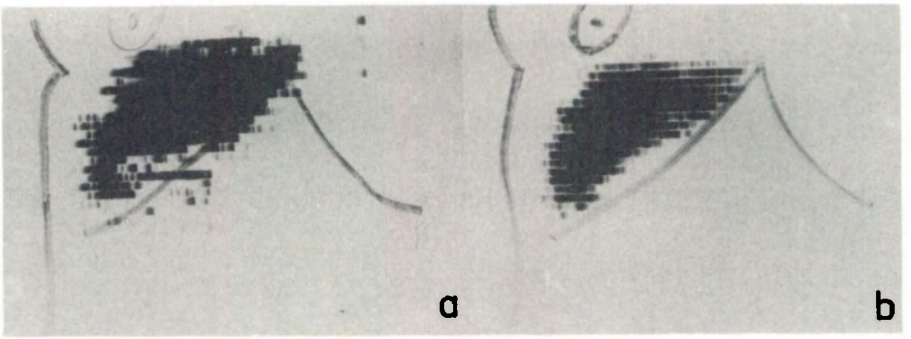

Fig. 4

Scans of normal liver
(a) With I^{125}-labelled Rose Bengal
(b) With colloidal Au^{198}

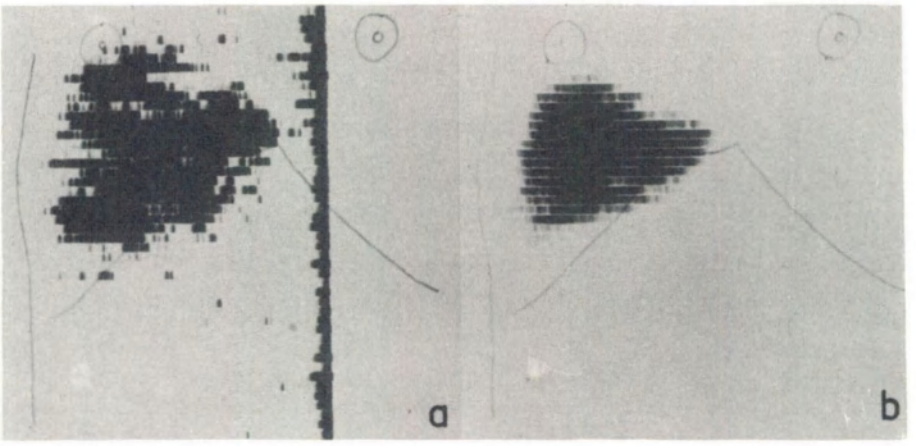

Fig. 5

Scans of liver with cyst in anterior right edge
(a) With I^{125}-labelled Rose Bengal
(b) With colloidal Au^{198}

Au^{198}, while absorbing a significant part of the soft 27.4-keV X-rays from I^{125}.

CONCLUSION

In in vivo studies of "cold" lesions in the thyroid and liver, I^{125} permits a more accurate and sensitive localization than I^{131} and Au^{198}. Similarly I^{125} gives a much more accurate localization of iodine-concentrating metastases of thyroid carcinoma, permitting differentiation of lesions occurring at differing depths in the body.

ACKNOWLEDGEMENTS

We acknowledge the valuable technical assistance of E. M. Reich and Mrs. S. Kornitzer-Baron.

REFERENCES

[1] MYERS, W.G. and VANDERLEEDEN, J.C., Radioiodine-125, J. nucl. Med. 1 (1960) 149.

[2] ENDLICH, M., HARPER, P., BECK, R., SIEMENS, W. and LATHROP, K., The Use of I-125 to Increase Isotope Scanning Resolution, Amer. J. Roentgenol. 87 (1962) 148.

[3] FELLINGER, K., HÖFER, R. and VETTER, H., Scintigraphie der Schilddrüse mit I^{125}, Nucl.-Med. 3 1 (1962) 20.

[4] CHARKES, N.D. and SKLAROFF, D.M., The Use of I-125 in Thyroid Scintiscanning. Amer. J. Roentgenol. 90 (1963) 1052.

[5] DEWEY, W.C. and SINCLAIR, W.K., Criteria for Evaluating Collimators Used in "In Vivo" Distribution Studies with Radioisotopes, Int. J. appl. Rad. Isotopes 10 (1961) 1.

VIII

CLINICAL APPLICATIONS: BRAIN

DESIGN AND FUNCTION OF A BRAIN SCANNER FOR CLINICAL USE *

W. PAUL AND T. P. MORLEY
DEPARTMENT OF PATHOLOGICAL CHEMISTRY AND DEPARTMENT OF SURGERY, UNIVERSITY OF TORONTO, CANADA

Abstract — Résumé — Аннотация — Resumen

DESIGN AND FUNCTION OF A BRAIN SCANNER FOR CLINICAL USE. Since the human brain is bilaterally symmetrical and possesses unusual resistance to many substances in the blood stream, it has been suggested that radioactive scanning for this region may be best performed with an instrument made especially for the purpose. A scanner is described which was designed to be used as a screening device for brain-tumour suspects, so that high sensitivity, simplicity of patient preparation and ease of reading and interpretation were primary requirements.

Brownell's equation relating radioactivity concentration to diameter of resolution indicates that the required radioactivity per unit volume is inversely related to the sixth power of the resolution diameter. Accordingly, a maximum permissible diameter of resolution was chosen consistent with satisfactory localization of areas of increased radioactivity. Precise delineation was not required. Since the number of detected disintegrations per unit time is an inverse function of the square of distance, two detectors each with a short "focus" are used rather than one detector which must be made optimal for the mid-sagittal plane.

The 2-in-diam. crystal and photomultiplier assemblies are mounted opposite one another on a rigid scanning frame, each fitted with a seven-hole (hexagonal) focusing collimator designed for a 1.5-cm resolution diameter and a focus 8 cm from the collimator face. The frame scans rectilinearly in the sagittal plane. The scan record is presented as an asymmetrogammagram and as separate left and right photographic two-dimensional displays. Pulses from each detector are fed to an amplifier-discriminator circuit and thence to a difference circuit which prints a left or right marker to indicate a predominance of left or right radioactivity. Pulses from each amplifier-discriminator circuit also go to count-rate meters which in turn activate lamps mounted in a light-tight housing. The two lamps, the light intensity of which is a function of activity measured by the respective detectors, are mounted on a common arm moved by Selsyn motors synchronous with Selsyn generators on the detector frame, thus permitting the use of a remotely placed recording unit. Cylindrical lenses focus the lamp sources on film, both right and left records being made simultaneously on an 11-in × 14-in X-ray film. Although the operator may adjust mean lamp current to a proper predetermined value over a wide range of count rate, a great deal of latitude is given the operator by the inclusion of three sheets of film in the cassette each providing optimum contrast for a different range of count rate.

Patients are given 350 μc of I^{131} human serum albumin after previous treatment with Lugols solution and scanning is performed between 24 and 72 h later. A single scan is usually sufficient. Scans on some patients are repeated in the antero-posterior direction.

On 653 patients 789 scans were made from September 1961 to November 1962. There was a confirmed diagnosis in 109 of these patients, 88 having tumours. Twenty-three of 30 glioblastomas and 15 of 19 meningiomas were clearly located.

ÉTUDE D'UN APPAREIL DE SCINTIGRAPHIE DU CERVEAU - SON RÔLE CLINIQUE. Du fait de la symétrie du cerveau humain et de sa résistance particulière à de nombreuses substances du flux sanguin, il semble que la scintigraphie du cerveau puisse être effectuée dans les meilleures conditions avec un appareil spécialement conçu à cet effet. L'auteur décrit un scintigraphe destiné à vérifier la présence de tumeurs du cerveau, qui répond en premier lieu aux conditions suivantes; haute sensibilité, simplicité des opérations de préparation du patient et facilité de lecture et d'interprétation.

La relation de Brownell entre la concentration de radioactivité et le diamètre de résolution montre que la quantité de radioactivité nécessaire par unité de volume est inversement proportionnelle à la sixième puis-

* This development was supported by a series of grants-in-aid of the Ontario Cancer Treatment and Research Foundation.

sance du diamètre de résolution. C'est pourquoi on a choisi le plus grand diamètre de résolution compatible avec une localisation satisfaisante des zones de radioactivité accrue. Une délimitation précise n'était pas nécessaire. Le nombre de désintégrations détectées par unité de temps variant en fonction inverse du carré de la distance, on utilise deux détecteurs ayant chacun une courte focale, de préférence à un détecteur qui doit être réglé sur le plan médian du cerveau.

Le détecteur à cristal de 5 cm de diamètre et le photomultiplicateur sont montés l'un en face de l'autre sur un cadre rigide, chacun d'entre eux étant muni d'un collimateur à focalisation à sept canaux (hexagonal) ayant un diamètre de résolution de 1,5 cm et un foyer à 8 cm de sa face antérieure. L'exploration est faite linéairement dans le plan sagittal. Le scintigramme se présente sous la forme d'un asymétrogammagramme et de représentations photographiques séparées, gauche et droite, à deux dimensions. Les impulsions de chaque détecteur passent dans un circuit amplificateur-discriminateur, puis dans un circuit différenciateur qui imprime un signe à gauche ou à droite pour indiquer une prédominance de radioactivité à gauche ou à droite. Les impulsions sortant de chaque circuit amplificateur-discriminateur passent également dans des débitmètres qui, à leur tour, actionnent des lampes dans une chambre noire. Les deux lampes, dont l'intensité lumineuse est proportionnelle à l'activité mesurée par le détecteur correspondant, sont montées sur un même support mû par des moteurs Selsyn synchronisés avec des générateurs Selsyn fixés sur le cadre du détecteur, ce qui permet d'utiliser un dispositif enregistreur placé à une grande distance. Des lentilles cylindriques focalisent la lumière émise par les lampes sur un film, les enregistrements à droite et à gauche étant effectués simultanément sur un film à rayons X de 36 x 28 cm. Bien que l'opérateur puisse régler le courant moyen des lampes à une valeur déterminée à l'avance d'une gamme étendue de taux de comptage, il dispose d'une grande latitude grâce à l'insertion dans le magasin de trois films donnant chacun le contraste optimum pour une gamme différente de taux de comptage.

On administre aux patients 350 μc d'albumine de sérum humain marquée avec ^{131}I, après traitement préalable avec la solution de Lugols, et on procède à la scintigraphie après un délai de 24 à 72 h. Normalement, un seul scintigramme est suffisant. Dans certains cas, on en fait un second dans la direction antéro-postérieure.

De septembre 1961 à novembre 1962, l'auteur a effectué 789 scintigrammes sur 653 patients. Dans 109 cas, le diagnostic a été confirmé, 88 patients présentant des tumeurs. L'auteur a nettement localisé 23 glioblastomes sur 30, et 15 méningiomes sur 19.

УСТРОЙСТВО И ФУНКЦИЯ ПРИБОРА ДЛЯ СКЕННИРОВАНИЯ МОЗГА И ЕГО КЛИНИЧЕСКОЕ ИСПОЛЬЗОВАНИЕ. Так как мозг человека обладает двусторонней симметрией и необычной сопротивляемостью в отношении многих веществ, содержащихся в крови, предполагается, что радиоактивное сканнирование этой области лучше всего осуществлять с помощью специального прибора. Дается описание сканнера, предназначенного для выявления больных с предполагаемыми опухолями мозга. При этом основными требованиями к прибору являлись высокая чувствительность, простота подготовки пациента, чтения и интерпретации данных.

В уравнении Брауннелла о соотношении между концентрацией радиоактивности и диаметром разрешения указывается, что уровень необходимой радиоактивности на единицу объема обратно пропорционален шестой степени диаметра разрешения. Соответственно максимально допустимый диаметр разрешения выбирался в зависимости от удовлетворительной локализации областей с повышенной радиоактивностью. Точных контуров не требовалось. Поскольку количество обнаруживаемых распадов на единицу времени представляет собой обратную функцию квадрата расстояния, целесообразнее использовать два детектора с коротким "фокусом", а не один детектор, который должен быть оптимальным в средне-сагиттальной плоскости.

Кристаллическая сборка диаметром 5 см и фотоумножительная сборка монтируются друг против друга в жесткой схеме сканнирования, причем каждая сборка снабжается фокусирующим коллиматором с семью отверстиями (в гексагональном порядке), предназначенным для получения диаметра разрешения 1,5 см и фокуса на расстоянии 8 см от поверхности коллиматора. Сканнирование ведется прямолинейно в сагиттальной плоскости. Сканнограммы представляются в виде асиметрогаммаграмм и раздельных левого и правого фотографических двухразмерных изображений. Импульсы от каждого детектора подаются на контур усилитель-дискриминатор и затем на дифференциальный контур, который печатает левую или правую отметки с целью показа преобладания концентрации радиоактивности слева или справа. Импульсы от каждого контура усилитель-дискриминатор подаются также на пере-

счетные устройства, которые в свою очередь возбуждают лампы, установленные в светонепроницаемом помещении. Две лампы, интенсивность света которых представляет собой функцию активности, измеренной соответствующими детекторами, монтируются на общей подставке, передвигаемой с помощью двигателей Сельсина в системе детектора синхронно с генераторами Сельсина, тем самым давая возможность применять установленную на расстоянии регистрирующую установку. Цилиндрические линзы фокусируют ламповые источники на пленку, при этом регистрация как справа, так и слева осуществляется одновременно на рентгеновской пленке размером 28 × 36 см. Хотя оператор может установить соответствующую предварительно определенную величину средней силы тока лампы в широком диапазоне скорости счета, оператору предоставляется большая свобода в связи с наличием в кассете трех пленок, каждая из которых обеспечивает оптимальную контрастность в различном диапазоне скорости счета.

Пациентам вводились 350 мкюри йода-131 с сывороточным альбумином человека после предварительной обработки раствором Люголя. Сканнирование осуществлялось через 24—72 часа. Обычно было достаточно получения одной сканнограммы. У некоторых пациентов сканнограммы снимались повторно в передне-заднем направлении.

В период с сентября 1961 года по ноябрь 1962 года у 653 пациентов было снято 789 сканнограмм. У 109 пациентов из этого числа диагноз подтвердился, у 88 пациентов были обнаружены опухоли. Была установлена локализация 23 из 30 глиобластом и 15 из 19 менингиом.

DISEÑO Y FUNCIÓN DE UN APARATO DE EXPLORACIÓN DEL CEREBRO PARA USO CLINICO. Como el cerebro humano tiene una simetría bilateral y es excepcionalmente resistente a muchas de las sustancias contenidas en la corriente sanguínea, su exploración radiactiva debe efectuarse con un instrumento especialmente concebido para este fin. El autor describe un dispositivo para la detección de tumores cerebrales, cuyas principales ventajas son: elevada sensibilidad, sencillez de las operaciones de preparación del paciente y facilidad de lectura e interpretación de los datos.

La ecuación de Brownell, que establece la relación entre la concentración de radiactividad y el diámetro de resolución, indica que la radiactividad necesaria por unidad de volumen es inversamente proporcional a la sexta potencia del diámetro de resolución. En consecuencia, el autor eligió un diámetro máximo compatible con la localización satisfactoria de las regiones de mayor radiactividad, siendo posible prescindir de una delimitación muy exacta. Como el número de desintegraciones detectadas por unidad de tiempo varía en función inversa del cuadrado de la distancia, se utilizan dos detectores de «foco» corto en lugar de un solo detector que debería adaptarse a un valor óptimo para el plano sagital medio.

Los cristales de 2 pulg de diámetro, unidos a sus fotomultiplicadores, están montados frente a frente en un bastidor rígido de exploración; cada uno de ellos está dotado de un colimador enfocado de siete canales hexagonales, con un diámetro de resolución de 1,5 cm a una distancia focal de 8 cm desde su plano anterior. El aparato explora rectilíneamente el plano sagital. El registro se presenta en forma de un gammagrama asimétrico y de representaciones fotográficas bidimensionales separadas para el lado izquierdo y para el lado derecho. Los impulsos procedentes de cada detector pasan a un circuito amplificador-discriminador y, de éste, a un circuito diferenciador que imprime una señal a la derecha o a la izquierda para indicar el predominio de la radiactividad en uno u otro de estos dos lados. Los impulsos procedentes de cada circuito amplificador-discriminador pasan también a integradores de impulsos que encienden lámparas montadas en una cámara oscura. Las dos lámparas, cuya intensidad luminosa es función de la actividad medida por los respectivos detectores, están montadas en un mismo brazo movido por motores sincrónicos Selsyn, con generadores Selsyn montados sobre el bastidor del detector, lo que permite utilizar un dispositivo de registro situado a distancia. Varios lentes cilíndricos enfocan la luz de las lámparas sobre película radiográfica de 11 × 14 pulg, obteniéndose simultáneamente un registro del lado derecho y del izquierdo. El operador puede ajustar la intensidad media de la corriente que circula por la lámpara a un valor previamente determinado en un amplio intervalo de intensidad de recuento, pero dispone de un vasto margen de trabajo, ya que puede introducir en el cargador tres películas, cada una de las cuales posee un contraste óptimo para una gama diferente de intensidad de recuento.

Entre 24 y 72 h antes de efectuar la exploración se administran a los pacientes 350 μc de seroalbúmina humana marcada con ^{131}I después de un tratamiento con solución de Lugol. Una sola exploración suele ser suficiente. En ciertos casos la exploración se repite en dirección anteroposterior.

Entre septiembre de 1961 y noviembre de 1962 se efectuaron 789 exploraciones en 653 pacientes. Para 109 de ellos el diagnóstico se confirmó: 88 tenían tumores. De 30 glioblastomas, se localizaron claramente 23; de 19 meningiomas se localizaron 15.

Entre septiembre de 1961 y noviembre de 1962 se efectuaron 789 exploraciones en 653 pacientes. Para 109 de ellos el diagnóstico se confirmó: 88 tenían tumores. De 30 glioblastomas, se localizaron claramente 23; de 19 meningiomas se localizaron 15.

1. INTRODUCTION

After several years of experimental work in brain scanning it became apparent that there was a need for a brain scanning system that would meet the requirements of simplicity and reliability associated with a routine scanning procedure. About 25 patients per week were available as suitable subjects for a safe, painless test for a possible intracranial space-occupying lesion. High cost and limited availability as well as certain limitations in lesion affinity ruled out arsenic-74, which had been previously investigated [1, 2] as the tracer for a standard test. The most readily available tracer was I^{131} human serum albumin for which there was a well documented experience in brain tumour detection. This source in the medium energy range was chosen as the basis for the instrument development, with provision to be made for other anisotropic sources of higher and lower gamma energy.

A display system was required which would present high visual contrast between the levels of count rate measured in the "target" and "non-target" regions wherever they occurred, yet there had to be a minimum loss of information since the operator could not easily determine beforehand at which level of count rate the high contrast was needed. This paper will describe the instrument developed for the purpose and the assessment of the instrument based upon the findings in 1187 patients scanned in a period of 26 months.

2. THE SCANNER

2.1. Detector arrangement

Since the instrument was to be used primarily for brain scanning there was no need to compromise the physical arrangement for scanning of other areas of the body. With the patient supine the symmetry of the head about a mid sagittal plane permits the use of two detectors. Two opposite detectors offer at least two advantages. The first is dependent on the short focal distance for which the collimators may be designed. Count rate in a gamma detector is proportional to the inverse square of the distance from the source. Each detector collimator is focussed for a distance of 13 cm from the crystal face instead of the 25 cm necessitated by a single detector focussing to the mid sagittal plane. The second advantage is the lateralization information which may be obtained by continuous direct comparison of activity in the two detectors.

2.2. Detector resolution and sensitivity

According to Brownell's analysis [3] the number of recorded quanta per resolution area $\pi\, d^2/4$ for a focussing collimator is proportional to the

fourth power of the resolution diameter d. It therefore seemed desirable to use the largest value of resolution diameter, for the new scanner, which would still be acceptable for diagnostic purposes.

The detector system finally evolved, consisted of 2-in diam. crystals mounted permanently in Harshaw "integral line assemblies" with a collimator of seven hexagonal holes in 2 in (51 mm) of lead. The effective resolution diameter is of the order of 2 cm, measured in a water phantom, as shown in Fig. 1.

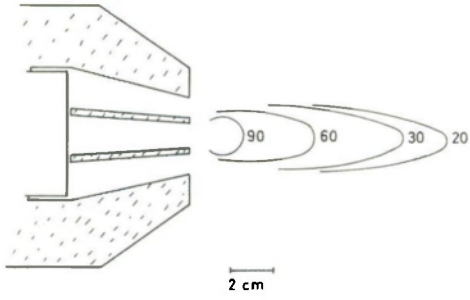

Fig. 1

The isosensitivity curve of the 7-hole collimator in water, as obtained with a "point" source of iodine-131

2.3. Mechanical operation

The detectors are mounted in opposition with the distance between them adjustable so that they can be positioned as closely as possible to each patient's head. The detector units are held at the top of two steel columns (Fig. 2) mounted on a common crossbar which is driven horizontally by a lead screw activated by a reversible constant speed motor. The speed is

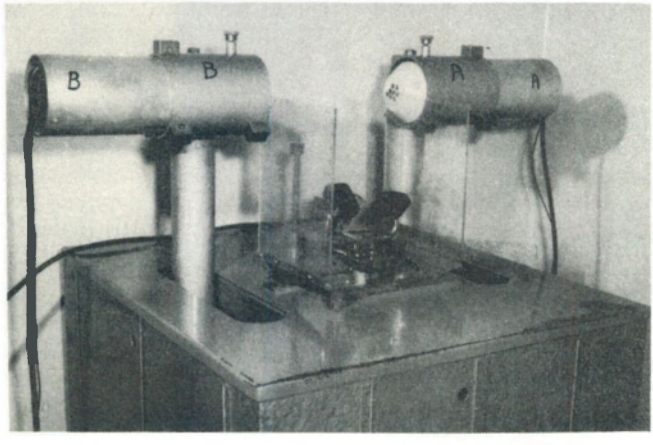

Fig. 2

View of the opposed detectors, with stretcher removed, showing the adjustable head-rest

adjustable by change gears, but all the scans cited in this report were performed at 2.1 mm/s.

The entire horizontal drive system is mounted on a counter-balanced carriage which is moved vertically by a lead screw activated by another reversible motor.

Although the scan may be performed with the uniform motion in either the vertical or horizontal direction, the scans reported here were all made with the detectors starting at the top in the horizontal direction with a step downward of 8 mm as each horizontal excursion was completed.

Horizontal and vertical adjustable limit switches, which may be adjusted to the head shape and size of each patient, are provided.

Each of the drive systems is connected by a chain drive to a magslip transmitter which in turn activates a receiver on the two-dimensional recording system located at a convenient distance from the scanner. Gears linking the various drives and lead screws are so arranged that the recording carriage moves at the same speed as the detector carriage (Fig. 3).

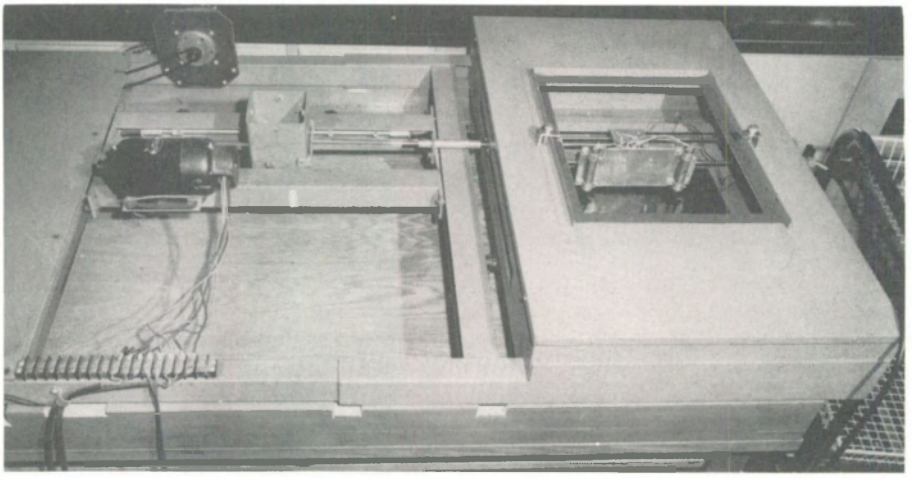

Fig. 3

View of the remote display unit
The magslip receivers are on the left, the light-tight box is on the right with the cover removed to show the arrangement of the lamp enclosures.

2.4. Circuitry

A block diagram of the pulse handling systems is set out in Fig. 4. The detector assemblies include cathode follower output circuits which feed into conventional pulse amplifiers. The Schmidt discriminators are set to pass pulses corresponding to 0.25 MeV and over. The discriminator output pulses of fixed amplitude and shape are fed to a count-rate meter and a 16 : 1 scaler. The scaled pulses from the left and right detectors enter a glow transfer tube subtraction circuit which indicates left or right predominance of radioactivity.

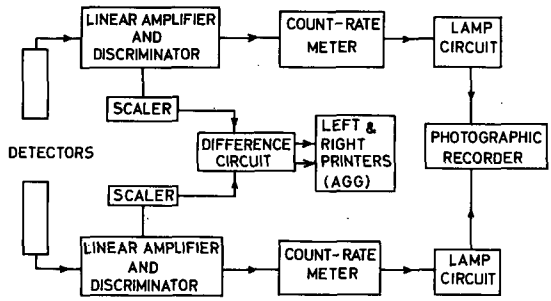

Fig. 4

Block diagram of the pulse handling and recording systems

Each count-rate meter operates a lamp mounted on the remote display unit through a lamp control circuit. The adjustable control is provided so that lamp current can be changed through a small range for any given count rate.

2.5. Display

(a) Asymmetrogammagram (AGG)

The difference circuit operates two solenoid-actuated levers mounted on the common crossbar (section 2.3) of the scanner. When the right detector registers 80 pulses more than the left the right lever is driven to the platten printing a curved mark on the paper fastened to it, at the same time electrically resetting the difference circuit to zero. When the left detector registers 80 pulses more than the right detector the adjacent left lever registers a straight mark on the paper and resets the circuit to zero.

When the detectors operate at exactly equal count rates neither right nor left marking lever is actuated. BROWNELL and SWEET [4], who first described this type of display called it an "Asymmetrogammagram" (AGG).

(b) Photographic records

The count-rate meters are provided with a visual display used by the operator to verify that radioactivity in the detector field is within usable limits. The lamps operated by the lamp circuit shown in the block diagram (Fig. 4) are housed in adjustable tubes mounted on a carriage of low mass which is moved in a horizontal plane by the magslip receivers cited in section 2.3 (Fig. 3). The lamp carriage is moved within a light-tight housing on the underside of which is mounted a cassette containing a pack of three 11 in × 14 in X-ray films (28 cm × 36 cm). The filament of each lamp is focussed on the film with a cylindrical lens. A mask fitted at the end of each lamp housing adjusts the line of light to the required length.

3. PROCEDURE

3.1. Time relationship of scan to tracer administration.

Each patient was given 350 μm of I^{131} labelled human serum albumin intravenously after previous treatment with 1 cm^3 of aqueous solution of iodine, B.P. Ordinarily a lateral scan was performed from 24 to 72 h later. If a vascular malformation was suspected the first scan was made right after administration followed by another after the usual lapse of time. Additional scans whether lateral or antero-posterior were performed in only a small percentage of cases.

3.2. Preparative details

With the patient supine and head on the three point head rest a vertical and rotational adjustment of the head rest was made to obtain the most comfortable head position. The detectors were then moved to the temporal area of the patient's head and the lamp currents set to 20 mA, by the lamp current adjustment potentiometer (section 2.4.). The temporal region usually displays the highest level of radioactivity in the scanned area. The 20-mA current generates a light intensity which exposes the most remote of the three films to a density of 0.5 (Figs. 5 and 6).

The detector carriage was then returned to the "start" position and scanning begun at the superior frontal corner of the scan rectangle. The detectors move horizontally between adjustable limit switches stepping downward (posteriorly) 8 mm at each traverse. The scan is finished when the lower vertical limit switch is reached. The period needed for scanning was rarely more than 30 min.

3.3. Positioning and recording

(a) For the AGG the operator sketches an outline of the patient's head on a centimeter-ruled graph paper with the aid of a rectangular grid etched on the two transparent plastic plates between which the patient's head is held. This outline is traced on to the printed AGG record itself at the end of the examination (Fig. 7).

(b) In order to have an accurate outline of the head a soft radiograph of the head is made to superimpose precisely on the photoscan. Reference points on the radiograph and the photoscans ensure accurate super-imposition. The radiograph is taken at the end of the examination: the detectors are placed out of the way at their lowest position and a standard X-ray cassette is clipped to the plastic plate on the left; exposure is by means of an X-ray tube placed as far away from the head as possible (in our examining room this distance is 170 cm).

3.4. Interpretation

Records were read and reported in writing on the basis of the scan records alone, with no information as to the neurological findings or those of other special investigations. Verbal reports on positive or suspicious

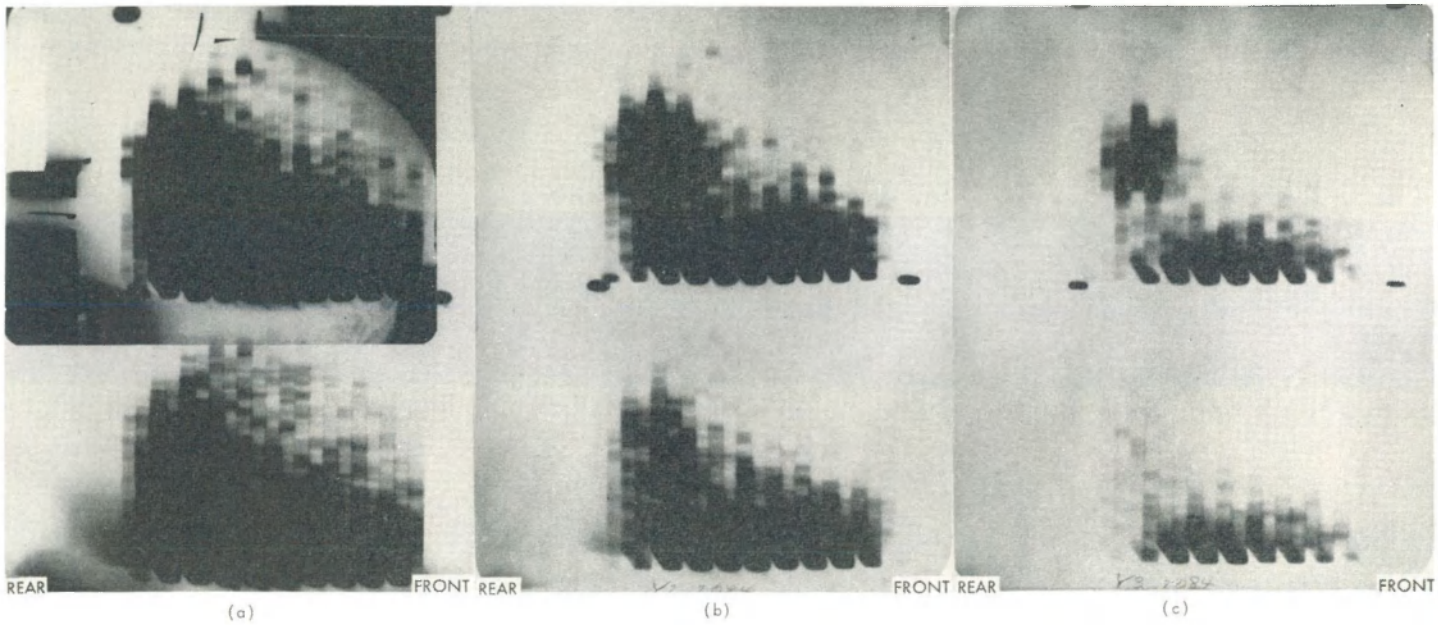

Fig. 5

The three photographic records showing the gradation of density. The film farthest from the lamp is shown in (c), the closest is shown in (a) with the radiograph shown superimposed on the left-side record. In all three records the upper photograph is a view from the left side of the head and the lower a view from the right side of the head.

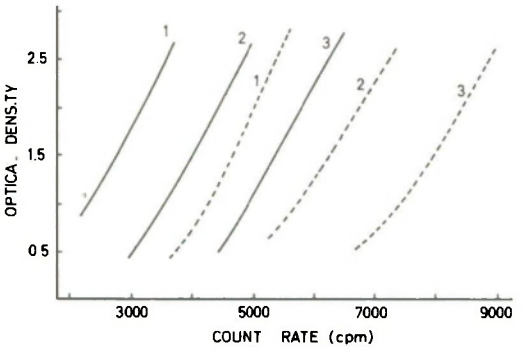

Fig. 6

Optical density of film plotted against counts per minute
The numbers designate proximity of the film to the light source. "1" is nearest the lamp and "3" the most remote. The solid curves represent optical density versus count rate with the lamp control at its most sensitive setting. The dotted curves show the least sensitive setting.

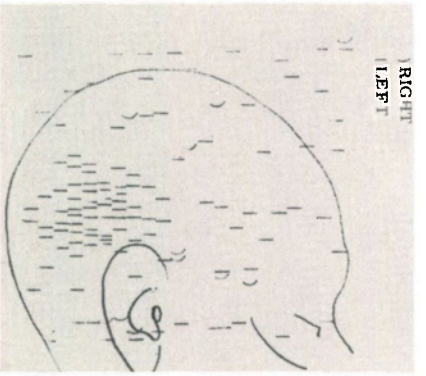

Fig. 7

The AGG record showing the left occipital localization observed in the photographic records.

records were made directly to the physicians requesting the scan, by the technician. This verbal communication was a clinical necessity but it was invariably followed by the written report of one of the authors (W. P.) and this formed part of the permanent record.

4. RESULTS

A follow-up of the 1187 patients scanned is divided as shown in Table I. The records for 62 patients were not obtainable. Most of these were out-patients who have not returned for further treatment. Most of the 928 patients having negative (or questionable) scans were shown by subsequent investigation not to have a space-occupying intracranial mass, but a small

TABLE I

SUMMARY OF 1187 CASES

Verified brain tumours	161
Positive scans, verified non-neoplastic, or unverified brain tumours	36
Negative scans, diagnosed or still in question	928
Negative scans, subsequent history not available	62

number remained under suspicion for cerebral tumour and were placed in the 'brain tumour suspect' category. Thirty-five patients had positive localizations with verified non-neoplastic lesions in most cases. Several remain unverified. Some of the unverified cases were known to have primary metastasizing tumours with a high probability of intracerebral secondary growths but surgery was considered inadvisable.

A further breakdown of the 161 proven intracranial neoplasms is set out in Table II according to pathological type and the numbers of positive localizations.

5. DISCUSSION

The objective of this study is to determine the extent to which the limitations in design imposed on the instrument, to permit routine use, interfered with its effectiveness in detecting intracranial mass lesions. Effectiveness can only be judged by comparison with reported results of other investigations since at the present time there is no universally acceptable phantom for the purpose.

The overall percentage of correct localizations, 65%, is lower than the 73% reported by McAFEE and TAXDAL [8], or the 85% reported by SCHLESINGER et al. [5]. The results may not be strictly comparable because it may be assumed in both reports that records were read with knowledge of the clinical findings, since there was no statement to the contrary in either report. A further factor affecting the final percentage figure is the acceptance, in the reports cited, of neuroradiological evidence as sufficient verification of positive findings. A much more significant determining factor is the nature of the cases referred for brain scanning. If the 12-month period from November 1962 to November 1963 were used instead of a 26-month period (Table II), the overall correct localization figure rises from 65 to 75%. This is so because a much smaller number of patients with possible pituitary tumours or posterior fossa tumours were referred for scanning, after the first 14 months' experience. It will be observed in

TABLE II

ANALYSIS OF SCANS IN 161 VERIFIED BRAIN TUMOURS

	14-month period		Succeeding 12 months		26 months	
	Pos.	Neg.	Pos.	Neg.	Pos.	Neg.
Glioblastoma multiforme and malignant astrocytoma	23	7	23	2	46	9
Meningioma	15	4	15	3	30	7
Metastatic carcinoma	6	7	13	5	19	12
Gliomas, benign	3	4	1	1	4	5
Posterior fossa tumours (acoustic neuroma 5, haemangioendothelioma 5, astrocytoma 1, metastatic carcinoma 1, ependymoma 1)	0	8	1	4	1	12
Pituitary tumours	0	7	1	1	1	8
Epidermoid cyst			0	1	0	1
Cysticercosis cyst			0	1	0	1
Pineal tumours	1	1			1	1
Cerebral microgliomatosis	1	0	1	0	2	0
Meningeal carcinomatosis	0	1			0	1
Totals:	49	39	55	18	104	57

Table II that the inferiorly placed neoplasms are most difficult to detect as are benign gliomas, in agreement with the observations of other investigators [5] and [7].

It would appear then that the percentage figure of accuracy is below the reported range considering the whole series, but if the last year only is considered, with its reduced incidence of inferiorly placed tumours, an accuracy equal to the careful study of McAfee and Taxdal is attained.

An alternative approach is to examine more closely those proven lesions which were missed. In addition to pathological type and location, further factors of size, whether or not there is cyst fluid, the lapse of time between tracer administration and scanning [5], the number of repeated scans and the performance of an A-P (antero-posterior) scan, influence the outcome of the radioactive scan procedure.

The benign gliomas (astrocytomas), the epidermoid cyst and the cysticercosis cysts show low levels of radioactivity rendering their localization unlikely unless they are associated with formation of cyst fluid which may concentrate I^{131} [6].

The posterior fossa tumours and pituitary tumours are masked by scalp muscle and shielded by bone. The acoustic neuromas in this area take up a moderate amount of tracer but were not easily located in the lateral scans. SHY in reference [7] was able to demonstrate these lesions by scanning in the A-P direction. Haemangioendotheliomas too take up a moderate amount of tracer but are difficult to localize because of their location in the posterior fossa.

The meningeal carcinomatosis case was of a thin layer of cells in the meninges and with its diffuse symmetrical distribution of neoplastic cells was not likely to absorb enough tracer to provide a contrast in the photographic records.

There were twelve metastatic tumours; three were suprasellar, one a thin (small volume) growth and in two the multiple deposits were so widely distributed that localization was not possible. Of the remaining six, two were considered very suspicious in the correct site, and four were missed completely. Two were malignant melanomas for which there is little information available concerning the uptake of I^{131}.

The seven meningiomas included three tuberculum sellae and olfactory groove, and one suprasellar. The fifth was a very thin en plaque growth. We do not know why there were false negative findings in three cases.

The nine false negatives of fifty-five malignant gliomas included two which had to be scanned soon after tracer administration; one which at the time of scanning several months prior to surgery was probably still a benign glioma and one which had so widely infiltrated a large area that it was considered simply as an error in orientation of the patient's head. The remaining five were read with varying degrees of suspicion, but by our standards were negative.

It may be assumed that the twelve falsely negative scans of gliomas, meningiomas and metastatic tumours were missed because of small size, or low uptake of tracer. These may have been localized with the aid of larger crystal detectors, collimators with a narrower resolution and a more time-consuming scanning programme, both for a single scan and with repeated scanning. A further improvement might have been obtained by the use of a tape recorder to retain all the scan information for repeated playback and high contrast recording. There is, however, no reason to believe that all of these would have been localized.

Similarly the five acoustic neuromas may have yielded some positive findings with A-P scanning. It should be noted that the added time and effort would have been applied as well to all 1187 patients to achieve the improved

incidence of positive findings and this would nullify the premise that the system to be devised was for routine investigation and screening.

6. SUMMARY AND CONCLUSIONS

A scanning instrument was designed and constructed for particular application to routine scanning of brain tumour suspects. Maximum sensitivity is achieved by the use of two opposite detectors with wide focussing collimators. Photographic recording is effected on three films to retain maximum scan information. A left-right difference circuit with printout (AGG) is used to assist in lateralization of areas of localization. This feature is particularly useful in determining whether a localization is to the left or right when the photographic records are nearly equal. Inferiorly placed asymmetries which may not appear on the photographic record because of the masking effect of the overlying temporalis muscles will often be demonstrated in the AGG.

An analysis of 1187 cases is presented with particular reference to the proven cases of intracerebral neoplasms in which a positive diagnosis was not made by the scanner.

The number of 'false negatives' could have been significantly reduced only by spending much more time over each examination, that is, by repeating the scan over a larger interval and by conducting A-P scans. Using the technique and instrumentation here described we decided that in our clinical setting the few extra correct results so obtained would not have justified slowing up the whole programme. We look to improved instrumentation and other radioisotope preparations to overcome the deficiencies in our examinations. For example, the use of collimators of narrow resolution together with larger crystals would give more clearly defined localizations. Improvement in detection can also be expected when a large-crystal, stationary detector of proven superior performance is available.

On the whole, the system described here for routine operation by non-professional technicians has been a very satisfactory method of screening for cases of brain tumour suspects and as an examination for pre-operative anatomical localization of the lesion. In its latter application it is supplanting arteriography and pneumography in an increasingly higher proportion of cases.

REFERENCES

[1] BOTTERELL, E. H., LOUGHEED, W. M., MORLEY, T. P., TASKER, R. R. and PAUL, W., The Canad. Med. Ass. J. 85 (1961) 1-8.

[2] PAUL, W. and BOTTERELL, E. H., J. nucl. Med. 4 (1963) 1-8.

[3] BROWNELL, G. L., "Theory of radioisotope scanning", these Proceedings I.

[4] BROWNELL, G. L. and SWEET, W. H., Nucleonics 11 (1953) 40-45.

[5] SCHLESINGER, E. B., de BOVES, S. and TAVERAS, J., Amer. J. Roentgenol. 87 (1962) 449-62.

[6] TATOR, C. H., The uptake of radioactive isotopes by intracranial lesions in vivo and in vitro, M. A. Thesis, Univ. of Toronto, 1 June 1963.

[7] SHY, G. M., BRADLEY, R. B. and MATTHEWS, W. B., External Collimation Detection of Intracranial Neoplasia with Unstable Nuclides, E. and S. Livingstone Ltd., London (1958) 107-18.

[8] McAFEE, J. G. and TAXDAL, D. R., Radiology 77 (1961) 207-22.

RESULTS OF POSITRON SCANNING IN 1200 CASES FOR DIAGNOSIS OF INTRACRANIAL LESIONS

O. WILCKE
NEUROCHIRURGISCHE UNIVERSITÄTSKLINIK,
COLOGNE, FEDERAL REPUBLIC OF GERMANY

Abstract — Résumé — Аннотация — Resumen

RESULTS OF POSITRON SCANNING IN 1200 CASES FOR DIAGNOSIS OF INTRACRANIAL LESIONS. The positron scanning method with Cu^{64} and As^{74} for the diagnosis of brain tumours has the advantage over γ-scanning methods that it needs a shorter test time and moreover involves less irradiation hazards. This is especially true with Cu^{64} (half-life 12.8 h), which may be used in studies on out-patients. From the degree of concentration of the radioactive substance in the tumour, its type may be determined. In combination with cerebral angiography, the diagnosis of the type of tumour is still better established, a fact which is very important in determining the indication for operation. In the present study, the exactness of the diagnosis amounted to 75-80% of all cases of brain tumours.

The most easily recognized lesions, through their high ability to concentrate the isotopes, were the meningiomas, abscesses and glioblastomas, while the oligodendrorogliomas and astrocytomas showed less ability to concentrate the radioactive substance and hence were less easily recognizable. A group of astrocytomas and almost all epidermoid tumours did not show any ability to concentrate the radioactive substance and in this group the combination with cerebral angiography is important for determining the diagnosis. The method of positron-scanning has proved of great value in excluding tumours in cases of suspected symptomatic epilepsy; the exactness of diagnosis here amounted to 90%. The combination of electro-encephalography with scanning showed similar accuracy in tumour diagnosis as well as tumour exclusion, so that arteriography and/or hospital admission could be dispensed with whenever combined negative findings and lack of clinical symptoms were found. The value of this method in examination of out-patients is thus clearly demonstrated.

DIAGNOSTIC DE 1200 CAS DE LÉSIONS INTRACRÂNIENNES PAR SCINTIGRAPHIE AU MOYEN DE POSITONS. Pour le diagnostic des tumeurs du cerveau, la scintigraphie au moyen des positons émis par ^{64}Cu et ^{74}As présente l'avantage sur la gammagraphie de réduire la durée de l'exploration et de diminuer les risques d'irradiation. Il en est surtout ainsi pour ^{64}Cu (période de 12, 8 h), qui peut être utilisé sur des patients non hospitalisés. Le degré de concentration de la substance radioactive dans la tumeur permet d'identifier le type de cette tumeur. En combinant cette méthode avec l'angiographie cérébrale, on peut augmenter encore la sûreté du diagnostic du type de tumeur, ce qui est très important pour décider de l'opportunité d'une intervention chirurgicale. Dans l'étude qui a fait l'objet du mémoire, on a obtenu une précision de 75 à 80% dans le diagnostic de tumeurs du cerveau de toutes sortes.

Les lésions les plus faciles à reconnaître du fait de leur aptitude à fixer les radioisotopes sont les méningiomes, les abcès et les glioblastomes; les oligodendrogliomes et les astrocytomes présentent une tendance moindre à fixer la substance radioactive et sont donc moins aisément décelables. Certains astrocytomes et presque toutes les tumeurs épidermiques n'ont aucune tendance à fixer la substance radioactive; pour ce groupe, il est indispensable de combiner la scintigraphie avec l'angiographie cérébrale pour poser le diagnostic.

La scintigraphie au moyen des positons a fait ses preuves lorsqu'il s'agit d'éliminer l'hypothèse d'une tumeur dans des cas d'épilepsie; la sûreté du diagnostic atteint 90%. On a obtenu la même précision en combinant l'électroencéphalographie et la scintigraphie, tant pour identifier une tumeur que pour écarter l'hypothèse de son existence. On peut ainsi éviter l'artériographie et l'hospitalisation chaque fois que l'ensemble des conclusions est négatif et qu'il n'existe aucun symptôme clinique. La valeur de cette méthode dans le cas de patients non hospitalisés est donc bien établie.

РЕЗУЛЬТАТЫ 1200 СЛУЧАЕВ ПОЗИТРОННОГО СКЕННИРОВАНИЯ ДЛЯ УСТАНОВЛЕНИЯ ДИАГНОЗА ВНУТРИЧЕРЕПНЫХ ЗАБОЛЕВАНИЙ. Метод позитронного сканнирования с использованием меди-64 и мышьяка-74 для установления диагноза опухолей мозга

имеет преимущество перед методами γ-сканнирования, так как требует меньше времени и кроме того связан с меньшей опасностью облучения. Это особенно справедливо в отношении меди-64 (период полураспада 12,8 часов), которая может применяться для исследования амбулаторных больных. Вид опухоли может быть определен по концентрации в ней радиоактивного вещества. Еще лучше разработана диагностика типа опухоли в комбинации с антографией сосудов головного мозга, что очень важно при определении показаний к операции. В данном исследовании точность диагноза составляла 75—80% всех случаев опухолей головного мозга.

К заболеваниям, которые легче всего распознаются вследствие их высокой способности концентрировать указанные изотопы, относятся менингиомы, абсцессы и глиобластомы, тогда как олигодендроглиомы и астроцитомы в меньшей степени способны концентрировать радиоактивные вещества и поэтому распознаются труднее. Группа астроцитом и почти все эпидермоидные опухоли не способны концентрировать радиоактивные вещества и в этих случаях комбинация с антографией сосудов головного мозга имеет важное значение для установления диагноза. Метод позитронного скеннирования оказался очень ценным при исключении диагноза опухоли в случаях предполагаемой симптоматической эпилепсии; точность диагноза составляет здесь до 90%. При комбинации электроэнцефалографии со скеннированием обнаружена одинаковая точность как при установлении, так и при исключении диагноза опухоли, что позволит обойтись без артериографии и/или госпитализации во всех случаях, когда получена комбинация отрицательных данных и отсутствуют симптомы болезни. Это подтверждает ценность метода при обследовании амбулаторных больных.

EXPLORACIÓN POSITRÓNICA PARA EL DIAGNÓSTICO DE LESIONES INTRACRANEANAS: RESULTADOS DE 1200 CASOS. La exploración positrónica con ^{64}Cu y ^{74}As para diagnosticar tumores cerebrales ofrece la ventaja de que requiere menos tiempo y entraña menos riesgos de irradiación que los métodos gammagráficos, especialmente cuando se recurre al ^{64}Cu (período: 12, 8 h), que puede emplearse en enfermos ambulantes. El grado de concentración de la sustancia radiactiva en el tumor permite determinar el tipo de este último. Si se combina ese método con la angiografía del cerebro se puede diagnosticar aún mejor el tipo del tumor, lo que tiene suma importancia para determinar si una intervención quirúrgica está indicada. En el estudio que se describe en la memoria los diagnósticos fueron correctos en el 75-80% de todos los casos de tumores cerebrales.

Las lesiones que con mayor facilidad se reconocen debido a su gran tendencia a concentrar los isótopos son los meningiomas, los abscesos y los glioblastomas, mientras que los oligodendrogliomas y los astrocitomas, que son menos capaces de concentrar la sustancia radiactiva, resultan más difíciles de reconocer. Un grupo de astrocitomas y casi ninguno de los tumores epidermoideos son capaces de concentrar la sustancia radiactiva así que, en este grupo, es importante confirmar el diagnóstico por angiografía del cerebro. El método de la exploración positrónica ha demostrado su gran utilidad para descartar la presencia de tumores en casos en que se sospecha epilepsia sintomática; el diagnóstico ha resultado correcto en el 90% de dichos casos. La combinación de la electroencefalografía y la exploración ha sido tan eficaz para diagnosticar como para descartar la presencia de tumores, gracias a lo cual se ha podido renunciar a la arteriografía y a la hospitalización del enfermo cuando los resultados han sido negativos y no se han observado síntomas clínicos. El valor de ese método para examinar pacientes ambulantes ha quedado, por lo tanto, claramente demostrado.

The positron-scanning method as it has been used for 5 yr in the Neurosurgical University Hospital of Cologne has proved to be a valuable method for the diagnosis of brain tumours as well as for the exclusion of the presence of a brain tumour. This diagnostic method is quickly performed and comfortable for the patient. The radiation dose is very low, particularly if Cu^{64} with a half-life of 12.8 h is used. The whole procedure lasts only 15 min. This method is therefore easily applied to outpatients also. For recording the scintigram two scintillation counters register by coincidence-measurement simultaneously the incident radiation from the zones of local isotope accumulation in side projection on the one hand, and by a special counter-system the γ-impulses on the other. If the impulses of the right hemisphere predominate curved markers are printed, and with a prevalence of the impulses

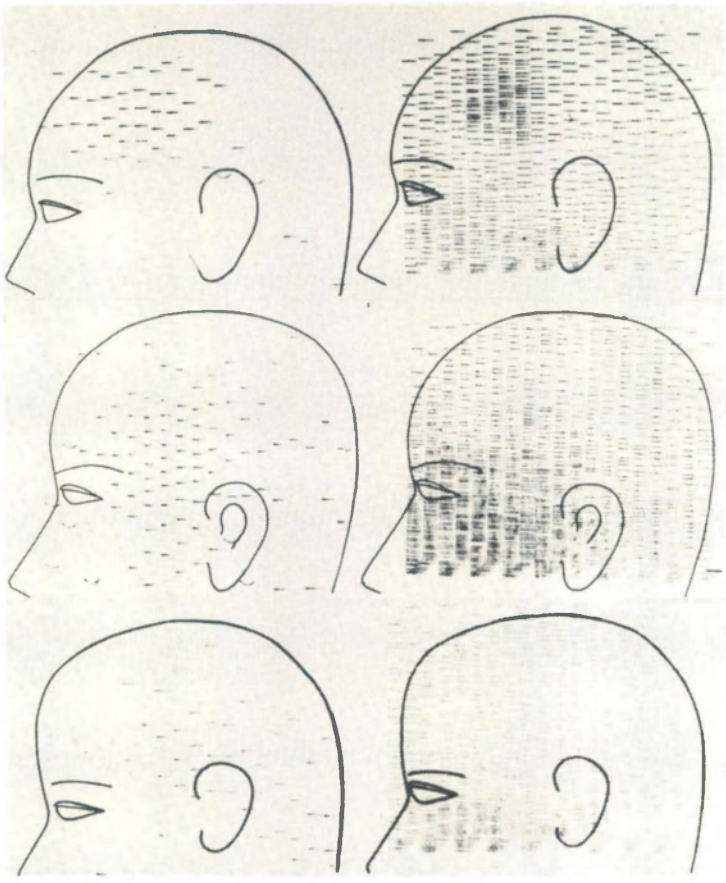

Fig. 1

Upper	Left-sided precentral meningioma
Middle	Left temporal glioblastoma
Lower	Left te nporal astrocytoma

from the left hemisphere straight markers are printed. In this way a precise localization of the site of local isotope accumulation is possible.

The most definite evidence for the presence of a brain tumour lies in the localized accumulation of radioactivity. The degree of accumulation allows one to draw conclusions on the type of tumour. (Fig. 1). The upper picture in Fig. 1 shows a left-sided precentral meningioma which, because of the strong uptake of activity, differentiates itself clearly from the middle one which shows a left fronto-lateral glioblastoma, while the lower picture shows a left temporo-parietal astrocytoma.

Meningiomas are always characterized by high uptake of radioactivity and are therefore easily diagnosed, as is shown in Fig. 2. This is a left-sided sphenoidal meningioma and Fig. 3 shows a parasagittal meningioma. Also in cases in which the angiography does not give a definite diagnosis of

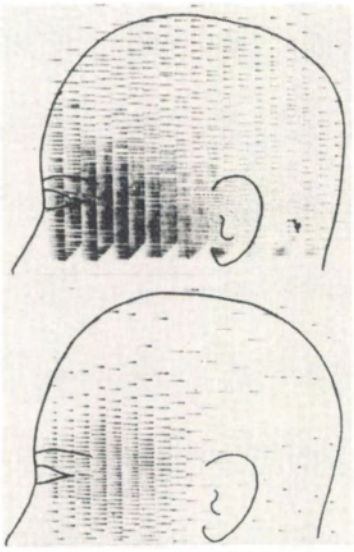

Fig. 2

Left-sided sphenoidal meningioma

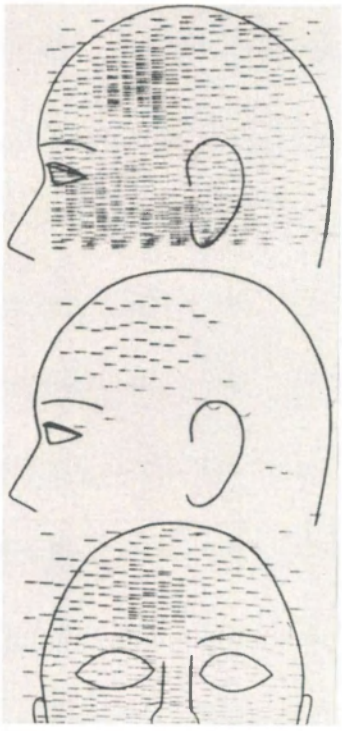

Fig. 3

Parasagittal meningioma

the type of tumour it is possible to diagnose a left-sided parietal meningioma from the scan, as is shown in Fig. 4. The same is true for a cerebello-pontine-angle meningioma as is demonstrated in Fig. 5. However, small suprasellar meningiomas cause diagnostic difficulties.

Glioblastomas (Fig. 6) show a definitely lower uptake of radioactivity as in this case of left-sided parietal glioblastoma. It is not always possible to differentiate between glioblastomas, oligodendrogliomas and astrocytomas on the grounds of activity uptake alone. In such conditions the angiography and clinical course must be taken into consideration. Sometimes even astrocytomas of the fibrillary type show lower activity than the normal side. Figure 7 shows the angiogram and the positrocephalogram of a 40-yr-old female patient in whom, because of the clinical course, a temporal astrocytoma was suspected. The angiogram showed a left-sided temporal space-occupying lesion and the positrocephalogram showed more activity on the right side than on the left, allowing a diagnosis on the left side. In such cases our experience shows that the lesion is usually either a congenital tumour or an astrocytoma. Operation and pathological examination thereafter verified the presence of an astrocytoma. The possibility of diagnosing the type of the tumour in such cases is valuable for determining the indication for operation.

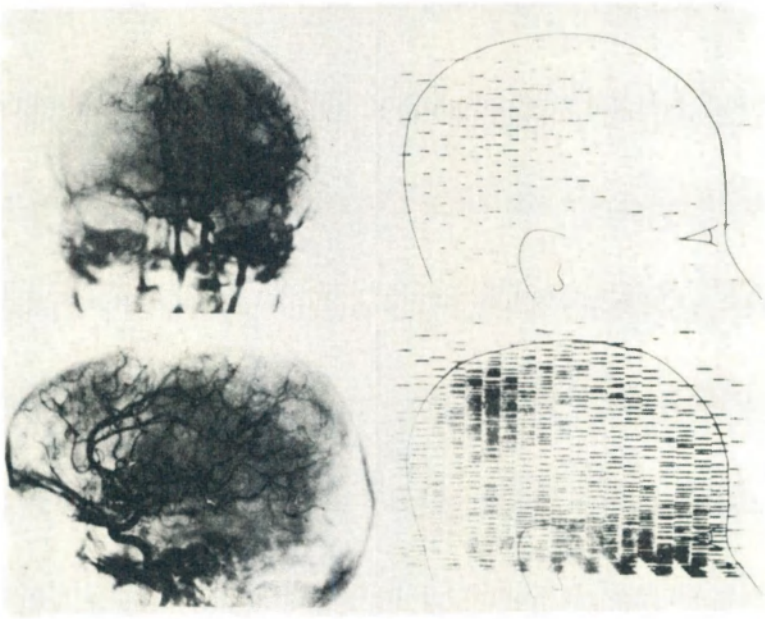

Fig. 4

Angiogram and scan of a left parietal meningioma.
the angiogram does not permit a diagnosis of the type of tumour, whereas the high uptake of radioactivity apparent from the scan, is considered typical for meningioma.

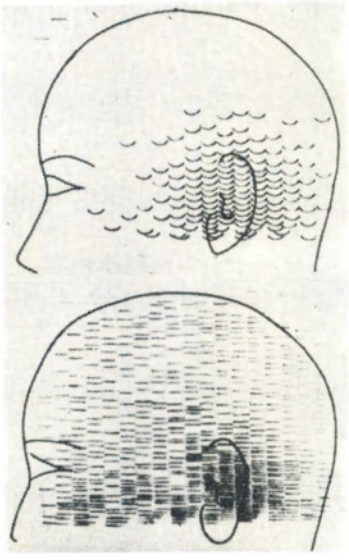

Fig. 5

Cerebello-pontine-angle meningioma

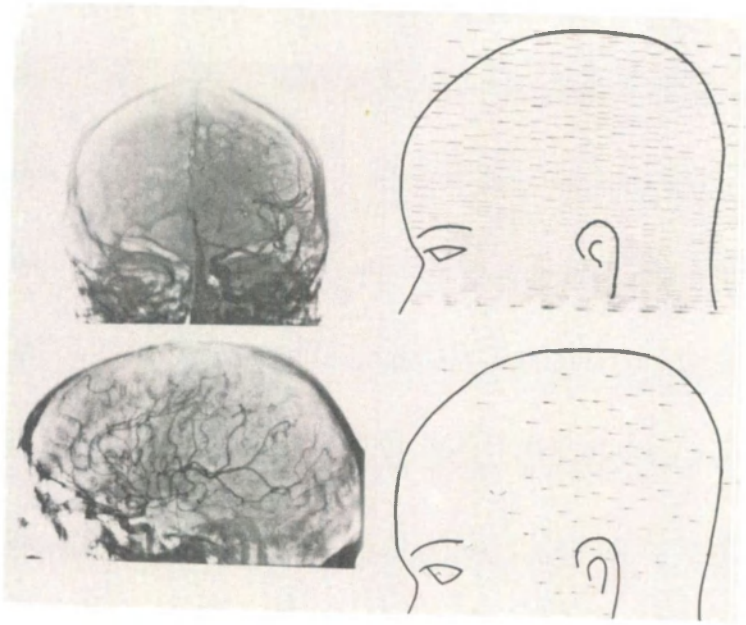

Fig. 6

Angiogram and scan showing a left-sided parietal glioblastoma

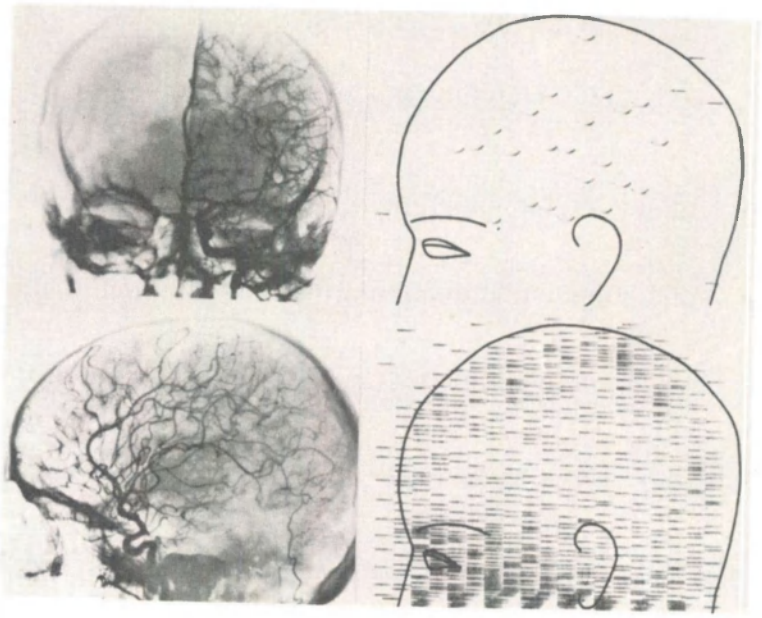

Fig. 7

Angiogram and scan of a left-sided temporal astrocytoma.
Tumour uptake is low compared with the right side.

This case indicates that a diagnosis of the type of tumour is possible by a combination of positrocephalogram and angiogram even if an isotope accumulation is lacking. Particularly in the case of epidermoids which do not take up radioactivity the diagnosis of the type of tumour is possible because

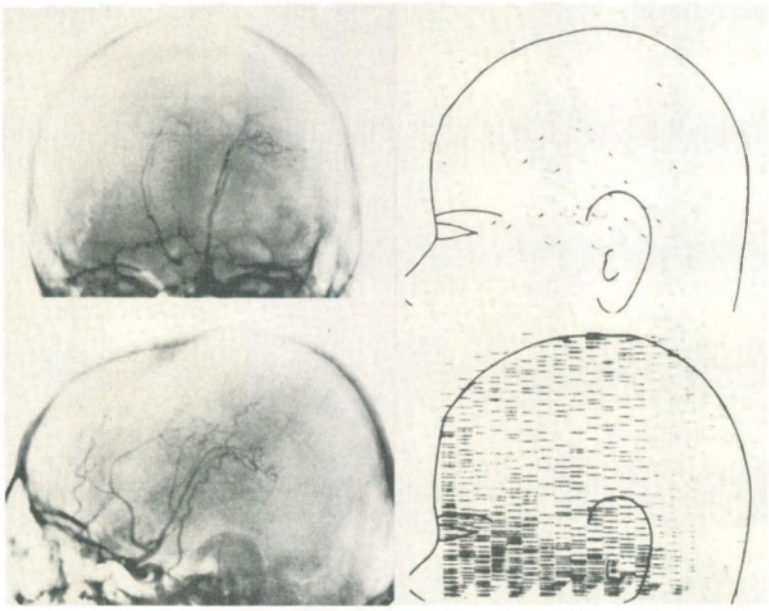

Fig. 8

Angiogram and scan of a left-sided temporal epidermoid. The tumour does not take up radioactivity.

of the typical angiogram and the higher number of impulses in the normal side (Fig. 8).

While the combination of angiogram and positron scanning in the clinical examination provides important conclusions on the type of tumour, it is the combination of EEG and positron scanning which permits an improved diagnosis of the presence or the exclusion of a brain tumour in the outpatient clinic. If the positron scanning as well as the EEG examination is negative, and if in addition there are no signs of increased intracranial pressure, pneumencephalography and angiography can be abandoned.

In 416 patients with clinically confirmed brain tumours (Table I) we found the greatest diagnostic accuracy in meningiomas followed by brain abscesses, and some rare tumours like gangliocytomas, neurofibromas, sarcomas and metastatic brain tumours. We are able to diagnose glioblastomas in 78%, and oligodendrogliomas in 75%, of the cases, while astrocytomas accumulate radioactivity in only 58% of all cases. Altogether 76% of the cerebral tumours showed an accumulation of activity.

In 56 patients suspected of tumour recidivation (Table II), a recidivist could be ascertained by clinical examination (EEG, angiography and encephalography) in 41 cases, and a recidivist could be excluded in 15 cases.

TABLE I

RESULTS OF POSITRON SCANNING FOR 416 CLINICALLY CONFIRMED BRAIN TUMOURS

Brain tumours	Total	Abnormal isotopic concentration	No isotopic concentration	Correct diagnosis (%)
Meningioma	76	70	3	96
Glioblastoma	37	29	8	78
Oligodendroglioma	28	21	7	75
Astrocytoma	45	26	19	58
Spongioblastoma	9	6	3	67
Ependymoma	8	5	3	62
Neurinoma	27	21	6	78
Sarcoma	6	5	1	83
Pituitary adenoma	19	15	4	79
Cranio-pharyngioma	8	4	4	50
Epidermoids	8	1	7	12
Gangliocytoma Neurofibroma Zylindroma	8	7	1	88
Metastatic tumours	35	28	7	80
Brain-stem tumours	30	17	13	57
Undetermined (not operated) tumours	56	43	11	77
Abscesses	16	14	2	88
	416	317 (76%)	99 (24%)	

TABLE II

RESULTS OF SCANNING IN PATIENTS SUSPECTED OF BRAIN TUMOUR RECURRENCE

Suspicion of tumour-recidivation	Confirmed	Not confirmed
Clinical examination	41	15
Scanning	36	20

TABLE III

RESULTS OF POSITRON SCANNING IN PATIENTS WITH CEREBELLAR TUMOURS AND INFLAMMATORY DISEASE IN THE POSTERIOR CRANIAL FOSSA

Cerebellar tumours	Abnormal isotopic concentration	No isotopic concentration	Total
Angioblastoma	3	3	6
Medulloblastoma	3	4	7
Spongioblastoma	5	2	7
Ependymoma	1	1	2
	12	10	22
Inflammatory disease (arachnitis) in the posterior cranial fossa	10	11	21

In 36 patients, i.e. 89% of the confirmed cases, the diagnosis was made possible by a one-time positron scanning. Since an accurate diagnosis of a tumour recidivist often needs the combination of EEG, angiography and pneumencephalography, the positron scanning has a special advantage in relation to outpatient examinations.

On the other hand the diagnostic value of the positron-scanning method in the case of cerebellar tumours is poor (Table III). In only just above half the cases the radioactivity uptake by the cerebellar tumour was large enough to be distinguished from the normal uptake by the muscles of the neck. A differentiation from inflammatory processes in the region of the posterior cranial fossa is impossible.

In order to exclude the presence of brain tumours 665 patients were examined by positron scanning (Table IV). In 12% of the cases with a variety of symptoms, as listed in the table, radioactivity uptake occurred, while 88% of the patients had a normal positron scan. A localized activity uptake was frequently found in the case of angiomas and in those cases in which bleeding or cerebral softening processes suggested a disturbance of the function of the blood brain barrier and a consequent accumulation of radioactivity. Tumours could be excluded with a diagnostic accuracy of 88%.

We can summarize our results thus: According to a localized activity uptake 76% of the cerebral tumours could be diagnosed by the positron-scanning method. From the degree of radioactivity accumulation the type of tumour could already be estimated. By the combination of angiogram and scan a further improvement of diagnosis of the type of tumour could be achieved, which is of considerable importance for the indication for operation. Tumour recidivists can be diagnosed with great accuracy. In non-neoplastic diseases the correct diagnosis was possible in 88% of the cases. However, for cerebellar tumours the diagnostic value of the positron-

TABLE IV

RESULTS OF POSITRON SCANNING IN 665 PATIENTS WITH VARIOUS CLINICAL SYMPTOMS

Non-neoplastic disorders	Total	Abnormal isotopic concentration	No isotopic concentration
Convulsive seizures	88	8	80
Vegetative disorder Headache Psychogenic disorder	318	28	291
Menière	14	2	12
Trigeminal neuralgia	10	1	9
Brain-atrophy (Alzheimer, Pick)	8	1	7
Papilloedema (Pseudotumour cerebri)	38	7	31
Encephalomyelitis disseminata Encephalitis	29	7	22
Brain trauma	8	3	5
Vascular disorders:			
Aneurysm	8	1	7
Angioma	12	7	5
Subdural hematoma	6	4	2
Intracerebral hematoma	6	4	2
Vascular occlusion	7	3	4
Cerebral softening	29	7	22
Sclerotic disease	83	5	78
Total	665	78 (12%)	587 (88%)

scanning method is poor. Although the positron-scanning method cannot replace the conventional angiography and pneumencephalography it is a very valuable contribution to diagnosis.

DISCUSSION

(On the two foregoing papers)

J. BRICE: I was very much interested in Dr. Paul's paper because I think there is a real need for cheap efficient machines for clinical use in

neurosurgery. I have been a little disturbed to note the trend towards complexity in the devices described at this Symposium. Many of the units we have heard about could hardly be used outside the larger centres. What we particularly require is a small efficient unit which we can readily handle ourselves or in association with the physics department of a larger institution.

I was also intrigued by the technique of superimposing a soft radiograph of the head on the photoscan. One of the difficulties facing the surgeon who examines these apparently rather crude outlines of the skull is to decide exactly where the tumour is and to plan his surgical attack accordingly.

We have found that the type of case under investigation has a considerable effect on the results and I should be interested to hear what experience Dr. Paul has had in cases of epilepsy of late onset. In such cases we sometimes find that our initial scans fail to indicate the tumours. Very obvious tumours can be seen, however, when a subsequent scan is made after the appearance of clinical signs.

W. PAUL: I can recall only a few instances of this kind. In these cases our scans were also negative at first, but positive when the patient returned some months later with a malignant tumour.

Our theory about these lesions is that they were initially grade-1 astrocytomata, which could not be demonstrated by I^{131}-albumin. By the time the patient returned a malignancy had developed which was able to pick up the tracer.

D. KUHL: I very much admire the way in which Dr. Paul was able to interpret these scans without prior knowledge of the case history, the physical findings, etc. On the other hand, I submit that this is not the ideal way to study a patient when the real purpose of the investigation is to collect the maximum of information about his clinical status. In my opinion, the study should be planned and interpreted by someone who is in full possession of all the relevant data. The right man to do this is the physician.

W. PAUL: All this information is available to the physicians or surgeons responsible for the patient and they naturally read the scans taking all the relevant information into account. Only the data in Tables I and II were derived by reading without knowledge of the patient's history. This was done to assess the value of the method.

G. TORI: Have you compared your scan data with information obtained by means of carotid arteriography?

W. PAUL: We have made direct comparisons of the over-all value of scans, arteriograms and ventriculograms. I have no exact figures with me but I have a good idea that the scans were at least as successful as the other two methods.

M. AKERMAN: We use Dr. Planiol's technique of numerical counting at symmetrical points. One advantage of this method is that it yields a large number of positive results - in our case 83%, which is slightly better, I think, than the results obtained with the methods described by Dr. Paul and Dr. Wilcke.

Another important advantage is that it very often gives us an indication of the histological nature of the tumours under investigation from the uptake curve of I^{131}-albumin (RISA) by the lesion. I should be very interested to hear whether either Dr. Paul or Dr. Wilcke have made any attempts to establish

the nature of the tumours they have detected and, if so, what scanning data they used for this purpose. Incidentally, I am very surprised that Dr. Paul's results were nearly all negative for tumours of the posterior fossa. We had almost 60% positive results for this region.

Finally, I notice that frontal-plane sweeping is not possible with the techniques described in these two papers. Does not this mean that you lose valuable information on the depth and exact localization of the tumours?

O. WILCKE: It is possible to diagnose deep-seated brain tumours using this method by making an A-P scan with the patient lying on his side. Information on the nature of the tumour can be obtained by studying the relative amount of accumulated activity. One can differentiate fairly definitely between malignant and benign tumours in this way. Another way of obtaining information on the nature of the tumour is to use a combination of angiography and scanning.

W. PAUL: Our equipment does not lend itself to the localization of tumours of the posterior fossa. This could probably be done by making suitable alterations to the apparatus. One may wonder whether this is worth while in view of the large number of patients that have to be examined. If this were a problem of pure research, our results could obviously be improved but the apparatus I described is intended for routine use only.

Repeated scans in the A-P direction and lateral directions at intervals, as well as scans with narrower collimation, would undoubtedly yield more information.

F. BECCHINI: In connection with Dr. Akerman's remarks, I should like to comment on our experience with the Planiol method, which we have been using very successfully at Pisa for three years. I would, however, disagree with Dr. Akerman's view that it is always possible to diagnose the nature of the tumour with this technique. We have had meningiomata where the hyperactivity was only apparent at a fairly late stage and we have found that highly vascularized glioblastomata can be demonstrated even at the time of the initial measurement.

B. MALAMOS: The results for the detection of metastatic lesions of the brain are different in these two papers. For metatstatic carcinomata Dr. Paul's scans were largely negative whereas Dr. Wilcke's scans were about 80% positive, if I remember rightly. As our Radioisotope Department at the Alexandra Hospital, Athens, is attached to a Department of Internal Medicine, I should be interested in hearing the authors' comments on this difference. Do they think it is due to the different measuring techniques employed or to a different uptake of the tracers used, I^{131}-albumin in the first method and Cu^{64} in the second.

W. PAUL: I think our proportion of positive findings would have been higher if we could have used some of the 36 positive scans listed in our Table I. Many of those were almost certainly of secondary lesions but we did not operate on them. We would naturally miss small multiple lesions because of our high resolution diameter.

H. GLASS: As I understand it, Dr. Paul tries to obtain all his information from a single scan. Surely one is liable to lose valuable information this way?

W. PAUL: Certainly. Therefore we carry out careful studies in par-

ticular cases to supplement the data obtained from our routine screening investigation.

D. ECONOMOS: In our experience, a series of scans taken at intervals following administration of the tracer can reveal the pattern of uptake by the tumour demonstrated by Dr. Planiol in her method. We have found this to be true both with RISA and with Hg^{203} and Hg^{197}. We find that scan data are at least as good as if not better than neuroradiological data both for locating and for identifying the tumour. In at least 60% of cases, data obtained by repeated scanning provide an indication of the nature of the tumour.

J. BRICE: Dr. Wilcke, you suggest in your paper that scanning is not a substitute for angiography or encephalography in neurological investigations. I am not sure that I agree with this point of view. One great advantage of scanning is that it does not disturb intra-cranial pressure relationships. We have been using it for this reason in combination with clinical examinations as the sole investigation prior to surgery. Obviously, because of its present error rate this technique cannot be used as a method of excluding brain tumours but it is certainly useful for the diagnosis and treatment of the more obvious malignant tumours.

O. WILCKE: The only tumours that can definitely be identified by positron scanning are meningiomata. For other tumours you can obtain a diagnostic accuracy of about 90% if you combine this technique with angiography. We find that it is impossible to dispense with angiography if the investigation is preparatory to an operation. We therefore regard scanning as a useful auxiliary technique but nothing more. Compared to gamma scanning, positron scanning has a number of advantages. Examinations take only 15 minutes and the radiation exposure is low, so that the method can easily be used on out-patients. If you use it in combination with encephalography, you can obtain a high degree of diagnostic accuracy, especially for tumour exclusion.

EVALUATION OF FLUORINE-18 AS A SCANNING AGENT FOR INTRACRANIAL TUMOURS*

W. ENTZIAN**, S. ARONOW, A.H. SOLOWAY AND W.H. SWEET
MASSACHUSETTS GENERAL HOSPITAL, BOSTON, MASS.,
UNITED STATES OF AMERICA

Abstract — Résumé — Аннотация — Resumen

EVALUATION OF FLUORINE-18 AS A SCANNING AGENT FOR INTRACRANIAL TUMOURS. F^{18}, a 110-min half-life, positron emitter was studied as a possible agent for brain-tumour localization. It was prepared in a nuclear reactor by thermal neutron irradiation of Li_2CO_3 ($Li^6(n, \alpha) H^3$, $O^{16}(H^3, n) F^{18}$). Tissue studies in mice bearing subcutaneously-transplanted ependymomas indicated that labelled sodium fluoride (NaF^{18}) gave excessive concentrations in bone and was therefore unsuitable as a brain-scanning agent. However, labelled potassium fluoborate (KBF^{18}_4) showed good preferential uptake in tumour compared with brain, uptake ratios ranging from 8 to 11. No excessive concentrations were found in other organs in either mice or cats.

Toxicity studies were carried out in mice and rabbits at levels of 300 mg/kg and 120 mg/kg respectively. No adverse effects were observed provided the solution was neutralized to a physiological pH. The chemical amounts needed for patient scanning were less than 0.5 mg/kg of body weight.

A comparative clinical study of 10 patients, each scanned with KBF^{18}_4 and other isotopic agents, corroborated the findings of Askenasy et al. that this is a useful compound for brain-tumour localization. Intravenous injection was optimally performed 30 min before scanning at a dosage of 15 μc/kg of body weight. Tissue samples of tumour and normal brain were obtained from one patient at operation. The uptake ratio was 3.5. While this is lower than that found in the mouse, it is still in a useful range.

Blood samples obtained from patients at varying time intervals after injection yielded a blood clearance curve which had two time constants. The first was very rapid and the second slower. This sequence is typical of useful scanning agents.

EMPLOI DU FLUOR-18 EN SCINTIGRAPHIE DES TUMEURS INTRACRÂNIENNES. Les auteurs ont étudié la possibilité d'employer ^{18}F, émetteur de positons ayant une période de 110 min, pour localiser les tumeurs du cerveau. Cette substance a été préparée dans un réacteur par irradiation de Li_2Co_3 par des neutrons thermiques ($^6Li(n, \alpha)^3H$, $^{16}O(^3H, n)^{18}F$). Il ressort d'études faites sur des tissus de souris présentant des épendymomes implantés par greffes sous-cutanées que le fluorure de sodium marqué ($Na^{18}F$) se concentre de manière excessive dans les os et qu'il ne convient donc pas pour explorer le cerveau. Par contre, on a constaté que le fluoborate de potassium marqué ($KB^{18}F_4$) se concentrait nettement plus dans les tumeurs que dans le tissu normal du cerveau, les rapports de concentration allant de 8 à 11. Aucune concentration excessive n'a été observée dans d'autres organes, tant chez les souris que chez les chats.

Les auteurs ont fait des études de toxicité sur des souris et des lapins pour 300 mg/kg et 120 mg/kg, respectivement. Aucun effet nocif n'a été observé tant que le pH de la solution était maintenu à une valeur physiologique. Les quantités de substance nécessaire pour procéder à la scintigraphie du sujet étaient inférieures à 0,5 mg/kg de poids du corps.

Une étude clinique comparative menée sur 10 patients, qui ont tous été examinés à l'aide de $KB^{18}F_4$ et d'autres agents radioisotopiques, a confirmé la conclusion d'Askenasy et autres: ce composé est utile pour localiser les tumeurs du cerveau. On a fait des injections intraveineuses dans des conditions optimales 30 min avant la scintigraphie, à raison de 15 μc/kg de poids du corps. Des échantillons de tissus de tumeur et de tissus normaux du cerveau ont été prélevés sur un malade qui subissait une opération. Le rapport de concentration était de 3,5. Bien que ce rapport soit inférieur à celui qui avait été observé chez la souris, il n'en demeure pas moins convenable.

---

* This work was supported in part by grants from the United States Atomic Energy Commission (AT(30-1)-1242), the USPHS (C-3174) and the John A. Hartford Foundation.

** German Research Council Fellow. Present address: Neurochirurgische Universitätsklinik, Bonn, Federal Republic of Germany.

L'examen d'échantillons de sang prélevés sur des malades à divers intervalles après l'injection a permis d'établir une courbe d'élimination du sang à deux constantes de temps. La première était très rapide et la seconde plus lente, ce qui est caractéristique des bons agents de scintigraphie.

ОЦЕНКА ФТОРА-18 КАК СКЕННИРУЮЩЕГО АГЕНТА ДЛЯ ВНУТРИЧЕРЕПНЫХ ОПУХОЛЕЙ. В качестве вероятного агента для локализации мозговых опухолей изучался фтор-18, излучатель позитронов с периодом полураспада 110 мин. Фтор-18 получали в ядерном реакторе путем облучения Li_2CO_3 ($Li^6(n,\alpha)H^3$, $O^{16}(H^3, n)F^{18}$)тепловыми нейтронами. Тканевые исследования на мышах с пересаженной подкожно эпендимомой показало, что меченый фторид натрия (NaF^{18}) создает избыточные концентрации в костях и поэтому не удовлетворяет в качестве сканирующего агента для мозга. Однако при применении меченого фторбората калия (KBF_4^{18})обнаружено избирательное поглощение его опухолью по сравнению с мозгом, причем величина поглощения изменялась в диапазоне от 8 до 11. Как у мышей, так и у кошек не обнаружено избыточной концентрации в других органах.

Изучение токсичности проводилось на мышах и кроликах при концентрации 300 мг/кг и 120 мг/кг соответственно. При нейтрализации раствора до уровня физиологического pH не наблюдалось никаких неблагоприятных эффектов. Химические количества, необходимые для сканнирования пациентов, составляли менее 0,5 мг/кг веса тела.

Сравнительные клинические исследования у 10 пациентов, каждый из которых подвергался сканнированию с KBF_4^{18} и другими изотопными веществами, подтвердили выводы Ашкенази и др. о том, что это соединение является полезным для определения локализации мозговых опухолей. Внутривенное введение осуществлялось оптимально за 30 минут до сканнирования при дозе 15 мккюри/кг веса тела. У одного пациента при операции были взяты образцы тканей опухоли и здоровой ткани мозга. Коэффициент поглощения составлял 3,5. Хотя это соотношение ниже, чем у мышей, но эта величина практически пригодна.

При исследовании крови, взятой у пациентов через разные промежутки времени после инъекции, получена кривая клиренса крови, имеющая две постоянных времени. Первая—очень кратковременная, вторая—медленнее. Такая характеристика типична для пригодных сканнирующих агентов.

EXAMEN DE LAS CARACTERÍSTICAS DEL FLUOR-18 COMO AGENTE DE EXPLORACIÓN DE LOS TUMORES INTRACRANEALES. Los autores estudiaron la posibilidad de utilizar ^{18}F (período: 110 min) para localizar tumores cerebrales. Prepararon este isótopo en un reactor por irradiación de Li_2CO_3 con neutrones térmicos ($^6Li(n,\alpha)^3H$, $^{16}O(^3H,n)^{18}F$). Los estudios realizados con tejidos de ratón en el que se había transplantado ependimomas por vía subcutánea mostraron que el fluoruro de sodio marcado ($Na^{18}F$) se concentra excesivamente en los huesos y que, por tanto, no es adecuado para explorar el cerebro. Sin embargo, el tumor captó una proporción mayor de fluoborato potásico marcado ($KB^{18}F_4$) que el tejido normal del cerebro; la razón de captación fue de 8 a 11. En los experimentos efectuados con ratones y gatos no se observó ninguna concentración excesiva en otros órganos.

Los autores efectuaron estudios de toxicidad sobre ratones y conejos con dosis de 300 mg/kg y 120 mg/kg respectivamente. No se observó ningún efecto adverso cuando la solución estaba neutralizada hasta alcanzar un pH fisiológico. La cantidad de productos químicos necesaria para la exploración fue inferior a 0,5 mg/kg de peso corporal.

Un estudio clínico comparativo de 10 pacientes, explorados después de administrarles $KB^{18}F_4$ y otros agentes isotópicos, corroboró los resultados obtenidos por Askenasy y sus colaboradores, según los cuales este compuesto es útil para localizar tumores cerebrales. La inyección intravenosa dio resultados óptimos cuando se administraron 15 μc por kg de peso corporal 30 min antes de proceder a la exploración. Se sacaron muestras de tumor y de tejido cerebral normal de un paciente durante la operación. La razón de absorción tumor/tejido normal fue de 3,5. Si bien este valor es inferior al correspondiente al ratón, presenta todavía utilidad diagnóstica.

Las muestras de sangre extraídas a diferentes intervalos después de la inyección permitieron trazar una curva de depuración sanguínea con dos constantes de tiempo. La primera era muy breve y la segunda más larga. Esta secuencia es típica de los agentes de exploración eficaces.

In many neurosurgical centres radioisotopic scanning has become a routine diagnostic procedure in patients with suspicion of intracranial space-occupying lesions [1, 2]. The use of positron-emitting isotopes rather than simple gamma-emitters has some theoretical advantages [3], particularly

TABLE I

SOME POSITRON-EMITTING RADIOISOTOPES USEFUL FOR SCANNING

Isotope	Half-life	Chemical form	Prod.
Ga^{68}	68 min	Ga-DTPA	Cycl.
F^{18}	112 min	KBF_4	Reac.
Zn^{62}	9.3 h	ZnCl	Cycl.
Cu^{64}	12.8 h	Cu-DTPA	Reac.
Zr^{89}	80 h	Citrate	Cycl.
I^{124}	4.5 d	Gamma Glob.	Cycl.
As^{72}	26 h	Na_3AsO_3	Cycl.
As^{74}	17.5	Na_3AsO_4	Cycl.
Na^{22}	2.6 yr	NaCl	Reac.

in a symmetrical organ such as the brain. Coincidence detection of the annihilation radiation from positron decay yields high sensitivity for a given resolution width and a fairly uniform transverse detection region.

A number of positron-emitting radioisotopes which have been evaluated as potential tumour-localization agents are listed in Table I. Of these, arsenic-74 as sodium arsenate has been the isotope of choice [4]. However, its long half-life, 17.5 d, and the fact that it is cyclotron-produced, are major disadvantages. Copper-64 chelates have been used to circumvent these two drawbacks of As^{74} [5]. With the development of camera-type imaging devices [6, 7] new opportunities for high-speed external visualization of isotopic concentrations and dynamic processes are presented. Under such conditions isotopes with half-lives shorter than 12.8-h Cu^{64} have distinct utility.

The work of ANBAR et al. in producing [8] and utilizing [9,10] fluorine-18 as a scanning agent is of great significance in this recent development. F^{18} is a pure positron-emitter with a 112-min half-life. Because of its short half-life and rapid excretion large single doses may be administered and repeated tests performed within short time intervals. The whole-body dose to the patient receiving the suggested amount of 1 mc of F^{18} is 0.05 rad compared with 0.42 rad for the usual dose of 3.0 mc of Cu^{64} and 1.8 rad for the diagnostic dose of 1.3 mc of As^{74}.

The present work is a series of studies with animals and with human patients using potassium fluoborate labelled with F^{18} and some comparisons with F^{18} ion. It corroborates the excellent work of ASKENASY et al. [11] in the localization of intracranial lesions using the BF_4^{18-} anion. In addition to the physical advantages of F^{18}, short half-life and pure positron emission, its chemical properties suggest some intriguing possibilities. The two-stage reaction described below may be used to convert oxygen atoms in complex

organic materials into fluorine by irradiating the lithium salts of these materials. The size of the fluorine atom is so small that fluorine-substituted compounds of biologically-active substances are active themselves (e.g. fluorinated steroids, fluorinated pyrimidines). This presents the possibility of new types of organic scanning agents.

METHODS

F^{18} was prepared at the Massachusetts Institute of Technology reactor by the irradiation of lithium carbonate in the following sequential reaction:

$$Li^6(n,\alpha)H^3; \quad O^{16}(H^3, n)F^{18}.$$

The standard procedure used in the preparation of $KBF_4{}^{18}$ consisted of the irradiation of 3.0 g of unenriched Li_2CO_3 at a flux of 2×10^{13} n/cm^2 s for a period of 7.5 h, until saturation was achieved. The total yield was 35 mc of F^{18}. The lithium carbonate was dissolved in 13.5 ml of 6N hydrochloric acid and in this mixture was dissolved 113 mg of stable KBF_4. The potassium fluoborate was crystallized in an ice bath, filtered, washed with 2 ml of ice water and recrystallized twice more. The crystallization also removed tritium produced in the reaction. The total F^{18} activity at the time of biological studies was about 6 mc with a specific activity of 130 μc F^{18}/mg KBF_4. For its use in man the compound was dissolved in 10 ml of isotonic pyrogen-free saline adjusted to the physiological pH.

In preparing the fluoride ion, the acidified solution of Li_2CO_3 was passed through a cation exchange column* to remove not only lithium but also the sodium-24 arising from the activation of trace amounts of sodium present in analytical-grade Li_2CO_3. In this manner 90–95% of F^{18} produced was recovered in the eluant.

Toxicity studies with fluoborate ion were carried out in white Swiss albino mice and in rabbits. Tissue distribution of $BF_4{}^{18}$ and F^{18} ions was examined utilizing C_3H mice bearing subcutaneously implanted tumours which were originally gliomas. Tissue studies were also performed in cats.

A limited series of scans using the mechanical brain scanner previously described [2, 3] was performed with $KBF_4{}^{18}$ on 10 patients who were tumour suspects. The administered dose in each case was 1–3 mc. The scans were performed at short time intervals after the intravenous injection.

In a number of these patients blood and urine samples were collected at intervals after injection to determine blood clearance as a function of time.

RESULTS

(1) Toxicity

In the toxicity studies no apparent acute toxic symptoms were seen in mice receiving intravenously 300 mg/kg and rabbits 120 mg/kg of KBF_4.

* Dowex 50

The animals were kept alive over a period of six weeks without sequelae. These tests were carried out with a solution neutralized to pH 7, for at a pH range of 1 to 3 large volumes of KBF_4 are extremely toxic. Doses of the order of 5-6 mg/kg of neutral KBF_4 were injected into terminal glioblastoma patients with no adverse effects.

The chemical amounts needed for routine patient scanning were less than 0.5 mg/kg and from the above data no problems of pharmacological toxicity were expected or observed in the patient study.

(2) Mouse tissue studies

The isotopic uptake in the organs of the mice bearing subcutaneously transplanted tumours is shown in Table II. Six groups of animals were used, three receiving labelled-fluoborate ion and three groups receiving F^{18-}. Sacrifice times were 15, 30 and 60 min after injection.

The tissue concentrations are presented in three different ways. Section A shows the average blood uptake for each group of animals as per cent of total injected dose per kilogram of tissue normalized to total animal weight of 70 kg*. This normalization is the standard compromise used for comparative tissue studies between individuals and species. The mouse values are sufficiently similar to human values to show a probable common metabolic mode.

Section B gives the tumour-to-brain uptake ratio. For fluoborate ion this ratio was approximately 10 throughout the time-interval 15 to 60 min, indicating that fluoborate ion might be a useful scanning agent.

Section C presents the ratios of the uptake in other tissues to that in blood. The greatest percentage uptake of the fluoborate was in blood and the least in brain, while in other tissues and in tumour the distribution was nearly the same with no organ having an exceptionally high level.

During this time-interval fluoride ion showed a high concentration in blood compared to all other tissues studied except bone. The level in skull was about 6 times the blood level at 15 min and 12 times at 60 min. This high concentration of fluoride ion in bone militated against its use as a brain-scanning agent since the heavy concentration in the skull would mask any variations in the underlying brain.

A similar tabulation is given in Table III of the average values of the tissue uptakes of $KBF_4{}^{18}$ in four cats sacrificed 30 min after injection. These values agree reasonably well with the mouse data in that the fluoborate ion did not concentrate specifically in any particular organ.

(3) Scanning results

A typical scan of one of the patients is shown in Fig. 1. A clearly defined parietal concentration is indicated in the coincidence scan in 1(a). Figure 1(b), the unbalance scan, shows a concentration of curved marks indicating that the activity was on the right side. At operation a glioblastoma multiforme was found at the location indicated in the scan.

* Tissue Concentration (Normalized) = Concentration (Observed) $\times \frac{\text{Total wt. in kg}}{70}$

TABLE II

RADIOISOTOPIC UPTAKE IN MICE PER UNIT WEIGHT OF TISSUE*

Interval after intravenous injection		15 min		30 min		60 min	
Compounds		BF_4	F	BF_4	F	BF_4	F
Number of animals in group		17	6	12	4	12	4
A	% remaining in blood per kg normalized to 70 kg	2.3	1.7	1.7	4.6	1.4	2.4
B	Ratio of tumour to brain	10.0	7.5	8.5	6.8	11.0	5.4
C	Ratio of specified organ to blood						
	Blood	1.0	1.0	1.0	1.0	1.0	1.0
	Brain	0.05	0.1	0.04	0.1	0.04	0.2
	Tumour	0.5	0.8	0.3	1.0	0.5	0.9
	Skull	0.4	6.3	0.3	8.6	0.3	11.7
	Muscle	0.6	0.6	0.1	0.9	0.2	0.4
	Scalp	0.6	0.6	0.4	0.6	0.5	0.7
	Thyroid	0.4	0.6	0.3	0.5	0.5	0.3
	Kidney	0.6	-	-	-	-	-
	Liver	0.3	--	-	-	-	-

* Values are averages for the animals in each group.

The data on the 10 patients scanned are summarized in Table IV. The range of ages was from 6 to 72 yr and included a series of neoplasms as well as one case of benign intracranial hypertension (pseudotumour). All these patients were also scanned with arsenic or copper within a few days before or after the fluorine scan. The fluorine scan evaluations are indicated in the table with comments comparing the results obtained with the other tracers.

The blood-clearance curve for the one patient (J.V.) from whom multiple samples were obtained, as well as 12 samples from seven other patients, are plotted in Fig. 2. There is a high degree of randomness in the data indicating that the absorption and excretion processes are highly individual. Using the data for J.V. the clearance curve seems to have two dis-

TABLE III

FLUOBORATE CONCENTRATION PER UNIT WEIGHT OF TISSUE IN CATS*

	Ratios to blood	Ratios to brain
Blood	1.0	27
Brain	0.04	1
Skull	0.2	6
Muscle	0.3	7
Scalp	0.6	16
Lung	0.9	
Kidney	0.8	
Heart	0.7	
Skin	0.7	
Liver	0.3	
Intestines	0.5	
Adrenals	0.5	
Pancreas	0.5	
Fat	0.1	

* Values are averages for four animals sacrificed 30 min after injection.

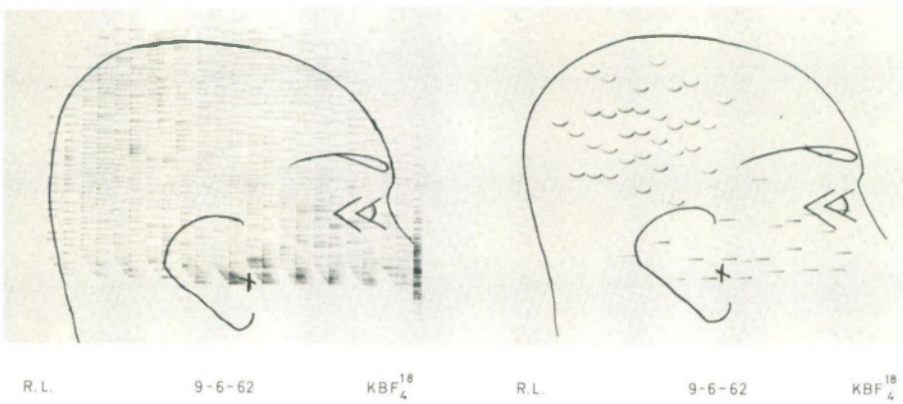

Fig. 1

KBF_4^{18} scan of patient with glioblastoma multiforme
(a) Coincidence scan showing posterior-parietal concentration
(b) Unbalance scan showing curved marks indicating right concentration

TABLE IV

SCAN RESULTS

Patient	Age	Diagnosis	Conf.	F^{18}	As^{74}	Cu^{64}	Comments
A	48	Glio. mult.	Opn.	1	1	-	F^{18} similar to As^{74}
B	38	Glio. mult.	Opn.	2	-	1	Cu^{64} better than F^{18}
C	6	Glio. mult.	Opn.	1	1	-	F^{18} similar to As^{74}
D	46	Astrcy. II	Opn.	4	-	4	Miss both isotopes
E	57	Astrcy. II	Opn.	1	1	-	As^{74} pre-op.; F^{18} post-op.; question opn. artifact
F	52	Pet. pyr. Mening.	Arter-gram	1	-	3	Question if we see bony involvement with F^{18}
G	32	Meta. melanoma	Auto.	3	-	1	Cu^{64} better than F^{18}
H	42	Meta. carcinoma	Opn.	2	2	2	All scans equally poor
I	72	Chordoma	Radiol.	1	2	4	F^{18} better than As^{74} or Cu^{64} Question uptake in bone erosion
J	12	Pseudo tumour	-	4	-	-	True negative

Notes: 1 = definitely abnormal
2 = probably abnormal
3 = probably normal
4 = definitely normal

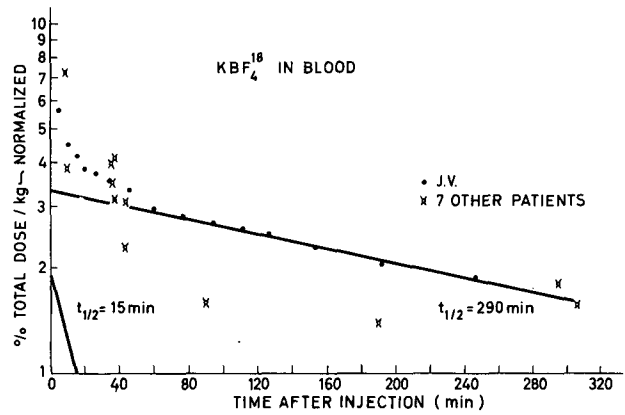

Fig. 2

Blood clearance study

tinguishable time constants, a fast component with half-time of about 15 min and a slow one with half-time of 290 min.

Figure 3 is the cumulative urinary-excretion curve for patient J.V. In the first few hours after injection the curve corresponds to an exponential excretion with half-time of about 470 min. The rate becomes slower at longer times, but is difficult to evaluate numerically due to the short half-life of F^{18}.

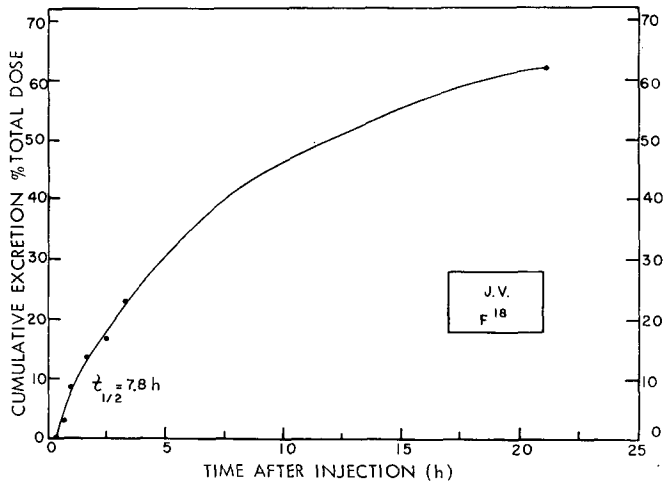

Fig. 3

Urinary excretion study of BF_4^{18} anion

DISCUSSION

The animal tissue studies showed a high tumour: brain uptake-ratio for fluoborate ion, no unusually large concentration in any specific organ

and no marked species variation. For these reasons it was considered suitable for evaluation in man.

The blood-concentration curve is also favourable since it is similar to that found in other useful scanning agents [4]. Such curves characteristically display two or more time constants. The first should be very rapid, in the order of minutes, and the second much longer, in the order of hours. These time constants must be examined on the basis of several competing processes. The first time constant represents rapid initial removal from the blood and should be caused by a general rapid interchange between blood and body tissue rather than excretion or selective removal by a specific organ. The urinary-excretion curve and the tissue studies indicate that for BF_4^- the last two processes are unlikely. The second constant should represent the excretory removal of the agent from the blood, reducing the radiation dose to the patient. If a third, much longer, time constant is observed, it represents the long-term steady-state interchange of the tracer between blood and body tissue, and the gradual excretion of the tracer.

With some isotopes, for example ionic copper and ionic fluorine, the tracer is found in specific organs, liver and bone respectively, so that this general time sequence does not apply. However, the animal-tissue studies of specific organs indicate that for KBF_4 there is no excessive preferential uptake in any organ.

Previous studies of blood clearance of arsenic indicate a similar curve with a fast component having a half-time of 46 min and a second component having a half-time of 27 h. The more rapid initial component in the case of the fluoborate, 15 min, should assist in allowing scans to be made at much shorter intervals after injection. This hypothesis is borne out in the scans performed where a time lapse of about one-half hour seems to be optimal. This contrasts to $1\frac{1}{2}$ h with arsenic. The rapid initial fall-off should also be of assistance when the isotope is used for high-speed camera studies of dynamic processes.

While the number of scans performed (10) is limited and therefore allows no generalizations, we do confirm the results obtained by ASKENASY et al. [11]. In all cases, except the benign intracranial hypertension in which there was no evidence of focal disease, the F^{18} scan was checked against a scan with arsenic or copper, or both.

The glioblastomas were clearly localized. In patient B the fluorine scan was somewhat poorer than the copper, possibly because the scan was begun 10 min after injection. This seems to be too short a time for good localization. In one case an astrocytoma was clearly missed with both isotopes and in another case was seen. This is consistent with the analysis of arsenic scans – that astrocytomas are frequently not seen. In patients F and I there was some bony involvement of the neoplasms. In both cases the visualization with fluoborate was better than with other isotopes. There is a possibility, which is being investigated further, that some fluorine may be split off biologically from the complex ion and appear as fluoride ion going preferentially to such bone or that the BF_4^{18-} was contaminated with F^{18-} and a more rigorous purification of BF_4^{18-} is required. Patient G with metastatic melanoma was missed with fluorine though seen with copper, and patient H with metastatic carcinoma was visualized with all isotopes but equally poorly.

Summarizing these cases we think that labelled-fluoborate ion may prove to be a satisfactory scanning agent and should be explored further. It is suggested that for intravenous use the injection be performed $\frac{1}{2}$–1 h prior to scan at a dosage of 15 μc/kg (approx. 1 mc per 150 lb). With this dosage, scanning may be performed on a mechanical scanner at a speed higher than usual, requiring approx. 25 min per scan.

Although this series of scans reveals no unusual advantages of BF_4^{18} as a conventional scanning agent, its physical properties must be emphasized. Administration of 20 - 40 mc, giving a whole-body dose of only 1 - 2 rad, would be permissible for routine scanning and even higher doses would be appropriate for patients with known focal lesions. These high doses would allow appreciably reduced scanning times or greatly refined resolution. Such improvements could open new avenues for scanning procedures.

SUMMARY

F^{18}, a 112-min half-life positron-emitter, was studied as a possible agent for brain-tumour localization. Tissue studies in mice bearing subcutaneously transplanted tumours indicated that labelled potassium fluoborate showed good preferential uptake in tumour compared to brain with no excessive concentration in other organs. F^{18}-labelled sodium fluoride gave very high concentrations in bone and is not suitable as a brain-scanning agent. Tissue studies in cats with the fluoborate ion confirm that there is no appreciable preferential tissue uptake. A preliminary study of a small number of patients scanned with fluoborate and other isotopic agents indicates that the former appears to be a suitable compound for brain-tumour localization and merits further study.

ACKNOWLEDGEMENTS

The authors wish to thank Dr. Robert G. Ojemann for his important assistance. The technical aid of Mrs. Janette Messer is gratefully acknowledged.

REFERENCES

[1] ARONOW, S., BROWNELL, G.L., LOVO, S., and SWEET, W.H., Proc. 9th Annual Meeting, Soc. of nucl. Med., Dallas, Tex. (1962).

[2] SWEET, W.H., MEALEY, J., ARONOW, S. and BROWNELL, G.L., Clinical Neurosurgery 7, Williams and Wilkins, Baltimore (1957) 159-99.

[3] BROWNELL, G.L., Medical Radioisotope Scanning, IAEA, Vienna (1959) 1-12.

[4] MEALEY, J., BROWNELL, G.L. and SWEET, W.H., A.M.A. Arch. of Neurol. Psych. 81 (1959) 310-20.

[5] BAGNALL, J.H., BENDA, P., BROWNELL, G.L. and SWEET, W.H., J. Neurosurg. 15 (1958) 411-26.

[6] ANGER, N.O. and GOTTSCHALF, A., J. nucl. Med. 4 (1963) 326-30.

[7] ARONOW, S., Proc. 2nd Int. Conf. of Med. Electron, Paris, Iliffe and Sons, London (1959).

[8] ANBAR, M. and NETA, P., J. Amer. chem. Soc. 84 (1962) 2673-78.

[9] ANBAR, M., ASKENASY, H.M., GUTTMANN, S., KOSAY, I.Z., LAOR, Y. and LEWITUS, Z., Semi-Annual Reports, Israel Atomic Energy Commission, July-Dec. (1960) 75-78.

[10] ANBAR, M. and ERNST, N., Int. J. appl. Rad. Isotopes 13 (1962) 47.

[11] ASKENASY, H.M., ANBAR, M., LAOR, Y., LEWITUS, Z., KOSAY, I.Z. and GUTTMANN, S., Amer. J. Roentgenol. 88 (1962) 350.

DISCUSSION

M. BLAU: Dr. Entzian is quite correct when he states that F^{18} is a very attractive isotope. A further attraction which I might mention is that it is, as far as I know, the only isotope that can be produced in clinically useful quantities in small university reactors. This is a point well worth bearing in mind when preparing a proposal for a new reactor or enlisting the co-operation of individuals who operate a reactor.

Dr. Entzian is incorrect, however, when he implies that it is possible to prepare F^{18}-labelled organic compounds by irradiating the equivalent oxygen compound. The recoil energy of the activation process is always orders of magnitude above the bond energy holding the F^{18} atom in the original molecule.

M. TER-POGOSSIAN: I should like to point out that F^{18} can also be prepared in small accelerators, which are even cheaper than medical reactors.

P.C.R. TURNER: May I comment on this question of preparing F^{18} in accelerators. F^{18} can be prepared by the reaction: $O^{16}(\alpha, np)F^{18}$. However, this reaction has a threshold at about 20 MeV, and to achieve an appreciable yield α-particles of about 30-MeV energy are required. This means that one needs quite a large accelerator, such as a 45-in cyclotron, which is not usually regarded as cheap.

F^{18} is prepared routinely with the Medical Research Council's 45-in cyclotron at Hammersmith Hospital using the above reaction. With current techniques maximum activities of about 10 mc at end of bombardment can be obtained.

SCANNING TECHNIQUES FOR BRAIN-TUMOUR LOCALIZATION

M.H. DUGGAN, J. BRICE*, E. JONES, J.R. MALLARD AND M.I. MYERS
DEPARTMENT OF MEDICAL PHYSICS, POSTGRADUATE MEDICAL SCHOOL, HAMMERSMITH HOSPITAL, LONDON, UNITED KINGDOM

Abstract — Résumé — Аннотация — Resumen

SCANNING TECHNIQUES FOR BRAIN-TUMOUR LOCALIZATION. The colour scanner * has been used to scan two small clinical series of brain tumour cases, one by means of As^{74} using positron detection, the other with I^{131}-labelled albumin using gamma detection and a focusing collimator. The results of these series are given and the value of the procedure to the clinician is presented. Matthews has shown, in studies on tumour-bearing rats, that Bi^{206} citrate should be a particularly favourable material for brain tumour localization and a preliminary attempt has been made to scan with this material using gamma detection and a focusing collimator. Preliminary results of this study are presented.

The focusing collimators used with the gamma-emitting isotopes have a deep geometrical focus and isocount responses are obtained on point sources which are almost depth independent for 20 cm. Experimental results on a series of collimators lead to design data for building such collimators to a given specification.

Stationary detector scanning has been carried out on brain-tumour cases using a gamma camera with storage-tube display. The advantages of such machines lie in greater sensitivity and more rapid visualization of the pattern of distribution of radioactivity, which in turn enables dynamic studies to be carried out. Problems which occur with such machines include the difficulty in marking anatomical features and the geometric distortions which occur. These are compared for pin-hole and matrix viewing apertures. The improvement in performance resulting from circuit modifications to remove the dependence of picture size on gamma-ray energy is discussed.

The analysis of cerebral scans presents difficulties when the suspected region is only slightly greater in count-rate than its surroundings. A "normal" count-rate pattern for a head has been determined by dividing scans into regions which are approximately anatomically equivalent from patient to patient, and counting scintiscan marks in each region. Any abnormal scan may then be compared with this pattern. Such analysis lends itself to computer techniques.

The use of continuous averaging techniques may also prove to be of value in improving the perception of abnormalities near the limits of detection in moving detector systems. The possible use of multichannel analysers to apply this and at the same time make possible a valuable new display system for both moving and stationary systems is presented.

TECHNIQUES SCINTIGRAPHIQUES POUR LA LOCALISATION DES TUMEURS CÉRÉBRALES. On a utilisé l'appareil de gammagraphie en couleurs* pour la scintigraphie de deux séries cliniques de tumeurs cérébrales, dans le premier cas au moyen de ^{74}As (détection des positons), dans le deuxième cas au moyen de l'albumine marquée avec ^{131}I (détection des rayons gamma, avec un collimateur à focalisation). L'auteur compare les résultats obtenus dans les deux séries. Matthews a montré, dans des études sur des rats ayant des tumeurs, que le citrate de ^{206}Bi devrait être un matériau particulièrement favorable pour la localisation des tumeurs cérébrales; aussi fait-on actuellement une troisième série clinique avec ce produit (détection des rayons gamma, avec un collimateur à focalisation). L'auteur présente les résultats préliminaires de cette étude.

Les collimateurs à focalisation utilisés pour les émetteurs gamma ont un foyer géométrique profond et donnent, pour des sources ponctuelles, des courbes d'isoréponse qui sont presque indépendantes de la profondeur sur une distance de 20 cm. Les résultats des expériences faites avec une série de collimateurs ont fourni les données nécessaires à la réalisation de collimateurs de ce genre destinés à des fins déterminées.

* MALLARD, J.R. et al. "An analysis of quantitative colour display for scanning", these Proceedings.

Des tumeurs du cerveau ont été explorées avec un détecteur stationnaire, en ayant recours à la photographie gamma et à l'enregistrement par un oscilloscope à mémoire. Les avantages de ce procédé résident dans une plus grande sensibilité et une visualisation plus rapide de la répartition de la radioactivité, ce qui permet de procéder à des études dynamiques. Ses inconvénients sont, notamment, la difficulté de noter les caractéristiques anatomiques et les distorsions géométriques qui se produisent. On les compare dans le cas des sténopés et de certaines ouvertures réglables. L'auteur examine les améliorations de rendement résultant des modifications de circuit pour faire disparaître la dépendance du format de l'image à l'égard de l'énergie des rayons gamma.

L'analyse des scintigrammes du cerveau présente des difficultés lorsque le taux de comptage pour la zone suspecte est à peine plus élevé que pour les zones avoisinantes. On a établi un schéma «normal» du taux de comptage pour le crâne en divisant les scintigrammes en régions à peu près équivalentes du point de vue anatomique d'un patient à l'autre, et en comptant les traces scintigraphiques dans chaque région. On peut comparer tout scintigramme anormal à ce schéma. Une telle analyse est faite au mieux avec un ordinateur.

L'utilisation de méthodes d'établissement continu des valeurs moyennes peut également présenter un interet pour l'amélioration de la visualisation des anomalies au voisinage des limites de la détection. Les auteurs étudient la possibilité d'utiliser des sélecteurs multiconaux aux fins décrites ci-dessus; cet emploi permet la réalisation d'un nouveau dispositif de visualisation efficace tant pour des systèmes mobiles que pour des systèmes stationaire.

ТЕХНИКА СКЕННИРОВАНИЯ ПРИ ОПРЕДЕЛЕНИИ ЛОКАЛИЗАЦИИ ОПУХОЛЕЙ МОЗГА. Установка для цветного сканнирования (Аннотация SM-51/25) использовалась для сканнирования двух видов опухолей мозга: в одном случае по позитронному излучению As^{74}, в другом — по гамма-излучению меченного J^{131} альбумина с использованием фокусирующего коллиматора.

Сравниваются результаты этих двух видов исследований. Мэтьюс, при исследовании опухолей у крыс, показал, что лимоннокислый Bi^{206} является особенно удобным материалом для определения локализации опухолей мозга, и в настоящее время проводится третья серия клинических исследований с применением этого материала, использованием гамма-детектирования и фокусирующего коллиматора. Приводятся предварительные результаты этих исследований.

Фокусирующие коллиматоры, примененные вместе с гамма-излучающими изотопами, имеют глубокий геометрический фокус; получены изосчетные характеристики для точечных источников, не зависящие от глубины до 20 см. Экспериментальные результаты, полученные для целого ряда коллиматоров, явились основой для конструкции таких коллиматоров с заданной спецификацией.

Стационарное детекторное сканнирование у больных с опухолями мозга было проведено с помощью гамма-камеры с воспроизводящим запоминающим устройством. Преимущества такой аппаратуры заключаются в большей чувствительности и более быстрой визуализации картины распределения радиоактивности, что дает возможность проведения исследований в динамике. К проблемам, возникающим в связи с этой аппаратурой, относятся трудность маркировки анатомических структур и встречающиеся геометрические искажения. Они возникают и в отношении булавочных и матричных апертур наблюдения. Обсуждаются улучшения, достигнутые в результате ряда изменений, направленных на устранение зависимости размера изображения от энергии гамма-лучей.

Анализ данных сканнирования мозга представляет трудности, если скорость счета в исследуемой области только немного выше, чем в окружающей ткани. "Нормальная" диаграмма скорости счета для головы была определена на основании разделения сканнограммы на ряд областей, которые являются приблизительно эквивалентными анатомически у ряда пациентов и путем измерения скорости счета в пределах сцентисканнографических отметок в каждой области. Поэтому любую патологическую сканнограмму можно сравнивать с этой диаграммой. При таком анализе прибегают к счетно-вычислительным методам. Использование метода постоянного усреднения также имеет значение для улучшения визуального наблюдения отклонений от нормы вблизи границ детектирования в подвижных детекторных системах. Рассматриваются возможности применения с этой целью многоканальных анализаторов и использования в то же время нового ценного воспроизводящего устройства как для подвижной, так и стационарной систем.

TÉCNICAS CENTELLEOGRÁFICAS PARA LA LOCALIZACIÓN DE TUMORES CEREBRALES. La centelleografía policroma* se ha empleado para explorar dos series clínicas de tumores cerebrales, una con ^{74}As, por detección de positrones, y la otra mediante albúmina marcada con ^{131}I por detección gamma con ayuda de un colimador enfocado. Se indican los resultados obtenidos en ambas series y se explica la utilidad clínica del procedimiento. Estudiando tumores en ratas, Matthews ha demostrado que el citrato de ^{206}Bi debería ser una sustancia particularmente adecuada para localizar tumores cerebrales; por esta razón se ha realizado una primera tentativa para efectuar exploraciones con esa sustancia por detección gamma con ayuda de un colimador enfocado. En la memoria se presentan los primeros resultados de ese estudio.

Los colimadores enfocados que se emplean para los emisores gamma tienen un foco geométrico profundo y con ellos se obtienen líneas de isorrespuesta a fuentes puntiformes que son casi independientes de la profundidad en una extensión de 20 cm. Los resultados experimentales han permitido obtener datos para construir colimadores que reúnen ciertas características específicas.

Algunos casos de tumor cerebral han sido explorados con un detector estacionario de cámara de rayos gamma y presentados en un osciloscopio con memoria. Las ventajas de estos instrumentos estriban en su mayor sensibilidad y en la rapidez con que permiten visualizar el esquema de distribución de la radiactividad, lo cual permite a su vez efectuar estudios dinámicos. Los inconvenientes que entraña el empleo de esos dispositivos son, entre otros, la dificultad de marcar características anatómicas y las deformaciones geométricas a que dan lugar. En la memoria se comparan estas últimas al utilizar cámaras estenoscópicas y cámaras de matriz. Se discuten las mejoras obtenidas modificando los circuitos para lograr que el tamaño de la imagen sea independiente de la energía de los rayos gamma.

El análisis de los centelleogramas del cerebro presenta dificultades cuando la región sospechosa acusa un índice de recuento sólo ligeramente superior al de las zonas que la rodean. Se ha determinado un esquema «normal» de índice de recuento para una cabeza, dividiendo los centelleogramas en regiones que desde el punto de vista anatómico son casi equivalentes de un paciente a otro, y contando los datos centelleográficos en cada región. Todo centelleograma anormal se puede comparar con este esquema. Estos tipos de análisis pueden efectuarse con provecho mediante calculadoras.

También puede ser útil emplear técnicas de promediación continua para facilitar la percepción de anomalías no muy alejadas de los límites de detección en sistemas detectores móviles. En la memoria se estudia la posibilidad de utilizar analizadores multicanales para aplicar esas técnicas y permitir al mismo tiempo un nuevo y útil procedimiento de presentación del centelleograma tanto en los sistemas móviles como en los estacionarios.

1. INTRODUCTION

For the past four years we have been carrying out cerebral scanning at Hammersmith Hospital. Because there is not a large neurosurgical unit in the hospital the majority of cases have come from other hospitals, and only about 40% have been Hammersmith patients. The extra difficulties which inevitably result from such an arrangement, e.g. transport, has made our series much smaller than those of other speakers in this section of the Symposium.

The series falls into two sections:

(1) 1960–1962 when cyclotron-produced isotopes of arsenic were used with positron detection; and

(2) 1962–1963 when reactor-produced iodine labelled albumen was used with a focusing collimator.

---

* MALLARD, J.R. et al. "An analysis of quantitative colour display for scanning", these Proceedings.

2. THE ARSENIC-POSITRON TECHNIQUE

The presence of the Medical Research Council 20-MeV cyclotron at Hammersmith made the choice of cyclotron-produced arsenic isotopes an obvious one particularly in the light of the improved resolution obtainable at that time with positron detection as reported by BROWNELL [1] and the very successful series using arsenic-74 reported by SWEET and BROWNELL [2], and SWEET, MEALEY, BROWNELL and ARONOW [3].

The technique and early results of the Hammersmith As series have been reported elsewhere [4-6]. To detect the pair of annihilation γ-ray photons, two $1\frac{1}{2}$-in-diam., 1-in-thick sodium iodide crystals were used as an opposed pair with cylindrical collimators 11 cm in length; the crystals were separated by approximately 17 in for A.P. scans and 15 in for lateral scans. The pulses from each counter were passed to a coincidence unit, the output of which was fed to the printing unit of the scanning machine. As a result only those pulses resulting from radiation arriving simultaneously in both detectors from a well-defined core between the counters were recorded. The same counting system but with a crystal separation 22 in has been investigated by DYSON [7] who found that the 50% resolution diameter in a water phantom was 2.1 cm and the 5% diameter 4.5 cm (see Table I).

TABLE I

COMPARISON OF ISOCOUNT CHARACTERISTICS OF POSITRON AND "DEPTH-INDEPENDENT" COLLIMATOR SYSTEMS

	Arsenic positrons		300-400 keV gamma rays 'Depth-independent' 19-hole focusing collimators	
	After DYSON (1960)	ARONOW (1062)	(MYERS and MALLARD 1964)	
	(cm)	(cm)	(cm)	
70% isocount diam.	1.6	1.2	2.0	1.6
50% isocount diam.	2.1	1.8	2.8	2.2
10% isocount diam.	3.9	3.3	4.7	3.7
70% isocount depth (cm)	= 18.0	11.5	18.2	13.4

The point-source resolution of the system is good and in addition it has the advantage that the count-rate does not vary much along the axis joining the two counters. For Dyson's counters, at a rather larger separation than we have used for brain-tumour localization, the count-rates were never less than 70% of the maximum for a thickness of 24 cm along with central axis in a water phantom and can be expected to be 18 cm or more in our conditions. ARONOW [8] has given the isoresponse curves of his system which

uses smaller scintillating crystals of 2 cm diam. and as a result his 50% resolution diameter is somewhat smaller at 1.8 cm; the longitudinal response distance along the central axis enclosed within the 70% isocount surface is 11.5 cm (Table I).

The most generally used isotope of arsenic is As^{74} [1, 3, 8] with a half-life of 17.4 d, but we were interested in using the shorter-lived As^{72}, with a half-life of 26 h, because it emits, on average, 2.7 times as many positrons per disintegration. The radiation dosimetry of As^{72} has been calculated by TURNER [9] and compared with that for As^{74} by MEALEY, BROWNELL and SWEET [10]. The critical organ is the kidney, and for the As^{74} dose (2.5 mc) used by MEALEY et al. [10] the kidney dose is almost 13 rad and if this is taken as the limiting dose per examination then 1.3 mc of As^{72} can be administered which, because of the much greater positron emission of As^{72}, gives 1.6 times as many positron coincidence counts over the brain than As^{74}. This increased count-rate, together with a reduced whole-body dose from 3.1 to 1.0 rad, was worth having and every effort was made to use As^{72} in the series.

However, because of its short half-life it was necessary to produce and prepare the material shortly before each scanning session, and, inevitably, in spite of great efforts by all concerned, it could not always be available at the moment a scan was needed. To overcome this, a stock solution of As^{74} was maintained, again made by the M.R.C. cyclotron team. Of the 93 cases scanned with arsenic, 18 were carried out with As^{72} and, for the purpose of the series, they have been taken together with those using As^{74}.

The scanning machine used was the colour-scanning machine described elsewhere in this Symposium [5, 5a]. The count-rates obtained in the scans were in the low count-rate range with about 2 cps over normal brain. Intravenous injections were given, the patient adjusted in position and the head held steady by a webbing band (see [6] Fig. 1). The patients are not normally sedated and the scan is commenced as soon as possible after injection because the greatest concentration of isotope in biopsy specimens has been shown by MEALEY et al. [10] to be immediately after injection. The lateral scan takes about 45 min and the A.P. scan about 30 min which is usually carried out after the lateral one if there appears to be a region of interest.

We have noticed on occasions during the A.P. scan, that the count-rate falls from one side to the other, the side scanned first being higher. This effect is also found to a lesser extent in the lateral scan; for example, there is usually a relatively higher level over the occipital region when scanning from posterior to anterior than from anterior to posterior. Presumably this is due to clearance of the arsenic from the system. It leads to more difficulty in the interpretation of scans and has, in a few cases, led us to state the wrong side for a lesion localized correctly in the lateral. Incidentally, we agree with the comment by ARONOW [8] that it is not always easy to obtain the medical staff at the right moment to give the injection which is a small point in favour of using albumen which is given the previous day.

3. THE ALBUMEN-FOCUSING COLLIMATOR TECHNIQUE

In mid-1962 the M.R.C. cyclotron was not operational whilst major modifications were made to it for a neutron therapy programme and it became necessary to use another technique for cerebral scanning. At that time the published results of DICHIRO [11] were sufficiently good to suggest that I^{131} labelled human serum albumen was the next material of choice after arsenic.

Since this material is not a positron emitter a new detecting system was required and it was necessary to design a collimator to achieve the desired resolution. It was decided to attempt to design one able to give not only a resolution laterally, which agreed as closely as possible with that of the arsenic positron technique that was thought to be adequate, but which had a longitudinal characteristic which was, as much as possible 'depth independent' in phantom, again, to be similar to the arsenic positron technique. For brain, or other deep organ scanning, we consider that 'depth independence' is required over as much as 20 cm in phantom and the collimators designed here closely approach this; they approach the ideal theoretical contours discussed by BROWNELL [12]. ARONOW [8] has commented that the shape of the arsenic characteristics already discussed are ideal for brain scanning when one has no prior knowledge of the position of the suspected lesion. It is important that there should be a good chance of detecting an abnormality far from the collimator and deep in the head as well as more superficially. The positron technique possessed this attribute as a result of using two counters, one on either side of the head, and some workers have used two counters connected as parallel [13] or as difference (or out-of-balance) counters [13-14]. One could, of course, scan both sides with a single counter but the time taken becomes prohibitive. Even so, using these techniques it is essential to ensure that abnormalities can be detected reasonably well in the centre of the head at 8-19 cm deep in tissue.

Most focusing collimators designed for scanning have been designed with a geometrical focal distance for the holes equal to the length of the collimator; the point-source characteristics of these collimators show that the radiation focal distance is at about 75-80% of the geometric focal distance and lie between 4 and 8 cm depth in air (300-400 keV) [15-18]. Table II compares their properties with those of the long-focusing ones designed here [19]. Although the shorter focusing collimators give a very good lateral 50% resolution diameter ranging from 0.6 to 1 cm, the longitudinal response falls to 70% of the maximum count-rate at depths from 5 to 9 cm in air which would be about 4 to 7 cm in phantom. These collimators are therefore excellent for scanning thin organs or for scanning where the depth of the abnormality is known and can be placed near the depth of the radiation focus but cannot be expected to do so well in detecting more deep-seated abnormalities.

The long-focusing collimators have a geometrical focal distance of twice the length of the collimator and the 70% response line occurs at depths of 13 to 18 cm in a water phantom. This improved depth response has been achieved at the expense of the point-source lateral 50% resolution diameter which becomes somewhat greater than 2 cm in order to retain adequate sensitivity, due to the appreciable attenuation of radiation from the much

TABLE II

LONGITUDINAL RESPONSE OF VARIOUS CONVERGENT MULTI-CHANNEL COLLIMATORS
(Energy range 300–400 keV)

Collimator description	'Depth-independent' collimators			Other scanning collimators from literature			
	I 19-hole 19 Crystal	II 19-hole 19 Crystal	III 19-hole $3\frac{1}{2} \times 3$ in Crystal	CRADDUCK and FEDORUK [20] 19-hole	FRANCIS et al. [15] 37-hole	DEWEY and SINCLAIR [16] 91-hole	MYHILL [17] 61-hole
	MYERS and MALLARD [19]						
Length of collimator (cm)	10	10	10	15.2	7.5	7.2	5.0
Geometric focal distance f (cm)	16	20	20	15.2	7.5	8.4	5.0
Radiation focal distance in air f_a (cm)	12.2	15.5	15.5	13	6.5	7.5	3.8
$f_a/f \times 100\%$	76	78	78	86	87	89	76
70% depth in air d_a (cm)	16.6	22.2	23	17.5	8.5	9.2	5.5
70% depth in tissue d_t (cm)	13.4	18.2	15.7	14.5	-	-	-
$d_a/d_t \times 100\%$	81	82	68	83	-	-	-
50% resolution diam. (in air 400 kV) at radiation focal distance (cm)	2.2	2.8	2.2	1.6	0.9	0.6	1.0

greater depths. However, these resolution diameters compare well with the resolution of the positron detector system.

Figure 1 shows the isocount lines for the collimator-counter system used for this series together with the longitudinal central-axis depth response in a phantom. We have found that the lateral 50% resolution diameter of long-focusing collimators in air is only increased by 7% when measured in phantom. The longitudinal characteristics are found to be those of 'in air' multiplied by the appropriate attenuation factor $e^{-\mu d}$, for depth d, in agreement with CRADDUCK and FEDORUK [20].

It is now hoped that it will prove possible to design a long-focusing collimator with better resolution characteristics; this should be possible by the use of smaller holes but a better collimator material than lead may prove to be necessary (compare HARRIS [18], with shorter focusing collimators).

The counter used for the clinical series had 19 individual small crystals set behind each hole of the collimator and encased in lead to attenuate background counts. The room background is considerably lower than for a single-crystal system employing the same collimator and shielding. A figure of merit similar to that of DEWEY and SINCLAIR [16] was used to indicate the probability of detecting a tumour and values were found which agreed closely with those found using a $3\frac{1}{2}$-in-diam., 3-in-thick crystal also using a 19-hole long-focusing collimator of similar characteristics. In high count-rate scans a 1.6-cm-diam. sphere containing 8 times the background concentration of radioactivity should be detected at a depth of 13 cm [5a].

The albumen doses were given approximately 24 h before scanning, the the average dose being 300 μc. The radiation dose to the patient has been estimated by DI CHIRO [11] as being 0.5 rad which is considerably less than for As^{74}. The count-rates found over normal brain in the scans were of the order of 10-20 cps, some 5-15 times greater than for arsenic.

4. RESULTS OF THE ARSENIC AND ALBUMEN SERIES

In this trial study the physicists performing the investigations and interpreting the isotope scans were situated in one hospital whilst most of the patients were referred from an entirely separate institution and were sent for examination with no clinical details apart from their name, age and the possibility that they might be suspected of harbouring a space-occupying lesion within the skull. Normals were included in the series without the knowledge of the physicists. In this way any possible aid from clinical examination or radiological data was eliminated from the trial.

The results of the scans reported at the time of examination have been checked and assessed by the clinicians in the light of subsequent clinical knowledge. Only those patients in whom a definite diagnosis has been made as a result of biopsy, craniotomy or autopsy, are included in the figures presented. In this way 44 of the total number of 133 still await verification.

The scans were assessed as accurate, inaccurate, false positive or false negative. Only those scans which provided information enabling the clinician to place a craniotomy directly on the tumour were considered accurate. 'Near misses' were rejected and were classed as inaccurate, to-

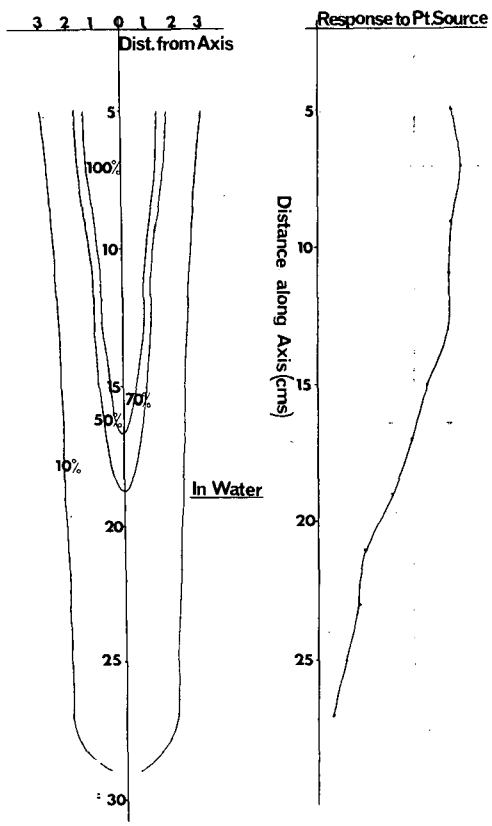

Fig. 1

Point-source isoresponse lines (Au^{198}; 411 keV) and central axis response in tissue equivalent phantom for 19-hole long-focusing collimator ('depth-independent').

gether with localization in incorrect sites. False negative scans were those in which no abnormal increases in count-rate were reported although a space-occupying lesion was discovered subsequently by other investigations. All 'normal' patients had further investigation performed which failed to reveal the presence of a space-occupying lesion. Such patients have also been followed up for at least a year without further evidence coming to light. Scans on these patients demonstrating areas of abnormally high count-rates were regarded as falsely positive.

The results of the two series are shown in Table III. Accurate scans are shown as a fraction of the total performed in that group. Several features are prominent in the Table. The series is small and shows a high proportion of normal patients. This results from a deliberate attempt on the part of the clinicians to send a representative selection of case material for examination. This fact undoubtedly affects the overall results and also affected the course of the trial because, as confidence in the method increased more difficult clinical problems were presented. Thus it will be seen that the proportion of gliomata in the later iodinated albumen series

TABLE III

RESULTS IN 89 PATIENTS SCANNED

Type of lesion	As^{72} and As^{74}	I^{131}	Total
Gliomata			
Benign	0/3	2/2	2/5
Malignant	10/15	2/4	12/19
Meningiomata	3/3	3/3	6/6
Pituitary tumours	2/2	1/1	3/3
Metastases	10/13	6/8	16/21
False negatives for all tumours	6/36	3/18	9/54
Haematomata	1/1	2/4	3/5
Infarcts	2/4	0/1	2/5
Angiomata	0/1	-	0/1
Total pathology	28/42	16/23	44/65
'Normals'	10/14	7/10	17/24
False positives	4/14	3/10	7/24

is lower than in the earlier arsenic series, suggesting that a greater proportion of clinically borderline cases were examined using radioactive iodinated albumen.

In common with other workers in this field, benign lesions such as meningiomata and pituitary adenomata were localized with ease, whilst the inaccurate results were more frequent with slower growing infiltrative types of glioma. This is of importance to the clinician, since early diagnosis and therapy affects the ultimate outcome for the patient a great deal more in the former than the latter group. Another interesting feature is the greater accuracy in patients with metastatic lesions of the brain. The presence of multiple areas of high uptake enabled the clinician to make a definite diagnosis and the patient was spared less pleasant procedures. Errors in this group of metastatic lesions occurred when the secondary lesions were smaller than the minimum size needed for detection by our counting method.

Increased count-rates were also found over haematomata and occasionally from cerebral infarcts. Indeed it was not possible to distinguish between space-occupying lesions due to neoplasia or to vascular causes although it is hoped that more refined techniques may ultimately make this possible. Similarly one cannot predict the likely histological characteristics of the

Fig. 2

A.P. and lateral colour scans of an obvious tumour (meningioma) using I^{131} H.S.A.

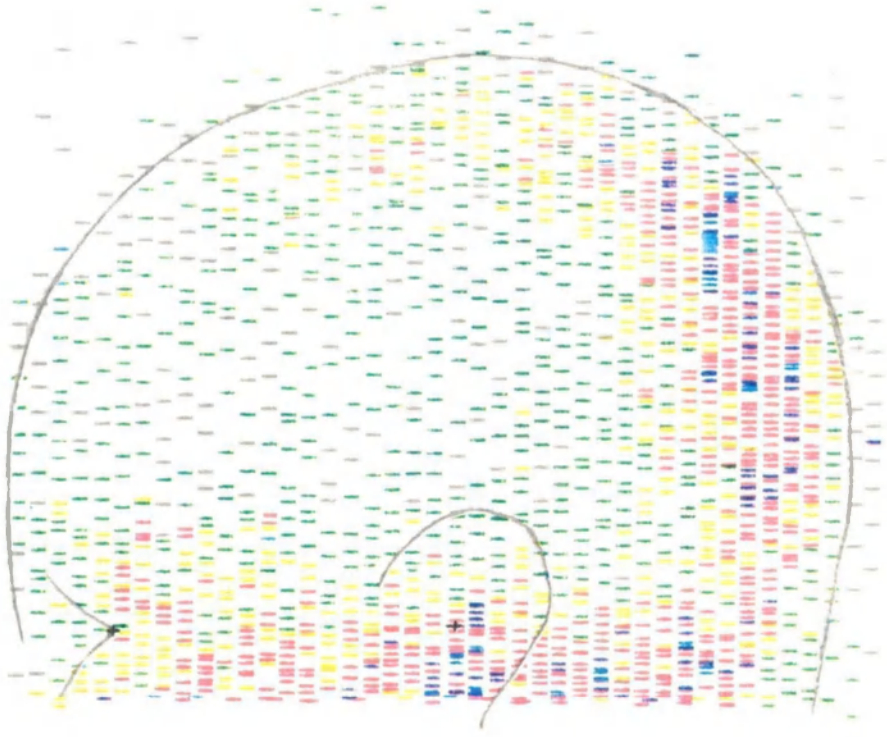

Fig. 3

Lateral scan using As^{74} showing a high count-rate (red, mauve and blue marks) in the post-parietal region over the site of a burr hole.

lesion although meningiomata appeared to give the highest count-rate increases relative to surrounding tissue of all the tumour types (Fig. 2).

The anatomical situation of the tumour had some bearing on the results in that lesions on the floor of the middle fossa or in the posterior fossa were found difficult to detect because of the normal high count-rate over these areas. Similarly recent operative procedures on the scalp, such as burr holes or even recent injury from epilepsy, led to false positive readings, due presumably to inflammatory changes in the scalp (Fig. 3). We have observed that if the scan was carried out after radiological air studies, or angiograms, there was more chance of recording a false negative. As many as 7/9 (80%) of our false negatives whilst only 24/43 (55%) of correct localizations followed such a test. It may be that the scan should be used as an initial investigation.

The high incidence of false positive and false negative results in our hands will no doubt diminish with experience but the presence of these errors and the inherent difficulty of detecting lesions below a certain size means that cerebral scanning cannot be used as the moment as a method of excluding intracranial pathology. Our overall performance is seen from Table III to be about 70% correct, a figure somewhat lower than that re-

ported by other workers [3, 8, 11, 27]. We believe that this has resulted from the small series, the very strict criteria used to score a success and the fact that definite normals were deliberately mixed in the series without prior knowledge of the physicist so that each case was scanned as if it were a suspected lesion.

This method of localization of space-occupying lesions within the head has the great advantage of being painless and harmless. It does not disturb the patient in any way apart from the inconvenience of an intravenous injection. It does, however, require the co-operation of the patient for a period of about one and a half hours, during which time the patient must lie still. In confused or restless patients this may be impossible and we were unable to use the method for the acutely ill. This resulted in the exclusion of acute lesions such as cerebral abscesses from our trial. The use of a gamma camera may shorten the period required for examination and enable the range of the method to be extended.

This examination does not disturb the intracranial hydrodynamics in any way. In no patient did we observe neurological deterioration following the procedure. Other conventional radiological methods of localization undoubtedly cause such deterioration and these conventional methods are therefore better used in a neurosurgical centre with facilities for immediate operation, if this becomes necessary. Brain scanning with isotopes will enable definite diagnostic work to be carried on outside a neurosurgical department and reduce the demand on such a department considerably.

The method may be used in two ways to aid the clinician. It can be used as an initial investigation on many patients and if a clear-cut scan is obtained over the area suspected clinically, a surgeon may be prepared to carry out a therapeutic procedure on this evidence alone. We have already started to treat patients successfully along these lines. Other patients will clearly require further radiological investigations. This method cannot give precise anatomical information concerning neighbouring structures which the surgeon may need in planning operative treatment.

Secondly, brain scanning may be used as a complement to conventional radiological methods when these fail. Early or small lesions are difficult to detect radiologically in the parietal parasagittal regions and the occipital lobes. These situations are readily accessible to scanning techniques and such lesions as early meningiomata or gliomata may be easily seen when other methods fail. Figure 4 shows an occopital glioma infiltrating the posterior half of the corpus callosum with its accompanying scan. In this patient both ventriculography and arteriography failed to locate the tumour and successful biopsy was carried out on the result of the brain scan.

It must not be forgotten that the method can only be carried out in centres where trained physicists, clinicians and other staff with the necessary experience and facilities to handle radioactive isotopes are available. Problems such as incontinence of patients, for example, with contamination of hospital equipment needs careful supervision. However, within these limitations and those mentioned above it is a useful addition to the diagnostic armamentarium.

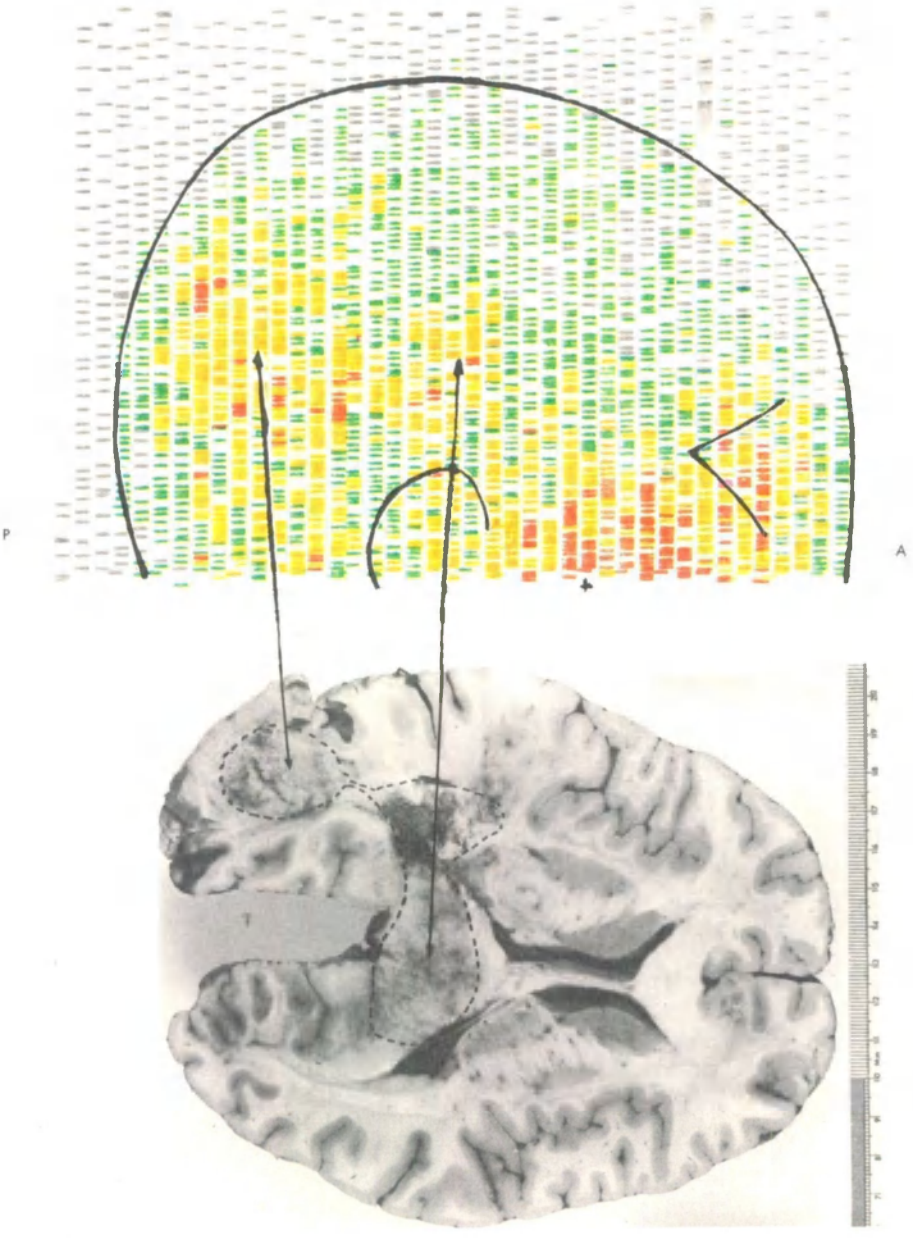

Fig. 4

Section showing occipital glioma infiltrating the posterior half of the corpus callosum with the lateral colour scan (I^{131} H.S.A.). The tumour is seen as the higher count-rate yellow marks.

5. A QUANTITATIVE APPROACH TO THE ANALYSIS OF CEREBRAL SCANS

A technique has been developed primarily to help in the interpretation of those cerebral scans in which there is no strikingly obvious abnormality but in which a visual inspection suggests that there may be an abnormality but one which requires some statistical analysis for its confirmation.

5.1. The A.P. scan

Interpretation of the borderline A.P. scans is generally based on symmetry or lack of symmetry between the left and right sides. In the borderline cases a count is made of the number of marks in equal areas of a grid in anatomically equivalent positions, as shown in Fig. 5. The difference

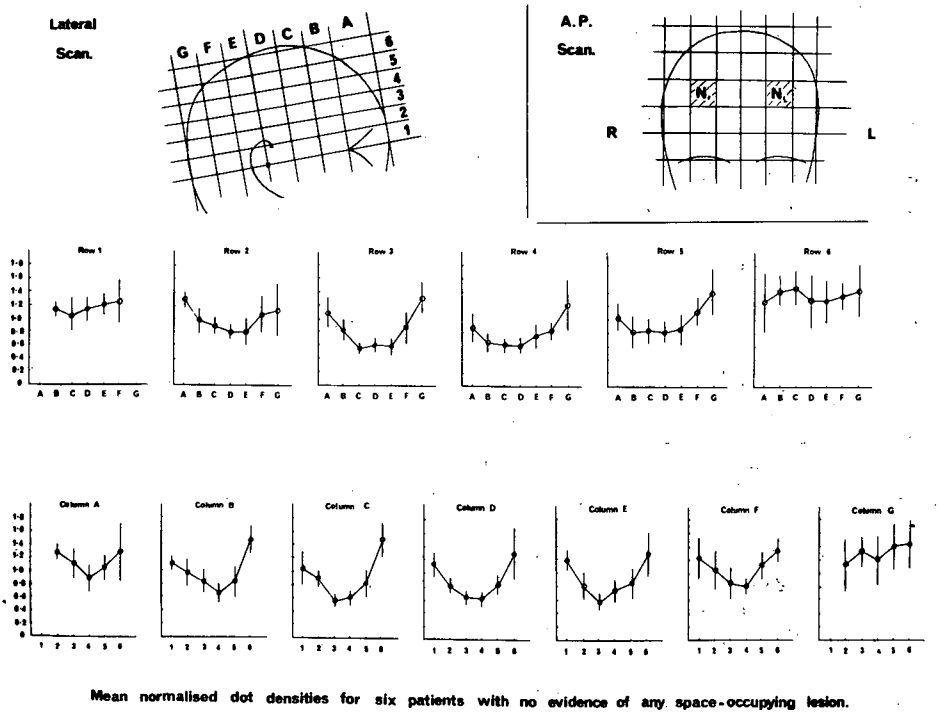

Fig. 5

The quantitative analysis of brain scans. In A.P. scans, equivalent areas on either side are compared. The method of constructing the grid used for the lateral scan is shown. The family of profile curves along the lines of the grid show the variation of normalized dot densities from area to area of the grid averaged for six patients with no evidence of any space-occupying lesions.

in count-rate $N_R - N_L$ is reported as abnormal if it is 4 or more standard deviations of the difference ($\sqrt{(N_R + N_L)/P}$ where P is the print-out number), probably abnormal if between 3 and 4, borderline normal from 2 to 3 and

normal if less than 2. For borderline abnormalities on the mid-line a procedure similar to that given below for lateral scan interpretation must be adopted.

5.2. The lateral scan

The borderline lateral scan is more difficult to interpret than the A.P. scan and each one must be viewed in comparison with the normal pattern. Because of variations in the normal pattern it is seldom satisfactory to interpret by inspection, that is, by comparing the appearance of the scan in question with a selection of normals. This is particularly so if the region of interest lies in or near regions which normally have high count-rates for it is then difficult to decide by inspection whether the pattern is a normal variant of abnormal.

A procedure has been developed to obtain the mean normal dot density pattern in quantitative terms for comparison with the scan in question. The grid shown in Fig. 5 gives areas which, as far as possible, are anatomically similar from patient to patient. It is obtained by dividing the distances between certain external bony features of the skull into equal parts, as seen in Fig. 5. The dot density is determined for each of the areas produced and each one is normalized by dividing by the average dot density for the whole head (i.e. total dots/total area).

The normal dot density pattern has been determined by considering six cases with no known space-occupying lesion. The findings are most conveniently displayed as a family of profile curves in which the average normalized dot density together with a standard deviation is plotted against position in the head (see Fig. 5). The profile curves for a suspect scan may be superimposed on the appropriate normal curves, and any increase in dot density is then immediately apparent. The increase may be expressed as as a multiple of the standard deviation (S.D.) of the difference between the normalized dot density in a given grid position for the suspect scan and the corresponding average normalized dot density for the normal scans.

Figure 6 shows the lateral scan of a patient in which, by inspection, the colour and dot density appeared to be slightly higher than normal in the parietal region. The scan was analysed, as above, and Fig. 7 shows the appropriate curves for comparison with the normal; grid position 3C (5 S.D.), and possibly 3D, 2C, 2D, 4C and 4D (range 1.5-2.7 S.D.) are regions of abnormally high uptake. A tumour, thought to be a glioblastoma, was subsequently found in this region.

In order to assess the value of this technique the lateral scans of 8 patients with proven lesions selected at random have been analysed in this way. Each of these eight scans might have been interpreted as being normal on the basis of qualitative inspection of the black and white pattern alone. The results are given in Table IV. Column 5 gives the number of grid positions adjacent to the one with the largest dot density difference from normal (Col. 4) where the difference is greater than 1.5 S.D. Although one single grid position may not show a significant dot density difference by itself, several questionable differences will increase the significance. This is illustrated by patient A.C. where in five grid positions the difference was

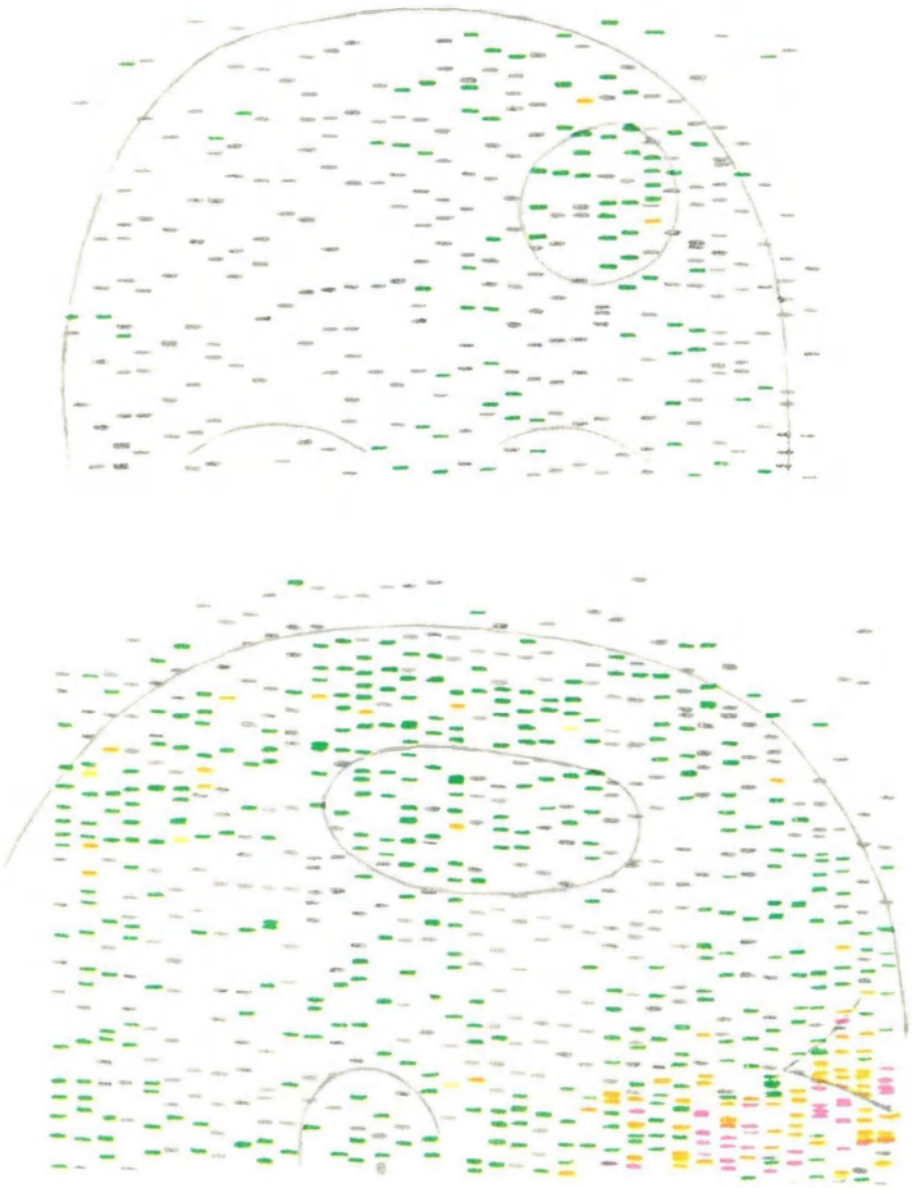

Fig. 6

A.P. and lateral scan (As^{74}) of the patient analysed in Fig. 7, showing a slightly increased count-rate in the parietal region. A tumour, thought to be a glioblastoma was found in this region.

only 80–90% significant in each one but nevertheless the region showed an overall significant increase which corresponded to a proven lesion.

Of these eight difficult cases, the colour scan gave the correct answer in five of them. For the other three, the lesions were in the temporal re-

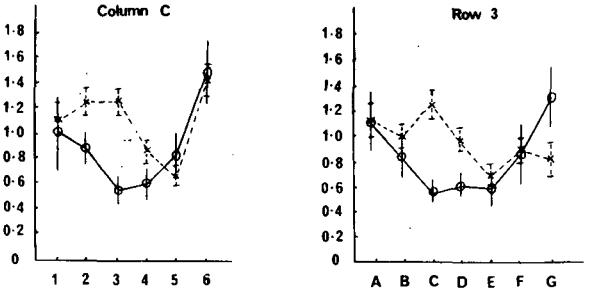

Fig. 7

The profile curves obtained from the scan shown in Fig. 6 superimposed on the mean curve for six patients with no evidence of any space-occupying lesion

——O—— Normal (mean of 6)

– – – x – – – Patient W.G.

The normalized dot densities in anatomically equivalent regions for patient W.G. compared with the mean for six patients with no evidence of any space occupying lesion

gion and two of them were still not detected by the analysis, but for the third (L.S.) the analysis showed a significant increase over the tumour site (there were other areas showing increases, however, which could have been considered abnormal). It may be that the apparent increases found in some scans (e.g. A.R.) are due to inaccurate positioning of the outer canthus and external auditory meatus, movement of the patient on previous investigations disturbing the intracranial dynamics. The validity of this method of interpretation depends on the use of a grid, variable from patient to patient, based on external bony structures and assuming that it is related to internal anatomy. In the case of count-rates obtained in cerebral scanning, the small S.D. of the mean values found for six normals suggests that this is not far from the truth. We have been encouraged by the work of DI CHIRO [21] who has paid much attention to the relationship between the normal anatomy of the brain and the normal isotope scan.

It may prove to be possible to present the information of the normal dot density pattern to a computer so that when a patient's scan is fed directly into it areas of abnormality can first be found by the computer. Perhaps this method of analysis may have applications to scans of other regions of the body.

6. PRESENT DEVELOPMENTS

6.1. The use of Bi^{206}

The Medical Physics Department is currently engaged in investigating the possible use of cyclotron-produced Bi^{206} for cerebral scanning. MATTHEWS and MOLINARO [22] have carried out experiments in which both the uptake of a subcutaneous fibrosarcoma and that of normal brain has been measured in rats for 17 different radioactive substances. Figure 8 shows the ratio of tumour: brain concentration for these substances at stated times after

TABLE IV

QUANTITATIVE ANALYSIS OF EIGHT SCANS USING THE METHOD DESCRIBED IN SECTION 5

Patient	Site of lesion	Type of lesion	Max. no. of S.D. difference over site of lesion	No. of adjacent grid position 1.5 S.D. diff.	First report from colour scan
A.C.	Temporal	Haematoma	1.9	2	Correct
W.G.	Parietal	Glioblastoma	5.0	4	Correct
H.G.	Parietal	Secondary cancer	2.7	1	Correct
D.M.	Posterior frontal	Astrocytoma IV	4.3	4	Correct
D.R.	Parietal	Astrocytoma III	3.4	5	Correct
A.R.	Temporal	Astrocytoma III	0.4 (1.4)*	0 (0) *	Incorrectly placed
L.S.	Temporal	Oligodendroglioma II	2.4 (4.1) *	5 (8) *	Reported normal
E.W.	Temporal	Astrocytoma II	0.0 (2.0) *	0 (4) *	Incorrectly placed over site of burr hole

* Refers to regions of increased dot density other than over site of lesion

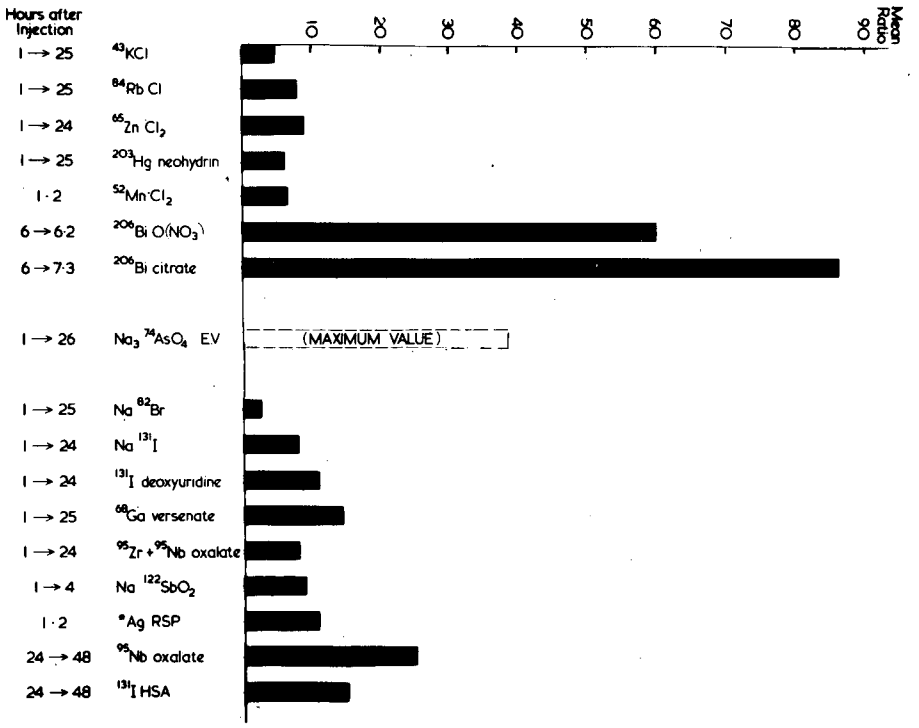

Fig. 8

The ratio of concentration in a subcutaneous fibrosarcoma to that in normal brain in rats for 17 radioactive substances. (MATTHEWS and MOLINARO [22].)

intravenous injection. The value found for iodine-labelled albumen is 16 whilst that for arsenate is more than twice as great at 38, but Hg^{203}-neohydrin was only 7. By far the greatest ratio was found for bismuth citrate at about five times the albumen ratio. This improvement was due primarily to a low brain uptake of bismuth rather than an increased tumour uptake and is accompanied by a lower muscle and blood level as compared with the other materials. As a result the brain background should be reduced as also the masking effect of muscle; the bone level is similar to that of the other materials.

Bi^{206} has been used for brain-tumour localization by MUNDINGER [14] but not using scintiscanning. He determined timed counts in 18 positions over the head and recorded the difference between counts taken on the right and left side; in 56 patients he claims 87.5% efficiency. He also found that the variation of count-rate over the lesion with time depended on the type of lesion and the localized vascular lesions could be differentially diagnosed.

Bi^{206}, with a half-life of 6.3 d, has a complex spectrum of γ-rays from 180 kV to 1.7 MeV but a large proportion of the radiation is from 77 keV X-rays formed by internal conversion. Preliminary attempts were made to scan patients using doses of 250 μc of Bi^{206}. The body background was excessively high, not only due to radiation penetration of the shield, which

was as thick as could be tolerated, but also because of a high retention of the isotope in the body. Measurements of the urinary excretion of bismuth from three patients indicated that only about 10% of the dose had been excreted by this route at the time of the scan (20 h). As a result it will be necessary to devise techniques to reduce the body background counts by a factor of 10 before this material can be used satisfactorily for scanning.

6.2. The use of a gamma camera

A prototype gamma camera using a 5-in-diam. $\frac{1}{2}$-in thick crystal with a 3/8-in-diam. pinhole and a storage tube display [23-24] was used to examine some of the patients sent for scintiscanning with iodine-labelled albumen. Figure 9 shows A.P. and lateral camera pictures taken in only about one third of the time of the scintiscanning technique. This particular

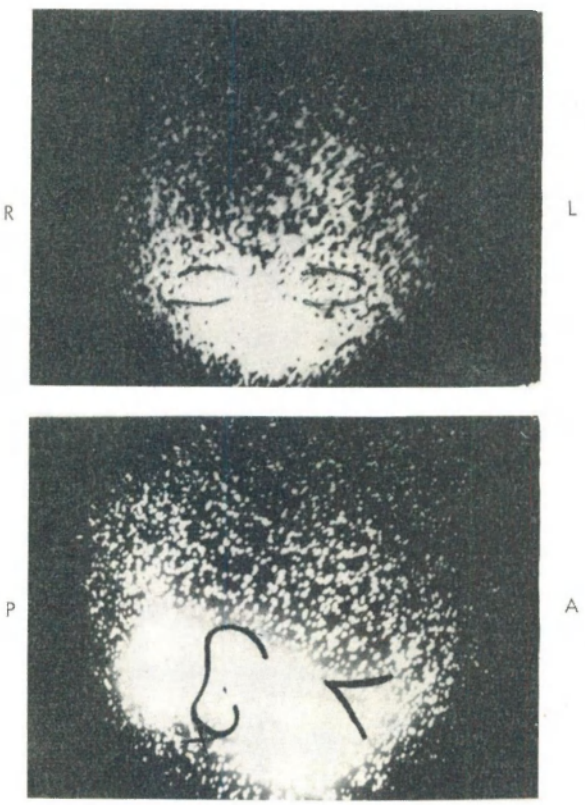

Fig. 9

A.P. and lateral scans (I^{131} H.S.A.) of the same patient as Fig. 4 taken with a gamma camera in one third of the time needed for the colour scintiscan. The tumour was seen much more clearly in the A.P. gamma camera picture than in the colour scan. (The lateral scan shown here has been damaged in reproduction but the tumour can still be perceived in the occipital region.)

tumour was clearly perceived on both machines but was much more visible in the A.P. view taken with the camera than with the colour scan.

We have found the difficulties arising from geometrical distortion to be quite considerable and, combined also with the difficulty of marking anatomical features satisfactorily on the pinhole camera display, have not yet used it routinely. We agree with the findings of BENDER [25] that the use of a grid collimator reduces geometrical distortion of the image and have also used a grid providing three times the sensitivity of the pinhole system.

We are at the moment constructing a 7-in crystal camera and intend to incorporate into it logarithmic amplifiers instead of the usual linear ones which follow the photomultipliers. The dependence of the positioning signals on γ-ray photon energy should be removed which should make it possible to use much wider channel widths than hitherto and thereby improve sensitivity for the same crystal size.

6.3. *Profile scanning of the head*

The method of quantitative analysis of cerebral scintiscans described in section 5 results in the presentation of a series of count-rate profiles along different lines across the head. It is possible that in the typical cerebral scan, much time is spent acquiring information in regions of comparatively little interest which could be devoted to a more important region.

The use of continuous averaging techniques to improve the signal-to-noise ratio should be of value. A line of several highly collimated collimators could be moved to and fro across the head at fairly rapid speeds their pulse outputs being fed into a multichannel analyser. Each channel of the analyser accepts only the pulses from a small portion of the traverse across the head from a given counter and at each traverse, the pulses received from the same portion are summed. The random background will increase as the square root of the number of traverses whilst the tumour-to background count-rate difference increases linearly; the tumour-to-background ratio is thereby improved at each traverse. For a given area scanned over a given time there is no extra information acquired compared with conventional scanning but it may enable one to spot the suspicious area more quickly and therefore allow one to spend much more time traversing this important region alone.

Finally, the use of multichannel analysers together with such a scanning system makes it possible to present a display in the form shown in Fig. 10 which is taken directly from a manufacturer's data sheet. X and Y co-ordinates present the area of scan whilst count-rate at a point appears as a height displacement of the appropriate spot. An effect of hills and valleys like a contour map is produced, which is very similar to the three-dimensional representations of composite profile scans (taken in the conventional way) by MacINTYRE, CRESPO and CHRISTI [26] and DOERING [28]. In addition, because of bunching of spots on one side of the hills and valleys, an extra visual contrast is displayed. The count-rates can be read off at will for any chosen co-ordinates. This display could also possibly be used with gamma cameras. It would be very exciting to apply this technique to cerebral scanning.

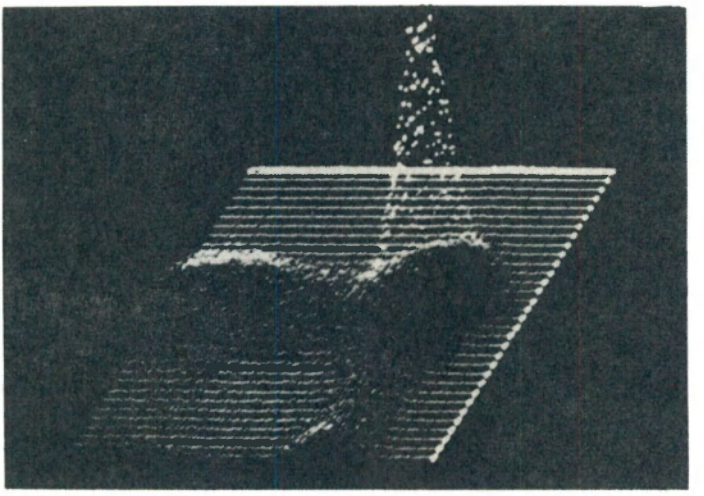

Fig. 10

Possible form of display using multichannel analyser. Count-rate is displayed as a height displacement from the xy plane and can be read out for any point. Used in conjunction with a multicounter system (one for each line) moving to and fro fairly rapidly. continuous averaging will improve tumour-to-background ratio. The display could also be used with a gamma camera.

7. CONCLUSION

The results of a small clinical series of cerebral scans carried out using two different radioactive materials have been presented. The two techniques were different, one using a positron emitter with coincidence circuitry, the other using a focusing collimator with a gamma emitter, but their point-source isocount characteristics were made very similar by the use of a long-focusing 'depth-independent' 19-hole collimator. The percentage of successful localizations shown in Table III is somewhat lower than that of other workers with much larger clinical series but the criteria used to score a success have been very rigid.

An analysis technique is described to aid the more accurate reporting of the presence or otherwise of abnormalities in cerebral scans and current work to improve the scope and accuracy of the isotope localization technique include the use of Bi^{206}, the gamma camera, and continuous averaging techniques.

We are confident that the method will take its place in the diagnostic side of a neurological and neurosurgical department, principally because of its relatively harmless nature and secondly as a further aid in the solution of problems that patients with neurosurgical disease present.

ACKNOWLEDGEMENTS

Our thanks are due to the British Empire Cancer Campaign for a grant to one of us (J.B.) and to the Medical Research Council who have granted

equipment and financial support to J.P.M. and M.M. respectively, which made this study possible. We are indebted to Mr. Wylie McKissock and Mr. L.S. Walsh of the Neurosurgical Department of St. George's Hospital at Atkinson Morley's Hospital and members of the Department of Medicine, Postgraduate Medical School and Radiotherapy Department, Hammersmith Hospital for permission to study and publish their cases. Our thanks are finally due to the technical, photographic and secretarial staff for their invaluable help, and finally to the Director and staff of the Medical Research Council Cyclotron Unit for supplying radioactive materials and advice.

REFERENCES

[1] BROWNELL, G.L., Int.J. appl. Rad. Isotopes 3 (1958) 181.
[2] SWEET, W.H. and BROWNELL, G.L., J. Amer. Med. Ass. 157 (1955) 1183.
[3] SWEET, W.H., MEALEY, J., BROWNELL, G.L. and ARONOW, S., Medical Radioisotope Scanning, IAEA, Vienna (1959) 136.
[4] TURNER, P.C.R., D'ARCY, J., MALLARD, J.R. and FOWLER, J.F., Proc. 3rd Int. Conf. Med. Elect., London (1960) 513.
[5] MALLARD, J.R., FOWLER, J.F. and SUTTON, M., Brit. J. Radiol. 34 (1961) 562.
[5a] MALLARD, J.R. et al., An analysis of quantitative colour display for scanning, these Proceedings.
[6] MALLARD, J.R., Proc. Roy. Soc. Med. 56 (1963) 680.
[7] DYSON, N.A., Phys. Med. Biol. 4 (1960) 376.
[8] ARONOW, S., Progress in Medical Radioisotope Scanning, Oak Ridge, USA (1962) 371.
[9] TURNER, P.C.R., Phys. Med. Biol. 7 (1962) 329.
[10] MEALEY, J., BROWNELL, G.L. and SWEET, W.H., Arch. Neurol. Psychiat, Chicago 81 (1959) 310.
[11] DI CHIRO, G., Acta Radiol. Suppl. 201 (1961)
[12] BROWNELL, G.L., Medical Radioisotope Scanning, IAEA, Vienna (1959) 1.
[13] BASCHIERI, I. and D'ARUZZO, B., Nucl. Medizin 2 (1962) 290.
[14] MUNDINGER, F., Nucl. Medizin 1 (1959) 167.
[15] FRANCIS, J.E., HARRIS, C.C. and BELL, P.R., J. Nucl. Med. 3 (1962) 10.
[16] DEWEY, W.C. and SINCLAIR, W.K., Int.J. appl. Rad. Isotopes 10 (1961) 1.
[17] MYHILL, J., Int. J. appl. Rad. Isotopes 12 (1961) 10.
[18] HARRIS, C.C., BELL, P.R., FRANCIS, J.E., SATTERFIELD, M.M., JORDAN, J.C. and MURRAY, J.P., Progress in Medical Radioisotope Scanning, Oak Ridge, USA. (1962) 25.
[19] MYERS, M.J. and MALLARD, J.R., Int. J. appl. Rad. Isotopes (1964) in press.
[20] CRADDUCK, T. and FEDORUK, S.O., J. Con. Ass. Radiol. 13 (1959) 9.
[21] DI CHIRO, G., Progress in Medical Radioisotope Scanning, Oak Ridge, USA (1962) 347.
[22] MATTHEWS, C.M.E. and MOLINARO, G., Brit. J. Exp. Path. 44 (1963) 260.
[23] MALLARD, J.R. and MYERS, M.J., Phys. Med. Biol. 8 (1963) 165.
[24] MALLARD, J.R. and MYERS, M.J., Phys. Med. Biol. 8 (1963) 183.
[25] BENDER, M.A. and BLAU, M., Nucleonics 21 (1963) 52.
[26] MACINTYRE, W.J., CRESPO, G.G. and CHRISTIE, J.H., J. Nucl. Med. 1 (1960) 262.
[27] BENDER, M.A. and BLAU, M., Progress in Medical Radioisotope Scanning, Oak Ridge, USA (1962) 388.
[28] DOERING, P., Medical Radioisotope Scanning, IAEA, Vienna (1959) 159.

DISCUSSION

H.A.B. SIMONS: Have you tried a more sophisticated statistical technique to analyse your brain-scanning results? Have you compared the efficiency of scanning with other clinical techniques, such as angiography, for tumour detection?

J. MALLARD: We have not done this, but our neuro-surgeon, Mr. Brice, has compared all our reports with the data obtained by other procedures on the same patients. Surely the important questions here are whether the scan can show information which is missed by other methods and whether there is less risk to the patient in cases where the information obtained is similar.

SELECTIVE NEOPLASM LOCALIZATION WITH MERCURY-197 NEOHYDRIN

D.B. SODEE
DOCTORS HOSPITAL AND RENNER CLINIC FOUNDATION, CLEVELAND HEIGHTS, OHIO, UNITED STATES OF AMERICA

Abstract — Résumé — Аннотация — Resumen

SELECTIVE NEOPLASM LOCALIZATION WITH Hg^{197} NEOHYDRIN. Hg^{197}, a low-energy X- and gamma-ray emitter (2.7-d half-life, 69-keV conversion X-rays, 77-keV gamma-rays) was tested as a scanning agent in a large series of patients. Five hundred patients suspected of neuro-surgical disease were scanned with Hg^{197}-Neohydrin. Utilizing photoscanning techniques that brought out vascular lesions as well as tumours, this procedure had a 96% correlation with the final diagnostic evaluation. This screening procedure was done before all other diagnostic tests.

As an outgrowth of this brain-scanning procedure, we have found localization of Hg^{197}-Neohydrin in lymphomas as well as in carcinomas. There seems to be selective deposition of the radioactive substance intercellularly. Areas of increased uptake of radioactivity can easily be delineated with standard commercial scanners.

Hg^{197}-Neohydrin was also found to be useful as a screening agent in the differentiation of eye tumours in a series of 88 patients and recently this low-energy radiopharmaceutical was found to concentrate in naso-pharangeal tumours which could then be delineated by photoscanning.

The diagnostic dose of Hg^{197}-Neohydrin for brain scanning delivers a radiation dose of 3 rad to the kidneys as compared to the 70 rad delivered to the kidneys by that of Hg^{203}-Neohydrin.

The high counting efficiency and ease of collimation of Hg^{197} make this isotope far better for scanning purposes than all other standard diagnostic scanning agents.

LOCALISATION SÉLECTIVE DE NEOPLASMES A L'AIDE DE LA NÉOHYDRINE MARQUÉE AVEC ^{197}Hg. Le mercure-197, émetteur de rayons X et de rayons gamma de faible énergie (période de 65 h, rayons X de 69 keV, rayons gamma de 77 keV), a été essayé comme agent d'exploration scintigraphique sur un grand nombre de patients. On a utilisé la néohydrine marquée avec ^{197}Hg pour la scintigraphie de 500 cas de neurochirurgie. Par des procédés de photoscintigraphie qui permettaient la visualisation des lésions vasculaires aussi bien que celle de tumeurs, on a obtenu des résultats confirmés dans 96% des cas par le diagnostic final. La scintigraphie était toujours faite avant tous les autres tests.

L'application de cette méthode de scintigraphie du cerveau a permis, en outre, de constater que la néohydrine marquée avec ^{197}Hg était localisée aussi bien dans les lymphomes que dans les carcinomes. Il semble y avoir dépôt sélectif de la substance radioactive au niveau intercellulaire. Les zones de fixation accrue de la radioactivité peuvent être aisément délimitées avec des agents scintigraphiques courants.

Des essais sur 88 patients on montré que la néohydrine marquée avec ^{197}Hg était également utile comme agent de détection pour différencier les tumeurs des yeux; enfin, on a constaté tout récemment qu'elle se concentrait dans les tumeurs rhino-pharyngiennes, que l'on pouvait alors délimiter par photoscintigraphie.

La quantité de néohydrine marquée avec ^{197}Hg nécessaire à une scintigraphie du cerveau délivre au reins une dose de 3 rad, contre 70 rad pour la néohydrine marquée avec ^{203}Hg.

Du fait de la grande efficacité de comptage et de la facilité de collimation, ^{197}Hg convient mieux que tous les autres agents classiques de diagnostic par scintigraphie.

ОБНАРУЖЕНИЕ ОПУХОЛЕЙ С ПОМОЩЬЮ НЕОГИДРИНА, МЕЧЕННОГО РТУТЬЮ-197. Ртуть-197—излучатель рентгеновских и гамма-лучей малой энергии (период полураспада 2,7 дня, конверсионное рентгеновское излучение мощностью 69 кэв, гамма-излучение 77 кэв) был опробован в качестве сканнирующего средства у большого количества больных. У 500 больных с предполагаемыми нервохирургическими заболеваниями произведено сканнирование по излучению неогидрина, меченного Hg^{197}. С помощью метода фотосканнирования удалось выявить поражение сосудов и опухоли, причем эта методика в 96% обеспечивала корреляцию с окончательным диагнозом. Эта методика рентгенологического исследования предшествовала всем другим видам диагностического обследования.

С помощью метода сканнирования головного мозга авторы обнаружили локализацию Неогидрина-Hg^{197} как в лимфомах, так и в карциномах. По-видимому, имеет место межклеточное селективное отложение радиоактивного вещества. Участки усиленного поглощения радиоактивности можно легко определить с помощью стандартных имеющихся в продаже сканнирующих устройств.

Неогидрин, меченный Hg^{197}, оказался пригодным средством для радиологического исследования при установлении дифференциального диагноза глазных опухолей у 88 больных. Недавно было обнаружено, что этот радиофармацевтический препарат с мягким излучением концентрируется в опухолях носоглотки, контур которых можно затем определить с помощью фотосканнирования.

Диагностическая доза неогидрина – Hg^{197} для сканнирования головного мозга создает дозу облучения почек, равную 3 рад, в то время как диагностическая доза неогидрина – Hg^{203} создает дозу облучения в 70 рад.

Благодаря высокой эффективности счета и легкости коллимации Hg^{197}, этот изотоп в гораздо большей степени отвечает целям сканнирования, чем все другие стандартные средства диагностического сканнирования.

LOCALIZACIÓN SELECTIVA DE NEOPLASMAS CON NEOHIDRINA-^{197}Hg. El autor ensayó como agente de exploración el ^{197}Hg, emisor de rayos X y gamma de baja energía (período: 2,7 d; rayos X de conversión: 69 keV; rayos gamma: 77 keV). Quinientos pacientes, que presentaban síntomas de afecciones neuroquirúrgicas, fueron examinados mediante neohidrina-^{197}Hg. Aplicando técnicas de fotoexploración que revelan tanto las lesiones vasculares como los tumores, se comprobó que entre los resultados así obtenidos y el diagnóstico definitivo había una correlación del 96%. Ese procedimiento de examen se aplicó antes de proceder a las demás pruebas diagnósticas.

Como resultado de la aplicación de ese procedimiento de exploración del cerebro, el autor descubrió localizaciones de neohidrina-^{197}Hg en linfomas y carcinomas. Al parecer, la sustancia radiactiva tiende a depositarse selectivamente en regiones intercelulares. Con los aparatos de exploración de tipo comercial se pueden delinear fácilmente las zonas de mayor absorción de radiactividad.

También se comprobó la utilidad de la neohidrina-^{197}Hg para la diferenciación de tumores oculares en una serie de 88 pacientes; recientemente se ha observado que este compuesto radiofarmacéutico de baja energía se concentra en los tumores nasofaríngeos que luego pueden delinearse por fotoexploración.

La dosis diagnóstica de neohidrina-^{197}Hg administrada para la exploración del cerebro entraña la absorción de 3 rad por el riñón; la de neohidrina-^{203}Hg entraña la absorción de 70 rad por este último órgano.

El elevado rendimiento de recuento del ^{197}Hg y la facilidad con que se colima las radiaciones que emite, hacen que este isótopo resulte mucho más útil para la exploración gammagráfica que cualquier otro de los agentes habitualmente empleados.

Screening methods for the detection of carcinoma are always being sought. Radioisotope methods utilized in the past for the detection of carcinoma have been tedious due to the choice of isotopes and, in some cases, the inadequacy of the equipment used [1, 2, 3]. Recently, during our routine, studies of brain scanning and renal scanning utilizing mercury-197 Neohydrin, we found that this compound was also localized in other tumours in all areas of the body [4]. Our studies on the scintillation detection of carcinoma utilizing mercury-197 Neohydrin will be presented.

METHODOLOGY

Picker Nuclear Magnascanners, Model 1108 B, were utilized throughout this study. For the last portion of the study, a 5×2-in sodium-iodide crystal was substituted for the 3 × 2-in crystal. For all large organ scanning, a lead 19-hole collimator was used.

When mercury-203 was utilized, an 80-keV window was centred on the 279-keV photopeak of this isotope. For all studies when mercury-197 was

utilized, a window of 60-90 keV was used. In vitro tissue-counts were done with a 2×2-in sodium-iodide crystal and pulse-height analyser.

DISTRIBUTION OF RADIOMERCURY-197 NEOHYDRIN

Shortly after the injection mercurial compounds are protein bound, and in the tracer amount utilized for scanning are primarily bound to the active sulph-hydral amino acids cysteine and glutathione [5, 6]. Soon after injection, an increasing amount of mercury-labelled chlormerodrin is found in the red cell fraction and the peak concentration of 33% of the total blood radioactivity is found in the red cell fraction at 2 h. The clearance of chlormerodrin in blood has been found in patients to be between 3-6 h and the 24-h urinary excretion is 80% of the administered dose. The normal tissue concentrations of mercurials are found where active enzymatic activity is taking place, with decreasing concentrations being found in the kidney, liver, spleen and intestine. The mercurials are readily diffusible into and out of cells; however in all tissues a percentage of the mercury entering the cell remains as this heavy metal combines with active protein moieties and this reaction causes denaturization of proteins intracellularly [7].

The mercurial denaturization of protein has been utilized to identify specific active mercaptan groups of proteins. This mercurial localization in the renal tubule cell has been utilized by our group and other investigators to detect unilateral renal disease by following the concentrations of radioactive mercury-labelled chlormerodrin in the kidney by uptake and scanning.

RADIATION DOSIMETRY OF Hg^{197} NEOHYDRIN

Using whole-body counts the effective half-life of Hg^{197} Neohydrin in the body was calculated to be 0.23 d. Utilizing the Hg^{197} characteristics described above, the whole-body radiation dose is 17 mrad/mc patient dose.

The renal retention of mercury has been found by ourselves and others to be approximately 10%. In sacrificed normal dog kidneys and in externally counted human kidneys the effective half-life of mercury in the kidneys has been found to be 18 d. However, with Hg^{197} the effective renal half-time cannot be greater than the physical half-life of the nuclide which is 2.7 d. The radiation dosage to the kidneys is then 0.80 rad/150-μc patient dose. Thus the renal radiation dose of Hg^{203} Neohydrin of 42 rad is greatly reduced by utilizing mercury-197 Neohydrin [8].

CANCER DETECTION WITH MERCURY-197 NEOHYDRIN

In the beginning of this study, we scanned areas suspected of carcinomatous change at various times during a 72-h period. We found that in the majority of cases, the 24-h post dose scan was most acceptable for several reasons. The blood background at 24 h had been reduced to a minimum, and for reasons being investigated the carcinoma cell retained the

most radioactive mercury, therefore making a good target-to-non-target ratio for clinical scintiscanning. In tumour areas in proximity to areas which normally concentrate mercury, we utilized thin lead shielding over the normal area, thus allowing us to concentrate on the tumour-involved area. Superimposition X-rays were done with small pieces of lead placed around the suspicious tumour area. Throughout this study we utilized 1 mc of mercury-197 Neohydrin intravenously.

RESULTS

Mercury accumulation, at 24-h post dose with 15-20% differential between the tumour and the uninvolved skin, was found in the squamous cell carcinomas (Table I). The malignant tumours of the nasopharynx were visualized and particularly in this anatomic position the positive photoscans were quite useful to the radiation therapist in planning his field of therapy. The scans of the lymphomas were useful in classifying the extent of these diseases, and therefore in the planning of their therapy. Bone tumours, both primary and metastatic, were visualized by scan before X-ray changes could be seen.

In the eye patients where the areas of tumefaction were quite small, we did confirmatory counting studies with a $\frac{1}{4}$-in scintillation crystal and ratemeter at 2-, 5- and 24-h post dose as well as photoscanning the orbital areas. It was found at an early time that the malignancies concentrated mercury best in the 24-h count and there was as much as 100% difference between the involved area and the uninvolved area of the eye. Two of the eye tumours were missed by the counting and scanning procedures because of their small size.

The bowel adenocarcinomas were the most difficult to visualize because the normal bowel mucosa also accumulates mercury. However, in the bowel tumours different rates of tumour turnover could be detected by scanning 24- and 48-h post dose of mercury-197 Neohydrin.

The false positives in this series of patients were found in the granulomatous diseases. The histoplasmomas and tuberculomas concentrated more mercury on in vitro count of the lesions than did the carcinomas. This was particularly noticeable when evaluating coin lesions of the lung.

MECHANISM OF MERCURY LOCALIZATION IN MALIGNANT TISSUE

Mercurial compounds are almost completely protein bound in vivo, with the protein binding being non-specific with the exception of the very reactive sulph-hydral amino acids such as cysteine and glutathione. The non-specificity of reaction of heavy metal cations such as mercury with proteins deserves stress, although at low concentrations the reaction with -SH does appear the most significant [9]. It has been well documented that mercury concentration then progressively increased in order of concentration in the renal tubular cell and the hepatic cell. These are two cells where sulph-hydral enzymes are found in great concentration. However, intracellular

TABLE I

CANCER DETECTION WITH Hg^{197}-Hg^{203} CHLORMERODRIN (Primary-Metastatic)

Organ	Malignant	Benign	Hg Conc.	No Hg Conc.	False positive	False negative
Eye	32	59	30	61	-	2
Lung	7	10	12	5	5*	-
Nasopharyngeal	20	36	20	36	-	-
Lymphoma	7	-	7	-	-	-
Leukemia	1	-	1	-	-	-
Pancreas	1	2	1	2	-	-
Stomach	3	3	3	3	-	-
Skin	5	4	5	4	-	-
Bowel	5	2	5	2	-	-
Bone	5	1	5	1	-	-
Breast	5	4	4	4	-	1
Prostate	2	-	2	-	-	-

* Histoplasmomas and tuberculomas

combination with certain protein moieties form insoluble compounds that remain in the cell.

Mercury when linked through one covalent bond to an organic moiety reacts essentially with one -SH per molecule according to the simple equation R-Hg-X+R'S→R-Hg-S'-R'+x.

Like inorganic Hg^{++}, organic mercurials have a high affinity for anions or groups with an available pair of electrons.

Organic mercurials can cause inhibition of enzymes other than by reaction with -SH groups, and interact with thyroxine and related compounds.

The following possibilities for mercury cellular localization are being explored:

(1) The increased mercurial content and retention we find in tumour tissue can have multiple explanations. Cancer cells have a higher amino acid content than normal cells, therefore, more -SH are available for mercury association [9].

(2) The presence of a trace amount of the chelating metal Mn has been shown to enhance amino acid transfer into cells, and the cellular uptake of this element by the cell was faster if the cells had been preloaded with amino acid. The A and B amino acids were accumulated whereas gamma amino acids were not. A second nitrogenous group removed 2-3 atoms from the amino group, greatly intensifying uptake. Structural features that increased ease of proton displacement from the amino group intensified uptake. A metal cation would be expected to displace this proton in forming a neutral chelate. Thus, mercury may be taking part in this transfer, and accumulating in the cell.

(3) Cysteine and glutathione are basic amino acids and have specificity for mercury association, therefore, more mercury may be carried into the tumour.

(4) Cancer mitochondria have deficient cell membrane with ion transfer changes as well as increased fragility. Mercury itself will have detrimental effects on membranes, therefore causing eflux of proteins making more complexes with mercury or allowing mercury influx across the membrane. Wenner has shown that the link uniting DPN to mitochondria is not as strong in cancer as normal tissues allowing easier passage to cytoplasm [7].

(5) The cancer cell has increased DNA production, therefore increasing the utilization of the oxidative enzymes which utilize cysteine and glutathione for electron transfer. As mentioned before, these amino acids are mercury carriers [10].

(6) The intense proteins synthesis in cancer cells makes it probable that more mercury will be bound intracellularly [11].

DISCUSSION

For the past 20 yr, isotopic methods for speeding diagnosis have been developed and recently photoscanning, utilizing labelled pharmaceuticals, has grown in popularity. The commercial instrumentation and radiopharmaceuticals have joined in our effort to make the radioisotope detection of disease processes a practical, inexpensive shortcut to surplant our now te-

dious diagnostic methods. For the last 2 yr we have been utilizing mercury-197 Neohydrin as a useful brain scanning pharmaceutical and as a practical renal scanning compound. Recently, we found that this radiopharmaceutical is concentrated by tissue that has undergone carcinomatous change. This 24-h measurable accumulation has been found in all areas of the body that have become carcinomatous with the exception of those organs that normally concentrate mercury to a high degree, such as the liver and kidney. This mercury accumulation has been demonstrated by in vitro counting techniques and by our clinical photoscanning techniques. It is hoped that this preliminary clinical study will promote interest in the biochemical reasons behind this accumulation. We present several theories that may explain this mercury concentration by the carcinomatous cell.

It is hoped that this simple scanning technique for the detection of cancer will have wide application and it is obvious that with accurate delineation of

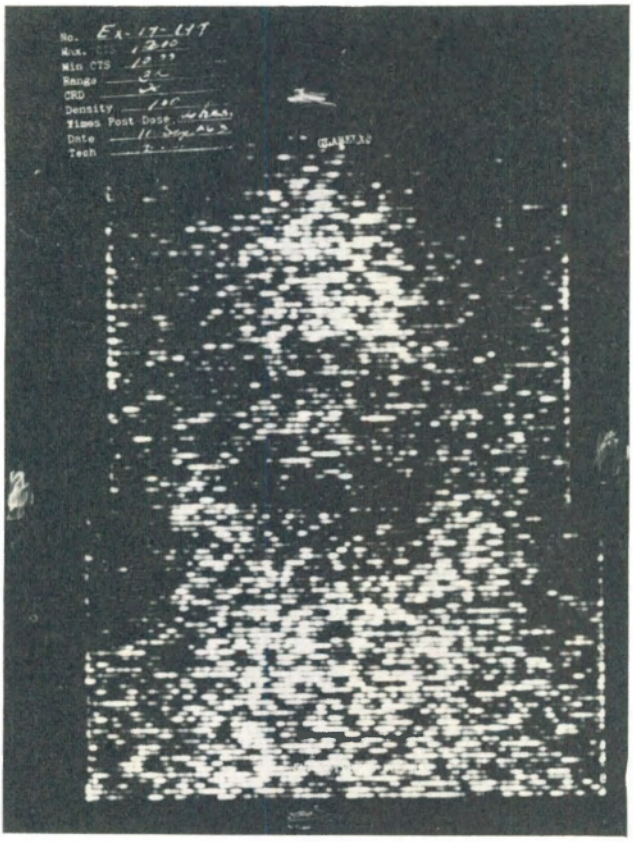

Fig. 1

Below the glabella the concentration of mercury is in the nasopharynx mass of sarcoma invading the soft palate.
The lateral and central concentrations are in palpable lymph nodes involved with reticulum cell sarcoma.

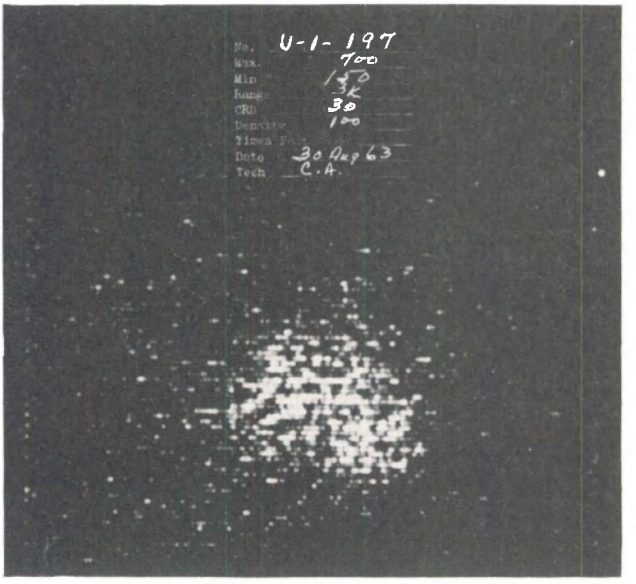

Fig.2

(A) The concentration of mercury-197 visualized on this photoscan is in an area of squamous cell carcinoma involving the right labia majoria and labia minora. The left labia majoria and minora were involved with biopsy-proven leukoplakia.

(B) The second scan is of the surgical specimen showing the distribution of radiomercury on the photoscan. There was no concentration of mercury above normal skin concentration in the area involved with leukoplakia.

the area carcinoma that the fields for radiation therapy may be more accurately planned and the therapeutic results better determined.

SUMMARY

Preliminary clinical work describing the accumulation of mercury-197 Neohydrin in all tumours is presented. Accumulation was found in all tumours; however, in those organs where mercury is normally concentrated this ability is lost with carcinomatous change. Granulomas, probably because of their areas of necrosis, are also found to have a high mercury accumulation.

CASE REPORTS

(1) Progressing symptoms of nasopharyngeal obstruction over a two-month period in a 66-yr-old male. A large tumour mass could be visualized in the nasopharynx and the patient had firm 2 cm×3 cm nodes in the right and left cervical chains. Photoscan done three hours post dose of mercury-197 chlormerodrin revealed concentration of the isotope in the nasopharyngeal mass, its extension into the soft palate and into the cervical node chains.

Scan repeated at 24 h revealed residual concentration in the described area of tumour. Biopsy revealed reticulum cell sarcoma. Well counts revealed the concentration in tumour to be 20 times the concentration in normal surrounding tissue. (See Fig. 1)

(2) White female, 82-yr-old, with a three-month history of pruritus and enlargement of an erythematous mass in the area of the right labia majoria. Physical examination revealed an angry erythematous area of infiltration of connecting tissue in the area. The left labia appeared to be involved with leukoplakia. Photoscan of the area 24 h post dose of mercury-197 Neohydrin revealed mercury uptake in the area of the lesion on the right. Scan of the surgery specimen, it was squamous cell carcinoma, revealed mercury only in the area of the anaplastic tissue. (See Fig. 2)

REFERENCES

[1] THOMAS, C.I., KROHMER, J.S. and STORAASLI, J.P., Detection of Intraocular Tumors with Radioactive Phosphorus, Arch. Ophth. 47 (1952) 276.

[2] WREN, F.R., GOOD, M.D. and HANDLER, P., The Use of Positron-emitting Radioisotope for Localization of Brain Tumors, Science 113 (1951) 525-7.

[3] BALE, W.F., SPAR, I.L. and GOODLAND, R.L., "Research directed toward the use of I^{131}-labeled fibrinogen and antibody to fibrin in the localization and treatment of tumors", Use of Radioisotopes in Animal Biology and the Medical Sciences II, IAEA, Academic Press, London (1962) 271.

[4] SODEE, D.B., "Delineation of Anatomic Structures and the Detection of Carcinoma Utilizing Low Energy Mercury Labeled Chlormerodrin", VIth Int. Symp. Radioaktive Isotope in Klinik und Forschung 6 (1964).

[5] REBA, R., McAFEE, J. and WAGNER, H., Radiomercury labeled Chlormerodrin for in vivo Uptake Studies and Scintillation Scanning of Unilateral Renal Lesions Associated with Hypertension, Medicine 42, No.4 (1963).

[6] MILNOR, J.P., Proc. Soc. exp. Biol. N.Y. 75 (1950) 63.

[7] BOYER, P., LARDY, H. and MYEBACK, K., The Enzymes 1, Academic Press 511-88.
[8] SODEE, D.B., Radiation Dosimetry of Mercury-197 Neohydrin, J. nucl. Med. 5 (1964) 74-5.
[9] CHRISTENSEN, H.N. and RIGGS, T.R., J. biol. Chem. (1956) 220. 265.
[10] Le BRETON, Elaine and MOVLE, Yvonne, "Biochemistry and Physiology of the Cancer Cell, The Cell 2, Academic Press (1961) 498-588.
[11] TAPLEY, D.F., J. biol. Chem. (1956) 222, 325.

DISCUSSION

C. KELLERSHOHN: In your work on the visualization of tumours and anatomical structures, have you tried using mercuric chloride in place of Neohydrin?

D. SODEE: We used mercuric chloride earlier in our work for brain tumour investigations and found that it was concentrated in the same way as Hg^{197}-Neohydrin. We stopped using it because of the high blood background produced for some time following administration. We needed a tracer that would clear rapidly from the blood and so Neohydrin was the obvious choice.

R. WOLF: We have been using Hg^{197} in the form of mercuric chloride to investigate cancer patients. We have found it extremely useful for tumour detection and have obtained good results in cancer of the lung, tongue and ovaries. In one case we were able to visualize a malignant struma that could not be seen with I^{131}. There is, of course, a relatively high blood level for a period of 24 h following administration.

M. AKERMAN: To what extent do you think that the uptake of the tracer by the tumour is affected by hyper-vascularization and neo-vascularization? One always finds these phenomena in malignant tumours.

D. SODEE: I am sure that these vascular changes would increase the delivery of the tracer to the tumour. In our studies of the uptake of Hg^{197}-Neohydrin, however, the concentration was just as high in non-vascular grade-1 astrocytomata as in tumours of other types. Intracellular localization must therefore also be involved.

M. TER-POGOSSIAN: In your study of the basic phenomena involved in the concentration of Hg^{197} in tumours, have you considered using autoradiography by means of the Auger electrons emitted? The resolution would, I think, be very good because of the low energy of the electrons.

D. SODEE: We are starting autoradiographic studies now, using cell cultures of tumour and normal tissue.

M. TER-POGOSSIAN: I should like to mention here that, following your lead, we switched from Hg^{203} to Hg^{197} for the localization of brain tumours. We find that because of the lower muscle background the results are better with the latter, particularly for tumours of the posterior fossa.

L. DONATO: Have you studied the time course of the uptake of Neohydrin in tumours?

D. SODEE: This has been done for several types of tumour. In several of the bowel tumours the mercury in the tumour was detectable for longer than in the normal bowel, which has been shown to turn over in approximately 48 h. The lymphomata seemed almost like the renal tubular cell in that the intra-cellular retention of the mercury was quite prolonged. Obviously, further information on turn-over times in tumours would be of

vast importance and it is clear that a great deal of work will have to be done on this problem.

C. HARRIS: For a time there was a good deal of confusion in the United States about the decay scheme of Hg^{197} and we were asked to investigate this scheme. This was done, apparently successfully. In the course of the work, however, we discovered that the previously accepted values for the mean beta ray energy, $\overline{E}_\beta$, and the gamma-ray dose-rate constant, Γ, for this isotope were in error. We investigated further and began to lose confidence in the classical methods of calculating radiation dose to tissue as applied to Hg^{197} in the kidney, because of the highly localized deposition of mercury in the organ. We are rather worried about this and I should be extremely interested to hear whether anyone else has done any work on this problem.

C. KELLERSHOHN: This question can be discussed in terms of the influence of (a) the decay scheme of Hg^{197} and (b) the spatial distribution of Hg^{197} within the kidney on the distribution of radiation dose to the kidney. In connection with (b), autoradiography shows that mercury is concentrated mainly in the cortex of the kidney. If we consider this zone to be a spherical corona with a uniform concentration of Hg^{197}, we shall not be going too far wrong in dosimetric calculations. Use can then be made of the classical formulae for calculating the radiation dose within a homogeneously radioactive sphere. The dose in the corona, i.e. in the renal cortex, can then be deduced. For an injection of 0.5 - 1 mc of Hg^{197}, the dose to the renal cortex would be of the order of 1 rad.

RADIOIODINATED (I^{131} AND I^{125}) FIBRINOGEN FOR THE DETECTION OF MALIGNANT TUMOURS IN MAN*

G. MONASTERIO, M.F. BECCHINI AND N. RICCIONI
CENTRE OF NUCLEAR MEDICINE,
MEDICAL CLINIC, UNIVERSITY OF PISA, ITALY

Abstract — Résumé — Аннотация — Resumen

RADIOIODINATED (I^{131} AND I^{125}) FIBRINOGEN FOR THE DETECTION OF MALIGNANT TUMOURS IN MAN. A high fibrin content has been shown in a large number of malignant tumours, both experimental and human; this finding has been referred to the high thromboplastin content within the tumour, inducing the polymerization of fibrinogen into fibrin.

On the basis of these data, human fibrinogen labelled with I^{131} and I^{125} has been tested as a possible agent for detecting malignant tumours in man.

The uptake of radioiodinate fibrinogen has been studied in malignant and benign tumours, as well as non-neoplastic space-occupying lesions. Seventy-three cases have been so far examined; 53 of these were represented by malignant tumours localized in the skeleton, lungs, brain, abdominal organs etc. The I^{131}-fibrinogen uptake test gave correct results in 79% of the cases examined; no false positive results were obtained in the whole series. The technique and the results are briefly discussed. From the data obtained, it seems that fibrinogen-I^{131} may be usefully applied for the early detection of malignancies in man; possible improvements of the detection technique may markedly increase the diagnostic value of the method.

EMPLOI DE FIBRINOGÈNE MARQUÉ AVEC ^{131}I OU ^{125}I POUR LA DÉTECTION DE TUMEURS MALIGNES CHEZ L'HOMME. Une teneur élevée en fibrine a été mise en évidence dans un grand nombre de tumeurs malignes, tant chez l'homme que chez des animaux de laboratoire; on a imputé ce phénomène au fait que la tumeur contient une forte proportion de thromboplastine qui provoque la formation de fibrine par polymérisation du fibrinogène.

Sur cette base, les auteurs ont utilisé du fibrinogène humain marqué avec ^{131}I ou ^{125}I pour la détection de tumeurs malignes chez l'homme.

Ils ont étudié la fixation du fibrinogène marqué dans des tumeurs malignes et des tumeurs bénignes, ainsi que dans des lésions en volume non-néoplastiques. Sur les 73 cas examinés jusqu'à présent, 53 étaient constitués par des tumeurs malignes localisées dans le squelette, les poumons, le cerveau, les organes abdominaux, etc. Le test de fixation du fibrinogène marqué avec ^{131}I a donné des résultats corrects dans 79% des cas examinés; aucun résultat faussement positif n'a été enregistré sur toute la série. Le mémoire expose succinctement le procédé et les résultats. D'après les données obtenues, il semble que le fibrinogène marqué avec ^{131}I puisse être utilisé avec succès pour la détection précoce de tumeurs malignes chez l'homme; en améliorant la technique de détection, il sera peut-être possible d'augmenter sensiblement la valeur du diagnostic établi par ce procédé.

ПРИМЕНЕНИЕ МЕЧЕННОГО РАДИОАКТИВНЫМ ЙОДОМ-131 И ЙОДОМ-125 ФИБРИНОГЕНА ДЛЯ ОБНАРУЖЕНИЯ ЗЛОКАЧЕСТВЕННЫХ ОПУХОЛЕЙ У ЧЕЛОВЕКА. В большом количестве злокачественных опухолей как экспериментальным путем, так и теоретически установлено высокое содержание фибрина. Этот вывод основан на том, что в злокачественной опухоли содержится большое количество тромбопластина, вызывающего полимеризацию фибриногена в фибрин.

На основе этих данных фибриноген человеческого организма, меченный йодом-131 и йодом-125, был подвергнут испытанию как возможный агент для обнаружения злокачественных опухолей у человека.

Поглощение меченного радиоактивным йодом фибриногена изучалось в доброкачественных и злокачественных опухолях, а также и в тканях, не являющихся новообразованиями, но занимающими определенное пространство. До сих пор изучены 73 случая; 53 из них составляют злокачественные опухоли, расположенные в скелете, легких, головном мозгу, орга-

* Supported by EURATOM Association Contract 026-63-4-BIAC

нах брюшной полости и т.д. Изучение поглощения фибриногена меченного йодом-131 дало точные результаты в 79% изучавшихся случаев. Ни в одном случае не получено неправильных положительных результатов. Кратко обсуждаются методы и результаты. На основании полученных данных явствует, что фибриноген меченный йодом-131 может успешно применяться для ранней диагностики злокачественных опухолей у человека. Возможные усовершенствования метода обнаружения могут существенно повысить диагностическую ценность метода.

EMPLEO DEL FIBRINÓGENO RADIOYODADO (^{131}I y ^{125}I) PARA LA DETECCIÓN DE TUMORES MALIGNOS EN EL HOMBRE. Se ha demostrado que en muchos tumores malignos, tanto en los inducidos en animales de laboratorio como en los formados espontáneamente en el hombre, hay un elevado contenido de fibrina; se ha establecido una relación entre este hecho y la gran cantidad de tromboplastina presente en el tumor, que sería lo que provoca la formación de fibrina por polimerización del fibrinógeno.

Teniendo esto en cuenta, los autores emplearon fibrinógeno humano marcado con ^{131}I y ^{125}I para detectar tumores malignos en el hombre.

Estudiaron la absorción del fibrinógeno radioyodado en tumores malignos y benignos y en lesiones no neoplásticas extensas. Han examinado hasta ahora 73 casos, constituidos 53 de ellos por tumores malignos localizados en el esqueleto, los pulmones, el cerebro, el tubo digestivo, etc. El ensayo de absorción del fibrinógeno-^{131}I dio resultados correctos en el 79% de los casos; en toda la serie no se dio ningún resultado erróneamente positivo. Los autores discuten brevemente la técnica y los resultados obtenidos. Los datos que ha sido posible reunir parecen indicar que el fibrinógeno-^{131}I puede utilizarse con éxito para la detección temprana de formaciones malignas en el hombre; es probable que perfeccionando la técnica de detección se logre aumentar notablemente el valor diagnóstico del método.

A high fibrin content has been reported both in experimental [1] and human [2] malignant tumours. Experimental neoplasms have also been shown to concentrate radioactivity after administration of I^{131}-labelled fibrinogen [3, 4]. In cases in which the level of fibrinolysis prevents the observation of this phenomenon, the simultaneous administration of an antifibrinolytic substance, epsilon amino caproic acid (EAC), allows a detectable concentration of radioactivity to be attained in the experimental tumour [5].

Starting from the above observations, preliminary studies were performed in the Medical Clinic of Pisa in 1962, in order to explore the possibility of detecting malignant tumours in man by external counting using I^{131} fibrinogen. The first results were encouraging [6].

Before undertaking wider experimentation in humans, it was thought advisable to compare the uptake of I^{131} fibrinogen with that of other labelled macromolecules (DIF, PVP and RIHSA) in an experimental tumour of the rat (chloromyeloma of Oberling-Guérin).

In Table I is reported the "tumour/non-tumour" radioactive concentration ratio (per g of tissue), observed 24 h after injection of the indicators. I^{131} fibrinogen yielded the highest figures although no antifibrinolytic agent had been used [7]. These findings seemed to justify an extensive appraisal of the method in man [8, 9].

TECHNIQUE

Radioiodinated fibrinogen was supplied by SORIN, labelled with I^{131} and I^{125} using the electrolytic technique [10]. Five μc/kg body weight were given intravenously to patients premedicated with Lugol solution, which was given for the entire duration of the study. In the early studies, EAC was also

TABLE I

UPTAKE OF RADIOACTIVE INDICATORS IN THE CHLOROMYELOMA OF THE RAT

Indicators	No. of rats	T/nT ratio*
NaI^{131}	10	3.92
I^{131} diiodofluorescein	15	3.16
I^{131} PVP	12	8.94
I^{131} RIHSA	10	9.26
I^{131} fibrinogen	15	26.50

* T/nT = Tumour/non-tumour concentration ratio per g of tissue.

given orally, at a dosage of 4 g every 4 h. More recently EAC was administered only when a negative result was obtained at 24 h.

The counting instrumentation included a 2 in × 2 in NaI scintillation counter with conic collimator (external opening 15 mm ϕ, internal opening 20 mm ϕ, length of channel 55 mm).

When the lesion was located away from the mid-line of the body, radioactive measurements were carried out on the suspected area and the symmetrical controlateral zone. In the case of lesions close to the mid-line of the body, measurements were carried out over the lesion and in closely surrounding zones.

ANALYSIS OF RESULTS

Results were expressed as % difference between the counting-rate over the suspected site and that over the symmetrical controlateral or the surrounding zone, depending on the location of the lesion. The results were considered as positive for the presence of malignancy if differences equal to or greater than 25% were attained and maintained (or further enhanced) in the successive measurements.

PATIENTS EXAMINED

A total of 96 cases of space-occupying lesion was studied, of which 59 were with malignant neoplasms, 7 with benign tumours, 17 with localized inflammatory processes, and 13 with localized lesions of different nature (cysts, etc.). The diagnoses were established on clinical, X-ray, and hystological grounds.

RESULTS

The results obtained in the above series are reported in Tables II – V. Out of 59 cases with malignant neoplasms (Table II), 42 yielded positive

TABLE II

MALIGNANT NEOPLASMS EXAMINED WITH RADIOFIBRINOGEN

Localization	No. of cases	Results	
		positive	negative
Skeleton	14	11	3
Lungs	14	8	6
Lymph nodes	9	9	-
Brain	5	4	1
Liver	1	1	-
Stomach	3	1	2
Colon	3	2	1
Breast	3	3	-
Kidney	2	1	1
Skin	2	2	-
Pleura	1	-	1
Uterus	1	-	1
Ovaries	1	-	1
Total	59	42	17

results. All 7 cases with benign tumours (Table III) were classified as negative. Localized inflammatory processes (Table IV) yielded negative results in 11 out of 17 cases of other types of space-occupying lesions (Table V), while, in this group, a bone cyst yielded a positive result, although on the borderline of significance. Only 2 cases with malignant neoplasms in which the results were negative at 24 h became positive after EAC administration.

In the entire series, correct results were obtained in 72 cases out of 96 examined (75%). The 24 cases in which an incorrect result was obtained comprise 17 false negative results in malignant neoplasms (Table II) (mostly located close to the mid-line of the body), and 7 false positive results (6 inflammatory lesions and 1 bone cyst).

Further work was then planned in an attempt to improve the diagnostic efficiency of the method for malignant lesions, making it independent of the availability of a controlateral reference point; and to establish the possible differential pattern between malignant lesions and lesions of other types, among the latter mostly the inflammatory processes.

DETECTION OF TUMOURS USING PRECORDIAL REFERENCE

The choice of the reference point, the counting-rate on which is taken as the baseline for the calculation of the percentage difference over the sus-

TABLE III

BENIGN TUMOURS EXAMINED WITH RADIOFIBRINOGEN

Localization	No. of cases	Results	
		positive	negative
Skeleton	3	-	3
Breast	1	-	1
Thyroid	1	-	1
Kidney	1	-	1
Lymph nodes	1	-	1
Total	7	-	7

TABLE IV

INFLAMMATORY LESIONS EXAMINED WITH RADIOFIBRINOGEN

Diagnosis	No. of cases	Results	
		positive	negative
Pulmonary tbc infiltrate	4	-	4
Tubercoloma of the lung	1	-	1
Broncopneumonia	1	-	1
Lung abscess	1	-	1
Renal abscess	1	-	1
Interstitial chronic hepatitis	1	-	1
Subacute pneumonia	1	-	1
Osteitis	2	1	1
Periostitis	1	1	-
Chronic osteomyelitis active	3	3	-
Chronic osteomyelitis	1	1	-
Total	17	6	11

pected region, necessarily entails a certain amount of uncertainty; this is maximal for lesions localized in body areas without a symmetrical counterpart. Attempts were made to limit this degree of uncertainty by using the precordial counting-rate as a reference level.

TABLE V

NON-NEOPLASTIC, NON-INFLAMMATORY LESIONS EXAMINED WITH RADIOFIBRINOGEN

Localization	No. of cases	Results	
		positive	negative
Bone cyst	5	1	4
Exostosis	2	-	2
Osteoporosis	2	-	2
Tendon calcification	1	-	1
Simple lymph node hyperplasia	2	-	2
Cerebral thrombosis	1	-	1
Total	13	1	12

The normal course of the radioactivity level in the epigastrial region was studied in 10 normal subjects, the counting-rate over 12 contiguous zones being measured and expressed in percent of the precordial counting-rate 1 h and 48 h after the injection of I^{131} fibrinogen. It was found that the difference between the percentage measured at 48 h and that at 1 h after injection never exceeded a value of +20 over the entire area.

The same type of study was carried out for a standard area over the right hypochondrium: the increment of the ratio $\frac{r \cdot \text{hypochondrium}}{\text{precordium}} \times 100$ from 1 to 48 h never exceeded +10.

These values (+20 for the epigastrium and +10 for the right hypochondrium) were taken as limits of the normal range. The technique was then applied to the study of 7 space-occupying lesions with epigastrial localization (6 malignancies and 1 case of gastric ulcer) and 13 cases with liver or biliary disease (6 of which were malignant neoplasms). The results are reported in Tables VI and VII respectively. Correct results were obtained in 6 out of 7 cases in the epigastrium (including 5 out of 6 malignant tumours) and in all cases in the right hypochondrium.

DIFFERENTIATION OF INFLAMMATORY FROM MALIGNANT SPACE-OCCUPYING LESIONS

The findings at 24 and 48 h for inflammatory lesions often resemble that of neoplastic lesions, thus preventing the differentiation of the two types of lesions.

It was observed, however, that inflammatory lesions tended to show an early positive difference (within the first hour), in comparison with the opposite side, usually greater than that observed in tumours, although afterwards the difference tended to a much larger increase in the latter.

TABLE VI

SPACE-OCCUPYING LESIONS WITH LOCALIZATION CLOSE TO THE MID-LINE EXAMINED WITH RADIOFIBRINOGEN USING PRECORDIAL REFERENCE

Diagnosis	No. of cases	Results	
		positive	negative
Gastric carcinoma	3	2	1
Peritoneal neoplasm	1	1	-
Metastasis retroperitoneal lymph node	1	1	-
Reticuloendotheliosis (periaortic lymph nodes)	1	1	-
Gastric ulcer	1	-	1
Total	7	5	2

TABLE VII

LIVER- AND BILIARY-SYSTEM LESIONS EXAMINED WITH RADIOFIBRINOGEN

Diagnosis	No. of cases	Results	
		positive	negative
Liver metastasis of mammary adenocarcinoma	4	4	-
Liver carcinoma	1	1	-
Gall-bladder cancer	1	1	-
Interstitial chronic hepatitis	2	-	2
Fatty liver	2	-	2
Hepatic tuberculosis	1	-	1
Chronic hepatocholangitis active	1	-	1
Icteric cholelithiasis	1	-	1
Total	13	6	7

In 4 out of the 6 inflammatory lesions of bone which had given false positive results the difference exceeded +25% in the first hour.

It was then decided to give more detailed consideration to the time course of radioactivity over the lesions, starting from 10 min and continuing for several days after injection.

The time course of the activity was simultaneously followed over the opposite side and the precordium; by taking the latter as representative of the intravascular activity, and assuming the counting-rate at 10 min over the suspected and controlateral regions as due to purely intravascular activity, the time courses of both intra- and extravascular activity over the suspected and opposite areas were obtained.

This type of study was carried out in 3 cases of malignant neoplasms (2 of femur metastasis from mammary cancer and one case of femur osteosarcoma), 3 of inflammatory lesions (2 erysipeloid and one of tibia-osteomyelitis) and in one of benign tumour (meningioma).

In the malignant tumours (Fig. 1) the extravascular activity over the neoplasms increased progressively until 24 - 36 h, after which it remained essentially unchanged for 160 - 180 h, when a progressive decrease took place. Over the normal opposite side the initial rise was followed by a downslope essentially parallel to that of the blood activity.

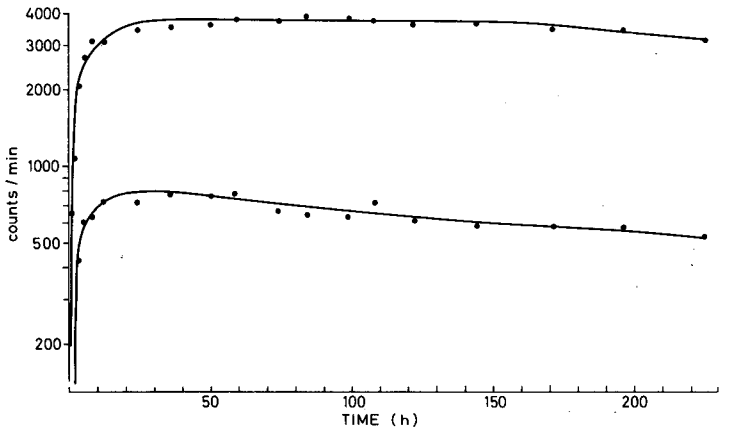

Fig. 1

Calculated extravascular activity curves in a case of osteosarcoma of the femur; upper curve on the tumour, lower curve on the normal opposite side

In the 3 inflammatory lesions (Fig. 2) extravascular activity rose progressively until the 20th h, up to a maximum of the same order of magnitude of that observed in tumours. The peak was followed by a gradual reduction of the extravascular activity; the curves of extravascular activity on the lesion showed a course essentially parallel to that over the opposite side, although at higher absolute levels.

The same pattern was observed in the case of meningioma (Fig. 3).

It is worth pointing out that the counting-rate differences (lesion versus controlateral) observed 10 min after injection tended to be much larger in the inflammatory processes than in the malignant neoplasms (15%, 65%, 70% respectively, versus 3%, 8%, 17%).

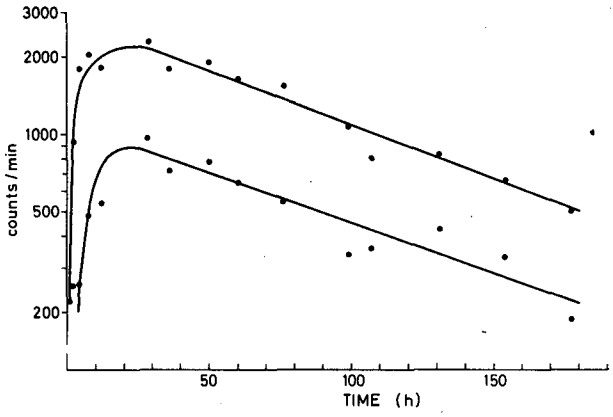

Fig. 2

Calculated extravascular activity curves in a case of erysipeloid of the forearm; upper curve on the lesion, lower curve on the normal opposite side

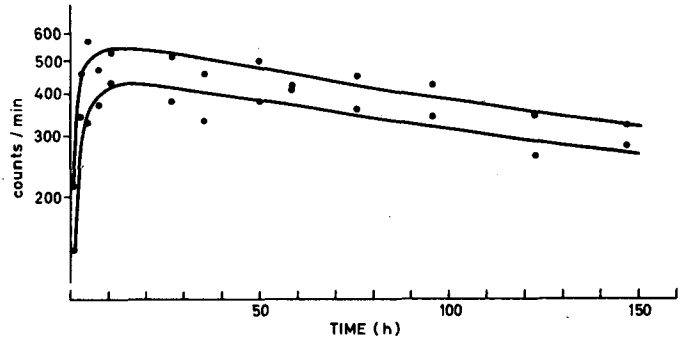

Fig. 3

Calculated extravascular activity curves in a case of meningioma; upper curve on the tumour, lower curve on the normal opposite side

Attempts were made to gain some information concerning the significance and the causes of the differences observed in the course of extravascular activity in the two types of lesions. An analogue computer was used to test the various hypotheses that could fit the observed data.

The model used is outlined in Fig. 4. Fibrinogen may diffuse from the blood into the interstitial space of the region explored by the counter, where it may coagulate into fibrin. Extravascular activity is taken away from the site of the lesion both by removal of fibrinogen as such and of the iodinated products of fibrin breakdown. It is also assumed that inflowing and outflowing activity at the explored site does not influence the course of body activity because of the small magnitude of the explored lesion.

When all the processes are assumed to take place as first-order reactions, the model easily fits the curves of extravascular activity observed in normal and inflammatory tissue, the latter requiring higher values for the blood-to-interstitial space transfer constant.

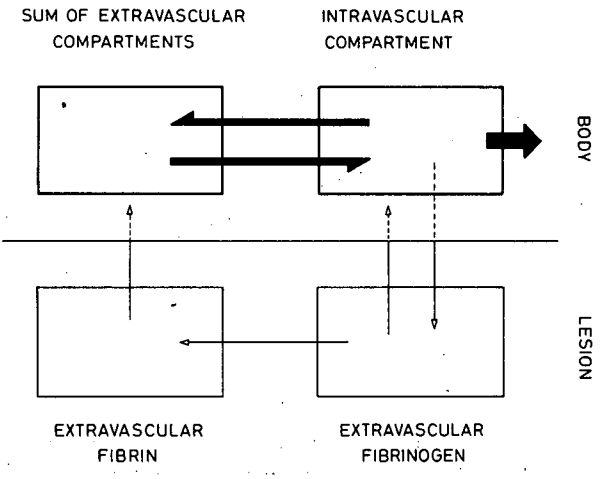

Fig. 4

Model assumed for describing fibrinogen uptake as recorded by external counting

On the contrary, the shape of the extravascular activity curves observed in tumours cannot be accounted for by such a model, no matter how the rate constants are adjusted. On the other hand, the tumour curve is easily reproduced if one assumes that fibrin breakdown occurs as a time discriminating process, implying a finite delay between incorporation and release of radioiodine from fibrine. It is enough to assume that about 5% per day of the fibrinogen present in the tumour interstitium precipitates to fibrin to account for the observed course of extravascular activity in tumours.

The following hypothesis may then be formulated to explain the time course of activity recorded by an external counter at the various sites and types of lesions:

(a) Over a normal site, the shape of the curve results from the decrease of intravascular activity caused by the turnover of body fibrinogen, and from the penetration and removal of fibrinogen itself in the interstitial spaces of the explored tissues, both processes occurring essentially as first-order reactions.

(b) Over the inflammatory processes and the highly vascularized benign neoplasm that were examined, the components of the curve are the same as in normals, with the exception of a higher transfer-rate from the blood to the interstice of the lesion.

(c) In the malignant neoplasms a new component is added to the higher blood-interstice transfer-rate which seems to be the distinctive pattern of inflammatory processes; i.e. the persistency of a fraction of the activity at the site of the lesion for a finite time, caused by the precipitation of a small fraction of I^{131} fibrinogen.

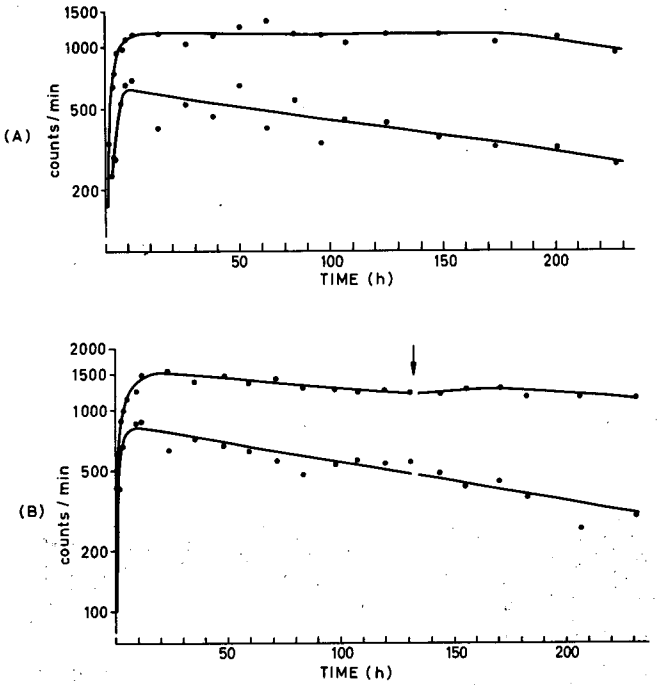

Fig. 5

A. Calculated extravascular activity curves in a case of femural metastasis from breast cancer; upper curve on the tumour, lower curve on the normal opposite side.

B. One case of Fig. 5A during heparin treatment; upper curve on the tumour, lower curve on the normal opposite side. The arrow indicates time of withdrawal of heparin and administration of protamine sulphate.

To test the latter hypothesis an attempt was made to prevent fibrinogen coagulation using heparin. In one of the cases of femur metastasis from mammary cancer in which the activity course had been studied and plateau pattern had been observed, the experiment was repeated during heparin treatment which was continued for the entire duration of the experiment; coagulation time ranged from 110 and 130 min. The obtained curve for extravascular activity (Fig. 5) shows a definite deviation from that observed without heparin: after the initial peak extravascular activity starts to fall as it occurs on the normal opposite side, although with a lower slope. Heparin was withdrawn and protamine sulphate administered five days after fibrinogen injection; this procedure, which brought about the normalization of blood-coagulation time, was followed by a definite rise of extravascular activity in the following hours.

The results of this latter experiment seem to confirm the hypothesis which has been formulated.

This series of experiments may offer some clue to the problems of differentiating malignant neoplasms from inflammatory processes. The two distinctive patterns seem to be:

(a) The longer persistence of an elevated extravascular radioactive content in the malignant tumours (a consequence of fibrin precipitation) as opposed to relatively rapid decay in the inflammatory processes, in a manner similar to that which can be observed in normal areas.

(b) The higher percentage difference from the reference site, observed 10 min after injection over the inflammatory processes in comparison with malignant neoplasms, apparently related to the larger blood supply in the former.

False positive results in inflammatory lesions might thus be prevented by combining an early (10 min) measurement and a very late one (after 5 or 6 d).

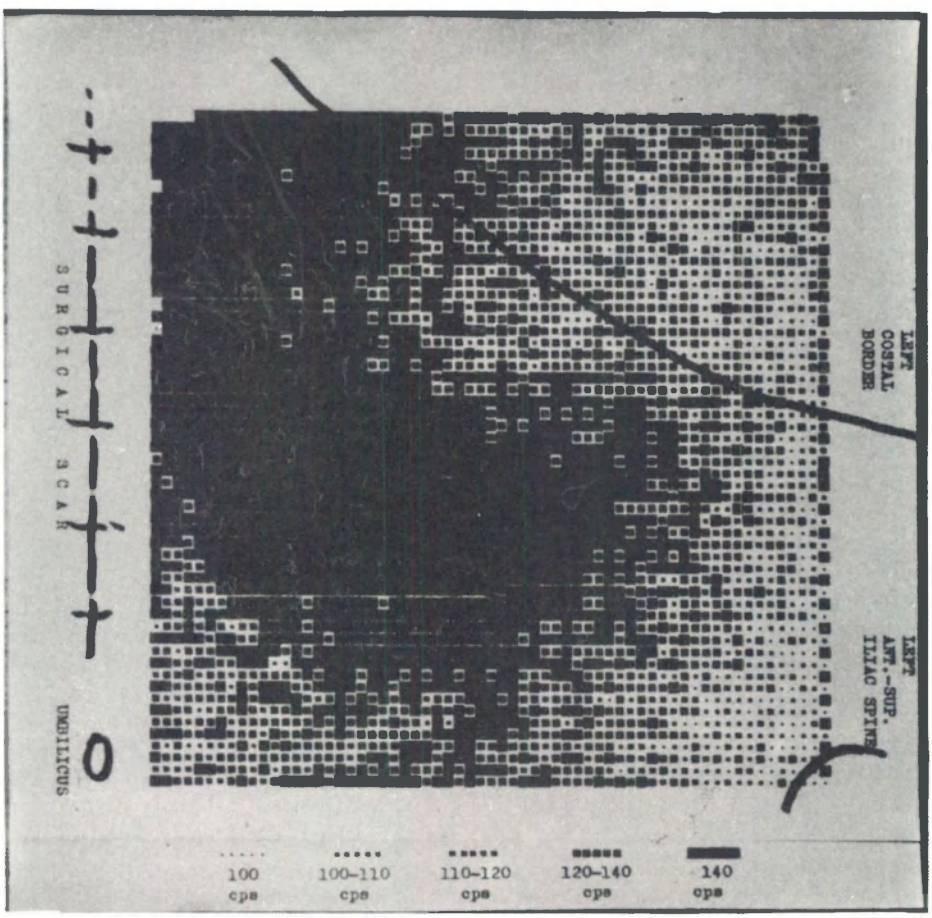

Fig. 6

Large tumour occupying part of the epigastrium and upper left abdominal quadrant detected by I^{131} fibrinogen scanning. Preset time, variable contrast scanning, was used.

CONCLUSION

I^{131} fibrinogen, because of its peculiar biological characteristics, seems to be a radioactive indicator particularly useful for the detection of malignant neoplasms using external counting.

I^{125} fibrinogen does not seem to have particular advantages, with the possible exceptions of tumours of superficial organs. Thanks to the technical and analytical improvements which have been described (namely the use of precordium counting-rate as reference) radiofibrinogen may detect malignant neoplasms in a higher percentage than that calculated on the basis of our first 59 cases; it also permits a better differentiation from other processes.

The application of scanning systems capable of detecting relatively small radioactive concentration differences [11] might enhance the practical value of the method, making possible direct visualization of the tumour (as shown in Fig. 6), and also in cases in which the location or diffusion of the tumour are unknown.

REFERENCES

[1] HIRAMOTO, R., YAGI, Y. and PRESSMAN, D., Canc. Research 19 (1959) 874 - 9.
[2] HIRAMOTO, R., BERNECKY, J., JURANDOWSKI, J. and PRESSMAN, D., Canc. Research 20 (1960) 592 - 3.
[3] DAY, E., PLANINSEK, J. and PRESSMAN, D., J. nat. Canc. Inst. 22 (1959) 413 - 26.
[4] DAY, E., PLANINSEK, J. and PRESSMAN, D., J. nat. Canc. Inst. 23 (1959) 799 - 812.
[5] BALE, W.F., SPAR, L. and GOODLAND, R.L., "Research directed toward the use of I^{131}-labelled fibrinogen and antibody to fibrin in the localization and treatment of tumours", Use of Radioisotopes in Animal Biology and the Medical Sciences II, IAEA, Academic Press, London (1962) 271.
[6] GIORDANI, R., BECCHINI, M.F. and RICCIONI, N., Boll. Soc. Ital. Biol. Sper. 38 (1962) 35 - 7.
[7] GIORDANI, R., DE RENZI, G., LAMARCHE, V., GIAGNONI, P., RICCIONI, N. and BECCHINI, M.F., Minerva nucl. 7 (1963) 538 - 41.
[8] MONASTERIO, G., BECCHINI, M.F. and GIORDANI, R., Minerva nucl. 7 (1963) 115 - 23.
[9] MONASTERIO, G., Proc. int. Soc. Surgery, Rome, Sep. 1963 (in press).
[10] ROSA, U., SCASSELLATI, G., PENNISI, F., RICCIONI, N., GIAGNONI, P. and GIORDANI, R., Minerva nucl. 7 (1963) 398 - 9.
[11] DONATO, L., GIORDANI, R., GENNARO, G. and SALVADORI, P., Minerva nucl. (1964) (in press).

DISCUSSION

E. LUBIN: I notice that in your paper you list five references referring to investigations that were performed with labelled anti-human fibrin globulin. What was the reason for your choice of fibrinogen instead of anti-human fibrin?

F. BECCHINI: We used fibrinogen because it was more readily available. I should add that our references also include investigations that were carried out with labelled fibrinogen.

E. LUBIN: Have you compared the relative value of both substances with reference to the tumour/non-tumour activity ratio?

F. BECCHINI: We have not made any direct comparisons.

M. BLAU: I think I can answer this question as far as biological behaviour is concerned. For uptake in tumour there is very little biological

difference between fibrinogen and anti-fibrinogen antibodies. When the antibody is injected, it attaches itself to the circulating fibrinogen and follows it as it is deposited in the tumour.

The chemical stability of anti-fibrinogen makes this compound preferable when storage of the labelled material or shipping to other laboratories has to be taken into account.

IX

CLINICAL APPLICATIONS: STOMACH, BONE MARROW, LYMPH NODES, KIDNEYS

STUDY ON THE LOCALIZATION OF IODINE IN THE STOMACH

W. H. CLODE*, M. SIMÃO RODRIGUES, M. A. PEREZ FERNANDEZ*, M. A. MURTEIRA AND A. M. BAPTISTA*
INSTITUTO PORTUGUÊS DE ONCOLOGIA, LISBON, PORTUGAL

Abstract — Résumé — Аннотация — Resumen

STUDY ON THE LOCALIZATION OF IODINE IN THE STOMACH. The authors have studied the localization of iodine in the stomach after intravenous injection of I^{131}-iodide, using a high-contrast photo-scanning system.

The study was performed at different times after injection (ordinarily 2, 24 and 48 h) in patients without any gastric disease, in patients with cancer of the stomach and in patients with peptic ulcers.

The distribution of radio-iodine was also studied in dog and human stomachs surgically removed at different times after the radio-iodine injection. In the surgically removed stomachs, the specific activity of the tissue corresponding to areas of interest revealed by scanning was determined in order to assist in interpreting the findings.

From the results the authors conclude that there are certain areas of the normal stomach which play a particular part in iodine metabolism. Localization of the zones of highest radioactivity concentration suggests more than one mechanism for iodine excretion. These observations support the findings of other workers using different methods.

Scanning at 24 h after administration of I^{131} allows gastric cancer to be detected in most of the patients with this disease who were studied. The explanation of these results is not only related to the iodine concentration by the tumour cells but also to some retention of iodine in the stomach walls. In most cases the radio-iodine concentration in the tumour was not higher than in the normal mucosal areas where increased iodine uptake occurs.

ÉTUDE DE LA LOCALISATION DE L'IODE DANS L'ESTOMAC. A l'aide d'un appareil de photo-exploration à fort contraste, les auteurs ont étudié la localisation de l'iode dans l'estomac après injection intraveineuse d'iodure marquée avec ^{131}I.

Ils ont fait cette étude à différents moments, après l'injection (habituellement après 2, 24 et 48 h) sur des sujets exempts de toute affection gastrique, sur des malades atteints d'un cancer de l'estomac et sur des malades ayant des ulcères gastriques.

Ils ont également étudié la distribution du radioiode dans des estomacs humains et canins après ablation à différents moments après l'injection du radioiode. Pour faciliter l'interprétation des résultats, ils ont déterminé dans ces estomacs l'activité spécifique du tissu correspondant aux zones d'intérêt révélées par scintigraphie.

Les résultats obtenus ont permis aux auteurs de conclure que certaines zones d'un estomac normal jouent un rôle particulier dans le métabolisme de l'iode. La localisation de ces zones de concentration de la radioactivité semble indiquer qu'il existe plusieurs mécanismes d'excrétion de l'iode. Ces constatations confirment les observations faites par d'autres chercheurs avec des méthodes différentes.

La scintigraphie 24 h après l'injection de ^{131}I permet de détecter le cancer de l'estomac chez la plupart des sujets atteints. Les résultats ne s'expliquent pas seulement par le fait que l'iode se concentre dans les cellules tumorales, mais encore par une certaine rétention de l'iode dans les parois de l'estomac. Dans la plupart des cas, la concentration du radioiode dans la tumeur n'était pas plus forte que dans les régions muqueuses normales, où se produit une fixation accrue d'iode.

ИЗУЧЕНИЕ ЛОКАЛИЗАЦИИ ЙОДА В ЖЕЛУДКЕ. Авторы изучали локализацию йода в желудке после внутривенной инъекции иодида, меченного йодом-131, используя для этого высококонтрастную систему фотосканирования.

* Comissão de Estudos de Energia Nuclear do Instituto de Alta Cultura, Lisbon

Исследование проводилось через различные промежутки времени после инъекции (обычно через 2, 24 и 48 часов) у больных, не страдающих никакими желудочными заболеваниями, больных с раком желудка и больных с пептической язвой.

Изучалось также распределение радиоактивного йода в желудках собаки и человека, удаленных хирургическим путем в различное время после инъекции радиоактивного йода. В удаленных хирургическим путем желудках для объяснения полученных данных определялась удельная активность тканей, относящихся к представляющим интерес областям, обнаруженным сканированием.

На основании полученных данных авторы делают вывод, что в нормальном желудке существуют области, которые играют особую роль в метаболизме йода. Локализация зон самой высокой концентрации радиоактивных изотопов предполагает существование более чем одного механизма выделения йода. Эти наблюдения подтверждают выводы других исследователей, использовавших различные методы.

Сканнирование через 24 часа после введения йода-131 позволяет обнаружить рак желудка у большинства обследованных больных, страдающих этой болезнью. Эти результаты объясняются не только концентрацией йода клетками опухоли, но также и некоторой задержкой йода в стенках желудка. В большинстве случаев концентрация радиоактивного йода в опухоли была не выше, чем в участках слизистой оболочки, где наблюдается повышенное поглощение йода.

ESTUDIO DE LA LOCALIZACIÓN DEL YODO EN EL ESTÓMAGO. Los autores estudiaron con un dispositivo de fotoexploración de gran contraste la localización del yodo en el estómago después de una inyección intravenosa de yoduro marcado con ^{131}I.

El estudio se realizó a diferentes intervalos después de la inyección (por regla general, a las 2, a las 24 y a las 48 h) en pacientes sin ninguna afección gástrica, en pacientes con cáncer de estómago y en pacientes con úlceras gástricas.

Estudiaron también la distribución del yodo radiactivo en estómagos humanos y de perro extirpados a diferentes intervalos después de la inyección. Para facilitar la interpretación de los resultados, midieron la actividad específica del tejido correspondiente a las zonas de interés delimitadas por la exploración.

Basándose en los resultados de esos estudios los autores han llegado a la conclusión de que ciertas regiones del estómago normal desempeñan un papel importante en el metabolismo del yodo. La localización de las zonas en que la concentración de radiactividad es más elevada indica que la excreción de yodo puede ser regida por varios mecanismos. Estas observaciones corroboran los resultados obtenidos por otros investigadores con métodos diferentes.

La exploración efectuada 24 h después de administrar ^{131}I permitió detectar el cáncer del estómago en la mayoría de los pacientes afectados por esa enfermedad. Estos resultados se explican no sólo por el hecho de que el yodo se concentra en las células tumorales sino también porque las paredes del estómago retienen cierta cantidad de este elemento. En la mayor parte de los casos, la concentración de yodo radiactivo en el tumor no fue superior a la observada en aquellas regiones de la mucosa gástrica en que se produce una absorción incrementada de este elemento.

1. INTRODUCTION

For several years we have been interested in the gammagraphic images observed over the stomach after administration of NaI^{131} in cases of gastric ulcer [1, 2]. Further data showed the need for a better knowledge of the iodine uptake and excretion by the gastric wall in order to assess the relevance of these surface measurements.

LIPSCHITZ [3] and ELMER [4] detected higher concentrations of iodine in the gastric juice than in the plasma. These findings were confirmed by DAVENPORT [5] in dogs with gastric pouches of Heidenheim and Pavlov. In 1947 SCHIFF et al. [6] using I^{131} studied the relation of radioiodine in the gastric juice and plasma in various gastric diseases but the data did not permit the correlation of the results with the disease. HONOUR, MYANT

and ROWLANDS [7] in 1952 continued this work and could not decide whether the concentration of iodine was a function of the cells responsible for the formation of acid or of pepsin. In 1956 LOGOTHETOPOULOS and MYANT [8] made an autoradiographic study of the stomach of the hamster after administration of radioiodine and noticed localization of iodine in the superficial cells of the mucosa. As MASON, KIRSCHBAUN and COLLINS [9] had shown that tiocianate inhibits concentration of iodine in the stomach, Logothetopoulos and Myant were able to demonstrate the presence of tiocianate with S^{35} labelled precisely at the points where the iodine was present.

We thought that the gammagraphic methods were particularly suitable for the study of the macroscopic distribution of radioiodine in the stomach and the purpose of this paper is to present data obtained with these techniques on the localization of radioiodine in the stomach of patients, and on the other hand to study the concentration of radioiodine in the different regions of the stomach of humans and dogs after administration of NaI^{131}.

2. MATERIAL AND METHODS

2.1. In vivo studies in humans

Studies were made of 57 patients of both sexes (15 without gastric disease, 3 after total gastrectomy, 30 with gastric cancer (adenocarcinomas), 6 with gastric ulcer and 3 with duodenal ulcer), all of them more than 50 yr old.

Intravenous injections of 300 μc of I^{131} were made (carrier-free NaI from the Radiochemical Centre, Amersham, with specific radioactivity of about 10 c/mg of iodine). After intravenous administration of the radionuclide a photoscanning was obtained at predetermined intervals with the patients in a supine position. In some cases the scanning was performed after a gastric lavage (volume not less than 1 l) with a Levine tube. The day before administration a liquid diet was established and on the day of the scanning tests the patient was fasting.

2.2. Studies in vitro

(a) Photoscanning of stomachs of dogs

No selection of the 14 dogs according to sex, weight, age or breed was made. We injected 2 mc of I^{131}, intravenously, from the same source as in 2.1. Dogs were sacrificed at 30 min, 2 h, 6 h, 24 h, 3 d and 7 d after injection. In all cases the animals were fasting at least 3 h before gastrectomy. The dogs were bled to death after having been anaesthetized with 0.5 g of Luminal +0.1 g of Petidine. The stomach was removed by section of the oesophagus 1 cm above the stomach and of the duodenum 3 cm below it. Freeing the large and lesser curvature from the respective omentum, the stomach was then opened through the large curvature and flushed out under running water in order to remove as much as possible of the residual gastric secretions after which it was blotted dry with filter paper. It was

then spread out on a cork board and pinned down, maintaining the folds in their original position. The gastric gammagraphy was then performed.

Some of the stomachs were stretched so as to undo the folds in an attempt to find out if these had any influence on the results.

(b) Photoscanning of human stomachs

1 mc of I^{131} was given intravenously to 11 patients more than 50 yr old, 2 h and 12 h before partial gastrectomy. Before the photoscanning the stomach that had been removed was treated as described above.

(c) Measurement of specific radioactivity

Samples 0.5 cm in diam. from the stomachs were obtained by punching after photoscanning. The weighted fragments, to which were added 5 drops of Lugol's solution, were digested with concentrated sulphuric acid for 3 d. Radioactivity of the samples was measured in a well-type scintillation detector. Radioactivity per unit weight was normalized for the time of injection.

2.3. Photoscanning system

The photoscanning system of the type developed by BENDER and BLAU [10] has been described in a previous paper [2] and Fig. 1 shows the optical

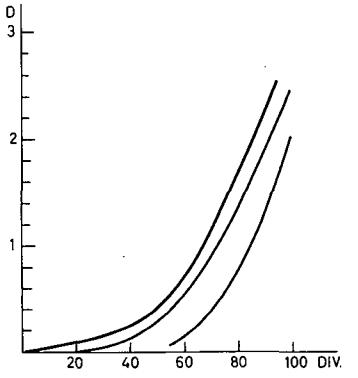

Fig. 1

Optical density (D) versus recorder deviation.
We used in this work the highest contrast (lowest curve).

contrast curves we can obtain using Ilford Red Seal, safety base, X-ray film.

In this work we operate under conditions to give the highest possible optical contrast (lowest curve of Fig. 1). We can see that below about 50% of the point of maximum radioactivity no information was registered.

We used a NaI(Tl) scintillation crystal (Harshaw, 3 in × 2 in) and a focusing collimator with seven tapered channels and the focal point 7.5 cm beyond the face.

3. RESULTS

3.1. In vivo studies

(a) Stomachs with no gastric disease

In seven patients the photoscanning was obtained 2 h after the radioiodine administration. In six we observed a well-defined image related to an iodine concentration in the stomach of elongated (Fig. 2) or of round form.

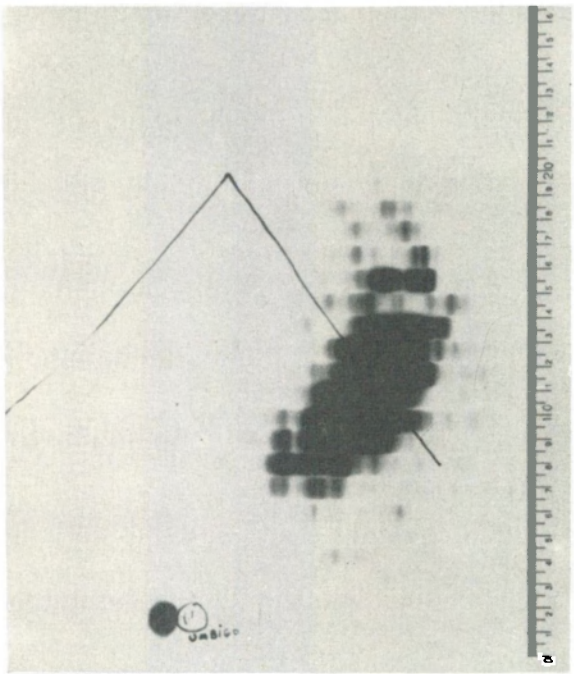

Fig. 2

Gastric photoscanning in a patient with no gastric disease, 2 h after injection of radioiodine

In one case we obtained a diffuse image like the one observed 24 h afterwards, as will be shown.

In 13 patients with photoscanning 24 h after administration the images obtained were of two fundamental types: a diffuse distribution (Fig. 3) or a more defined area extending between the two kidney surface projections (Fig. 4) probably related to iodine renal excretion. In five of the patients we repeated the photoscanning after gastric lavage. No appreciable alteration in the scanning images was observed. When in the same patient we performed photoscannings 2, 24 and 48 h after radioiodine administration we did not observe the concentration images of the 2-h scanning, either at 24 or 48 h, the 48-h scanning not differing greatly from the 24-h one, although more difficult to obtain because of the diminished radioactivity present.

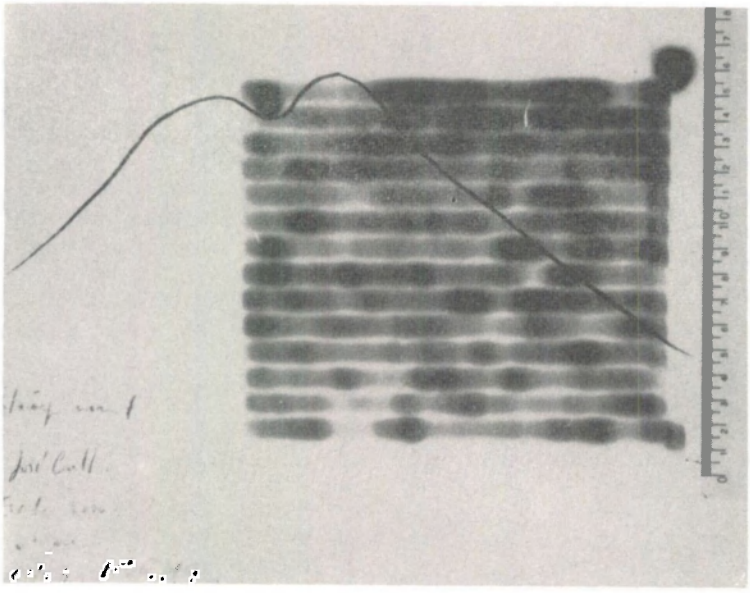

Fig. 3

Gastric photoscanning in a patient with no gastric disease, 24 h after injection of radioiodine

(b) Scanning after total gastrectomy

In patients with total gastrectomy following Lima Basto's technique in which a reservoir is constructed [11] we obtained 24-h scanning images over the abdomen similar to those observed in normal patients (Fig. 5).

(c) Scanning in patients with gastric cancer

The photoscannings obtained 24 h after injection of I^{131} showed an image that in many cases was very similar to the one we described at 2 h in normal stomachs (Fig. 6). However, sometimes the radioiodine distribution was not so well defined, pointing to a concentration of radioiodine in the stomach although not so uniformly distributed as in the 2-h scannings. In a group of 17 patients with gastric cancer 15 showed these images ("positive" images) which we consider related to the presence of cancer. In two of the cases we were not able to detect the particular iodine concentration referred to above. One case was a cancer of the fornix with invasion of the cardia and the other had an early stage adenocarcinoma of the antrum.

In another group of 17 patients gastric lavage was performed before scanning. The results were considered positive for the presence of cancer in only 7 of the patients. Figure 7 shows images obtained 24 h after injection of radioiodine before and after gastric lavage. As may be seen, there was no important alteration in the nature of the image.

It is to be noticed that in some of the cases we have not found a relationship between the maximum of radioactivity and the palpable mass of

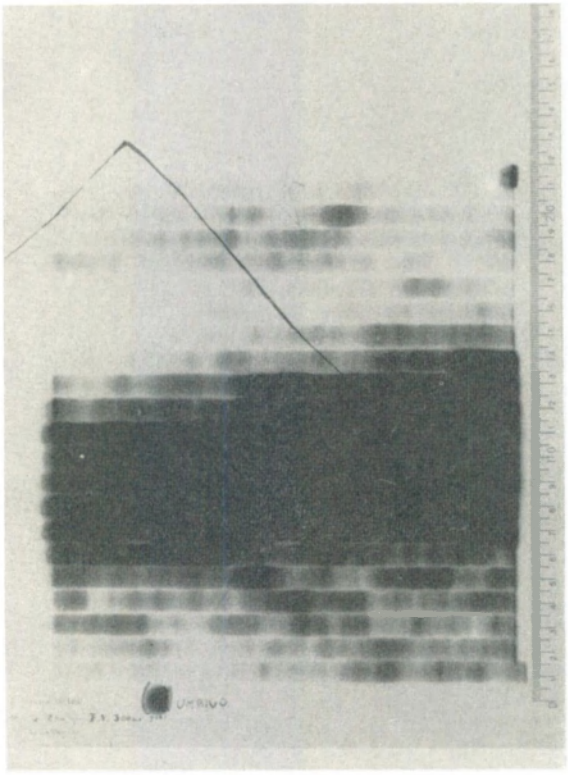

Fig. 4

Gastric photoscanning in a patient with no gastric disease, 24 h after injection of radioiodine

the tumour. This showed the need for an in vitro scanning of the stomach after gastrectomy. We shall return to this matter later.

(d) Scanning in patients with ulcer

Of the six cases of gastric ulcer, the scanning was negative for cancer in three. Of the other three with positive images, in one the diagnosis was established at operation and confirmed anatomo-pathologically, in the other two, who were not operated, gastric citology was negative.

All three cases of duodenal ulcer had a negative 24-h scanning.

3.2. In vivo studies

(a) Stomachs of dogs

Figure 8 shows the image obtained of the stomach of a dog removed and washed free of food, 6 h after injection of radioiodine. In order to get a clearer idea of the iodine distribution we usually performed the scanning

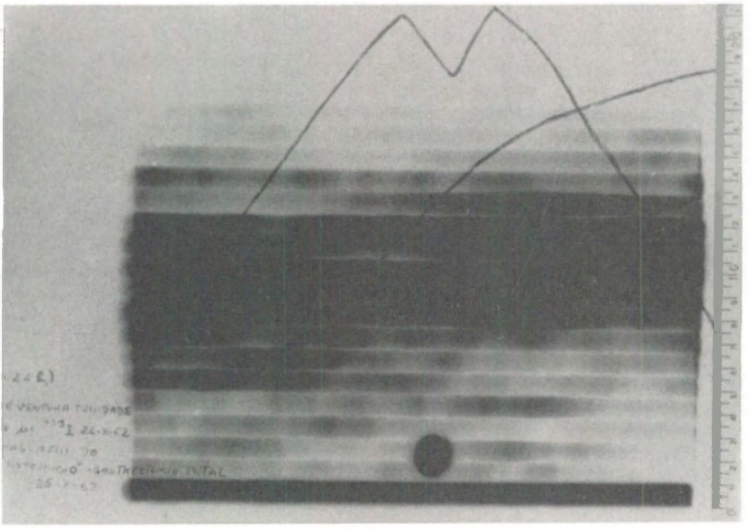

Fig. 5

Photoscanning obtained over the abdominal region after total gastrectomy, 24 h after injection of radioiodine

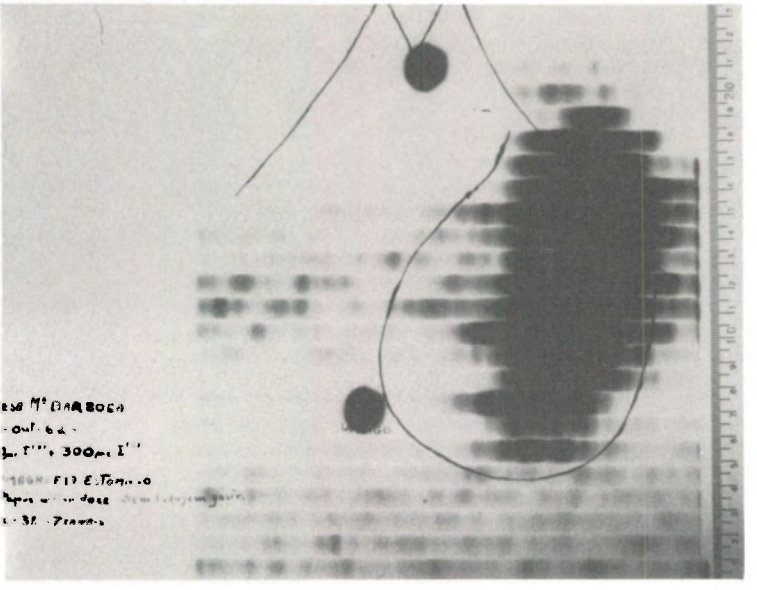

Fig. 6

Gastric photoscanning in a patient with cancer of the stomach, 24 h after injection of radioiodine

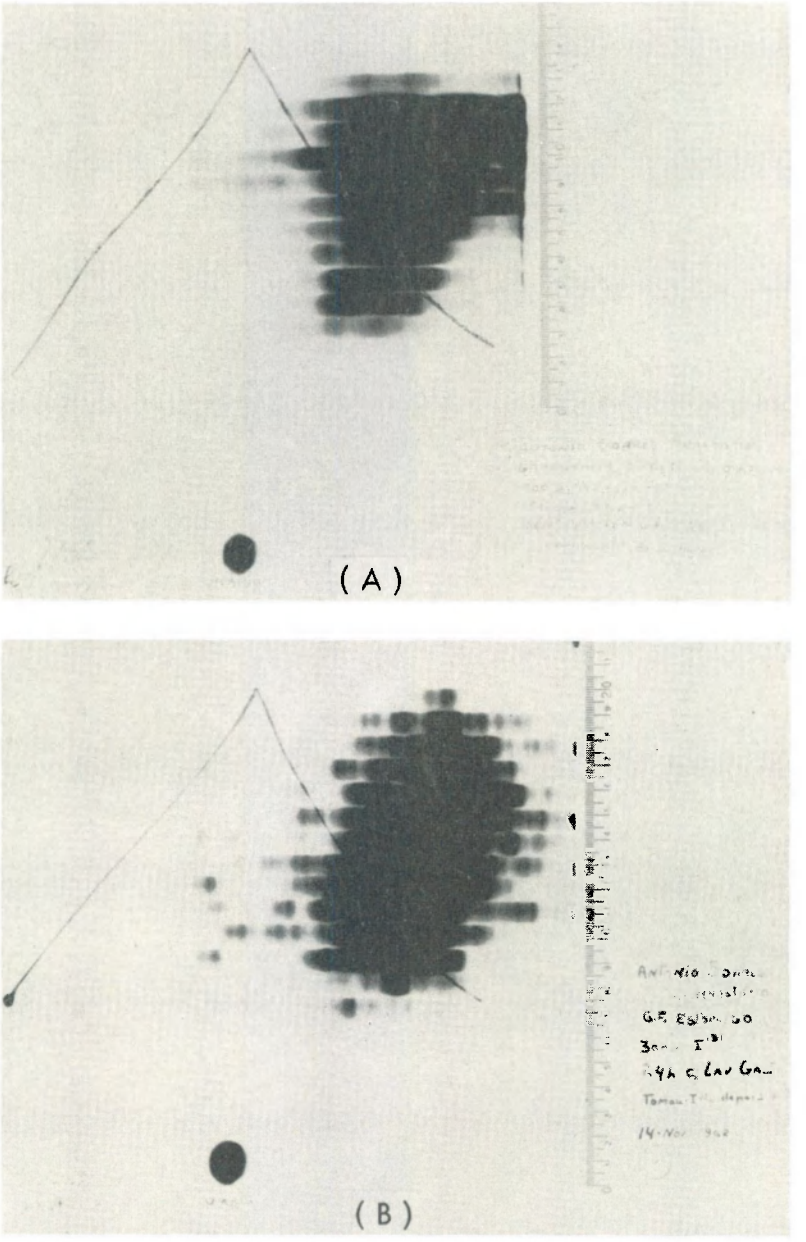

Fig. 7

Gastric photoscanning of a patient with cancer of the stomach, 24 h after injection of radioiodine
(A) before gastric lavage
(B) after gastric lavage

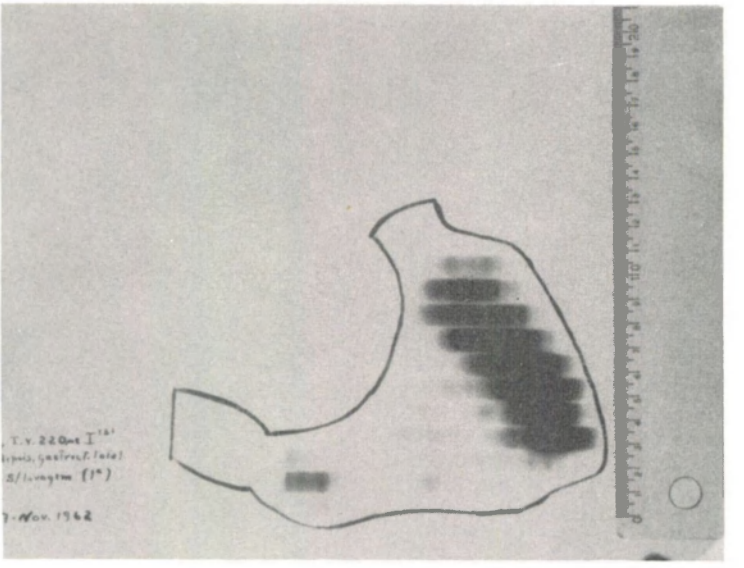

Fig. 8

In vitro photoscanning of a stomach of a dog, removed 6 h after injection of radioiodine

in stomachs opened through the greater curvature. Except for diminished radioactivity with time, there were no noticeable differences in scannings obtained 30 min, 2 h, 6 h and 24 h after radioiodine administration. Figure 9 shows a typical result where it is possible to see the concentration of iodine in the regions corresponding to the fundus of the stomach and the antrum. It must be added that the image of the antrum was not so clearly marked in all cases. The region of the lesser curvature was relatively "cold" (it must be remembered that a high contrast scanning system was used). Since the higher radioactivity observed in the fundus of the stomach could be ascribed not to a higher radioiodine concentration but only to a greater tissue thickness of the folds, we repeated the scannings stretching the stomach and levelling the surface. The topographical distribution was unaltered.

(b) Human stomachs

In four patients with gastric cancer we had the opportunity to compare the photoscannings before and after gastrectomy when we observed the removed stomach. Figure 10 shows the photoscanning before operation and Fig. 11 the result after gastrectomy. The highest radioactivity was observed over the tumour area.

In order to compare the distribution of radioiodine in the human stomach with the one observed in dogs we made the photoscannings of stomachs partially removed from patients with duodenal ulcers. Figure 12 shows the result and it is possible to see that radioactivity is concentrated mainly in the folds.

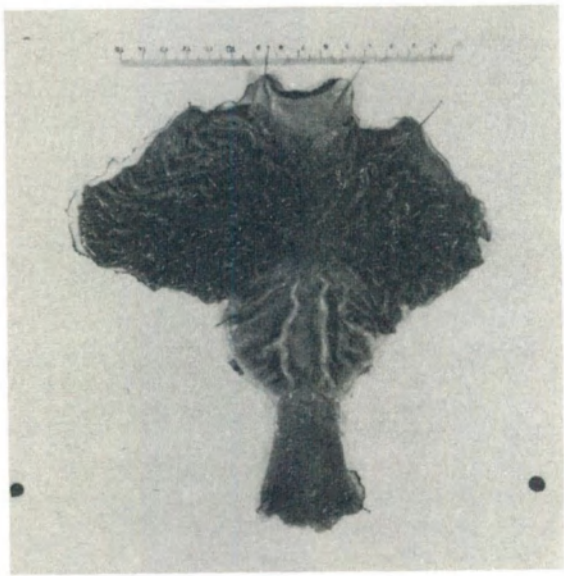

A

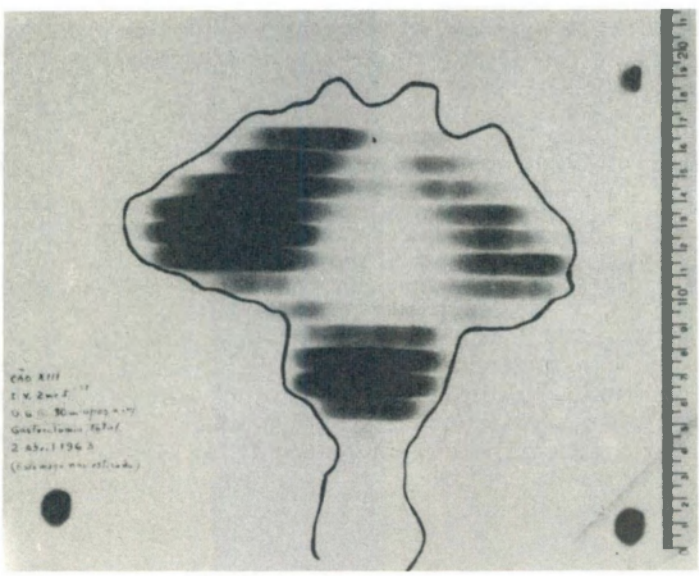

B

Fig. 9

A Stomach of a dog opened through the large curvature and removed 30 min after injection of radioiodine

B Photoscanning of the same stomach

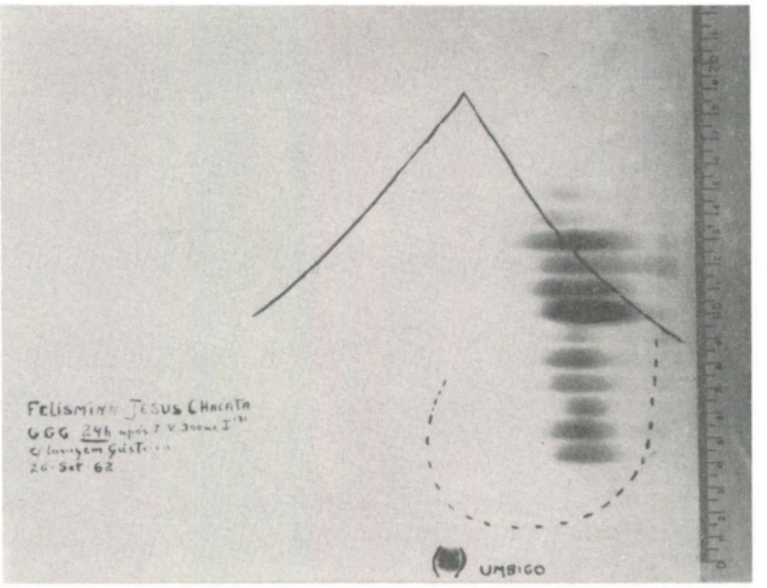

Fig. 10

Gastric photoscanning of a patient with cancer of the stomach
24 h after injection of radioiodine and after gastric lavage

(c) Specific radioactivity measurements

(i) In dogs

Following the gammagraphy images we punched out equal area fragments from the more active area and from the duodenum. Figure 13 shows the results at 30 min, 2 h, 6 h, 24 h, 3 d and 7 d after injection of radioiodine. Each point is the average obtained from two dogs and represents the relationship between radioactivity per gram of the most active area of the stomach and the radioactivity per gram of duodenum tissue. The relationship reached its highest value 2 h after injection and decayed with an effective half-life of about 1 d. Figure 14 shows the evolution of the specific radioactivity of the duodenum tissue with time.

(ii) In man

It was, of course, not possible to reproduce in man the study performed in dogs. We measured the radioactivity per gram of equal area fragments from the tumour and the normal tissue in 11 operative specimens of gastric cancer. Radioiodine was concentrated in the tumour but not always at significantly higher levels as compared with normal tissue.

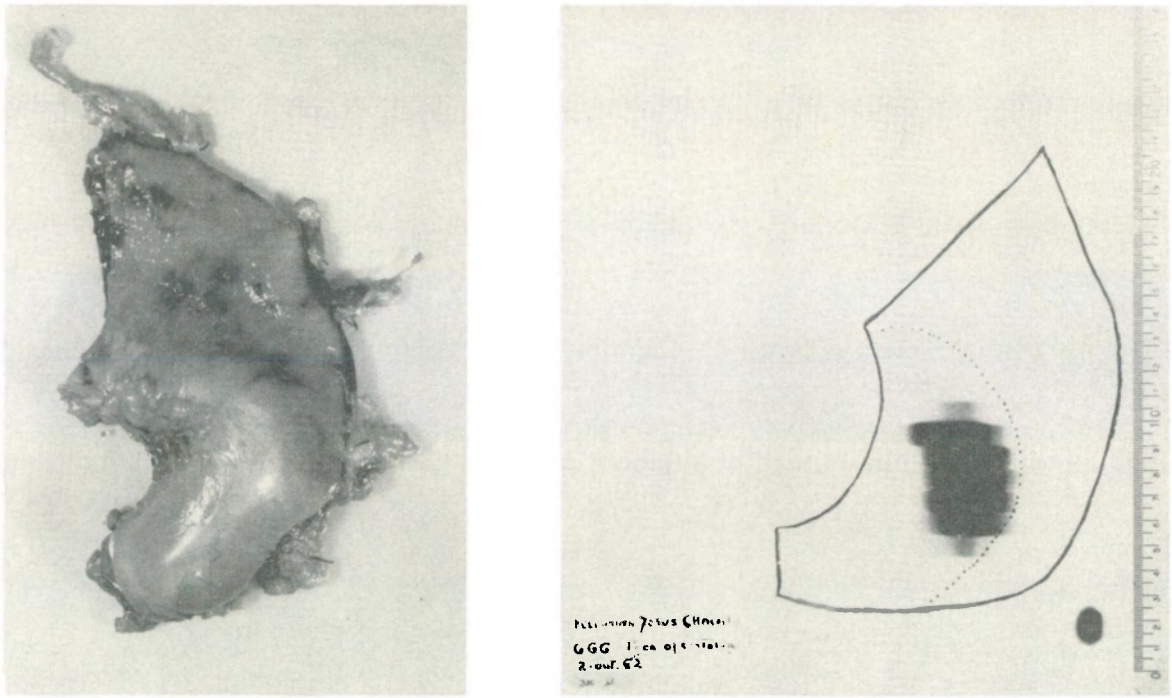

A B

Fig. 11

A Operative specimen from same patient as in Fig. 10
B Photoscanning of the operative specimen

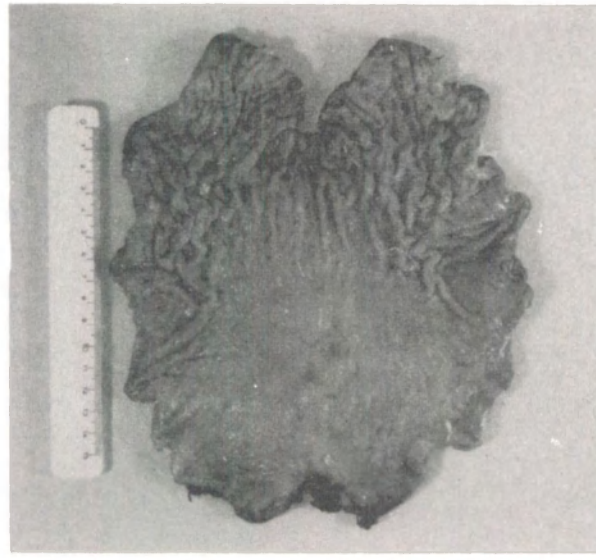

A

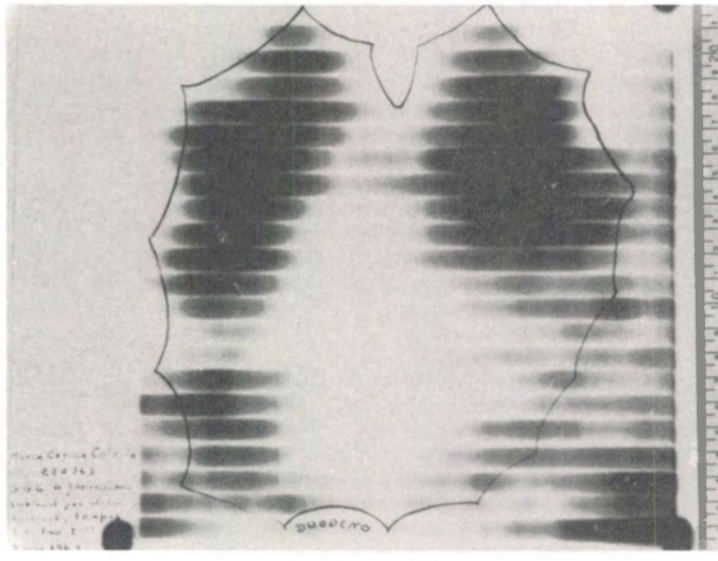

B

Fig. 12

(A) Operative specimen of a patient with duodenal ulcer, opened through the large curvature and removed 2 h after injection of radioiodine
(B) Photoscanning of the operative specimen

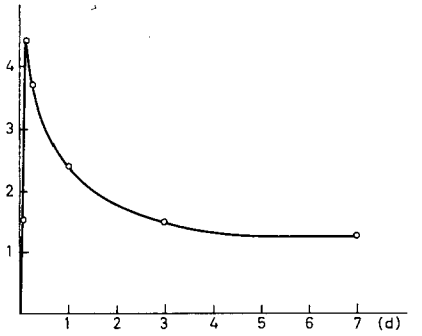

Fig. 13

The relation between the radioactivity per gram of the highest activity zone of the stomach and the radioactivity per gram of duodenum tissue of dogs as a function of time

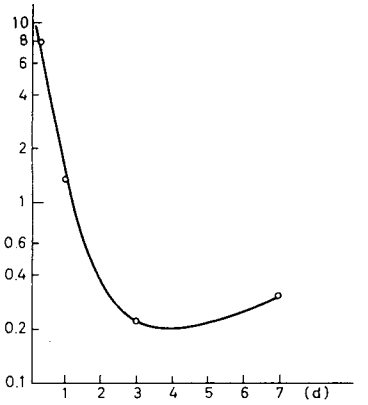

Fig. 14

Radioactivity per gram of duodenum tissue of dogs as a function of time

4. DISCUSSION AND CONCLUSIONS

The experimental photoscanning study in the stomachs removed from dogs at different times after injection of NaI^{131} revealed an iodine concentration particularly in the fundus and the antrum regions (Fig. 9) that decayed very rapidly as shown by the curves of Fig. 13 and Fig. 14. Since BERNARD [12] histochemical techniques for the localization of the secretion of chloridric acid is in use, images very similar to the ones we obtained by photoscanning have been observed by BRENCKMANN [13] using, as Bernard did, Prussian Blue. This is not surprising since the mechanisms of secretion of iodine and chlorine must be closely related. However, we must point out that we observed a very high concentration of iodine over the antrum area and as far as we know no secretion of chloridric acid has been attributed to this region. This result suggests the possibility of two mechanisms for the iodine secretion in agreement with an hypothesis of HOWELL

and MIDDESWORTH [14]. It is possible that the same mechanisms are present in man although in the few cases studied we could not detect the existence of both of them.

In all the cases of stomachs with gastric cancer (adenocarcinoma) that were removed, gammagraphy revealed higher radioactivity levels over the tumour. The specific radioactivity of fragments of these stomachs showed that there was concentration of radioiodine over the tumour although not at significantly higher levels than in the normal tissue. In a previous study [1] we found out that in all cases the specific radioactivity of the tumour was very much higher than in normal tissue. We now know that these values came from the use of formol as a fixative. All the measurements presented in the actual paper were obtained using fresh specimens, as described above. The photoscanning images accordingly must be related to a greater thickness of cancer tissue concentrating radioiodine. That 15 of the 17 cases gave positive images for the presence of cancer could be interpreted as the presence of tumour masses. The fact that the gastric lavage changed the scanning images in 10 out of 17 patients with gastric cancer could be explained by the presence of radioiodine in the gastric juice. As in some patients there was a small amount of residual gastric juice, we think that lavage removed the radioiodine with the gastric juice and/or from the stomach wall. In some cases alterations of the wall could hinder the removal of radioiodine and account for the permanence of the characteristic scanning images. We cannot explain the "positive" images observed in some of the ulcer cases. The small number of cases studied warrant further consideration of this problem.

It must be emphasized that in normal stomachs "positive" images were never found 24 h after the radionuclide injection. Clearly defined images were obtained 2 h after injection in agreement with the results obtained in stomachs of dogs (Figs. 2 and 8). The results obtained in patients after total gastrectomy exclude saliva as a responsible factor for the images, and lead to the conclusion that images obtained in many normal individuals 24 h after radioiodine injection could indeed be related to the presence of the kidneys in the scanned region.

Summing up, we can conclude that the stomach plays an active part in the metabolism of iodine related to a different functional capacity of some of its regions. Cancer of the stomach is responsible for radioactive images from which we could detect its presence.

ACKNOWLEDGEMENTS

We would like to thank Professor E. Lima Basto for his interest and help as well as all the members of the Surgical Department of the Instituto Português de Oncologia.

Only with the generous help of the Calouste Gulbenkian Foundation was this work made possible and it is our pleasure to thank it for its support.

REFERENCES

[1] CLODE, W.H., SOBRAL, J.M.V., LIMA BASTO, E. and BAPTISTA, A.M., Surg. 50 (1961) 725.
[2] BAPTISTA, A.M., CLODE, W.H., LIMA BASTO, E., SOBRAL, J.M.V. and MURTEIRA, M.A., Proc. VIII Intern. Cancer Congr., Moscow (1962).
[3] LIPSCHITZ, W., Arch. exper. Path. Pharmakol. 147 (1929) 142.
[4] ELMER, A.W., Iodine Metabolism and Thyroid Function, Oxford University Press, London (1938).
[5] DAVENPORT, H.W., Gastroenterol. 1 (1943) 1055.
[6] SCHIFF, L., STEVENS, C.D., MOLLE, W.E., STEINBERG, M.D., KUMPE, C.W. and STEWART, P., J. Nat. Canc. Inst. 17 (1947) 349.
[7] HONOUR, A.J., MYANT, N.B. and ROWLANDS, E.N., Clin. Scien. 11 (1952) 447.
[8] LOGOTHETOPOULOS, J.H. and MYANT, N.B., J. Physiol. 133 (1956) 213.
[9] MASON, E., KIRSCHBAUN, T. and COLLINS, S., Surgical Forum (1951) 58.
[10] BENDER, M.A. and BLAU, M. Int. J. appl. Rad. Isotopes 4 (1959) 154.
[11] LIMA BASTO, E., Arq. Pat. 28 (1956) 203.
[12] BERNARD, C., Leçons sur les Propiétés Physiologiques des Liquides de l'Organisme, J.B. Baillière Fils, Paris (1859).
[13] BRENCKMANN, in COSTA, A.C. da and CHAVES, P.R., Tratado Elementar de Histologia e Anatomia Microscópica 2, Luso Espanhola, Lisbon (1947) 88.
[14] HOWELL, G. and MIDDESWORTH, L.V., Proc. Soc. exp. Biol. N.Y. 93 (1956) 602.

DISCUSSION

C. KELLERSHOHN: At a meeting about 18 months ago Dr. Harper showed that, as far as the iodide space is concerned, the behaviour of Tc^{99m}-pertechnetate is very similar to that of I^{131}-iodide. As I understand it, there is an appreciable uptake of Tc^{99m} by the mucosa of the stomach, so that it is possible to make a scintigram of the latter organ. Since Tc^{99m} is the better isotope with regard to radiation dose and scinti-scanning, would it not be better to use it, rather than I^{131}, for the type of investigation discussed by Dr. Baptista?

P. HARPER: We have been interested in the localization of pertechnetate in the stomach because this is probably the principal site of localization in the body, containing 25 - 30% of the injected dose in mice. We have done no scintigrams deliberately, but we have carried out various secretion studies with a Heidenhain pouch dog under a variety of circumstances of rest and histamine stimulation using double tracers of iodide and pertechnetate. We found that the secretion curves for the two ions were remarkably similar. When serum levels were normalized the curves were superimposable to within a few per cent under all observed conditions. As far as the stomach is concerned, the ions are indistinguishable.

B. MALAMOS: In how many cases were you able to detect cancer of the stomach by scanning when conventional methods such as clinical examination, gastric-juice examinations and radiographic examination had failed?

A. BAPTISTA: We obtained a positive image indicative of malignancy in at least two or three cases where radiological and other tests suggested a different condition.

B. MALAMOS: You referred to the detection of a metastasis near the thyroid. Was this an adenocarcinoma or a scirrhus?

A. BAPTISTA: It was an adenocarcinoma.

M. TUBIANA: Is there any correlation between the radioactivity in the plasma iodide and that in the stomach? When one is looking for the metastases of a thyroid cancer, it is during the first few hours that gastric radioactivity tends to interfere. This indicates that the radioactivity of the stomach decays rapidly.

A. BAPTISTA: As we have pointed out in our paper, this is indeed the case. Some interference is, of course, to be expected. This problem has been studied by Schiff et al. [6].

M. TUBIANA: Have you considered using anti-thyroid drugs to reduce the radiation dose received by the thyroid? This would not prevent the "iodine pump" from working but it would inhibit the incorporation of I^{131} into organic compounds. The I^{131} would thus leave the thyroid at a much faster rate.

A. BAPTISTA: We have used a few anti-thyroid drugs but our experience is very limited. In the few cases which we studied we found that we did not gain very much by administering such drugs.

P. CZERNIAK: We use the following procedure for increasing the uptake of I^{131} by the stomach. Patients are given Lugol's solution before the examination and 0.5 mg of histamine half an hour before injection of I^{131}. The injection is given in two doses at an interval of 15 min. Patients are fed after the injection and again 2 - 3 h before the scan is performed. A further dose of histamine can be given, if necessary, using an anti-histamine drug such as Phenergan. In this way a good scinti-scan of the stomach can be obtained.

In cases of cancer of the stomach we generally find regions of reduced, not increased, I^{131} uptake.

A. BAPTISTA: We have tried similar procedures. The reason our pictures are not clearer is that we have been concentrating on 24-h scans.

BONE-MARROW SCANNING AFTER INTRAVENOUS INJECTION OF COLLOIDAL Au^{198}

L. -G. LARSSON AND L. JONSSON
UNIVERSITY OF UMEÅ, SWEDEN

Abstract — Résumé — Аннотация — Resumen

BONE-MARROW SCANNING AFTER INTRAVENOUS INJECTION OF COLLOIDAL GOLD-198. Colloidal Au^{198} is, after intravenous injection, rapidly removed from the blood by reticulo-endothelial activity. Most of the injected colloid is taken up by liver, but a small part is taken up by spleen and bone marrow. Bone-marrow uptake was studied in a large number of patients by means of total body scintigrams and total body profile counting. Three main patterns of distribution could be distinguished.

(1) Normal pattern: In patients without bone-marrow disease, uptake of Au^{198} was limited to the central parts of bone system (thorax, spine, pelvis, skull and proximal epiphyses of femur and humerus), i.e. normal sites for active red bone marrow. With the exception of the proximal epiphyses of femur and humerus no, or only a very slight, uptake was found in the bones of arms and legs.

(2) Hyperplastic pattern: This type of distribution was found in polycythaemia vera and haemolytic conditions. Bone-marrow uptake was increased and, besides the central parts of bone system, considerable uptake was often demonstrated in the long bones of arms and legs.

(3) Destructive pattern: This pattern was regularly found in myelofibrosis and very often in leukaemia, bone-marrow carcinomatosis and malignant lymphoma with bone-marrow involvement. It was characterized by general reduction of bone-marrow uptake in central parts of the body, combined with increased uptake in the long bones of legs and arms due to compensatory peripheral haematopoiesis. All degrees of bone-marrow destruction and compensatory peripheral hyperplasia could in this way be visualized.

By means of total body profile counting it was possible to obtain a more quantitative and reproducible expression for bone-marrow uptake. Repeated examinations were performed in cases of polycythaemia vera; in some cases it was possible to follow the changes in bone-marrow uptake which occurred when polycythaemia vera developed into a stage of myelofibrosis. In detailed scintigrams of the pelvis, it was also possible to study the extent of local abnormalities, such as bone tumours and bone metastases. Some improvements regarding collimator design and method of registration are also reported.

SCINTIGRAMME DE LA MOELLE OSSEUSE APRÈS INJECTION INTRAVEINEUSE D'OR-198 COLLOÏDAL. Après injection intraveineuse, l'or-198 colloïdal est rapidement éliminé du sang par activité réticulo-endothéliale. La plus grande partie du colloïde injecté est fixée par le foie, mais la rate et la moelle osseuse en absorbent une petite partie. On a étudié l'absorption par la moelle osseuse sur un grand nombre de sujets par scintigraphie du corps humain et par traçage du profil de radioactivité du corps humain. On a pu distinguer trois types principaux de répartition:

1. Type normal. Chez les sujets ne présentant pas de troubles de la moelle osseuse, l'absorption de ^{198}Au était limitée aux parties centrales du squelette (thorax, épine dorsale, bassin, crâne et épiphyses proximales du fémur et de l'humérus), c'est-à-dire aux emplacements normaux de la moelle osseuse rouge active. Sauf aux épiphyses proximales du fémur et de l'humérus, on n'a décelé qu'une très faible absorption dans les os des bras et des jambes.

2. Type hyperplasique. On a observé ce type de répartition dans les polyglobulies vraies et les hémolyses. L'absorption par la moelle osseuse était plus importante et une absorption considérable s'est souvent manifestée, non seulement dans les parties centrales du squelette, mais aussi dans les os longs des bras et des jambes.

3. Type destructif. On a rencontré ce type régulièrement dans les cas de myélofibrose et très souvent dans les cas de leucémie, de carcinomatose de la moelle osseuse et de lymphogranulomatose affectant la moelle osseuse. Ce type était caractérisé par une diminution générale de l'absorption par la moelle osseuse dans les parties centrales du corps, accompagnée d'un accroissement de l'absorption dans les os longs des bras et des jambes dû à l'hématopoïèse périphérique compensatrice. On a pu observer de cette façon tous les degrés de destruction de la moelle osseuse et d'hyperplasie périphérique compensatrice.

Par traçage du profil du corps humain, on a pu obtenir une expression plus quantitative et mieux reproductible de l'absorption par la moelle osseuse. On a procédé à plusieurs examens dans les cas de polyglo-

bulies vraies; dans certains cas, il a été possible de suivre les variations de l'absorption par la moelle osseuse qui se produisaient lorsque la polyglobulie évoluait vers une phase de myélofibrose. Dans des scintigrammes détaillés du bassin, on a pu également étudier l'étendue d'anomalies locales, telles que les tumeurs et métastases osseuses. Le mémoire fait également état de plusieurs améliorations apportées au collimateur et à la méthode d'enregistrement.

СЦИНТИГРАММЫ КОСТНОГО МОЗГА ПОСЛЕ ВНУТРИВЕННОГО ВВЕДЕНИЯ КОЛЛОИДАЛЬНОГО ЗОЛОТА-198. Коллоидальное золото-198 после внутривенного введения быстро выводится из крови в результате деятельности ретикуло-эндотелиальной системы. Большая часть введенного коллоида поглощается печенью, однако небольшая часть поглощается селезенкой и костным мозгом. Для изучения поглощения коллоида костным мозгом, проводилось исследование большого количества пациентов с помощью сцинтиграмм всего организма и профильного измерения уровня радиоактивности всего организма. Установлено три основных типа распределения:

1. Нормальный тип. У пациентов, не страдающих заболеваниями костного мозга, поглощение золота-198 было ограничено областями центральных отделов костной системы (грудная клетка, позвоночник, таз, череп и проксимальные эпифизы бедренной и плечевой костей), т.е. обычными участками активного красного костного мозга. За исключением проксимальных эпифизов бедренной и плечевой костей не обнаружено никаких или обнаружены очень небольшие следы поглощения в костях рук и ног.

2. Гиперпластический тип. Такой вид распределения был обнаружен при истинной полицитемии и в условиях гемолиза. Поглощение в костном мозгу увеличивалось и помимо центральных отделов костной системы значительное поглощение зачастую имело место в длинных костях рук и ног.

3. Деструктивный тип. Этот тип распределения постоянно обнаруживался при миелофиброзе и очень часто при лейкемии, карциноматозе костного мозга, злокачественной лимфоме с поражением костного мозга. Он характеризовался общим снижением поглощения в костном мозгу в центральных отделах организма наряду с увеличением степени поглощения в длинных костях ног и рук в связи с компенсаторным периферическим гематопоэзом. В этом случае можно было наблюдать все степени разрушения костного мозга и коменсаторной периферической гиперплазии.

В результате профильного измерения радиоактивности всего организма можно было получить более полное количественное и воспроизводимое выражение для поглощения в костном мозгу. В случаях истинной полицитемии проводились повторные исследования. В некоторых случаях удавалось проследить изменения степени поглощения в костном мозгу при превращении истинной полицитемии в стадию миелофиброза. На основании подробных сцинтиграмм таза можно было также исследовать степень развития местных нарушений, например костных опухолей и костных метастазов. Сообщается также о некоторых усовершенствованиях конструкции коллиматора и метода регистрации.

CENTELLEOGRAMAS DE LA MÉDULA ÓSEA DESPUÉS DE UNA INYECCIÓN INTRAVENOSA DE ORO-198 COLOIDAL. El ^{198}Au coloidal inyectado por vía intravenosa es rápidamente eliminado de la sangre por la actividad del sistema reticuloendotelial. La mayor parte del coloide inyectado se fija en el hígado, pero el bazo y la médula ósea absorben una pequeña cantidad. El autor ha estudiado la absorción medular en un gran número de pacientes mediante centelleogramas del cuerpo entero y por trazado del perfil de radiactividad del cuerpo entero, y ha observado tres tipos principales de distribución.

1. Tipo normal. En los pacientes que no sufrían ninguna afección de la médula ósea sólo absorbieron ^{198}Au las partes centrales del esqueleto (tórax, columna vertebral, pelvis, cráneo y epífisis proximales del fémur y del húmero), es decir, las zonas donde normalmente se encuentra la médula ósea roja en actividad. Exceptuando las epífisis proximales del fémur y del húmero, la actividad en los huesos de los brazos y de las piernas fue nula o sumamente leve.

2. Tipo hiperplástico. El autor encontró este tipo de distribución en los casos de policitemia vera y de enfermedades hemolíticas. La absorción medular fue mucho mayor y con frecuencia pudo observarse una absorción considerable, no sólo en la parte central del esqueleto sino también en los huesos largos de los brazos y de las piernas.

3. Tipo destructivo. El autor lo observó regularmente en los casos de mielofibrosis y muy a menudo en los de leucemia, carcinomatosis de la médula ósea y linfomas malignos con repercusiones en la médula ósea. Se caracteriza por una reducción general de la absorción medular en las partes centrales del cuerpo y un aumento de la captación por los huesos largos de las piernas y de los brazos debido a una hematopoyesis periférica com-

pensadora. De esta manera se pudieron visualizar todos los grados de destrucción de la médula ósea y de hiperplasia periférica compensadora.

Por trazado del perfil de radiactividad del cuerpo entero fue posible obtener para la absorción medular una expresión más exacta y reproducible. Se efectuaron repetidos exámenes en casos de policitemia vera; en algunos de ellos fue posible observar los cambios en la absorción medular debidos a la evolución de la policitemia vera hacia la fase de mielofibrosis. Por medio de centelleogramas detallados de la pelvis, se pudo también estudiar la extensión de anomalías locales tales como tumores y metástasis óseos. El autor expone algunos perfeccionamientos introducidos en el diseño del colimador y en el método de registro.

The active, red bone marrow can be visualized by radioactive scanning procedures after intravenous injection of a radioactive colloid (which is taken up by the reticulum cells) or radioiron (which is metabolized in the erythropoetic cells). In this paper only the first-mentioned method will be discussed.

After intravenous injection of colloidal Au^{198} about 90% of the injected material is normally taken up by the liver, while the remaining part is shared between the spleen and the bone marrow. In 1956, while doing some liver scintigrams after relatively large doses of Au^{198}, we observed a slight uptake in the bone marrow (Fig. 1). Using a total-body scintigraph and a detector with a cylindrical collimator (width 2.4 cm, length 8 cm), we examined patients with polycythemia vera, myelofibrosis and different malignant bone marrow diseases after intravenous injection of 1–2 mc colloidal Au^{198}. Good correlation was found between the uptake of colloidal Au^{198} in the bone marrow and the occurrence of active haematopoesis. Three types of distribution patterns could be demonstrated:

1. Normal pattern

In patients without bone marrow disease the uptake of Au^{198} was limited to the central parts of the body (chest, spine, pelvis, skull and proximal epiphyses of femora and humera), i.e. normal sites for active, red bone marrow. With exception of the proximal epiphyses of femur and humerus usually no uptake was demonstrated in the bones of arms and legs.

2. Hyperplastic pattern

This type of distribution was found in polycythemia vera and haemolytic conditions, and probably also occurs in other diseases with hyperplasia of the bone marrow. It was characterized by increased uptake in the bone marrow and, besides the central part of the body, considerable uptake was often demonstrated in the arms and the legs (Fig. 2).

3. Destructive pattern

This pattern was regularly found in myelofibrosis and occurred very often in leukaemia, myeloma, malignant lymphoma and bone-marrow carcinomatosis. In these cases a general reduction of the bone-marrow uptake in the central parts of the body was observed often combined with increased uptake in the legs and the arms due to compensatory peripheral haematopoesis (Figs. 3, 4 and 5).

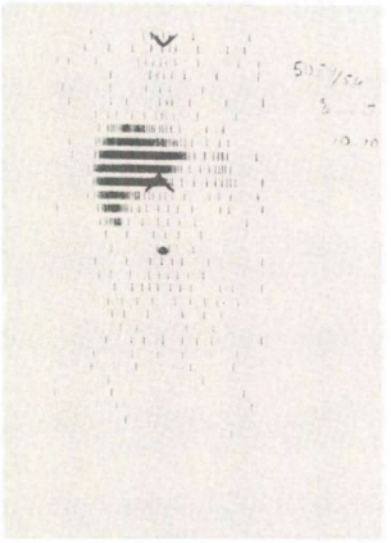

Fig. 1

The original scintigram made in 1956, in which a slight uptake of colloidal Au^{198} in the bone marrow was observed

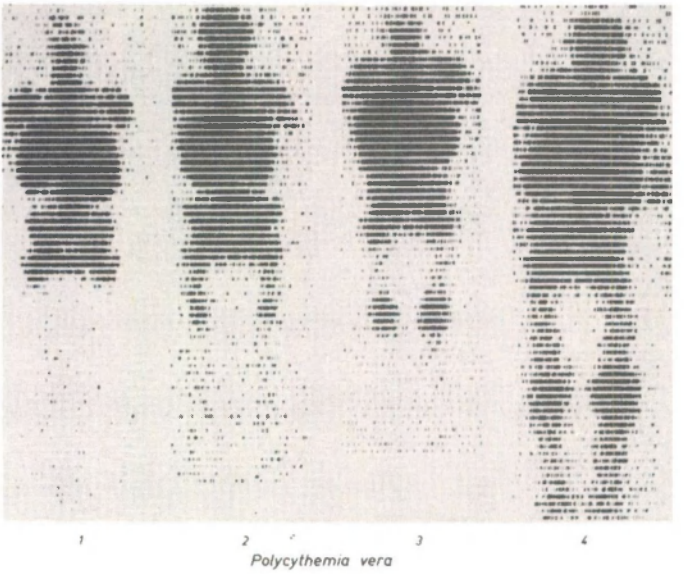

Fig. 2

Bone-marrow scintigrams after intravenous injection of Au^{198}
Hyperplastic patterns in polycythemia vera.

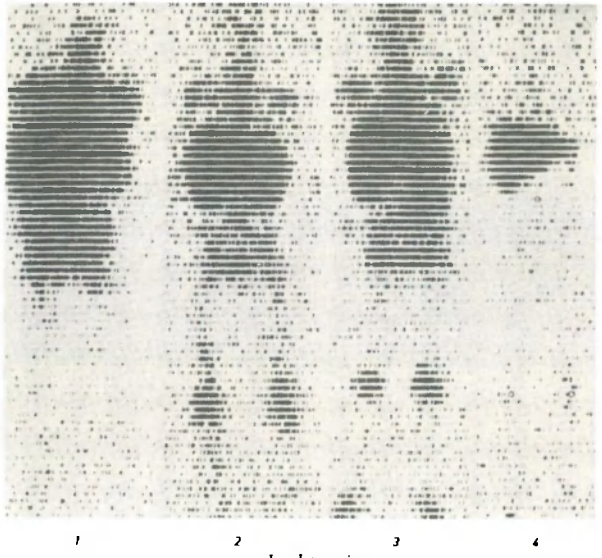

Leukaemia

Fig. 3

Bone-marrow scintigrams after intravenous injection of Au^{198}
Destructive patterns in leukaemia.

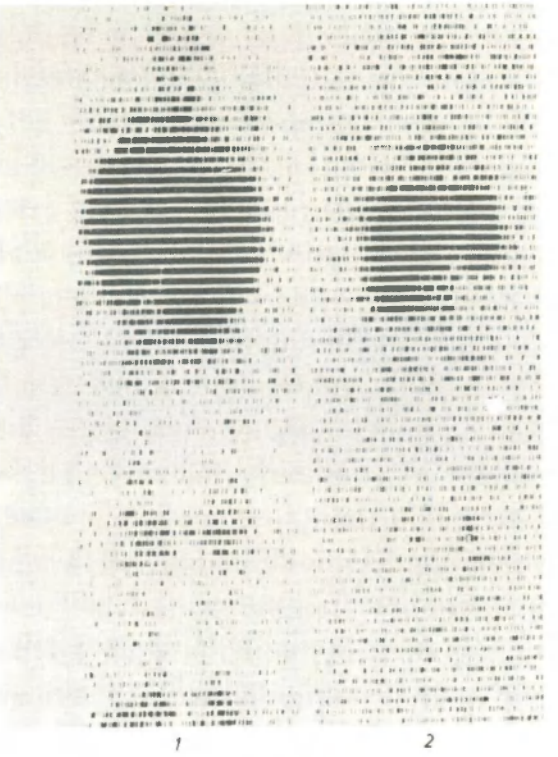

Myelofibrosis

Fig. 4

Bone-marrow scintigrams in two cases of myelofibrosis revealing pronounced reduction of bone-marrow reticulum

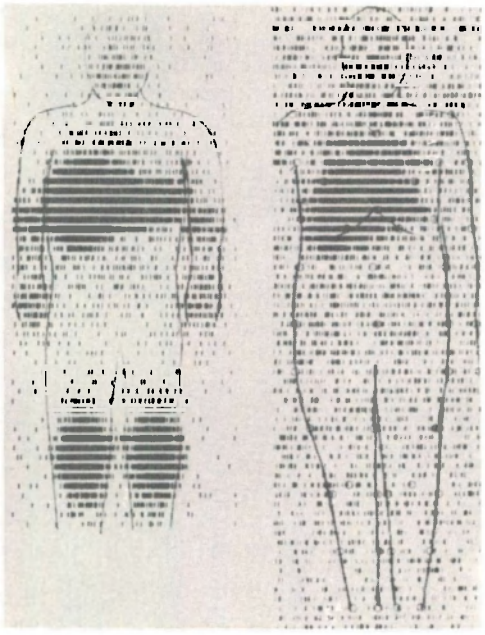

Fig. 5

Bone-marrow scintigrams in two patients with bone-marrow carcinomatosis. The left case had widespread roentgenologic bone metastasis. In the right case no metastases could be observed on the roentgen films, but the carcinomatosis was verified by bone-marrow puncture.

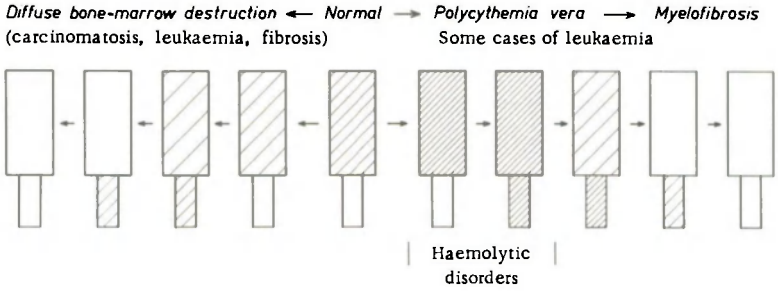

Fig. 6

Scheme of development of different patterns of bone-marrow uptake of colloidal Au[198]
The large rectangles represent the normal site for haematopoesis and the small rectangles represent peripheral haematopoesis.

The probable development of the different patterns is schematically presented in Fig. 6.

In order to obtain better resolution and sensitivity we have modified the technique in several ways during the last few years. The original small

NAI(Tl) crystal ($1\frac{3}{4}$ in × 1 in) was replaced by a larger crystal ($4\frac{1}{4}$ in × 2 in) supplied with multi-channel collimators (Fig. 7), which improved the scanning picture considerably (Fig. 8). For registration we simultaneously used a mechanical printer and a magnetic tape recorder (BERNE et al.[1]), which allowed the reproduction of a series of scans with different degree of impulse-rate suppression. This gave a semiquantitative impression of the uptake in various regions (Figs. 9 and 10). The scanning speed was 60 cm/min and the spacing 2.4 cm.

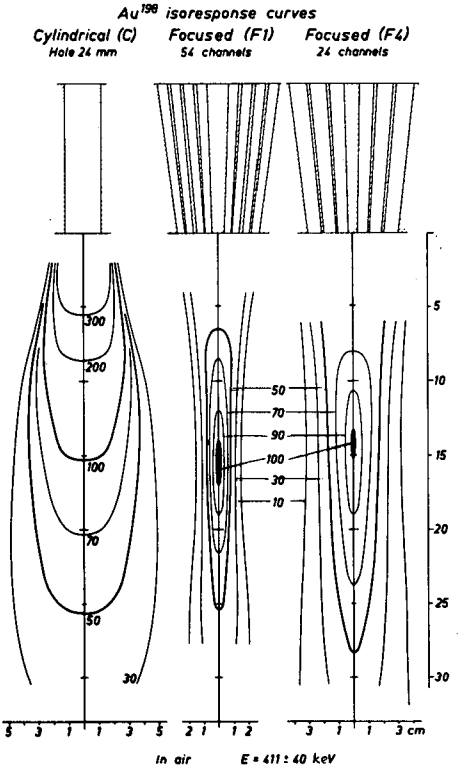

Fig. 7

Isosensitivity curves (in air) for the different collimators

To obtain a reproduceable and numerical expression for the bone-marrow uptake we used profile scanning ad modum POCHIN [2]. For that purpose the detector was supplied with a slot collimator with a width of 1 cm. The distance between the crystal and the jugular fossa was standardized to 30 cm and the detector was moved with a speed of 10 cm/min from head to feet with the patient in supine position. The impulse rates were recorded by means of two linear ratemeters and a dual-channel pen recorder, allowing simultaneous recording of the high impulse rates over the liver and the much lower rates over various parts of the bone marrow (Fig. 11). The curve was calibrated by measurement of a standard dose of Au^{198}. For numerical

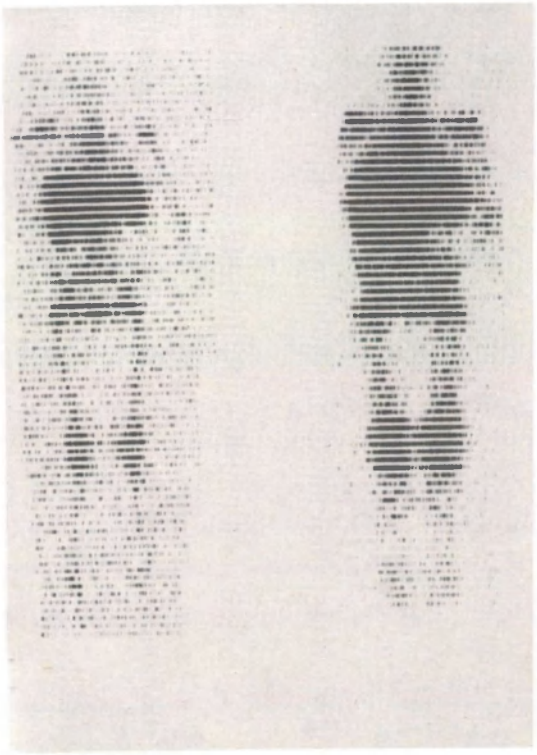

Fig. 8

Improvement of resolution obtained with a multichannel collimator (F1) compared with cylindrical collimator (right scintigram)

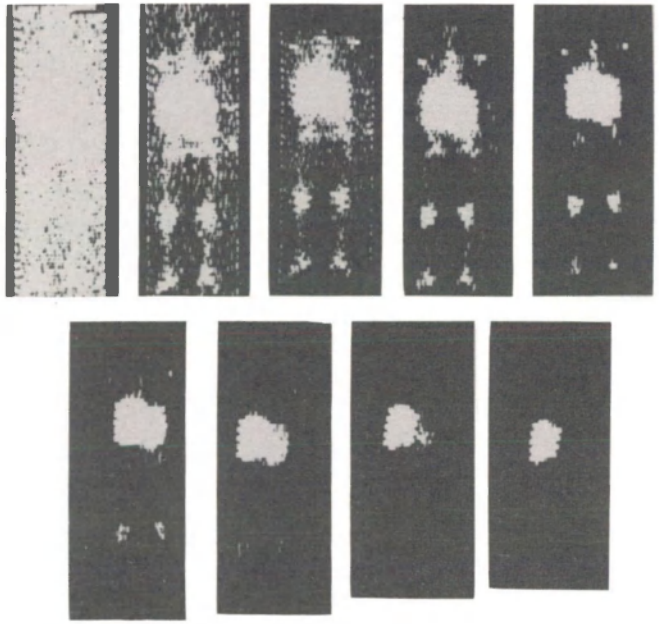

Fig. 9

Polycythemia vera with pronounced peripheral haematopoesis
Magnetic tape recording.

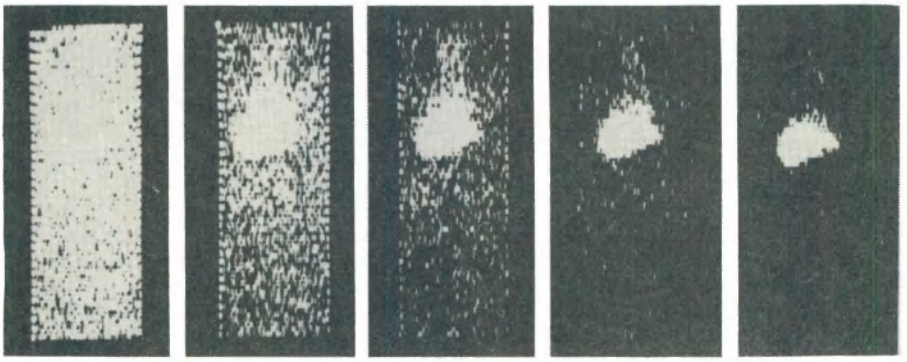

Fig. 10

Bone-marrow carcinomatosis with pronounced bone-marrow destruction. Magnetic tape recording.

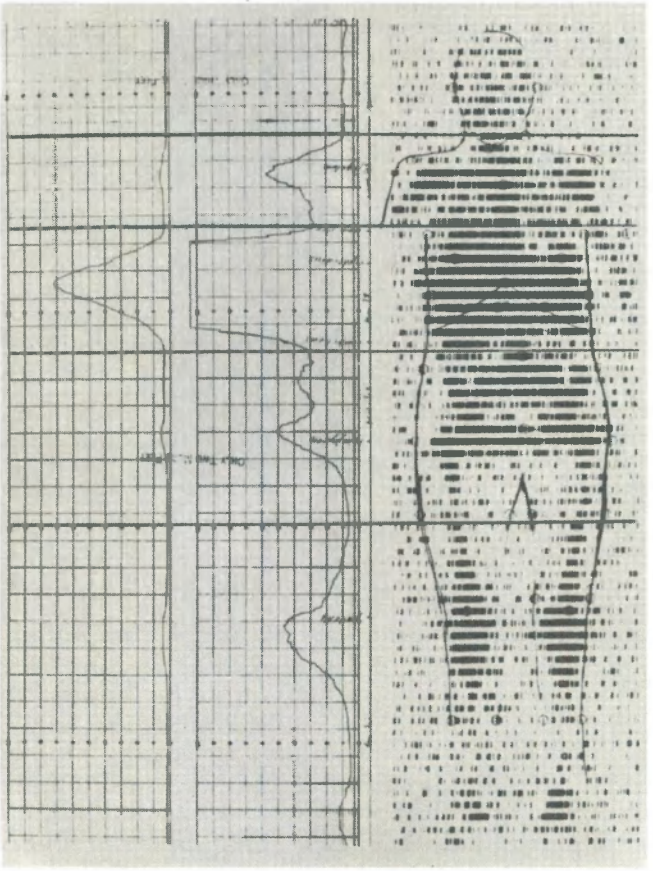

Fig. 11

Profile scanning in patient with polycythemia vera

interpretation the surfaces below five different parts of the curve were measured corresponding to the head, the upper part of the chest including the shoulder girdle, liver and spleen, pelvis (including the proximal parts of femora) and the remaining parts of the legs. To calculate these different areas we used an arrangement with two scalers and a read-out unit. The impulses were alternately counted in the two scalers with time intervals corresponding to 1 cm of the profile scan. The numerical expression thus obtained gave in some way more information than the scintigram, especially regarding the uptake in the normal sites for active bone marrow. An example of the value of this method is demonstrated in Fig. 12, which gives the result in ten consecutive controls, 25 cases of polycythemia vera in active stage and 25 cases of leukaemia. Most cases of polycythemia vera had increased relative uptake in the bone marrow and many leukaemias had decreased uptake. Also, however, some cases with increased bone-marrow uptake were found among the leukaemia patients.

Profile counting made it also possible to follow individual patients during different phases of their disease. We had for instance the opportunity to follow the development of myelofibrosis in some cases of polycythemia vera and observed a good correlation between the degree of fibrosis and the reduction of Au^{198} uptake in the bone marrow. As might be expected, treatment with P^{32} usually caused depression of the bone-marrow uptake (Fig. 13).

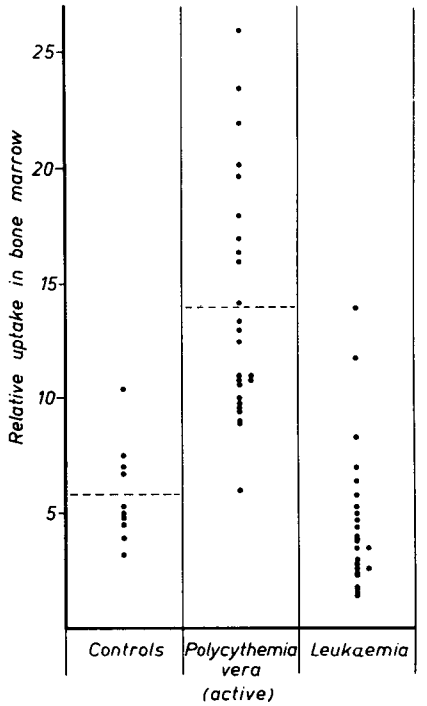

Fig. 12

Relative bone-marrow uptake in controls, polycythemia vera and leukaemia

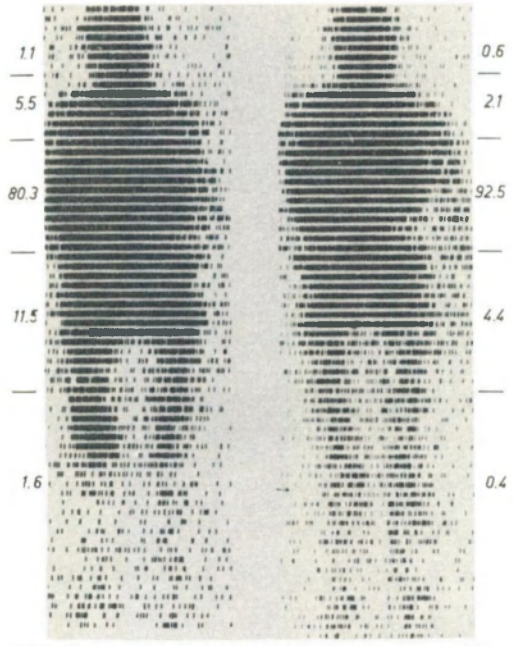

Fig. 13

Depression of bone-marrow uptake after P^{32} -treatment in a case of polycythemia vera

Sometimes, however, the pattern of distribution changed also after the treatment, with reduction of the uptake in the central parts of the body and simultaneous increase of uptake in the more peripheral parts (Fig.14). This and several other observations gave the impression that the activity of the bone-marrow reticulum might be regulated by some hormonal mechanism of feed-back type.

By scanning technique it was also possible to obtain a more detailed picture of special parts of the bone-marrow system (Fig.15), including possibilities for demonstration of localized lesions such as tumours and metastases (Fig.16).

Even with the improvements described above the method requires too large tracer doses for a more extensive use in benign diseases. A good total-body scintigram can seldom be obtained after less than about 0.5 mc Au^{198} in cases with normal uptake and 0.2-0.3 mc in patients with increased uptake (for instance polycythemia vera). The profile counting requires doses in the order of 0.1-0.2 mc. We think, however, that the method can be further improved by development of the detector and registration system, by the use of more short-lived radioisotopes or, perhaps, by the use of colloids with less affinity to the liver and more affinity to the bone-marrow reticulum. It is also possible that radioisotopes of iron will be more suitable for bone-marrow scanning.

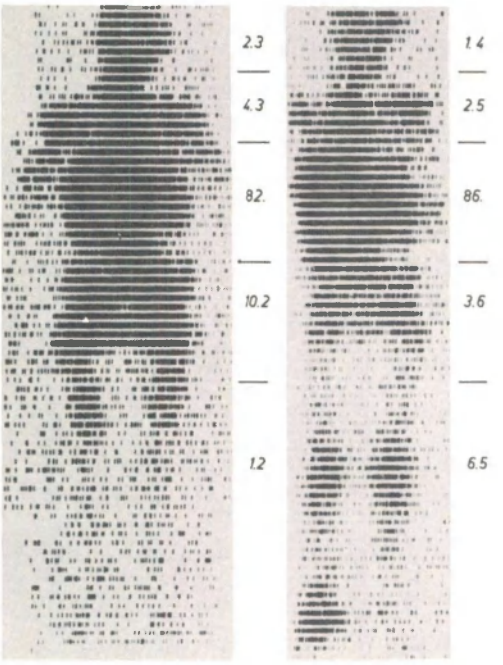

Sep. 22, 1960 Sep. 5, 1962

Polycythemia vera

Fig. 14

Changes in the pattern of distribution of colloidal Au^{198} in the bone marrow of a patient with polycythemia vera treated four times with P^{32} between Sep. 1960 and Jan. 1962 (total dose 24 mc P^{32})

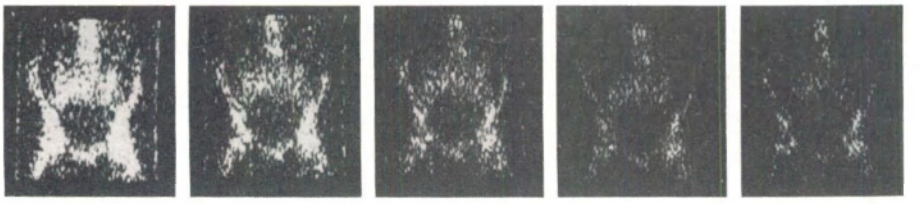

Fig. 15

Scintigram of the pelvis. Magnetic tape recording.

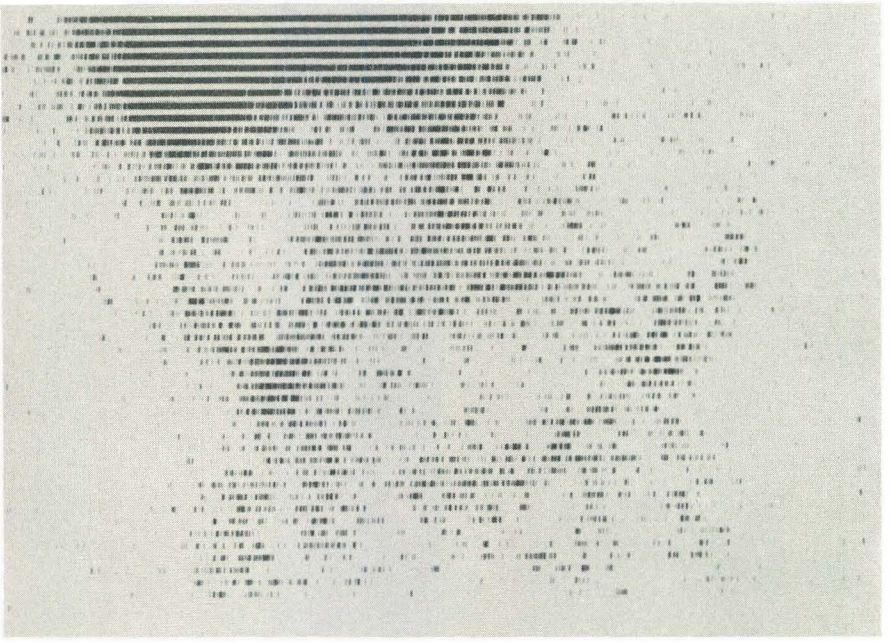

Fig. 16

Bone metastasis in a patient with carcinoma of the rectum
The defect visualized in the left iliac bone in the scintigram was verified as a metastasis by a bone-marrow aspiration but could not be demonstrated on the radiographs.

REFERENCES

[1] BERNE, E. and JONSSON, U., "Ein magnetischer Analysator für die quantitative Auswertung von Scintigrammen", Nucl.-Med. 1 (1959) 80.
[2] POCHIN, E. E., "Profile counting", Medical Radioisotope Scanning, IAEA, Vienna (1959) 143.

BIBLIOGRAPHY

ENGSTEDT, L., FRANZÉN, S., JONSSON, L. and LARSSON, L.-G., "In vivo localization of colloidal Au^{198} intravenously injected in polycythemia vera", Acta radiol. 49 (1958) 66.
JONSSON, L., LARSSON, L.-G. and RAGNHULT, L., "A scanning apparatus for the localization of gamma emitting isotopes in vivo", Acta radiol. 47 (1957) 217.
LARSSON, L.-G., Medical Radioisotope Scanning, IAEA, Vienna (1959) 117.
LARSSON, L.-G., ENGSTEDT, L., FRANZÉN, S. and JONSSON, L., "Bone marrow scintigrams. An in vivo study of the bone marrow reticulum in malignant bone marrow diseases", Acta Union contre Canc. 16 (1960) 1473.
LARSSON, L.-G. and JONSSON, L., "Totalscintigram av människokroppen", Svenska LäkT. 54 (1957) 1817.

SCANNING OF BONE MARROW IN HAEMATOPOIETIC DISORDERS

R. M. KNISELEY, G. A. ANDREWS, C. L. EDWARDS* AND R. TANIDA
OAK RIDGE INSTITUTE OF NUCLEAR STUDIES**
TENN., UNITED STATES OF AMERICA

Abstract — Résumé — Аннотация — Resumen

SCANNING OF BONE MARROW IN HAEMATOPOIETIC DISORDERS. Scanning can help evaluate size and distribution of the haematopoietic marrow, a difficult task by aspiration or biopsy. With the 61-hole focusing gold-tungsten Oak Ridge National Laboratory Scanner, the marrow organ has been clearly delineated by means of intravenous colloidal Au^{198}, it being known that reticulo-endothelial function in the marrow correlates with areas of haematopoiesis. Patients with normal haematopoiesis and with a variety of blood disorders such as focal marrow lesions, acute and chronic leukaemia, polycythaemia vera, myelofibrosis, multiple myeloma, and lymphoma have been scanned. Because of the reticulo-endothelial activity in liver and spleen, the marrow pattern is obscured in the mid-trunk. Vertebral bodies, intervertebral discs, pelvis and long bones are outlined, and, in the thorax, the sternum and thoracic vertebrae. Focal lesions have also been found. Because of respiratory motion, individual ribs are not seen. In expanded marrow, the knee region can be shown, including the joint space. It has been possible to correlate these scans with aspiration biopsy and with linear scans. Because relatively large doses of Au^{198} are required, other isotopes are being investigated. An improved whole-body scanner is being tested for more practical scans.

GAMMAGRAPHIE DE LA MOELLE OSSEUSE DANS LES TROUBLES HÉMATOPOÏÉTIQUES. La gammagraphie permet d'évaluer plus aisément l'importance quantitative et la répartition de la moelle hématopoïétique, tâche qu'il est difficile de réaliser par biopsie. Au moyen du scintigraphe or-tungstène, à collimateur avec 61 canaux à focalisation, du Laboratoire national de Oak Ridge, on a pu nettement délimiter l'organe médulleux à la suite d'une injection intraveineuse d'or-198 colloïdal; on sait, en effet, que la fonction réticulo-endothéliale de la moelle correspond à des zones d'hématopoïèse. On a fait des gammagraphies sur des sujets présentant une hématopoïèse normale mais divers troubles sanguins: lésions focales de la moelle, leucémie aiguë et chronique, polyglobulie vraie, myélofibrose, myélomes et lymphomes. Etant donné l'activité réticulo-endothéliale dans le foie et la rate, la structure médullaire est obscurcie au milieu du tronc. Les vertèbres, les disques intervertébraux, le bassin et les os longs apparaissent très nettement ainsi que – dans le thorax – le sternum et les vertèbres thoraciques. On a aussi relevé des lésions focales. En raison du mouvement respiratoire, on ne distingue pas les diverses côtes. Il a été possible de mettre les scintigrammes en corrélation avec des biopsies par aspiration et des scintigrammes linéaires. Comme il faut des doses de ^{198}Au relativement importantes, on étudie actuellement certains autres radioisotopes. On essaie un appareil perfectionné de scintigraphie de l'ensemble du corps en vue d'obtenir des scintigrammes plus pratiques.

СКЕННИРОВАНИЕ КОСТНОГО МОЗГА ПРИ ГЕМАТОПОЭТИЧЕСКИХ НАРУШЕНИЯХ. Скеннирование может помочь при оценке объема и распределения гематопоэтического костного мозга – трудной задаче для аспирации или биопсии. С помощью скеннера с золотым-вольфрамовым фокусирующим коллиматором диаметром 61 мм в Окриджской национальной лаборатории после внутривенного введения коллоидального золота-198 были получены четкие очертания костного мозга, причем известно, что ретикуло-эндотелиальная функция костного мозга соответствует областям гематопоэза. Скеннирование проводилось у пациентов с нормальным гематопоэзом и с разными нарушениями крови, например с очаговым поражением костного мозга, острой и хронической лейкемией, истинной полицитемией, миелофиброзом, множественной миэломой и лимфомой. В связи с ретикулоэндотелиальной активностью в печени и селезенке изображение костного мозга затемнено в центральном отделе. Очерчены тела позвонков, межпозвоночные диски, кости таза и длинные кости, а в грудной клетке гру-

* Present address: United States Public Health Service, Staten Island, N. Y.

** Under contract with the United States Atomic Energy Commission.

дина и грудные позвонки. Обнаружены также очаговые поражения. Отдельные ребра не видны из-за дыхательных движений. При разрастании костного мозга его можно видеть в коленной области, включая область сустава. Появилась возможность связать эти скенограммы с данными аспирационной биопсии и с линейными диаграммами. В связи с тем, что требуются сравнительно большие дозы золота-198, исследуется возможность применения других изотопов. Для получения скеннограмм, имеющих большее практическое значение, в настоящее время испытывается усовершенствованное устройство для скеннирования всего организма.

EXPLORACIÓN DE LA MÉDULA ÓSEA EN CASOS DE TRASTORNOS HEMATOPOYÉTICOS. La centelleografía puede constituir una ayuda valiosa para evaluar el tamaño y la distribución de la médula hematopoyética, operación difícil de realizar por aspiración o por biopsia. Con el centelleógrafo del Oak Ridge National Laboratory (colimador de oro-wolframio enfocado, de 61 canales) los autores han podido delinear claramente la médula inyectando oro-198 coloidal por vía endovenosa, ya que se sabe que la función reticuloendotelial de la médula está relacionada con zonas de hematopoyesis. Han sometido a exploración gammagráfica a pacientes con función hematopoyética normal y a otros con diversos trastornos de la sangre: lesiones focales de la médula, leucemia aguda o crónica, policitemia vera, mielofibrosis, mieloma múltiple y linfoma. La actividad reticuloendotelial del hígado y del bazo no permiten distinguir bien la médula en la parte central del tronco. En los centelleogramas se perciben claramente las vértebras, los discos intervertebrales, la pelvis y los huesos largos y, en el tórax, el esternón y las vértebras torácicas. Se han hallado también lesiones focales. Los movimientos respiratorios no permiten ver individualmente las costillas. Cuando la médula está dilatada se puede visualizar la zona de la rodilla, incluido el espacio articular. Los autores han logrado establecer una correlación entre estos centelleogramas, los resultados de biopsias por aspiración y centelleogramas lineales. Como se requieren dosis relativamente elevadas de oro-198, se está estudiando la posibilidad de emplear otros isótopos. También se está ensayando un antropogammámetro perfeccionado con el fin de facilitar la exploración.

1. INTRODUCTION

The organ of haematopoiesis is difficult to locate and quantitate. Its response to stimuli such as haemorrhage, infection, altitude, or disturbances in homeostasis is difficult to measure: (a) the peripheral blood often does not reveal the bone-marrow picture accurately, and (b) there are limits to the numbers and sites of bone-marrow aspirations. Single bone-marrow aspirates, although a valuable procedure in studying disorders of haematopoiesis, may not provide a representative aliquot of the organ. Moreover, roentgenology, although it is evolving useful adjunct information for the field of haematology [1], usually gives little information on the sites or functional activity of bone marrow.

Refinements in scintillation scanning have stimulated our group to investigate patients with a variety of haematopoietic disorders. ENGSTEDT et al [2] showed the feasibility of total-body scintigrams after intravenous injection of colloidal Au^{198}. We also have been able to demonstrate the distribution of haematopoietic marrow with considerable detail [3], exploiting the observation [4] that the distribution of intravenously injected colloids in the bone marrow correlates well with the areas of active haematopoiesis. POCHIN [5] has suggested the uses of profile scanning in giving a rapid and quantitative measure of radioisotope distribution throughout the body.

2. MATERIALS AND METHODS

2.1. Instrumentation

Area scans were obtained with the Oak Ridge National Laboratory (ORNL) research scanner. This device is equipped with a tungsten-alloy shield,

3 in × 2 in NaI crystal with a 37-tapered-hexagonal-hole-gold collimator focusing 3 in from its front face [6, 7]. Photoscans were recorded using a 1:1 dot factor with the spectrometer setting at the 410-keV energy peak for Au^{198} and a window opening of 100 keV. Scans were made at the speed of 0.3 in/s and the collimator was placed to traverse at minimum clearance across the surface of the patient. Profile scans were obtained with the ORINS linear scanner [8]. This instrument consists of twelve 2-in NaI crystals arranged in two opposing lines of six each, shielded with movable jaws of lead 2-in thick, and placed at a distance from each other of 39 in. The patient is placed on a motor-driven platform, which passes between the two sets of detectors at a table speed of 12 in/min. Signals from the detectors are fed into a spectrometer with an energy band set at 410 keV and a window width of 100 keV. The profile of radioactivity is recorded on a recording ratemeter.

2.2. Procedure

Intravenous doses of usually 1 - 2.5 mc of colloidal Au^{198}* are administered. Since the reticuloendothelial system clears the gold from the circulation with a half-time of 3 - 5 min, scanning can begin 15 - 30 min after intravenous injection. Test material once phagocytosed remains fixed and apparently does not redistribute; hence scanning can be carried out at any time during the next day or so. Routinely the following views were obtained; anterior chest, anterior pelvis, posterior pelvis. Serial linear scans were made at three different ratemeter scale settings to provide three levels of sensitivity. In patients for whom the linear scan indicated abnormal distribution of radioactivity into the extremities, area scans of the skull and upper and lower extremities were also obtained.

2.3. Patients

A total of 60 groups of scans have been prepared on 51 patients with a variety of haematopoietic disorders, as summarized in Table I.

3. RESULTS

We have observed a range of patterns from no visible marrow to a greatly expanded marrow organ with uptake even in the distal bones of the extremities. The experience also includes increases and decreases of uptake in the usual marrow areas and compensatory extension of the marrow organ in certain patients with destructive processes in the sites of usual haematopoiesis. Focal marrow lesions, some of small size, have also been visualized.

* Abbott Laboratories, Oak Ridge, Tenn.

TABLE I

SCANNING OF BONE MARROW

Diagnosis	No. of patients	Summary of findings
Acute leukaemia	10	Pattern varies from low uptake or patchy focal lesions to normal or increased uptake in an expanded organ
Subacute granulocytic leukaemia	2	Normal or expanded organ with increased uptake
Chronic granulocytic leukaemia	1	Somewhat increased uptake and expanded organ
Chronic lymphocytic leukaemia	3	Concentration diminished in advanced stage; normal in one patient with haemolytic complication; patchy decrease in sites of radiation therapy with compensation in long bones
Polycythemia vera	1	Normal or slightly expanded
Polycythemia vera, late stage	3	Varies: expanded organ into long bones; decreased uptake
Myelofibrosis	3	Very low to absent concentration in marrow
Anaemia; acquired haemolytic	1	Increased concentration in usual sites
Anaemia; refractory, sideroblastic	1	Profound expansion of organ and increased uptake
Multiple myeloma	3	Activity in head and in extremities; evidence of attempt to compensate for destroyed marrow
Local radiation therapy for soft-tissue neoplasms	5	Usually low or absent concentration persistent (up to 3-yr observation post radiotherapy) at sites of treatment
Metastatic tumour in bone	2	Defect at site of lesion and radiation therapy
Hodgkin's disease	5	Varies: good visualization with expanded organ in some; focal areas of decreased to absent uptake at site of bone lesion
Lymphosarcoma	4	Focal and regional decrease in some sites; decrease or absence at sites of radiotherapy
No haematologic disease or marrow lesion	7	Activity mainly confined to bones of trunk with small amounts in proximal humeri and femurs. One 18-yr-old patient with lupus had a small amount of activity in the region of the knees

3.1. Normal patterns

Although no truly normal patients were studied, we established approximations of the normal pattern by observing patients without primary blood diseases or known metastases to the marrow. Scans of the pelvic region show the greatest detail and this view has usually provided the most information. Here there is no obscuring of the skeleton by liver or splenic activity. The normal area scans showed most of the activity (outside the large amounts in the liver and spleen) to be in the bones of the trunk. Small amounts were seen in the proximal parts of the humeri and femurs and in the neck and skull. The normal linear scans showed a large peak caused by the liver and spleen; activity was seen in the marrow of the trunk, and with the more sensitive scale settings, very small amounts of the skull, neck and proximal femurs. In the region of the liver and spleen any activity present in marrow was obscured by the large amount in these organs. The amount of colloid deposited in the lungs varied appreciably. In those patients with a relatively large amount in the lungs, and little in the bones of the chest, the heart outline could be seen as a pale area. We have confirmed our suspicion that significant activity may be in the pulmonary parenchyma noting decreased activity on the side of operation in a patient who had had a pneumonectomy. Respiratory motion contributed to the indistinct outline of the ribs. In one emphysematous patient with a relatively fixed chest, the pronounced concentration in individual ribs was seen (Fig. 1c).

3.2. Expansion of marrow

In some patients a general expansion of the marrow organ was clearly shown. This was conspicuous in patients with erythroid hyperplasia; it was most striking in a patient who had a refractory anaemia associated with ineffectual erythropoiesis (Fig. 1) and in a patient who had an extreme erythroid myeloproliferative state subsequent to polycythemia vera. Other examples of less pronounced marrow expansion were seen in certain patients with acute and chronic leukaemia (Fig. 5c).

Compensatory hyperplasia was associated with impairment of function of the marrow in its usual sites. The most notable example was a patient with multiple myeloma (Fig. 2) who had replacement of much of the marrow of the trunk and extension of haematopoietic function to the long bones. The validity of the interpretation of the marrow scans was confirmed by aspiration from multiple sites [3]. Other examples of compensatory marrow expansion, less pronounced, were seen in another patient with myeloma and in three patients with large radiation ports over the trunk. An additional patient with lymphosarcoma, and one with lymphocytic leukaemia, had some extension of marrow into the long bones, possibly related either to radiation therapy of the trunk or to effects of the primary disease.

3.3. Contraction of marrow

Widespread impairment of radioisotope deposition was seen in late stages of polycythemia with marrow fibrosis and in patients with myelofibrosis lacking any earlier history of polycythemia (Fig. 3). A similar picture was

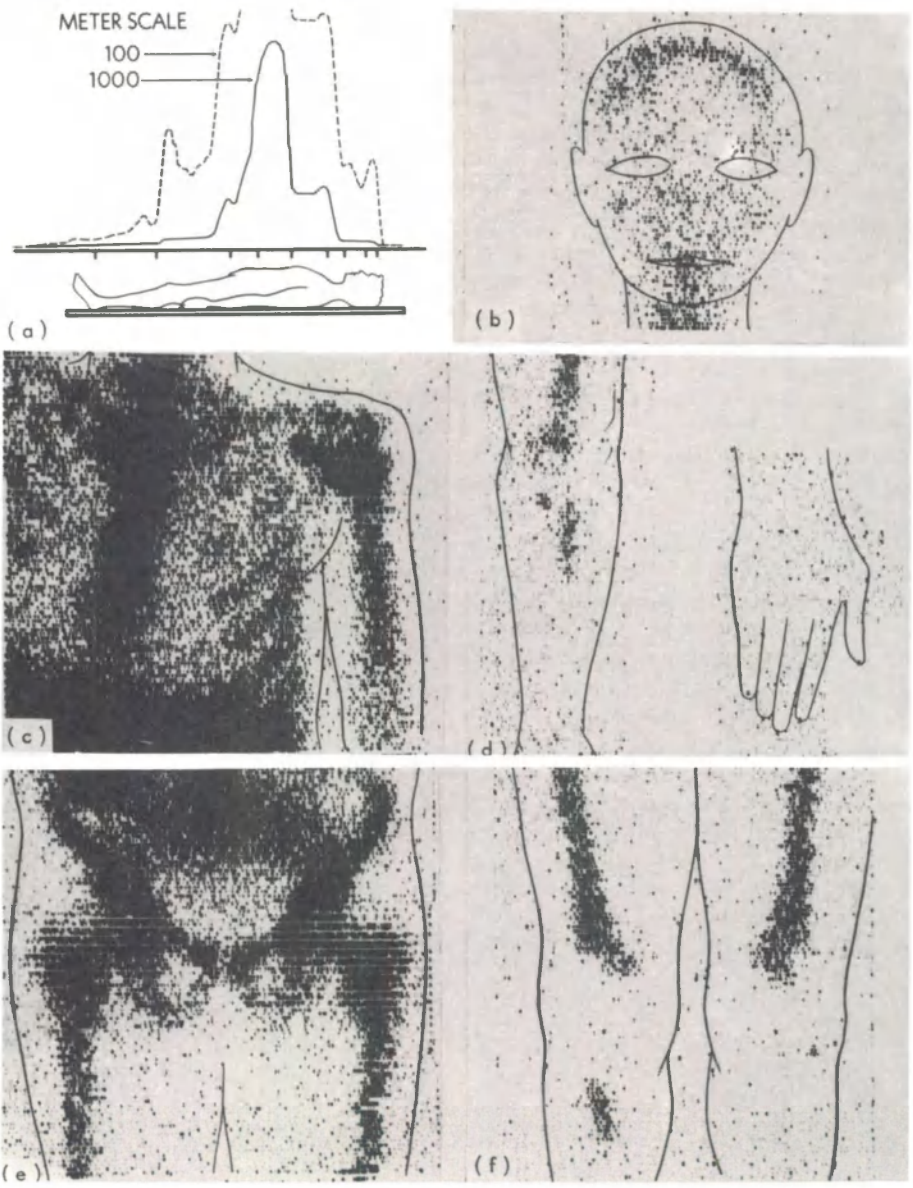

Fig. 1

A 65-yr-old man with chronic refractory sideroblastic anaemia

(a) Linear scan. Expansion of marrow space into head and extremities.
(b) Increase in calvarium and base of skull.
(c) Chest, anterior view. Pronounced increase in bones and expansion into humerus. Note unusually clear outline of ribs. In this patient emphysema prevented usual excursion of chest.
(d) Marrow in distal humerus and proximal forearm.
(e) Anterior view of pelvis with heavy, increased concentration in normal sites and extension into shafts of femurs.
(f) Marrow expanded to knees and proximal right tibia; lateral condyles in this instance not participating. (Marrow aspiration of right lateral condyle of humerus showed fatty marrow with suggestion of necrosis.)

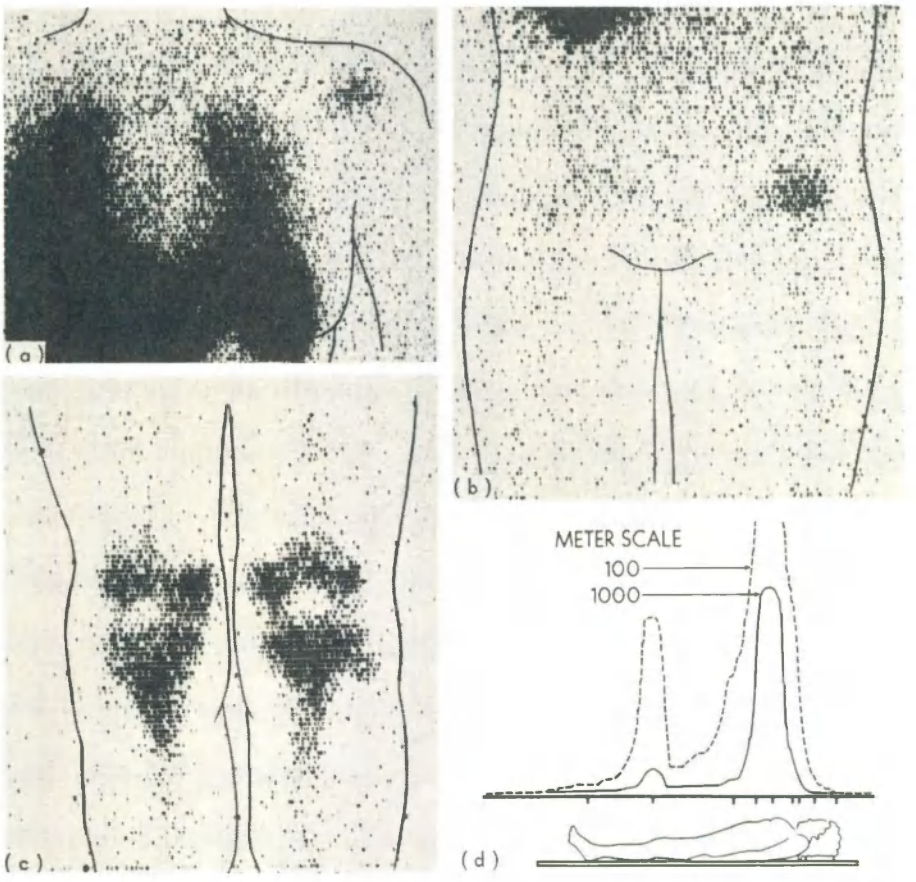

Fig. 2

Multiple myeloma, 52-yr-old woman. Follow-up scans 7 months after previous series [compare illustration in ref. 3]. The disease has progressed and the compensatory haematopoiesis in the periphery is now less pronounced. The patient lost 12 in in height from myeloma widespread in trunk.

(a) Anterior view of chest, increase in lung fields with clear cardiac silhouette, absence of usual thoracic concentration; focal activity, head of humerus.
(b) Anterior view of pelvis; absent uptake in usual bony sites owing to widespread destruction of trunk; foci in heads of femurs.
(c) Compensatory activity in knee region; correlates with aspiration biopsy showing active normal haematopoiesis.
(d) Linear scan showing abnormal distribution of functioning marrow.

also seen in certain cases of acute leukaemia and one patient with a late stage of chronic lymphocytic leukaemia. A mild degree of generalized impaired uptake was seen in one patient with Hodgkin's disease.

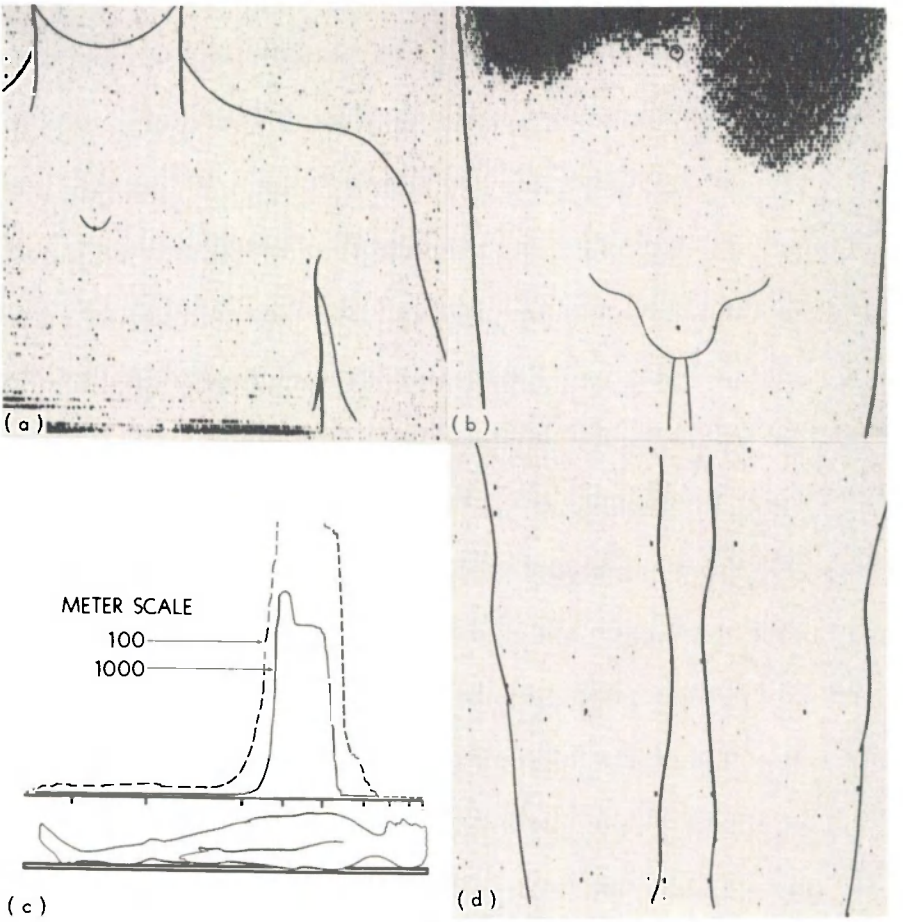

Fig. 3

Myelofibrosis, 30-yr-old man.

(a) Chest scan, absence of usual uptake
(b) Pelvis, anterior view; absence of usual uptake. Note massively enlarged spleen.
(c) Linear scan. Usual liver-spleen peak; absence of bone-marrow localization.
(d) Absence of functioning marrow on area scans of knees.

3.4. Localized destruction

More localized areas of decreased radioactivity were seen in several situations. One unusual patient with acute leukaemia previously reported [3] had extensive necrosis of pelvic marrow associated with complete lack of uptake of the isotope. Areas of impaired concentration of the isotope were seen in multiple myeloma, Hodgkin's disease (Fig. 4), lymphosarcoma, and metastatic carcinoma of the breast.

We observed bone marrow in local irradiation fields; in some instances normal marrow was included incidentally in treatment of lesions not in-

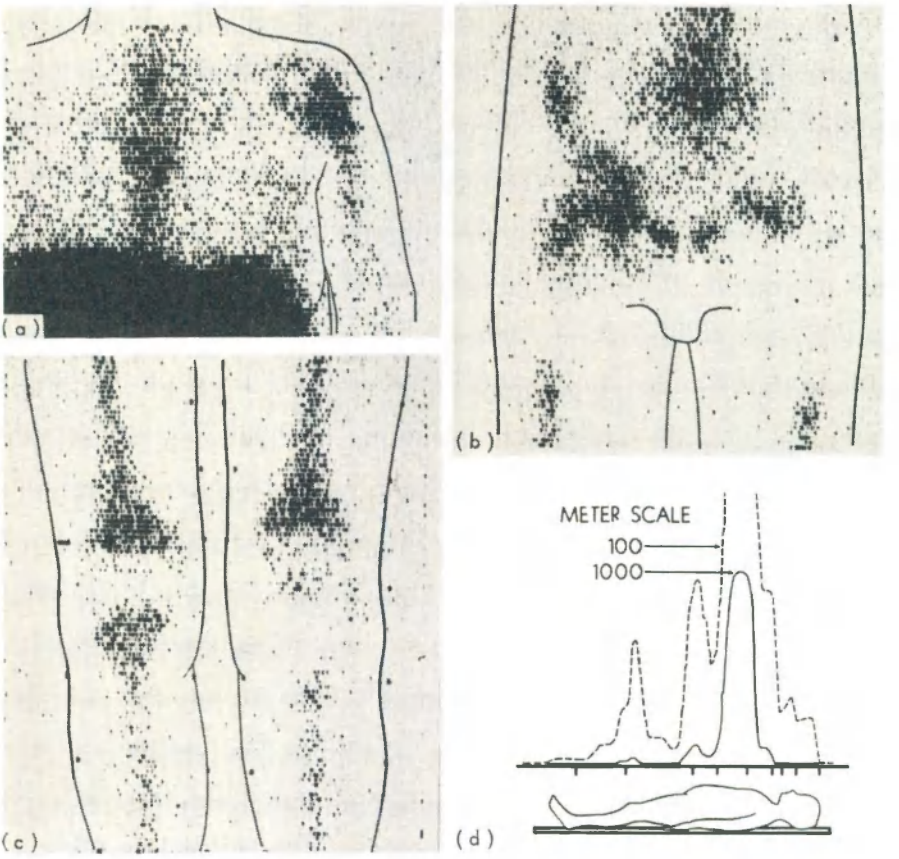

Fig. 4

Hodgkin's disease, 12-yr-old boy. Multiple courses post radiotherapy to chest, pelvis past 2 yr.

(a) Chest with normal concentration in bony thorax. Extension in humerus, normal (?) for age.
(b) Anterior view pelvis: note absence of uptake in left ilium, site of radiotherapy, 3000 r, Co^{60}, completed 10 d before scan.
(c) Anterior view of legs. Extension into extremities pronounced, possibly to be expected in a child; note defect in right tibia, site of pathologic fracture, from Hodgkin's disease.
(d) Linear scan. Increased activity in lower extremities.

volving bone. Our experience with 11 patients demonstrates a range from slight impairment to complete absence of isotope deposition of these sites treated with either palliative or cancerocidal doses. The impairment of uptake has been seen to persist for periods of 2 - 3 yr; longer observations have not been possible. In one 12-yr-old boy with Hodgkin's disease, a normal pattern was seen in marrow in treatment fields within 1 - 2 yr after irradiation; this was considered to be unusually complete and rapid marrow regeneration (Fig. 4).

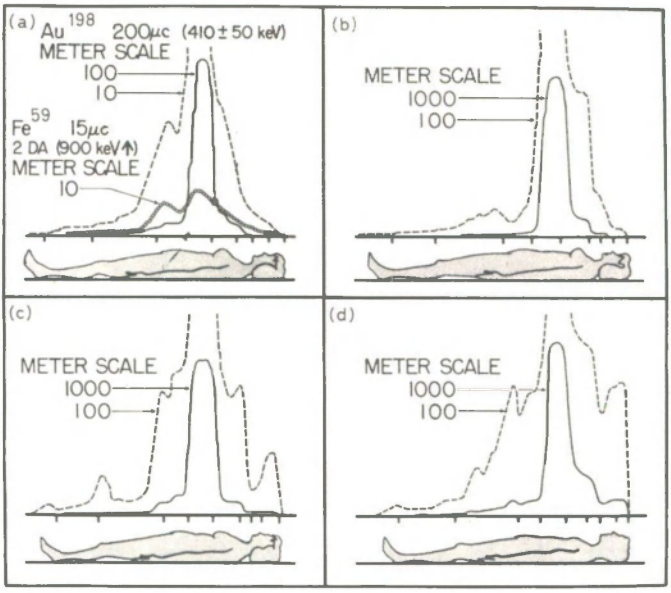

Fig. 5

Linear scans showing characteristic patterns obtained. The liver-spleen peak is most prominent.

(a) Normal profile, 58-yr-old woman with history of obscure anaemia but now free of findings. Dotted line is profile 2 d after 15 μc of Fe^{59}. Solid and dashed lines are after 200 μc of Au^{198}.
(b) Pelvic irradiation for carcinoma of ovary; note crater at site of usual pelvic uptake
(c) Acute leukaemia in 78-yr-old woman; note peripheral expansion into skull and lower extremities
(d) Multiple myeloma, peripheral increase in marrow concentration.

The profile scans (Fig. 5) showed the main peak representing radioactivity in liver and spleen. Bone-marrow activity was seen as lesser elevations above the base line cephalad and caudad to the liver-spleen peak. With more sensitive ratemeter settings (which put the liver-spleen peak off scale) the quantitative distribution along the skeleton was demonstrated.

Normally a peak representing pelvis was the most prominent marrow zone. Patterns in general showed the amount of uptake and the distribution of the organ, except where hidden by the liver-spleen peak. It was of help to show expansion of marrow into the head and long bones of the lower extremities. Small focal lesions were not discernible but large areas of impaired function were recorded (Fig. 5b).

4. DISCUSSION

We anticipate that mapping out and quantitating the haematopoietic bone marrow may be feasible eventually by a combination of the techniques that have been demonstrated in this paper. Even at autopsy such information has been difficult to obtain heretofore. Multiple local surface measurements

with hand-placed scintillation detectors fail to present the required information in a form that can be correlated conveniently with anatomic structures. A number of complex variables must still be worked out for the scanning method and improvements in instrumentation and tracers must be evolved before the procedure will have a broad application. For example, an apparently increased uptake in normal marrow sites as seen on area scans may be the result of increased marrow function; but conceivably contributing to this result might be diminished hepatic blood flow. If a greater fraction of the dose is circulated through the marrow during the early rapid clearance of the colloid from the plasma, then one might expect an apparent enhancement of function of the bone marrow. Particle size, amount of stable carrier, and uniformity of the colloidal preparation also will affect the rates of plasma clearance as well as the sites of localization. In fact, these factors might be exploited for greater relative localization in the bone marrow. The physical characteristics of the radioisotope and the capabilities of the equipment also influence the picture obtained. The size of the patient is significant in relation to absorption and scatter. Area scanning even with optimal focusing collimators [7] does not provide a quantitative record of the radioactivity at various depths in the body. The profile scans were of specific value in certain situations where quantitation is needed. They indicate the extent of expansion or contraction of the marrow organ and may show areas of compensatory haematopoiesis. The profile scans, because of the great sensitivity of the instrument, may show small peaks over the extremities representing concentrations of activity too slight to be seen in area scans. They are not helpful in showing small focal areas of negative uptake in the areas of usual concentration. The profile scans can be made with much smaller test doses (200 μc or less) of colloidal Au^{198}, and thus can be made in patients for whom the larger doses would not be suitable. The profile scans can be made much more rapidly and are less tiring for the patients.

Practically, scans assist in finding the best site for bone-marrow aspiration studies. In a number of the patients, needle-aspiration studies or autopsy findings were available after scans; the observations and interpretations made from the scan records were confirmed, providing a better basis for understanding the nature of the local lesions or abnormal sites of haematopoiesis.

Colloidal Au^{198} has been the most useful tracer isotope in this study, but it is still far from ideal. Colloidal Au^{199} with a lower gamma energy was tried, but scans were unsatisfactory, possibly because of a less than optimal colloidal preparation. Heat-denatured human serum albumin labelled with I^{131} was tried also. However, the release of the iodine label from the reticuloendothelial system within an hour or so after injection creates a high body background and localization of the iodide in the urinary tract obscures the pelvic region. The disadvantages of most colloidal preparations now available have the common failing that the bulk of the dose localizes in the liver and spleen, thus obscuring the midtrunk. Moreover, the colloidal preparations are a direct measure of reticuloendothelial function and only indirectly give evidence on haematopoietic function. In patients of many types a good correlation has been seen between haematopoietic activity and phagocytic activity in the bone marrow. However, we have not had the op-

portunity to study aplastic anaemia or acute marrow depressions caused by chemotherapy; it is possible that in these situations or others the correlation between these two functions is imperfect.

Another disadvantage to the use of colloidal Au^{198} is the relatively high test dose required. Although this dose does not produce any demonstrable haematologic depression, admittedly it is too high for routine use. Hence, in these studies, it has been confined to patients with disorders that would require marrow-depressing therapy or whose outlook is such that the possibility of late radiation effects is not important. Therefore we are seeking ways to improve the method. If a suitable colloid of technetium-99m can be prepared it will have significant advantages over Au^{198}. With the 6-h half-life the radiation exposure is a small fraction of that obtained from Au^{198}. The 140-keV gamma emission would demand much less collimator shielding. The short half-life would also permit relatively frequent serial studies to observe the changes in a patient who is responding to therapy or whose disease process is in rapid transition. Other colloidal preparations with selected amounts of carrier (for example, rare earths) may eventually also offer advantages over Au^{198}.

Ideally an isotope of iron would offer a direct means of observing erythropoiesis. Unfortunately iron-59, in addition to its high gamma-ray energy, has a long half-life so that a dose sufficient to obtain area scans with comparable resolution and reasonable scanning times is not feasible. Informative profile scans can be made with moderate-sized tracer doses (Fig. 5a); however, when iron-52 can be made available, its 8-h half-life will allow significantly larger doses and it should be possible to obtain a direct view of the erythropoietic marrow organ and its size and distribution.

Another area for potential improvement is in refinement of instrumentation. The scanner used in the studies reported here is actually designed for high-resolution area scanning of organs such as brain, thyroid, kidney, and liver. At ORINS a new whole-body scanner has recently been constructed in collaboration with the ORNL group. It uses a 5-in scintillation crystal and a high-resolution lead-focusing collimator, which is described elsewhere in these proceedings [9]. From preliminary scans it has been possible to obtain a whole-body scan in approximately 1 h using doses of Au^{198} similar to those required for the area scanner (Fig. 6). With testing and refinement of this equipment, it is anticipated that rather detailed views of the skeleton can be obtained with considerably greater efficiency, although some loss of resolution will be expected.

5. SUMMARY

Radioisotope scanning techniques promise to be of considerable assistance in determining the size and distribution of the haematopoietic marrow organ. With the 61-hole focusing gold-tungsten research collimator, the marrow organ has been clearly delineated using intravenous colloidal Au^{198}. Patients with normal haematopoiesis and with a variety of haematologic disorders have been studied: focal marrow lesions, acute and chronic leukaemia, polycythemia vera, myelofibrosis, multiple myeloma, and lymphoma. The reticuloendothelial activity in the liver and spleen obscures

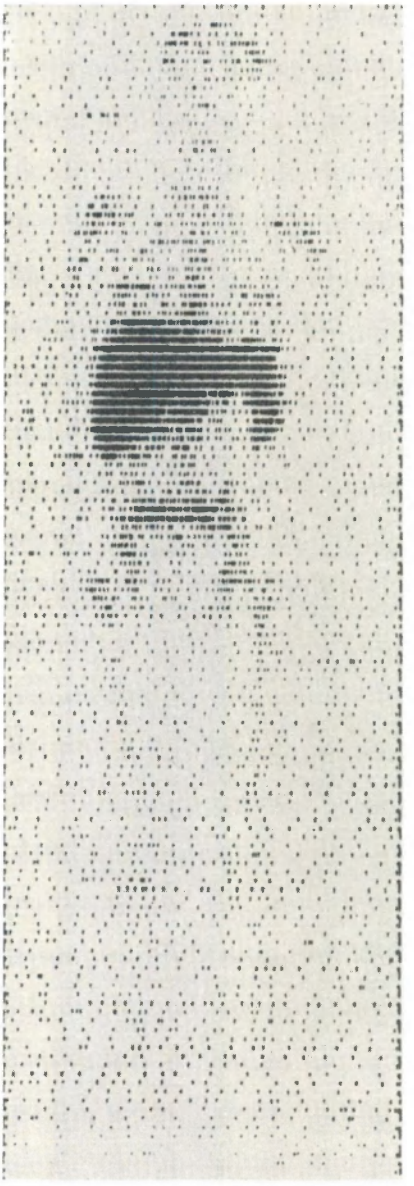

Fig. 6

Whole-body scan, a 78-yr-old woman with acute leukaemia (same as Fig. 5(c)). ORINS whole-body scanner. Scanning time, 1 h, Au^{198}, 2 mc. Distinct expansion of marrow into long bones and head as indicated indicated in linear scan. Some spurious counts on the record are machine artifacts.

the marrow pattern of the midtrunk. Vertebral bodies, intervertebral discs, pelvis, and long bones are outlined, and in the thorax, the sternum, and thoracic vertebrae. In expansion of the marrow organ, the calvarium

and the peripheral long bones can be delineated. Relatively small focal lesions have also been found. Because of respiratory motion individual ribs are not usually seen. Sometimes significant activity in lungs has been demonstrated.

Linear scans give some quantitative estimation of the distribution of marrow along the trunk and are useful in showing abnormal extension of the marrow outside of the trunk. In addition, contractions or regional destruction of the marrow outside of the liver peak can be estimated semiquantitatively.

Aspiration biopsy and autopsy studies confirm the interpretations made on the scans. Thus a broader more comprehensive view of the blood-forming organ can be obtained. Because of the relatively large doses of Au^{198} now required, other tracer isotopes are being investigated. Improved instrumentation for the linear scanner and for area scanning promises more practical and more quantitative techniques.

REFERENCES

[1] MOSELEY, J.E., Bone Changes in Hematologic Disorders, Grune and Stratton, New York (1963).

[2] ENGSTEDT, L., FRANZEN, S., JONSSON, L. and LARSSON, L.-G., "Reticuloendothelial activity studied in vivo in humans by means of whole-body scintigrams after intravenous injection of colloidal Au^{198}", Reticuloendothelial Structure and Function (HELLER, J.H., Ed.), Roland Press Co., New York (1960) 221-32.

[3] EDWARDS, C.L., ANDREWS, G.A., SITTERSON, B.W. and KNISELEY, R.M., Clinical bone marrow scanning with radioisotopes. Accepted (1963) for publication in Blood.

[4] ROOT, S.W., ANDREWS, G.A., KNISELEY, R.M. and TYOR, M.P., The distribution and radiation effects of intravenously administered colloidal Au^{198} in man, Cancer 7 (1954) 856 - 66.

[5] POCHIN, E.E., "Profile counting", Medical Radioisotope Scanning, IAEA, Vienna (1959) 143 - 62.

[6] FRANCIS, J.E., HARRIS, C.C. and BELL, P.R., A Focusing Collimator for Research in Scanning, J.nucl. Med. 3 (1962) 10 - 17.

[7] HARRIS, C.C., BELL, P.R., FRANCIS, J.E., Jr., SATTERFIELD, M.M., JORDAN, J.C. and MURRAY, J.P., Jr., "Collimators for Radioisotope Scanning", Progress in Medical Radioisotope Scanning (KNISELEY, R.M., ANDREWS, G.A. and HARRIS, C.C., Eds.) USAEC Rep. TID-7673 (1963) 25 - 65.

[8] MORRIS, A.C., Jr., "A Linear Scanner for Human Radioisotope Research", USAEC Rep. ORINS-33, (1960) 26 pp.

[9] HARRIS, C.C., BELL, P.R., SATTERFIELD, M.M. and JORDAN, J.C., The design and performance of a large high-resolution focusing collimator, these Proceedings I.

DISCUSSION

(On the two foregoing papers)

R. HÖFER: It may be of interest if I briefly discuss a non-scanning technique we have been using to investigate the uptake of colloids by the bone marrow. We were prompted to do this work after seeing the bone-marrow scans shown by Dr. Larsson* at the Seminar on Medical Radioisotope Scanning organized by the International Atomic Energy Agency in 1959 and by the later observations of Kellershohn and Desgrez demonstrating a high Au^{198}-colloid uptake in the bone marrow of patients with liver cirrhosis. The advantage of our method over the scanning procedures presented by Dr. Larsson

* Medical Radioisotope Scanning, IAEA, Vienna (1959) 117 - 120.

and Dr. Kniseley is that one only needs a Au^{198} dose of 50 - 100 μc. The information it provides will answer many if not all of the questions which can be answered with scanning techniques.

Our technique is as follows. We inject a tracer dose of colloidal Au^{198} and then determine the disappearance curve of the colloid from the blood in two ways, firstly by external counting over the head, and secondly by counting blood samples taken at intervals of 1 to 10 min. The initial counting rate for both disappearance curves is determined by extrapolating to zero time. The results of both types of measurement are then expressed as percentages of initial activity and plotted against time.

Since the counter used for the body-surface measurements over the head "sees" not only blood but also reticulo-endothelial cells in the bone marrow of the head, the curve measured by external counting reflects both disappearance from the blood and uptake by the bone marrow. At any particular time the difference between the percentage initial counting rate measured over the head and the percentage initial counting rate measured in the blood gives an indication of the proportion of the tracer dose taken up by the extrahepatic reticulo-endothelial system in the bone marrow.

It is interesting to note that the figures obtained by this method for the relative bone-marrow uptake (RBU) are in agreement with those that Dr. Larsson obtained by quantitating his profile-counting results. In normal cases our RBU values ranged between 6.9 and 14.8%. The RBU values for polycythaemias were usually high - up to 39%. In some cases, however, where the condition merged into osteomyelosclerosis, low uptakes were found; the lowest we ever observed was 2%. I agree with Dr. Larsson that myelogenous leukaemias may exhibit normal as well as very high RBU-values. In our experience this also applies to lymphogenous leukaemias and Hodgkin's disease.

I should be interested to hear the views of both Dr. Larsson and Dr. Kniseley on the mechanism involved in cases of abnormally high colloid uptake by the bone marrow. We feel that there are only three possibilities: (a) impaired uptake of the colloid by the liver leading to a compensatory extrahepatic uptake in the reticulo-endothelial system; in liver cirrhosis we found values for the RBU as high as 70%; (b) a blood flow through the bone marrow that is, in absolute terms, higher than normal; and (c) increased efficiency of the reticulo-endothelial cells in the bone marrow. From experience with the reticulo-endothelial system in the liver it seems likely that efficiency is constant over a wide range of pathological conditions. I am, therefore, of the opinion that a high RBU is in most cases indicative of an increased bone-marrow blood flow; this presupposes, of course, that liver blood flow and liver efficiency are normal.

L. G. LARSSON: I am sure you are right in saying that blood flow through the bone marrow plays an important part in the uptake of Au^{198}-colloid into the marrow. I think, however, that the really important factor in this increased uptake is the hyperplasia of the bone-marrow reticulum which occurs in connection with general hyperplasia of the marrow. There is a very good correlation between the degree of hyperplasia seen in histological bone-marrow sections and the uptake of Au^{198} by the bone marrow.

R. KNISELEY: I agree that liver blood flow is a factor that affects uptake into the marrow, but this is certainly not the whole story. All sorts

of other factors must be involved, e.g. the uniformity of the size of the colloidal particles. The uptake will, I think, be affected if the particles are not homogeneous. I am also certain, however, that there is a good correlation between marrow hyperplasia and reticulo-endothelial activity in the bone marrow. Whether or not it is out of phase in some situations, it is difficult to say.

We should be reluctant to use any one site such as the head for the purpose of obtaining representative data on marrow uptake or changes in marrow uptake. On the basis of fairly wide experience we feel that the patterns of expansion of marrow tend to be complicated and non-uniform. In arm counting studies we have found this same variation in the patterns of disappearance from the blood and retention in the forearm. The phenomena involved are too complicated to enable tests to be carried out at any one site.

P. HARPER: We have not observed any localization of Tc^{99m} sulphur colloid in bone marrow in our patients but this may be because we have been concentrating on other problems. There has been some indication of such localization in large rats and we are sure that, given large enough doses of this isotope, it would be possible to visualize active bone marrow in patients.

I was interested, Dr. Kniseley, in the case of the patient who exhibited increased phagocytosis in the lungs. We have found this same phenomenon with four elderly emphysematous patients and also in one old rat. I wonder what the reason for this could be.

R. KNISELEY: In this connection I might perhaps mention that the patient whose ribs were clearly shown (Fig. 1C) had pronounced emphysema but there was no increase in pulmonary concentration.

A. DESGREZ: Dr. Höfer, do you not think it might be possible to increase the sensitivity of your method by studying the uptake of the colloid in the sternum, in particular in the manubrium? In our experience, the uptake is greater here than in the skull and it can be observed more readily.

R. HÖFER: I agree that there are a number of reasons why the sternum is probably more suitable than the head for measuring the relative bone-marrow uptake with out method. We used the head because in this position it is easier to shield the counter against the relatively high activity of the liver.

P.C.R. TURNER: I should like to mention some investigations with Fe^{52} that have been carried out by Dr. L. Szur at Hammersmith Hospital, London. In these investigations the distribution of activity along one of the long bones, usually of the leg, was determined by means of a coincidence-counting technique. Only a small number of patients have been studied but this includes both normal and abnormal subjects. The distributions obtained along the leg are in general agreement with those reported by Dr. Larsson and Dr. Kniseley.

Apart from the fact that the supply of Fe^{52} is limited, the use of this isotope poses a number of other problems. The decay product of Fe^{52} is itself radioactive. In 95% of the disintegrations 21-min Mn^{52m} is produced and in the other 5% 6-d Mn^{52}. The manganese concentrates in the liver so that the same kind of difficulty arises as with colloidal gold.

Another difficulty is the actual production of Fe^{52}. We have prepared it by α-bombardment of Cr^{50}. Because the abundance of Cr^{50} is only 4%, the yield is low whilst samples are contaminated with 2.9-yr Fe^{55} formed from

Cr^{52} which has an abundance of 84%. The radiation dose from Fe^{55} is the limiting factor in clinical applications. The use of enriched Cr^{50} would be useful but inconvenient and expensive. Prof. W. G. Myers has indicated that he has prepared Fe^{52} through the $Cr^{52}(He^3, 3n)Fe^{52}$ reaction. We should like to investigate this possibility since this should make it possible to obtain higher yields with less contamination with Fe^{55}.

A. DESGREZ: I should like to ask Dr. Larsson a question about his "normal-pattern" patients. Were these absolutely normal persons or were they simply patients who were not suffering from bone disease, like the controls used by Dr. Kniseley? I am prompted to ask this by the results we have obtained at the Service Frédéric Joliot since 1961 in various investigations carried out in conjunction with Dr. Delaloye. We have found that if doses of Au^{198}-colloid of the order of 200 μc, i.e. the quantity normally used for liver scintigrams, are administered to cirrhotic patients, it is possible, with the help of an ordinary cylindrical collimator, to visualize such central parts of the skeleton as the thorax, the vertebral column and the pelvis, which cannot be seen normally.

We have also noticed that this uptake in bone tends to decrease as treatment proceeds. Figure 1 shows scans of a cirrhotic patient. In spite of the fact that the dose used was slightly less than 200 μc, you can see remarkably clearly a considerable uptake by the vertebral column.

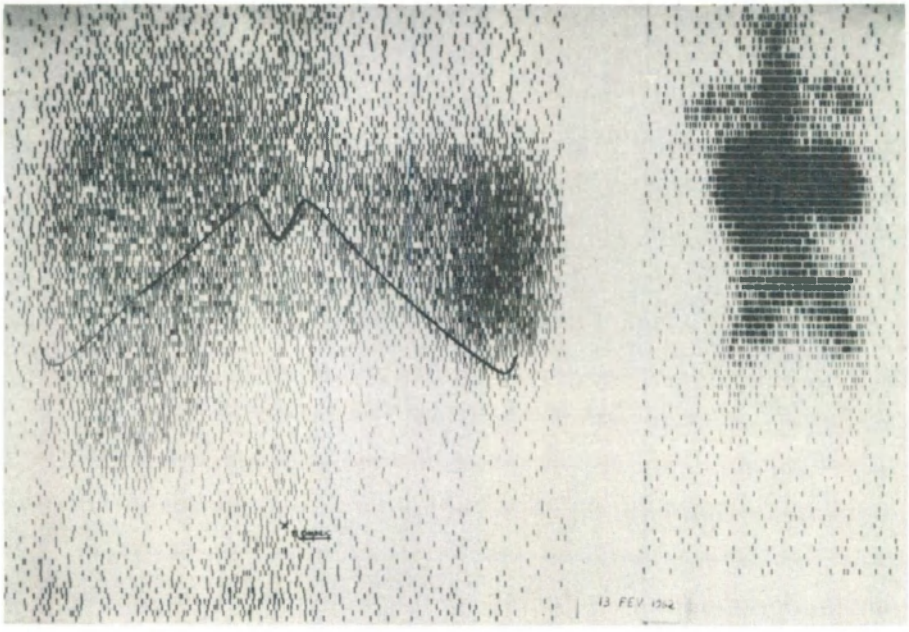

Fig. 1

Abdominal and whole-body scans in a cirrhotic subject after administration of 200 μc Au^{198}-colloid

Figure 2 shows scans made almost a year following treatment of an ordinary case of cirrhosis.

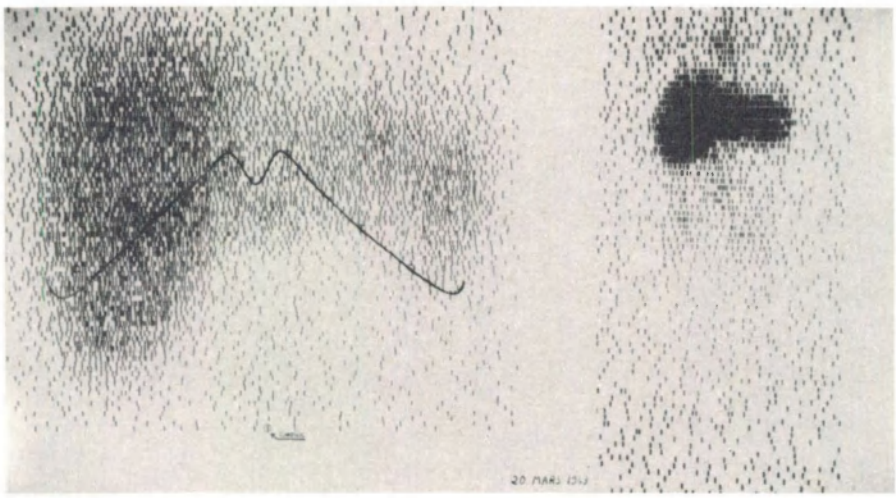

Fig.2

Abdominal and whole-body scans in a treated cirrhotic subject after administration of 200 μc Au^{198}-colloid

The uptake in bone is now considerably less and the picture is much closer to what one would expect from a normal person. Uptake in liver is correspondingly greater. The techniques used in both cases were exactly the same.

L.G. LARSSON: We have not examined any completely normal subjects because of the relatively large tracer doses involved. Our controls are persons who are not suffering from any known bone-marrow disease; they are mostly patients with localized malignant tumours.

Patients suffering from cirrhosis and other liver complaints probably do take up relatively more Au^{198} in the bone marrow than normal subjects. We have not, however, had any experience of this ourselves, perhaps because cirrhosis of the liver is much less prevalent in Sweden.

C. PAPAVASILIOU: I should like to present a representative case report from our records in which bone-marrow scanning was extremely useful in the diagnosis and subsequent treatment of a case of Cooley's disease. The patient, a 14-yr-old girl, entered our hospital suffering from spastic paraplegia of the lower extremities. Myelography was carried out and a complete block was found at T5-T6. Films of the chest and thoracic spine revealed a mass 3 cm in diam. at the level of T5 - T6 that was paraspinally located on the right side. Bone-marrow scanning after injection of 250 μc of Au^{198}-colloid revealed considerable concentration of the radioactive material in this mass, showing that the shadow on the film was a mass of extramedullary marrow which was causing the paraplegia. The mass was irradiated with a dose of 900 rad and the paraplegia was resolved.

B. MALAMOS: I was very interested by these papers since information on the bone marrow is very often needed, not only in cases of malignant diseases but also in haemolytic disorders. In the Mediterranean area, for instance, we find many congenital haemolytic anaemias with hyperactive but often insufficiently productive marrows. However there is the problem of

permissible doses. In the case of malignant diseases, for example, a high dose such as that used by Dr. Kniseley would perhaps not be harmful. In cases of haemolytic anaemia on the other hand it would not be permissible. Our physicists insist that doses of 400 - 500 μc to adult subjects must not be exceeded. Since the doses used by Dr. Kniseley differed considerably from those used by Dr. Larsson, I should be interested to hear their comments on this.

R. KNISELEY: As we point out in the paper, these high doses are only used for patients who require myelo-suppressive therapy. They do not give rise to any detectable haematopoietic depression. For more general use in patients with good prognosis one has to use lower doses.

L. G. LARSSON: The radiation dose to the liver after an intravenous injection of 1 mc Au^{198} is about 48 rad; the dose to the bone marrow is of the order of 2 - 5 rad. In cases of severe haemolytic disease you can certainly perform good bone-marrow studies with 0.1 - 0.2 mc Au^{198}. I do not think there is any cause for worry with doses of this order.

LA LYMPHOGRAPHIE INDIRECTE ET SON INTÉRÊT EN ONCOLOGIE

B. DELALOYE ET P. MAGNENAT
LABORATOIRE DES RADIOISOTOPES,
CLINIQUE MÉDICALE UNIVERSITAIRE DE LAUSANNE,
LAUSANNE, SUISSE

Abstract — Résumé — Аннотация — Resumen

INDIRECT LYMPHOGRAPHY AND ITS IMPORTANCE IN ONCOLOGY. Indirect lymphography, which only requires a subcutaneous injection of colloidal gold-198 with a particle diameter of 50 Å in the tributary region of the lymphatic system being explored, makes possible, by scintigraphic recording, a clear representation of the ganglionic lymphatic chains. The problems of collimation in getting optimum definition are discussed.

With this method of investigating the lymphatic system, measurement of the time of appearance of the gold in the blood yields indirect information regarding the rate of transit of the colloidal gold particles in the lymphatic vessels. Useful information is also obtained on neoplastic infiltrations of the ganglia and hence it is possible to determine the extent of a metastatic infiltration. Clinical examples are described. In addition, the authors describe a new technique for hepatic lymphography by the transcutaneous, sub-capsular injection of colloidal gold-198. This technique reveals the anterior and posterior mediastinal lymphatic chains.

LA LYMPHOGRAPHIE INDIRECTE ET SON INTÉRÊT EN ONCOLOGIE. La lymphographie indirecte, qui ne nécessite qu'une injection sous-cutanée d'or-198 colloïdal dont le diamètre des particules est de 50 Å dans le territoire tributaire du système lymphatique que l'on veut explorer, permet par enregistrement scintigraphique une bonne mise en évidence des chaînes ganglionnaires lymphatiques. Les problèmes de collimation sont discutés afin d'obtenir la meilleure définition possible.

Ce mode d'investigation du système lymphatique permet, lorsqu'on mesure le temps d'apparition de l'or dans le sang, d'obtenir indirectement des renseignements sur la vitesse du transit des particules d'or colloïdal dans les vaisseaux lymphatiques. On obtient également d'utiles renseignements sur les infiltrations néoplastiques des ganglions et, de ce fait, il est possible de connaître l'étendue d'une infiltration métastatique. Des exemples cliniques sont décrits. De plus, les auteurs décrivent une nouvelle technique de lymphographie hépatique par injection sous-capsulaire d'or-198 colloïdal par voie transcutanée. Cette technique permet de mettre en évidence la chaîne médiastinale lymphatique antérieure et postérieure.

КОСВЕННАЯ ЛИМФОГРАФИЯ И ЕЕ ЗНАЧЕНИЕ В ОНКОЛОГИИ. Косвенная лимфография, которая требует лишь подкожного введения коллоидального золота-198 (диаметр частиц 50 Å) в соответствующем участке лимфатической системы, дает с помощью сцинтиграфической регистрации возможность с достаточной очевидностью выявлять цепи лимфатических узлов. Обсуждаются проблемы коллимации в целях наилучшего определения.

Такой метод исследования лимфатической системы позволяет при измерении времени появления золота в крови получать косвенным путем сведения о скорости переноса частиц коллоидального золота по лимфатическим сосудам. Так же были получены полезные сведения о неопластической инфильтрации узлов, что дает представление о протяженности метастазов. Описываются клинические случаи. Кроме того, авторы дают описание нового метода лимфографии печени путем введения коллоидального золота-198 через кожный покров под капсулу печени. Такой метод позволяет выявлять цепь лимфатических узлов в переднем и заднем средостении.

LA LINFOGRAFÍA INDIRECTA Y SU INTERÉS EN ONCOLOGÍA. La linfografía indirecta, para la cual sólo se requiere una inyección subcutánea de oro-198 coloidal, cuyas partículas tienen un diámetro de 50 Å, en los tributarios del sistema linfático que se quieren explorar, permite visualizar por registro centelleográfico las cadenas ganglionares linfáticas. Los autores examinan los problemas de colimación a fin de obtener la mejor definición posible.

Esta técnica de investigación del sistema linfático facilita indirectamente, cuando se mide el tiempo de aparición del oro en la sangre, informaciones sobre la velocidad de circulación de las partículas de oro coloidal por los vasos linfáticos. Permite también obtener informaciones útiles sobre las infiltraciones neoplásticas de los ganglios, con lo que es posible conocer el alcance de una infiltración metastática. Los autores presentan algunos ejemplos clínicos. Describen, además, una nueva técnica de linfografía hepática por inyección intracapsular de oro-198 coloidal por vía transcutánea. Esta técnica permite visualizar la cadena mediastínica linfática anterior y posterior.

L'intérêt d'une bonne mise en évidence des ganglions lymphatiques n'est plus à souligner.

Pour ce faire, deux méthodes de lymphographie s'offrent à nous. L'une, directe [1, 2] nécessite la dénudation et le cathétérisme d'un petit vaisseau lymphatique; l'autre, indirecte, permet de suivre la migration lymphatique d'une substance déterminée, injectée dans l'espace interstitiel [3, 4].

La lymphographie indirecte repose sur des données anatomiques et physiologiques qu'il semble utile de rappeler brièvement.

C'est à McCALLUM en 1903 [5] que revient le mérite d'avoir démontré qu'il n'existait pas de connexion directe entre l'espace interstitiel et les capillaires lymphatiques qui doivent être considérés comme un espace clos; alors que la théorie de VIEUSSENS [6], communément admise jusque là, voulait qu'il y ait des vasa serosa entre la circulation sanguine et le système lymphatique. Par la suite les travaux de LEWIS [7], DRINKER et al., [8], EPPINGER [9], ZHDANOV [10], ont précisé que le rôle essentiel des lymphatiques réside dans le transport des protéines de l'espace interstitiel.

La vitesse de ce transport varie suivant l'endroit considéré; en effet, au niveau de la cavité péritonéale il se fait beaucoup plus rapidement qu'au niveau de la peau, de la plèvre ou des poumons [11]. Mais la mobilisation, les mouvements actifs peuvent augmenter le débit de la lymphe [12], tout comme l'hypoxémie [13].

Par ailleurs, les capillaires lymphatiques ont une paroi discontinue, sans membrane basale, pourvue de pores qui permettent un passage très aisé du liquide interstitiel dans les voies lymphatiques, POLICARD [14].

Sur le parcours de ces vaisseaux lymphatiques se trouvent groupés des ganglions formés de follicules, qui baignent dans la lymphe. Les cellules littorales des sinus sont douées de phagocytose et peuvent se libérer du ganglion pour émigrer dans le système sanguin et atteindre tant le foie que la rate par exemple [14].

En conséquence, il ressort que pour obtenir une mise en évidence des ganglions lymphatiques, il faut déposer dans l'espace interstitiel du territoire que l'on veut explorer, des particules dont le diamètre équatorial est proche de celui des albumines, c'est-à-dire 36 Å. Ces particules en suspension colloïdale, franchissent les pores des capillaires lymphatiques et migrent avec la lymphe. Puis elles sont phagocytées dans les ganglions par les cellules littorales du système réticulo-endothélial [15-16]. Ce phénomène se répète de ganglions en ganglions sur la chaîne envisagée. Les fluides, les lipides et les protéines circulent pour leur part sans être retenus dans les ganglions, jusqu'à l'abouchement des lymphatiques dans le courant sanguin.

Pour réaliser une telle lymphographie, à la suite d'autres auteurs [17, 18, 19, 20, 21, 22], nous injectons par voie sous cutanée, dans une zone tributaire du territoire lymphatique à explorer, sous un petit volume (0,2 à 0,4 ml) et sous une faible pression, une suspension de particules d'or 198 colloïdal dont le diamètre équatorial se situe entre 20 et 60 Å (Saclay – France). L'activité à injecter varie suivant les régions à explorer, de 50 μc à 100 ou 200 μc. L'or utilisé ayant une haute activité spécifique, il est dilué dans de la xylocaïne à 2% pour éviter que l'injection soit douloureuse. Après l'injection on procède à un léger massage local ou à une mobilisation active, quand elle est possible. Cet examen étant généralement pratiqué chez des malades atteints de cancer, nous n'utilisons jamais de hyaluronidase ou de streptokinase pour favoriser la migration du colloïde en raison du danger de dissémination tumorale possible.

L'enregistrement de la lymphographie se fait à l'aide d'un scintigraphe type MECASERTO, qui a un détecteur protégé par une masse de 70 kg de plomb, l'angle de vision étant défini par un collimateur focalisé de type «Honey Cone» à 19 canaux, dont le foyer se trouve à 22 cm du cristal. Après bien des essais in vivo avec d'autres types de collimateurs, tels que les cylindriques de 18 ou de 21 mm de diamètre, nous avons choisi le système focalisé.

De façon usuelle, nous utilisons une vitesse de balayage de 460 mm/min, avec un espacement de 2,5 mm.

Une fois l'injection faite, il faut attendre un certain temps pour que la chaîne ganglionnaire ait capté le colloïde. Pour la lymphographie hépatique on peut commencer l'enregistrement après 2 ou 4 h, l'optimum se situant vers 6 h, on voit alors apparaître le plus souvent la chaîne ganglionnaire thoracique antérieure. Pour la lymphographie mammaire et jugulaire, ce délai est de 6 à 12 h, alors que nous l'avons trouvé de 12 à 24 h pour les lymphographies périphériques des membres. Des enregistrements réalisés à intervalles répétés permettent de suivre la migration de l'or colloïdal le long du chemin lymphatique.

Nous avons procédé à plus de 211 enregistrements de lymphographies qui intéressent les territoires suivants:

les membres supérieurs	:	2 cas
les membres inférieurs	:	55 cas
la chaîne jugulaire	:	4 cas
la capsule du foie	:	46 cas
la capsule splénique	:	2 cas.

Nous allons examiner tout d'abord les lymphographies périphériques des membres inférieurs que nous avons classées en quatre groupes:

1. Dans ce premier groupe, nous avons classé les enregistrements qui présentaient une bonne mise en évidence des ganglions inguinaux, iliaques externes et para-aortiques des deux côtés (fig. 1).

Nous trouvons ici 10 malades dont 8 pouvaient être considérés comme normaux, bien que l'un présentait un amartome du foie et l'autre une mononucléose infectieuse. Le neuvième avait une cirrhose alors que le dixième était suspect d'un cancer à la suite de présence de cellules atypiques dans le sang.

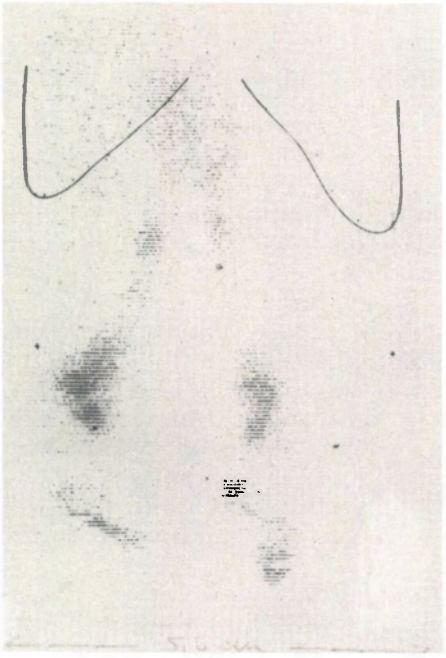

Figure 1

Lymphographie normale des membres inférieurs.

2. Dans le deuxième groupe, nous avons réparti les lymphographies qui présentaient une zone muette au niveau de l'une des chaînes iliaques externes (fig. 2).

Parmi ces 23 sujets nous relevons 9 cas de tumeurs, cancers du col de l'utérus, du vagin, de la prostate, du sein, 1 mélanome du talon, dont 6 présentaient des métastases abdominales. Nous retrouvons encore dans ce groupe 1 cas de Hodgkin, 3 états fébriles, 4 pancréatites dont 2 étaient chroniques, 1 sclérose vasculaire et 5 cirrhoses.

3. Le troisième groupe intéresse des lymphographies qui présentaient une migration moins satisfaisante encore avec un stop au niveau des chaînes para-aortiques (fig. 3).

Sur 16 malades, nous trouvons 9 cas de cancers dont 5 présentaient des métastases para-aortiques, 1 maladie de Hodgkin pour laquelle le diagnostic a été posé sur biopsie inguinale, 1 état fébrile, 1 leucémie lymphoïde, 2 cirrhoses, 1 angine et 1 pancréatite aigue.

4. Le quatrième groupe comprend tous les cas où nous avons observé une migration quasiment nulle du colloïde.

Sur 6 cas, nous avons 4 malades atteints de cancer dont 3 présentaient de larges infiltrations ganglionnaires iliaques et para-aortiques, 1 pancréatite chronique et 1 insuffisance cardiaque avec présence d'œdèmes importants aux membres inférieurs.

Les quatre lymphographies des membres supérieurs que nous avons pratiquées le furent chez 2 malades atteints de cancer. L'un présentait une

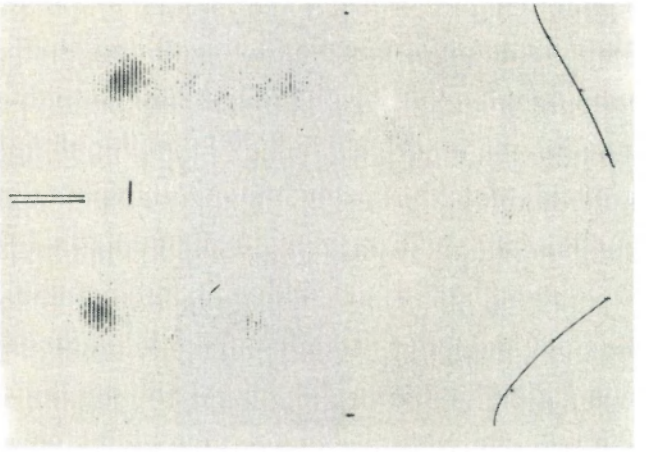

Figure 2

Lymphographie des membres inférieurs avec lacune iliaque externe gauche.

Figure 3

Lymphographie des membres inférieurs sans mise en évidence des ganglions para-aortiques.

masse tumorale médiastinale, avec compression de la veine cave supérieure; dans ce cas nous avons constaté une très faible mise en évidence des ganglions axillaires des deux côtés. L'autre malade était atteint d'un épithélioma trabéculaire de la bronche souche droite avec métastase axillaire externe droite, nous avons pu vérifier que la métastase ne fixait pas le colloïde alors qu'un paquet ganglionnaire était bien visible au niveau de la face interne du creux axillaire (fig. 4).

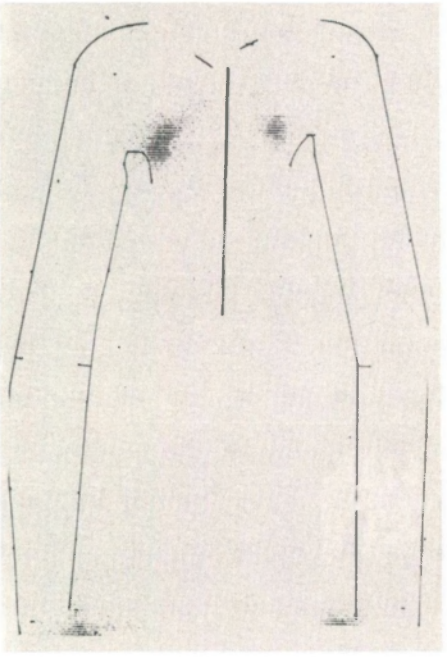

Figure 4

Lymphographie des membres supérieurs
(explication dans le texte).

Les lymphographie de la chaîne jugulaire, enregistrées au scintigraphe après une double injection sous muqueuse à chaque extrémité de la lèvre inférieure, ont permis dans un cas de maladie de Hodgkin, de montrer qu'après évidement jugulaire droit l'on avait oublié un ganglion alors qu'à gauche on constatait une faible migration du colloide (fig. 5 (a et 5 b)).

Nous avons par ailleurs procédé à 92 enregistrements de lymphographie hépatique isotopique, chez 46 malades grâce à une technique personnelle précédemment décrite [22, 23], permettant par voie transthoracique, une injection intracapsulaire au niveau de la face supérieure du foie droit.

1. Chez 11 malades, nous avons obtenu 28 bons enregistrements (fig. 6), avec mise en évidence de la chaîne thoracique antérieure jusqu'au confluent jugulo-sous-clavier droit. Parmi ces cas, nous voyons un cancer de la prostate avec métastase médiastinale et une tumeur de la bronche souche droite, les autres sujets peuvent être considérés comme normaux.

Figure 5. a)

Lymphographie de la chaîne jugulaire après évidement (explication dans le texte).

Figure 5. b)

Lymphographie normale de la chaîne jugulaire.

2. Chez 10 malades, nous avons obtenu une très faible migration du colloïde dans la capsule sans migration thoracique.

Les différentes affections qui se répartissent dans ce groupe intéressent une lymphangite thoracique carcinomateuse, un cancer bronchique affectant la lobaire inférieure droite, un cas suspect de Hodgkin abdominal, trois cirrhoses et une maladie de Besnier Boeck Schaumann.

3. Dans le troisième groupe qui comprend 8 malades, nous n'avons pas constaté de migration du colloïde, même après 97 h, seul le point d'injection apparaissait à l'enregistrement scintigraphique. Parmi ces malades nous

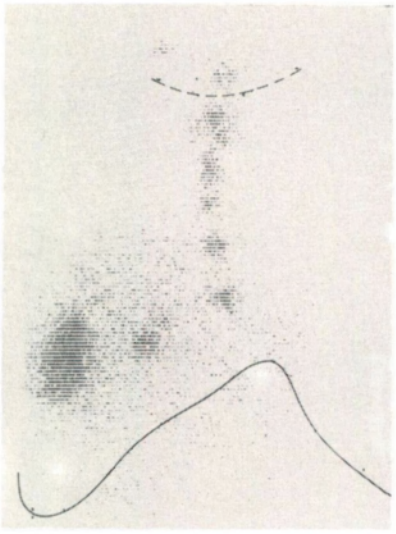

Figure 6

Lymphographie hépatique capsulaire avec migration du colloïde jusqu'au confluent jugulo sous-clavier droit.

relevons la présence d'un cancer du pancréas avec métastases multiples, un cancer de l'estomac, trois cirrhoses, une hépatite, un diabète et une bronchopneumonie.

Chez 18 malades, nos lymphographies hépatiques étaient interprétables car la technique que nous avons utilisée au début de nos investigations n'était pas satisfaisante.

Par ailleurs, dans 5 cas l'injection a été pratiquée dans la cavité pleurale, dans 5 autres cas l'activité injectée était insuffisante et dans 1 cas le colloïde s'est répandu dans la cavité péritonéale.

Il convient maintenant de tenter une critique de ces résultats. ZEIDMANN [24] a montré que les cellules cancéreuses étaient arrêtées dans le sinus marginal des ganglions, et ce fait a été confirmé expérimentalement sur l'animal par le travail de TJERNBERG [25] qui a révélé que 5 j après la greffe d'une tumeur V × 2 on constatait une hyperplasie des ganglions lymphatiques qui coïncidait avec une apparition de follicules pseudo-secondaires. D'autre part, les autoradiographies des ganglions après injection d'or colloïdal, montrent que lorsqu' ils sont métastatiques, ils ne fixent pas l'or. Les ganglions de voisinage, même sains, ne fixent pas davantage parfois le colloïde, la circulation lymphatique subissant à leurs niveaux des modifications qui sont encore mal connues .

Il serait ainsi logique de penser que l'on ne devrait rencontrer de stop ou de zones muettes lors d'une lymphographie isotopique que chez les malades atteints de néoplasies ou d'hémopathies malignes.

Toutefois dans un certain nombre d'affections telles que les cirrhoses, les pancréatites, certains états fébriles, nous trouvons des lymphographies isotopiques pathologiques. De plus d'autres auteurs, parmi lesquels nous

citerons GEST [21], ont comparé les résultats de la lymphographie directe radiologique avec ceux de la lymphographie indirecte isotopique, et ils ont constaté qu'une absence de fixation ganglionnaire d'or colloïdal ne coïncidait pas toujours avec un processus néoplasique, remarque que nous avons également faite.

Il est possible d'envisager plusieurs hypothèses pour expliquer l'absence de migration dans les cas qui ne présentent pas d'infiltration métastatique, on pourrait invoquer soit la présence de microembolies carcinomateuses, ce qui n'est pas vraisemblable d'ailleurs à la lumière des résultats de la lymphographie directe radiologique; soit une action du type toxinique qui inhiberait l'activité phagocytaire des cellules du SRE au sein des ganglions tributaires de l'organe touché par une tumeur. Dans les affections non tumorales, l'absence de migration est encore plus difficile à justifier, et la seule explication demeure du domaine des hypothèses. Il serait en effet possible d'invoquer soit une réaction inflammatoire qui, en modifiant le milieu, empêcherait tant le phénomène de phagocytose que celui de pinocytose de se produire, soit une inhibition purement fonctionnelle de l'activité phagocytaire.

Ces quelques observations montrent les limites de la lymphographie indirecte isotopique. En tant que moyen d'investigation ne perturbant pas la circulation lymphatique, elle nous donne des renseignements d'ordre physiologique sur la capacité phagocytaire des ganglions. A ce titre, elle présente un grand intérêt qui mérite une étude portant sur un très grand nombre de cas atteints d'affections tumorales ou d'autres maladies.

En oncologie, elle ne donne pas les mêmes renseignements que la lymphographie directe radiologique. Mais il convient de rappeler ici que les lymphographies radiologiques sont loin d'être d'une interprétation toujours facile. En effet, TJERNBERG [25] pense que le lymphadénogramme est encore la meilleure technique que nous pouvons utiliser pour faire un véritable diagnostic différentiel entre cancer et infection, à moins que l'on puisse aisément procéder à plusieurs lymphographies directes.

Nous croyons que l'utilité de la lymphographie isotopique se trouve résumée dans les trois indications suivantes:

1. L'exploration d'une chaîne lymphatique inaccessible à la lymphographie directe.
2. Pour mettre en évidence un curage ganglionnaire incomplet.
3. La dernière indication est l'application thérapeutique de doses élevées en oncologie, ainsi que plusieurs auteurs l'ont préconisé [26-31].

RÉFÉRENCES

[1] KINMONTH, J. B., Ann. Roval Coll. Surg. Engl., 15 (1954) 300.
[2] KELLERSHOAN, C. et BENICHOUX, J., Min. Nucl. 2 (1958) 159.
[3] WALKER, L. A., J. Lab. and Clin. Med. 36 (1950) 440.
[4] SAGE, H. H. and FORUN, B. V., Proc. Soc. Exper. Biol. and Med., 97 (1958) 895.
[5] MAC CALLUM, Bull. John Hopkins Hosp. 14 (1903) 105.
[6] VIEUSSENS, R., Norum vasorum corporis humani systema, Amstelod (1705).
[7] LEWIS, J. H., J. Amer. med. Ass. 76 (1921) 1342.

[8] DRINKER, C. K. and JOFFEY, J. M., Lymphatics, Lymph and Lymphoid Tissue, Harvard Univ. Press Cambridge, Mass. (1941).
[9] EPPINGER, H., Permeabilitaetspathologie, Springer, Vienne (1949).
[10] ZHDANOV, D. A., General Anatomy and Physiology of the Lymphatic System, Medgiz, Leningrad (1952).
[11] JOFFEY, J. M. and COURTICE, F. C., Lymphatics, Lymph and Lymphoid Tissue, Edw. Arnold Ltd., London (1956) 107.
[12] WHITE, J. C., FIELD, M. E. and DRINKER, C. K., Amer. J. Physiol. 103 (1933) 34.
[13] MAURER, F. W., Amer. J. Physiol. 131 (1940) 331.
[14] POLICARD, A., Physiologie et pathologie du système lymphoïde, Masson & Cie., Paris (1963).
[15] SÖRENSON, G. D., Anat. Rec. 139 (1961) 276.
[16] RUSZNYÁK, I., FÖLDI, M. and SZABÓ, G., Lymphatics and lymph Circulation, Pergamon Press Ltd., Londres, (1960).
[17] SCAMAN, W. B. and POWERS, W. E., Cancer 8 (1955) 1044.
[18] FARINET, G. e CARALOT, A., Min. Fisioter. 4 (1959) 282.
[19] THOMAS, C. G. Jr., Surg. Gynec. and Obstet. 103 (1956) 51.
[20] GEST, J. et DELOUCHE, G., J. Radiol. Electr. 44 (1963) 86.
[21] GEST, J., Bull. Acad. Suisse Sci. Méd. 19 (1963) 97.
[22] MAGNENAT, P. et DELALOYE, B., à paraître dans Radioaktive Isotope in Klinik und Forschung, Vol. VI (1964).
[23] MAGNENAT, P. et DELALOYE, B., à paraître dans La Revue Médico Chirurg. des Maladies du Foie, de la Rate et du Pancréas (1964).
[24] ZEIDMANN, I. and BUSS, J. M., Cancer Res. 14 (1954) 403.
[25] TJERNBERG, B., Acta Radiol. Scand. Suppl. 214 (1962).
[26] BRASFIELD, R. D. and HENSCHKE, U. K., Amer. J. Roentgenol., Radium Ther. and Nuclear Med., LXXXV (1961) 849.
[27] CHIAPA, S., GALLI, G., BARBAINI, S. e RAVASI, G., Radiol. Med., 48 (1962) 663.
[28] RATTI, A., Radiol. Clin. 31 (1962) 220.
[29] SCHWARTZ, S. I., GREENLAW, R. H., ROB, C. and RUBIN, P., Cancer 15 (1962) 623.
[30] VECCHIETTI, G. e ONNIS, A., Attual. Ostet. e Ginec. 9 (1963) 609.
[31] LENZI, E., Riv. Ital. Ginec. 46 (1962) 343.

DISCUSSION

A. BAPTISTA: I am a little sceptical as to whether it is possible to use the method described for therapeutic purposes. It has been shown by autoradiography that colloïds collect peripherally around nodes with metastases. It is difficult to see how the high doses required could be delivered to the metastases themselves.

B. DELALOYE: Therapeutic applications come last in the list given in our paper because there is little point in trying to utilize endolymphatic therapy with isotopes in the case of metastases. Nevertheless, although I have no direct experience of this problem, I think that this method could be used in specific cases, e.g. for reticulosarcomas, where it would be possible to fill the sinuses using I^{131}-Lipiodol.

DIAGNOSIS OF INTRASPINAL NEUROLOGICAL SYNDROMES BY MYELOSCINTIGRAM

G. PANTAZIS, J. TAPTAS. H. MIKROPOULOS, N. KORDIOLIS, V. SAMARAS, E. PARASCHOU, C. SAVVAS AND F. DERMENTZOGLOU
DEMOCRITUS CENTRE AND AGHIOS SAVVAS HOSPITAL
ATHENS, GREECE

Abstract — Résumé — Аннотация — Resumen

DIAGNOSIS OF INTRASPINAL NEUROLOGICAL SYNDROMES BY MYELOSCINTIGRAM. Thirty-eight patients presenting signs of intraspinal neurological syndromes were examined by myeloscintigram at the Greek Anticancer Institute ("Agios Savvas" Hospital). They were suffering from intervertebral disc protrusions, tumours, congenital and inflammatory lesions. Most of them were studied with myelograms as well and the relative advantages of the two methods were discussed. The findings of the myeloscintigram consisted either in decrease or increase of radioactivity locally, depending on the different types of lesions. Provided a careful and detailed examination is done the myeloscintigram may, in a large proportion of cases, prove considerably helpful in the diagnosis of intraspinal lesions.

DIAGNOSTIC PAR MYÉLOSCINTIGRAMME DES SYNDROMES NEUROLOGIQUES INTRASPINAUX. A l'Institut anticancéreux hellénique (hôpital «Agios Savvas»), 38 patients présentant des syndromes neurologiques intraspinaux ont été examinés par myéloscintigramme. Ils souffraient de protrusions de disques intervertébraux, de tumeurs, de lésions congénitales et de lésions inflammatoires. La plupart d'entre eux ont été examinés également au moyen de myélogrammes et on a comparé les avantages respectifs des deux méthodes. Les résultats obtenus par le myéloscintigramme consistaient en décroissements ou accroissements locaux de la radioactivité, selon les divers types de lésions. Dans une forte proportion de cas, le myéloscintigramme peut rendre de très grands services pour le diagnostic des lésions intraspinales, à condition que l'on procède à un examen minutieux et détaillé.

ДИАГНОЗ СПИННОМОЗГОВОГО НЕВРАЛГИЧЕСКОГО СИНДРОМА С ПОМОЩЬЮ СЦИНТИГРАММЫ СПИННОГО МОЗГА. Исследовались 38 пациентов с признаками спинномозгового невралгического синдрома методом сцинтиграммы спинного мозга в Греческом противораковом институте (Госпиталь "Агиос Саввас"). Больные страдали от выбухания межпозвоночного диска, опухолей, врожденных и воспалительных поражений. Большинство пациентов было также исследовано методом клеточной картины костного мозга, и были обсуждены сравнительные преимущества обоих методов. Показания сцинтиграммы спинного мозга свидетельствовали либо о понижении, либо об увеличении локальной радиоактивности, зависящей от различных типов поражений. При условии тщательного и подробного исследования сцинтиграмма спинного мозга может в большинстве случаев оказаться весьма полезной в определении диагноза поражений спинного мозга.

DIAGNÓSTICO DE SÍNDROMES NEUROLÓGICOS INTRAESPINALES POR MIELOCENTELLEOGRAFÍA. En el Instituto griego de lucha contra el cáncer (Hospital «Agios Savvas») se han examinado por mielocentelleografía 38 pacientes que presentaban indicios de síndromes neurológicos intraespinales. Sufrían protusiones de discos intervertebrales, tumores y lesiones congénitas e inflamatorias. La mayor parte de los casos se estudiaron también con ayuda de mielogramas, y se analizaron las ventajas relativas de ambos métodos. La mielocentelleografía permite observar una disminución o un aumento local de la radiactividad, según los diferentes tipos de lesiones. Siempre que se examine detallada y cuidadosamente, el mielocentelleograma puede en gran número de casos, resultar de considerable utilidad para el diagnóstico de lesiones intraespinales.

Symptoms and signs of intraspinal neurological syndromes are frequently inadequate for correct diagnosis and localization. Since even CSF (cerebral-spinal fluid) examination and plain roentgenograms often do not solve

the diagnostic problems, myelography using various oily substances has become an indispensable diagnostic tool. Along the same lines as myelography (the introduction into the spinal canal of a substance whose distribution can be followed from outside), the myeloscintigram was introduced in 1956 by BAUER and YUHL [1] using RISA, a radioiodinated human serum albumin, and following its course along the spinal canal with a scanner. This substance, after its introduction into the lumbar sac, usually diffuses easily into the subarachnoid space and demonstrates on the myeloscintigram an area of increased dot density corresponding to the greater concentration of the radioactivity, while along the sides of this column the dot density is lower because of the gradual diminution of the radioactivity (Figs. 1 and 2).

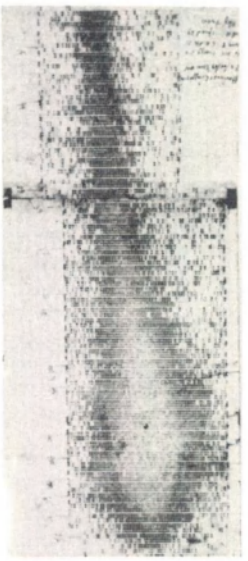

Fig. 1
Normal myelogram

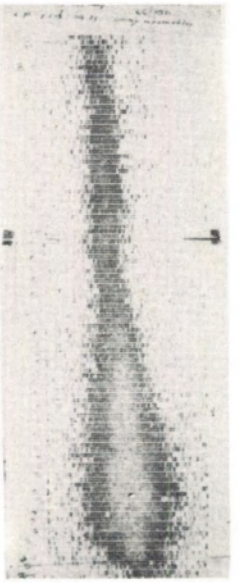

Fig. 2
Normal myelogram

This normal column of increased radioactivity is usually better demonstrated at the lumbar canal area, where the spinal canal has its maximum width.

Alterations in the above described pattern are of significance in various lesions and can be demonstrated in two different and distinct ways: (a) complete or incomplete block or narrowing of the spinal canal because of a space-occupying lesion or adhesions that interrupt circulation into the subarachnoid space, thus showing a decrease of the recorded activity at the site of the lesion; (b) increase of the recorded activity at the site of the lesion suggesting absorption of the RISA by abnormal tissues.

The latter manner of demonstration is the chief distinctive feature of the myeloscintigram which has not been, to our knowledge, investigated in the few similar works that have been previously published.

Though the RISA may well diffuse into the subarachnoid space, at times it does not, and in such cases tilting of the patient's head downwards is advisable as well as repeated withdrawals of the injected fluid for better mixing with the cerebral-spinal fluid (CSF) in order to avoid the demonstration of artefacts.

According to PERRYMAN et al. [2], within 24 h 40-50% of the RISA leaves the CSF. Most of the I^{131} will remain bound to the protein, while 5% will be picked up by the thyroid, if this gland is not already blocked.

No toxic side effects were noted, except the usual mild complaints that frequently follow any lumbar tap.

Among other reasons the method has been tried as an attempt to avoid the disadvantages of oil myelography, in which a radio-opaque medium is introduced into the spinal canal. This is the preferred method; however it is not so easy to withdraw the medium after the examination, and this in some circumstances has been considered the cause of various inflammatory reactions.

It has also to be kept in mind that routine myelography does not always demonstrate an existing lesion, and the oil at times disperses into small bubbles thus making findings unreliable while an accidental extradural injection of it, in contrast with RISA, may alter findings if the examination is to be repeated. And last, but not least, neither the patient nor the personnel is exposed to as much radiation during the recording of a myeloscintigram as during myelography under careful fluoroscopic observation and when many roentgenograms are taken.

On the other hand, myelography can be more easily performed at almost any hospital with an X-ray department, and is relatively cheap while myeloscintigrams can only be done in hospitals with advanced radioisotope equipment and with a radioactive substance of relative short life that results in high costs or shortages of supply.

Regardless of the above considerations for or against the method its real value has rather to be evaluated from its results on clinical grounds, and this will be done during the discussion that follows the description of the technical details of the method and the summaries of the case histories of the 38 patients studied. These suffered from disc protrusions, tumours, myelitis, arachnoiditis, tuberculosis or congenital anomalies causing a variety of neurological syndromes of spinal origin.

TECHNIQUE

In order to protect the thyroid gland of the patient from absorption of I^{131}, either 20-30 drops of Lugol's solution were given for 1 d prior to the examination or an intravenous or intramuscular injection of sodium iodide was given the same day of the examination.

The RISA in a quantity of 300-350 μc was injected through a regular spinal needle into the lumbar subarachnoid space, usually at the L_3-L_4 level, after mixing with CSF withdrawn at the same time into a 5-ml syringe. For even better mixing 2-3 withdrawals and re-injections of CSF mixed with RISA were made.

The spinal tap was done with the patient lying on his side and we soon discovered from personal experience, that tilting of the patient for several minutes was advisable as BELL and HERTCH [3] also recommend and for which an automatic tilt table would have been an advantage.

The scanning was always done in the prone position and usually after 20-30 min. Whenever possible we verified the location of the injection by anterio-posterior roentgenograms.

The time of the actual recording depended on the findings during the scanning. For lumbar area lesions approximately 30 min was necessary, and upper thoracic or cervical lesions needed up to 70 min for recording of the whole spine from the lumbar region upwards.

SCANNER

In this study we used a Nucor Mediscanner Model C4004C. This Mediscanner includes a highly directional focusing scintillation detector, a motor-driven scanning and recording system, and a highly superior pulse height analyser.

The scintillation counter HSA500A includes:

(1) A thallium-activated sodium iodide crystal of 2×2-in diam.

(2) A photomultiplier tube associated with the circuitry of the pulse height analyser and with the print-out circuit to produce printing pulses.

The crystal is heavily shielded by lead and provides maximum directional sensitivity with minimum sensitivity to background.

The focusing collimator has a honeycomb series of 18 openings, which exposes the face of crystal to radiation from a small focal point of radioactivity.

The circuit of the single channel analyser contains two discriminators, a lower and an upper one. The lower discriminator level can be varied from 0-100 V and the upper discriminator is biased 0-10 V above the lower discriminator. We set the lower discriminator level at 21 V and the upper one at 2.5 V (channel width). The high voltage setting used was 910 V.

The amplifier gain was set at 8 times. A scaling factor of four was used.

The speed of the scintillation detector was 24 cm/min. This is the maximum speed of our scanner.

During scanning of the spinal canal, the count-rate at various places along its course from the lumbar to the cervical spine was also recorded manually on the paper.

The optimal distance from the collimator to the radioactive source is 5 cm. In order to keep this distance as stable as possible, taking into consideration the normal curvature of the back of the patient, we had manually to move the collimator up or down.

CASES

1. (H.C., male, age 36)

History for the past year of lower back pains radiating to both lower extremities with weakness of peroneal groups bilaterally. On examination

there was also hypoaesthesia in the distribution of L_4-L_5 bilaterally. Plain X-ray plates showed diminution of the space between L_4-L_5. A discolipiodol myelogram showed a block at the L_3-L_4 area (Fig. 3), and the myeloscinti-

Fig. 3

Case 1. Myelogram showing block at the L_3-L_4 level

gram showed diminution of the recorded radioactivity of the level of L_4 (Fig. 4). During surgical exploration, a protruding mid-line disc was found at the L_3-L_4 interspace. In this case there was thus a complete agreement between clinical and laboratory findings including the myeloscintigram.

2. (E.V., female, age 24)

History of mild back pains for the past 2 yr without neurological findings. Plain roentgenograms showed narrowing of the L_4-L_5 interspace. The myelogram was not done and the myeloscintigram was normal. At operation a disc was found protruding to the right at the L_4-L_5 interspace. In this mild case of lumbar disc protrusion the myeloscintigram was negative.

3. (S.T., male, age 63)

Mild symptoms of right sciatica with a right Lasseque sign only. Myeloscintigram was normal. No myelogram or operation was performed.

4. (E.P., male, age 29)

A lumbar disc was between L_4-L_5 with only a Lasseque sign and normal roentgenogram. The myelogram clearly demonstrated the lesion, while the myeloscintigram showed an area of decreased radioactivity of the same

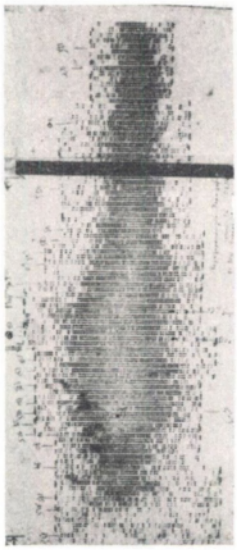

Fig.4

Case 1. Myeloscintigram showing partial block at the L_4 level

level, but this latter finding has not been considered adequate per se to warrant an exploration.

5. (G.T., male, age 42)

A case of surgically proven post-traumatic disc protrusion at the L_4-L_5 level. Myelogram was not done. The patient had back pains and the myeloscintigram was abnormal with decreased radioactivity in a wide area, but the findings were not of a pathognomonic nature.

6. (S.Z., male, age 34)

Case of a surgically proven right disc protrusion of the T_{12}-T_{11} area and right Lasseque sign with minimal hypoaesthesia, the myelogram showed the lesion and the myeloscintigram was normal.

7. (G.M., male, age 36)

With minimal clinical signs the myeloscintigram was normal. Myelogram was not done and plain roentgenogram showed narrowing of the L_4-L_5 interspace.

8. (G.S., male, age 42)

Intermittent clinical symptomatology due to a disc protrusion at the L_4-L_5 level with minimal signs of hypoaesthesia. Both the myelogram and the myeloscintigram were inconclusive. Surgery was not performed.

9. (A.D., female, age 33) and 10. (A.A., male, age 41)

Cases of surgically proven lumbar disc protrusions with positive myelogram had inconclusive myeloscintigram, probably due to inadequate distribution and circulation of the RISA. No tilting of the patient was done at this time.

11. (G.P., female)

Primary carcinoma of nasopharynx and early signs of spinal cord involvement progressing to right-sided weakness. On myelography there was a retention of Discolipiodol at the C_7-T_1 level, and the myeloscintigram showed evidence of diminution of radioactivity at the C_6-T_1 level.

12. (V.S., male, age 65)

Metastatic carcinoma to the lumbar region with destruction of L_5 vertebra with back pains, loss of ankle reflexes and diminution of right patelar reflex. Myelogram showed block at the L_4-L_5 level and myeloscintigram showed block of the radioactivity below L_3 level. Palliative surgery was performed.

13. (A.Z., male, age 58)

A gross extradural haemangioma or lymphangioma found during operation at the L_1-L_2 level. The patient had paraparesis, the myelogram showed block at the L_2-L_3 level (Fig. 5), and the myeloscintigram showed a block at the L_2 level (Fig. 6).

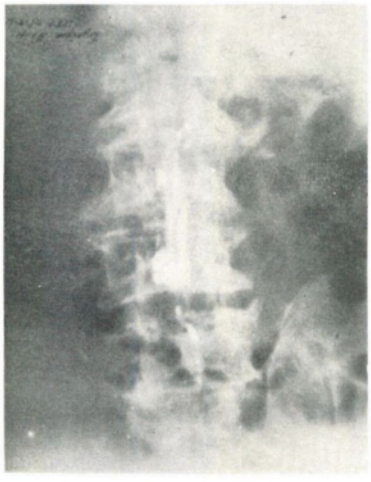

Fig. 5

Case 13. Myelogram showing block at the L_2-L_3 level

Fig. 6

Case 13. Myeloscintigram showing block at the L_2 level

14. (C.S., male, age 23)

Signs of right hemiparesis due to a neurinoma of the cervical area below the C_3 level. Myelogram done after the introduction of Discolipiodol in the cisterna magna showed the upper limit of the block to be at the C_2-$C_?$ level. On the other hand RISA introduced from the lumbar area showed a block at the C_6 level from below, and this level should be considered approximately the lower end of the lesion or even somewhat lower.

15. (X.D., male, age 39)

Bilateral pyramidal signs of the lower extremities and hypoaesthesia up to the umbilicus level. Lipiodol myelography showed a complete block at the T_{10} level, and myeloscintigram showed a diminution of the recorded radioactivity from L_1-L_2 and a complete block at the T_{12} level. An intrameningial melanoma was found at the T_9-T_{10} level.

16. (P.C., female, age 26)

Paraplegia and a sensory level at the umbilicus level. Myelogram showed filling abnormalities from the T_{12}-T_{11} area, with a complete block at the T_{11} level (Fig. 7). The myeloscintigram showed increase of recorded radioactivity apparently due to increased absorption from the tumour at the T_{11}-L_2 level (Fig. 8). During operation an extensive glioma was found at the T_{11}-L_2 area.

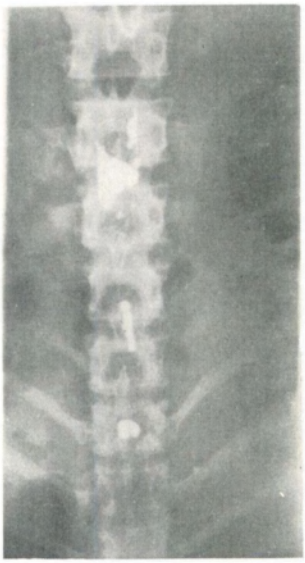

Fig. 7

Case 16. Myelogram showing block at the T_{11} level

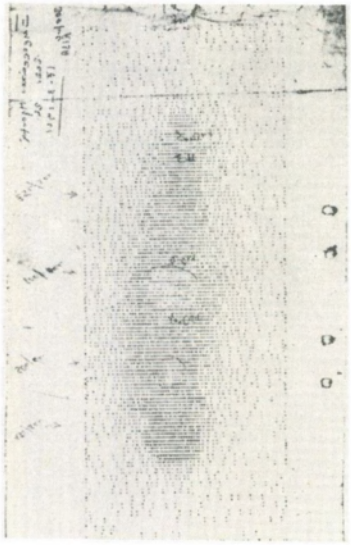

Fig. 8

Case 16. Myeloscintigram showing evidence of increased absorption of RISA at the T_{11}-L_2 level

17. (T.L., female, age 38)

Mild pyramidal signs of the lower extremities due to an haemangioma on the dura at the T_2-T_7 area. Lumbar myelogram showed a block at the T_9, the myeloscintigram showing it at the T_{10} area.

18. (S.D., female, age 39)

Weakness and atrophy of right leg. Myelogram showed a block at the L_2-L_3 level, and the myeloscintigram showed a block at the T_9-T_{11} level. An extradural tumour was found at the L_2-L_4 level.

19. (T.M., male, age 38)

Flaccid paraplegia and losses of urine and faeces from 20 days with xanthochromic CSF. On myelogram an incomplete block was found at the L_3 up to T_{11} area as well as narrowing of the spinal canal above the T_{10}

Fig. 9

Case 19. Myelogram showing incomplete block from L_3-T_{11} and T_{10}-T_8

vertebra extending at least for another 2 vertebrae (Fig. 9). Myeloscintigram showed an area of increased selective absorption between L_2-T_{10} and another between the T_9-T_6 area (Fig. 10).

During operation only the lower area of the spine was opened between T_{10}-L_2 and an ill-defined intramedullary glioma was partially removed. No exploration was done between T_6-T_{10} where the tumour was possibly extending.

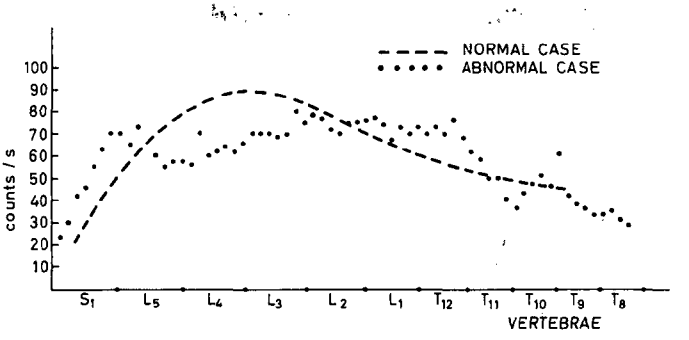

Fig. 10

Case 19. Curves made from recording the counting rate in the myeloscintigram showing the distribution of RISA

20. (F.T., female, age 71)

Case of intrameningial tuberculomas at the T_{12} level. A relationship was found between clinical signs of the paraplegia and the myeloscintigram and myelogram with signs of block at the same level. The case was also proven histologically.

21. (A.P., female, age 43)

Suffering from syringomyelia and signs of paresis of the upper extremities primarily and sensory dissociation. Myelogram showed areas of abnormal retention of Discolipiodol at the cervical and thoracic area. Myeloscintigram showed decreased radioactivity at the cervical area.

22. (A.G., female, age 50)

Pyramidal signs of lower extremities, more so on the left and sensitivity diminution at the L_4 area. Myelogram showed a narrowing of the spinal canal above the L_3 level and the myeloscintigram showed increase of the recorded radioactivity of the L_3 level. At operation diastematomyelia was found at the same level.

23. (A.Z., female, age 50)

With clinical and surgical findings of arachnoiditis and two myelograms done during her two admissions, only the second of which was abnormal, with evidences of abnormal retention of the Discolipiodol. The first myeloscintigram was done without tilting of the patient towards the head and evidence of decrease of the recorded radioactivity was found above the T_6 level. During the second myeloscintigram done after considerable tilting of the patient, repeated withdrawals of the RISA mixed with CSF and reinjections, the myeloscintigram proved normal although at this latter admission the symptoms of the patient were more marked. Comment: differences of technique lead to different results.

24. (T.T., male, age 58)

Had a fracture of the T_{11} 5 yr previously. Eight months previously weakness of the lower extremities with pyramidal signs bilaterally and destruction of the T_{11} with CSF protein of 1 g and 2 cells. Myelogram

Fig. 11

Case 24. Myelogram showing block at the T_{11} level

showed a complete block at the T_{11} (Fig. 11). Myeloscintigram showed decreased recorded radioactivity above the L_1 and a complete block at the T_{11} (Fig. 12).

25. (I.A., female, age 55)

There was an absence of radioactivity locally. Arachnoiditis was found during an operation at the cervical and thoracic area done one year prior to the myeloscintigram. This result was interpreted as probably due to post-operative adhesions.

26. (A.G., male, age 36)

In another case of arachnoiditis surgically proven at the lower thoracic area both the myelogram and the myeloscintigram showed it to be at the same level at T_{11} although the myelogram revealed that it was an incomplete one.

27. (S.S., male, age 36)

In this last case of surgically proved leptomeningitis both the myelogram and the myeloscintigram showed abnormalities of circulation of the recording materials at the same lumbar area, resulting in areas of decreased and increased density of recorded activity at the myeloscintigram and areas of retention of Lipiodol at different spots.

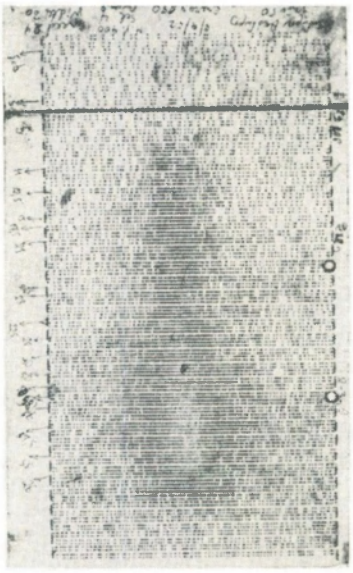

Fig. 12

Case 24. Myeloscintigram showing block at the T_{11} level

28. (M.M., female, age 58), 29. (K.K., male, age 17), 30. (D.A., male, age 51), 31. (G.K., male, age 53)

These were cases of chronic myelitis of undetermined aetiology where the myeloscintigram was normal.

32. (T.G., male, age 53)

Clinically a diagnosis of myelitis was made, the myelogram was normal, and the myeloscintigram showed a block probably caused by inadequate technique (no tilting was carried out).

33. (M.R., female, age 47)

A case of suspected tumour (no operation was accepted by the patient) where both the clinical and laboratory findings of the myelogram and myeloscintigram were in agreement that a block was presented in the T_{12} level.

34. (D.P., female, age 40) and 35. (A.K., male, age 36)

Probable diagnosis of myelitis and intercostal neuralgia respectively; the myeloscintigram proved to be normal only after adequate tilting of the patient.

TABLE I

PROTRUDED INTERVERTEBRAL DISCS

Case	Myelography	Myeloscintigram	Findings
1	Block L_3-L_4	Incomplete block L_4	Mid-line disc L_3-L_4 (surg.)
2	None	Normal	Disc 2E L_4-L_5 (surg.)
3	None	Normal	Conservative treatment
4	Block L_4-L_5	Incomplete block L_{4-5}	Disc L_4-L_5 (surg.)
5	None	Incomplete block, wide area	Disc L_4-L_5 (surg.)
6	Incomplete block	Normal	Disc T_{12}-L_1 (surg.)
7	None	Normal	Disc suspect L_4-L_5 Conservative treatment
8	Inconclusive	Inconclusive	Disc suspect L_4-L_5 Conservative treatment
9	Narrowing of column	Inconclusive	Mid-line disc L_4-L_5 (surg.)
10	Block L_4-L_5	Inconclusive	Mid-line large disc L_4-L_5 (surg.)

36. (P.P., male, age 70)

A diagnosis of metastatic carcinoma at the T_6 was made and the patient had paraplegia. The myeloscintigram was normal, and no myelogram was done.

37. (D.K., male, age 35) and 38. (A.T., male, age 68)

In these cases of sciatica and probable disc protrusion at the cervical area respectively no positive conclusions from the myeloscintigrams were possible probably because of technical errors.

DISCUSSION

In the present study ten cases of lumbar disc protrusions were presented, eight of which were surgically treated.

TABLE II

TUMOURS AND CONGENITAL LESIONS

Case	Myelography	Myeloscintigram	Findings
11	Incomplete block C_7-T_1	Incomplete block	Metastatic carcinoma cervical, no operation
12	Block L_4-L_5	Block	Metastatic carcinoma (palliative surg.)
13	Block L_2-L_3	Block L_2	Haemangioma or lymphangioma (surg.)
14	Discolipiodol cisterna magna, block C_2-C_3	RISA lumbar, block C_6	Neurinoma C_3-C_5 (surg.)
15	Block T_{10}	Block T_{12}	Melanoma T_9-T_{10} (surg.)
16	Block T_{11}	Increase in activity T_{11}-L_2	Glioma T_{11}-L_2 (surg.)
17	Block T_9	Block T_{10}	Haemangioma T_2-T_7 (surg.)
18	Block L_2-L_3	Block T_9-T_{11}	Extradural tumour L_2-L_4
19	Incomplete block T_{11}-L_3 Narrowing T_{10}-T_8	Increase in activity L_2-T_{10} and T_9-T_5	Intramedular glioma T_{10}-L_2; possibly above also (surg.)
20	Block T_{12}	Block T_{12}	Tuberculoma (surg.)
21	Syringomyelia; retention of drops cervical	Decrease in activity cervical	Syringomyelia; conservative treatment
22	Narrowing L_3	Increase in activity L_3	Diastematomyelia (surg.)

In six of the cases myelography was also done as well as myeloscintigram. In five the myelogram was positive, and the myeloscintigram showed evidence of incomplete block in only two of them. Another two had a normal myeloscintigram and the fifth was inconclusive. In one case both myelography and myeloscintigram were inconclusive (no operation performed).

TABLE III

ARACHNOIDITIS

Case	Myelography	Myeloscintigram	Findings
23	Abnormal retention of drops	Normal	Arachnoiditis Thoracic (surg.)
24	Block T_{11}	Decrease in activity L_1-T_{12} Block T_{11}	Leptomeningitis T_{11}
25	None	Block	Post-operative adhesive arachnoiditis
26	Incomplete block T_{11}	Block T_{11}	Arachnoiditis (surg.)
27	Abnormal retention of drops, lumbar area	Areas of increase and decrease of activity lumbar area	Leptomeningitis (surg.)

In four of the milder cases only myeloscintigram was done and in three of them it was normal (one of these cases had a proven disc at operation). The fourth case showed an incomplete block and a protruded disc was found.

Thus the myeloscintigram was normal or inconclusive in the mild cases, except in one case, when it was inconclusive and at surgery a large mid-line disc was found.

BAUER and YUHL [1] found the myelogram to be correct in disc cases in 20 out of 25 patients and false negative in 5 cases. They also found myeloscintigram to be correct in 30 out of 34 cases.

We found the myelogram to be correct in five out of six cases, and the myeloscintigram was correct in three out of ten cases. Most of the failures were among cases with mild symptomatology.

Among our series of nine tumour cases in all regions of the spinal canal, myelogram was performed in all cases and evidences of complete or incomplete block were found in all cases. Myeloscintigrams were also abnormal in all cases, showing complete or incomplete block in seven cases.

The localization was accurate in five of the cases, and on the sixth case the block was somewhat lower, probably due to pre-existing Discolipiodol between the lesion and the RISA. On the seventh case however with an extradural tumour of the L_3-L_4 area and slight clinical signs, the myeloscintigram was thought to be at the T_9-T_{11} level. In retrospect we are wondering whether this was not a technical error or whether it was due to incomplete obstruction of the spinal canal for the CSF, taking into consideration that the heavier oil substance we use for myelography may show blocks in areas where the thinner CSF mixed with RISA can in any case pass.

In one of the five cases noted above, where Discolipiodol was introduced from the cisterna magna and showed only the upper limit of the block to be

at C_2-C_3 level, RISA was found between C_2-C_5, thus proving the value of combined examinations in special cases.

In the remaining two of the nine cases of tumours, where block or incomplete block was found by myelography, the myeloscintigrams showed evidences of increased activity rather than block and this latter finding occurred in the only two cases of intramedullary glioma included in these series. The same findings occurred in a case of diastematomyelia and in one case of arachnoiditis.

In the glioma cases the increased radioactivity was interpreted as due to selective absorption of the RISA by the gliomas and in case No. 20 the tumour was localized quite accurately in its whole size, and from the number of dots in the myeloscintigram a curve can be reproduced (Fig. 10) showing exactly the location of the tumour.

We are not in a position to explain the mechanism of selective absorption of RISA by abnormal tissues. We thought though that the RISA may perhaps penetrate the nervous tissue by following the route of Virchow's perivascular spaces.

In the only other case where such an increase of radioactivity was found, one was in the described case of diastematomyelia and another in a case of arachnoiditis, but in both cases the appearance of the myeloscintigram was different. There was rather a spotty increase of radioactivity among areas of decreased activity and this appearance is interpreted as caused by adhesions and/or small cavities where a greater amount of RISA was trapped without adequate diffusion within the CSF.

Though we realize that the number of cases of glioma we include in these series is not adequate to warrant final conclusions for a possible prognosis of the type of lesion by myeloscintigram, we think that this is an interesting point for further efforts in the diagnosis of gliomas or, more generally, the possible diagnosis of intramedullary tumours by the myeloscintigram.

If this hypothesis proves to be correct and even better demonstrated in the future by using photoscanning or other radioactivated substances combined with greater effort in simultaneous and even more accurate marking of anatomical landmarks on the myeloscintigram, we think that it will be a real step forward in comparison with the standard methods of myelography.

Regarding more accurate localization, we consider a method similar to the one proposed by BAUER and YUHL [1] should be used more generally. It consists of recording two standard anatomical points both by the scanner and by anterio-posterior roentgenograms of the spine.

Another point that we want to make is that though recording of the cervical area is somewhat less satisfactory from the technical viewpoint, we think that it can be done with more effort and giving the examinations much more time than 30 min or less reported in most of the published works [1, 4, 5, 6].

In one case of cervical syringomyelia, clinically diagnosed, decreased activity was found at the site of the lesion and retention of some oil drops was found in myelography.

In one case of tuberculoma a block was found by both myelography and myeloscintigram at the same lower thoracic segment.

In our series of arachnoiditis or leptomeningitis that were serious enough to cause incapacitating neurological symptoms and to need explo-

ration, the myelogram performed in four cases was abnormal with retention of oily drops at the site of the lesion. The myeloscintigram correctly demonstrated the site of the lesion with a block or simply decreased activity in three cases, in one case it showed spotty areas of decreased or increased activity, and in one case it proved to be normal while the myelogram showed simply abnormal retention of oily drops. This last case was apparently mild. In four cases of myelitis the myeloscintigram was normal and no myelograms were done. In another case the myeloscintigram showed a block probably because no tilting was carried out, and the myelogram was normal.

The last five cases of our series are not described in any detail since either a complete diagnosis was not made because of inadequate time or for other reasons (the myeloscintigrams were normal or in two cases were not technically satisfactory).

CONCLUSION

The myeloscintigram is a method with potentialities, not fully explored up to the present time, and which may become in the future even more helpful in the diagnosis of spinal neurological syndromes.

In the lumbar disc cases in which we used it, the results were inferior to oil myelography, especially in mild cases, but in tumour cases it may prove to be comparatively more helpful, especially if future studies demonstrate in a larger number of cases the validity of our findings of selective absorption of the RISA by certain tumours.

This latter finding may be useful for prognosis as well. In arachnoiditis and leptomeningitis the findings are as a rule positive, and in myelitis negative.

Finally, further efforts to improve present technical facilities would be worthwhile.

REFERENCES

[1] BAUER, F.K. and YUHL, F.T., Radioisotope Myelography, Int.J.appl. Rad. Isotopes 2 (1957) 52-8.
[2] PERRYMAN, C.R., NOBLE, P.R. and BRAGDON, F.H., Myeloscintigraphy: a useful procedure for localisation of spinal block lesions, Amer. J. Roentgenol. 80 (1958) 104.
[3] BELL, R.L. and HERTCH, G.H., Automatic contour scanner for myelography, Int. J. appl. Rad. Isotopes 7 (Nov. 1959) 19-22.
[4] BELL, R.L., Automatic contour myelography in infants, J. nucl. Med. 3 (1962) 288.
[5] LIASS, F.M., Isotope myelography in the diagnosis of herniation of the intervertebral disc, Vopr. Neirokhir 25 (May-June 1961) 28-30.
[6] PECKER, J and JAVALET, A Diagnosis of cervical neoplasms by gamma-myelography and vertebral arteriography, Neurochirurgie 6 (1960) 284.

DISCUSSION

M. TUBIANA: Have you compared the results obtainable by the myeloscintigram method with those that can be obtained by means of profile counting along the vertebral column? We did some work with the latter technique

in 1951*. Our impression was that profile counting was the better method for two reasons. In the first place, it is able to provide a quicker and more precise answer to the one question that is of importance, namely whether the radioactive substance spreads along the spine. Secondly, it is a quantitative method and, if repeated at regular intervals, it provides a means of following the passage of a radioactive substance through an incomplete block.

H. MIKROPOULOS: We have only used dot counting in a small number of cases so far. Our visual results were adequate for our purposes.

J. BRICE: It was scarcely surprising that you were not able to demonstrate laterally placed discs. Your normal scans did not show detailed anatomical structures such as the nerve-root dural cuff and it is these anatomical structures that are disturbed by discs.

A more important limitation of this technique is that you cannot be certain that a subdural injection has not been made inadvertently. This is a recognized difficulty which occasionally occurs in conventional myelography and I think it could give rise to false positive and negative results.

H. MIKROPOULOS: We had the impression that we were in the subarachnoid space and we generally injected and withdrew the CSF mixed with RISA a few times on each occasion.

W. ENTZIAN: Have you obtained any specimens from cases under operation which might provide some indication of the relative uptake of the radioactive compound by intradural tumour or normal tissue?

H. MIKROPOULOS: No. It must be remembered, of course, that operations are not performed immediately after scanning but frequently some days later.

---

* TUBIANA, M., BENDA, P. et CONSTANS, J., «Sodium radioactif et liquide céphalo-rachidien, applications diagnostiques des méningites tuberculeuses et des compressions médullaires», Revue neurol. 85 (1961) 17.

RENAL SCINTISCANNING WITH Hg^{203}-NEOHYDRIN IN UROLOGIC DISEASES

V. BOLLINI AND G. TORI
RADIOLOGY INSTITUTE OF THE UNIVERSITY OF BOLOGNA, ITALY

Abstract — Résumé — Аннотация — Resumen

RENAL SCINTISCANNING WITH Hg^{203}-NEOHYDRIN IN UROLOGIC DISEASES. Renal scintiscanning has been carried out using Hg^{203}-labelled Neohydrin. The equipment used is the Nuclear Chicago Isotope Scanner Type 1700 with 2 x 2-in crystal and a 7-cm focal-length honeycomb collimator. Usually the scintigrams are registered both on paper and on photographic film. Hg^{203}-labelled Neohydrin is usually employed in doses of 120-160 μc (about 2 μc/kg). The scanning examination starts about 2 h after the injection and lasts about 40-50 min.

The selective storage of labelled Neohydrin at the level of the renal cortex makes it possible to obtain a graphic representation of the two kidneys and to identify their position, orientation and shape, and the homogeneity of the actively functioning parenchyma. In some cases, autoradiographic investigations have been carried out on diseased kidneys after surgical removal.

By this method anomalies in position and orientation, both congenital and acquired, can be ascertained. As regards shape, the limits of the renal patterns are the more clearly defined as the renal function is better. Technical aspects such as the width of the crystal, type of collimator (whose focal plane should pass through the transverse medial plane of the kidneys), and dose - which should be not too high nor too low - are essential conditions for a correct graphic reproduction of the renal patterns.

Failure in tabular activity in the parenchyma is shown by a lack in the uptake of radioactivity. The position, extent and shape of such defects in uptake vary according to the entity of the renal structures and their derangement due to various pathological processes: tumours, cysts, hydronephrosis, tuberculosis etc.

In normal subjects a homogeneous scintigram is usual, although a clearer hilar region is not a rare occurrence. Any circumscribed decrease of scintigraphic density outside the hilum is the expression of a less actively functioning zone. Among kidney patterns larger than normal, the homogeneous ones which point to a compensatory hypertrophy should be distinguished from the dishomogeneous and irregular ones. These last pictures suggest the presence of large hydronephroses, tumours or multiple cysts. In renal vascular disease, the character of the uptake in the two kidneys can be of significant value in assessing the reduced function and in differentiating unilateral from bilateral diseases. Renal scintiscanning thus shows promise of proving a useful clinical technique, particularly if combined with radiological examination of the kidneys by traditional means (urography, ascending pyelography, retropneumoperitoneum, tomography, aortography, etc.).

SCINTIGRAPHIE DU REIN DANS LES MALADIES DES VOIES URINAIRES AU MOYEN DE NÉOHYDRINE MARQUÉE AVEC ^{203}Hg. Les auteurs ont procédé à des scintigraphies du rein au moyen de néohydrine marquée avec ^{203}Hg. Ils ont utilisé le dispositif de scintigraphie «Nuclear Chicago», type 1700, à cristal de 5 x 5 cm et collimateur alvéolaire de 7 cm de distance focale. En général, les scintigrammes sont enregistrés à la fois sur papier et sur film photographique; la néohydrine marquée avec ^{203}Hg est administrée en doses de 120 à 160 μc (environ 2 μc/kg). L'examen scintigraphique commence deux heures environ après l'injection et dure de 40 à 50 min.

Le fait que la néohydrine marquée se fixe sélectivement au niveau du cortex rénal permet d'obtenir une représentation graphique des deux reins et de déterminer leur position, leur orientation et leur forme, ainsi que le degré d'homogénéité du parenchyme normal. Dans certains cas, des examens autoradiographiques ont été effectués sur des reins malades, après ablation.

Cette méthode permet de déterminer les anomalies, congénitales ou acquises, dans la position et l'orientation des reins. En ce qui concerne la forme de l'organe, les contours de l'image du rein sont d'autant plus nets que la fonction rénale est meilleure. Des caractéristiques techniques telles que la largeur du cristal, le type de collimateur (dont le plan focal doit couper le plan médian transversal des reins) et la dose (qui ne doit être ni trop élevée ni trop faible) représentent les conditions déterminantes d'une reproduction graphique correcte de la structure rénale.

Une mauvaise fixation de la radioactivité dénote une insuffisance de l'activité tubulaire dans le parenchyme. La position, l'étendue et la forme des zones de mauvaise fixation varient suivant le degré d'intégrité des structures rénales et leur altération sous l'effet de divers processus pathologiques: tumeurs, kystes, hydronéphrose, tuberculose, etc.

Chez des sujets normaux, le scintigramme est généralement homogène, bien qu'il ne soit pas rare d'observer une plus faible densité dans la région du hile. Toute tache plus claire en dehors du hile indique une zone où la fonction rénale n'est pas normale. Parmi les images du rein plus grandes que la normale, il convient d'établir une distinction entre les images homogènes, qui dénotent une hypertrophie compensatoire, et les images non homogènes et irrégulières. Ces dernières semblent indiquer une forte uronéphrose ou la présence de tumeurs ou de kystes multiples. Dans les affections réno-vasculaires, le caractère de la fixation de la radioactivité dans les deux reins peut beaucoup aider à évaluer la diminution de la fonction rénale et à établir si un seul rein ou les deux sont atteints. On peut donc s'attendre que la scintigraphie du rein constituera une méthode intéressante d'exploration clinique, surtout en association avec l'examen radiologique des reins par les méthodes classiques (urographie, pyélographie ascendante, rétropneumopéritoine, tomographie, aortographie, etc.).

СЦИНТИЛЛЯЦИОННОЕ СКЕННИРОВАНИЕ ПОЧЕК С ПОМОЩЬЮ НЕОГИДРИНА, МЕЧЕННОГО РТУТЬЮ-203, ПРИ УРОЛОГИЧЕСКИХ ЗАБОЛЕВАНИЯХ. Для сцинтилляционного скенирования почек использовался неогидрин, меченный ртутью-203. Был применен ядерный Чикагский изотопный скеннер типа 1700 с кристаллом 5 × 5 см и коллиматор "Ханикоум" с фокусным расстоянием 7 см. Обычно сцинтиграммы регистрируются одновременно на бумаге и на фотопленке. Неогидрин, меченный ртутью-203, *применяется обычно в дозах* 120—160 мккюри (около 2 мккюри/кг). Скеннирование начинают спустя 2 часа после инъекции и продолжают 40—50 минут.

Селективное скопление меченого неогидрина в корковом слое почек дает возможность получить графическое изображение обеих почек и определить их положение, ориентацию и форму, а также гомогенность активно функционирующей паренхимы. В некоторых случаях были проведены авторадиографические исследования пораженных почек после хирургического удаления.

С помощью такого метода можно диагносцировать как врожденные, так и приобретенные аномалии положения и ориентации. Что касается формы, то границы почек можно определить тем точнее, чем лучше функционирует почка. Такие технические аспекты, как ширина кристалла, тип коллиматора (фокальная плоскость которого должна проходить через среднюю поперечную плоскость почек) и доза, которая не должна быть слишком высокой или слишком малой, составляют существенное условие для правильного графического воспроизведения очертаний почек.

Нарушение деятельности канальцев в паренхиме определяется благодаря нарушению поглощения радиоактивности. Положение, размеры и форма таких дефектов поглощения колеблются в соответствии с характером почечной структуры и ее нарушений вследствие различных патологических процессов: опухолей, кист, гидронефроза, туберкулеза и т.д.

У здоровых людей обычно получают однородные сцинтиграммы, хотя получение более четкой области ворот органа не является редким случаем. Какое-либо ограниченное уменьшение сцинтиграфической плотности вне ворот представляет собой функционирующую менее активно зону. При более крупных размерах почек, по сравнению с нормальными, следует отличать однородные скенограммы, которые указывают на компенсаторную гипертрофию, неоднородных и имеющих неправильную форму. Изображения этих последних указывают на наличие крупных участков гидронефроза, опухолей или множественных кист.

При почечных сосудистых заболеваниях определение характера поглощения в обеих почках представляет большую ценность для оценки снижения их функции и для разграничения односторонних и двусторонних поражений.

Таким образом, сцинтилляционное скеннирование почек обещает дать полезные клинические методы, особенно в сочетании с радиологическим исследованием почек традиционными средствами (урография, восходящая пиэлография, ретропневмоперитонеум, томография, аортография и т.д.).

EXPLORACIÓN CENTELLEOGRÁFICA DEL RIÑÓN CON NEOHYDRINA-^{203}Hg EN LAS AFECCIONES UROLÓGICAS. Los autores han efectuado exploraciones centelleográficas del riñón empleando neohidrina marcada con ^{203}Hg. Para ello, utilizaron el Nuclear Chicago Isotope Scanner, tipo 1700, con un cristal de 2 x 2 pulg

y un colimador alveolar de 7 cm de distancia focal. Los centelleogramas se registran generalmente simultáneamente en papel y película fotográfica. La neohidrina marcada con ^{203}Hg suele administrarse en dosis de 120 a 160 μc (aproximadamente 2 μc/kg). La exploración se empieza unas dos horas después de la inyección y dura de 40 a 50 min.

La concentración selectiva de la neohidrina marcada en la corteza renal permite obtener una representación gráfica de ambos riñones, comprobar su posición, orientación y forma, y verificar la homogeneidad del parénquima en actividad. En algunos casos se han efectuado investigaciones autorradiográficas en riñones después de extirparlos quirúrgicamente.

Gracias a ese método se pueden determinar anomalías, congénitas o adquiridas, en la posición y la orientación. Por lo que respecta a la forma, los límites del diagrama quedan más claramente definidos cuanto mejor es la función renal. Ciertas condiciones técnicas tales como la anchura del cristal, el tipo de colimador (cuyo plano focal debe cortar el plano transversal mediano de los riñones) y la dosis (que no debe ser ni excesiva ni demasiado baja) son esenciales para obtener un centelleograma correcto.

Las deficiencias en la actividad tubular del parénquima dificultan la captación de radioactividad. La situación, la extensión y la forma de esos defectos de la captación varían en función de las estructuras renales y según los procesos patológicos que los determinan: tumores, quistes, hidronefrosis, tuberculosis, etc.

Para las personas sanas se obtienen centelleogramas homogéneos, aunque no es raro que la región hilar aparezca más clara. Cualquier disminución circunscrita de la densidad centelleográfica fuera del hilio indica una zona de actividad atenuada. Cuando los riñones aparecen dilatados hay que distinguir entre los homogèneos, que indican una hipertrofia compensatoria, y los no homogéneos e irregulares. Estos últimos sugieren la presencia de hidronefrosis extensas, de tumores o de quistes múltiples. Cuando se trata de enfermedades vasculares, el carácter de la captación en ambos riñones puede contribuir considerablemente a determinar una disminución de la función renal y a diferenciar los casos unilaterales de los bilaterales. Así, la centelleografía del riñón constituye al parecer una técnica clínica de gran utilidad, especialmente si se combina con el examen radiológico por medios tradicionales (urografía, pielografía ascendente, retroneumoperitoneo, tomografía, aortografía, etc.).

Renal scintiscanning using Neohydrin labelled with Hg^{203} has been widely applied in these last years in the diagnosis of various renal diseases. In many cases of renal malformations, cystic dysplasia, hydronephrosis, renal neoplasms, and obstructive arteriopathy of the renal artery, the scintiscan can be a very useful aid in diagnosing the case. This signifies that the semeiotic elements demonstrated by scintiscanning in these cases can complement and clarify the radiological findings obtained with the various traditional and special techniques.

The renal scintiscan with radiomercury is the expression of the parenchymography of the cortical structure of the kidney. The radiomercury accumulates specifically in the tubular cells, provided that these are assured of an adequate blood supply and are functioning properly. If the renal parenchyma or a part of it presents an altered tubular function, caused by anatomical or functional compromission, or is indeed truly hypovascularized, there will not be any fixation at such level or the fixation will be more or less diminished. Therefore, in numerous diseases that determine a functional or anatomical damage of the tubular activity, one will note various results of altered fixation, which may be diffused or localized with true and proper defects of uptake.

Most of the time, these results are not pathognomonic of a given disease but they are often aspecific.

Their significance and their value, however, require greater experience in order to reduce the percentage of interpretative errors. For this same reason, one must keep in mind certain technical factors, such as the type

of collimator, the distance of the kidney from the plane of focalization, the thickness of the interposed soft parts, the administered dose, the velocity of movement, etc.

A detailed description of the diagnostic possibilities of the scintiscan in various renal diseases is not possible because of the limited time allowed.

Nevertheless, numerous papers concerning this subject can be found in medical literature.

Today the renal scintiscan is being brought to universal attention as one of the most useful aids in urographic examination. To demonstrate this, we will present some observations of the polycystic kidney and renal tuberculosis. We have chosen the first of these diseases because it presents scintiscan findings which are almost pathognomonic. The second was chosen because its indications for scintiscanning have, till now, not been given due consideration.

POLYCYSTIC KIDNEY

The result of the scintiscanning is very variable and it is characterized by bilateral renal shadows, more or less enlarged, with polycyclic margins. The continuity of these margins is sometimes interrupted in the peripheral part of the organ where cystic formations, extrinsically developed, exist.

The density of the scan pattern is not homogeneous due to the presence of defects of uptake with lacunar aspect, of various dimensions and topography, which alternate themselves with areas that fix the radionuclide in various degree. In some points the patterns appear scarce. In others they appear more or less normal and in still other points, they appear denser than normal (Fig. 1, a and b).

The scan picture, besides giving significant results from a diagnostic point of view, permits a good approximate evaluation of the grade of functional activity of each of the two kidneys and determines the topography of the areas of the parenchyma which still conserve the capacity of fixing the radionuclide (Fig. 2, a and b). These observations, coupled with urographic findings permit a more reliable interpretation and constitute precious information on which therapy can be based.

The case of a post-operative polycystic kidney, which we have observed at various intervals of time, demonstrates how the operated kidney loses a great deal of its ability to fixate the radionuclide, even to the extreme extent of total exclusion (Fig. 3, a and b). These observations can constitute important elements of judgement on the still open discussion of whether the surgical intervention in cases of polycystic kidneys is feasible or not.

RENAL TUBERCULOSIS

The results vary according to the pathological forms, the seriousness and extension of the tubercular process and its duration.

In the initial forms, which are characterized by papillary erosion, the scintiscan can appear completely normal. Scintigraphic alterations become more evident with the progression of the renal lesion. The forms of middle

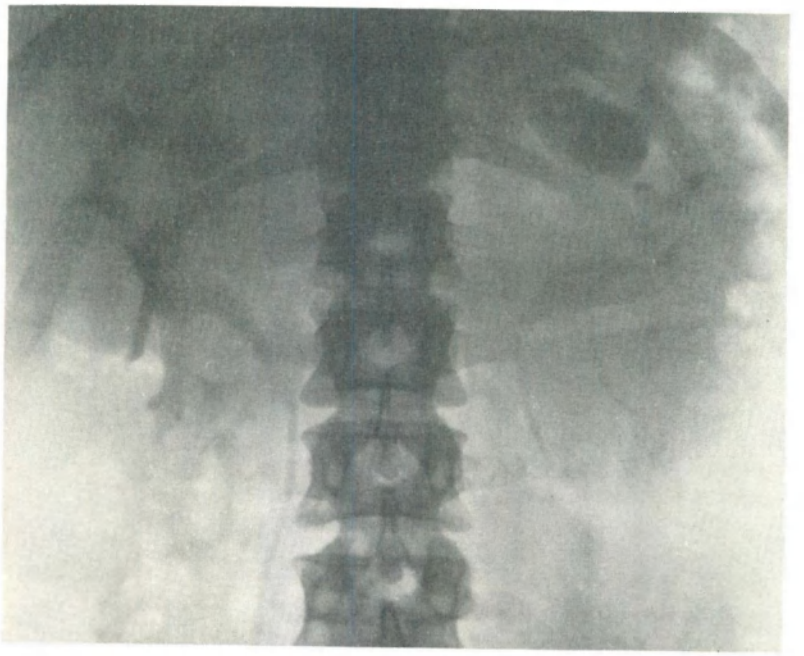

Fig. 1(a)

Bilateral polycystic kidney (urography)

Fig. 1(b)

Bilateral polycystic kidney

The photoscan shows that the renal shadows, and particularly the right one, are increased in size and have a somewhat irregular contour. Distribution of the radionuclide is not homogeneous: lacunar defects of uptake are to be seen, alternating with areas of normal or even increased density.

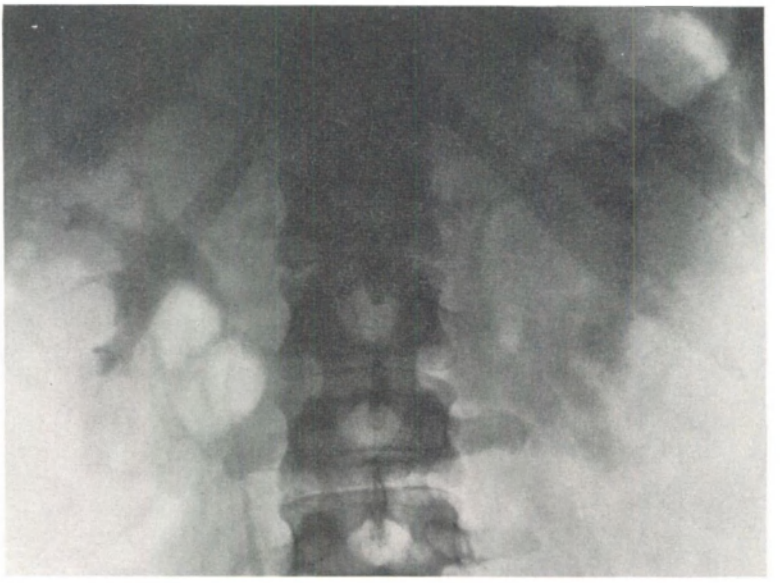

Fig. 2(a)

Bilateral polycystic kidney (urography)

severity with cavitary lesions can still present an almost normal morphology of the organ but with diffused reduction of the fixation to a variable degree.

Erosive forms with the production of caverns and destruction of the parenchyma, or reduction of the same because of serious atrophic-hypotrophic phenomena, give rise to results of altered fixation, with areas of reduced uptake or true defects of uptake (Figs.4, a and b; 5, a and b; 6, a and b).

These findings are particularly interesting because they complete the urographic findings and provide a more exact evaluation (Figs. 7, a and b; 8, a and b). In fact, the renal scintiscan can be useful in establishing if a calyx visualized on the excretory urogram constitutes a genuine expression that the corresponding portion of the kidney is functioning or does not truly represent a retrograde filling from the renal pelvis.

In the forms of chronic progression, with the extensive reduction of the parenchyma and concomitant phenomena of cicatrization, one has results of more or less complete functional exclusions (Fig. 9, a and b). The margins of the kidney are not clearly evident and the renal area presents a radioactive level which is poorly distinguished from that of the background.

CONCLUSIONS

The presentation of this paper appears to document better than other examples of renal diseases, the importance of the renal scintiscanning in order to ascertain the lesions present and also to evaluate the grade of ac-

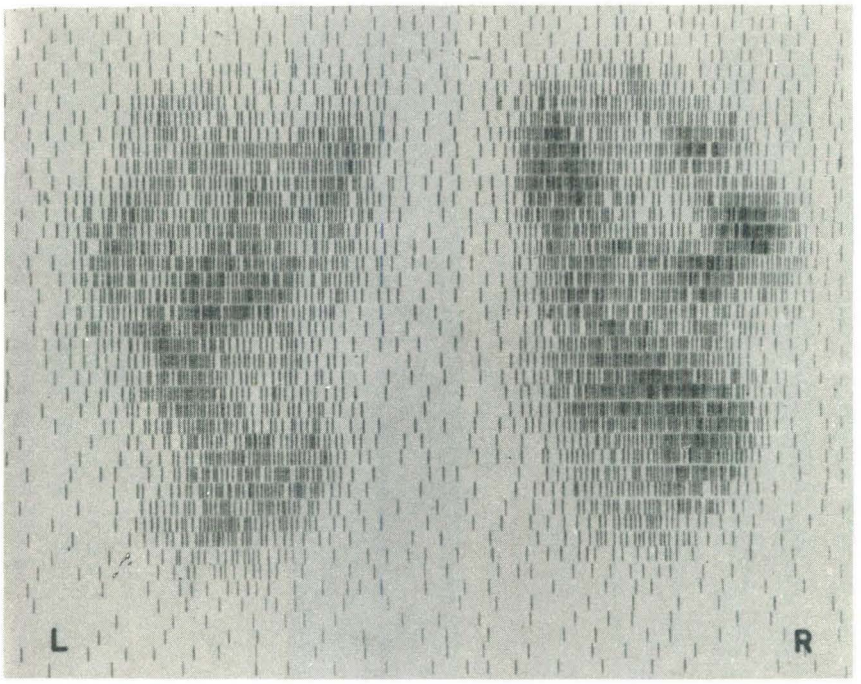

Fig. 2(b)

Bilateral polycystic kidney

The scintiscan, besides showing a typical picture of cystic dysplasia, allows us to ascertain the functional degree of the two kidneys much better than by urography. A higher uptake is in fact evident on the right side where the areas of residual parenchyma show a thicker tracing.

tivity of the parenchymal portions which fix the radionuclide. These facts have a decisive importance for therapeutic decisions, particularly in the field of surgery.

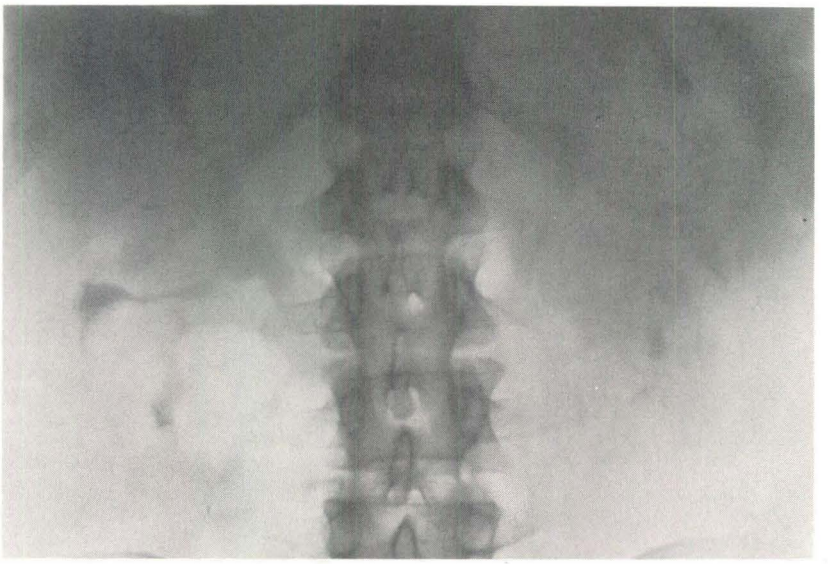

Fig. 3(a)

Bilateral polycystic kidney surgically treated (urography)

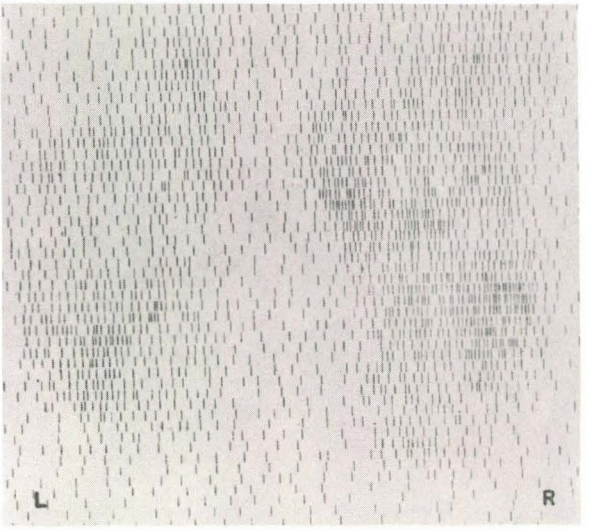

Fig. 3(b)

Bilateral polycystic kidney surgically treated

The corresponding scintiscan shows a very low uptake of radionuclide on both sides of the residual parenchyma. The scanning has been carried out six months after surgery. Although a reliable comparison with pre-surgery conditions is not possible, due to the non-availability of a previous scintigraphic examination, from the findings on the post-surgery scintiscan we can however assume that the bilateral operation did not bring about a favourable result on the functional activity of the residual parenchyma, which in fact is poor.

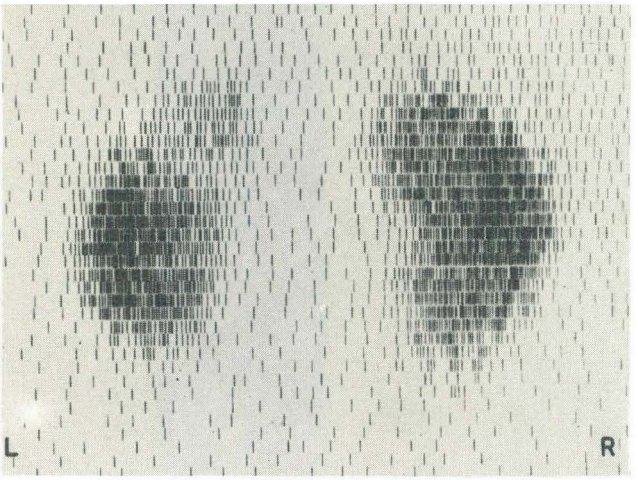

Fig. 4 (a)

Ulcero-caseous tuberculosis of the left kidney

The scintiscan shows a lacunar uptake defect at the level of the superior pole of the left kidney.

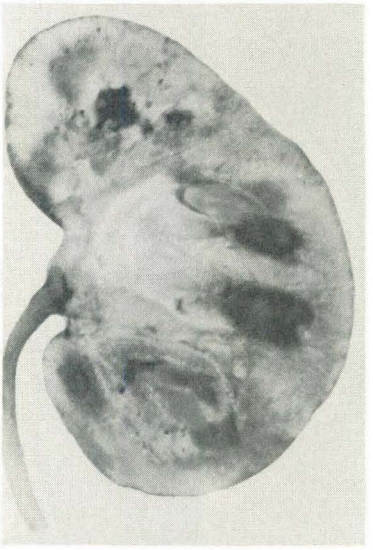

Fig. 4 (b)

Ulcero-caseous tuberculosis of the left kidney

A photograph of the operatory specimen shows destruction of the parenchyma of the superior pole and the presence of a cavitary formation .

Fig. 5 (a)

Ulcero-caseous tuberculosis of the left kidney

Urography combined with tomography, shows the presence of a lesion on the intermediate tract of the upper calyx, most probably of a specific nature

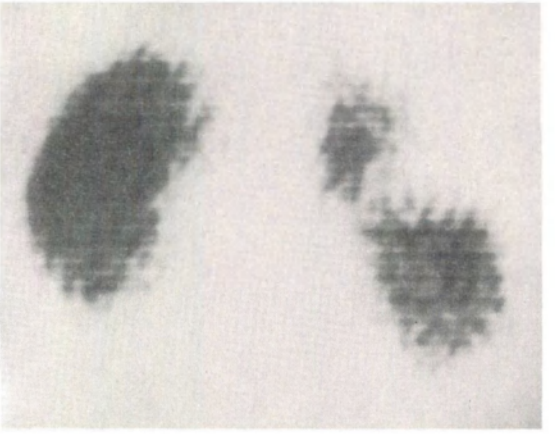

Fig. 5 (b)

Ulcero-caseous tuberculosis of the left kidney

The photoscan shows a roughly round-shaped uptake defect on the upper half of the left kidney. The remaining parenchyma of the superior pole and the lower half of the organ show a certain decrease in uptake activity.

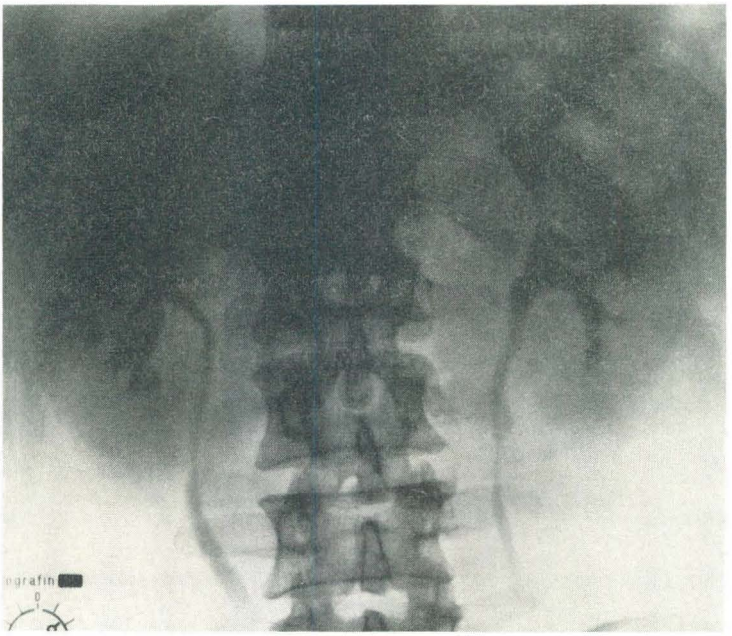

Fig. 6(a)

Sclero-atrophic tuberculosis of the right kidney
The urography shows lack of injection of the right upper calyx.

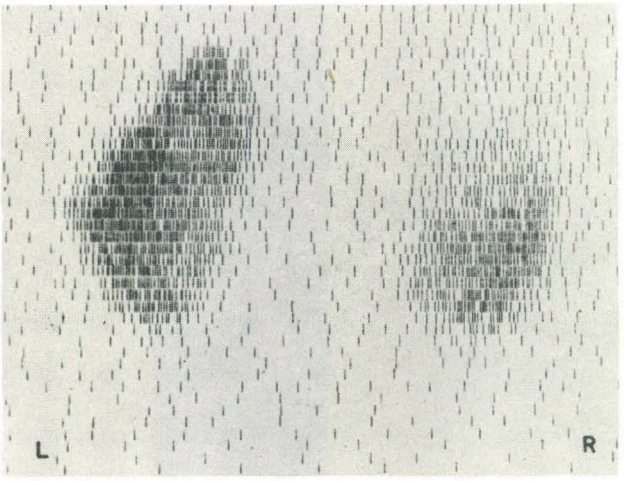

Fig. 6(b)

Sclero-atrophic tuberculosis of the right kidney

The scintiscan shows absence of uptake on the upper half of the right kidney. This explains the meaning of the urographic finding and allows appraisal of the size of the parenchymal lesion on the upper half of the organ.

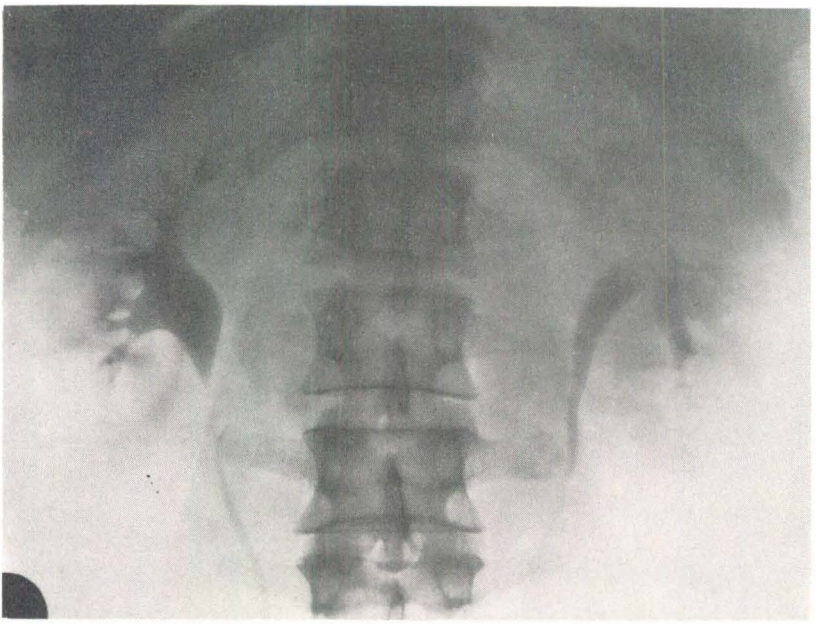

Fig. 7 (a)

Ulcero-cavitary tuberculosis

The urography shows the presence of a serious specific lesion on the upper half of the left kidney.

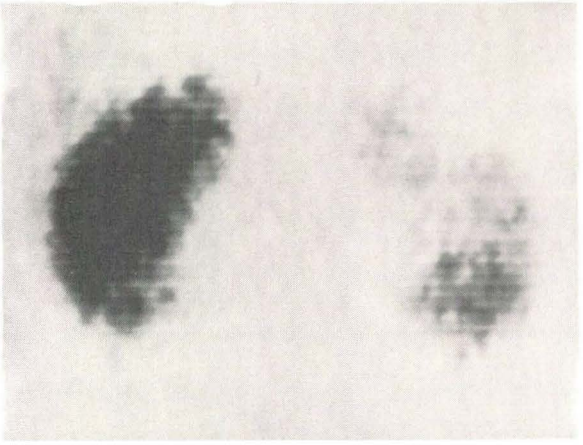

Fig. 7 (b)

Ulcero-cavitary tuberculosis

The photoscan shows a remarkable decrease in uptake activity; particularly in the superior half of the left kidney. The fact bears out the urographic finding as regards the lesion on the upper half of the organ. It is to be noted besides that on the scintiscan the lower half of the left kidney shows a conspicuous decrease of function. This is a finding not ascertained by urography.

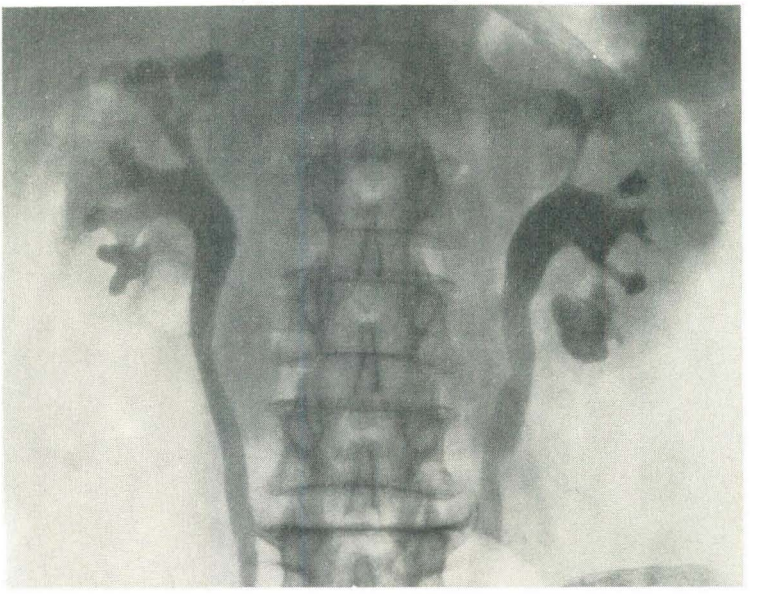

Fig. 8 (a)

Bilateral renal tuberculosis

On the right side urography shows the presence of a lesion on the intermediate tract of the lower calyx, as well as a calycectasia on the superior pole; on the left side a cavitary lesion of the inferior pole and a thinning of the intermediate tract of the upper calyx are to be seen.

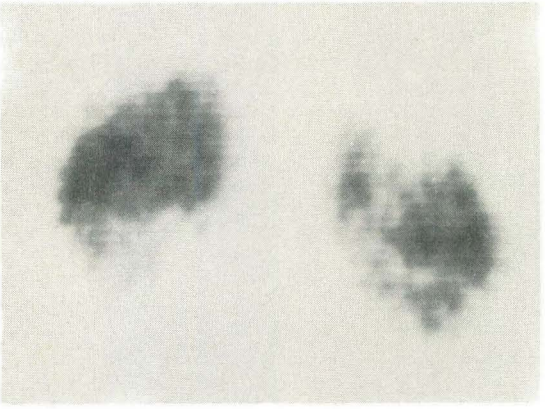

Fig. 8 (b)

Bilateral renal tuberculosis

The photoscan completes and supplements the radiological finding, showing that on the right side the most relevant lesion is on the lower renal pole where uptake is practically absent. On the left side the lower renal pole, where radiologically the lesion is more conspicuous, shows a fairly good uptake, while at the level of the superior pole a wide uptake defect is to be seen. The last finding explains the remarkable radiological narrowing of the intermediate tract of the upper calyx caused by a sclero-atrophic process spreading to almost all of the superior pole of the left kidney.

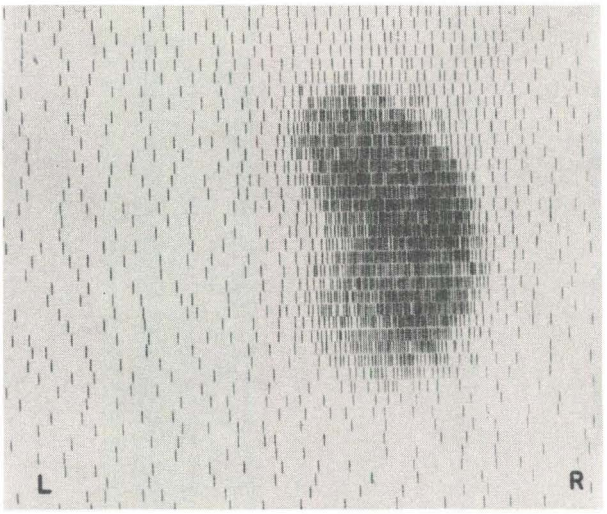

Fig. 9(a)

Sclero-atrophic generalized tuberculosis of the left kidney

Scintiscan shows the complete absence of uptake in the left kidney.

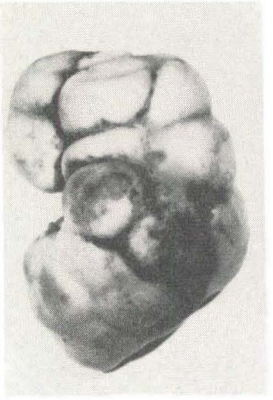

Fig. 9(b)

Sclero-atrophic generalized tuberculosis of the left kidney

Photograph of the operatory specimen.

BIBLIOGRAPHY

ALLEN, T. D. and RILEY, F. W., J. Urol. 90 (1963) 617-30.
BORGHGRAEF, R. R. M., KESSLER, R. H. and PITTS, R. F., J. clin. Invest. 35 (1956) 1055-66.
BROOKS, R. T., Jr., DETTMAN, P. M. and GALUSZKA, A. A., J. Urol. 90 (1963) 107-12.
COHEN, M. B., PEARMAN, R. O., MIMS, M. M. and BLAHD, W., J. Urol. 89 (1963) 360-5.
DESGREZ, A., RAYNAUD, C., BLANCHON, P. et KELLERSHOHN, C., Bull. et Mém. Soc. Méd. Hôp., Paris 77 (1961) 536-42.
DESGREZ, A., RAYNAUD, C. et KELLERSHOHN, C., Presse Méd. 70 (1962) 2194-7.
HAYNIE, T. P., STEWART, B. H., NOFAL, M. M., CARR, E. A. Jr. and BEIERWALTES, W. H., J. Amer. Med. Ass. 179 (1962) 137-40.
McAFEE, J. G. and WAGNER, H. N., Jr., Radiology 75 (1960) 820-1.
REBA, R. C., WAGNER, H. N., Jr. and McAFEE, J. G., Radiology 79 (1962) 134-5.
RICHET, G. et ARDAILLOU, R., in: Actualités néphrologiques de l'Hôpital Necker, Ed. Flammarion, Paris (1963).
SIMMONS, J. L. and JONES, M. A., Jr., J. Urol. 90 (1963) 642-57.
SKLAROFF, D. M., BERK, N. and KRAVITZ, C., J. Amer. Med. Ass. 178 (1961) 418-21.
TORI, G., Radiobiol. Radioter. e Fis. Med. 18 (1963) 3-24.
WESPHAL, R. D., SCOTT, R., Jr., ERICKSON, E. E. and MOTZKIN, D., J. Urol. 87 (1962) 519-26.
WOODRUFF, M. W., KIBLER, R. S., BENDER, M. A. and BLAU, M., J. Urol. 89 (1963) 746-52.
ZUM WINKEL, K. und SCHEER, K. E., Nucl. Med. 2 (1961) 71-9.

DISCUSSION

A. DESGREZ: While I fully agree with all that has been said on the subject of Hg^{203}-Neohydrin, I think it might be worth while to draw attention to the possibilities of Hg^{197}-Neohydrin, the use of which was suggested just over a year ago by Dr. Kellershohn and ourselves.

Using this substance makes it possible to inject much higher doses of radioactivity, e.g. 1.5 mc, whilst even reducing slightly the radiation dose. With these doses normal scanning equipment will produce scans with a much improved resolution. As a result, one is in a better position to interpret details of the parenchyma as well as the general shape of the organ. In Fig. 1, for example, the curved contours visible on the left kidney correspond to dilated calyces, the existence of which we have in fact been able to check. These features could certainly not have been visualized with a permissible dose of Hg^{203}.

G. TORI: I agree that Hg^{197}-Neohydrin has a number of definite advantages. One drawback is its short half-life. Hg^{203} has a longer half-life and hence is economically more attractive.

P. HARPER: The photo-scans shown by Dr. Tori have sufficient resolution and contain sufficient statistical information to show very clearly the artefact due to respiratory movements, which makes a saw-tooth appearance of the upper and lower borders of the organ - in some instances this amounts to about 2 cm. If the representation of the organ is to be refined, the motion of the kidneys will have to be controlled in some way. One possibility is to block the appropriate phrenic nerve. We have been doing this ourselves routinely for liver and spleen scans. Unfortunately, however, this cannot be done bilaterally.

C. KELLERSHOHN: I think this can be done without resorting to temporary paralysis of the phrenic nerve to suppress the effect of thorax move-

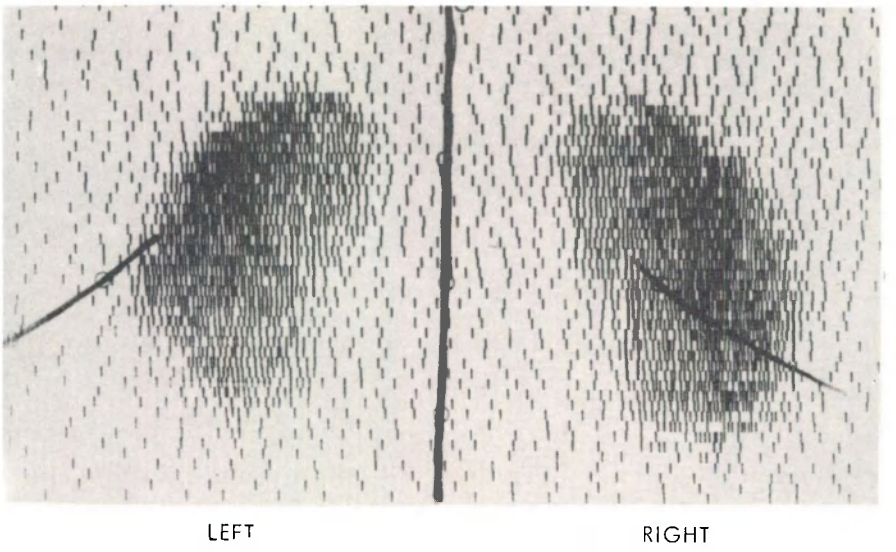

Fig. 1

Renal scans obtained with Hg^{197} -Neohydrin

ment on kidney scans. As has been pointed out by Bender and by Anger, you can obtain a very high degree of sensitivity by using scintillation cameras fitted with a grid-type optical system. If a camera of this sort is used in conjunction with an electron-capture nuclide of relatively short half-life, e.g. Hg^{197}, it is possible to obtain kidney scans in a matter of seconds. If necessary, the patient can always be asked to stop breathing for a few seconds.

I should also like to draw attention to another way of investigating renal function. This method bears a certain formal similarity with the thyroid uptake studies; a curve is traced showing the uptake of the mercurial compound in each kidney, as detected externally. This method has been developed in the last few months by Dr. Raynaud at the Service Hospitalier Frédéric Joliot; the results so far have been encouraging.

X

CLINICAL APPLICATIONS: PANCREAS, LUNGS, SPLEEN

PANCREAS SCANNING WITH Se^{75}-SELENOMETHIONINE

M. BLAU
DEPARTMENT OF NUCLEAR MEDICINE, ROSWELL PARK MEMORIAL INSTITUTE, BUFFALO, N. Y., UNITED STATES OF AMERICA

Abstract — Résumé — Аннотация — Resumen

PANCREAS SCANNING WITH Se^{75}-SELENOMETHIONINE. Amino-acids show a high degree of localization in the pancreas during the first few hours after administration. This specificity is related to the rapid synthesis and turnover of the digestive enzymes. Since none of the elements in the structure of amino-acids (C, H, N, O and S) have suitable gamma-emitting isotopes, they cannot be used for scanning. Several I^{131} derivatives of amino-acids were prepared and tested, but the pancreas-localizing property of the original amino-acid was lost in every case. The chemical similarity of selenium and sulphur suggested that the selenium analogue of methionine might resemble methionine closely enough to take its place in protein synthesis. Se^{75} (half-life, 128 d; principal gamma-ray, 0.27 MeV) is suitable for scanning.

Selenium-75-selenomethionine was prepared by yeast biosynthesis. The yeast was grown on a low sulphur medium containing high specific activity Se^{75} as selenite. After extraction with ether and hot trichloracetic acid, the protein residue was hydrolysed with hydrochloric acid. The resulting amino-acid mixture was separated by column chromatography.

Selenium-75-selenomethionine prepared in this manner showed biological properties of a natural amino-acid. The uptake in pancreas was about 7% of the administered dose and the concentration in a gramme of pancreas was seven times that in a gramme of liver. Blood and other organs had even lower uptakes.

The clinical usefulness of pancreas scanning is now being evaluated. Tumours of the pancreas have been found as areas of decreased uptake. There is no concentration of selenomethionine in cases of acute pancreatitis. It is too early to give a statistical estimate of our ability to find tumours of the pancreas by this technique. The estimated total body dose from this procedure is less than 1 rad. The selenium dose is only a few microgrammes and represents no toxicity hazard.

SCINTIGRAPHIE DU PANCRÉAS AVEC DE LA SÉLÉNOMÉTHIONINE MARQUÉE AU SÉLÉNIUM-75. Les acides aminés ont une forte tendance à se concentrer dans le pancréas dans les premières heures qui suivent l'administration. Cette spécificité va de pair avec la synthèse et le renouvellement rapides des enzymes digestifs. Etant donné qu'aucun des radioisotopes des éléments qui entrent dans la composition des acides aminés (C, H, N, O et S) n'est un émetteur gamma intéressant, on ne peut pas s'en servir en scintigraphie. On a préparé plusieurs dérivés des acides aminés contenant de l'iode-131, mais on a constaté à chaque essai que l'acide aminé avait perdu sa propriété de se concentrer dans le pancréas. Etant donné que la sélénium et le soufre ont des propriétés chimiques très voisines, on a pensé que de la méthionine contenant du sélénium à la place de soufre pouvait ressembler suffisamment à la méthionine ordinaire pour prendre sa place dans la synthèse des protéines. Le sélénium-75, qui a une période de 128 j et qui émet des rayons gamma de 0,27 MeV, convient très bien pour la scintigraphie.

On produit la sélénométhionine marquée au sélénium-75 par biosynthèse de la levure. On fait proliférer la levure dans un milieu pauvre en soufre contenant du sélénium-75 à forte activité spécifique sous forme de sélénite. Après extraction à l'éther et à l'acide trichloracétique chaud, on hydrolyse le résidu protéinique avec de l'acide chlorhydrique. On obtient ainsi un mélange d'acides aminés qu'on sépare par chromatographie sur colonne.

La sélénométhionine marquée au sélénium-75 préparée de cette manière possède les mêmes propriétés biologiques qu'un acide aminé naturel. La quantité fixée dans le pancréas correspond à environ 7% de la dose administrée; la concentration spécifique dans le pancréas est sept fois plus élevée que dans le foie. Le sang et les autres organes ont des taux de fixation encore plus faibles que le foie.

Les auteurs procèdent maintenant à l'évaluation de la valeur clinique de cette méthode de scintigraphie du pancréas. On a détecté des tumeurs du pancréas qui sont des régions où la fixation est plus faible. En cas de pancréatite aiguë, le pancréas perd sa propriété de fixer la sélénométhionine. Il est encore trop tôt pour procéder à une évaluation statistique du dépistage des tumeurs du pancréas par cette méthode. La dose

totale à l'organisme entier est inférieure à 1 rad. La quantité de sélénium administrée (quelques microgrammes) n'entraîne aucun risque de toxicité.

СКЕННИРОВАНИЕ ПОДЖЕЛУДОЧНОЙ ЖЕЛЕЗЫ С ПОМОЩЬЮ СЕЛЕНОМЕТИОНИНА, МЕЧЕННОГО СЕЛЕНОМ-75. Обнаружена высокая степень концентрации аминокислот в поджелудочной железе в течение первых нескольких часов после введения. Эта особенность связана с быстрым синтезом и кругооборотом пищеварительных ферментов. Поскольку ни один из элементов в структуре аминокислот (C,H,N и S) не имеет соответствующих гамма-излучающих изотопов, их нельзя использовать для скеннирования. Были подготовлены и испытаны несколько производных аминокислот-йод-131, но в каждом случае терялось свойство исходной аминокислоты сосредоточиваться в поджелудочной железе. Химическое сходство селена и серы дает основание считать, что селеновый аналог метеонина близок к метионину по строению в достаточной степени, чтобы занять его место при синтезе белка. Селен-75 (период полураспада 128 дней, основные данные: гамма-лучи, 0,27 Мэв) пригоден для скеннирования. Приготавливался селенометионин-селен-75 с помощью биосинтеза дрожжей. Дрожжи выращивали на среде с низким содержанием серы и высокой удельной активностью селена-75 в виде селенита. После экстрагирования эфиром и горячей трихлоруксусной кислотой белковый остаток подвергали гидролизу с помощью соляной кислоты. Результирующую смесь аминокислот разделяли методом хроматографии на колонке.

Селенометионин-селен-75, подготовленный таким образом, имел биологические свойства природных аминокислот. Поглощение в поджелудочной железе составляло около 7% введенной дозы, а концентрация на грамм поджелудочной железы была в 7 раз больше чем на грамм печени. Поглощение в крови и других органах было еще ниже.

печени. Поглощение в крови и других органах было еще ниже.

В настоящее время производится клиническая оценка методов скеннирования поджелудочной железы. Опухоли поджелудочной железы представляли участки с меньшим поглощением. Не наблюдалось концентрации селенометионина в случаях острого панкреатита. Еще слишком рано давать статистическую оценку этого метода обнаружения опухолей поджелудочной железы. Предполагаемая общая доза, получаемая организмом в результате этой процедуры, составляет менее 1 рада. Доза селена составляет несколько микрограмм и не представляет опасности в отношении токсичности.

EXPLORACIÓN DEL PÁNCREAS CON SELENOMETIONINA-^{75}Se. Los aminoácidos tienden a localizarse en el páncreas durante las primeras horas que siguen a su administración. Esta especificidad está relacionada con la rapidez de la síntesis y de la renovación de las enzimas digestivas. Como ninguno de los elementos que componen los aminoácidos (C, H, N, O y S) tiene isótopos emisores de rayos gamma apropiados, no es posible recurrir a ellos para la exploración centelleográfica. Los autores prepararon y ensayaron varios derivados de aminoácidos marcados con ^{131}I, pero en todos los casos comprobaron la desaparición de la propiedad de localizarse en el páncreas característica del aminoácido original. La semejanza química entre el selenio y el azufre sugirió a los autores la posibilidad de que el análogo seleniado de la metionina se pareciese a ésta lo suficiente para poder sustituirla en la síntesis proteica. El selenio-75 (período: 128 d; rayos gamma principales: 0,27 MeV) es adecuado para la exploración.

La selenometionina-^{75}Se fue preparada biosintéticamente mediante levaduras. Estas levaduras se cultivaron en un medio con poco azufre que contenía ^{75}Se de alta actividad específica, en forma de selenito. El residuo proteínico extraído con éter y ácido tricloracético en caliente, se hidrolizó con ácido clorhídrico. La mezcla de aminoácidos obtenida se separó por cromatografía en columna.

La selenometionina-^{75}Se así preparada tiene las propiedades biológicas de un aminoácido natural. El páncreas absorbió el 7%, aproximadamente, de la dosis administrada y la concentración por gramo de tejido fue siete veces mayor en el páncreas que en el hígado. Menor aún que en éste fue la concentración en la sangre y en otros órganos.

Los autores están ahora evaluando la utilidad clínica de la exploración del páncreas. Han comprobado que los tumores del páncreas constituyen zonas de absorción disminuida. En los casos de pancreatitis aguda no se produce concentración de selenometionina. Sería prematuro estimar estadísticamente la posibilidad de aplicar esta técnica para descubrir tumores del páncreas. Se estima que la dosis corporal total imputable a la aplicación de este procedimiento es inferior a 1 rad. La dosis de selenio es de algunos microgramos solamente y no entraña ningún riesgo de toxicidad.

INTRODUCTION

In the 5 yr since the first IAEA conference, medical radioisotope scanning has grown from a research interest to a commonly employed clinical diagnostic procedure. This advance is principally a reflection of the widespread availability of sophisticated scanners equipped with large, well-shielded crystals, focusing collimators, and effective data-presentation systems. The improvements in instrumentation have been accompanied by a search for new and better radioactive compounds with suitable organ or tissue specificity. To the original brief list of organs scanned (thyroid, liver and brain) we must now add kidney, spleen, heart, lung, bone and pancreas.

This paper summarizes our work in the development and use of Se^{75}-selenomethionine for pancreas scanning.

THE SEARCH FOR A PANCREAS SPECIFIC AGENT

Investigators searching for pancreas specific agents always start in the same place: ionic Zn^{65}. For some reason or other a mythology has grown up about the remarkable specificity of zinc for the pancreas. A few distribution studies quickly show that this "specificity" is shared by many organs including liver and kidney. Complexing agents and pre-loading with zinc improve the distribution somewhat [1], but the specificity is still inadequate for scanning.

Berberine, an alkaloid prepared from colombo root, was reported to have a very high pancreas selectivity [2]. When the abdominal organs of berberine-injected rats were examined under ultraviolet light, only the pancreas showed the characteristic bright yellow berberine fluorescence. We prepared a radioactive derivative of berberine, but this had no pancreas specificity [3]. To eliminate the possibility that chemical changes during the labelling procedure altered the biological properties of the berberine, the radio-assays were followed by a series of distribution studies in which the berberine was measured spectrophotometrically. We never found more than 1% of the injected berberine in the pancreas. In addition thin sections of liver, kidney, spleen and pancreas were examined by fluorescence microscopy. The amounts of berberine visible in all tissues were comparable to that in the pancreas. We concluded from these experiments that berberine has no pancreas specificity. The localization apparent by gross fluorescence was due to quenching of the fluorescence in other organs but not in the pancreas. The high sensitivity of fluorescence observations can be very misleading.

Another non-productive approach to pancreas localization was the use of localizing antibodies. Antibodies to a specific rat tissue (kidney, liver, or lung) can be prepared by the immunization of rabbits with various tissue fractions. These antibodies, purified and labelled with I^{131}, show remarkable specificity when injected into rats. Up to 50% of the injected dose can be found in the target organ. However, in spite of many attempts, using a variety of pancreas antigens (whole homogenate, sediment, mitochondria, lipid extracts), we were unable to prepare an antibody with even modest

in vivo pancreas specificity. This failure is probably due to the relatively small blood flow through the pancreas compared with the flow through the liver, kidney and lung. Even small amounts of cross-reacting antigens in these organs result in uptake of the circulating antibody before appreciable flow through the pancreas has occurred.

Another possible localizing agent is the pancreas-stimulating hormone secretin. This hormone is a polypeptide with a molecular weight of about 3000. It cannot be iodinated directly, but a radioactive derivative was prepared by coupling with I^{131} p-iodo benzoate groups. One or two preparations did show definite pancreas specificity. Because of the delicate nature of the hormone, we were unable to repeat these results with any regularity. It seems possible that a gentler tagging procedure might result in a usable pancreas specific agent.

AMINO ACID UPTAKE IN PANCREAS

The uptake of amino acids by the pancreas has been recognized for some time [4]. It has been shown that the high degree of concentration in the pancreas during the first few hours after administration is related to the synthesis of the digestive enzymes [5]. These enzymes do not represent a large portion of the total protein in the body at any given time. However, the very rapid utilization and destruction of the digestive enzymes compared with other body proteins accounts for the high rate of synthesis.

Table I shows the pancreas uptake and pancreas-to-liver concentration ratios for three amino acids. The uptake of cystine and methionine is quite high. The specificity of tryptophan is remarkable, especially since the D, L mixture was used instead of the natural L form. Also listed in Table I are data for a few readily available amino-acid derivatives. It can be seen that external substitution on the amino-acid molecule destroys the pancreas-localizing properties. The 5-OH-tryptophan maintains a good concentration ratio but the total amount localized in the pancreas is only one-tenth that of the parent compound. It is possible that other substituted tryptophans might retain adequate pancreas uptake, but these derivatives are difficult to prepare and none were available for testing.

Se^{75}-L-SELENOMETHIONINE

From the studies on externally substituted amino acids it seemed clear that to take part in the synthesis of the digestive enzymes a pancreas-specific amino acid would have to be internally labelled. Unfortunately none of the elements in the structure of amino acids (C, H, N, O, S) have isotopes with physical characteristics suitable for scanning. The chemical similarity of selenium and sulphur suggested that the selenium analogue of methionine (with selenium substituted for sulphur within the molecule) might resemble methionine closely enough to take its place in protein synthesis. There is an isotope of selenium, Se^{75} (half-life, 128 d; principal gamma-ray energy, 0.27 MeV), which is suitable for scanning.

TABLE I

PANCREAS LOCALIZATION OF AMINO ACIDS AND DERIVATIVES*

Amino acids	Dose in pancreas (%)	$\frac{\text{Pancreas}}{\text{Liver}}$ (per g)
C^{14}-L-methionine	6.4	8.8
S^{35}-L-cystine	5.1	7.2
C^{14}-D, L-tryptophan	12.5	11.2
Derivatives		
C^{14}-50H-L-tryptophan	1.3	8.6
N-I^{131} acetyl-tryptophan	0.3	0.9
I^{131}-mono iodo-L-tyrosine	0.3	1.2

* In rats, 1 h after intravenous administration.

Se^{75}-L-selenomethionine was prepared by yeast biosynthesis [6]. The yeast is grown on a low sulphur medium containing high specific activity Se^{75} as selenite. The Se^{75} is picked up by the yeast cells, converted to selenomethionine and incorporated into protein. The cells are harvested and after extraction with ether and hot trichloroacetic acid the protein is hydrolyzed with hydrochloric acid. The selenomethionine is separated by column chromatography on Dowex-50. High specific activity selenomethionine is very sensitive to oxidation and an antioxidant (B-mercaptoethylamine) is used during the preparation and in the final selenomethionine solution.

The distribution of Se^{75}-L-selenomethionine in dogs is shown in Table II. The pancreas uptake and specificity are characteristic of a natural amino acid with about 7% of the injected dose in the pancreas and a concentration ratio of eight times as much selenomethionine in a gram of pancreas as in a gram of liver. Figure 1 shows the time course of the pancreas localization of Se^{75}-L-selenomethionine in mice. The uptake is quite prompt, with a maximum reached in the first $\frac{1}{2}$ h. This peak is maintained for 4 h and then the selenomethionine gradually leaves the pancreas as the digestive enzymes are secreted. The mice had no access to food.

In cats cannulated for the collection of pancreatic juice, selenomethionine was directly incorporated into the digestive enzymes with no prior metabolic change [7]. The selenomethionine was synthesized into the enzymes at the same rate and in the same manner as methionine.

As a gamma-emitting amino acid with the biological behaviour of natural amino acids, Se^{75}-L-selenomethionine has possible applications quite apart from the pancreas studies. For example it has been shown that Se^{75}-L-selenomethionine and S^{35}-L-methionine are actively transported across the

TABLE II

Se^{75}-L-SELENOMETHIONINE DISTRIBUTION*

	Pancreas	Liver	Kidney	Spleen	Blood
% Dose in total organ	6.8	11.4	1.7	0.4	6.3
% Dose/g pancreas / % Dose/g organ	--	8.1	10.0	29	31

* In dogs, 2 h after subcutaneous injection.

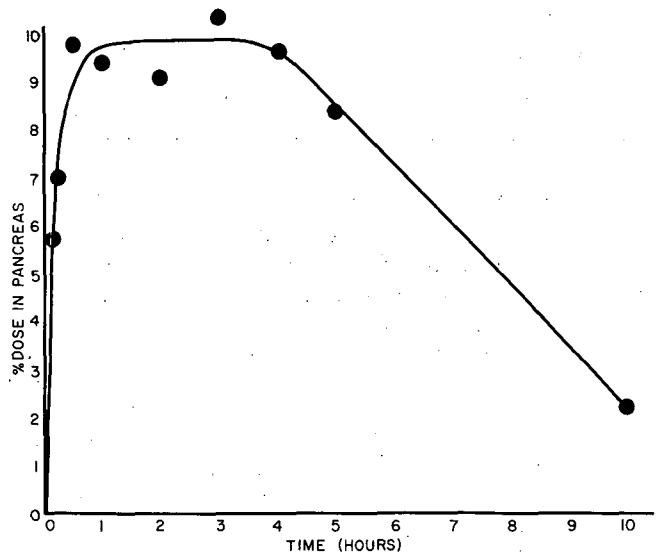

Fig. 1

Uptake of Se^{75}-L-selenomethionine in the mouse pancreas

intestinal wall at exactly the same rate [8] and therefore Se^{75}-L-selenomethionine could be used as a convenient indicator of amino-acid absorption from the gut. Similarly, proteins containing Se^{75}-L-selenomethionine would be a useful test material for protein digestion. Unlike I^{131} albumin, the radioactivity could not be separated from the protein without digestion. Using electrophoretic techniques we have been able to follow the incorporation of Se^{75}-L-selenomethionine into the various plasma proteins and the metabolic turnover of the various fractions with time. The results are essentially the same as those with S^{35}-methionine but the measurement techniques are much simpler. Se^{75}-L-selenomethionine can be used for the visualization

by scanning of other organs. We have been able to scan the prostate and parotid glands and visualization of the parathyroids has been reported [9].

RADIATION DOSIMETRY

The precise dosimetry of a radioactive compound with a changing distribution is extremely difficult to determine. In the case of Se^{75}-L-selenomethionine reasonably accurate estimates are possible when the following assumptions are made. When injected the radioactivity is taken up into the various protein synthesis systems. The principal initial localization is in pancreas (7%) and in liver (10%). The pancreas uptake is into the digestive enzymes which are secreted into the gut at the next meal. These enzymes are themselves digested and recycled. The liver uptake is principally into the plasma proteins being synthesized at the time of injection and these leave the liver within a day to enter the general circulation. Following the initial distribution there is extensive recycling of the isotope but no localization in any particular organ or tissue. The distribution after the first day can be considered as essentially total body. For the most part the radiation dose is from gamma rays and local concentrations do not play an important role in the dose considerations.

The biological half-life has not been accurately determined in humans. In the rat it is about 20 d but there is evidence that it is appreciably longer in man. The best evidence available at this time indicates a biological half-life of about 100 d.

The gamma-ray dose constant for Se^{75}, calculated for the seven gamma-ray energies with abundances above 0.5%, is 1.56 r/mc-h at 1 cm. In addition the short-range radiation from X-rays and conversion electrons has been estimated at 0.0105 MeV per Se^{75} disintegration [10].

Using these physical and biological factors the following integrated doses have been calculated, based on a routine scanning dose of 3 μc/kg:

Total body dose	=	1.3 r
Extra dose to pancreas	=	0.06 r
Extra dose to liver	=	0.05 r
Highest total body dose rate	=	0.11 r/week

These doses, while not insignificant, are well within the range considered acceptable for diagnostic procedures.

SELENIUM TOXICITY

Se^{75}-L-selenomethionine can be prepared with a specific activity of 10-20 mc/mg. The dose of selenium given with a standard scanning dose (200 μc) is only a fraction of a milligram. This is several orders of magnitude below the toxicity level and represents no hazard. We have observed no adverse reactions in over 200 injections.

SCANNING PROTOCOL

In order to improve the uptake of Se^{75}-L-selenomethionine in the pancreas and decrease the secretion of the radioactive pancreatic juices before scanning is completed, the following protocol has been evolved:

8.00 a.m.	Breakfast: 2 glasses of milk only
11.00 a.m.	Cecekin Vitrum (1 unit/kg) intravenously
12.00 noon	3 μc/kg Se^{75}-L-selenomethionine, intravenously, and 15 mg Probanthine, orally.
12.30 p.m.	Start scanning.

When it is necessary to establish the position of the liver margin, a liver scan using colloidal Au^{198} is done a day or two after the pancreas scan. We have experimented with many protocol variations and find that this one gives the most consistently satisfactory scans.

A light protein breakfast is required to provide the other amino acids for the synthesis of the digestive enzymes. When selenomethionine is given after overnight starvation, the liver uptake is enhanced and the pancreas uptake decreased. Presumably, even in mild protein deficiency, the synthesis of the plasma proteins takes precedence over the digestive enzymes. Heavy protein meals must be avoided to prevent the possibility of continued stimulation of pancreatic secretion during scanning.

Cecekin Vitrum is a preparation of intestinal hormones containing cholecystokinin, secretin and pancreozymin. In pancreas scanning it is used to empty the pancreas of enzymes, thus stimulating the synthesis of new proteins. Both secretin and pancreozymin are necessary for full enzyme secretion. The cholecystokinin activity is not required, but Cecekin is the only commercial preparation containing both pancreas-stimulating hormones. In cases of acute pancreatitis where pancreas stimulation is contra-indicated the Cecekin is not used.

One hour after the emptying of the pancreas the Se^{75}-L-selenomethionine is given. At this point the pancreas is synthesizing fresh digestive enzymes at a maximum rate and there is no longer any danger of stimulation from residual Cecekin activity. Probanthine, an anti-cholinergic drug, is given orally just after the selenomethionine injection. When absorbed it helps to prevent the newly formed radioactive digestive enzymes from leaving the pancreas during scanning.

CLINICAL RESULTS

The clinical usefulness of pancreas scanning is now being evaluated. It is much too early to draw accurate conclusions from the data, but a preliminary estimate is possible.

Over 150 scans have been done. The scanning protocol described above was used in only 58 of these patients. Table III presents the diagnostic results in these cases. Most of the patients referred for scanning complained of vague epigastric distress. The scans were interpreted without know-

TABLE III

CLINICAL RESULTS

Established diagnosis	Pancreas scan interpretation	
	Positive	Negative
Normal	0	19
Tumour, intrinsic	3	3
Tumour, extrinsic	1	0
Pancreatitis, active	3	0
Pancreatitis, inactive	0	5

Total scans evaluated	34
Insufficient time for follow-up	16
Technically unsatisfactory	8
Total	58

ledge of the clinical evaluation or access to the results of other diagnostic tests.

Interpretable scans were obtained in 85% of the cases. Half of the tumours were not found on the scans, but no false positive results were reported. With active pancreatitis the failure to take up Se^{75}-L-selenomethionine was diagnostic in every case. Inactive pancreatitis produced little or no inhibition of pancreatic uptake. One case of distortion of the pancreas outline by an extrinsic mass was correctly diagnosed. Because of the short follow-up many cases cannot be evaluated at this time.

Results similar to these have been reported from other laboratories [11, 12].

The pancreas scans have provided information helpful in the management of many patients, particularly by ruling out pancreatite as a possible diagnosis. With increasing experience in interpretation it is expected that this procedure will become even more useful. Figures 2-7 show selected pancreas scans.

SUMMARY

The selenium analogue of methionine, Se^{75}-L-selenomethionine, retains the pancreas specificity characteristic of natural amino acids. This

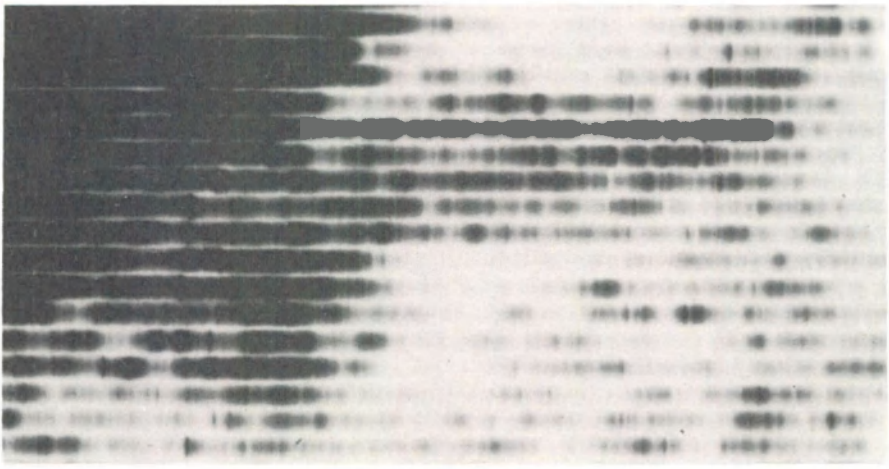

Fig. 2

Normal pancreas scan

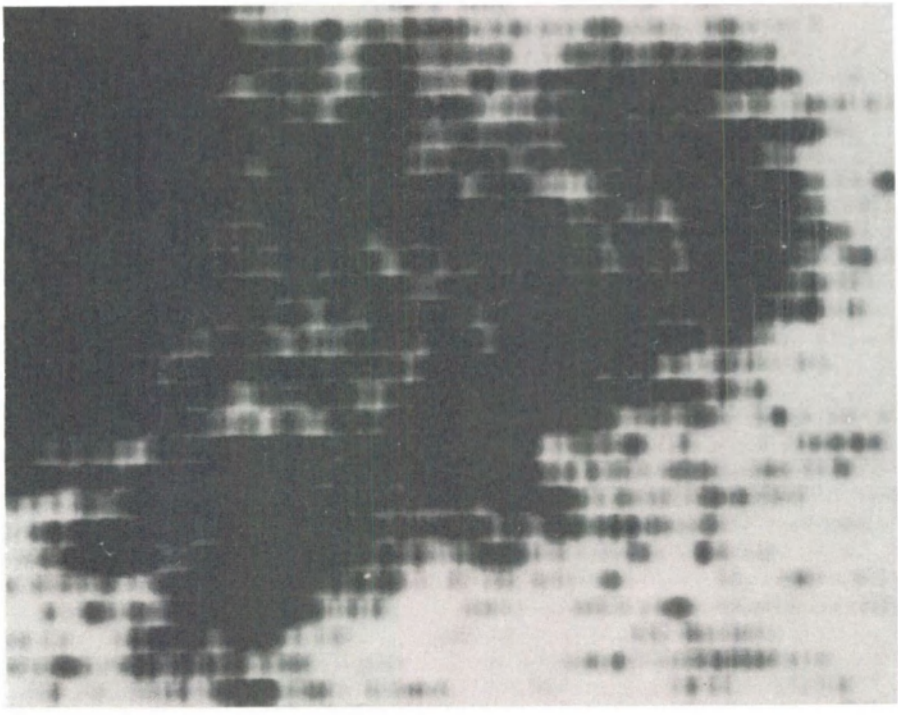

Fig. 3

Normal pancreas scan

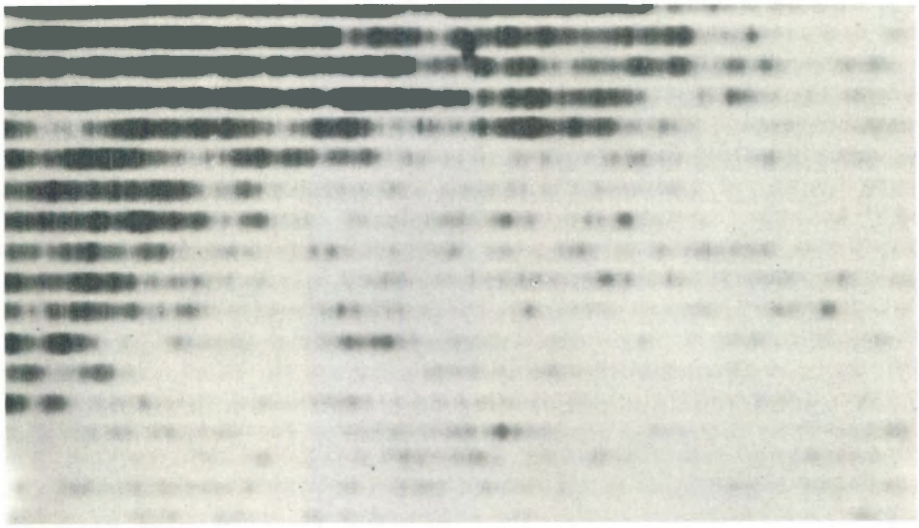

Fig. 4

Pancreas scan showing lack of pancreas uptake in pancreatitis

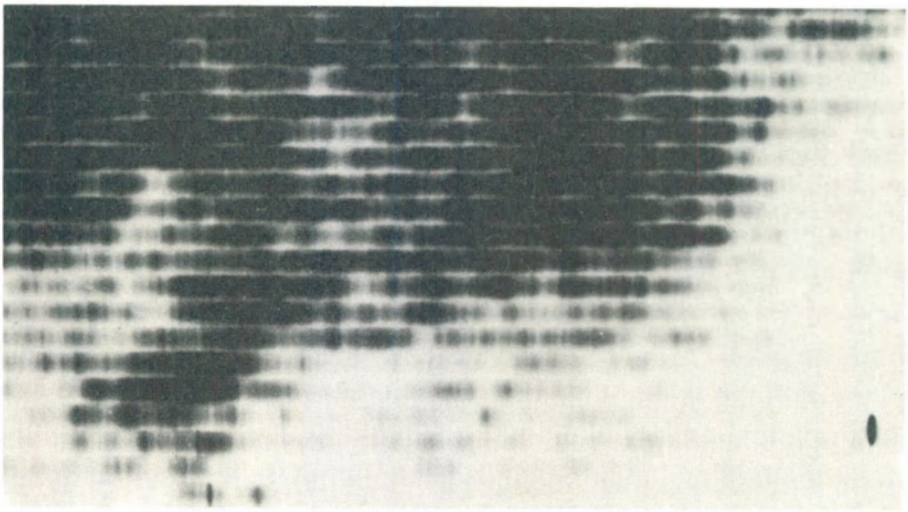

Fig. 5

Pancreas scan showing tumour deficit in head of pancreas

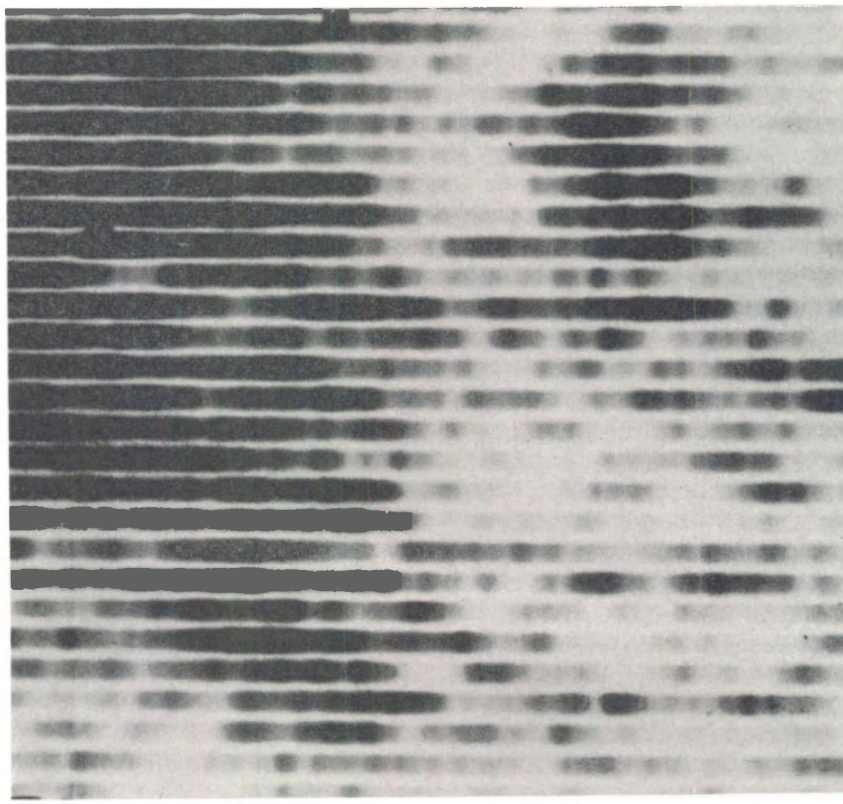

Fig. 6

Pancreas scan showing tumour deficit in body of pancreas

specificity is adequate for pancreas visualization. The scans provide useful information in benign and malignant disease of the pancreas.

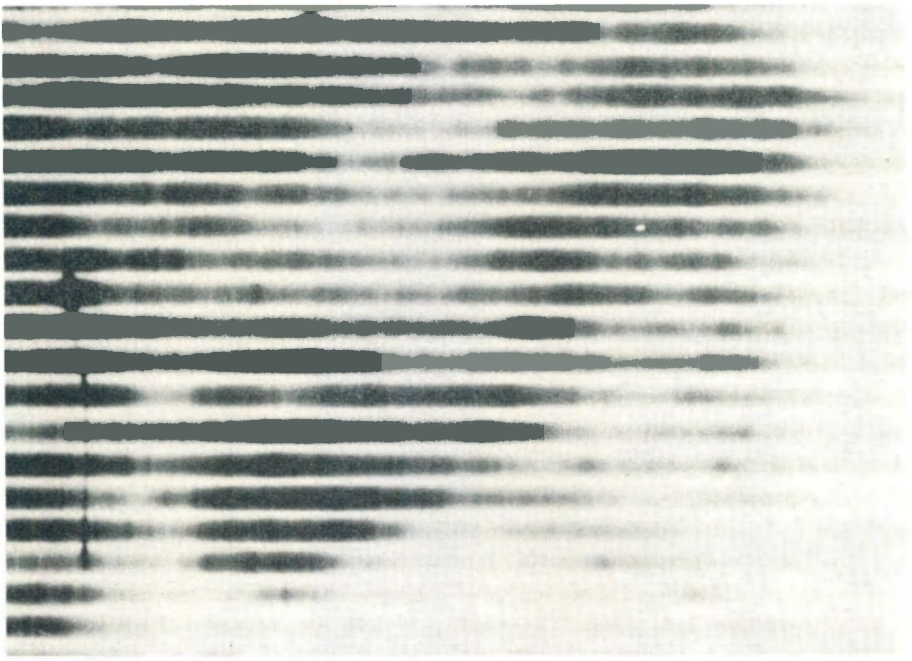

Fig. 7

Pancreas scan showing distortion of body of pancreas by extrinsic mass

REFERENCES

[1] GREENLAW, R. H. and STRAIN, W. H., J. nucl. Med. 1 (1960) 114.
[2] NARDI, G. L. and SEIPEL, J. H., Surg. Forum 6 (1955) 381.
[3] BLAU, M. and BENDER, M. A., Gastroenter. 38 (1960) 217.
[4] WHEELER, J. E. et al., Proc. Soc. exp. Biol. Med. 70 (1949) 187.
[5] HANSSON, E., Acta Physiol. scand. 46 (1959) Suppl. 161.
[6] BLAU, M., Biochim. Biophys. Acta 49 (1961) 389.
[7] HANSSON, E. and BLAU, M., Biochim. biophys. Res. Comm. 13 (1963) 71.
[8] SPENCER, R. P. and BLAU, M., Science 136 (1962) 155.
[9] POTCHEN, E. J. and DEALY, J. B., J. nucl. Med. 4 (1963) 203.
[10] HINE, G. J. and BROWNELL, G. L., "Radiation Dosimetry", Academic Press, New York (1956) 900.
[11] SODEE, D. B., Exhibit at Society of Nuclear Medicine 1963.
[12] HAYNIE, T. P. et al., J. nucl. Med. 5 (1964) 90.

RADIOISOTOPE SCANNING OF THE PANCREAS WITH SELENOMETHIONINE-Se^{75}

D. B. SODEE
DOCTORS HOSPITAL AND RENNER CLINIC FOUNDATION,
CLEVELAND HEIGHTS, OHIO, UNITED STATES OF AMERICA

Abstract — Résumé — Аннотация — Resumen

RADIOISOTOPE SCANNING OF THE PANCREAS WITH SELENOMETHIONINE-Se^{75}. Photoscanning of the pancreas utilizing selenomethionine-Se^{75} has recently been shown to be a practical technique. In a series of 100 patients who underwent 250 such photoscans, the pancreas was visualized in 90% of the cases. The physiological stimulation of the pancreas was found to be the most important factor in pancreatic selenomethionine-Se^{75} concentration. Utilizing a 30-g protein meal, physiological stimulation of the pancreas was begun one hour before the intravenous administration of 3 to 4-μc/kg selenomethionine-Se^{75}. Fifteen minutes later continued stimulation of the pancreas was ensured by the oral administration of 900 μg of glutamic acid hydrochloride. Before scanning the pancreas, a ¼-in curved lead shield was placed over the liver bed previously outlined by an Au^{198} liver scan. This lead shield blocks the radiation from the concentration of selenomethionine-Se^{75} in the liver that in the past impaired accurate delineation of the pancreas.

The authors have recently utilized a 5-in by 3-in crystal and a 121-hole lead collimator with a 5-in focal distance. This has further improved delineation of the pancreas and, as the technique is perfected, smaller lesions at greater depths may be visualized.

The results show that pancreatic carcinoma does not concentrate selenomethionine-Se^{75} as well as normal tissue. Five of six patients with pancreatic carcinoma had their disease correctly interpreted by this procedure. The smallest carcinoma not visualized was obscured by an enlarged liver. Acute and chronic pancreatitis are also confirmed by the pancreatic scan as the impaired cells of the pancreas do not concentrate selenomethionine-Se^{75}.

The author also reports selective uptake of selenomethionine-Se^{75} by parathyroid tissue. Utilizing the same scanning technique parathyroid adenomas in a small group of hyperparathyroid patients have been visualized.

Photoscanning of the pancreas is already a practical technique and an investigation of photoscanning of the parathyroid is now being undertaken. With the renewed interest in organs that previously could not be visualized by standard radiographic techniques, selective organ scanning, by means of labelled compounds chosen for their biochemical properties, becomes an important technique of the future.

GAMMAGRAPHIE DU PANCRÉAS A L'AIDE DE LA SÉLÉNOMÉTHIONINE-^{75}Se. On a démontré récemment que la photo-gammagraphie du pancréas à l'aide de sélénométhionine-Se était une méthode pratique. Chez un groupe de 100 sujets qui avaient subi 250 photo-gammagraphies de ce genre, le pancréas a été visualisé dans 90% des cas. On a constaté que la stimulation physiologique du pancréas constitue le facteur le plus important de la concentration de la sélénométhionine-^{75}Se dans cet organe. L'ingestion de 30 g de protéine avait déclenché la stimulation physiologique du pancréas une heure avant l'injection intraveineuse de 3 à 4 μc de sélénométhionine-^{75}Se par kilogramme. Un quart d'heure plus tard, cette stimulation était rendue constante par administration buccale de 900 μg de chlorhydrate d'acide glutamique. Avant la gammagraphie du pancréas, un écran courbé en plomb de 0,95 cm d'épaisseur a été placé au-dessus de la région hépatique préalablement déterminée par gammagraphie du foie à l'aide de ^{198}Au. Cet écran arrête le rayonnement émis par la sélénométhionine-^{75}Se concentrée dans le foie, qui empêchait autrefois de délimiter le pancréas avec précision.

L'auteur a utilisé récemment un cristal de 12,5 × 7,5 cm et un collimateur en plomb à 121 canaux ayant une distance focale de 12,5 cm. Il est ainsi parvenu à délimiter le pancréas avec plus de précision; en perfectionnant ce procédé, il sera peut-être possible de «voir» des lésions moins importantes à des profondeurs plus grandes.

Les résultats montrent que les carcinomes du pancréas ne fixent pas la sélénométhionine-^{75}Se aussi bien que le tissu normal. Grâce à cette méthode, on a pu déterminer le caractère cancéreux de tumeurs pancréatiques chez cinq des six personnes examinées. La plus petite de ces tumeurs, qui n'a pu être rendue visible,

se trouvait cachée par un foie hypertrophié. La gammagraphie du pancréas permet également de déterminer les pancréatites aiguës et chroniques du fait que les cellules atteintes ne retiennent pas la sélénométhionine-^{75}Se.

L'auteur signale en outre une fixation sélective de sélénométhionine-^{75}Se dans le tissu parathyroïdien. En faisant appel à la même méthode d'exploration, il a pu observer des adénomes de la parathyroïde chez un petit groupe de personnes atteintes d'hyperparathyroïdie.

La photo-gammagraphie du pancréas constitue d'ores et déjà une méthode pratique; on étudie actuellement la possibilité de l'appliquer à la parathyroïde. Etant donné le regain d'intérêt dont bénéficient les organes que l'on ne parvenait pas à visualiser par les procédés radiographiques ordinaires, la gammagraphie des divers organes à l'aide de composés marqués, choisis pour leurs propriétés biochimiques, est appelée à un bel avenir.

ДИАГНОСТИЧЕСКОЕ ФОТОСКЕННИРОВАНИЕ ПОДЖЕЛУДОЧНОЙ ЖЕЛЕЗЫ. Недавно было показано, что фотоскеннирование поджелудочной железы с помощью селенометионина, меченного Se^{75}, является практическим методом. У 90% из 100 больных, у которых было получено 250 подобных фотоскенограмм, можно было отчетливо видеть поджелудочную железу. Было обнаружено, что физиологическая стимуляция поджелудочной железы является главным фактором концентрации селенометионина – Se^{75} в поджелудочной железе. За час до внутривенного введения в организм 3 – 4 мкк/кг селенометионина – Se^{75} с помощью 30 граммов белковой пищи была начата физиологическая стимуляция поджелудочной железы. Через 15 минут была достигнута непрерывная стимуляция поджелудочной железы путем введения через рот 900 мкг гидрохлорида глутаминовой кислоты. До скеннирования поджелудочной железы над областью печени, предварительно определенной при скеннировании с помощью золота-198, был помещен изогнутый защитный экран из свинца размером 0,9 см. Этот экран блокирует возникающее в результате концентрации селенометионина – Se^{75} в печени излучение, которое в прошлом мешало точному определению контура поджелудочной железы.

Недавно авторы использовали кристалл размером 12,5 × 7,5 см и 121-канальный свинцовый коллиматор с фокусным расстоянием 12,5 см. Это улучшило качество изображения, и по мере усовершенствования методики можно будет, вероятно, видеть меньшие повреждения на большей глубине.

Оказалось, что карцинома поджелудочной железы концентрирует селенометионина – Se^{75} . хуже, чем нормальная ткань. С помощью этой методики удалось правильно истолковать заболевание у 5 из 6 больных, страдающих карциномой поджелудочной железы. Неподдающиеся обнаружению мельчайшие карциноматозные узлы были затемнены увеличенной печенью. Диагноз острого и хронического панкреатита также подтверждается скеннированием поджелудочной железы, поскольку поврежденные клетки поджелужочной железы не концентрируют селенометионин – Se^{75}.

Автор также описывает избирательное поглощение селенометионина – Se^{75} тканью паращитовидной железы. С помощью этого же метода скеннирования были обнаружены аденомы паращитовидной железы у небольшой группы больных с повышенной функцией паращитовидной железы.

Фотоскеннирование поджелудочной железы уже является практическим методом, и в настоящее время ведется изучение фотоскеннирования паращитовидной железы. Наряду с вновь пробудившимся интересом к органам, которые были невидимы при обычных радиографических методах, селективное скеннирование органов с помощью соединений, содержащих меченые атомы и подобранных по их биохемическим свойствам, становится важным методом будущего.

GAMMAGRAFÍA DEL PÁNCREAS MEDIANTE RADIOISÓTOPOS. La eficacia de la fotoexploración del páncreas utilizando selenometionina-^{75}Se ha sido recientemente demostrada. Se han efectuado 250 fotoexploraciones de ese tipo en una serie de 100 pacientes y el páncreas se ha visualizado en el 90% de los casos. Se ha observado que el estímulo fisiológico del páncreas es el factor más importante en la concentración pancreática de la selenometionina-^{75}Se. Administrando 30 g de comida proteica, el estímulo fisiológico del páncreas empezó una hora antes de inyectar por vía intravenosa de 3 a 4 μc/kg de selenometionina-^{75}Se. Quince minutos después se logró el estímulo continuo por administración oral de 900 μg de clorhidrate de ácido glutámico. Antes de proceder a la exploración se colocó un blindaje de plomo de 3/8 pulg de espesor, adaptado a la región hepática previamente delimitada por una exploración del hígado mediante ^{198}Au. Este blindaje intercepta la radiación emitida por la selenometionina-^{75}Se concentrada en el hígado, radiación que antes impedía la delimitación exacta del páncreas.

El autor ha utilizado recientemente un cristal de 5 x 3 pulg y un colimador de plomo de 121 canales, con una distancia focal de 5 pulg. Este instrumento ha permitido mejorar la delimitación del páncreas y localizar lesiones más pequeñas situadas a mayor profundidad.

Los resultados obtenidos demuestran que la concentración de la selenometionina-^{75}Se es menor en los carcinomas pancreáticos que en el tejido normal. Examinados con esa técnica seis pacientes afectados de carcinoma pancreático se diagnosticó correctamente le enfermedad en cinco casos. El carcinoma más pequeño que no pudo visualizarse estaba ocultado por el hígado hipertrofiado. La exploración pancreática permite también confirmar la pancreatitis aguda y crónica, ya que las células lesionadas no concentran la selenometionina-^{75}Se.

El autor trata además de la concentración selectiva de la selenometionina-^{75}Se en el tejido paratiroideo. Con la misma técnica de exploración se han visualizado adenomas paratiroideos en un pequeño grupo de enfermos de hiperparatiroidismo.

La fotoexploración del páncreas es ya una técnica de uso corriente; actualmente se estudia la posibilidad de una fotoexploración de la paratiroides. Debido a la mayor importancia médica atribuida a órganos que antes no podían visualizarse con las técnicas radiográficas tradicionales, la exploración selectiva de órganos por medio de compuestos marcados, elegidos según sus propiedades bioquímicas, va adquiriendo cada vez mayor importancia.

Pancreatitis and pancreatic tumour are disease processes that are difficult to diagnose by standard clinical laboratory determinations and radiographic techniques [1, 2]. Early diagnosis of carcinoma of the pancreas is seldom accomplished by such methods and by the time the presence of tumour is known there is little chance for cure, even by surgery. The high morbidity and mortality of pancreatic disease, and the difficulties in diagnosis by standard methods, have stimulated considerable interest in radioisotope methods of visualization of the pancreas for clinical diagnosis.

Radioactive zinc has been evaluated [3] because of the relative high zinc content of the pancreas; however, the physical properties of the commonly used isotope of the element (Zn^{65}) apparently make its use as a pancreatic localizing agent not feasible.

The high concentrations of amino acids in the secretions of the pancreas are well known. In 1961, BLAU [4] in an original technique utilized a common amino acid, methionine, to develop a new radiopharmaceutical selenomethionine-Se^{75} labelled with a gamma-emitting radioisotope. Se^{75} has excellent scanning characteristics as 79% of its disintegrations are in the range of 279 keV and there is no beta emission [5]. In animal studies, BLAU and MANSKE [6] showed that slightly less than 10% of the administered dose of selenomethionine-Se^{75} localized in the pancreas and that the concentration of the radioactivity in the pancreas per gram is approximately nine times that found in the liver. In 1962, BLAU and BENDER [7] reported the clinical use of selenomethionine-Se^{75} for scanning of the pancreas in a small series of patients, with visualization of pancreas in the majority of cases.

During the past year we have investigated Se^{75}* as an agent for radioisotope scanning of the pancreas in clinical diagnosis. At first, we followed the protocol outlined by BLAU and BENDER [7] but we encountered some technical difficulties in its use.

We have since devised an entirely new technique in the use of this compound which has not only provided visualization of the pancreas but offers considerable promise as a practical procedure for the diagnosis of pan-

* Supplied through the courtesy of Dr. Paul Numerof of E. R. Squibb & Sons.

creatic tumour and pancreatitis, both on an in-patient and an out-patient basis. This report describes our clinical experience in the use of selenomethionine-Se^{75} for radioisotope scanning of the pancreas.

RADIATION CHARACTERISTICS AND DOSIMETRY OF SELENOMETHIONINE-Se^{75}

Se^{75} has no beta radiation, and has a primary gamma energy of 279 keV. The physical half-life of Se^{75} is 128 d. The biological half-life of selenomethionine-Se^{75} is 23 d. As utilized in our protocol described, the effective half-life of selenomethionine-Se^{75} in the pancreas is approximately 24 h. The whole-body radiation dose using 250 μc of selenomethionine-Se^{75} is approximately 0.9 rad. The radiation dose to the pancreas is 0.2 rad. The following are the γ-ray dose calculations for 250 μc intravenous selenomethionine-Se^{75}:

Total γ-ray dose, D_γ (rad) = concentration (μc/g) $\times$ effective half-life, T_{eff} (days) [0.0346 $\times$ geometrical factor $\times$ γ-ray dose constant]

Pancreas:

$$D(\gamma) = \frac{15}{250} \times 1\,[0.0346 \times 43.1 \times 2.1] = 0.2 \text{ rad}$$

Whole body:

$$D(\gamma) = \frac{250}{70\,000} \times 27 [0.0346 \times 126 \times 2.1] = 0.99 \text{ rad.}$$

RATIONAL

The original protocol of BLAU and BENDER [7] for scanning of the pancreas with selenomethionine-Se^{75} called for an overnight fast, two glasses of skim milk for breakfast the next morning, followed in 3 h by the intravenous injection of 70 dog units of Cecekin (Vitrum, Sweden), which is a mixture of secretin, pancreozymin and cholecystokinin. One hour later selenomethionine-Se^{75} was administered intravenously in a dose of 3.5 μc/kg of body weight and the scan was started 1 h after injection. With this technique these investigators obtained visualization of the pancreas in two-thirds of the subjects scanned.

During the initial phase of our investigation the protocol of Blau and Bender was followed in 25 scanning procedures, but we had less success then they with this technique. For large organ scanning we found that better scans were obtained if the concentration of isotope in the organ was kept more constant. With the early protocol, Cecekin stimulated the pancreas to secrete the tagged enzymes rapidly and therefore the radioactivity was secreted towards the head of the pancreas and into the intestine so that pancreatic differentiation was poor. The transit time for the selenomethionine-

Se^{75} was approximately 2 h. Furthermore, Cecekin is a mixture of duodenal hormones, and we found that in addition to stimulating the pancreas it also stimulated the liver and the gall-bladder maximally with resulting increased uptake of selenomethionine-Se^{75} by these organs.

Due to the anatomical relationships of the liver, gall-bladder and pancreas this high uptake of radioactivity by the liver made pancreatic scanning more difficult. In the majority of cases, the liver is in close proximity to the pancreas, and using our commercial scanner, penetration of the lead side shielding by the 0.411-MeV γ-rays of Se^{75} in the liver distorted the pancreatic scan. Furthermore, the large concentration of Se^{75}-methionine in the liver made it technically difficult to bring out small variations of contrast in the pancreas.

For the above reasons, we have made the following changes in the protocol for pancreatic scanning with selenomethionine-Se^{75}:

1. To stimulate the pancreatic uptake of selenomethionine-Se^{75} the fasting patient receives a high protein meal containing 30 g of protein and less than 0.5 g of fat and carbohydrate (see Table I). One hour later, 250 μc of selenomethionine-Se^{75} is administered intravenously; 15 min later 900 mg

TABLE I

A HIGH PROTEIN MEAL TO STIMULATE PANCREATIC UPTAKE OF SELENOMETHIONINE-Se^{75}

Item	Amount (g)	Protein content (g)	Fat content (g)
Skimmed milk powder	735	261.7	0.73
Strained veal	250	40.0	4.2
Water	1200	---	---
Total	2185	301.7	4.93

Note: 218 g of formula, containing 30.1 g of protein and 0.49 g of fat are used for each test.

of glutamic acid hydrochloride is given orally. The hydrochloric acid portion stimulates the secretion of the small intestine, thereby enhancing Se^{75}-methionine incorporation into pancreatic tissue [1, 2, 3].

2. If the liver is enlarged over the pancreas, the pancreas is not well visualized by scanning methods because of the concentration of selenomethionine-Se^{75} in the liver. Since there is no reason to visualize the liver at the time of the pancreatic scan, malleable lead shielding made of three thicknesses of 1/8-in lead is placed over the liver whose site has been previously determined by a liver scan utilizing colloidal Au^{198}. As the majority of energetic γ-radiation is stopped by the lead shielding, the selenomethio-

nine-Se^{75} concentrated in the liver no longer greatly interferes with the scanning of the pancreatic area.

METHODOLOGY

A total of 61 patients took part in this investigation. They included both hospitalized patients and those who were seen at this clinic as out-patients. In the majority of cases the following procedure was used. Before the scheduled scanning of the pancreas a liver scan was performed with colloidal Au^{198}. On the morning of the pancreatic scan, the patient reported to the clinic without breakfast and was administered a cold blended high-protein meal. One hour after the high protein meal, 250 μc of selenomethionine-Se^{75} were administered intravenously. Fifteen minutes later the patient was given orally 900 mg of glutamic acid hydrochloride. The scanning procedure was then attempted (see Figs. 1-5).

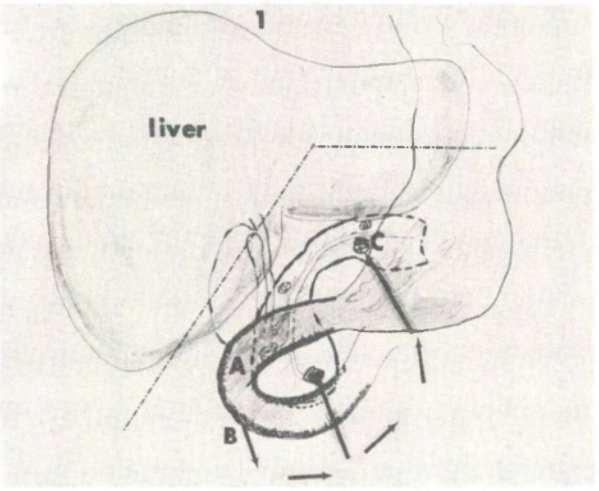

Fig. 1

Before the pancreatic scan can be performed a liver scan with 100 μc of Au^{198} is performed. This can be done any time before the pancreatic scan is done. A lead shield made of a double thickness of rubber lead or a 3/8-in malleable lead shield fitting the body is placed to coincide with where the liver is found on liver scan. If the liver is enlarged to the level of the umbilicus the pancreatic scan cannot be done as the pancreas is covered by the liver. The patient is fasted after midnight and is fed the ice-cold 30-g protein meal in the morning. (A) The protein, as it enters the duodenum, causes stimulation to the intestine to secrete (B) secretin and pancreozymin. These enzymes in turn promote the secretion of the pancreatic enzymes by (C) acinar cells.

SCANNING TECHNIQUE

With the patient in the true antero-posterior position a liver shield was placed over the previously outlined liver area. Fifteen minutes after the

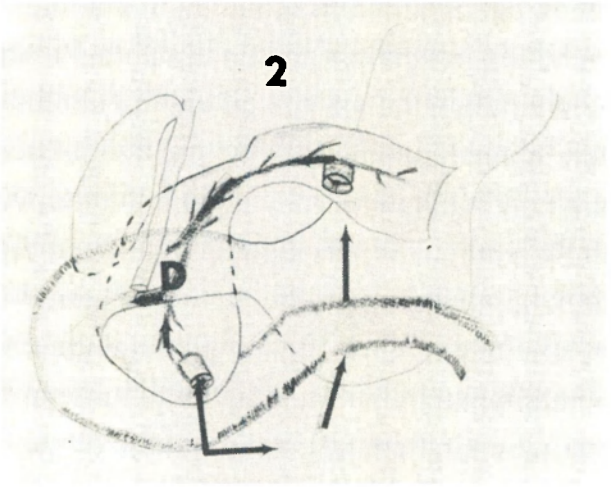

Fig. 2
The pancreas is now functioning normally with the acinar cells secreting pancreatic enzymes into the duodenum (D).

dose of selenomethionine-Se^{75} the maximum concentration in the pancreas was usually in the tail, which was found to the left of the xiphoid process. The maximum count-rate at this time was approximately 3000 counts/min and the blood background was usually 2000 counts/min. We utilized photoscanning devices; therefore methods of contrast enhancement were stressed. The scanning time of the pancreatic area was approximately 30-40 min. The scanning procedure was then repeated as needed. At 2 h after dose the spleen begins to be visualized on scan, and at 4 h the renal outline may be seen. Our most accurate anatomical pancreatic scans were done before 4 h after the dose, but the later scans gave indications of obstruction to pancreatic flow.

EQUIPMENT

Picker Magnascanners, Model 1108 B, were utilized for scanning procedures.

RESULTS

A total of 200 pancreatic scans were performed with selenomethionine-Se^{75} on the 61 patients of the series. Visualization of the pancreas was obtained in 97% of the cases in which the pancreatic scan protocol was followed. Four of the 61 patients of the series had pancreatic carcinoma, and in three cases diagnostic scans were obtained.

In one patient, the pancreatic tumour was large enough to have radiographic signs, but in the other patients gastrointestinal radiographs were

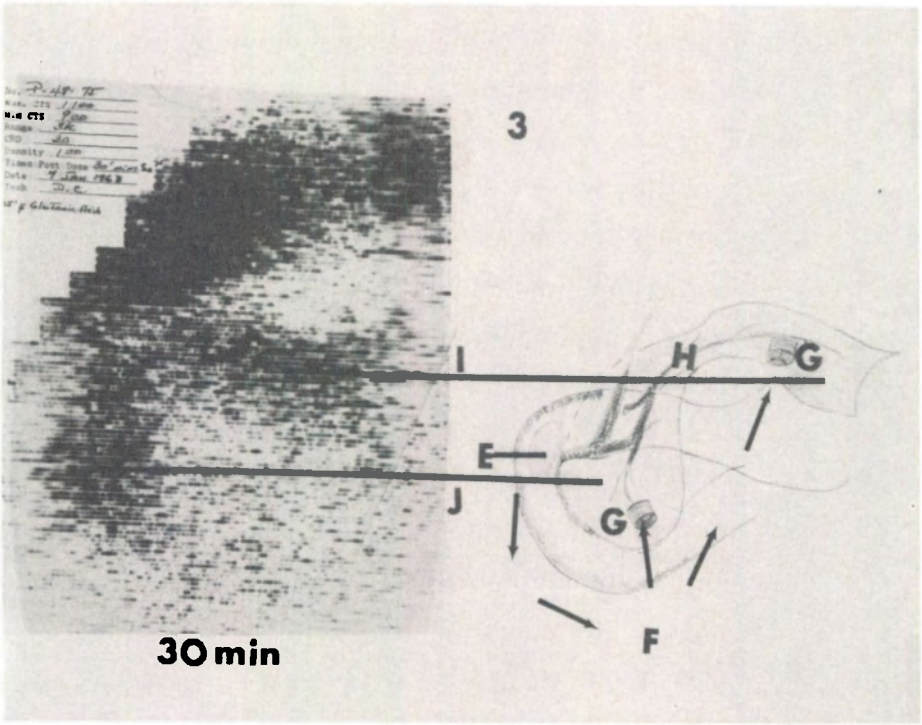

Fig. 3

250 μc of selenomethionine is administered intravenously 1 h after the pancreatic meal. Fifteen minutes later (E) 900 mc of glutamic acid hydrochloride is administered by mouth. The hydrochloric acid helps to promote the continuous secretion by the intestine of secretin and pancreozymin which will continue to aid the passage of selenomethionine-Se^{75} into the duodenum (F). Pancreatic enzymes (G) and radioactive enzymes (H) are then slowly secreted through the ductal system towards the duodenum. As can be seen on the 30-min scan, the pancreas is now well visualized with the head on the lower left, the middle thin portion being the body and the tail crossing the mid line going to the reader's right. The liver edge can be seen above the pancreas and the effect of the liver shield may be seen along the upper edge of the scan.

interpreted as being within normal limits. In all six of the patients with pancreatitis the pancreatic photoscan corroborated the clinical impression. The pancreatic scan obtained in this disease looked most promising. The uptake of selenomethionine-Se^{75} by the damaged pancreas is decreased much in the same way that the uptake of I^{131} is decreased in thyroiditis, so that in the areas of pancreatitis there is little or no concentration of the selenomethionine-Se^{75}.

DISCUSSION

For many years methods of visualization of the pancreas that do not require surgery have been sought, but up to the present time all have proved

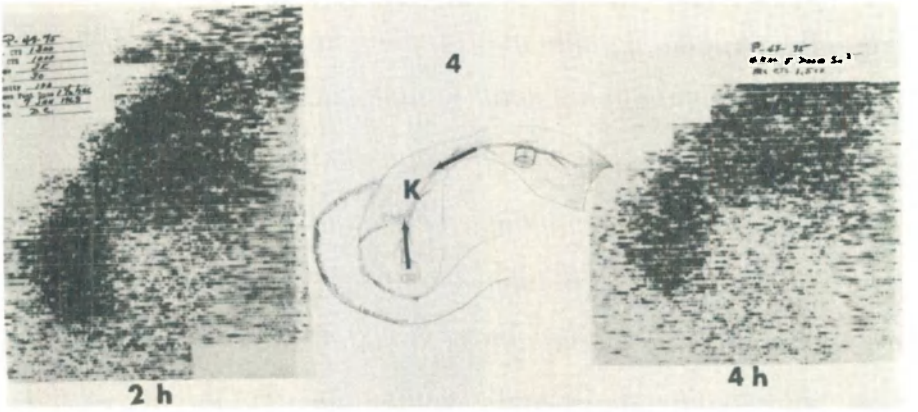

Fig. 4

The 2-h and the 4-h scans show a good visualization of the pancreas and it will be noted that the liver edge is moving and on the 2-h scan is actually impinging on the edge of the pancreas. It will be noted that the liver shield was moved closer to the pancreas in these 2-h scans to help on the scanning technique. It will be noted that less radioactivity is outside the pancreas in the lower portion of the scan corresponding to the loop of the duodenum.

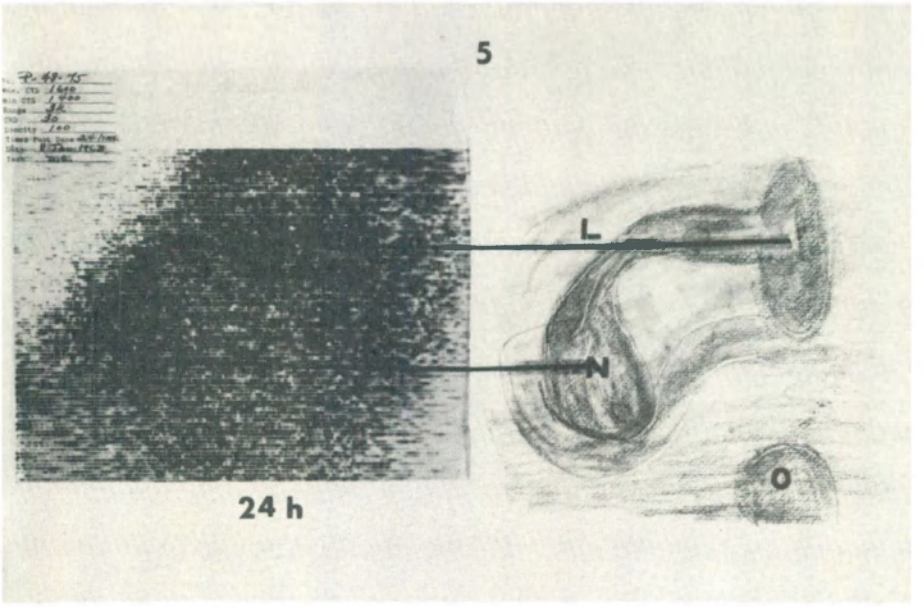

Fig. 5

In the normal pancreas very little of the administered dose of selenomethionine-Se^{75} is still in the pancreas at 24 h and now the background activity of the blood is approaching the activity of the pancreas. However on this scan the barest outline of the pancreas is still visible.

unsuccessful. Pancreatic scanning with selenomethionine-Se^{75} is the first successful approach to non-surgical visualization of the pancreas that has been made so far. The scanning technique described above is not difficult to follow and the entire diagnostic procedure requires approximately 3 h and can be applied to out-patients as well as in-patients. With our present scanning knowledge it is now possible to visualize a lesion in the pancreas as small as 2 cm in size. With the anticipated advances in collimation and increased size of scintillation crystals,we may expect in the future visualization of even small tumours. The fact that pancreatitis may be verified by the simple scanning technique is in itself a major advance in the diagnosis of pancreatic disease. It is hoped that, since this procedure may find small pancreatic tumours, their early detection may help to reduce the high mortality from this disease. Pancreatic scanning may also prove to be a satisfactory diagnostic test of pancreatitis and thereby make unnecessary many surgical explorations indicated under present methods of diagnosis. It is obvious that the ability to diagnose acute pancreatitis by pancreatic scanning will undoubtedly help to decrease mortality from surgical intervention in that disease. It may be possible also to alleviate the distress of chronic pancreatitis by using the scanning apparatus as a guide to specific areas of surgical ir.tervention.

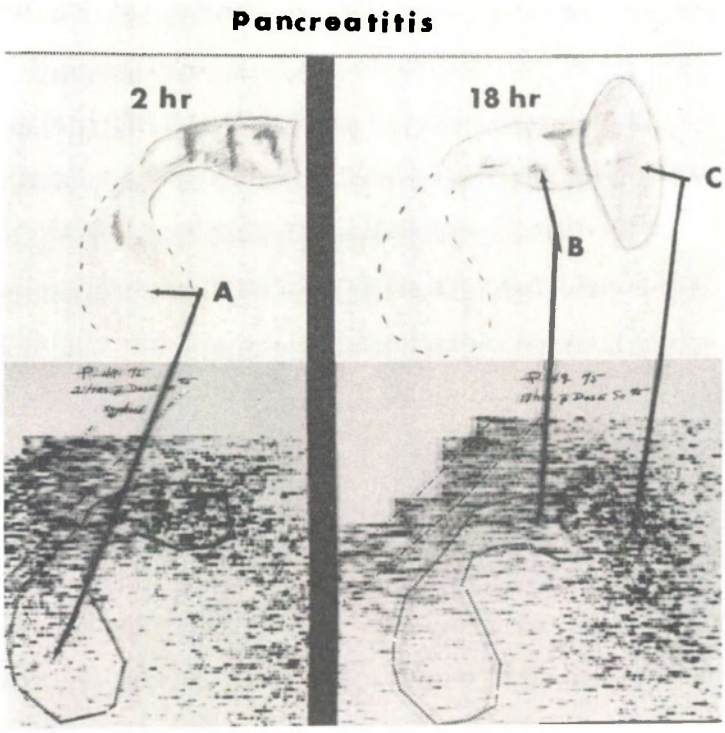

Fig. 6

2-h and 18-h scans of patient in case report 1

It is hoped with this development of a method to successfully scan the pancreas utilizing the concentration of selenomethionine-Se^{75} in pancreatic tissue that renewed interest may be stimulated among medical and paramedical personnel in this very important but long silent organ.

CASE REPORTS

1. Mr. G.was a 52-yr-old labourer with a history of alcoholism and repeated episodes of what was clinically pancreatitis. He had clinical bouts and flare-ups of his pancreatic disease process every 2-3 months. Pancreatic scan revealed concentration of the selenomethionine-Se^{75} only in the area of the tail of the pancreas. At surgery, the entire head and body of the pancreas was noted to be destroyed by chronic inflammatory disease.

The 2-h scan revealed continued absence of activity in the head and slight activity in the tail (Fig. 6). Activity in the tail and in the spleen is well visualized 18 h later.

2. Mrs. D. was a 75-yr-old retired nurse who had had 6 weeks of crampy mid-abdominal pain with some radiation to the back and no weight loss. She had just noted the onset of anorexia. CBC liver function studies and all contrast studies were normal. Pancreatic scan done $\frac{1}{2}$-h after a dose of selenomethionine-Se^{75} revealed a defect in the medial portion of the head of the

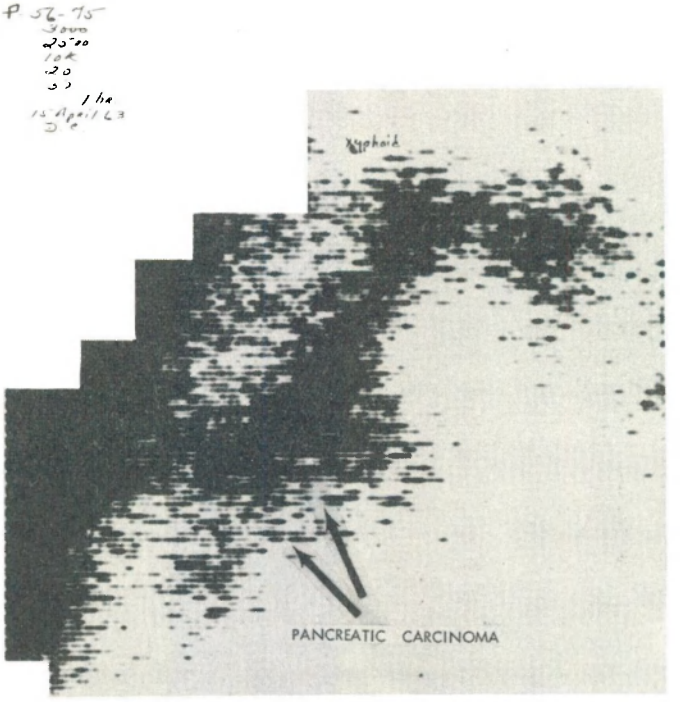

Fig. 7

1-h scan of patient in case report 2

pancreas (see Fig. 7). This defect persists on the 2-h scan. The 6-h scan was done posteriorly and in this position a large cold area was noted in the head of the pancreas. The 24-h scan revealed that very little of the radioactivity had left the area of the pancreas. This was compatible with obstruction. The same 2 to 3-cm defect could be noted in the medial head of the pancreas. At surgery a $2\frac{1}{2}$-cm carcinoma of the pancreas was noted at the level of the ampulla with complete obstruction of the pancreatic duct.

REFERENCES

[1] DI SANT'AGNESE, P.A., "Disease of the Pancreas", A Textbook of Medicine (CECIL, R.L. and LOEB, R.F. Eds.) 10th ed., W.B. Saunders, Philadelphia (1959) 907-19.

[2] GOLDSTEIN, F., The Gallbladder and Pancreas", Pathologic Physiology (SODEMAN, W.A., Ed.) 3rd ed., W.B. Saunders, Philadelphia (1961) 801-7.

[3] MESCHA, I., QUINN, J.D., WITOCOFSKI, R.L. and HOSICK, T.A., The Utilization of Radioactive Zinc and Manganese in an Effort to Visualize the Pancreas, Radiology 73 (1959) 63.

[4] BLAU, M., Biosynthesis of Se^{75}-Selenomethionine and Se^{75}-Selenocystine, Biochim. Biophys. Acta 49 (1961) 389.

[5] ORNL Catalog

[6] BLAU, M. and MANSKE, R.F., The Pancreas Specificity of Se^{75}-Selenomethionine, J. nucl. Med. 2 (1961) 102.

[7] BLAU, M. and BENDER, M.A., Se^{75}-Selenomethionine for Visualization of the Pancreas by Isotope Scanning, Radiology 78 (1962) 974.

DISCUSSION

(On the two foregoing papers)

A. DESGREZ: Dr. Sodee seems to interpret the radioactive areas, which can sometimes be seen in the region of the left rib edge, as being due to the spleen. Our interpretation at Orsay is that these areas correspond to the first, second and third jejunal loops which project at this point. This interpretation is based on observations of similar images with I^{131}-Rose Bengal, which is known to be eliminated by way of the intestine.

D. SODEE: I believe we may both be right. In this region there is superimposition of the spleen and gastro-intestinal tract. One can certainly observe secretion into the duodenum on the scan.

A. BAPTISTA: Does Dr. Blau consider that L-selenomethionine or a similar substance could be used as a simple radiological contrast medium?

M. BLAU: No. Selenium is not radio-opaque. If another atom were substituted to make the compound radio-opaque, it would no longer behave as an amino acid and there would be no pancreatic uptake.

I. BASCHIERI: Would there be any advantage in using two opposing coupled detectors? Since that part of the liver which is superimposed on the pancreas is anterior to it, the increased counting efficiency thus obtained would be everywhere higher for the pancreas than for the liver. Even if the central part of the organ were not so dark as the head and the tail, because of the intervention of the spine between the posterior detector and the active zone, I think that the resulting image of the pancreas would be clearer.

D. SODEE: This is a good suggestion, but we have not tried it out. We have, however, used a 5-in crystal instead of the 2 × 3-in crystal we previously employed. With the 5-in crystal we are able to use a focusing collimator whose focal distance is optimal in pancreas scanning. With this combination we hope to observe more detail in the organ.

P. HARPER: Since this procedure appears to provide satisfactory information in cases of pancreatitis, how does the complicated protocol fit into the routine clinical situation of an acute abdominal crisis during the night?

D. SODEE: We have done this operation in the middle of the night, using a simplified procedure which excludes the feeding of the protein meal.

M. BLAU: The detailed protocol will produce the best scans, but acceptable scans can usually be obtained without any preparation. Failure to visualize the pancreas indicates a diagnosis of acute pancreatitis. However, this diagnosis cannot be made with the same certainty if there is no visualization in the case of a patient scanned without proper preparation as when the pancreas fails to be visualized in a properly prepared patient.

D. SODEE: What Dr. Blau has just said is true if the patient has not been acutely ill for a period of 24 h. Usually a patient suffers from acute pancreatitis as a result of excessive drinking or some other form of overindulgence. In such cases, the pancreas must be stimulated; otherwise all the selenomethionine goes to the liver.

R. GONGORA: Does the absence of a pancreatic image on a scintigram in Dr. Blau's procedure definitely indicate a pathological condition, or can it sometimes be caused by individual physiological variations?

M. BLAU: In our experience the absence of visualization has always indicated pancreatic disease.

D. SODEE: We were surprised to find that we could not clearly visualize the pancreas in many patients who had suffered from diabetes for from ten to fifteen years. It seems that in diabetes, although the main abnormality is in the islet cells of the pancreas, there may also be a low-grade pancreatitis with infiltration of the pancreatic tissue by a mucopolysaccharide related to the disease. It is also interesting to note that we have scanned three patients with gastric or duodenal ulcers before surgery and observed defects on the scan in the region of the head of the pancreas corresponding to an ulcer penetrating into the pancreatic bed.

G. TORI: Have you any experience with chronic cholecystitis or chronic hepatitis?

D. SODEE: We have not routinely examined patients suffering from these conditions, mainly because of the high cost of the Se^{75}-selenomethionine at present available.

M. BLAU: We have not examined such patients either. In cases with extensive liver metastases there is less uptake in liver. The pancreas is visualized as usual. With regard to the availability of Se^{75}-selenomethionine, as far as I know there are only two reliable suppliers. One is E.R. Squibb and Sons, New Brunswick, United States of America and the other is the Radiochemical Centre, Amersham, England.

D. SODEE: What is the selenium content of the Radiochemical Centre product as compared with the Squibb product?

M. BLAU: The former has only about one fifth of the specific activity of the latter, but this is still sufficiently high to enable one to administer

200 μc and still give less than 1 mg of selenium, which is well below the toxicity level.

M. GONGORA: What precautions have to be taken when storing Se^{75}-selenomethionine?

M. BLAU: Se^{75}-selenomethionine must be carefully protected against oxidation. We add 1 mg/cm^3 of β-mercapto-ethylamine as an anti-oxidant to all solutions. The Squibb product is supplied with added anti-oxidant. The Radiochemical Centre material is not but, having a lower specific activity, it is not quite so susceptible to oxidation.

DIAGNOSIS OF MASSIVE PULMONARY EMBOLISM IN MAN BY RADIOISOTOPE SCANNING

H. N. WAGNER, Jr., D. C. SABISTON, Jr., M. IIO AND J. K. LANGAN
DEPARTMENTS OF MEDICINE, SURGERY AND RADIOLOGY,
THE JOHNS HOPKINS UNIVERSITY SCHOOL OF MEDICINE,
BALTIMORE, MD., UNITED STATES OF AMERICA

Abstract — Résumé — Аннотация — Resumen

DIAGNOSIS OF MASSIVE PULMONARY EMBOLISM IN MAN BY RADIOISOTOPE SCANNING. Macroaggregated human-serum albumin particles labelled with either I^{131} or chromium-51 have been utilized to determine regional blood flow to the lungs in dogs and man. Following intravenous injection, the particles accumulated in the lung, permitting clear delineation of the lung fields by scintillation scanning. In patients with lung abscess, pneumonia, atelectasis, tumours and thromboembolic disease of the lung, there was a decreased accumulation of the radioactivity in the regions of the lungs involved. The technique was found to be clinically useful in the diagnosis of massive pulmonary emboli in man and in the demonstration of vascular occlusion in certain patients with cor pulmonale. Studies in dogs made possible the determination of the rate at which revascularization occurred following experimental pulmonary emboli. Scintillation scanning was carried out at various times after the removal of the experimental emboli. The circulation was restored through the lungs within a period of several weeks after the removal of chronic pulmonary emboli in dogs. Although aggregated human-serum albumin retained its antigenicity in rabbits, guinea pigs and dogs, extensive studies failed to reveal any antigenicity of the particles to man. Because of the rapid metabolism of the macroaggregated albumin particles, the radiation to the patient was well within permissible levels. The use of albumin of high specific activity permitted injections of small chemical quantities; consequently no cardiovascular effects, such as increases in pulmonary artery pressure, changes in electrocardiogram or respiratory rate, were noted.

DIAGNOSTIC PAR SCINTIGRAPHIE DE L'EMBOLIE PULMONAIRE MASSIVE CHEZ L'HOMME. Pour déterminer chez le chien et chez l'homme le flux sanguin vers les poumons, on a utilisé des macroparticules d'albumine de sérum humain marquée avec ^{131}I ou ^{51}Cr. A la suite d'une injection intraveineuse, les particules s'accumulaient dans les poumons, permettant ainsi de délimiter nettement les régions pulmonaires par scintigraphie. Chez les sujets atteints d'abcès pulmonaires, de pneumonie, d'atélectasie, de tumeurs ou de thromboembolie des poumons, on observait une accumulation moins intense de la radioactivité dans les régions pulmonaires affectées. Du point de vue clinique, cette méthode s'est révélée utile pour le diagnostic des embolies pulmonaires massives chez l'homme et pour la mise en évidence d'une occlusion vasculaire chez certains sujets atteints de cœur pulmonaire. Les études sur des chiens ont permis de déterminer le rythme auquel une vascularisation nouvelle se produisait à la suite d'embolies pulmonaires induites. On a fait des scintigraphies à diverses reprises après embolectomie. Chez les chiens, la circulation dans les poumons était rétablie dans les quelques semaines qui suivaient l'embolectomie. Si les macroparticules d'albumine de sérum humain gardaient leur caractère antigène chez les lapins, les cobayes et les chiens, des études très poussées n'ont pu déceler un tel caractère chez l'homme. Par suite du métabolisme rapide des macroparticules d'albumine, la dose de radioactivité reçue par les sujets restait bien en deça des niveaux admissibles. L'emploi d'albumine à forte activité spécifique permettait de faire des injections de petites quantités de produit chimique; de ce fait, on n'a pas relevé d'effets cardio-vasculaires, tels que des augmentations de la tension dans l'artère pulmonaire, des modifications de l'électro-cardiogramme ou du rythme respiratoire, etc.

ДИАГНОСТИКА МАССИВНОЙ ЛЕГОЧНОЙ ЭМБОЛИИ У ЧЕЛОВЕКА С ПОМОЩЬЮ РАДИОИЗОТОПНОГО СКЕННИРОВАНИЯ. Крупные частицы альбумина сыворотки человека, меченные йодом-131 или хромом-51, использовались для определения регионального тока крови в легких у собак и человека. После внутривенного введения частицы, накапливающиеся в легких, дают четкое изображение контуров легких при сцинтилляционном скенировании. У пациентов с легочными абсцессами, пневмонией, ателектазом, раком легких и

тромбоэмболической болезнью легких наблюдалось понижение накопления радиоактивности в пораженных участках. Был найден метод, который будет пригоден в клинике для диагностики массивной легочной эмболии у человека и демонстрации закупорки сосудов у некоторых пациентов с " cor pulmonale". Исследования на собаках сделали возможным определение скорости реваскуляризации после экспериментальной легочной эмболии. Сцинтилляционное скеннирование проводилось в различные периоды времени после удаления экспериментального эмбола. Циркуляция крови в легких у собак восстанавливалась в течение нескольких недель после удаления хронического легочного эмбола. Хотя крупные частицы альбумина сыворотки человека сохраняли свои антигенные свойства для кроликов, морских свинок и собак, широкие исследования не привели к обнаружению каких-либо антигенных свойств этих частиц для человека. Ввиду быстрого метаболизма крупных частиц альбумина доза облучения пациента находилась в пределах допустимых доз. Использование альбумина с высокой удельной активностью позволяло вводить небольшие химические количества; впоследствии не отмечено каких-либо изменений со стороны сердечно-сосудистой системы, как повышения давления в легочной артерии, изменения электрокардиограммы или частоты дыхания.

DIAGNÓSTICO DE LA EMBOLIA PULMONAR MASIVA EN EL HOMBRE POR EXPLORACIÓN RADIOISOTÓPICA. Los autores utilizaron macroagregados de partículas de seroalbúmina humana marcada con ^{131}I o con ^{51}Cr para determinar el caudal sanguíneo regional que afluye a los pulmones en el perro y en el hombre. Inyectadas por vía intravenosa, las partículas se acumulan en el pulmón y permiten delinear claramente los campos pulmonares por exploración centelleográfica. En pacientes con absceso del pulmón, neumonía, atelectasia, tumores y tromboembolias pulmonares, se observó una acumulación disminuida de radiactividad en las regiones afectadas. Se comprobó la utilidad clínica de esta técnica para diagnosticar embolias pulmonares masivas en el hombre y para descubrir oclusiones vasculares en ciertos pacientes afectados de cor pulmonale. Los estudios en perros permitieron determinar la rapidez con que progresa la revascularización después de una embolia pulmonar experimental. Se efectuaron varias exploraciones centelleográficas una vez retirados los émbolos experimentales. La circulación se restableció en todo el pulmón algunas semanas después de haber eliminado los émbolos pulmonares crónicos en los perros. Los agregados de seroalbúmina humana han conservado su poder antigénico en los conejos, los cobayos y los perros, pero los estudios realizados no han permitido comprobar que las partículas tengan poder antigénico alguno en el hombre. Gracias al rápido metabolismo de los macroagregados, la dosis de radiación recibida por el paciente se mantiene bastante inferior a los valores admisibles. El empleo de albúminas de elevada actividad específica permite limitar considerablemente las cantidades inyectadas; no se observan, por lo tanto, efectos cardiovasculares tales como aumentos de presión en la arteria pulmonar, ni alteraciones del electrocardiograma o del ritmo respiratorio.

The diagnosis of massive pulmonary embolism is frequently difficult and always uncertain, primarily because the symptoms and signs may mimic other diseases such as myocardial infarction or pneumonia. Ancillary examinations including chest X-ray and electrocardiogram, are rarely definitive. The diagnosis can be suspected when sudden dyspnea, pleural pain, haemoptysis, syncope or a bloody pleural effusion occur in patients who are predisposed to pulmonary embolism, i.e. in persons who are suffering from congestive heart failure or polycythemia, or who are bedridden, as during the post-operative or post-partum state.

A high degree of suspicion is no longer adequate. When therapeutic measures were relatively non-specific, absolute accuracy in diagnosis was not required. Today, however, the need for improved diagnostic ability has increased because we now have new means of treating pulmonary thrombo-embolism. These include anticoagulant drugs to prevent further thrombosis, proteolytic agents to dissolve thrombi which have already formed, and specific surgical therapy including ligation or plication of the inferior vena cava to prevent passage of peripheral thrombi into the lungs, and pulmonary embolectomy, the removal of obstructing clots from the pulmonary arteries themselves.

The present report describes the development and initial evaluation of a new radioisotope scanning procedure that has been found to be a safe and effective way of diagnosing massive pulmonary embolism in man. In addition to its use in thrombo-embolic diseases, the method has been used to obtain information concerning regional pulmonary blood flow in other pulmonary diseases.

GENERAL PRINCIPLES IN MEASURING REGIONAL PULMONARY BLOOD FLOW BY RADIOISOTOPE SCANNING

Despite differences in the details of various methods of measuring regional blood flow, most are based on the principle of conservation of material. A known quantity (Q) of material flowing into a region is divided three ways: some (Q_i) will accumulate in the region, some (Q_m) wil be metabolized, and the remainder (Q_e) will flow out of the region. This can be described by the equation: $Q = Q_i + Q_m + Q_e$. The inflow (Q) into a region is equal to the blood flow (F) into the region multiplied by the concentration of the substance in the arteries leading to the region (C_a). The basic equation can therefore be written $F \times C_a = Q_i + Q_m + Q_e$. If one injects a substance that is completely removed from the blood in a single passage through the region, $Q_e = 0$; if the substance is not metabolized during the period of observation, $Q_m = 0$; therefore the amount of the substance found in the region will be proportional to the blood flow to the region, i.e. $F \times C_a = Q_i$. This principle has been applied to the measurement of regional pulmonary blood flow. One injects macro-aggregates of human serum albumin labelled with either Cr^{51} or I^{131} and determines their concentration in various regions of the lungs by radioisotope scanning. The concentration of the aggregates in various parts of the lung is directly related to pulmonary blood flow.

MACRO-AGGREGATED HUMAN SERUM ALBUMIN (MAA)

In 1956, HALPERN and his associates introduced the use of aggregates of human serum albumin as a type of particle that offered important advantages in the study of phagocytosis [1]. In contrast to other particles such as carbon, thorium dioxide, saccharated iron oxide, chromic phosphate, and colloidal gold which remain in phagocytic cells almost indefinitely, the albumin aggregates can be metabolized after ingestion by these cells. This made it possible to administer large quantities of the albumin aggregates and derive information about the phagocytic capacity of the reticulo-endothelial system (RES) not obtainable with the use of minute quantities of non-metabolizable materials. To study phagocytosis, one uses particles whose average diam. is approximately 10 nm [2, 3]. By altering the conditions under which the albumin particles are aggregated, one obtains much larger aggregates, referred to as macro-aggregated albumin (MAA), which vary in size from 1-50 μm.

PREPARATION OF MACRO-AGGREGATED ALBUMIN (MAA)

(a) I^{131}-labelled MAA

Radioiodinated human serum albumin of high specific activity (1-2 mc/mg) was obtained from the Squibb Laboratories. A 0.1-% solution was made in 0.9% sodium chloride solution and adjusted to pH 5.5 with dilute hydrochloric acid. Since the size of the albumin aggregates was found to be highly dependent on pH, the latter was controlled within 0.1 pH units. Three to five milliliters of the acidified albumin solution were placed in glass vials and heated for 4 min at 100°C in an oscillating water bath (100 cycles/min). This resulted in the formation of visible macro-aggregates. The entire procedure was carried out under sterile conditions and the final product was tested for sterility and pyrogenicity. If subsequent dilutions of the material were required, it was necessary to use either glucose or sodium chloride solution that had been adjusted to pH 5.5. Subsequent alteration of the pH towards either greater or lesser acidity resulted in breakdown of the MAA into smaller albumin aggregates that concentrated in the liver and spleen.

(b) Cr^{51}-labelled MAA

Chromic chloride (Cr^{51}) of high specific activity was obtained from Atomic Energy of Canada. Human serum albumin was labelled by reaction with chromic chloride at pH 5.5. Aggregation was then carried out by heating at 100°C for 4 min in an oscillating water bath. Under these conditions, approximately 50% of the radioactive chromium was bound to the MAA. The unreacted radioactive chromic ions were removed by centrifugation and serial washing in glucose solution at pH 5.5.

DISTRIBUTION OF MAA AFTER INTRAVENOUS INJECTION

Pentobarbital anaesthetized dogs in a supine position were injected intravenously with 0.01-0.02 mg/kg MAA. Immediately after injection serial 1 ml blood samples were withdrawn from the femoral artery at 4-s intervals. Samples obtained during the 1st, 2nd and 3rd min were pooled and the radioactivity measured in a well-type crystal scintillation detector. Four minutes after injection, the dogs were killed by the rapid injection of saturated magnesium sulphate solution. The organs were immediately removed and weighed. At least 6 samples were taken from each organ for determination of the percentage of the injected dose of radioactivity per unit weight of tissue. The results are shown in Tables 1-3 and Fig. 1. When injected intravenously, MAA accumulated to a high degree in the lungs. The second highest concentration of radioactivity was in organs containing the highest concentrations of reticulo-endothelial cells, namely the liver and spleen. Presumably in preparing the MAA some particles of smaller size were formed. These behaved in a manner similar to the AA particles used to measure RES function, i.e. they passed through the pulmonary vessels and accumulated in the fixed phagocytic cells of the body, chiefly in the liver and spleen. Chromium-51 labelled MAA had a smaller proportion of the smaller aggre-

TABLE I

DISTRIBUTION OF I^{131} MAA
% dose in total organ

Dog No.	Body weight (kg)	R. Lung	L. Lung	Liver	Spleen	R. Kidney	L. Kidney	Heart	Brain	Pancreas
1	8.0	39.8	25.9	20.5	1.37	0.22	0.21	0.15	0.025	0.075
2	9.5	39.4	33.0	19.9	2.60	0.36	0.36	0.24	0.029	0.107
3	12.0	29.1	22.4	48.2	8.13	0.51	0.50	0.39	0.058	0.133
4	13.2	29.8	18.7	35.8	5.50	0.35	0.34	0.18	0.034	0.103
5	8.0	42.7	55.4	7.5	1.00	0.55	0.60	0.24	0.067	0.080
Mean		67.2		26.4	3.72	0.80		0.24	0.043	0.100
Standard deviation		17.59		15.66	3.03	0.28		0.09	0.017	0.023
Standard error		7.89		7.02	1.36	0.13		0.04	0.008	0.010

TABLE II

DISTRIBUTION OF Cr^{51} MAA
% dose in total organ

Dog No.	Body weight (kg)	R. Lung	L. Lung	Liver	Spleen	R. Kidney	L. Kidney	Heart	Brain
1	14.4	46.3	38.7	7.6	0.58	0.10	0.11	0.08	0.009
2	10.4	52.7	38.5	7.3	1.43	0.15	0.12	0.14	0.010
3	13.9	48.8	33.7	10.8	0.66	0.14	0.15	0.11	0.007
4	10.8	57.4	48.7	21.00	1.51	0.17	0.18	0.11	0.012
Mean		91.2		11.7	1.04	0.28		0.11	0.010
Standard deviation		10.59		6.41	0.50	0.02		0.03	0.003
Standard error		5.30		3.21	0.25	0.01		0.01	0.001

TABLE III

% DOSE PER GRAMME OF MAA IN SOME ORGANS

I^{131} MAA					Cr^{51} MAA				
Dog No.	Lungs	Liver	Splcen	Kidneys	Dog No.	Lungs	Liver	Spleen	Kidneys
1	0.905	0.095	0.050	0.025	1	0.985	0.019	0.010	0.003
2	0.962	0.071	0.072	0.015	2	1.122	0.022	0.014	0.005
3	0.535	0.152	0.104	0.017	3	1.103	0.028	0.016	0.004
4	0.454	0.095	0.057	0.009	4	1.505	0.066	0.060	0.004
5	1.506	0.032	0.023	0.024					
Mean	0.872	0.089	0.061	0.018	Mean	1.179	0.034	0.025	0.004
Standard deviation	0.4179	0.0436	0.0316	0.0133	Standard deviation	0.1759	0.0218	0.0235	0.0008
Standard error	0.1874	0.0196	0.0142	0.0060	Standard error	0.0880	0.0109	0.0118	0.0004

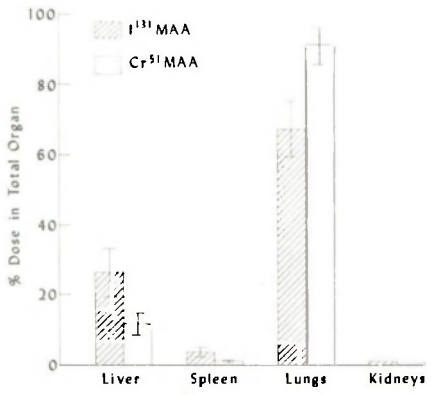

Fig. 1

Distribution of I^{131} and Cr^{51} macro-aggregated albumin (MAA) following intravenous injection in dogs
The standard error of the mean is indicated.
Other organs of the body had less than the kidneys.

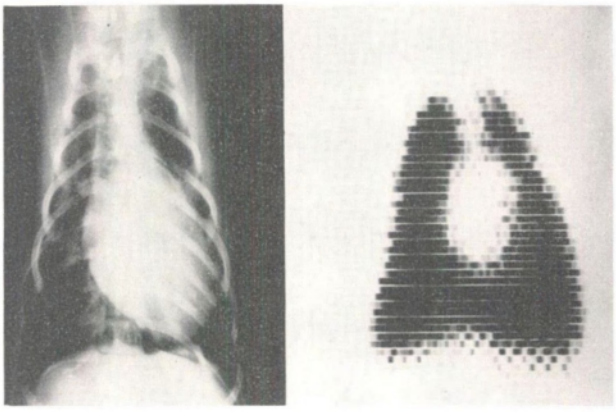

Fig. 2

Lung scan of a normal dog following the administration of 100 μc of I^{131} MAA

gated albumin (AA) than did the iodinated material, as evidenced by the higher fraction of the material in the lungs compared to the liver and spleen. The high concentration of the material in the lungs of a dog is illustrated in Fig. 2, which is the distribution of the radioactivity as determined by radioisotope scanning techniques described elsewhere [4]. The dark areas correspond to areas of high concentration of radioactivity.

Studies were performed to determine the mechanism of concentration of MAA in the lungs. When injections were made into the internal carotid artery of dogs or into the abdominal aorta of man the particles lodged in those organs whose blood supply was from the systemic side of the circulation, just as they had lodged in the lungs when injected intravenously. An

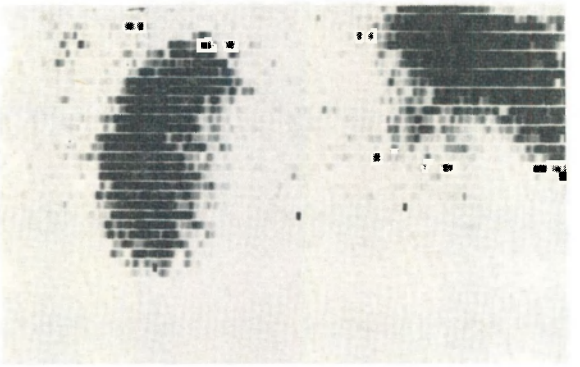

Fig. 3

Radioisotope scan of the abdomen in man following the injection of 300 μc of I^{131} MAA into the aorta of a patient with unilateral renal disease and hypertension
The left renal artery was subsequently found to be impaired.
A high concentration of radioactivity can be seen in the right kidney and the spleen.
A small concentration can be seen in the diseased left kidney.

example of a systemic injection in man is shown in Figure 3 which is the radioisotope scan of the abdomen following injection of I^{131} MAA into the thoracic aorta. Thus it seemed that the mechanism of concentration of the aggregates was that they became lodged in the first capillary bed which they encountered.

METABOLIC FATE OF RADIOACTIVE MAA

Measurements were made in 4 subjects to determine the rate of disappearance of the radioactivity from the lungs following the intravenous injection of I^{131} MAA. The rate of clearance was approximately exponential with half-times ranging between 5 and 10 h. Simultaneous measurements of hepatic radioactivity gave evidence that the particles in the lungs were being broken down into smaller aggregated albumin (AA) particles that returned to the circulating blood and were subsequently phagocytized by the RES cells of the liver and spleen.

Figures 4 A and 4 B illustrate typical studies of the cumulative urinary excretion of radioactivity in normal subjects following the intravenous injection of I^{131}-and Cr^{51}-labelled MAA. During these studies, which are representative of studies in 4 other people, the uptake of radioactive iodine by the thyroid was blocked by the administration of 10 drops of Lugol's solution per d for 4 d. The radioactive iodine was excreted at a more rapid rate than the chromium-51. Chromic ions (Cr^{51}) bound to albumin aggregates and phagocytized by the RES did not return immediately to the circulation, as did radioactive iodine, but rather remained in the liver and spleen for longer periods of time.

With I^{131} MAA, after 24 h, radioactivity was not present in the lungs and lung scanning could be repeated. With Cr^{51} MAA, the lung concentration of radioactivity after 24 h was less than 25% of that present immediately after injection.

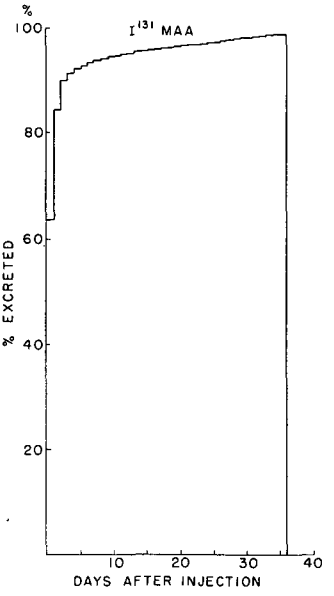

Fig. 4A

Cumulative urinary excretion of radioactivity in man
following the intravenous injection of 300 μc of I^{131} MAA
The thyroid gland had been blocked by the administration of Lugol's solution for 4 d.

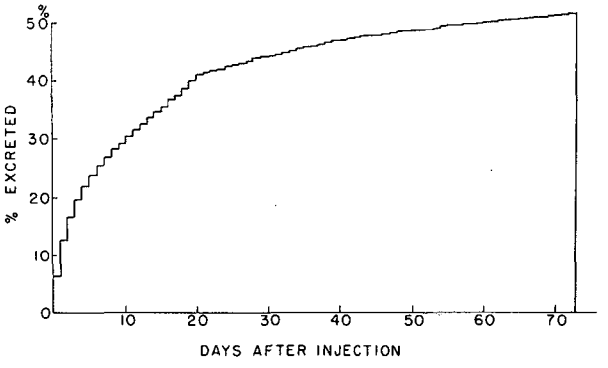

Fig. 4B

Cumulative urinary excretion of radioactivity in man
following the intravenous injection of 1 mc of Cr^{51} MAA

TOXICITY STUDIES

Radioisotope-labelled macro-aggregated albumin could be potentially toxic in 3 ways: alteration in the structure of the albumin molecule might render it antigenic to man; obstruction of pulmonary capillaries and arteri-

oles might result in deleterious cardiovascular effects; and, lastly, there might be a radiation hazard. Consequently, extensive testing for potential toxicity was carried out before its initial use in human beings. Before the study of MAA, we administered aggregated albumin (AA) in more than 1200 studies in over 300 individuals, and were unable to detect any evidence of antigenicity, although human albumin aggregates were antigenic to foreign species (dogs, rabbits, and guinea pigs), and cross-reacted with normal human serum albumin [3]. Studies with macro-aggregated albumin failed similarly to reveal evidence of antigenicity to man. Testing included skin reactions, albumin clearances and careful evaluation of symptoms or signs following repeated injections. One subject, a young girl known to have had angioneurotic oedema with hives on several occasions in the past, developed urticaria several hours after the performance of a lung scan. Since radioiodinated MAA had been used, the thyroid gland had been blocked by the administration of 0.5 ml of Lugol's solution. The hypersensitivity reaction may have been due to MAA or to iodine. Further studies to determine the offending antigen were not deemed justifiable. No untoward reactions were observed in any other subject.

In studies of cardiovascular toxicity, the LD_0 was determined in rats and found to be of the order of 5000 times the dose used to perform lung scans in man, i.e. over 10 mg/kg. Doses as high as 10 mg/kg were also administered to dogs without increases in pulmonary artery pressure or respiratory rate, and without a decrease in femoral arterial pressure. Rats which received up to 10 mg/kg of MAA were indistinguishable from control rats in histological examination of the lungs, immediately and one week after injection.

When radioiodinated MAA was used, the thyroid gland was blocked by the administration of 0.5 ml of Lugol's solution per d for 4 d in order to prevent accumulation of radioactive iodine. When this was done, over 80% of the radioactivity appeared in the urine within 48 h and the entire dose could be accounted for within a period of several weeks. When Cr^{51} MAA was used, the excretion into the urine was slower, approximately one half the dose remaining in the liver. With both I^{131} and Cr^{51}, the limiting organs from the standpoint of radiation dose were the lungs and the liver, the dose being 0.3 rad and 3.0 rad, respectively, for 300 μc of I^{131} and 1 mc of Cr^{51}.

RESULTS

I. Experimental pulmonary emboli in dogs

In a series of 50 dogs, latex balloons measuring approximately 3×1 cm were filled with radiopaque contrast media and introduced into the external jugular vein by means of a plastic tube and plunger which permitted the "embolus" to be pushed into the right atrium. When viewed by cinefluorography, the "emboli" could be seen to circulate within the right ventricle for a few minutes, at which time they made their way out into the pulmonary artery where they became fixed in either a major or lobar pulmonary artery. A silk string attached to the "embolus" and fastened to the skin of the neck

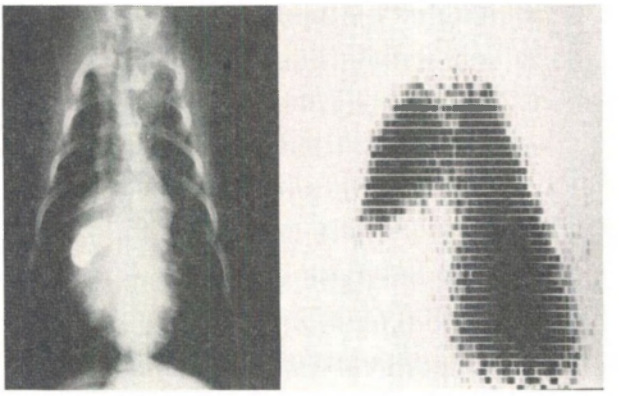

Fig. 5

Lung scan of a dog with an experimental embolus in the artery to the right lower lobe
The increased density on the radiograph is the rubber balloon filled with opaque contrast medium.

permitted removal of the embolus at a later date without opening the chest of the dog.

In every case the site of the vascular occlusion was determined correctly by scanning and confirmed by determining the radiographic location of the opaque embolus. In most cases the embolus went into the pulmonary artery leading to the right lower lobe (Fig. 5).

When the emboli were removed within 24 h, a scan performed 24 h after removal of the embolus usually indicated restoration of the circulation. However, when the embolus was left longer than 24 h, its removal did not restore blood flow within 24 h. Several weeks or even months were required before the circulation returned. In pathological studies we found in most cases that distal to the point of vascular obstruction in situ thrombosis had spread peripherally. This resulted in an arboreal network of occluded vessels distal to the embolus.

II. Characteristics of the lung scan in normal man

Figure 6 is the appearance of the normal lung scan from the anterior-posterior viewpoint. In all cases, a dose of 300 μc of I^{131} MAA or 1000 μc of Cr^{51} was injected while the patient lay supine. To obtain more quantitative data than that provided by the scanning procedure, the output of the detection system could be used as input to a ratemeter and chart recorder. As shown in Fig. 7, one obtained a series of "profiles" of the concentration of the radioactivity as the probe moved across the chest. The area under the curves could be obtained by planimetry. The designations L and R refer to the counting rates obtained when over the left and right hemithorax, respectively.

The anterior-posterior lung scan was characterized by the area of decreased radioactivity corresponding to the cardiac silhouette. The superior mediastinum was also visualized as an area of decreased concentration of radioactivity. When the scan was performed from the posterior-anterior

Fig. 6

Normal appearance of lung scan in man scanned by means of a 3-in crystal detector moving across the anterior chest.

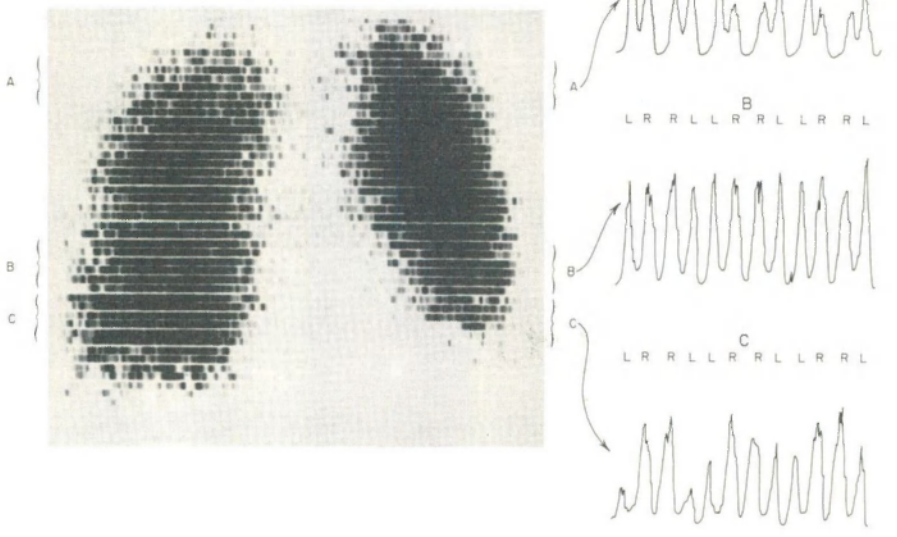

Fig. 7

Multiple profile scan of the lungs of a normal man
The radioactivity tracings were obtained by means of a ratemeter connected to the output of the spectrometer.
L and R refer to the left and right lung, respectively.

viewpoint, the cardiac area was diminished in size relative to that seen in the AP projection and a larger area of lung could be visualized.

III. Massive pulmonary embolism in man

Of the first 100 lung scans performed in man, 5 patients were proved by autopsy to have had massive pulmonary embolism. Figures 8A and 8B are the chest X-ray and lung scan of a 75-yr-old woman who developed extreme dyspnea 10 d after a mid-thigh amputation. The marked avascularity of nearly the entire left lung and several areas of the lower right lung con-

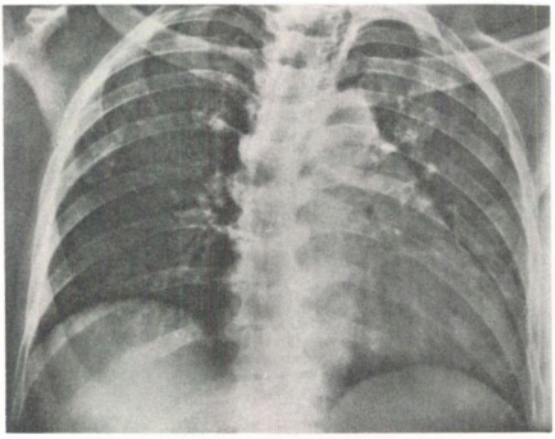

Fig. 8A

Chest X-ray of a patient with massive pulmonary embolism

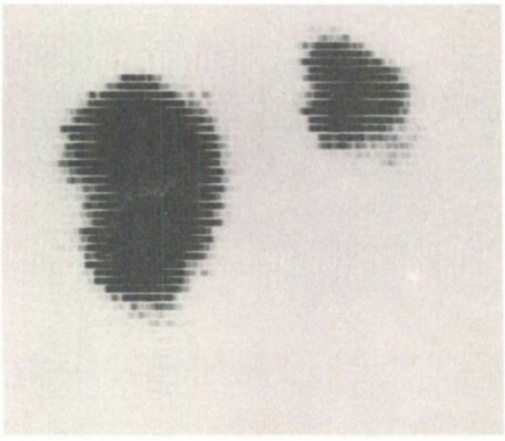

Fig. 8B

Lung scan of the same patient as in Fig. 8A
Avascular areas can be seen at the left lower lung field and in the middle and lower right lung fields.

firmed the suspicion of massive pulmonary embolism, not apparent on the chest X-ray. The patient was not considered a suitable candidate for surgery and died several days later. Autopsy confirmed the presence of multiple pulmonary emboli.

Figures 9A, 9B and 9C are anterior-posterior lung scans of 3 other patients who subsequently died and were found at autopsy to have multiple pulmonary embolism.

The characteristic pattern of massive pulmonary embolism was a gross irregularity of distribution of the radioactivity nearly always involving both lungs. Because of the diminished blood flow to other areas, the concentration of the MAA in the perfused reas of the lung was found to be greater than normal, thereby giving a striking contrast between the avascular and vascular areas.

IV. Chronic recurrent pulmonary embolism

Pulmonary arteriograms and lung scans were compared in a series of patients. Many had had ligation or plication of the inferior vena cava to present recurrence of pulmonary embolization. The patient whose studies are shown in Figs. 10A and 10B had had plication of his vena cava a year before the present study. Avascular areas were found at the right and left bases. Pulmonary arteriography also showed the vascular abnormalities in areas that corresponded to the filling defects on the scan.

The patient whose studies are shown in Figs. 11A, 11B and 11C was a 42-yr-old woman who complained of pleuritic pain on the right side of the chest and had transient fever. Lung scan (Fig. 11B) indicated that there was an avascular area at the left base. This was confirmed by subsequent pulmonary arteriogram (Fig. 11C).

DISCUSSION

In the present series of over 100 patients, either autopsy, operation or selective pulmonary arteriography confirmed the diagnosis of regional pulmonary avascularity in 14 cases where filling defects were observed in the lung scans. The size of the smallest lesion that could be detected is not known with certainty, although it is likely that lesions less than a few centimeters in diameter would be missed with present scanning equipment. This is not a serious limitation in diagnosing massive pulmonary embolism, because large areas of lung are usually involved. GORHAM found that 85% of patients with fatal pulmonary embolism have involvement of either one entire lung or large areas in both lungs [5]. Experiments in dogs also indicate that over 50% of the lung circulation must be impaired before significant pulmonary hypertension and respiratory distress ensue. We found large bilateral lesions in all 5 patients who died of massive pulmonary embolism. Of the patients who survived, 1 complete lung was involved in 1 patient while 8 others had bilateral defects. In our patients the degree of respiratory difficulty correlated well with the degree of impairment of the pulmonary vasculature as seen in the lung scans.

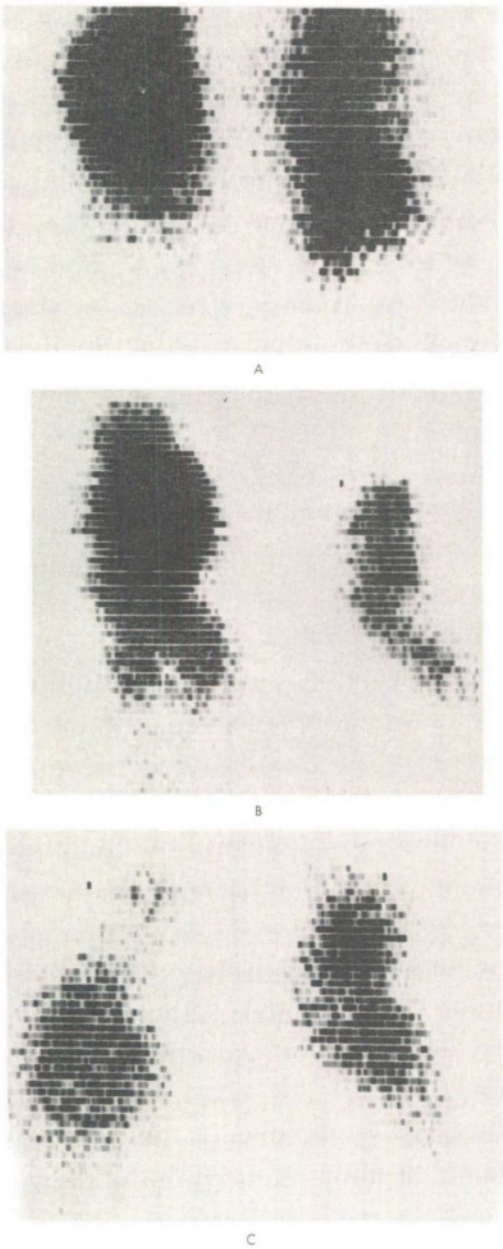

Figs. 9A-9C

Lung scans of three patients who were proved at autopsy to have multiple pulmonary embolism
The crescent-shaped lesions in the middle lateral portion of the left lung can be seen,
as well as impairment of the blood supply to the right lower lobe.

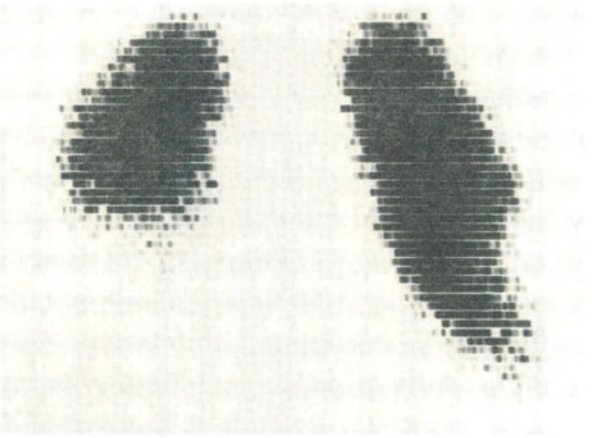

Fig. 10A

Lung scan of a patient who had had plication of his inferior vena cava for multiple pulmonary embolism

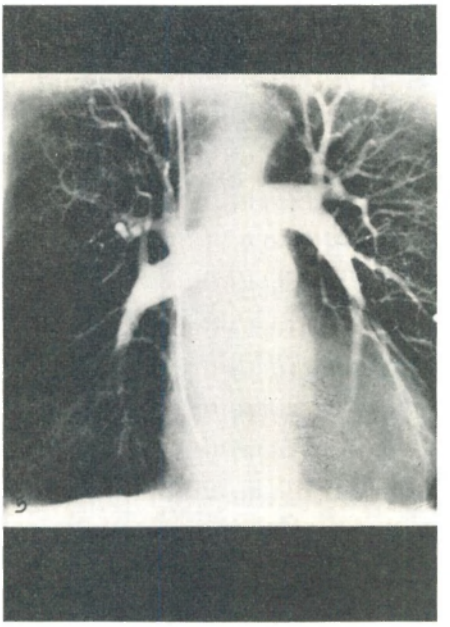

Fig. 10B

Lung scan of the same patient as in Fig. 10A

Since we have used selective pulmonary arteriography as a means of confirming the diagnosis of pulmonary embolism in the patients who did not come to autopsy, a reasonable question is what does lung scanning offer in making the diagnosis of pulmonary embolism that pulmonary arteriography

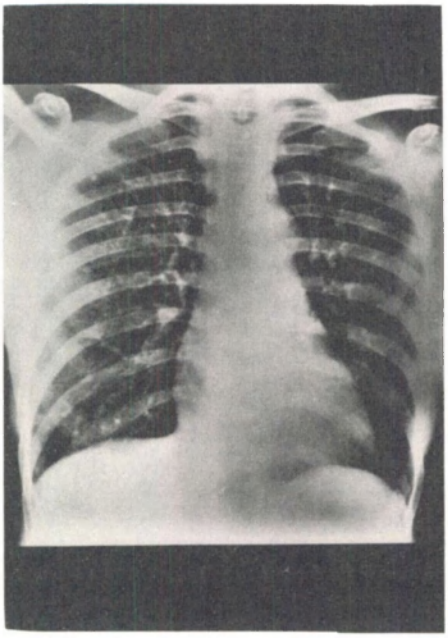

Fig. 11A

Chest X-ray of a patient with right-sided pleuritic chest pain and exertional breathlessness
An area of increased radiolucency could be seen at the left base.

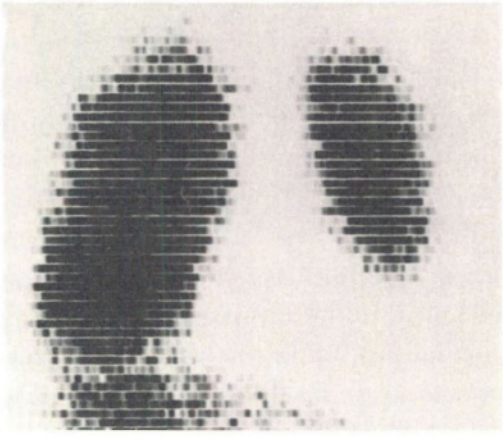

Fig. 11B

Lung scan of the same patient as in Fig. 11A
An avascular area could be seen at the left lower lung field.
Radioactivity could also be seen in the liver.

Fig. 11C

Selective pulmonary arteriogram in the same patient as in Figs. 11A and 11B, confirming the avascularity of the left lower lung

does not? Each technique has its own particular strong points and deficiencies. To be completely satisfactory, pulmonary arteriography must be performed by injecting relatively large volumes of radiopaque material directly into the pulmonary artery. Intravenous injections usually do not give sufficiently good definition of the vasculature. Therefore cardiac catheterization is required, which is cumbersome at best, and may result in the dislodgement of venous thrombi at worst. Furthermore, experience has shown that patients with pulmonary hypertension tolerate injections of X-ray contrast material very poorly. Up to the present, lung scanning has not been associated with any known toxicity and does not result in any morbidity. An important advantage is that serial studies can be performed at frequent intervals in the same subject, thereby providing follow-up information at intervals that would not be possible if one had to perform repeated pulmonary arteriography. Examples of follow-up studies now in progress are an evaluation of the natural history of pulmonary embolism with respect to revascularization, evaluation of the incidence of recurrences of pulmonary embolism after vena caval plication or ligation, and determination of the efficacy of thrombolytic drugs.

The scanning procedure is technically simple and at present we have a scanner available for immediate use as soon as the diagnosis is suspected. In at least 20 patients serious consideration of the diagnosis of massive pulmonary embolism was discarded when lung scans revealed normal pulmonary vasculature. On the other hand, whenever we have obtained strong evidence of multiple areas of pulmonary avascularity, selective pulmonary

arteriography was performed if consideration was given to the possible necessity of pulmonary embolectomy.

Is the scanning procedure sufficiently definitive to permit the diagnosis of massive pulmonary embolism on the basis of the scan alone? The answer to this question is a qualified no. No, because, as we have previously reported [6] most parenchymal lesions of the lungs result in avascularity of the pulmonary circulation, the blood supply presumably being provided by the bronchial circulation. A qualified no, because in a large number of patients, a characteristic pattern has been observed in massive pulmonary embolism. This pattern consists of avascularity of the right lower lobe, together with a crescent-shaped defect in the mid-lateral part of the left lung field.

In the studies in dogs, we found that the right lower lobe is by far the most commonly involved lobe when large emboli pass into the lungs. Frequent involvement of the right lower lobe has also been reported in pathological studies in man, and in the present patients we have confirmed this finding. The crescent-shaped defect may represent another frequent site of embolism in man, and we suspect, but have not yet proved, that this lesion results from involvement of the superior segment of the left lower lobe.

Even in the absence of the characteristic pattern one should suspect pulmonary embolism if one finds multiple avascular areas on the scan, particularly if no parenchymal lesions are seen on the chest X-ray. This has usually been the case, both in the experimental emboli in dogs and in patients subsequently proved to have massive embolism. Particularly helpful is the finding of a corresponding zone of increased radiolucency, a finding reported initially by WESTERMARK [7] and extended recently by TORRANCE [8].

On the other hand, if there is a lesion on the chest X-ray, from our past experience, regardless of whether the lesion is the result of an infarct, pneumonia, atelectasis, abscess or tumour, the area will be avascular with respect to the pulmonary arterial blood flow and an area of decreased radioactivity will be found on the lung scan. In these cases, while of considerable academic interest, the information is of no diagnostic value.

A particular word of caution must be mentioned with respect to lung bullae or cysts. These areas are both avascular and radiolucent on chest X-ray and may therefore mimic the findings in pulmonary embolism. An example of this type of patient was reported previously [6].

SUMMARY AND CONCLUSIONS

1. Radioisotope scanning of the lungs in 110 patients and 50 dogs following the intravenous injection of I^{131} or Cr^{51} macro-aggregated albumin (MAA) was a safe and effective way of diagnosing massive pulmonary embolism.
2. In many patients a characteristic pattern of avascularity was observed. This consisted of a decreased pulmonary blood flow to all or part of the right lower and to a crescent-shaped area on the lateral mid-portion of the left lung.
3. To date, no haemodynamic, immunologic or radiation hazard has been observed.

4. The method has been found to be an important adjunct to selective pulmonary arteriography, and has important advantages in being readily available, faster, technically easier, and free of morbidity. Consequently it was used as a rapid screening procedure and made possible serial studies at frequent intervals in the same individual.
5. The scanning technique was found to be particularly suitable to evaluate the natural history of massive pulmonary embolism, as well as to determine the effectiveness of surgical procedures such as vena caval ligation, or of drugs such as anticoagulants or fibrinolytic agents.

REFERENCES

[1] HALPERN, B.N., BIOZZI, G., BENACERRAF, B., STIFFEL, C. and HILLEMAND, B., C.R. Soc. Biol. 150 (1956) 1307-11.
[2] TAPLIN, G.V., DORE, E.K., JOHNSON, D.E. and KAPLAN, H., in Scientific Exhibit, 10th Annual Meeting of the Society of Nuclear Medicine, June 26, 1963, Montreal, Canada.
[3] WAGNER, H.N. Jr., IIO, M. and HORNICK, R.B., J. clin. Invest. 42 (1963) 427-34.
[4] WAGNER, H.N. Jr., McAFEE, J.G. and MOZLEY, J.M., J. Amer. med. Ass. 174 (1960) 162-6.
[5] GORHAM, L.W., Arch. int. Med. 108 (1961) 8-22; 189-207; 418-26.
[6] WAGNER, H.N. Jr., SABISTON, D.C., IIO, M., MEYER, J.K. and LANGAN, J.K., J. Amer. med. Ass. 187 (1964) Feb. 22
[7] WESTERMARK, W., Acta radiol. 19 (1938) 357-72.
[8] TORRANCE, D.J. Jr., The Chest Film in Massive Pulmonary Embolism, Chas. C Thomas, Springfield, Ill. (1963).

DISCUSSION

C.M.E. MATTHEWS: I should like to refer again to the lung-scanning studies which we carried out with Xe^{133} at Hammersmith Hospital. The slit collimators we now use have a resolution of about 2 cm, not 5 cm; these are similar to four-hole collimators in the vertical plane, and to a slit in the horizontal plane. One pair of these counters scans the right and another the left lung, and it is planned to increase the number of counters used. The scans can also be made after exercise or in different postures. The radiation dose with rebreathing for ventilation measurements is only about 70 mrad to the lungs; if Xe^{133} is merely injected for the measurement of blood flow it is very much smaller. The information obtained is quantitative and the different volumes of lung in the counting field can be allowed for.

H. WAGNER: We have had considerable experience in using Xe^{133} and think it is extremely valuable in studying both pulmonary circulation and pulmonary ventilation. However, using macro-aggregated albumin, pulmonary blood flow can be studied not only after, but also during, exercise. One needs only inject the material during whatever particular circumstances one wishes to study. The resulting distribution can then be examined at leisure within an hour or two of injection. It would, for example, be absolutely impossible to study the effect of gravitational forces with the equipment required for work with Xe^{133}. We believe that we have evidence regarding the distribution of the blood supply to the lung in cases of exposure to forces four times that of gravity.

G.V. TAPLIN: What is the particle-size distribution of your aggregates made at pH 5.5 and 100°C? Do you estimate mean size according to linear dimension or by volume? I should also like to ask what are the relative merits of Cr^{51} compared with I^{131} or I^{125} as a label for the albumin aggregates.

H. WAGNER: We consider that the particle-size distribution will vary from 1 μm up to 50 μm. We are absolutely certain that, in our best preparations, the minimum is 1 μm and we believe the maximum to be 50 μm. We measure the particle-size distribution by differential filtration with millipore filters and also by using a Coulter particle counter and thus we calculate the mean particle size.

As to your last question, we believe that a higher percentage of the particles remains in the lung when Cr^{51} is used. We also find that the extraction efficiency is higher and a greater percentage of the particles remains in the lungs after heating at 100°C for 4 min. We consider that the pH is a most critical factor. We heat the particles from the beginning at pH 5.5 and ensure precision to one tenth of a pH unit. If the material is diluted, for example, care must be taken to ensure that it remains at the isoelectric point of albumin; otherwise, the particles will deteriorate and the extraction efficiency in the lung will decrease. We also believe that with storage there may be a decrease in the number of particles going to the lungs. I should like to point out that this is not at all important in lung scanning. In the worst possible situation, there would still be approximately 60% accumulation in the lungs. However, if one wishes to quantitate the data, a very good extraction efficiency is required.

J.-C. ROUCAYROL: How frequently can this type of study be repeated?

H. WAGNER: Because of the very rapid metabolic breakdown of these materials in the lungs, the study can be repeated at 24-h intervals. With the iodine-labelled materials, there is nothing left in the lungs after 24 h.

PHOTOSCANNING OF THE SPLEEN BY HEAT-TREATED Cr^{51}-LABELLED ERYTHROCYTES IN CONGENITAL HAEMOLYTIC ANAEMIAS

H. GYFTAKI, C. PROUKAKIS, D. BINOPOULOS, C. ELIAS AND V. ALEVIZOU
ALEXANDRA HOSPITAL, ATHENS UNIVERSITY, ATHENS, GREECE

Abstract — Résumé — Аннотация — Resumen

PHOTOSCANNING OF THE SPLEEN USING HEAT-TREATED Cr^{51}-LABELLED ERYTHROCYTES IN CONGENITAL HAEMOLYTIC ANAEMIAS. The delineation of the spleen by photoscanning after the intravenous injection of heat-treated Cr^{51}-labelled erythrocytes is valuable when investigating congenital haemolytic anaemias, especially thalassaemia, a disease which is recognized as one of the most important public health problems in Greece.

Heat-treated Cr^{51}-labelled erythrocytes were prepared as follows: blood was taken from the subject by venepuncture and delivered into a sterile bottle containing acid-citrate-dextrose. The red cells were separated by centrifugation and the plasma discarded. 50 - 150 μc Cr^{51}-chromate was added to the red cells and the mixture allowed to stand for 30 min at room temperature. The labelled cells were washed once with saline and re-suspended in saline. The suspension was heated at 49.5°C for one hour. The heated cells were washed once with saline and re-suspended in saline. The suspension was then injected intravenously into the subject. Scanning was performed one hour later.

Cases of thalassaemia major, sickle cell haemoglobin/thalassaemia and thalassaemia trait have been investigated by this method. All the cases studied, with the exception of one carrier of thalassaemia trait, whose spleen was not palpable, showed varying degrees of splenomegaly. The size and configuration of the spleen could be well demonstrated. A constant finding in spleen scans on patients with congenital haemolytic anaemia, not observed in scans on normal subjects, was the presence of regions of lower average radioactivity throughout the organ. The interpretation of this finding is discussed.

GAMMAGRAPHIE DE LA RATE AVEC DES ÉRYTHROCYTES MARQUÉS AVEC ^{51}Cr ET TRAITÉS THERMIQUEMENT DANS L'ANÉMIE HÉMOLYTIQUE CONGÉNITALE. La gammagraphie de la rate après injection intraveineuse d'érythrocytes marqués avec ^{51}Cr et traités thermiquement constitue une méthode de choix pour étudier l'anémie hémolytique congénitale, notamment la thalassanémie, maladie qui constitue l'un des problèmes de santé publique les plus importants en Grèce.

Les érythrocytes marqués avec ^{51}Cr et traités thermiquement sont préparés de la manière suivante: après avoir prélevé du sang par ponction dans une veine, on le place dans un flacon stérile contenant un citrate acide et de la dextrose. On sépare à la centrifugeuse les globules rouges du plasma, que l'on jette; après avoir ajouté de 50 à 150 μc de ^{51}Cr sous forme de chromate, on laisse reposer le mélange pendant 30 min à la température de la pièce. Les cellules marquées sont lavées une première fois dans un sérum, puis remises en suspension dans du sérum. Cette suspension est chauffée à 49,5°C pendant une heure, puis lavée de nouveau avec du sérum et remise en suspension dans du sérum. Cette suspension est alors injectée dans une veine du sujet et on procède à la gammagraphie une heure plus tard.

Les auteurs ont étudié par cette méthode des cas de thalassanémie majeure, d'anémie à cellules falciformes et de thalassanémie hétérozygote. A l'exception d'un malade souffrant de thalassanémie hétérozygote, dont la rate n'a pu être palpée, on a constaté dans tous les cas divers degrés d'hypertrophie de la rate. On a pu bien déterminer la dimension et la configuration de la rate. Dans toutes les gammagraphies de la rate de malades souffrant d'anémie hémolytique congénitale, on a noté la présence de zones à radioactivité moyenne plus faible; cette particularité n'a jamais été constatée chez des sujets normaux. Les auteurs discutent l'interprétation de ce phénomène.

ФОТО-СКЕННИРОВАНИЕ СЕЛЕЗЕНКИ С ПОМОЩЬЮ ТЕРМИЧЕСКИ ОБРАБОТАННЫХ МЕЧЕННЫХ ХРОМОМ-51 ЭРИТРОЦИТОВ ПРИ ВРОЖДЕННЫХ ГЕМОЛИТИЧЕСКИХ АНЕМИЯХ. Получение контуров селезенки с помощью фото-сканнирования после внутривенного введения термически обработанных меченных хромом-51 эритроцитов имеет большое значение при исследовании врожденных гемолитических анемий и в особенности талас-

семии – заболевания, которое считается одной из наиболее серьезных, если не самой серьезной, проблемой здравоохранения в Греции.

Термически обработанные меченные хромом-51 эритроциты приготавливались следующим образом: кровь пациента, взятая путем венепункции, переливалась в стерильную колбу, содержащую лимоннокислую декстрозу. Эритроциты отделялись путем центрифугирования, и плазма отбрасывалась. К эритроцитам добавляли 50–150 мккюри хромата–хром-51 и эту смесь оставляли на 30 минут при комнатной температуре. Меченые клетки однократно промывали физиологическим раствором и снова суспензировали в физиологическом растворе. Эта суспензия нагревалась в течение одного часа при температуре 49,5 °С. Подогретые эритроциты промывали в физиологическом растворе и снова суспензировали в физиологическом растворе. Эту суспензию затем вводили пациенту внутривенно. Через час после этого проводилось сканнирование.

Таким методом были исследованы больные с классической талассемией, серновидноклеточной талассемией и пациенты, имеющие признаки талассемии. У всех обследованных больных, за исключением одного носителя признаков талассемии, селезенка которого не прощупывалась, обнаружена различная степень спленомегалии. Отчетливо определялся размер и конфигурация селезенки. На сканнограммах у пациентов с врожденной гемолитической анемией, не наблюдаемой на сканнограммах здоровых пациентов, постоянно находили области с низкой средней радиоактивностью на протяжении всего органа. Обсуждается толкование этих данных.

FOTOEXPLORACIÓN DEL BAZO EN CASOS DE ANEMIA HEMOLÍTICA CONGÉNITA EMPLEANDO ERITROCITOS SOMETIDOS A CALENTAMIENTO Y MARCADOS CON ^{51}Cr. El delineamiento del bazo por fotoexploración después de una inyección intravenosa de eritrocitos sometidos a calentamiento y marcados con ^{51}Cr es de suma utilidad para la investigación de las anemias hemolíticas congénitas y, especialmente, de la talasemia, enfermedad que constituye uno de los problemas sanitarios más importantes de Grecia.

Los eritrocitos tratados térmicamente y marcados con ^{51}Cr se prepararon de la siguiente manera: se extrajo sangre del paciente por punción de la vena y se trasvasó a un frasco esterilizado que contenía una solución ácida de citrato y dextrosa. Los hematíes se separaron por centrifugación y se desechó el plasma. A los hematíes se añadieron de 50 a 150 μc de cromato-^{51}Cr y la mezcla se dejó en reposo a la temperatura ambiente durante 30 min. Seguidamente se lavaron hematíes una sola vez con suero fisiológico y se pusieron en suspensión. Esa suspensión en suero fisiológico se calentó a 49,5°C durante una hora. Los hematíes se volvieron a lavar con suero fisiológico y se preparó una segunda suspensión que se inyectó intravenosamente al paciente. La exploración se efectuó una hora después.

Por este método se han investigado casos de talasemia mayor, anemia drepanocítica y talasemia heterocigótica. Todos los casos estudiados, exceptuando uno de talasemia heterocigótica, en el que el bazo no era palpable, presentaban grados diversos de esplenomegalia. Se pudo poner de relieve perfectamente el tamaño y la configuración del bazo. Una peculiaridad que aparece constantemente en los centelleogramas esplénicos de enfermos de anemia hemolítica congénita, y que no se observa en los de sujetos sanos, es la presencia, en toda la extensión del órgano, de regiones de radiactividad media reducida. En la memoria se procura interpretar ese dato.

The attempt to visualize different organs with radioisotopes has been extended to most internal organs. Thus the scanning of the thyroid, the first scanning technique to be applied, was followed by scanning of the liver, brain, kidney and of other organs. By scanning techniques the size, the exact position and the functioning tissue of the different organs examined can be estimated.

After the demonstration that red cells sensitized with anti-Rh (D) antibody [1, 2] and also heated red cells [3] were trapped selectively by the spleen, interest turned to the visualization of this organ.

The purpose of this communication is to report the study by scanning of the spleen exclusively in patients with congenital haemolytic anaemias and carriers of the trait of these anaemias, which besides the other abnormal findings usually show a more or less enlarged spleen.

METHOD

The method used consists of the intravenous injection of heat-treated, Cr^{51}-labelled erythrocytes. The method is as follows: 20 ml of the patient's blood are withdrawn and delivered into a sterile bottle, containing 4 ml of acid-citrate-dextrose. The mixture is then centrifuged for 15 min at 1500 rev/min and the supernate is discarded. Then 100-200 μc of $Na_2Cr^{51}O_4$ are added to the red cells and the mixture is allowed to stand for 30 min at room temperature. The labelled cells are washed once with isotonic saline and then re-suspended in saline and incubated in a water bath at a temperature of 49.5°C for 60 min. After the second incubation, the blood is centrifuged for 15 min at 1500 rev/min. The supernate is discarded and the red cells re-suspended in saline. After cooling to room temperature, the blood is administered to the patient intravenously.

One hour and sometimes 24 h after the intravenous injection of the Cr^{51}-labelled red cells scanning of the spleen is performed. A blood sample is taken before the performance of the scan and then its radioactivity is measured.

Position of the patient

All the scans were performed in the right lateral position of the patient except for one that was performed in the supine position.

Technique of photoscanning

As scanner the SC-500 scanner of BAIRD-ATOMIC was used. This scanner is equipped with a scintillation counter, with a 3×2-in sodium iodide crystal activated with thallium. The side shielding of the counter has 2-in lead and tungsten and the collimator is of a focusing type with 37 holes.

The use of a pulse height analyser permits the measurement of the primary radiation of Cr^{51}, and scattered radiation and high energy background are eliminated. The recording is made on paper (dot recording) and on photographic film (film recording). The method of recording is entirely different for the two types of recording.

On the paper, an electric stylus sends a spark through a sensitized paper each time a number of counts is collected, depending on the selected dot factor. A special electronic device permits recording on the paper only, when the counting rate exceeds a certain counting rate which can be predetermined. For out scans of the spleen this counting rate was 30% of the maximum.

The photorecording is obtained by means of a small beam of light with density depending on the counting rate. This density can be adjusted so that the maximum counting rate (called 100%) corresponds to the maximum of the blackening. The minimum of blackening can be adjusted to any counting rate between 0-90% of the maximum. In our scans it was 45%. For counting rates lower than 45% of the maximum, no blackening appeared on the film. Counting rates between 45-100%, covered the whole range of blackening from zero to maximum. By this technique, small relative differences in counting rate are more easily shown by differences in the blackening.

The maximum counting rate for different cases ranged between 500-2500 counts/min and the scanning speed between 5-7½ in/min.

Scanning was made in one direction only, with rapid return, to eliminate "scalopping". The patient was placed first on the bed and the margins of the spleen were then detected and marked.

By moving the scintillation counter over the spleen the maximum counting rate was determined and the density control then fixed to correspond to the maximum blackening.

The dimensions of the light source were 1/8×3/16 in and the scan spacing 3/16 in.

RESULTS

Morphologic changes of the erythrocytes

Dry smears were prepared from the blood samples before and after incubation at 49.5°C. Except for the morphological changes characterizing the disease, no changes were observed in the unheated red cells. The changes produced in the heated red cells were similar to those observed by others [4, 5, 6, 7] i.e. showing a knobby appearance or pseudopodial projections from the red cell surface (Figs. 1-4).

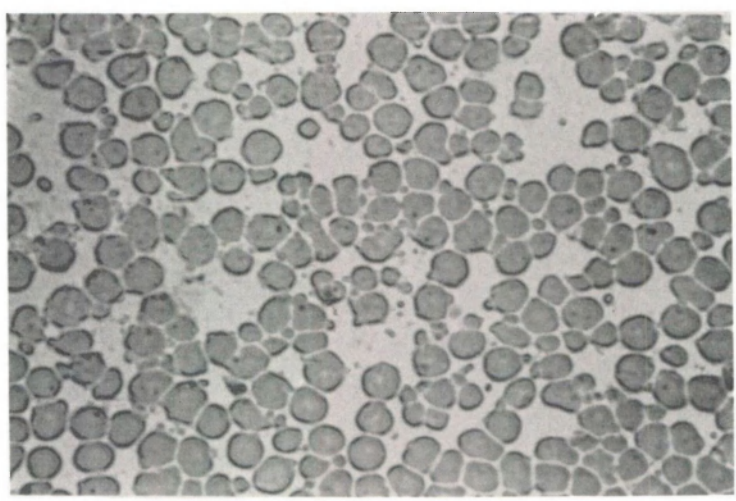

Fig. 1

Changes produced in the heated red cells of a normal subject

The Cr^{51} uptake of the red cells after heating at 49.5°C

The Cr^{51} uptake by the red cells, after heating at 49.5°C, ranged between 65-88% of the initial dose. We failed to observe, as did other investigators, a significant loss of Cr^{51} during heating [8].

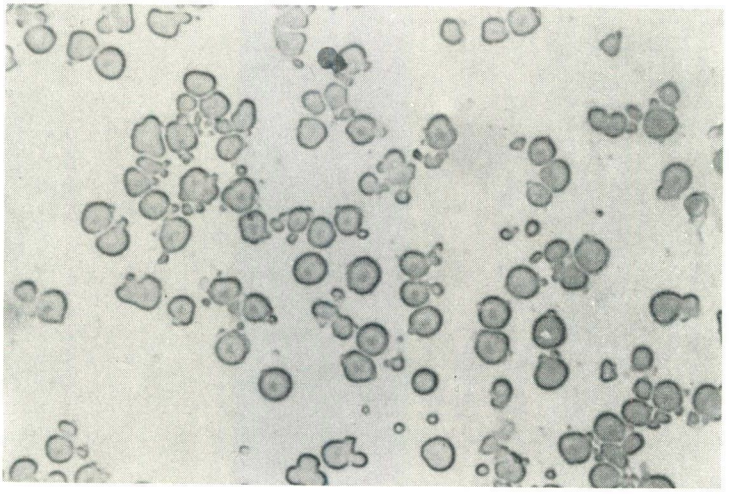

Fig. 2

Changes produced in the heated red cells of a subject with thalassaemia trait

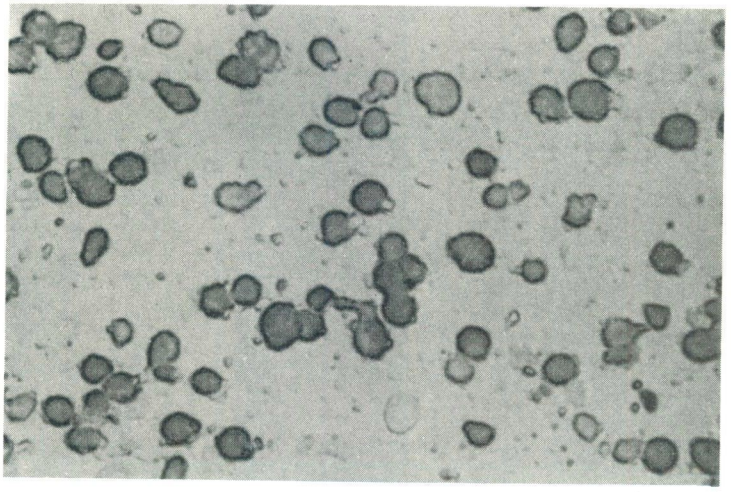

Fig. 3

Changes produced in the heated red cells of a patient with thalassaemia

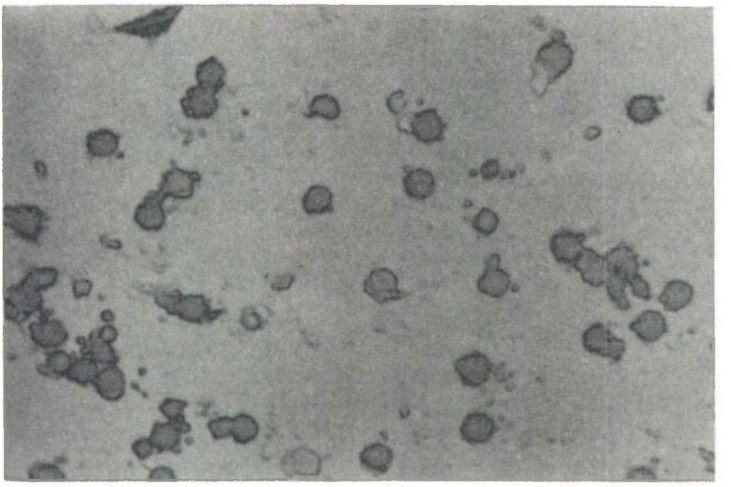

Fig. 4

Changes produced in the heated red cells of a patient with sickle-cell thalassaemia

Finally 41-79% of the initial dose (ranging from 100-200 μc and in two cases 50 μc) was injected into the patient.

The whole blood radioactivity at the time of scanning was found to amount to 0-3.2% of the administered dose, except in the four cases (one normal, one sickle-cell thalassaemia and two thalassaemia traits) in which the values were 5.4%, 6.9%, 13% and 10% respectively.

Scanning of the spleen

Scans of the spleen were obtained in all subjects with congenital haemolytic anaemias, except for one who was thought to have autosplenectomy, as well as in the carriers of the thalassaemia trait. The spleen was also visualized in all cases of normal subjects.

The scan was studied regarding its size and position, but mainly as to the uniform distribution of splenic radioactivity and the existence of space-occupying lesions.

Normal subjects

Ten normal subjects, with no evidence of splenic disease, were studied.

The mean value of the two dimensions of the photoscan, in two perpendicular dimensions, was 8.5×10.9 cm respectively.

The position of the spleen in the subjects was normal. The density of the splenic photoscan was homogeneous in the film, as has been observed by others [9, 10] (Fig. 5).

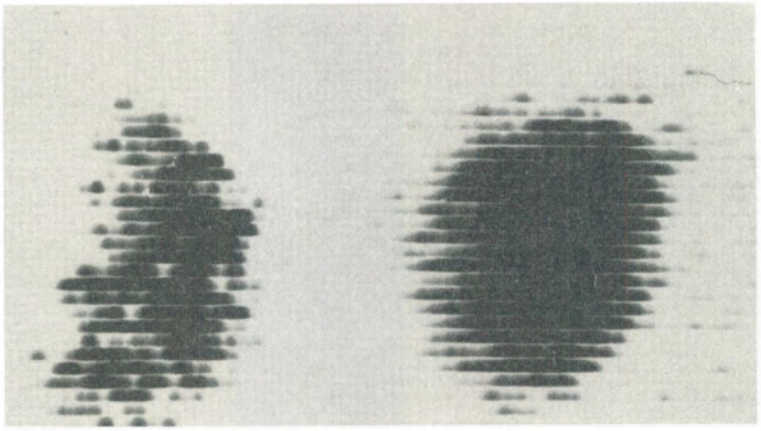

Fig. 5

Photoscanning of the spleen in two normal subjects with uniform distribution of radioactivity

Patients with congenital haemolytic anaemias

Eleven patients with congenital haemolytic anaemias (six with thalassaemia and five with sickle-cell thalassaemia) and eight carriers of the thalassaemia trait were studied.

Four of the five scans performed on the patients with sickle-cell thalassaemia demonstrated non-uniform distribution of radioactivity (Fig.6), whilst in the last the spleen failed to be visualized. This is attributed to autosplenectomy from repeated infarcts and not to any error in the technique, since the red cells possessed the characteristic signs of being trapped by the spleen. Also, we failed to detect significant radioactivity over the hepatic region. The spleen of two cases was enormous, extending to the iliac crest; in the third, it was markedly enlarged, and in the remaining two the spleen was not palpable.

Scanning of the spleen in the patients with thalassaemia did not show uniform distribution of splenic radioactivity in all cases. The photoscan in three of the six patients demonstrated homogeneous distribution of radioactivity (Fig. 7), but in the remaining three it was not homogeneous (Fig. 8). In all cases the spleen was markedly enlarged.

Two of the eight carriers of the thalassaemia trait that were studied had a palpable spleen. The distribution of radioactivity in the photoscan was uniform in five (Fig. 9), non-uniform in one (Fig. 10) and doubtful in the remaining two (Fig. 11).

COMMENTS

The observed non-uniform distribution of radioactivity in some of the cases of congenital haemolytic anaemias, which contrasted with the homogeneity of normal cases, requires special consideration.

Fig. 6

Photoscanning of the spleen in three cases of sickle-cell thalassaemia with space-occupying lesions

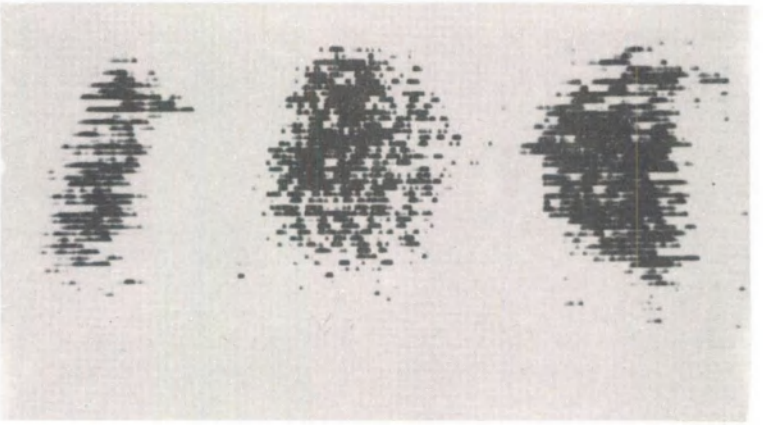

Fig. 7

Photoscanning of the spleen in three cases of thalassaemia with uniform distribution of radioactiviy

Fig. 8

Photoscanning of the spleen in three cases of thalassaemia with space-occupying lesions

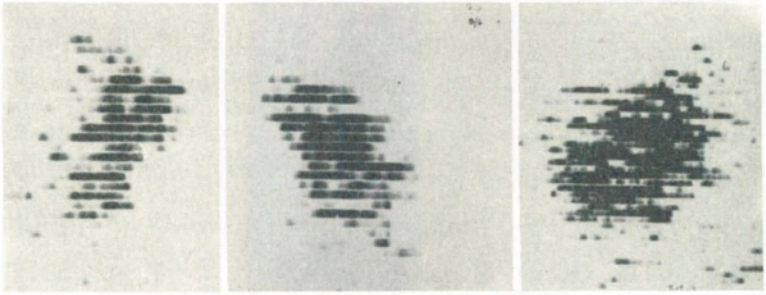

Fig. 9

Photoscanning of the spleen in three cases of thalassaemia trait with uniform distribution of radioactivity

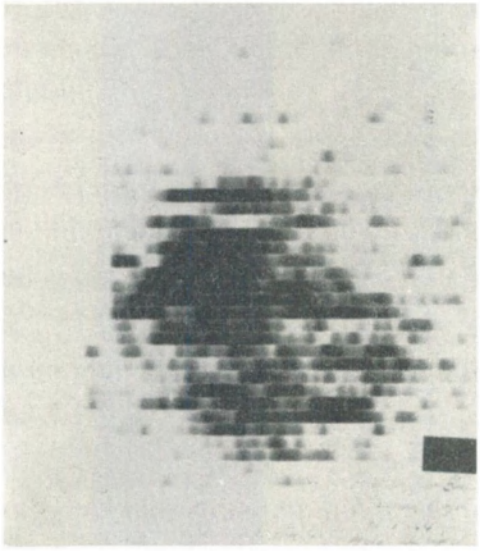

Fig. 10

Photoscanning of the spleen in one case of thalassaemia trait with space-occupying lesion

The observed counting-rate over the splenic region in scans characterized by non-uniformity was so high that the parts of the photoscan showing less radioactivity must be accepted as reliable and not caused by a statistical variation in the counting rate.

The enlargement of the spleen cannot be correlated with the non-uniform distribution of radioactivity. This is because some of the cases studied with splenomegaly showed a uniform distribution of radioactivity. In the references uniform rather than non-uniform distribution of radioactivity is emphasized in splenomegaly [6, 9].

The observed foci of less radioactivity in the photoscans of the cases of sickle-cell thalassaemia can well be explained through splenic infarcts and the replacement of their splenic parenchyma by fibrous tissue.

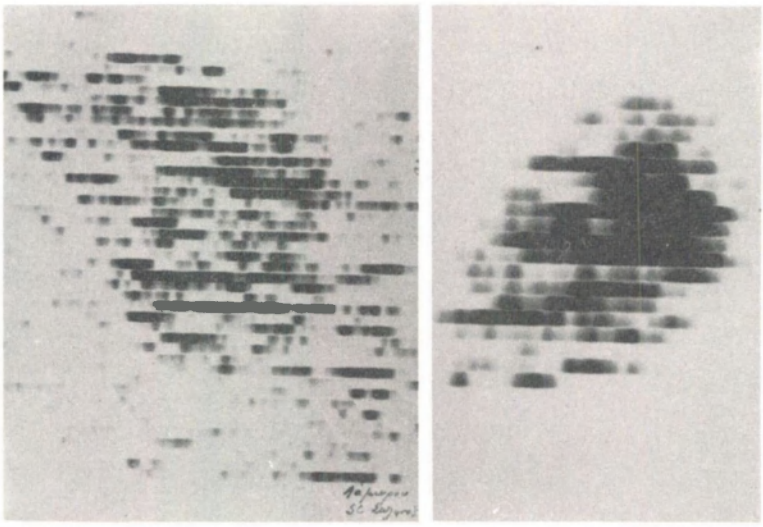

Fig. 11

Photoscanning of the spleen in two cases of thalassaemia trait characterized as doubtful

It has been observed in patients with sickle-cell disease that the clearance of heat-treated red cells from the blood was much slower than in normals [11].

We did not find in the references cases of sickle-cell thalassaemia, in which the clearance of heat-treated red cells was studied. The blood radioactivity at the time of scanning in the four cases in which the spleen was visualized was 0%, 1.2%, 0.3% and 1.1% of the injected dose. In the fifth case with autosplenectomy it was 6.9%. In the reference [6] a case of sickle-cell disease is reported in which the distribution of radioactivity in the photoscan of the spleen was homogeneous. This case concerns a 6-yr-old child in which the spleen probably did not show infarcts.

The pathology of the spleen in thalassaemia can explain the non-uniform distribution of radioactivity found in three cases of thalassaemia and in one case of the thalassaemia trait. It is reported that infarcts have been observed and microscopically areas of fibrous tissue. Also hyperplasia of the reticuloendothelial cells [12, 13] was noted.

The fact that the non-uniform distribution of radioactivity in the photoscans of the spleen in thalassaemia was not found in all cases permits the assumption that it depends on the degree and the extent of the above-mentioned pathologic changes.

The number of cases studied is too small to permit statistical analysis of the findings. Nevertheless the scanning of the spleen makes it possible to determine the size, location and amount of functional tissue, as well as the degree of fibrosis in the spleen.

ACKNOWLEDGEMENTS

We wish to express our thanks to Professor B. Malamos for this work, which was performed under his supervision. We wish to thank also Dr. M. Kesse for the microscopic examination of the blood smears.

REFERENCES

[1] JANDL, J.H., JONES, A.R. and CASTLE, W.B., J. clin. Invest. 36 (1957) 1428-59.
[2] JONES, N.C.H., MOLLISON, P.L. and VEALL, N., Brit. J. Haemat. 3 (1957) 125-33.
[3] HARRIS, I.M., McALISTER, J. M. and PRANKERD, T.A., Clin. Sci. 16 (1957) 223-30.
[4] HAM, T.H., SHEN, S.C., FLEMING, E.M. and CASTLE, W.B., Blood 3 (1948) 373-403.
[5] WAGNER, H.N., RAZZAK, M.A., GAERTNER, R.A., CAINE, W.P. and FEAGIN, O.T., Arch. int. Med. 110 (1962) 128-35.
[6] JOHNSON, P.M., WOOD, E.H. and MOORING, S.L., Roentgenology 86 (1961) 757-67.
[7] WINKELMAN, J.W., WAGNER, H.N., Jr., McAFEE, J.G. and MOZLEY, J.M., Radiology 75 (1960) 465-6.
[8] HOLZBACH, T., CLARK, R.E., SHIPLEY, R.A., KENT, W.B. and LINDSAY, G.E., J. lab. and clin. Med. 60 (1962) 902-13.
[9] JAMMET, H., GONGORA, R., BILSKI-PASQUIER, G., DUHAMEL, G. and MARCHAL, G., La Semaine des Hôpitaux 17 (1962) 1047-53.
[10] JOHNSON, P.M., HERION, J.C. and MOORING, S.L., Radiology 74 (1960) 99-101.
[11] WAGNER, H.N., McAFEE, J.G. and WINKELMAN, J.W., Arch. int. Med. 109 (1962) 77-88.
[12] BLAUSTEIN, A., The Spleen, McGraw-Hill Book Company, Inc., New York, Toronto, London (1963) 83.
[13] ROBBINS, S.L., Textbook of Pathology with Clinical Application, 2nd ed., W.B. Saunders Company, Philadelphia and London (1962) 253.

RÉSULTATS DE L'APPLICATION CLINIQUE DE LA SCINTIGRAPHIE DE LA RATE DANS 500 CAS: POSSIBILITÉS ET LIMITES

J. FISCHER
PREMIÈRE CLINIQUE ET POLYCLINIQUE MÉDICALE
ET
R. WOLF
INSTITUT DE RADIOLOGIE CHIMIQUE DE L'UNIVERSITÉ DE MAYENCE,

Abstract — Résumé — Аннотация — Resumen

RESULTS OF CLINICAL APPLICATION OF SCINTILLATION SCANNING OF THE SPLEEN ON 500 PATIENTS: POSSIBILITIES AND LIMITS. After injecting erythrocytes marked with radioactive substances and artificially damaged there is a rapid clearance of these cells from the blood-stream and sequestration in the spleen. The resultant high concentration of radioactivity in the spleen permits a good scintigraphic demonstration of the organ. For many reasons $Na_2Cr^{51}O_4$ seems at present to be the most suitable substance for labelling erythrocytes, and alteration by heat the most practical means of damaging the cells.

The systematic application of spleen scintigraphy on over 500 patients showed the following indications for this method:

(1) Demonstration of enlargement of the spleen is not possible by clinical or roentgenological methods; (2) Verification of tumours in the upper left abdominal region; (3) Demonstration of accessory spleens after splenectomy; (4) Demonstration of ectopic spleens (situs inversus, ptosis); (5) Demonstration of parenchymal defects in the spleen (e.g. intrasplenic bleeding, infarcts of the spleen, necrosis of the spleen and intrasplenic cysts).

By planimetric measurements of the scintigram area and by calculating the "splenic surface area index" (= scintigram area/body surface of the patient) a good quantitative estimation of the extent of spleen enlargement may be obtained. In healthy persons the surface area of the scintigram does not exceed 70 - 80 cm^2 and the splenic surface-area-index lies normally within $2.5 - 4.5 \times 10^{-3}$. A comparison with the clinical findings showed that only one third of the spleens which were found by scintigraphy to be positively enlarged could be detected by percussion and palpation. In various diseases the clinical estimation of spleen enlargement is false in an even higher percentage of the cases.

Only when the spleen has completely lost the ability to sequestrate heat-altered erythrocytes is the scintigraphic depiction of the spleen impossible. Such cases, however, seem to be extremely rare; we have so far observed only one. Up to now the information on form, size, position and parenchymal defects which are afforded by scintigraphy, cannot be obtained by any other method, including special roentgenological methods.

The process makes few demands on the patient, so that even very ill persons can tolerate it; it is not dangerous and can be performed on walking patients. The load of radiation dose to the patient is slight. For the spleen, depending on the volume, it is of the order of a few rad. The dose to the sexual organs and the whole body is on the average 40 mrad, which is far less than arises in many simple routine roentgenological examinations.

RÉSULTATS DE L'APPLICATION CLINIQUE DE LA SCINTIGRAPHIE DE LA RATE DANS 500 CAS: POSSIBILITÉS ET LIMITES. Après injection d'érythrocytes marqués avec une substance radioactive et altérés artificiellement, on constate une rapide élimination de ces cellules de la circulation sanguine et accumulation dans la rate. Il en résulte une forte concentration de radioactivité dans cet organe, ce qui permet d'en faire de bons scintigrammes. Pour plusieurs raisons, c'est $Na_2{}^{51}CrO_4$ qui semble constituer actuellement la substance la plus appropriée pour le marquage des érythrocytes; le traitement thermique est le meilleur moyen de provoquer une altération des cellules.

Une campagne d'emploi systématique de cette méthode sur plus de 500 malades a donné les résultats suivants:

a) Constatation d'une splénomégalie qu'il était impossible de déceler par des méthodes cliniques ou avec des rayons X; b) Vérification de l'existence de tumeurs dans l'hypochondre gauche; c) Constatation de l'existence de rates accessoires après splénectomie; d) Constatation de l'existence de rates ectopiques (situs inversus, ptose); e) Constatation de troubles dans le parenchyme de la rate (hémorragie, infarctus de la rate, nécrose de la rate, kyste intrasplénique).

Par mesure planimétrique de l'aire du scintigramme et calcul de l'«indice de surface» (aire du scintigramme/surface totale du corps), on peut obtenir une bonne estimation quantitative de l'hypertrophie de la rate. Chez un sujet sain, l'aire du scintigramme ne dépasse pas 70 à 80 cm^2 et l'«indice de surface» est normalement de l'ordre de $2,5$ à $4,5 \cdot 10^{-3}$. En comparant les résultats cliniques avec ceux de la scintigraphie, on a constaté que seulement le tiers des splénomégalies diagnostiquées par scintigraphie pouvaient être détectées par percussion et palpation. Pour diverses affections, le diagnostic clinique de l'hypertrophie de la rate était erroné dans un pourcentage encore plus élevé de cas.

Ce n'est que lorsque la rate a complètement perdu son pouvoir d'accumulation des érythrocytes traités thermiquement que la scintigraphie ne donne pas de résultats. Mais ces cas sont extrêmement rares; les auteurs n'en ont observé qu'un seul. Aucune autre méthode, même pas les techniques radiologiques spéciales, ne donne les renseignements sur la forme, les dimensions, la position et sur les altérations du parenchyme que l'on peut obtenir par scintigraphie.

La scintigraphie affecte très peu le patient, si bien que même des personnes très atteintes peuvent la tolérer; elle n'est pas dangereuse et peut même être pratiquée sur des sujets qui ne sont pas hospitalisés. La dose de rayonnement absorbée par le malade est faible. Pour la rate, elle est de l'ordre de quelques rad et varie suivant le volume de l'organe. Pour les organes sexuels et pour le corps entier, la dose est en moyenne de 40 mrad, ce qui est très inférieur à la dose reçue à l'occasion de nombreux examens radiologiques courants.

РЕЗУЛЬТАТЫ КЛИНИЧЕСКОГО ПРИМЕНЕНИЯ СЦИНТИЛЛЯЦИОННОГО СКЕННИРОВАНИЯ СЕЛЕЗЕНКИ У 500 БОЛЬНЫХ: ВОЗМОЖНОСТИ И НЕДОСТАТКИ. После введения эритроцитов, меченных радиоактивными веществами и искуственно поврежденных, наблюдалось быстрое выделение этих клеток из тока крови и захват их в селезенке. Результирующая высокая концентрация радиоактивных веществ в селезенке позволяет получить хорошее сцинтиграфическое изображение этого органа. По ряду причин $Na_2Cr^{51}O_4$ кажется в настоящее время наиболее подходящим веществом для мечения эритроцитов, а изменение температуры — наиболее практичным методом повреждения этих клеток.

Систематическое применение сцинтиграфии селезенки более чем у 500 больных установило следующие показания для применения этого метода:

1) Демонстрация увеличения селезенки невозможна клиническими или рентгенологическими методами. 2) Диагностика опухолей в левом верхнем отделе брюшной полости. 3) Демонстрация дополнительных селезенок после спленэктомии. 4) Демонстрация эктомии селезенки (situs inversus, опущение). 5) Демонстрация паренхиматозных дефектов в селезенке (например, внутриселезеночное кровотечение, инфаркты селезенки, некроз селезенки, внутриселезеночная киста).

Путем планиметрического измерения площади сцинтиграммы и расчета "индекса площади поверхности селезенки" (= площадь сцинтиграммы/поверхность тела больного) можно получить хорошую количественную характеристику степени увеличения селезенки. У здоровых людей площадь поверхности сцинтиграммы не превышает 70—80 $см^2$, а индекс площади поверхности селезенки находится обычно в пределах $2,5-4,5 \cdot 10^{-3}$. Сравнение с клиническими данными показало, что только в одной трети случаев увеличение селезенки, обнаруженное при сцинтиграфии, может быть диагносцировано путем перкуссии и пальпации. При различных заболеваниях клиническая оценка увеличения селезенки является ошибочной в еще большем проценте случаев.

Получение сцинтиграфического изображения селезенки невозможно лишь в случае полной утери селезенкой способности захвата измененных воздействием тепла эритроцитов. Однако такие случаи, очевидно, крайне редки; авторы наблюдали только один такой случай.

Данные о форме, размере, положении и паренхиматозных дефектах, полученные путем сцинтиграфии, не удалось получить до настоящего времени никаким другим методом, включая специальные рентгенологические методы.

Метод требует от больного немногое, его могут перенести даже очень больные люди; он не опасен и может быть применен у амбулаторных больных. Величина дозы облучения больного небольшая. Для селезенки, в зависимости от объема, она составляет порядка нес-

колько рад. Доза облучения половых органов и всего тела составляет в среднем 40 мрад, что значительно ниже доз, получаемых при многих простых обычных рентгенологических исследованиях.

RESULTADOS DE LA APLICACIÓN CLÍNICA DE LA CENTELLEOGRAFÍA DEL BAZO A 500 PACIENTES: POSIBILIDADES Y LÍMITES. Cuando se inyectan eritrocitos marcados con sustancias radiactivas y deliberadamente dañados, el bazo los capta con rapidez, eliminándolos de la corriente sanguínea. La concentración de radiactividad que este proceso provoca en el hazo permite obtener un buen centelleograma de dicho órgano. Por varias razones, el $Na_2{}^{51}CrO_4$ parece ser la sustancia más adecuada para marcar eritrocitos; la mejor manera de dañarlos es someterlos a la acción del calor.

Sistemáticamente aplicada a más de 500 enfermos, la centelleografía del bazo ha demostrado ser de suma utilidad para las investigaciones siguientes:

a) Comprobación de la dilatación del bazo cuando no es posible hacerlo por métodos clínicos o roentgenológicos; b) Comprobación de la presencia de tumores en la región abdominal superior izquierda; c) Demostración de la existencia de bazos accesorios después de la esplenectomía; d) Demostración de ectopías esplénicas (situs inversus, ptosis); e) Demostración de la presencia de defectos parenquimatosos en el bazo (por ejemplo: hemorragia intraesplénica, infartos del bazo, necrosis del bazo, quistes intraesplénicos).

Se puede obtener una buena estimación cuantitativa de la dilatación del bazo midiendo por planimetría la superficie del centelleograma y calculando el "índice de la superficie esplénica" (superficie del centelleograma/superficie del cuerpo del paciente). En las personas sanas, la superficie del centelleograma no es superior a 70-80 cm^2 y dicho índice está generalmente comprendido entre 2,5 y $4,5 \cdot 10^{-3}$. Una comparación con los resultados clínicos ha puesto de manifiesto que sólo en una tercera parte de los casos una dilatación del bazo determinada categóricamente por centelleografía ha podido ser detectada por percusión y palpación. Esta diferencia es todavía más acentuada en diversas enfermedades.

La visualización del bazo sólo resulta imposible cuando esta glándula ha perdido completamente la capacidad de captar los eritrocitos dañados por el calor. Esto, al parecer, ocurre con muy poca frecuencia; hasta ahora, los autores sólo han observado un caso. Ningún otro método, incluidos los métodos roentgenológicos especiales, permite obtener los datos que la centelleografía proporciona sobre la forma, el tamaño, la posición y los defectos parenquimatosos del bazo.

Esta exploración es tolerada incluso por personas gravemente enfermas; no es peligrosa y se puede someter a ella a enfermos ambulantes. La dosis de radiación que recibe el paciente es pequeña; para el bazo, es de unos pocos rad, según el volumen de la glándula. La dosis media a las gónadas y al organismo entero es de 40 mrad, es decir, muy inferior a la que el paciente recibe en muchos de los exámenes roentgenológicos corrientes.

1. INTRODUCTION

L'emploi de la méthode scintigraphique nous permet d'enregistrer des organes tels que la thyroïde, le foie, les reins ou le pancréas. Cette méthode consiste à marquer des substances accumulées plus ou moins sélectivement dans l'organe en question par un isotope radioactif. A l'heure actuelle, on ne connaît encore aucune substance s'accumulant sélectivement dans la rate. Après une injection d'or colloïdal radioactif en vue d'une étude scintigraphique du foie on observe parfois une fixation splénique et médullaire (Fig. 1). Toutefois ce phénomène, observé surtout lorsqu'il s'agit de formes avancées de cirrhoses, est inconstant [1, 2]; il exprime seulement l'activité phagocytaire générale du système réticulo-histiocytaire pour des substances colloïdales.

On obtient de même une image de la rate après l'injection de $Cl_2{}^{197}Hg$. Etant donné que cette substance s'accumule simultanément en concentration beaucoup plus forte dans d'autres organes parenchymateux, elle ne se prête pas non plus très bien à la gammagraphie splénique [3] (fig. 2).

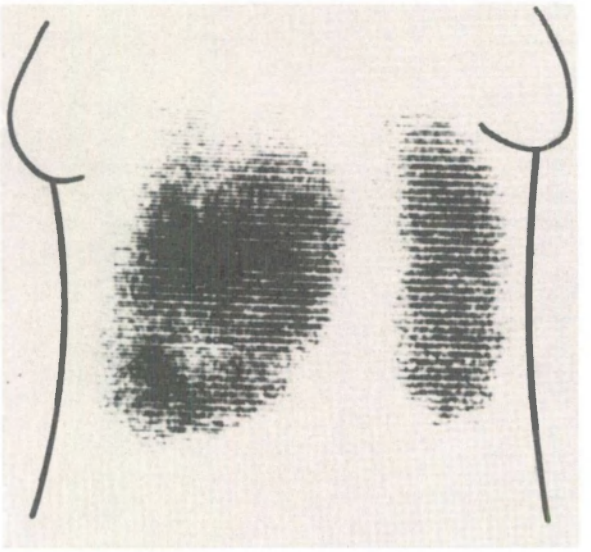

Figure 1

Photoscintigramme de face après injection intraveineuse de 200 μc d' ^{198}Au colloidal dans un cas de cirrhose hépatique. Bonne image du foie et de la rate.

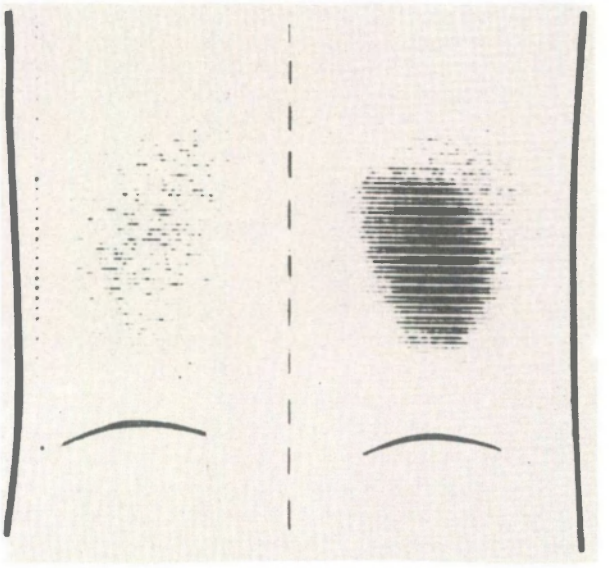

Figure 2

Photoscintigramme de dos 24 h après injection intraveineuse de 200 μc de $Cl_2{}^{197}Hg$ chez un malade, après néphrectomie du rein gauche. L'ombre du foie se projette à côté du rein droit; de plus, on voit la silhouette de la rate.

Deux faits connus depuis assex longtemps en hématologie sont les piliers de base de la scintigraphie sélective de la rate. Mais on ne les a mis en corrélation que depuis peu.

Depuis 1950, on sait que les hématies peuvent être marquées de manière irréversible par le ^{51}Cr [4]. Cette technique de marquage est actuellement utilisée dans le monde entier pour déterminer la survie érythrocytaire. Des mesures effectuées à la surface du corps après l'injection d'hématies marquée, ont montré que l'on trouve une haute activité du ^{51}Cr dans la rate, surtout chez les sujets porteurs de la tare sphérocytaire. HARRIS, McALISTER et PRANKERD [5] ont pu démontrer que des sphérocytes artificiels (par exemple, des érythrocytes revêtus d'anticorps anti-D incomplets ou des érythrocytes altérés par des moyens physiques ou chimiques) sont captés dans la rate de la même manière mais beaucoup plus rapidement que les sphérocytes d'origine naturelle [5].

En injectant des hématies marquées au ^{51}Cr et altérées par un procédé sérologique, chimique ou physique, on peut donc obtenir une haute concentration de ^{51}Cr dans la rate et réaliser de manière satisfaisante une image de cet organe par scintigraphie.

La première scintigraphie de la rate a été réalisée par JOHNSON et al. en utilisant des hématies marquées, revêtues d'anticorps anti-D incomplets [6, 7, 8]. Pour des raisons pratiques ce procédé convient moins bien que celui qui utilise des hématies altérées par le chauffage. Cette méthode fut employée pour la première fois par WINKELMAN et al. [9], WAGNER et al. [10, 11], JAMMET et al. [12]. Elle a trouvé entre temps une application de plus en plus étendue [13, 19, 20, 21, 22, 23, 24, 25, 26].

Ce nouveau procédé diagnostique a une très grande importance parce qu'il permet en toutes circonstances la mise en évidence de la rate, ce qui est souvent difficile ou impossible par les moyens cliniques ou par les techniques radiologies classiques.

2. TECHNIQUE

On marque environ 5 ml d'érythrocytes autologues avec 300 - 400 μc de $Na_2{}^{51}CrO_4$, selon les techniques habituelles. L'altération des hématies de préférence par chauffage, s'effectue dans un bain-marie à 49, 5°C pendant 20 min. Par le chauffage, la majorité des érythrocytes se transforme en sphérocytes et en même temps on voit apparaître des fragments érythrocytaires d'un diamètre inférieur à 2,5 μ. La préparation des hématies doit se faire sans hémolyse.

L'injection des hématies altérées par le chauffage est très bien tolérée. Jusqu'à présent, parmi nos 500 malades, nous n'avons observé aucune réaction secondaire, ni aucune complication.

L'appareil utilisé pour tous nos examens scintigraphiques est le MAGNASCANNER-PICKER. Par principe nous avons toujours établi deux scintigrammes synchronisés en utilisant un stylo pour l'un et la photographie pour l'autre. Chez chaque malade nous avons réalisé la scintigraphie en deux plans: en général de profil sur le côté droit et de dos, parfois aussi de face afin d'obtenir des données plus exactes sur l'étendue de l'organe (fig. 3).

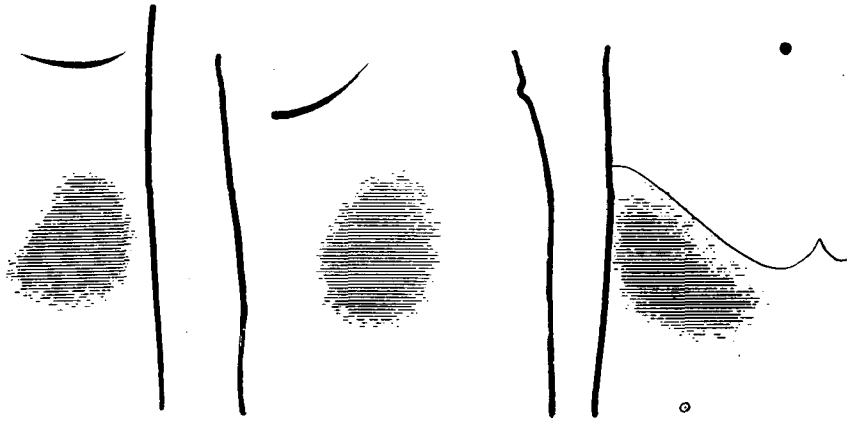

Figure 3

Scintigraphie de la rate après injection intraveineuse d'hématies altérées par chauffage. A gauche scintigraphie de face, au centre de profil (malade couché sur le côté droit), à droite scintigraphie de dos.

3. BASE BIOLOGIQUE

Chez les sujets normaux l'élimination des hématies altérées se traduit au cours de l'enregistrement par une courbe bi-phasique: 60 - 75% de l'activité injectée est éliminée du sang en une courte période de 3,0 - 5,5 min, le reste en une plus longue période de 30 - 50 min.

On retrouve régulièrement la courte période dans la courbe d'activité splénique (fig. 4). On peut donc la qualifier comme étant la période d'extraction spécifiquement splénique. Une étude approfondie de ce processus a montré que l'on peut tirer des conclusions sur le fonctionnement proprement dit de la rate et du système réticulo-histiocytaire [27] à partir de la vitesse d'élimination que l'on vient de mesurer.

Dans des cas pathologiques la décroissance de l'activité du sang peut être fortement retardée. Dans ces cas on constate sans exception une diminution dans l'accumulation de l'activité de la rate. Par contre la courbe de l'activité hépatique montre une augmentation.

Ces faits sont lourds de conséquences pour la scintigraphie de la rate.

a) Si le processus d'extraction selon lequel les hématies passent du sang dans la rate, est retardé ou fortment diminué, l'activité maximale de la rate est également diminuée; ceci entraîne des oscillations statistiques assez importantes et une différence de niveau moins prononcée entre la rate et les tissus environnants. Ainsi les conditions optimales ne sont plus réalisées [28].

b) Si l'accumulation de l'activité dans le foie est accrue, on voit apparaître cet organe dans le scintigramme. Dans le scintigramme de profil il est alors parfois bien difficile de délimiter la rate du foie et cela peut donner lieu à des confusions. Dans certains cas on est obligé d'augmenter le contraste pour obtenir une séparation nette entre la rate et le foie.

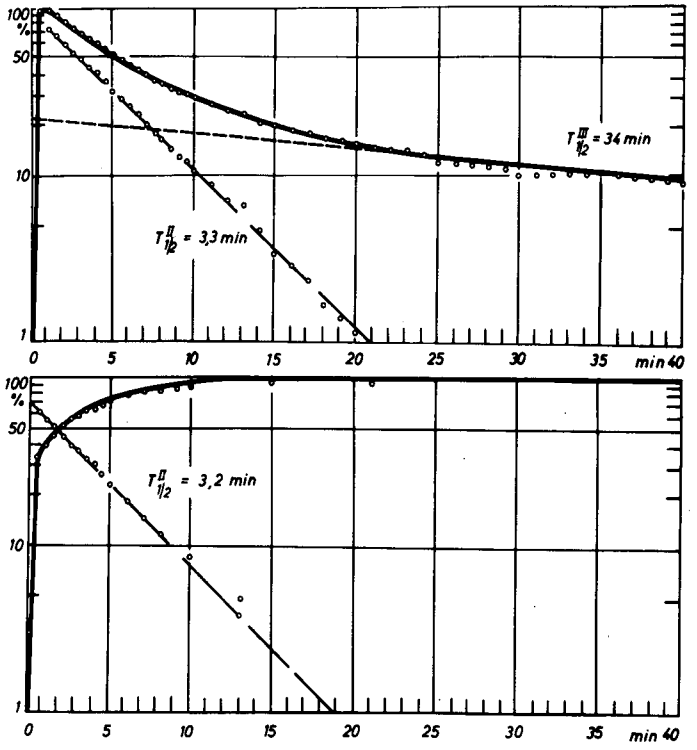

Figure 4

Courbe d'élimination des érythrocytes altérés du sang (diagramme du haut) et de leur accumulation dans la rate (diagramme du bas). Les courbes ont été normalisées dans leur maximum à 100%. Les lignes en pointillé représentent les composantes obtenues graphiquement à partir de la courbe bi-phasique.

4. LE SCINTIGRAMME ET SON INTERPRÉTATION

Le scintigramme est toujours l'expression visuelle d'une fonction bien déterminée d'un organe. En ce qui concerne la fonction de la rate, c'est son intensité d'absorption et de séquestration des sphérocytes qui est en cause. Les examens histologiques ont montré que la séquestration des hématies altérées par le chauffage se fait dans le réseau réticulaire périsinusal. Ces hématies altérées sont arrêtées dans ce filtre, parce qu'elles ont perdu leur plasticité qui normalement leur permet de passer à travers les pores qui ont un diamètre inférieur au leur. Il s'agit donc d'un filtrage qu'on pourrait qualifier de mécanique et qui arrête les sphérocytes dans la rate. Par contre, les fragments érythrocytaires d'un diamètre inférieur à 2,5 μ peuvent passer cette barrière et se réintégrer au sang. Leur élimination se place dans la longue période de la courbe bi-phasique que nous avons déjà mentionnée plus haut. Ils sont ensuite phagocytés par les cellules du système réticulo-histiocytaire.

Des changements de l'architecture histologique de la rate, notamment du réseau réticulaire périsinusal, peuvent entraîner une diminution de la capacité de séquestration. Ces changements histologiques peuvent être de nature différente: affection primaire des cellules réticulaires, prolifération des éléments lymphatiques pathologiques, métaplasie médullaire dans la rate ou destruction du tissu splénique et remplacement de ce dernier par du tissu conjonctif. Si les aréales de fixation défectueuses dépassent une certaine dimension, elles s'extériorisent dans le scintigramme.

Dans des cas exceptionnellement rares le tissu splénique normal peut être complètement bouleversé. La rate perd alors toute sa faculté de séquestrer les hématies altérées. Parmi 500 cas, nous avons observé une seule fois un tel cas chez une malade atteinte d'une leucémie myéloide en poussée myéloblastique. L'examen histologique de cette rate dont le volume était fortement augmenté (3700 g), a montré que le réseau réticulaire périsinusal avait été complètement remplacé par des plaques homogènes de myéloblastes. JOHNSON et al. ont décrit un cas analogue chez une malade également atteinte de leucémie myéloide chronique [7]. JAMMET et al. ont observé une fixation splénique défectueuse dans un cas de sarcome splénique, et l'impossibilité de la rate à fixer des hématies dans un cas de maladie de Hodgkin [12].

Mais il semble qu'il s'agisse ici de cas tout à fait exceptionnels, car nous avons observé plusieurs malades où la fixation splénique, bien qu'inférieure à 20% de la totalité de l'activité injectée, ne nous a nullement empêché d'obtenir une image scintigraphique satisfaisante de l'organe.

5. LES INDICATIONS DE LA SCINTIGRAPHIE DE LA RATE

La scintigraphie de la rate est la méthode de choix pour étudier la topographie, la forme et les dimensions de la rate. Etant donné qu'elle ne présente aucun risque pour le malade et qu'elle est très fidèle dans ses résultats, elle fait déjà partie du répertoire diagnostique de la clinique avec les indications suivantes:

a) mise en évidence des splénomégalies non décelables par les moyens cliniques et radiologiques,
b) appréciation quantitative des dimensions de la rate,
c) identification des tumeurs dans l'hypochondre gauche (fig. 5),
d) recherche des rates accessoires après la splénectomie (fig. 6),
e) mise en évidence des rates ectopiques (fig. 7),
f) mise en évidence des lésions spléniques, par exemple: infarctus, nécroses, kystes intraspléniques, rupture de la rate (fig. 8, 9, 10).

6. APPRÉCIATION QUANTITATIVE DES DIMENSIONS ET DU VOLUME DE LA RATE PAR LA SCINTIGRAPHIE

6.1. Appréciation quantitative des dimensions

Comme nous avons pu le démontrer, on peut obtenir une image scintigraphique très fidèle de la rate, en respectant certaines conditions lors de l'examen [28].

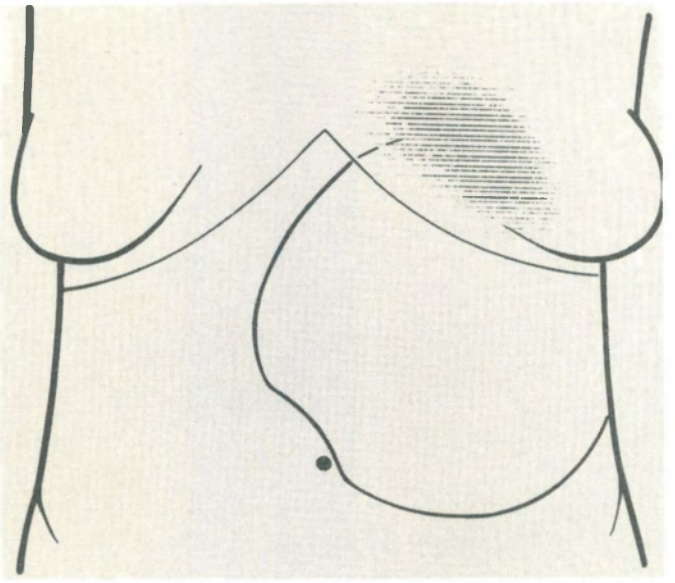

Figure 5

Styloscintigramme de face chez une malade avec une grosse tumeur de l'hypochondre gauche. La tumeur ne correspond pas à la rate. Il s'agissait d'un neurinome de l'espace rétropéritonéal, identifié lors de l'opération.

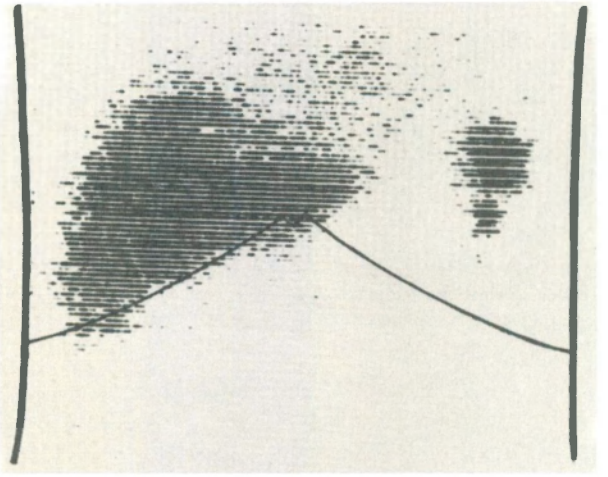

Figure 6

Photoscintigramme de dos, 18 ans après l'ablation de la rate en raison d'un traumatisme. On remarque une rate accessoire hypertrophiée ainsi qu'une forte fixation hépatique et médullaire.

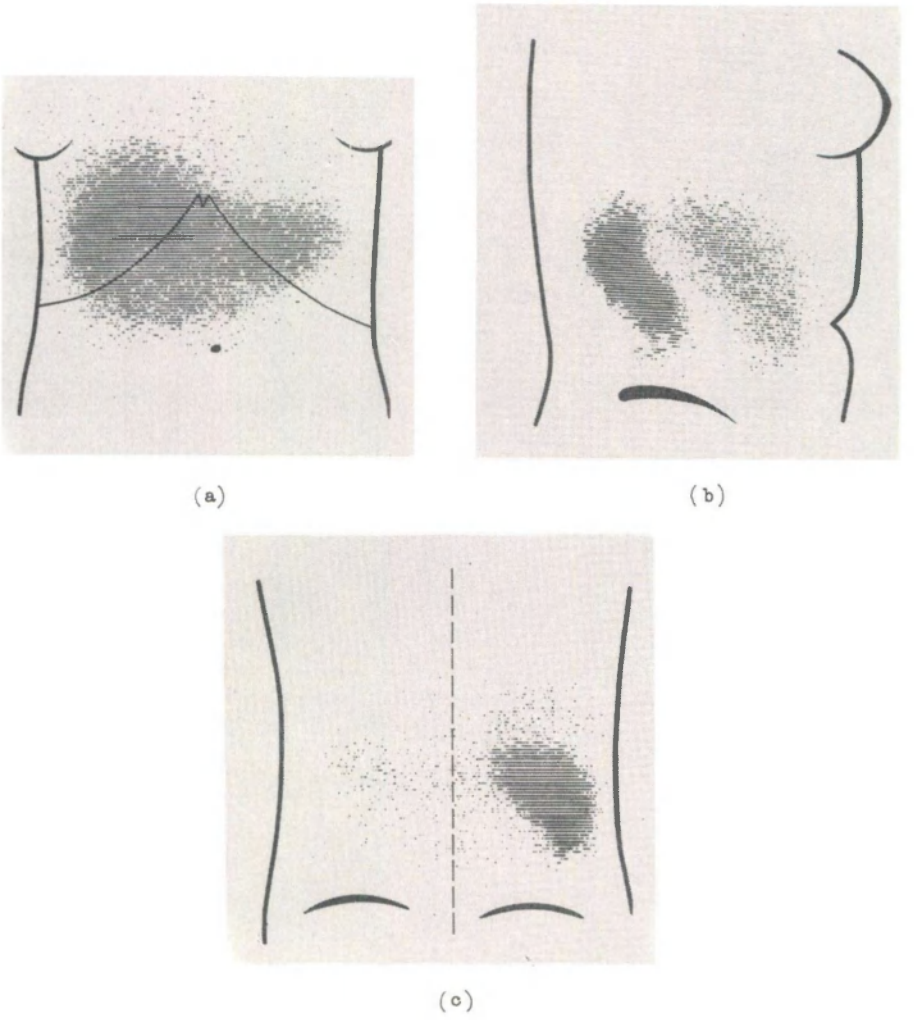

Figure 7

Styloscintigrammes chez une malade présentant une ectopie de la rate (situs inversus partialis) après injection d'hématies altérées par chauffage et marquées avec du ^{51}Cr: a) de face, b) de profil, la malade étant couchée sur le côté gauche, c) de dos.

Par la planimétrie, on peut facilement évaluer la superficie du scintigramme. Le scintigramme de profil sur le côté droit présente presque sans exception la plus grande superficie. Ceci correspond bien à la disposition anatomique de la rate. Chez des sujets normaux la superficie scintigraphique de la rate ne dépasse généralement pas 80 cm^2.

Pour pouvoir mieux comparer nous avons établi une relation entre la superficie scintigraphique de la rate et la superficie du corps du malade et nous avons ainsi défini un indice de superficie splénique (ISS), qui nor-

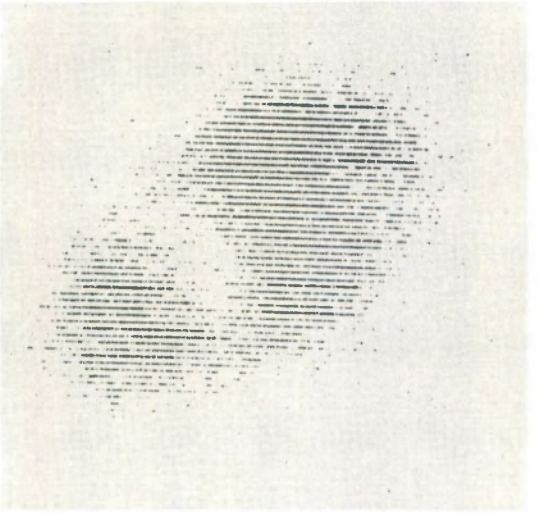

Figure 8

Styloscintigramme. Infarctus splénique.

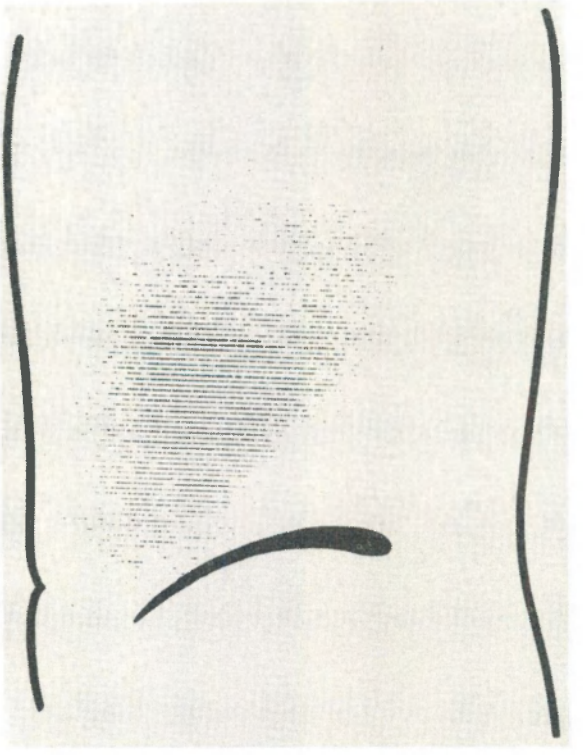

Figure 9

Styloscintigramme de profil. Forte augmentation de la rate dans un cas de mononucléose infectieuse avec de larges aréales de fixation défectueuse surtout dans le pôle supérieur.

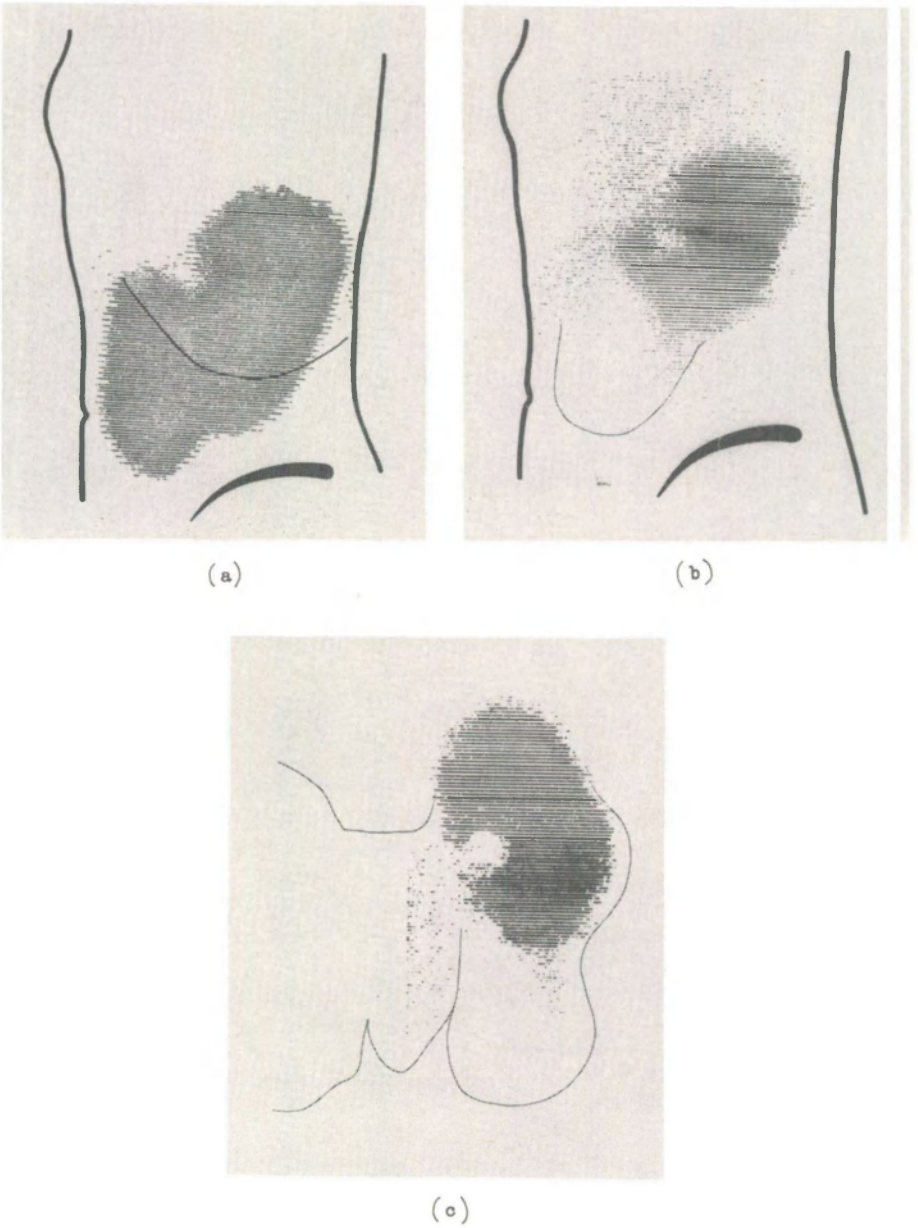

Figure 10

Styloscintigrammes d'une splénomégalie extrême: a) premier examen, b) deuxième examen dix mois après; il montre une large nécrose dans le pôle inférieur. c) le scintigramme de la pièce anatomique pathologique montre la concordance avec les lésions enregistrées in vivo.

malement varie entre 2, 8 et $4,5 \cdot 10^{-3}$, chez des sujets ayant une rate normale [16].

La détermination de l'indice de superficie splénique, permet pour la première fois d'établir des données quantitatives sur le degré de la splénomégalie. De plus il nous donne l'objectivité désirée pour savoir dans quelle mesure nous sommes capables de déceler une augmentation de la rate par les moyens cliniques de la percussion et de la palpation. En prenant comme critère pour une rate ayant certainement augmenté de volume, une superficie splénique supérieure à 80 cm^2 ou un indice de superficie splénique au-dessus de $4,5 \cdot 10^{-3}$, nous avons obtenu les chiffres indiqués dans le tableau I.

TABLEAU I

DÉTECTION DE SPLÉNOMÉGALIE

Maladies	Nombre de cas	Splénomégalie décelée par		Pourcentage de cas décelés par les méthodes cliniques
		scintigraphie	méthodes cliniques	
Maladie de Hodgkin	62	38	4	10,5
Polycythémie	47	37	4	10,8
Leucémie	62	56	29	51,7
Divers	291	186	48	25,8
Total	462	317	85	26,8

Nos résultats démontrent que dans 26,8% de nos cas seulement, les moyens cliniques ont permis de constater une augmentation de la rate. Ceci signifie que dans environ 75% des cas n'ayant pas été présélectionnés, l'augmentation de la rate se soustrait à la constatation clinique.

Il faut prendre aussi en considération le fait que certains états pathologiques comme par exemple l'agénésie ou l'atrophie, les ectopies ainsi que les rates accessoires, échappent totalement aux méthods d'investigation cliniques tout comme à l'investigation radiologique classique. De plus, il n'est pas rare de considérer à tort une tumeur de l'hypochondre gauche comme étant la rate.

Si l'on incorpore également ces derniers cas dans notre considération d'ensemble, nous en arrivons à la conclusion suivante que les méthodes cliniques et classiques de la radiographie ne nous donne que dans 17% des cas des précisions valables sur la topographie et les dimensions de la rate (tableau II).

Mis à part l'événement rarissime d'une asplénie fonctionnelle, telle que nous l'avons décrite dans un chapitre précédent, il nous est toujours possible par la scintigraphie de la rate de réaliser avec précision une image de cet organe, et c'est une loi constante,

TABLEAU II

RÉSULTATS DE LA SCINTIGRAPHIE DE LA RATE DANS 500 CAS

Nombre de cas	Résultats
14	La tumeur palpée ne correspond pas à la rate, contrairement à la supposition clinique
9	Rate de volume inférieur à la normal (ISS < 2,8).
12	Malades splénectomisés (2 à 31 and après l'ablation). En trois cas, mise en évidence de rates accessoires.
3	Situs inversus totalis (2 malades) Situs inversus partialis (1 malade).
462	La rate nettement augmentée de volume (ISS > 4,5) n'a été décelée cliniquement que dans 26,8% de cas.

6.2. Appréciation du volume

Il est difficile de déterminer directement le volume de la rate à l'aide de la scintigraphie. Pour en arriver là, il faudrait connaître la section transversale maximale de l'organe et perpendiculairement à celle-ci l'étendue en profondeur. Comme la rate est suspendue de façon très mobile dans l'organisme chaque changement de position du malade est suivi d'une rotation notable de l'axe splénique. De ce fait on ne peut pas connaître avec exactitude son étendue en profondeur, exception faite des splénomégalies importantes.

Théoriquement on peut établir une corrélation entre la superficie scintigrafique et le volume de la rate en postulant que l'augmentation de l'organe se fait selon un même accroissement dans les trois dimensions.

Pour ce cas on peut appliquer l'équation suivante:

$$V = a F^{3/2}$$

où a est le facteur de proportionalité et F est la superficie du scintigramme.

Cette équation correspond aux relations numériques qui ont été indiquées par DOERING, pour la détermination du poids de la thyroide à base du scintigramme [29].

Dans 19 cas, nous avons pu déterminer le poids de la rate prélevée par splénectomie (une fois par autopsie) peu après avoir fait une scintigraphie in vivo.

La courbe obtenue en mettant en relation la superficie scintigraphique et le poids de la rate, est représentée dans la figure 11. Comme le démontre ce diagramme les valeurs théoriques concordent fort bien avec les valeurs empiriques jusqu'à un poids d'environ 800 g. Pour des volumes

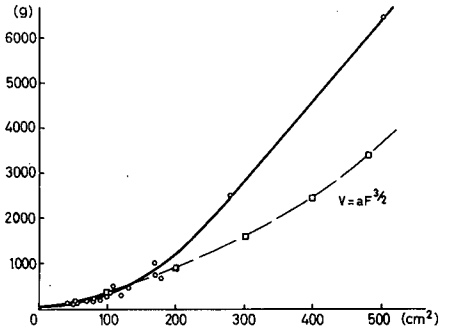

Figure 11

Nomogramme pour déterminer le volume splénique basé sur la superficie de scintigramme.
(O —— O: courbe empirique)
(□ ---- □: courbe théorique)

supérieurs, le poids réel semble être plus élevé que les valeurs calculées. Il faut cependant considérer que la courbe a été établie à partir d'un nombre relativement faible de cas. Des examens approfondis vont montrer si on peut arriver par ce moyen à établir un nomogramme qui permette de déduire le volume de la rate en se basant sur la superficie scintigraphique.

Dans les splénomégalies importantes on peut constater que le changement de position du malade n'est plus accompagné d'une rotation de l'organe. Ainsi on peut obtenir par la scintigraphie en deux plans les mesures nécessaires pour calculer le volume.

7. CONCLUSION

La scintigraphie de la rate est une méthode de recherches extrêmement importante pour la clinique. Les possibilités fondamentales qu'elle offre consistent en ceci: pouvoir reproduire pour la première fois de manière simple et toujours fidèle la forme, la position et les dimensions de cet organe. Elle permet en outre des diagnostics qu'il était impossible de formuler jusqu'à présent d'après les autres méthodes, comme par exemple prouver la perte de tissus parenchymateux en cas d'infarctus et de nécrose splénique. L'atrophie de la rate, des rates accessoires et des ectopies ne peuvent être pratiquement décelées que par cette méthode. Elle permet d'éliminer avec certitude toutes les tumeurs de l'hypochondre gauche, qui ne sont pas d'origine splénique.

En déterminant la superficie du scintigramme et en calculant l'indice de la superficie splénique, on peut obtenir des données quantitatives sur les dimensions de l'organe.

Outre les facteurs connus qui limitent en général les possibilités de la scintigraphie, l'état fonctionnel de la rate peut être lui aussi un facteur limitatif. Quand la rate n'est plus capable de séquestrer des sphérocytes, on ne peut pas, à partir de cette méthode, représenter cet organe par un scintigramme. Mais ceci ne joue aucun rôle dans l'emploi pratique de cette méthode car de tels cas sont extrêmement rares.

BIBLIOGRAPHIE

GRUNDMANN, E., Über die Stellung der Milz bei den hämolytischen Anämien, Acta hep.-splenol. (Stuttgart) 8 (1961) 34.

GRUNDMANN, E., Die normale und die pathologische Histologie der Milz unter Bezug auf die Milzfunktionen, Verh. dtsch. Ges. inn. Med. 1963, J.F. Bergmann, München (1963) 779.

JANDL, J.H., SIMMONS, R.L. and CASTLE, W.B., Red cell filtration and the pathogenesis of certain hemolytic anemias, Blood 18 (1961) 133.

RÉFÉRENCES

[1] MAGNENAT, P. et DELALOYE, B., La scintigraphie du foie et de la rate dans la cirrhose, in Szintigraphie und Radiokardiographie, Symp. Schweiz. Akad. Med. Wiss., Basel 1962, Schwabe & Co. Verlag Basel/Stuttgart (1963) 136.

[2] STROUN, J., MEYKADEH, F., SCHERER, J., LAPERROUZA, C. et WENGER, P., Apparition d'un splénogramme au cours de l'épatoscintillographie à l'or colloïdal radioactif, Helv. med. Acta 30 (1963) 557.

[3] FISCHER, J. et WOLF, R., Szintigraphie mit $^{197}HgCl_2$, German med. Research (Freiburg i. Br.) (in press).

[4] GRAY, S.J. and STERLING, K., The tagging of red cells and plasma proteins with radioactive chromium, J. clin. Invest. 29 (1950) 1604.

[5] HARRIS, I.M., McALISTER, J.M. and PRANKERD, T.A.J., The relationship of abnormal red cells to the normal spleen, Clin. Sci. 16 (1957) 223.

[6] JOHNSON, Ph.M., HERION, J.C. and MOORING, S.L., Scintillation scanning of the normal human spleen utilizing sensitized radioactive erythrocytes, Radiology 74 (1960) 99.

[7] JOHNSON, Ph.M., WOOD, E.H. and MOORING, S.L., Splenic scintillation scanning, Amer. J. Roentgenol. 86 (1961) 757.

[8] JOHNSON, Ph.M. and HERION, J.C., Technical considerations in scintillation scanning of the human spleen, Radiology 76 (1961) 438.

[9] WINKELMAN, J.W., WAGNER, Jr., H.N., McAFEE, J.G. and MOZLEY, J.M., Visualization of the spleen in man by radioisotope scanning, Radiology 75 (1960) 465.

[10] WAGNER, Jr., J.N., McAFEE, J.G. and WINKELMAN, J.W., Splenic disease diagnosis be radioisotope scanning, Arch. intern. Med. 109 (1962) 673.

[11] WAGNER, Jr., H.N., RAZZAK, M.A., GAERTNER, R.A., CAINE, jr., W.P. and FEAGIN, O.Th., Removal of erythrocytes from the circulation, Arch. Int. Med. 110 (1962) 90.

[12] JAMMET, H.R., GONGORA, G., BILSKI-PASQUIER, G., DUHAMEL, G. et MARCHAL, G., L'autogammagraphie splénique, Sem. Hôp. Paris 38 (1962) 1047.

[13] FISCHER, J., Radio-Isotope in der Hämatologie. I. Int. Symp. Freiburg i. Br. 1962, Friedrich-Karl Schattauer Verlag, Stuttgart (1963) 246.

[14] FISCHER, J., Klinik und Diagnostik der Milzerkrankungen, Verh. dtsch. Ges. inn. Med. 1963, J.F. Bergmann, München (1963) 798.

[15] FISCHER, J. et WOLF, R., Die szintigraphische Darstellung der Milz mit Radiochrom (^{51}Cr), Dtsch. med. Wschr. 88 (1963) 305.

[16] FISCHER, J. et WOLF, R., Die quantitative Abschätzung der Milzgrösse mit Hilfe der Szintigraphie, Dtsch. med. Wschr. 88 (1963) 1430.

[17] FISCHER, J. et WOLF, R., Grundlagen und Technik der Milzszintigraphie, Acta hep.-splenol. (Stuttgart) 10 (1963) 209.

[18] FISCHER, J. et WOLF, R., Die Szintigraphie der Milz mit ^{51}Cr, in Szintigraphie und Radiokardiographie, Symp. Schwiez. Akad. Med. Wiss. Basel 1962, Schwabe & Co. Verlag Basel/Stuttgart (1963) 184.

[19] FISCHER, J., SEVERIN, G. et WOLF, R., Die Stellung der Szintigraphie im Rahmen der radiologischen Milzdiagnostik, Acta radiol. (Stockholm) sous presse.

[20] HOLZBACH, R.Th., CLARK, R.E., SHIPLEY, R.A., KENT, W.B. and LINDAY, G.E., Evaluation of spleen size by radioactive scanning, J. Lab. & Clin. Med. 60 (1962) 902.

[21] HORST, W., SCHNEIDER, C. et VILLANUEVA-MEYER, H., Die szintigraphische Darstellung der Milz mit Cr^{51}-markierten, wärmegeschädigten roten Blutzellen und Untersuchungen über die quantitative Verteilung des Cr^{51} im Organismus, Radio-Isotope in der Hämatologie, I. Int. Symp. Freiburg i. Br. 1962, Friedrich-Karl Schattauer Verlag, Stuttgart (1963) 249.

[22] KUBA, J., CHARAMZA, O. and WIEDERMANN, M., Gamagrafie Sleziny, Ceskoslovenska Rentgenologie 17 (1963) 328.
[23] LUZZATTI, G., Lo splenoscintillogramma nella diagnostica delle masse dell'emiaddome di sinistra, Radiol. Med. 49 (1963) 513.
[24] SPINELLI-RESSI, F., Lo scintillogramma della milza mediante globuli rossi marcati con ^{51}Cr, Min. nucl. 6 (1962) 266.
[25] SPINELLI-RESSI, F. and FOSSATI, F., Splenic scintillation scanning with sensitized or heated red cells, in Szintigraphie und Radiokardiographie, Symp. Schweiz. Akad. Med. Wiss., Basel 1962, Schwabe & Co. Verlag Basel/Stuttgart (1963) 198.
[26] zum WINKEL, K. et KLUGE, A., Szintigraphie und Funktionsprüfung der Milz mit alterierten Erythrozyten, Radio-Isotope in der Hämatologie, I. Int. Symp. Freiburg i. Br. 1962, Friedrich-Karl Schattauer Verlag, Stuttgart (1963) 239.
[27] FISCHER, J. et WOLF, R., Über eine neue Methode zur quantitativen und differentiellen Erfassung einer spezifischen Sequestrationsleistung des retikulo-histiozytären Systems und ihre klinische Anwendung, sous presse.
[28] WOLF, R. and FISCHER, J., Studies on the relationship of organ size and scanning picture, voir ces comptes rendus.
[29] DOERING, P. et KRAMER, K., Strahlentherapie 105 (1958) 245.

SCINTILLATION SCANNING OF THE SPLEEN WITH RED CELLS LABELLED WITH CHROMIUM-51

F. SPINELLI-RESSI
ISTITUTO DI RADIOLOGIA E MEDICINA NUCLEARE, OSPEDALE MAGGIORE, MILAN, ITALY

Abstract — Résumé — Аннотация — Resumen

SCINTILLATION SCANNING OF THE SPLEEN WITH RED CELLS LABELLED WITH Cr^{51}. Satisfactory scintiscans of the spleen have been obtained using chromium-51-labelled red cells, modified by two methods. Initially red cells were sensitized in vitro by coating with incomplete anti-D antibody. In this method the concentration of sensitized red cells in the spleen is proportional to the volume of anti-D serum employed in the sensitization procedure. Satisfactory scintiscans were obtained using 0.50 ml of a 1:128 dilution of anti-D serum, having an original titre of 1:512/ml of red cells.

In spite of good results, the sensitization method, utilizable only in Rh positive patients, has been replaced by the method using red cells modified by heating, which is technically easier and may be used also in Rh negative patients.

The image of the spleen is clearly delineated in all the cases, without interference from hepatic radioactivity. The spleen: liver ratio ranges between 5:1 and 10:1.

To date scintillation scans of the spleen have been performed in about 60 patients. No immediate or delayed clinical reactions have been observed in the patients after the injection of sensitized or heated red cells.

Since the radiation dose delivered to the patient is lower than the dose delivered in many radiological and clinical examinations with radioactive isotopes, the scanning procedure has been widely used in the differential diagnosis of the masses of the left abdomen. Among the cases studied, it is worth while mentioning two cases of splenomegaly associated with a tumour of the left kidney, one case of Banti's disease in a patient, in which a neoplasm of descending colon was suspected and a case of neuroblastoma in a patient two years old, in which the scintiscan of the spleen and that of the kidneys were of great help in making the right diagnosis. Further, the scintiscan has been of unique utility to rule out an accessory spleen and to demonstrate the spleen in congenital malformations, like situs inversus viscerum. In patients affected by chronic leukaemia the scanning procedure has been used in objectively demonstrating modifications in spleen size after roentgen-ray therapy.

SCINTIGRAPHIE DE LA RATE AU MOYEN D'HÉMATIES MARQUÉES AU CHROME-51. L'auteur a obtenu des scintigrammes satisfaisants de la rate au moyen d'hématies marquées au chrome-51, altérées suivant deux méthodes différentes. La méthode utilisée en premier lieu consistait à sensibiliser les hématies in vitro en les revêtant d'anticorps anti-D incomplet. Avec cette méthode, la concentration dans la rate des hématies sensibilisées est proportionnelle au volume de sérum anti-D utilisé pour la sensibilisation. L'auteur a obtenu des scintigrammes satisfaisants en utilisant, par ml d'hématies, 0,50 ml de sérum anti-D dilué à 1:128, dont le titre initial était de 1:512.

Bien qu'elle ait donné de bons résultats, la méthode de sensibilisation, qui ne peut être utilisée que chez des patients à Rh positif, a été remplacée par une autre méthode dans laquelle les hématies sont altérées thermiquement; cette seconde méthode est techniquement plus facile et peut également être appliquée chez des patients à Rh négatif.

L'image de la rate est nettement délimitée dans tous les cas, sans interférence due à la radioactivité hépatique. Le rapport rate:foie varie entre 5 et 10.

A ce jour, l'auteur a établi des scintigrammes de la rate pour une soixantaine de patients. Aucune réaction clinique, immédiate ou différée, n'a été observée à la suite de l'injection d'hématies sensibilisées ou altérées thermiquement.

La dose de rayonnement délivrée au patient étant inférieure à la dose administrée dans de nombreux examens radiologiques et cliniques au moyen des radioisotopes, cette méthode scintigraphique est largement utilisée à l'hôpital de l'auteur pour le diagnostic différentiel des masses de la partie gauche de l'abdomen.

Parmi les cas étudiés, il convient de citer deux cas de splénomégalie associée à une tumeur du rein gauche, un cas de maladie de Banti chez un sujet présentant les symptômes d'un néoplasme du côlon descendant et un cas de neuroblastome chez un enfant de deux ans, que la scintigraphie de la rate et des reins a beaucoup aidé à diagnostiquer correctement. En outre, la scintigraphie peut seule permettre d'écarter l'hypothèse d'une rate accessoire et de visualiser la rate dans les malformations congénitales telles que l'inversion viscérale. Chez les sujets atteints de leucémie chronique, la scintigraphie a permis d'obtenir une preuve objective des modifications de la taille de la rate après rœntgenthérapie.

СЦИНТИЛЛЯЦИОННОЕ СКЕННИРОВАНИЕ СЕЛЕЗЕНКИ С ПОМОЩЬЮ ЭРИТРОЦИТОВ МЕЧЕННЫХ ХРОМОМ-51. Удовлетворительные сцинтиграммы селезенки были получены при использовании эритроцитов, меченных хромом-51, что осуществлялось двумя способами. Первоначально эритроциты сенсибилизировали in vitro путем воздействия неполного анти-D антитела. При таком методе концентрация сенсибилизированных эритроцитов в селезенке пропорциональна объему применяемой в процессе сенсибилизации сыворотки анти-D. Удовлетворительные сцинтиграммы были получены при использовании 0,50 мл сыворотки анти-D в разбавлении 1:128, при первоначальном титре 1:512, на 1 мл эритроцитов. Несмотря на хорошие результаты, метод сенсибилизации, применимый лишь у резус-положительных больных, был заменен методом с использованием эритроцитов, видоизмененных посредством нагревания, который в техническом отношении гораздо проще и может использоваться и у резус-отрицательных больных.

Изображение селезенки имело четкую конфигурацию во всех случаях без каких либо помех за счет радиоактивности печени. Соотношение селезенка-печень колеблется в пределах между 5:1 и 10:1.

К настоящему моменту сцинтиграммы печени получены почти у 60 больных. У больных после инъекции сенсибилизированных или подогретых эритроцитов не наблюдалось непосредственных или отдаленных клинических реакций. Поскольку доза радиации, полученная больным, меньше дозы, получаемой при многих радиологических и клинических исследованиях за счет радиоактивных изотопов, то процедура скеннирования широко использовалась для дифференциальной диагностики образований в левой половине брюшной полости. Среди изучавшихся случаев заслуживают упоминания два случая спленомегалии, сочетавшиеся с опухолью левой почки, один случай болезни Банти у больного, где предполагалось наличие новообразования в нисходящей петле толстой кишки, а также случай нейробластомы у двухлетнего ребенка, при которой сцинтиграмма селезенки и почек оказывают большую помощь для постановки правильного диагноза. Кроме того, сцинтиграмма явилась уникальным методом для исключения добавочной селезенки и для демонстрации селезенки при врожденных аномалиях, подобных обратному расположению внутренностей. У больных хронической лейкемией скеннирование использовалось для объективной демонстрации изменения размеров селезенки после рентгенотерапии.

EXPLORACIÓN CENTELLEOGRÁFICA DEL BAZO MEDIANTE ERITROCITOS MARCADOS CON CROMO-51. El autor ha obtenido centelleogramas satisfactorios del bazo empleando eritrocitos marcados con cromo-51, modificados por dos procedimientos. Al principio, sensibilizaba los eritrocitos in vitro recubriéndolos con un anticuerpo incompleto anti-D. Con este procedimiento la concentración en el bazo de eritrocitos sensibilizados resulta proporcional al volumen del suero anti-D empleado para su sensibilización. Con 0,50 ml de una solución de suero anti-D, diluida al 1:128 a partir de un título inicial de 1:512, por milímetro de eritrocitos, se han conseguido centelleogramas satisfactorios.

Pese a sus buenos resultados, este procedimiento de sensibilización, que sólo puede aplicarse a pacientes con Rh positivo, fue sustituido por un método basado en el empleo de eritrocitos modificados por la acción del calor, *método que es más fácil de utilizar* y que puede aplicarse también a pacientes con Rh negativo.

En todos los casos la imagen del bazo aparece claramente delineada, sin ninguna interferencia de la radiactividad hepática. La razón bazo/hígado varía entre 5:1 y 10:1.

Hasta ahora el autor ha procedido a la exploración centelleográfica del bazo de unos 60 pacientes. No ha observado en estos últimos ninguna reacción clínica inmediata ni retardada después de la inyección de los eritrocitos sensibilizados o calentados.

Como la dosis de radiación recibida por el paciente es inferior a la que se administra en muchos exámenes radiológicos y clínicos efectuados mediante isótopos radiactivos, este procedimiento de exploración ha sido muy utilizado para el diagnóstico diferencial de las masas de la mitad izquierda del abdomen. Entre los

casos estudiados, cabe mencionar dos de esplenomegalia acompañada de tumor del riñón izquierdo, uno de enfermedad de Banti en el que se sospechaba la presencia de un neoplasma del colon descendente, y otro de neuroblastoma en un niño de dos años, cuyo diagnóstico fue facilitado por el centelleograma del bazo y de los riñones. La exploración centelleográfica ha sido, además, de suma utilidad para descartar la existencia de un bazo suplementario y señalar malformaciones congénitas del bazo, tales como un situs inversus viscerum. En pacientes afectados por leucemia crónica este procedimiento de exploración ha servido para demostrar objetivamente la existencia de modificaciones del tamaño del bazo causadas por una aplicación terapéutica de rayos X.

1. INTRODUCTION

The scintigraphy of the spleen, introduced by JOHNSON et al. [1] and WINKELMANN et al. [2], has proved particularly interesting in clinical practice [3].

By means of an ordinary roentgenologic examination the visualization of the spleen is often unsatisfactory. Even with more complex techniques, such as retropneumoperitoneum and splenoportography, the differential diagnosis of a mass is not always possible. Furthermore, these examinations are rather troublesome for the patient.

During liver scanning with colloidal radiogold radioactivity is found also in the spleen. Most of the radiogold, however, is taken up by the reticuloendothelial tissue of the liver, so that the amount of Au^{198} concentrated in the spleen is often insufficient for scintillation scanning. Furthermore, by this method the radioactivity of the left hepatic lobe interferes with the splenic area and a satisfactory delineation of the spleen is not possible.

As we pointed out in previous reports [4, 5], the scintigraphy of the spleen, largely used in our hospital, has been found particularly useful in the differential diagnosis of the masses of the left abdomen.

2. TECHNIQUE

2.1. Preparation of red cells

Only occasionally in pathological conditions are unmodified red cells highly sequestered by the spleen. Therefore in order to concentrate in the spleen a sufficiently high radioactivity to visualize the organ red cells must be modified before injection. They may be modified by two methods.

In the first method red cells are sensitized in vitro by coating with incomplete anti-D antibodies. Red cells are washed several times, each time with 10 vol. of sterile isotonic saline. To the erythrocytes an equal volume of isotonic saline and the human anti-D serum are then added. The mixture is incubated at 37°C for 30 min. Care must be taken that in all the operations a sterile technique is employed. Splenic trapping of sensitized red cells is proportional to the volume of anti-D serum employed in the sensitization procedure. JOHNSON et al. [6] report that satisfactory red cell sensitization was obtained by adding to the entire red cell suspension 6 ml-0.5 ml of a 1 : 128 dilution of anti-D serum having an original titer of 1 : 512. Under these conditions Coombs' test performed on the red cell suspension was positive. With the quantity of serum used by JOHNSON et al. [1] we

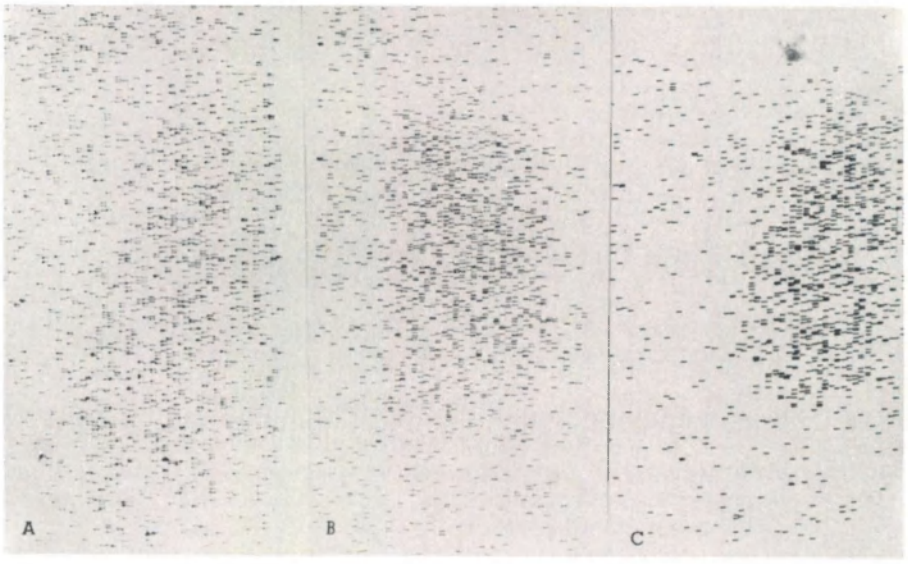

Fig. 1

(A, B, C) Scintiscans of the spleen performed with red cells sensitized with differing quantities of anti-D serum

could not obtain satisfactory scintiscans (Fig. 1A); radioactivity in the spleen was very low, whereas circulating radioactivity due to insufficiently sensitized labelled red cells, which were therefore not sequestered by the spleen, was relatively high. Furthermore, in these conditions, Coombs' test was negative. Also with a double quantity of anti-D serum the visualization of the spleen was still unsatisfactory (Fig. 1B). A high concentration of red cells in the spleen and a satisfactory delineation of the organ were obtained with greater quantities of anti-D serum, i.e. with 0.5 ml of anti-D serum per ml of red cells (Fig. 1C). Under these conditions Coombs' test was positive. The sensitization method is applicable only to Rh-positive patients. In the second method red cells are modified by heating. The whole blood is incubated in a water bath at 50°C for 30 min. This method is technically easier and may be used also in Rh-negative patients.

2.2. Labelling of red cells

A total of 200 μc of chromium-51 (as sodium chromate) are added to the red cells.

When the sensitization method is used, the labelling process is initiated after sensitization and is completed in 1 h at 37°C.

When the heated cell technique is used, the radioactive chromium is added to the blood before heating. In children, heated red cells and 2 μc/kg of Cr^{51} are used.

2.3. Scintillation scanning technique

We use a commercial scanning apparatus with lead-shielded 1-in scintillation crystal and with a cylindrical collimator measuring 20 mm in diam. and 100 mm in length. A spectrometer with "window" of 10 V, set on the peak of chromium-51, is used.

The probe is placed as close as possible to the skin. Scanning speed is 6 mm/s. The examination requires about 45 min.

2.4. Position of the patient

The patient is placed in supine, prone or lateral position. Therefore anterior, posterior and lateral projections of the spleen may be obtained by means of the scintiscan. The best delineation of the spleen is usually obtained in the posterior scintiscan. However, in the differential diagnosis of the abdominal masses the anterior scintiscan seems to us more valuable. The lateral scintiscan is useful in assessing the size of the spleen and probably in detecting intrasplenic localized lesions.

3. THE MECHANISM OF SEQUESTRATION OF RED CELLS BY THE SPLEEN

The mechanism by which modified red cells are almost totally sequestered by the spleen has been discussed in a previous report [4]. The cause of sequestration of red cells sensitized with incomplete anti-D antibodies is still not completely known. However, it would seem that the two best explanations of this sequestration are:

(a) agglutination of red cells and sequestration by the spleen, which acts as a passive filter;

(b) spherocytosis as the consequence of the damaged erythrocyte metabolism and sequestration of the spherocytes by the spleen.

The mechanism by which heated red cells are sequestered by the spleen is easier to understand. These cells undergo poikilocytosis, anysocytosis and spherocytosis, and are therefore easily sequestered by the spleen.

4. RESULTS AND DISCUSSION

4.1. General observations

To date scintillation scans of the spleen have been performed by us in about 60 patients. In the majority of cases the heated red cell technique has been used.

The image of the spleen is clearly delineated in all the cases. The anterior scintiscan of a normal spleen is shown in Fig. 2. The splenic area is roughly ovoidal in shape and defined by sharp margins. Figure 3 shows the posterior and lateral scintiscans of a splenomegaly in a patient with Laennec's cirrhosis.

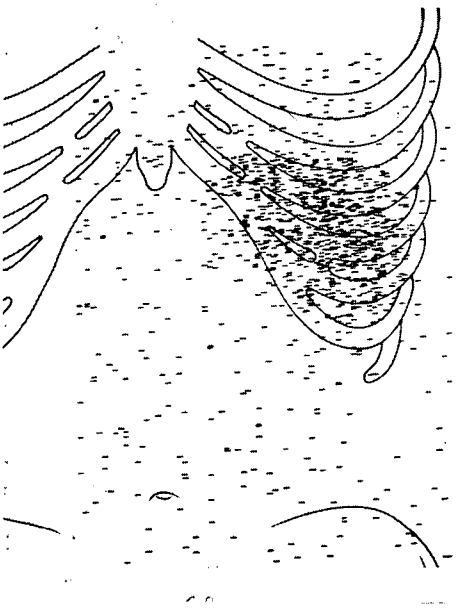

Fig. 2

Anterior scintiscan of a normal spleen

Usually sufficient radioactivity to obtain a satisfactory scintiscan is detectable in the splenic area within 1 h after injection. However at this time the level of circulating radioactivity is relatively high; therefore in order to obtain a better delineation of the splenic area the scintiscan is performed between the 6th and 24th h. In all cases radioactivity is detected in the hepatic area, since hapatic sinusoids also behave as a passive filter, However, hepatic radioactivity is always much lower than splenic radioactivity. Serial counts on the loci of maximum radioactivity in the spleen and liver show that within 1 h after injection the spleen-liver ratio ranges between 5 : 1 and 10 : 1. Moreover hepatic radioactivity does not interfere with the delineation of the spleen because it is detectable only in the centre of the right hepatic lobe and not in the left lobe.

On the basis of our experience an assessment of the clinical value of splenic scintillation scanning can be made. The scintillation scanning procedure may be utilized to study the morphology and, subordinately, the function of the spleen.

4.2. Morphological study

The scintillation scanning is the only method by which a direct visualization of the splenic tissue can be obtained.

The procedure is particularly useful in the differential diagnosis of the masses of the left abdomen. In most cases the spleen is easily detectable by means of a physical examination. In addition the organ can be indirectly

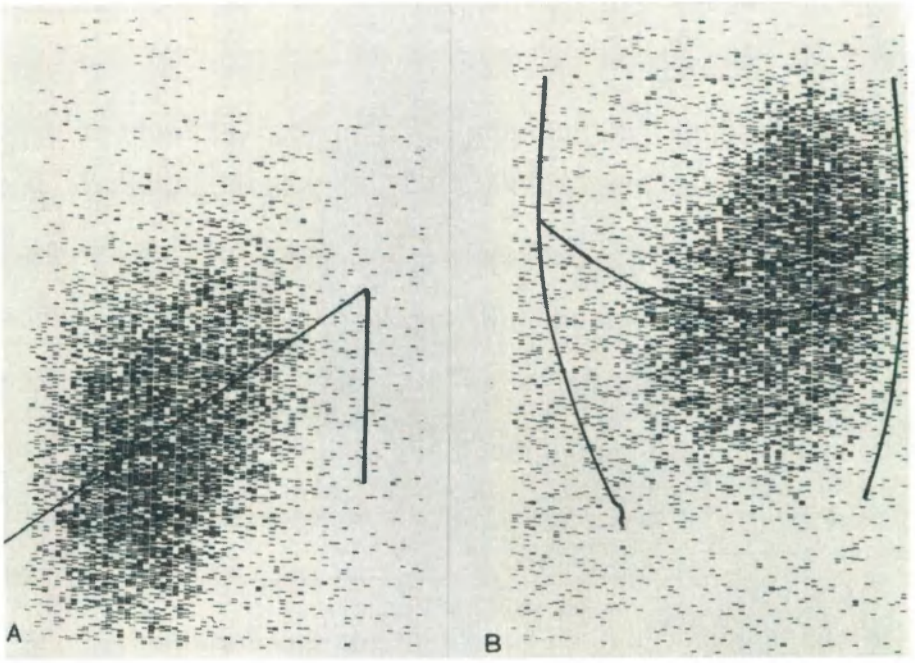

Fig. 3

Posterior (A) and lateral (B) scintiscans of a splenomegaly in a patient with Laennec's cirrhosis

visualized by means of ordinary roentgenological examinations. However, when these examinations are not conclusive or cannot be carried out owing to the condition of the patient, the scintiscan can be helpful for the differentiation of an abdominal mass. The utility of the radioisotope technique is illustrated by the following cases.

In a 2-yr-old child a huge mass was found upon physical examination. The mass could not be satisfactorily identified by means of several radiological examinations, including urography. The scintiscan showed that the mass was extrasplenic (Fig. 4).

Another patient, a 57-yr-old female, was admitted to hospital with severe anaemia and constipation. A few days before admission the patient had had a severe intestinal haemorrhage. In the left abdomen was found a mass, firm in consistency, which could not be indented with pressure. The first diagnosis of descending colon neoplasm was then thought questionable because of a laboratory finding revealing a severe trombocytopenia. Owing to the condition of the patient and especially to the recent intestinal haemorrhage a barium enema was thought dangerous. The scintiscan (Fig. 5) showed that the mass was a huge spleen, which occupied the entire left abdomen. The patient was operated on and the scintiscan diagnosis was confirmed. The case was classified as hypersplenism with secondary anaemia and thrombocytopenia.

In our opinion the scintiscan of the spleen replaces in many cases more complex radiological techniques, such as retropneumoperitoneum and sple-

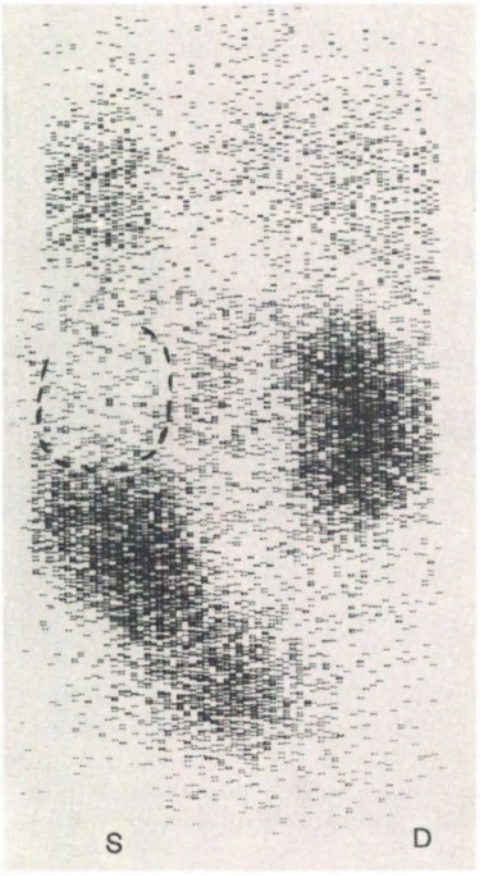

Fig. 4

Photographic composition of a posterior scintiscan of the spleen and of a renal scintiscan with Neohydrin-Hg^{197}, performed in a 2-yr-old child with a left abdominal mass. The scintiscans show that the mass is extrasplenic and extrarenal.

noportography. Undoubtedly the retropneumoperitoneum is of great value in the differentiation of some abdominal masses. However, in many cases the scanning procedure seems to be more practical as a routine method.

In one case examined by us the scintiscan and the retropneumoperitoneum were both indispensable for a correct diagnosis of a mass in the left abdomen. In this patient, after the physical and ordinary roentgenological examinations, an extrarenal tumour and a splenomegaly were thought to be associated. The scintiscan showed a slightly enlarged spleen; the inferior pole of the mass was roughly 5 cm below the inferior limit of the radioactive area (Fig. 6A). In order to better define the mass a retropneumoperitoneum was performed. The tomographic examination showed no solution of continuity between the spleen and the supposed extrarenal tumour (Fig. 6B). On the basis of this finding, a cyst at the inferior pole of the

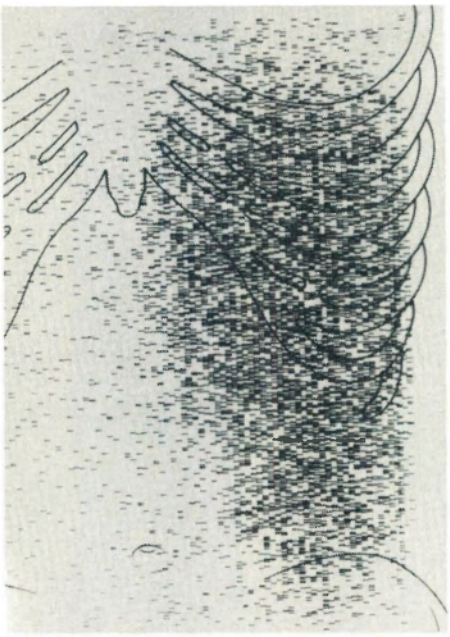

Fig. 5

Scintiscan of a huge spleen in a case of hypersplenism with secondary anaemia and thrombocytopenia

spleen, appearing on the scintiscan as a "cold" area, was diagnosed. With only one of the two examinations a correct diagnosis would have been impossible. The scintillation scanning is also of some utility in objectively demonstrating modifications in spleen size after antiblastic or roentgen-ray therapy in patients affected by chronic leukaemia.

Finally it is worth mentioning two cases in which scintillation scanning has been of some interest. In one patient, splenectomized some years previously and with a recent trombocytopenia, the scintiscan was performed in order to detect an accessory spleen and to study the liver behaviour when red blood cells sensitized with incomplete anti-D antibodies were injected into a splenectomized patient. The scintiscan (Fig. 7) shows in the splenic area a radioactivity not significantly different from that of the background. The hepatic activity is low and not different from that observed in other cases. No other area of radioactivity has been found.

In Fig. 8 the scintiscan of a child with situs inversus viscerum is shown. The spleen, normal in shape, is located in the right abdomen.

In all our scintiscans the distribution of the radioactive tracer in the parenchyma has been uniform, with the exception of one case of sarcoidosis with splenomegaly (Fig. 9). The scintiscan of this patient shows a large spleen: the radioactivity is uniformly distributed in the lower pole, whereas in the remaining parenchyma the distribution of the tracer is non-homogeneous. A similar case was reported by JOHNSON et al. [7].

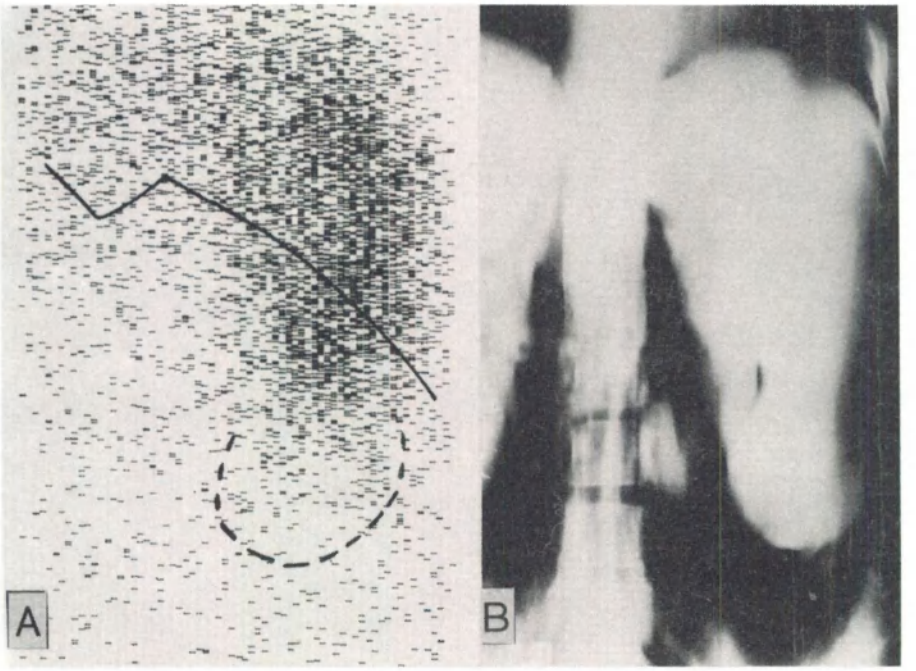

Fig. 6

(A) Hydatic cyst at the lower pole of the spleen, which appears on the scintiscan as a "cold" area
(B) Retropneumoperitoneum of the same case

4.3. Functional study

The modified red cell technique has also been used for studying the function of liver and spleen, utilizing the spleen-liver ratio. However, we do not believe that the spleen-liver ratio is a satisfactory measure of the function of these organs. Indeed, the function of the liver can be studied by means of more accurate investigations. However, it would be of great value if by this method the function of the spleen could be evaluated. Unfortunately, since hepatic sinusoids also are able to sequester the modified red cells the spleen-liver ratio can only be an index of a function common to both organs [7].

Furthermore, it is likely that the variation of spleen-liver ratio is partially due to technical factors. Geometrical errors involved in the detection of radioactivity of two organs very different in mass may be one factor responsible for the variation of spleen-liver ratio. Another factor, in our opinion, is the preparation of red cells. That is to say, it is possible that the degree of red cell alteration is not always the same, especially in pathological conditions. Consequently, the splenic and hepatic sequestration of red cells could vary independently of the function of the two organs. It is, of course, difficult to state to what extent the factors mentioned above are

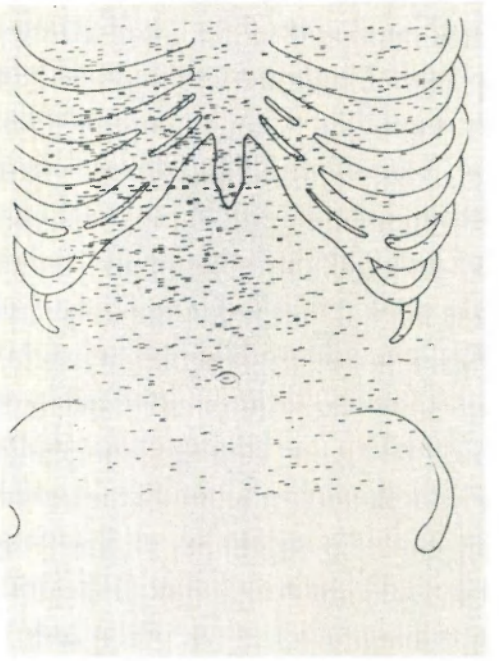

Fig. 7

Anterior scintiscan performed in a splenectomized patient

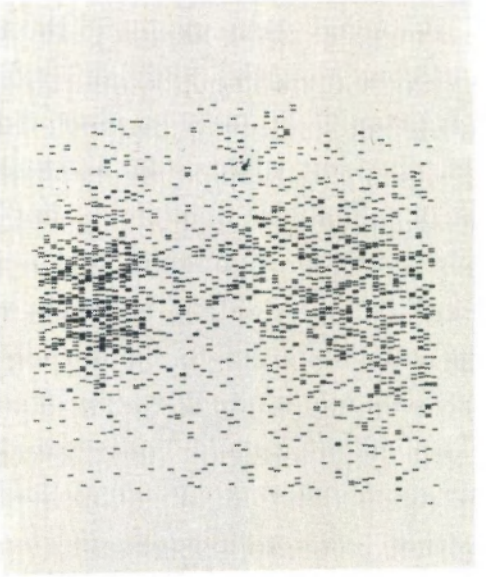

Fig. 8

Situs inversus viscerum: the anterior scintiscan shows that the spleen is located in the right abdomen

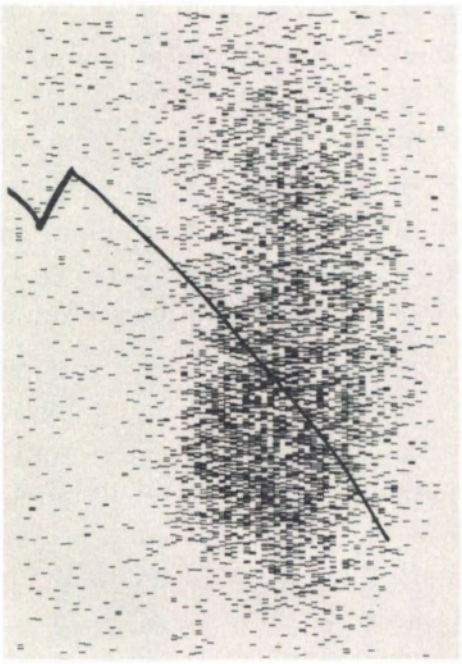

Fig. 9

Sarcoidosis with splenomegaly. Non-homogeneous distribution of radioactivity in the upper portion of the spleen.

responsible for the variation of the spleen-liver ratio. In our examinations we have not found a constant relationship between spleen-liver ratio and the type of disease studied, with the exception of cirrhosis with splenomegaly, in which the spleen-liver ratio was usually high. In this case the increased ratio is probably due to a decreased sequestration of red cells by the liver.

In any case it seems to us that this method is not sufficiently reliable to be used as a test for assessing the function of the spleen.

5. HAZARDS

We have never observed immediate or delayed clinical reactions after the injection of sensitized or heated red cells. In all cases we have used the patient's own cells.

The amount of radiation delivered to the patient depends mainly on the chromium-51 dosage and on the extent of sequestration of red cells by the spleen. According to our observations, the effective half-life of chromium-51 in the spleen ranged between 8 and 16 d, being shorter when sensitized red cells were used. Under these conditions, if 200 μc of Cr^{51} are injected, the whole body absorbs 30-50 mrad and the spleen absorbs 5-11 rad. In

evaluating the dose absorbed by the gonads, besides the dosage and the effective half-life of Cr^{51}, the distance of the spleen from the ovary or testis has also to be considered. Because of the variations of position and size of the spleen and the different distance of the ovary and testis from the spleen, the dose absorbed may vary between 20 and 60 mrad. It is interesting to point out that in the retropneumoperitoneum the dose delivered to the ovary is about 2 r and the dose delivered to the testis is 0.3-0.5 r; in splenoportography the dose delivered to the ovary is about 1 r and the dose delivered to the testis is about 0.1 r [8].

Therefore, the radiation dose delivered to the patient by means of this method is within the limits accepted in clinical procedures using radioactive isotopes and lower than the dose delivered in several radiological examinations used for the diagnosis of the abdominal masses, such as retropneumoperitoneum and splenoportography.

REFERENCES

[1] JOHNSON, P. M., HERION, J. C. and MOORING, S. L., Radiology 74 (1960) 99-101.
[2] WINKELMAN, J. W., WAGNER, H. N., Jr., McAFEE, M. D. and MOZLEY, J. M., Radiology 75 (1960) 465-6.
[3] FISCHER, J. and WOLF, R., Dtsch. med. Wschr. 88 (1963) 305-8.
[4] SPINELLI-RESSI, F., Minerva nucl. 6 (1962) 266-71.
[5] SPINELLI-RESSI, F. and FOSSATI, F., Bull. schweiz. akad. med. Wiss. 19 (1963) 82-91.
[6] JOHNSON, P. M. and HERION, J. C., Radiology 76 (1961) 438-43.
[7] JOHNSON, P. M., WOOD, E. H. and MOORING, S. L., Amer. J. Roentgenol. 86 (1961) 757-67.
[8] LUZZATTI, G., Radiol. med., Torino 49 (1963) 513-39.

DISCUSSION

(On the three foregoing papers)

R. WOLF: Dr. Proukakis mentioned one case of autosplenectomy in which he was not able to visualize the spleen. On the other hand, he failed to find any activity in the liver and the total blood activity at the time the scan was begun was 6.9% of the initial dose. Where was the activity?

C. PROUKAKIS: The case which was attributed to autosplenectomy showed a whole-blood radioactivity (expressed as a percentage of the administered dose) which was rather higher than that observed in most of the other cases. Radioactivity was detected over the hepatic region, but was not sufficient to allow a reliable liver scan to be made. It is possible that radioactivity was present in other organs of the reticulo-endothelial system. Since we did not make a whole-body count of Cr^{51} or collect urine, we do not know the amount of Cr^{51} that was excreted.

R. WOLF: One of Dr. Spinelli-Ressi's figures (Fig. 9) was interpreted as showing non-homogeneous distribution of radioactivity in the upper portion of an enlarged spleen. I think, however, that the effect in question was caused by the anatomical location of the organ. The spleen is situated at

the back of the body and, when it becomes enlarged, it grows in a ventral direction. When the patient scanned is in the supine position, there is much more intervening tissue over the upper portion of the spleen than over the lower. This leads to a corresponding drop in the count rate over the former region. I should like to ask Dr. Spinelli-Ressi whether he tried to scan the patient in the prone position.

F. SPINELLI-RESSI: We did not scan the patient in the prone position; on the other hand, the histological findings confirmed our interpretation.

M. BEN-PORATH: Could Dr. Proukakis say what criteria he uses in defining a space occupying lesion on a photoscan and what was the time-constant in relation to the counting rate on the scans shown?

C. PROUKAKIS: The criterion used in defining a space occupying lesion on a photoscan is the presence of an area in which there is less blackening of the film surrounded by an area where the blackening is denser. This is considered especially characteristic when the area in which there is less blackening is located in the central part of the organ examined.

I should like to ask my colleague, Dr. Binopoulos, to answer your second question.

D. BINOPOULOS: The time constant was one second or two seconds, depending on the counting rate.

K. EPHRAÏM: In Fig. 2 of Dr. Fischer's paper, which shows a spleen scan obtained with $Hg^{197}Cl_2$, there is a very sharply delineated area which is clearly lighter than the rest of the spleen. In some of the other scans he presents, there are other sharply delineated areas which are very much darker than the rest of the spleen. I should like to ask Dr. Fischer if these areas have any clinical significance or if they are just artefacts.

J. FISCHER: These are artefacts which sometimes appear in stylus scintigrams as a result of the adhesion of carbon (burnt paper) to the stylus. On the other hand, these defects never appear in the photo-scintigram which is made at the same time.

M. BEN-PORATH: Would you comment on your findings in scanning the spleens of patients suffering from leukaemia and polycythaemia?

J. FISCHER: The variations in spleen size in cases of leukaemia and polycythaemia are shown in Table I of our paper. The spleen is always enlarged in leukaemia and in 75% of cases of polycythaemia which have not undergone therapy. I should like once again to draw attention to the differences between clinical and scintigraphic findings. In both diseases the examination of the rate of elimination of damaged red cells from the blood is of special interest.

B. MALAMOS: In carrying out your spleen scans, numbering over 600, were you ever obliged because of technical difficulties to inject the heat-treated Cr^{51}-labelled red cells a second time?

J. FISCHER: Up to now we have not had to repeat a spleen scan as a result of technical difficulties connected with the preparation of red blood cells. I should like to point out, however, that it is sometimes necessary to scan a patient in three positions. We scanned two patients who had undergone Thorotrast examinations 20 years previously and in whom the spleen had been reduced to the size of a walnut. We could not demonstrate these spleens when the patients were scanned in the supine position, nor could we do so in a lateral scan, since most of the activity accumulates in the

liver. We could, however, observe the atrophic spleens when the patients were scanned in a prone position.

A. BAPTISTA: Did any of the authors of the papers under discussion inject Cr^{51}-labelled erythrocytes from patients suffering from such blood disorders as sickle-cell anaemia into normal subjects and, if so, what did they observe in the clearance curve and/or spleen scan?

H. GYFTAKI: The purpose of our study was to visualize spleen lesions in cases of congenital haemolytic anaemia. We did not inject heat-treated Cr^{51}-labelled erythrocytes from such patients into normal subjects, and, consequently, we have no information regarding clearances of these cells in normal subjects or scans following this procedure.

J. FISCHER: Heat treatment is the only method which simulates the normal aging of erythrocytes. All the alterations occurring in erythrocytes which have aged in the normal way or in erythrocytes which have been stored are also found in heat-treated erythrocytes. During 20 min of heating at 50°C the life-span of a normal erythrocyte is reduced by a factor of 5000 to 6000.

B. MALAMOS: Which of the two methods used by Dr. Spinelli-Ressi, i.e. sensitization and the heat-treatment technique, was found to be the more satisfactory?

F. SPINELLI-RESSI: It is certainly easier to use the heat-treatment technique.

B. MALAMOS: Did you find one of these techniques superior to the other in any diseases for the purpose of visualizing the spleen?

F. SPINELLI-RESSI: No.

XI

CLINICAL APPLICATIONS: LIVER

APPLICATION DE LA MÉTHODE SCINTIGRAPHIQUE A L'EXPLORATION MORPHOLOGIQUE DU FOIE AU COURS DE L'AMIBIASE

R. GONGORA ET H. JAMMET
FONDATION CURIE, PARIS, FRANCE

Abstract — Résumé — Аннотация — Resumen

USE OF THE SCINTIGRAPHIC METHOD IN MORPHOLOGICAL EXPLORATION OF THE LIVER DURING AMOEBIASIS. Increasing recourse is being had to the scintigraphic method of morphological exploration of the amoebic liver owing to the frequency of hepatic localizations of amoebiasis and to the difficulties of clinical and paraclinical diagnosis of amoebic abscess of the organ. The method yields data of great importance in this field.

The authors quote the statistics of examinations they have carried out and endeavour to draw conclusions from them.

They describe the examination technique from the following points of view:

(a) The choice of materials (I^{131}-labelled Rose Bengal and Au^{198} in colloidal solution) with their advantages and disadvantages;

(b) The apparatus used, with special reference to the problem of collimation;

(c) Actual performance of the examination, involving a functional study and the scintigram itself, which has to be carried out from different angles;

(d) Repetition of the examination after an interval of several months.

The authors then deal with the scintigraphic semiology of hepatic localizations of amoebiasis; they analyse the elementary abnormal images, study their topography, and describe their associations in the case of hepatitis and in cases of amoebic abscess.

They then study the development of these images with time and report a number of cases for which the scintigraphic examination was repeated after an interval of several weeks or months.

Finally, they enunciate the indications for application of the method, which provides essential data for the positive diagnosis of amoebic abscess of the liver and for topographical and morphological diagnosis (of particular interest surgically), and which makes it possible to observe the progress of the disease and the healing of the abscess after medical treatment.

APPLICATION DE LA MÉTHODE SCINTIGRAPHIQUE A L'EXPLORATION MORPHOLOGIQUE DU FOIE AU COURS DE L'AMIBIASE. La méthode scintigraphique est de plus en plus sollicitée pour l'exploration morphologique du foie amibien en raison de la fréquence des localisations hépatiques de l'amibiase et des difficultés du diagnostic clinique et paraclinique de l'abcès amibien du foie. La méthode fournit dans ce domaine des renseignements d'intérêt majeur.

Les auteurs rapportent la statistique des examens qu'ils ont effectués et se proposent de tirer les conclusions de ces examens.

Ils décrivent la technique d'examen envisageant successivement:

a) Le problème du choix des produits (rose bengale marqué avec ^{131}I et ^{198}Au en solution colloïdale), en soulignant leurs avantages et inconvénients respectifs;

b) L'appareillage utilisé en insistant sur le problème de la collimation;

c) Le déroulement de l'examen qui comporte une étude fonctionnelle et la scintigraphie proprement dite effectuée nécessairement sous plusieurs incidences;

d) La répétition de l'examen à plusieurs mois d'intervalle.

Les auteurs traitent ensuite de la sémiologie scintigraphique des localisations hépatiques de l'amibiase; ils analysent les images anormales élémentaires; étudient leur topographie et décrivent les associations de ces images dans le cas d'hépatite et dans les cas d'abcès amibien.

Ils étudient l'évolution de ces images dans le temps, en rapportant un certain nombre de cas pour lesquels l'examen scintigraphique a été répété à plusieurs semaines ou plusieurs mois d'intervalle.

Enfin, ils dégagent les indications de la méthode qui apporte des renseignements essentiels pour préciser le diagnostic positif des abcès amibiens du foie et pour le diagnostic topographique et morphologique (particulièrement intéressant sur le plan chirurgical), et qui permet de suivre l'évolution de la maladie et d'apprécier la guérison des abcès après traitement médical.

ПРИМЕНЕНИЕ СЦИНТИГРАФИЧЕСКОГО МЕТОДА ДЛЯ МОРФОЛОГИЧЕСКОГО ИССЛЕДОВАНИЯ ПЕЧЕНИ ПРИ АМЕБИАЗЕ. Сцинтиграфический метод находит все более широкое применение при морфологическом исследовании амебного заболевания печени в связи с частотой печеночных локализаций амебиаза и трудностями клинического и параклинического диагноза амебного абсцесса печени. В данной области метод дает возможность получать весьма интересные данные.

Приводится статистика проведенных опытов, предлагаются соответствующие выводы.

Изложение метода исследования дается в следующем порядке:

Проблема выбора индикатора (Бенгальская роза, меченная йодом-131 и золотом-198 в коллоидальном растворе), при этом указываются их соответствующие положительные и отрицательные качества.

Использованная аппаратура с указанием на проблему коллимации.

Процесс обследования, который включает в себя функциональные исследования, и собственно сцинтиграфию, проводимую в обязательном порядке под несколькими углами.

Повторение исследования с интервалом в несколько месяцев.

Излагается вопрос о сцинтиграфической симптоматике почечных локализаций амебиаза; анализируются элементарные патологические изображения; исследуется их типография и описываются ассоциации этих изображений в случаях гипатита и амебного абсцесса.

Изучается эволюция этих изображений во времени и приводится в связи с этим несколько случаев, когда сцинтиграфические исследования повторялись с интервалом в несколько недель или месяцев.

Наконец, указывается метод, который позволяет получать существенные данные для уточнения позитивного диагноза амебного абсцесса печени, причем их топографический и морфологический диагноз представляет особый интерес в хирургическом плане. Этот метод также позволяет следить за эволюцией болезни и устанавливать лечение абсцессов после общего медицинского лечения.

APLICACIÓN DE LA CENTELLEOGRAFÍA A LA EXPLORACIÓN MORFOLÓGICA DEL HÍGADO EN CASOS DE AMIBIASIS. Las amibiasis se localizan con gran frecuencia en el hígado y los abscesos que producen son difíciles de diagnosticar clínica o paraclínicamente. Por ello, en estos casos, la exploración morfológica del hígado se efectúa cada vez más por centelleografía, método que permite obtener datos de gran interés.

Los autores exponen los resultados estadísticos de los exámenes que han efectuado y las conclusiones correspondientes.

Describen la técnica de examen considerando, sucesivamente:

a) el problema de la elección de los productos (Rosa Bengala marcado con ^{131}I; ^{198}Au en solución coloidal) señalando sus ventajas e inconvenientes;

b) los aparatos empleados, insistiendo en el problema de la colimación;

c) el desarrollo del examen, que comprende un examen funcional y la centelleografía propiamente dicha efectuada, necesariamente, desde varias proyecciones;

d) la repetición del examen a intervalos de varios meses.

A continuación, los autores tratan de la semiología centelleográfica de las amibiasis hepáticas, analizan las imágenes anormales elementales, examinan su topografía y describen las asociaciones de esas imágenes en el caso de la hepatitis y en el de los abscesos amibianos.

Estudian la evolución temporal de esas imágenes y dan información sobre un cierto número de casos en que el examen centelleográfico se repitió a intervalos de varias semanas o de varios meses.

Por último, señalan en que casos está indicado este método, que facilita datos esenciales para precisar el diagnóstico positivo de los abscesos hepáticos amibianos y su diagnóstico topográfico y morfológico, particularmente interesante desde el punto de vista quirúrgico, y que permite seguir la evolución de la enfermedad y apreciar la curación de los abscesos después del tratamiento médico.

I. INTRODUCTION

La méthode scintigraphique appliquée à l'étude de l'amibiase hépatique fournit des renseignements d'un intérêt majeur. Elle est largement sollicitée en raison de la difficulté du diagnostic clinique et paraclinique de l'abcès amibien d'une part et de la difficulté d'apprécier la guérison d'une amibiase hépatique d'autre part. En effet, sur 1190 examens scintigraphiques effectués dans le Service de radioisotopes de la Fondation Curie, 84 examens ont été effectués chez 68 sujets amibiens, certains d'entre eux ayant subi 2 ou 3 examens successifs.

Il s'agissait: a) soit d'anciens amibiens pour lesquels était effectué un examen de «sécurité» afin de s'assurer de la non évolutivité de la maladie, b) soit d'amibiens présentant des signes cliniques de localisation hépatique et pour lesquels on demandait à la scintigraphie une confirmation diagnostique et c) soit d'amibiens hépatiques avérés, pour lesquels se posait le problème de la localisation d'un abcès ou de la surveillance de l'évolution sous traitement.

Les examens ont été effectués: a) avec du rose bengale marqué avec de l'iode 131 (25 fois) et b) avec du radio-or 198 en solution colloïdale (59 fois).

L'utilisation du radio-or 198 en solution colloïdale offre plusieurs avantages: elle permet d'obtenir une image hépatique pure dépourvue de toute superposition digestive et laisse le temps, en raison de la fixation définitive de l'or au niveau du tissu réticulo-endothélial hépatique, de pratiquer le balayage des différentes faces. Par ailleurs, la décroissance est telle qu'elle permet la répétition de l'examen à intervalle de temps suffisamment court pour suivre l'évolution sous traitement médical d'une hépatite ou d'un abcès.

Les examens ont été effectués en utilisant soit un collimateur cylindrique, soit le plus souvent un collimateur à plusieurs canaux convergents. Ce dernier, dont la hauteur est de 10 cm, comporte 31 canaux dont le foyer de convergence est situé à 7 cm du plan inférieur; il présente l'avantage, sur les collimateurs cylindriques, d'une meilleure définition, pour une perte relativement faible du rendement en profondeur. Cependant, la limite du rendement en profondeur implique la nécessité absolue d'explorer le foie selon trois balayages (fig. 1): a) balayage de la face antérieure, b) balayage de la face latérale droite et c) balayage de la face postérieure.
Tous les examens avec le radio-or 198 ont été soumis à cet impératif.

Quelques sujets ont été examinés à la fois à l'aide d'un scintigramme classique par balayage et à l'aide de la caméra à scintillations que nous avons décrite. Le tube à entretien d'image qui équipe l'un des deux oscilloscopes cathodiques que nous utilisons pour l'enregistrement des images, permet, par le jeu du seuil de lecture, d'examiner l'image avec une brillance variable de façon continue. Cette Manœuvre, en offrant la possibilité de choisir et de photographier plusieurs images différemment contrastées d'un même enregistrement facilite l'interprétation des images de tonalité des scintigraphies classiques (fig. 2).

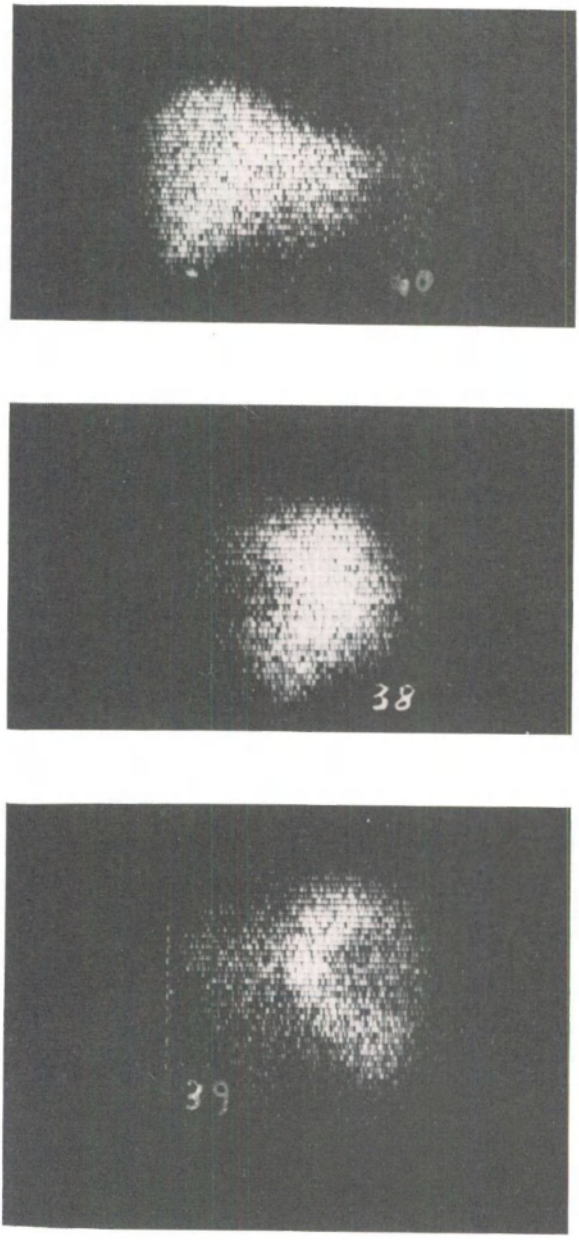

Figure 1

Scintigraphies du même sujet, effectuées suivant trois balayages : antérieur, latéral droit et postérieur.

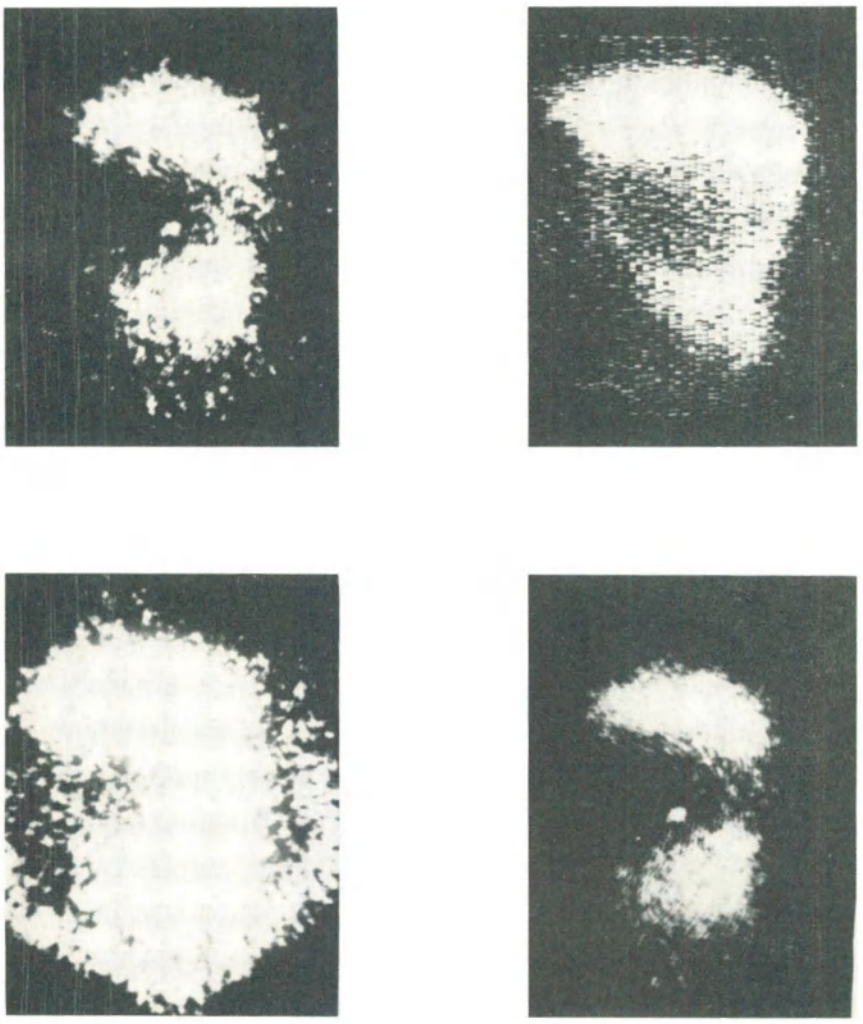

Figure 2

Scintigraphie par caméra à scintillations.

II. DONNÉES FONCTIONNELLES

L'épuration sanguine du produit utilisé a été étudiée au cours de ces examens, à partir de prélèvements de sang effectués à intervalle de temps défini, pendant la première heure qui a suivi l'injection.

Pour les 25 examens avec la rose bengale, nous avons retenu le taux de rétention à la première heure; dans 17 cas, soit 68% des cas, le taux est inférieur à 12%, se situant parfois au-dessous de 10%. L'épuration sanguine du rose bengale est donc ou normale ou accélérée. Dans huit cas, au con-

TABLEAU I

RÉPARITION DE LA «CLEARANCE» FRACTIONNELLE DU RADIO-OR

Valeur de la «clearance» fractionnelle	< 17%	17%	20%	23%	> 25%
Nombre de sujets	4	10	16	17	6

traire, elle est retardée: il s'agit toujours de sujets au long passé d'amibiase hépatique, trois d'entre eux ayant subi une ou plusieurs interventions chirurgicales pour abcès hépatique, un quatrième, examiné en laparoscopie présentant une hépatite scléro-inflammatoire du lobe gauche.

Chez 53 sujets, nous avons étudié la «clearance» fractionnelle du radio-or. Le tableau I indique la répartition des «clearances» fractionnelles du radio-or pour ces 53 sujets. Celle-ci s'est révélée diminuée dans 4 cas, normale ou légèrement supérieure à la normale dans 43 cas et nettement augmentée dans 6 cas. Là encore les diminutions se retrouvent chez des sujets ayant un long passé d'amibiase hépatique.

Il ressort de cette étude que l'épuration sanguine du rose bengale et du radio-or est rarement affectée au cours de l'amibiase hépatique, celle-ci est le plus souvent normale et quelquefois augmentée. Les diminutions s'observent après évolution prolongée de la maladie ou à titre de séquelles en particulier après intervention chirurgicale. Par contre, en cours de poussée évolutive, on observe volontiers un tendance à l'augmentation de l'épuration, ceci traduisant très vraisemblablement un état inflammatoire. La comparaison des cas d'hépatite pure et d'hépatite avec abcès n'a pas montré de différence significative.

L'étude de l'évolution des clearances chez les malades ayant subi, plusieurs examens a reflété dans l'ensemble l'évolution de la maladie. Le nombre de cas est cependant trop restreint pour que cette notion puisse être généralisée. Le tableau II indique les «clearances» du radio-or chez 8 sujets ayant subi 2 ou 3 examens; dans 6 des cas, les «clearances» primitivement augmentées diminuent et se normalisent sous traitement mécidal. Dans un cas, la «clearance» inférieure à la normale lors du premier examen subit une diminution après traitement.

Enfin dans un cas on assiste à une nette augmentation de la «clearance» malgré une amélioration spectaculaire des signes cliniques et biologiques.

III. SÉMÉIOLOGIE SCINTIGRAPHIQUE

L'analyse des images scintigraphiques nous a conduits à relever un nombre restreint d'images anormales élémentaires que l'on retrouve avec une grande fréquence et que nous classerons suivant leur topographie.

Il s'agit tout d'abord de modifications globales du volume et de la forme du foie caractérisées par une hépatomégalie et une accentuation de la con-

TABLEAU II

VARIATIONS DE LA «CLEARANCE» FRACTIONNELLE DU RADIO-OR CHEZ DES SUJETS AYANT SUBI PLUSIEURS EXAMENS

Cas	1er examen	2ème examen	3ème examen
1er cas	0,35	0,23	
2ème cas	0,40	0,20	
3ème cas	0,23	0,43	
4ème cas	0,23	0,17	0,20
5ème cas	0,27	0,23	
6ème cas	0,15	0,10	
7ème cas	0,23	0,17	
8ème cas	0,23	0,23	

vexité des bords et de l'encoche interlobaire. Ces modifications schématisées sur la figure 3 confèrent à la silhouette hépatique un aspect en «sabot»; elles sont illustrées par la série de scintigraphies de la figure 4. L'accentuation de l'encoche interlobaire et de la convexité du bord inférieur du lobe gauche peut être telle que ce dernier tend à s'individualiser et acquiert une morphologie quadrangulaire (fig. 5).

Nous avons relevé en second lieu des modifications lobaires qui portent essentiellement sur la structure: importante diminution de la densité du lobe droit ou du lobe gauche (fig. 6).

Enfin nous avons rencontré des modifications locales intéressant également la structure de l'image, caractérisées par des lacunes, des images de tonalité et des encoches. Ces images, de dimensions variables, pouvant atteindre 20 cm de diamètre, sont généralement mal limitées et siègent le plus souvent au niveau de la face postérieure du lobe droit; des trois balayages effectués, le balayage latéral droit est celui qui précise le mieux la morphologie de ces images (fig. 7).

Le tableau III indique le nombre de ces images anormales élémentaires. Aussi, nous avons relevé 41 images du type 1 (modification globale de la forme du foie); 5 images du type 2 (modification de la structure d'un lobe) et 40 images du type 3 (images de tonalité, encoches et lacunes).

Ces modifications élémentaires sont isolées ou plus fréquemment associées. Pour les 54 malades présentant une image anormale la répartition de ces images s'établit de la façon suivante (tableau IV) a) 15 sujets présentant uniquement une image du type 1 (anomalie globale de la morphologie du foie), b) 8 sujets présentant uniquement une image du type 3 (anomalie locale) et c) 31 sujets présentant plusieurs de ces anomalies associées.

La restitution ad integrum sous traitement médical même pour des images lacunaires volumineuses peut être obtenue en un temps relativement court. Les figures 8 et 9 illustrent le cas d'un malade qui présentait des antécédents de dysenterie amibienne, des signes cliniques d'hépatite et pour lequel une première scintigraphie a montré une très volumineuse lacune supéro-externe du lobe droit; ce malade a été traité par «emetine et antibiotiques» pendant quelques mois au terme desquels la guérison clinique

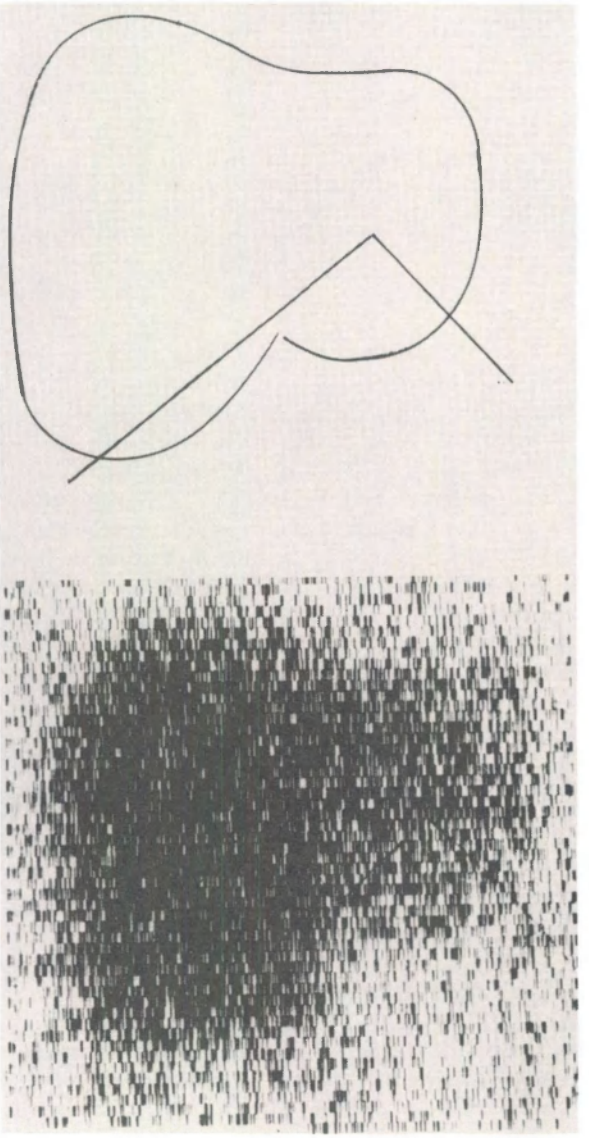

Figure 3

Déformation globale de l'image hépatique.

s'accompagnait d'une scintigraphie normale. Malheureusement, il n'en est pas toujours ainsi: la figure 10 montre la persistance d'images lacunaires chez des sujets qui après traitement médical étaient en état de guérison clinique apparente; dans ce cas l'examen scintigraphique revêt un intérêt majeur: il conduit à poursuivre le traitement médical ou oriente vers un acte chirurgical.

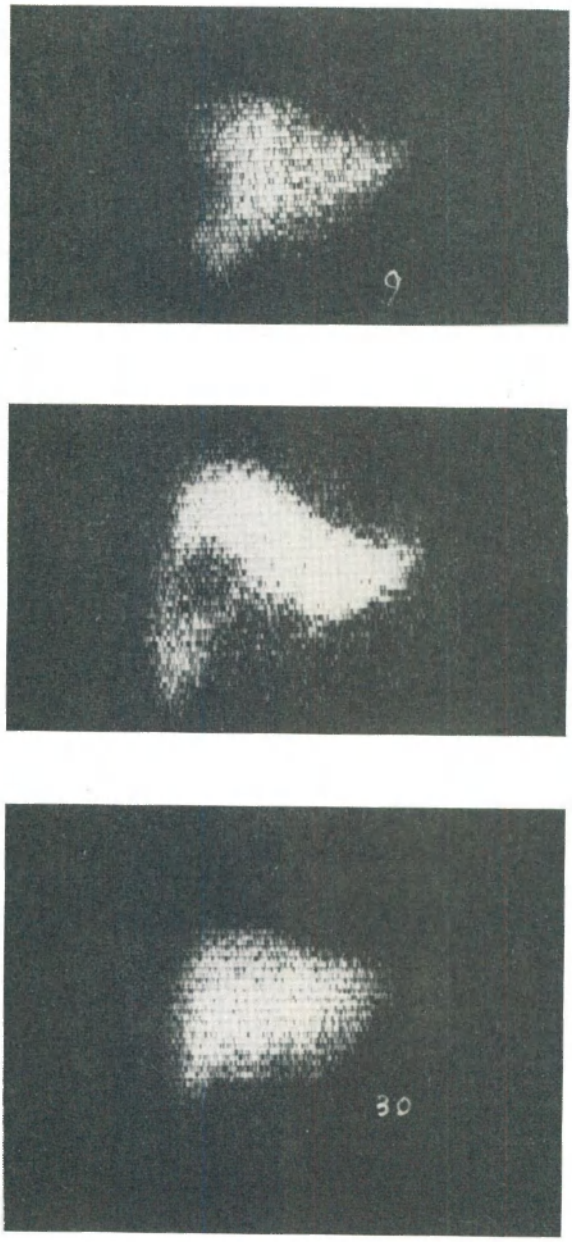

Figure 4

Illustration scintigraphique de la déformation globale du foie chez différents sujets.

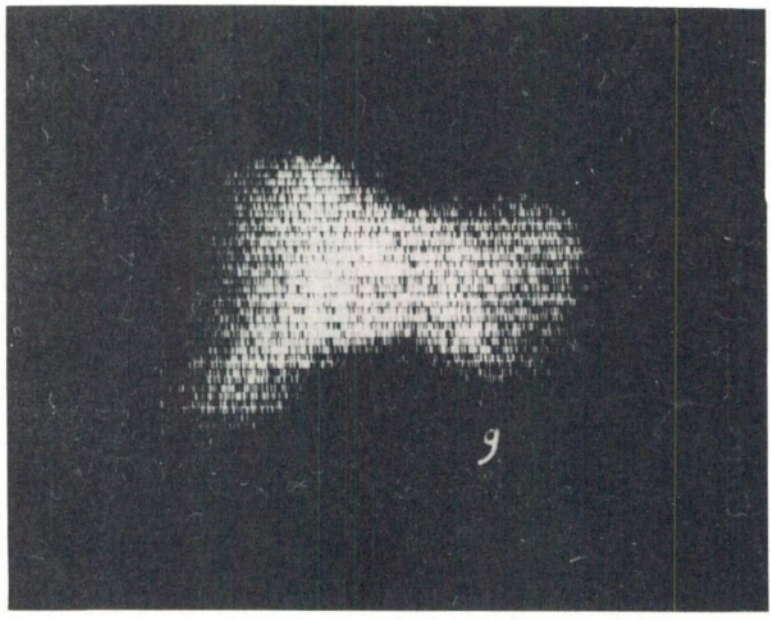

Figure 5

Individualisation du lobe gauche.

TABLEAU III

IMAGES ANORMALES ÉLÉMENTAIRES

Type 1	41
Type 2	5
Type 3	40

Note:

Type 1 : accentuation de la convexité des bords et de l'encoche interlobaire.
Type 2 : modifications lobaires: diminution de densité d'un lobe.
Type 3 : modifications locales: images de tonalité, lacunes, encoches.

V. CONCLUSION

L'aide apportés par la scintigraphie dans l'amibiase hépatique est considérable. Elle contribue à étayer le diagnostic d'atteinte hépatique au cours de l'amibiase en montrant des déformations globales de la silhouette hépatique quasi caractéristiques; elle permet la distinction entre hépatite et abcès dans des cas où la clinique est hésitante. Elle est indispensable à la surveillance de l'évolution de la maladie sous traitement médical car il y a souvent divergence entre l'évolution clinique et scintigraphique, l'in-

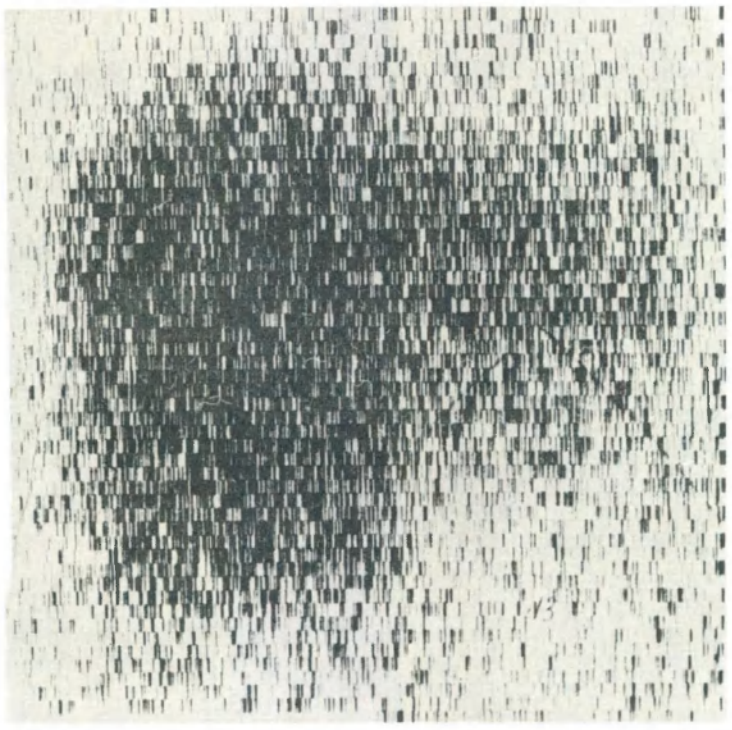

Figure 6

Diminution de densité localisée au lobe gauche.

TABLEAU IV

RÉPARTITION DES IMAGES ANORMALES ÉLÉMENTAIRES POUR 54 SUJETS PRÉSENTANT UNE IMAGE ANORMALE

Type 1 isolé	15
Type 2 isolé	0
Type 3 isolé	8
Association de plusieurs types	31

tégrité de l'image scintigraphique permettant seule d'affirmer la guérison. Pour apporter tous ses fruits, la scintigraphie doit se plier à un certain nombre d'exigences: utilisation du radio-or 198 et balayage de trois plans successifs: ce dernier impératif conditionne la durée de l'examen qui est de l'ordre de 3 h; l'utilisation de la caméra à scintillations semble devoir nous libérer partiellement de cet inconvénient en permettant l'exploration rapide sous plusieurs incidences des zones suspectes repérées sur la scintigraphie effectuée par balayage antérieur.

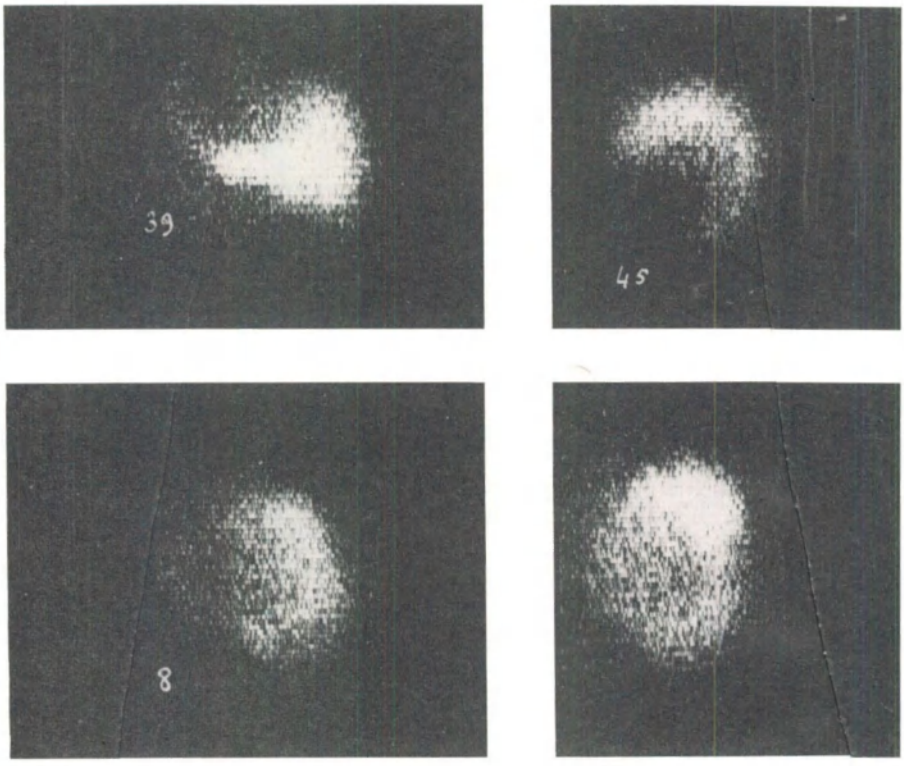

Figure 7

Scintigraphies de profil montrant la localisation postérieure des images lacunaires.

Bien entendu ces modifications morphologiques considérées isolémen ne sont pas pathognomoniques de l'amibiase hépatique, mais leur association jointe aux modifications de la «clearance» chez des sujets suspects constituent un faisceau d'arguments en faveur de la localisation hépatique de l'amibiase.

IV. INDICATIONS ET RESULTATS

Ces examens ont été effectués soit dans un but diagnostique, soit dans le but de surveiller l'évolution de la maladie sous traitement.

Quatorze des 68 malades examinés présentaient une image scintigraphique normale lors d'un premier examen; pour six d'entre eux l'existence d'antécédents de dysenterie amibienne et d'un syndrome douloureux de l'hypocondre droit motivaient l'examen dont les résultats ont permis d'éliminer une localisation hépatique. Les 8 autres, présentaient des antécédents d'hépatite amibienne et avaient reçu un traitement médical intensif; le problème

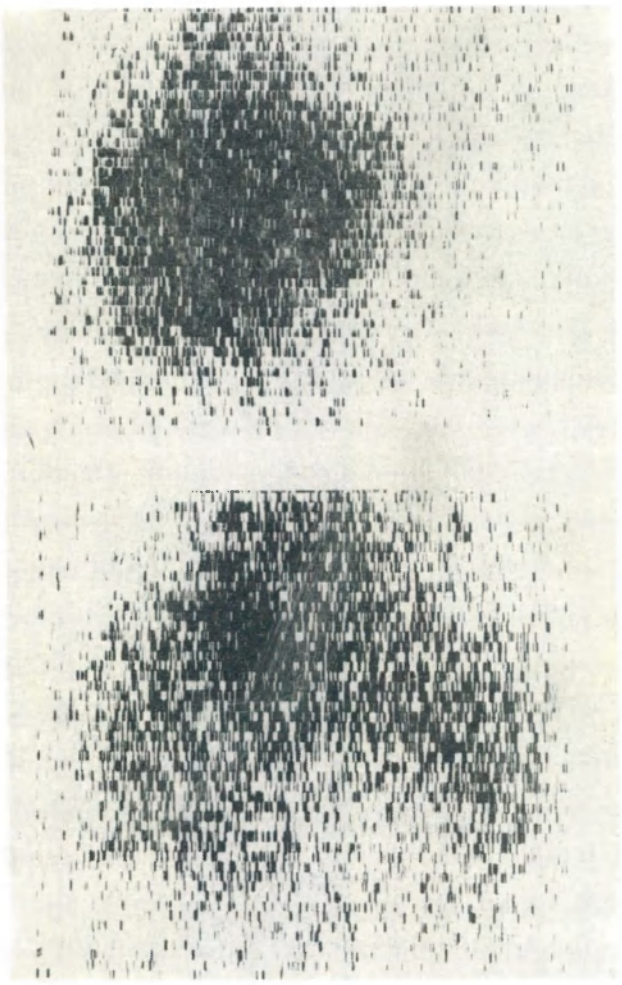

Figure 8

Scintigraphies de profil du même malade avant et après traitement médical montrant la restitution ad integrum à un an et demi d'intervalle.

était chez eux d'apprécier les séquelles de la maladie ou de rechercher un abcès résiduel; la scintigraphie a conclu à l'intégrité de l'image hépatique.

Cinquante quatre malades présentaient une image anormale lors d'un premier examen. Ces malades étaient: a) soit d'anciens amibiens chez lesquels on recherchait une localisation hépatique, hépatite ou abcès et pour ce groupe qui comprend 23 malades 14 ont une scintigraphie caractéristique d'une hépatite tandis que 9 ont une scintigraphie affectée par une image lacunaire; b) soit des malades dont la localisation hépatique était connue et chez lesquels on recherchait un abcès; pour ce groupe de 31 malades dans

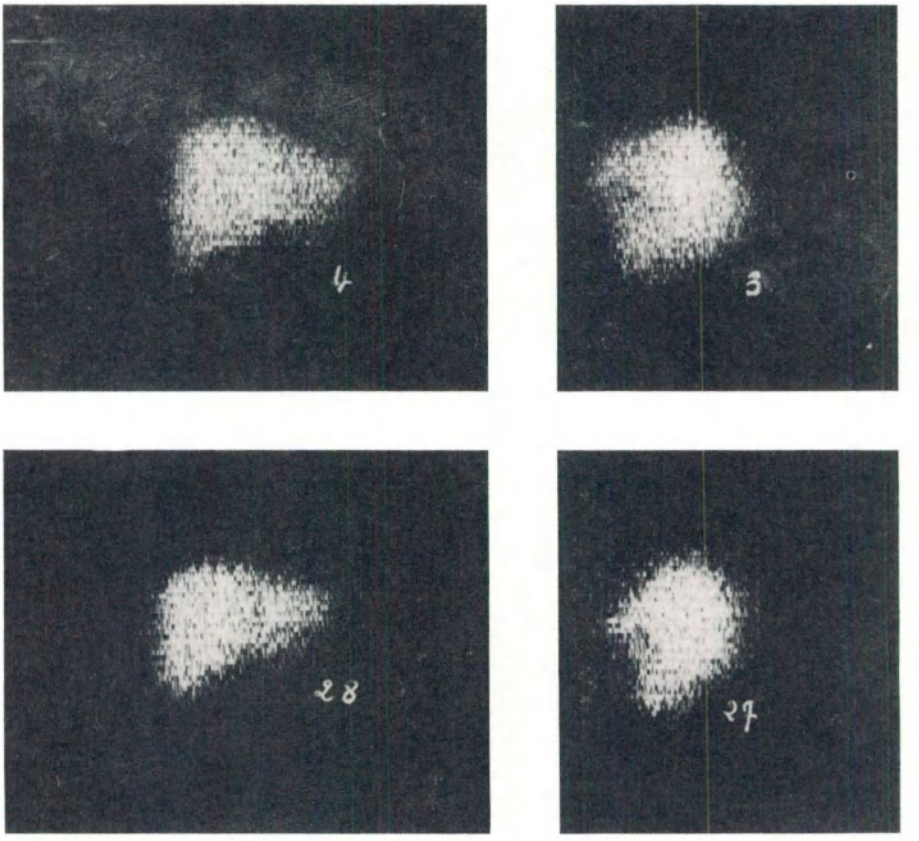

Figure 9

Scintigraphies de profil du même malade avant et après traitement médical montrant la restitution ad integrum à un an et demi d'intervalle.

25 cas la scintigraphie a objectivé un abcès tandis que dans 6 elle montrait seulement une image d'hépatite.

Ces données mettent en valeur l'intérêt diagnostique de la méthode qui a permis d'affirmer soit l'intégrité du parenchyme hépatique, soit une hépatite, soit un abcès.

Un certain nombre d'examens ont été effectués après traitement chirurgical d'un abcès; l'intégrité scintigraphique constituant un critère de guérison. Mais dans la majorité des cas, les examens répétés l'ont été chez des sujets soumis à un traitement médical et dans le but de suivre l'évolution d'un abcès. Ainsi 13 malades ont subi 2 ou 3 examens successifs. Dans 6 cas on a pu observer le retour à la normale de l'image scintigraphique dans 2 cas une légère régression des anomalies scintigraphiques et 3 fois la persistance d'images lacunaires.

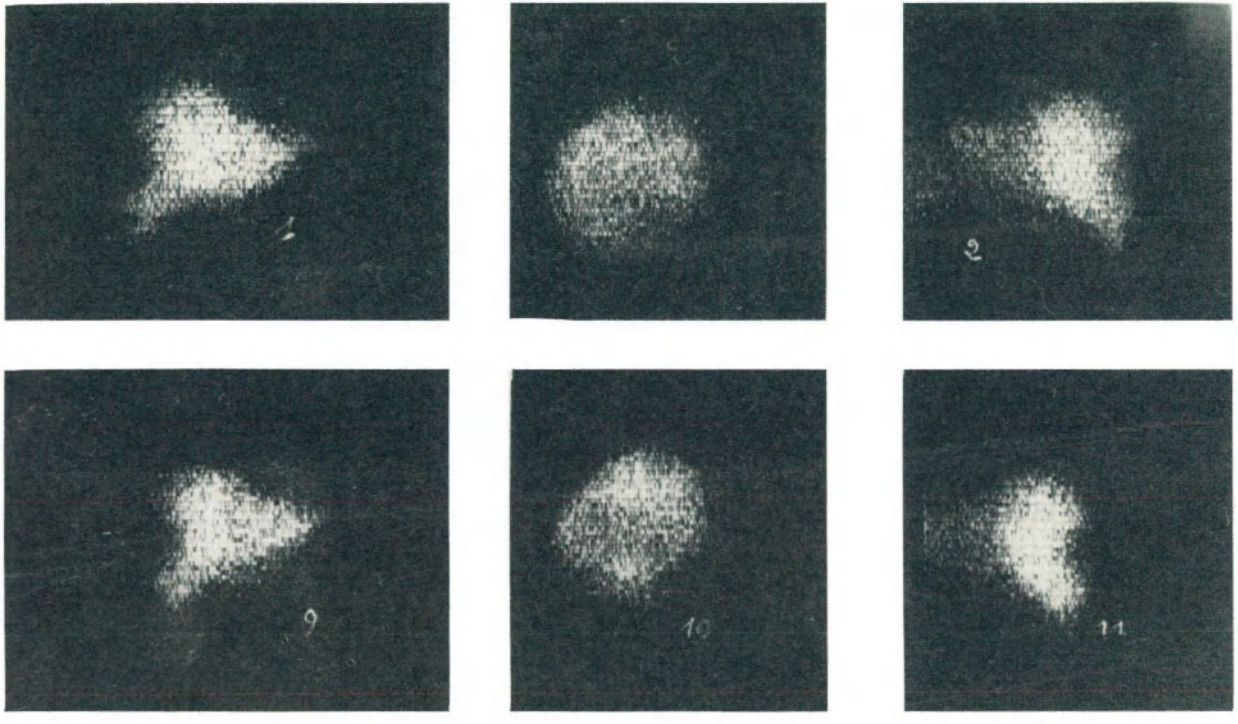

Figure 10

Les deux séries de scintigraphies effectuées selon trois faces et à un mois d'intervalle montrent la persistance d'image lacunaire malgré un traitement médical.

THE VALUE OF LIVER SCANNING IN THE DIAGNOSIS OF ECHINOCOCCUS DISEASE OF THE LIVER

T. DOXIADES, P. GATSOU, D. IKKOS, G. MERIKAS AND A. NASTOU
EVANGELISMOS HOSPITAL, ATHENS, GREECE

Abstract — Résumé — Аннотация — Resumen

THE VALUE OF LIVER SCANNING IN THE DIAGNOSIS OF ECHINOCOCCUS DISEASE OF THE LIVER. Echinococcus disease of the liver is quite common in Greece. During the past year, liver scanning was carried out in 40 patients with proven hydatid cysts of the liver.

These cysts appear as defects in the scan. Therefore, it is impossible to attribute with absolute certainty a liver-scan defect to a hydatid cyst, without the help of clinical and/or laboratory data. However, in the scans signs exist which help to decide whether a defect is probably due to a cyst or not.

Our experience shows that liver scanning is a most valuable method in the diagnosis of Echinococcus disease of the liver for the following reasons:

(1) It shows the presence or absence of a clinically important cyst;

(2) It defines satisfactorily the number, size and localization of cysts of clinically important size; and

(3) It is the only available method by which it can be decided whether an elevation of the right hemidiaphragm is due to an Echinococcus cyst or a normal variation in the shape and/or location of the liver.

RÔLE DE LA GAMMAGRAPHIE DANS LE DIAGNOSTIC DE L'ÉCHINOCOCCOSE DU FOIE. L'échinococcose du foie est une affection assez répandue en Grèce. Au cours de l'année écoulée, on a procédé à des gammagraphies du foie sur 40 sujets chez qui on avait constaté des kystes hydatiques du foie.

Ces kystes apparaissent comme des irrégularités sur le scintigramme. En conséquence, il est impossible d'attribuer avec certitude une irrégularité à un kyste hydatique, à moins de pouvoir disposer en même temps de certaines autres données cliniques ou de laboratoire. Néanmoins, le scintigramme comporte certains indices qui permettent de déterminer si une irrégularité est vraisemblablement due à un kyste.

Il ressort de l'expérience des auteurs que la gammagraphie du foie est une méthode des plus précieuses pour le diagnostic de l'échinococcose:

1. Elle indique la présence ou l'absence d'un kyste cliniquement important;
2. Elle définit de façon satisfaisante le nombre, la dimension et la localisation de kystes cliniquement importants;
3. Elle constitue la seule méthode permettant de déterminer si une élévation du côté droit du diaphragme est due à un kyste hydatique ou à une modification normale de la forme ou de la position du foie.

ЗНАЧЕНИЕ СКЕННИРОВАНИЯ ПЕЧЕНИ ПРИ ДИАГНОСТИКЕ ЭХИНОКОККОЗА ПЕЧЕНИ. Эхинококкоз довольно распространен в Греции. В прошлом году было проведено сканирование печени у 40 больных с установленными эхинококковыми цистами печени.

На сканнограмме цисты проявляются как дефекты. Поэтому дефект на сканнограмме печени нельзя с абсолютной уверенностью отнести за счет эхинококковой цисты без наличия других клинических и/или лабораторных данных. Однако на сканнограммах имеются признаки, которые помогают решить, объясняется ли дефект наличием цисты или нет.

Опыт авторов показывает, что сканирование печени является самым ценным методом диагностики эхинококкоза печени по следующим причинам:

1) оно показывает наличие или отсутствие клинически важных цист;
2) определяет с удовлетворительной степенью точности количество, размер и локализацию цист, имеющих клинически важные размеры;
3) сканирование – единственный метод, позволяющий определить, объясняется ли подъем правого купола диафрагмы эхинококковым пузырем или нормальным вариантом формы и/или локализации печени.

IMPORTANCIA DE LA EXPLORACIÓN GAMMAGRÁFICA EN EL DIAGNÓSTICO DE LA EQUINOCOCOSIS DEL HÍGADO. La equinococosis del hígado es muy común en Grecia. Durante el pasado año los autores exploraron el hígado de 40 pacientes afectados por quistes hidatídicos.

Esos quistes aparecen como defectos en el gammagrama, pero no es posible atribuir con toda seguridad a un quiste hidatídico uno de estos defectos sin ayuda de otros datos clínicos o de laboratorio. No obstante, ciertos indicios en el gammagrama del hígado permiten decidir con cierta probabilidad si un defecto se debe o no se debe a la presencia de un quiste.

Los experimentos efectuados por los autores demuestran que la exploración hepática es un método muy valioso para el diagnóstico de la equinococosis del hígado por las siguientes razones:

1. Revela la presencia o la ausencia de quistes importantes desde el punto de vista clínico.
2. Indica satisfactoriamente el número, el tamaño y la localización de los quistes de dimensiones clínicamente importantes.
3. Es el único método que permite decidir si una elevación del hemidiafragma derecho se debe a un quiste hidatídico o a una variación normal de la forma o de la situación del hígado.

INTRODUCTION

The diagnosis of echinococcus cyst of the liver can be considered as certain when: (1) a round, smooth mass is found by palpation or seen on X-ray films and (2) laboratory examinations show an increased number of eosinophils in the peripheral blood, a positive Casoni skin test and/or a positive Weinberg serological test. Centrally located cysts can neither be palpated nor seen by X-ray examination except if the cysts are calcified; a non-characteristic hepatomegaly is the only clinical finding in these cases. Splenoportography has been used successfully for the demonstration and/or localization of centrally located cysts. This method has not, however, been used very extensively because of its technical problems and its potential dangers. Some authors have used cholangiography in the diagnosis of echinococcus cysts of the liver, but this technique is seldom used for this purpose in Greece.

Positive laboratory tests for echinococcus are of no value in the diagnosis of liver cysts in cases showing cysts in other organs, e.g. the lungs. Positive laboratory tests may finally be found in cases with very small echinococcus cysts of the liver, i.e. in cases in which the cysts are so small that they cannot cause any symptoms to the patient.

But even when the clinical and/or laboratory findings demonstrate the presence of echinococcus cysts in the liver, the information available to the surgeon in planning his operation is usually not complete. The clinical and usual X-ray examination quite frequently do not permit an accurate knowledge of the number, size and location of clinically important cysts.

The visualization of echinococcus cysts of the liver in liver scans has been reported by different authors [1-8]. ADAMS and his co-workers [5-6] studied the diagnostic value of liver scanning in echinococciasis of the liver in a limited number of patients. Their conclusion was that the method was of significant value.

The aim of the present work was to examine critically the diagnostic value of liver scanning in echinococcus disease of the liver and for this purpose a comparison of the scan findings and the operative ones was undertaken. This work was considered of possible value since no similar data could be found in the literature.

MATERIAL AND METHODS

A. Material

The material of the present study comprises 104 patients, sent to the laboratory for liver scanning because of suspected echinococcus cysts of the liver. These 104 cases represent approximately 20% of the total number (516) of patients sent for liver scanning during the period July 1962 to January 1964 inclusive. Symptoms from the right hypochondrium (66 cases) or the epigastrium (6 cases) were the main complaints in these 104 cases. Eosinophilia was the presenting symptom in 4 cases. Nine of the patients were sent for examination because of the presence of hydatid cysts in the lung. Enlargement of the liver was the main cause for the liver scanning in the remaining 21 cases. The sex of the patients was male in 59 cases and female in 45 cases. Their age varied between 17 and 75 yr, with a mean age of 46 yr.

B. Methods

Liver scanning was performed by the usual technique [2, 9, 10] using I^{131}-labelled Rose Bengal* and a commercial apparatus**.

Thyroid uptake of I^{131} was blocked by administration of Lugol's solution for the 2-3 d preceeding the test; when iodine-containing material had been used previously (as for example for cholecystography), Lugol administration was omitted. Rose Bengal I^{131} was given intravenously in a dose of usually 130-140 μc. Scanning of the liver was performed with the patient in the supine position and the detector above the patient, except on rare occasions when lateral and/or posterior scans were obtained. Two liver scans were performed in nearly all cases: the first one was started 10-15 min after the administration of the Rose Bengal and the second one immediately after completion of the first. The collimator-to-skin distance was 4 cm for the first scan and less than 1 cm for the second scan. Since the collimator used (Picker 19-hole) has a focusing distance of 7 cm, the first scan concerned principally the anterior and the second one the deeper-seated parts of the liver. The whole examination lasted for approximately 90 min. The usual setting of the Magnascanner was: scanning speed 50 cm/min; EPM 80-100%; density 12, HV 700, when a Kodak royal blue medical X-ray film was used.

A reading of the obtained photoscans was performed after contrast enhancement by photo-copying, according to a previously described technique [11].

Planimetry was done using commercial equipment. The statistical methods used were the standard ones.

RESULTS

The results of the present study are summarized in Table I. The scanning findings were reported as negative in 45 cases and as positive in

* Commercially prepared by the Radiochemical Centre, England, or Phillips-Duphar, Holland.

** Magnascanner, manufactured by Picker Inc., USA.

TABLE I

RESULTS OF LIVER SCANNING FOR HYDATID CYSTS IN 104 CASES

Type of scan	No. of cases
Total number of liver scans	516
Scans on subjects with suspected diagnosis of hydatid cysts of the liver	104
Negative findings	45
Positive findings	59
Positive findings due to	
Post-operative scars in	2
Metastatic cancer in	5
"Idiopathic" liver cyst in	1
Most probably hydatid cysts in	51
Operated	34
Not operated as yet	17

the remaining 59 cases. It should be mentioned that, as here defined, positive scans were considered those in which single or multiple defects could be seen, the defects showing circular limits when located centrally or toxoid limits when found peripherally. All other scans were considered as negative for the present study, disregarding eventual presence of other findings, such as hepatomegaly, irregular fixation of Rose Bengal, etc.

Two of the cases with positive scans had been previously operated because of hydatid cyst of the liver and both showed a circular defect, located near the operative scar. The scan findings did not permit a decision as to whether the observed defects were due to post-operative scars of the liver or new cysts. Both patients were explored surgically and none of them had any new liver cysts.

In five other cases the scanning findings were considered as probably due to a malignant disease rather than echinococcus cysts. Explorative laparotomy and/or post-mortem examination verified the diagnosis of malignancy in all five cases.

One patient (Case No. 51) showed a huge, semicircular defect with smooth margins. The diagnosis of a very large echinococcus cyst was, therefore, considered as very probable. Exploratory laparotomy showed indeed the presence of a huge cyst. This cyst was not, however, due to echinococcus and its nature remained obscure.

In the remaining 51 patients the clinical and laboratory examinations

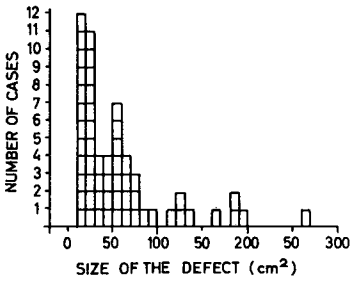

Fig. 1

Size of scan defects in hydatid cysts of the liver

as well as the scanning findings were in accordance with the diagnosis of echinococcus cysts of the liver. The number of the defects seen on the scan was: one in 37(74%) cases, two in 9(18%) cases and three or more in 4(8%) cases.

The size of the defects was approximated by measuring their surface in the scan by planimetry. The results of these measurements are shown in Fig. 1. As can be seen the size of the defect was quite small in approximately half of them; their surface varied between 10-30 cm^2 in 43% of the defects. In a second group, comprising 38% of the defects, the size varied between 30-80 cm^2. The remaining 11 defects had sizes up to 260 cm^2.

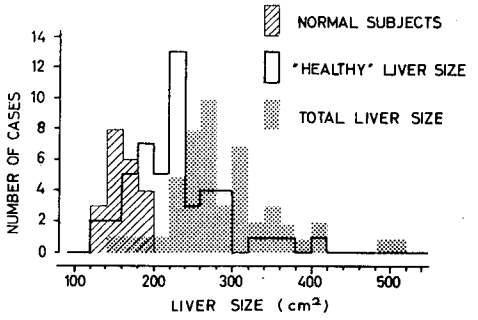

Fig. 2

Liver size in hydatid cysts of the liver

Figure 2 shows the surface area of the "healthy liver", i.e. the liver not occupied by the cyst, as well as the surface area of the total organ (includes the areas of both the healthy liver and the defect). For a comparison, the surface area of the liver of a group of normal persons is shown in the same figure. It is quite obvious that the size of the total area and the "healthy" area varied tremendously from case to case. Despite that, the more common value for the total area was 270 cm^2, i.e. a value 70% larger than that of the normal sized liver (160 cm^2).

The correlation between the size of the "healthy" liver and the whole liver is shown in Fig. 3. The high degree of correlation ($r = 0.83$, $P < 0.001$)

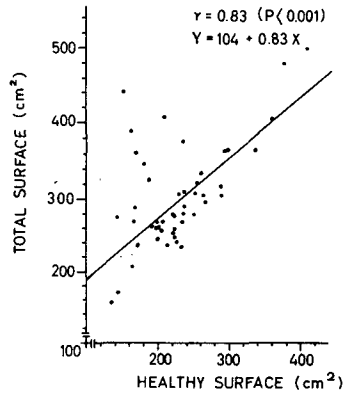

Fig. 3

Correlation between the "healthy" and total liver surface in hydatid cysts of the liver ("healthy" surface stands for the part of the liver surface not occupied by the scan defect).

could be expected since the first value, i.e. the one for the healthy liver, is included in the second one. Despite this high significant correlation, the deviation of the individual values from the regression line is quite pronounced. This finding can be interpreted as showing that the increase of the liver size does not always follow closely the increase of the size of the cyst.

Up to January 1964 an operation had been performed in 34 of the 51 cases considered as positive for the presence of hydatid cysts in the liver. In 22 (67%) of these 34 cases the agreements between the scan and operative findings as to the number of cysts was excellent. In the remaining 12 cases the number of cysts proven at operation was apparently or really different from the one predicted on the basis of the scan (Table II). In one patient, in whom the scan had been considered as negative, the operation showed the presence of a small cyst in the middle of the upper border of the liver. Re-evaluation of the scan (see Fig. 4 B) showed that the impression due to the heart was in this case more pronounced than usual. This change corresponds exactly to what could be expected on the basis of the operative findings. In this case a truly positive scan had been misinterpreted as negative. In one other patient (Case No. 85) two cysts were found at operation while only one cyst was visible on the scan (see Fig. 7 D). In another case (No. 103, Fig. 5 A) no cyst was found although the liver scan showed a well-defined defect in the lower border. In the remaining 9 of the 34 operated cases a single cyst was found by operation although two or more defects were visible in the scan (Figs. 6, 7 A-C and E-F).

DISCUSSION

The present work concerns only echinococcus disease of the liver caused by echinococcus unilocularis, since the other type of parasite – echinococcus multi-locularis – is unknown in Greece [12].

The visualization of echinococcus cysts of the liver in liver scans is

TABLE II

A COMPARISON OF THE RESULT OF LIVER SCANNING AND OPERATION AS REGARDS THE NUMBER OF HYDATID CYSTS

Case No.	Number of hydatid cysts of the liver found by	
	Liver scanning	Operation
72	One, eventually one more	One
73	One	One
74	One	One
75	One	One
76	Many	One
77	Eventually two (post-operative scars)	One
78	One	One
79	One	One
80	One	One
81	Probably two	One, ruptured to the lung
82	One	One
83	One	One
84	One, eventually one more	One
85	One	Two
86	One	One
87	One	One
88	One	One
89	One, eventually two more	One
90	One	One
91	One	One
92	Many	One
93	Two	Two
94	One	One
95	One	One
96	One	One
97	One, probably one more	Two
98	Two	Two
99	One, eventually one more	One
100	Two	Two
101	Two	Two
102	Two, eventually three	One huge
103	One	One
104	One	None

due to the fact that the substances usually employed in liver scanning do not penetrate into the cyst fluid. Therefore, a defect is found in the scan at the place corresponding to the cyst.

There is general agreement that liver tumourous masses smaller than 2-3 cm in diam. cannot be detected by the presently available liver scanning techniques, and especially the one used by us. The fact that the smallest defect detected by us in the present study had an area of 10 cm^2, i.e. an area corresponding to a mass approximately 4 cm in diam., is in complete agreement with the above statement. The possibility exists, therefore, that echinococcus cysts smaller than 4 cm in diam. might have been missed in

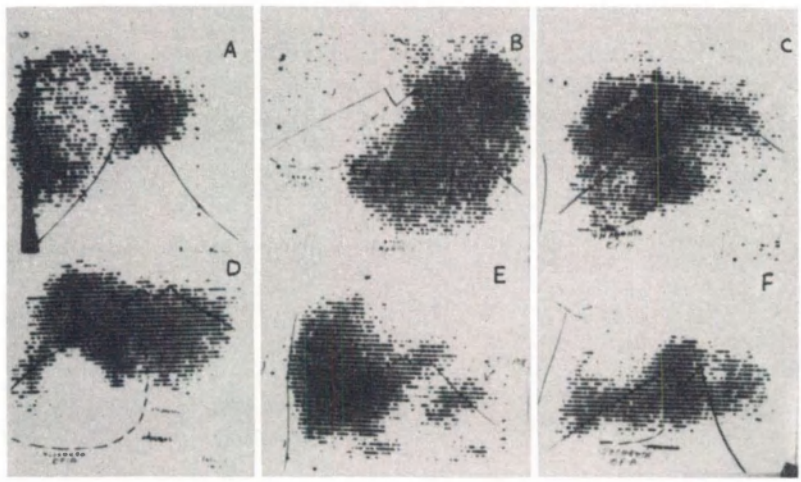

Fig. 4

Types of scan defects caused by hydatid cysts of the liver

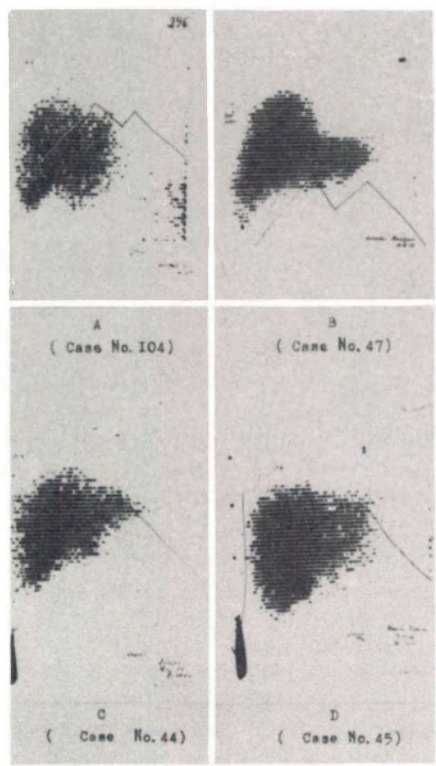

Fig. 5

Liver scans in a case of false positive result (A), false negative result (B) and two negative cases, explored surgically (C and D)

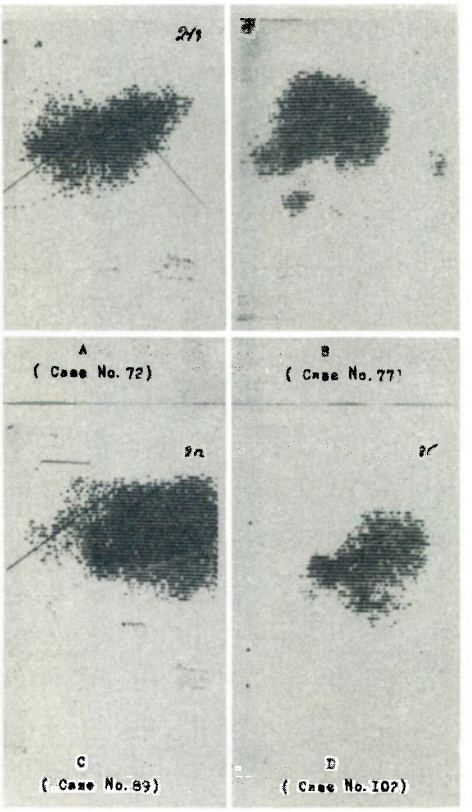

Fig. 6

Liver scans in solitary hydatid cysts of the liver
in cases previously operated for echinococcus of the liver

the cases examined by us. This size limitation seems, however, to be of no importance in clinical work, since echinococcus cysts must attain, in practically all cases, a diameter larger than 4 cm before they can cause any symptoms. One might, therefore, accept as true the idea that clinically important cysts are potentially detectable by the presently available liver scanning techniques.

Since the cysts are of spheroid shape, the typical defect caused by these cysts is cyclical or toxoid, according to whether the cyst is centrally or peripherally located. Furthermore, the boundary between the defect and the remaining liver picture is usually smooth (Fig. 4). None of these characteristics is, however, pathognomonic of echinococcus cysts. Defects with similar characters can be due to other causes, such as abscesses, malignant tumours, cysts of other etiology and so on. Rupture of the echinococcus cyst or suppuration might, on the other hand, change the typical appearance of the defect caused by the echinococcus cyst (see, for example Fig. 7 E). Echinococcus cysts are usually found in the right lobe (70% in the present material) but they might be located anywhere in the liver. Finally, liver

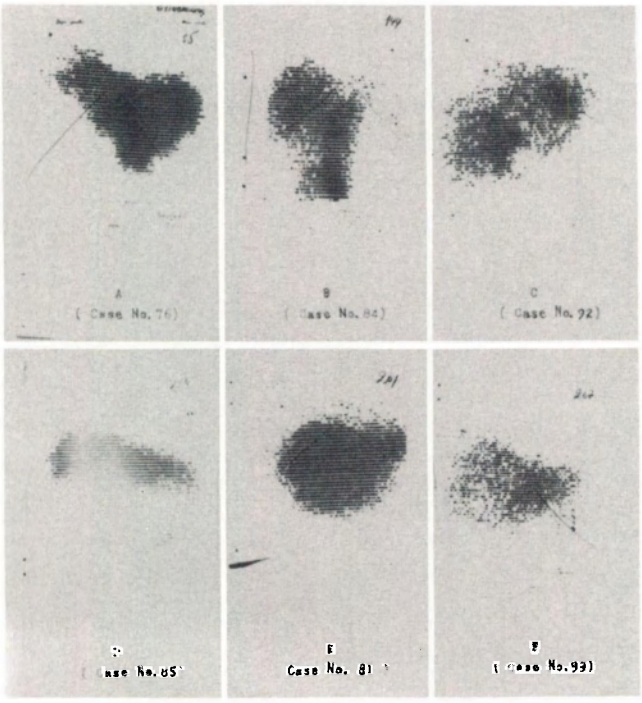

Fig. 7

Liver scans in hydatid cysts of the liver in cases in which there was a discrepancy between the scanning and operation findings with respect to the number of cysts

cysts due to echinococcus are usually single (74% in the present study) but two or more cysts are found in a considerable number of cases [12, 13]. Therefore, the diagnosis of echinococcus cysts of the liver cannot be done only on the basis of the scan.

CAROLI and BONNEVILLE [7] stressed the importance of the presence of a compensatory liver hypertrophy in the diagnosis of echinococcus liver disease. Our data do not, however, totally support this opinion. It should be mentioned here that our measurements are only approximations since a given increase in the area of the thin left lobe represents a much smaller increase in liver size than a corresponding change in the thicker right lobe. Despite this reservation we think, however, that the measurements done were good approximations of the true changes.

The overall accuracy of liver scanning as regards the presence or not of clinically important cysts seems to be very satisfactory. Of the 104 cases examined by us there was only one case where the cyst was missed in the scan although the operation proved later that a cyst was present (Case of Fig. 5 B). It might be argued that a negative scanning report might have influenced the final diagnosis so that patients with a liver cyst might not have been sent for operation. The follow-up period is as yet too short to exclude such a possibility. It can only be mentioned that until now no other

patients in whom the liver scanning was reported as negative for cysts was shown later to harbour such a cyst in the liver. It should also be mentioned that two of the patients with a negative liver scan were operated upon and that no cyst was found in them (Cases of Fig. 5 C-D). If only the 34 operated cases are taken into account, then the false negative results (1 out of 34, or 3%) seem to be very small. The same applies as regards the false positive results as well: a cyst could not be found in only one out of the 34 patients operated upon (Case of Fig. 5 A). So the overall diagnostic accuracy of liver scanning for the presence of clinically important echinococcus cysts – 94% – seems to be extremely high.

The accuracy of the method under discussion as regards the number of cysts seems at first to be decidedly lower, since the number of cysts was correctly predicted in only 24 of the 34 patients or 70% (see Table II). In 4 of the remaining 10 cases the cause of this discrepancy might have been the fact that these patients had been previously operated for liver cysts. It is understandable that some of the defects seen in the liver scans of these cases (Fig. 6 A-D) might have been caused by post-operative scars or other changes in the liver. Support of this view is provided from the observation that defects in the left lobe of the liver have been observed in a number of patients previously operated upon for peptic ulcer [14].

A certain explanation for the discrepancy in three of the ten cases is not possible. Examination of their liver scans (see Fig. 7 A-C) shows definitely the presence of more than one defect. None of these patients had been previously operated on the abdomen. The finding of only one cyst at operation might eventually be due to the fact that one of the cysts might have escaped detection during surgery. The possibility of such an event is amply attested from the relatively large number of patients operated upon for a second cyst a few years after a first cyst had been removed [13].

Case No. 85 was proven surgically to have two cysts while only one defect could be seen in the scan (Fig. 7 D). No explanation for this discrepancy can be provided, since the operation report is not very detailed as regards the size and the location of the two cysts. The scan of Case 81 (Fig. 7 E) was interpreted as showing two defects, one at the upper half and the other at the lower half of the right border of the liver. At operation only a large cyst, located posteriorly, could be found. This cyst had been spontaneously ruptured to the lungs and it is possible that the scan picture was the result of the change of the shape of the cyst consequent to the rupture. The discrepancy in the last case (Case No. 99) was proven to be the result of a technical error. The liver scan showed a large defect occupying most of the right lobe [Fig. 7 F]. Furthermore, the palpable lower limits of the liver were marked significantly lower than the limits found on scanning. Therefore the presence of two cysts was reported. At operation the liver was hardly enlarged below the costal margin. The second cyst supposedly occupying the lower half on the right lobe did not exist. Its spurious appearance on the scan was, thus, the result of an erroneous placement of the palpatory limits of the liver too low. Thus, the accuracy of the liver scanning as regards the number of cysts is probably higher than 70%.

The aforementioned excellent diagnostic accuracy of liver scanning as regards the presence or not of clinically important echinococcus cysts and its satisfactory accuracy as regards the definition of the number, size and

location of the cysts seem to justify the opinion that, when available, liver scanning is very helpful in the diagnosis and treatment of echinococcus cysts of the liver. The method is especially helpful in deciding whether a roentgenologically seen elevation of the right hemidiaphragm is due to an hydatid cyst or not.

REFERENCES

[1] CAROLI, J., JAMMET, H.J. and RENAULT, H., Sem. Hop. 34 (1958) 449/SP89.
[2] DONATO, L., BECCHINI, M.F. and PANICHI, S., in Medical Radioisotope Scanning, IAEA, Vienna (1959) 87-103.
[3] CZERNIAK, P. and LUBIN, E., Tind. v. Gastroenterol. 4 (1961) 42.
[4] ABAD, R., Acta Oncologica 1 (1962) 213.
[5] ADAMS, R., Med. Arts Sci. (1962) 9-12.
[6] ADAMS, R., HINDAWI, A.Y. and QUASSAB, Kh., J. nucl. Med. 3 (1962) 315.
[7] CAROLI, J. and BONNEVILLE, B., Arch. mal. appar. digest 51 (1962) 55.
[8] CZERNIAK, P., LUBIN, E., DJALDETTI, M. and DE VRIES, A., J. nucl. Med. 4 (1963) 35.
[9] STIRRETT, L.A., YUHL, E.T. and LIBBY, R.L., Surg. Gynec. Obsta 96 (1953) 210.
[10] FRIEDELL, H.L., MACINTYRE, W.J. and REJALI, A.M., Amer. J. Roentgenol. 77 (1957) 455.
[11] IKKOS, D., LIBBY, R., GATSOU, P. and DOXIADES, T., Evangelismos Hosp. Rev. 25 (1963) 257.
[12] OURIAS, B., Atti del VII Congresso Internazionale di Idatologia, Roma (1960) 699.
[13] DEVÉ, F., L'echinococcose primitive, Masson et Cie, Ed. Paris (1949).
[14] GATSOU, P. and IKKOS, D., Unpublished observations.

SCANNING STUDY OF 700 LIVERS EVALUATION OF EXISTING DIAGNOSTIC PROCEDURES

P. CZERNIAK
RADIUM AND ISOTOPE INSTITUTE, GOVERNMENT HOSPITAL,
TEL-HASHOMER, ISRAEL

Abstract — Résumé — Аннотация — Resumen

SCANNING STUDY OF 700 LIVERS (Evaluation of the existing diagnostic procedures). The livers of 700 patients have been examined. Clinical studies, laboratory tests, roentgenographic examinations and liver-scanning studies were performed. The patients were followed up and finally an objective diagnostic confirmation was obtained in most cases. In this way an evaluation of the performed tests was established. The liver scanning was done using Au^{198}, I^{131}-Rose Bengal and I^{131} PVP. Apart from the classical AP technique, special techniques were utilized, such as tri- or bi-plane stereoscanning and combined isotope studies with Au^{198} and I^{131}-Rose Bengal leading to a determination of the RLC (radioisotope liver coefficients). The patients were divided into eight clinical groups and the diagnostic data were accordingly compiled and evaluated. A summary of the results of this study is presented.

Each clinical group was separately analysed. For example, a space-occupying lesion was detected in 95% of the 65 cases of Echinococcus disease. X-ray examination detected calcifications in only 35% of these cases, but also in 14% of other liver diseases. Weinberg and Casoni reactions were positive in 64% of the cases of Echinococcus, but also in 22% of other diseases. In hepatic malignancy, a space-occupying lesion was detected in 44% of cases, a foggy scan in 30% and morphological changes in 29%. In two of the 158 tumour cases the scan falsely appeared to be normal, but in 40% of the same cases the laboratory results were negative.

By using the bi- and tri-plane stereoscanning technique, new and supplementary information on the state of the liver was obtained in 45% of cases.

Liver scanning was also used in the follow-up study. It was found that:

(1) After Echinococcotomy, a definite scar persists as a space-occupying lesion;

(2) Three months after a treated amoebic abscess, complete regeneration occurs;

(3) After a porto-caval shunt, the liver scan becomes smaller and the spleen larger – even when the general condition is satisfactory;

(4) Cytostatic agents may be temporarily effective in some diffuse hepatic lesions;

(5) A rescanned suspected lesion may reappear as a space-occupying lesion or disappear. Thus the time of scanning may affect the diagnosis.

Conclusions: (1) Liver scanning can be considered as a very useful method for clinical, morphological and topographical diagnosis in hepatopathology; and (2) The results may be improved by (a) advanced instrumentation and the use of stereoscanning techniques and (b) good collaboration between the internists and surgeons.

ÉTUDE SCINTIGRAPHIQUE DE 700 FOIES (Evaluation des procédures actuelles de diagnostic). On a examiné les foies de 700 malades (étude clinique, analyses en laboratoire, examens radiographiques, explorations scintigraphiques). On a continué à «suivre» les malades après ces examens; on a pu avoir la confirmation objective du diagnostic dans la plupart des cas et évaluer les résultats de la campagne. Pour la scintigraphie du foie, on a utilisé l'or-198, le rose bengale marqué avec ^{131}I et le polyvinylpyrrolidone également marqué avec ^{131}I. On a appliqué, non seulement la méthode classique, mais aussi des méthodes particulières comme l'exploration stéréographique dans deux plans ou trois plans et l'emploi combiné de l'or-198 et du rose bengale marqué à l'iode-131 pour déterminer les coefficients relatifs de fixation de ces radio-isotopes dans le foie. Les sujets avaient été répartis en huit groupes cliniques aux fins de compilation et d'évaluation des résultats du diagnostic, qui sont présentés succinctement dans le mémoire.

Chaque groupe clinique a été analysé séparément. Par exemple, on a détecté une lésion en volume dans 95% des 65 cas d'échinococcose. La radiographie a permis de constater des calcifications dans 35% seulement de ces cas, mais aussi dans 14% des autres cas de maladies hépatiques. Les réactions de Weinberg

et Casoni ont été positives dans 64% des cas d'échinococcose, mais aussi dans 22% des autres cas. En ce qui concerne le cancer du foie, on a détecté une lésion en volume dans 44% des cas, on a obtenu un scintigramme voilé dans 30% des cas et on a constaté des modifications morphologiques de l'organe dans 29% de cas. Dans deux des 158 cas de tumeurs malignes, le scintigramme semblait faussement normal, mais dans 40% de ces mêmes cas les résultats obtenus au laboratoire étaient négatifs.

Par la technique d'exploration stéréographique dans deux ou trois plans, on a obtenu dans 45% des cas des renseignements nouveaux ou complémentaires sur l'état de l'organe.

On a également utilisé la scintigraphie pour le contrôle ultérieur des résultats. On a fait les constations suivantes:

1. Après extirpation du kyste hydatique, une cicatrice caractérisée persiste sous forme de lésion en volume;
2. Trois mois après le traitement d'un abcès amibien, une régénération complète intervient;
3. Après une dérivation porto-cavale, le scintigramme du foie devient plus petit et celui de la rate plus grand – même lorsque l'état général est satisfaisant;
4. Les agents cytostatiques peuvent être momentanément efficaces pour certaines lésions hépatiques diffuses;
5. Il arrive qu'une lésion dont on n'avait pu affirmer la présence avec certitude devienne macroscopique ou qu'elle cesse totalement d'être visible; par conséquent, le moment de l'exploration peut affecter le diagnostic.

L'auteur tire les conclusions suivantes:

1. On peut considérer la scintigraphie comme une méthode très utile pour le diagnostic clinique, morphologique et topographique en hépatopathologie. 2. On peut améliorer les résultats: a) en utilisant des appareils perfectionnés ou en ayant recours aux techniques d'exploration stéréographiques; b) par une bonne collaboration entre le clinicien et le chirurgien.

ИССЛЕДОВАНИЕ ПЕЧЕНИ 700 БОЛЬНЫХ С ПОМОЩЬЮ СКЕННИРОВАНИЯ. (Оценка существующих диагностических методов). Проводились клинические исследования, лабораторные анализы, рентгенографическое обследование и скеннирование печени 700 больных. За больными было установлено наблюдение, и в большинстве случаев в конечном итоге диагноз подтвердился. Таким образом была дана оценка проведенным исследованиям. Скеннирование печени производилось с помощью бенгальской розы и поливинилпиролидона, меченных золотом-198 и йодом-131. Помимо классического АР-метода для определения радиоизотопных коэффициентов печени применялись специальные методы, такие как трех или двухплоскостное стереоскеннирование и комбинированное изотопное исследование с помощью меченной золотом-198 и йодом-131 бенгальской розы. Больные были разделены на восемь клинических групп, и соответственно производился сбор и оценка диагностических данных. Дается краткое изложение результатов этого исследования.

В каждой клинической группе анализы проводились отдельно. Например, в 95% из 65 случаев эхинококковой болезни был обнаружен ограниченный участок поражения. Рентгеновское обследование выявило обизвествление только в 35% этих случаев, а также в 14% случаев других заболеваний печени. Реакции Вайнберга и Касони были положительны в 64% случаев эхинококковой болезни, а также в 22% случаев других заболеваний. При злокачественных заболеваниях печени ограниченный участок поражения был обнаружен в 44% случаев, неясная скеннограмма в 30%, морфологические изменения – в 29%. В двух из 158 случаев скеннограмма ошибочно оказалась нормальной, однако в 40% этих же случаев лабораторные результаты были отрицательными.

Благодаря применению метода двух и трехплоскостного стереоскеннирования в 45% случаев были получены новые и дополнительные данные о состоянии печени.

Скеннирование печени применялось также при последующих исследованиях. Было обнаружено, что:

1) после эхинококкотомии остается отчетливый рубец как ограниченный участок поражения;
2) через три месяца после излечения амебного абсцесса происходит полная регенерация;
3) после создания порто-кавального анастомоза размер скеннограммы печени уменьшается, а селезенки – увеличивается, даже при удовлетворительном общем состоянии;
4) при некоторых диффузных поражениях печени цитостатические агенты могут быть временно эффективны;
5) при повторном скеннировании предполагаемое заболевание может оказаться ограниченным участком поражения или исчезнуть. Таким образом диагноз зависит от времени скеннирования.

Выводы: 1. Скеннирование печени может считаться очень полезным методом клинического, морфологического и топографического диагноза при патологических изменениях

печени. 2. Результаты могут быть улучшены путем: а) улучшения аппаратуры и применения методов стереоскеннирования, б) лучшего сотрудничества между терапевтами и хирургами.

EXPLORACIÓN HEPÁTICA DE 700 PACIENTES (Evaluación de los métodos actuales de diagnóstico). El autor ha examinado el hígado de 700 pacientes (estudios clínicos, análisis de laboratorio, exámenes roentgenográficos y exploraciones centelleográficas), ha seguido la evolución clínica de los pacientes y ha podido obtener en la mayoría de los casos una confirmación objetiva del diagnóstico. Esto ha permitido evaluar los ensayos realizados. Para la exploración del hígado se utilizó ^{198}Au, Rosa Bengala marcado con ^{131}I y polivinilpirrolidona marcada también con ^{131}I. Además de la exploración anteroposterior, se recurrió a técnicas especiales como la exploración estereoscópica en dos o tres planos y al empleo combinado del ^{198}Au y el Rosa Bengala marcado con ^{131}I para determinar los coeficientes relativos de fijación de estos radioisótopos en el hígado. Los pacientes habían sido distribuidos en ocho grupos clínicos con miras a la compilación y evaluación de los resultados del diagnóstico. En la memoria se presenta un resumen de estos resultados.

Cada grupo clínico se analizó por separado. Por ejemplo, se detectó una lesión macroscópica en el 95% de los 65 casos de equinococosis. La radiografía sólo permitió descubrir calcificaciones en el 35% de estos casos, pero también en el 14% de los otros casos de afecciones hepáticas. Las reacciones de Weinberg y Casoni fueron positivas en el 64% de los casos de equinococosis, pero también en el 22 por ciento de las otras enfermedades. En lo que respecta al cáncer del hígado, se detectó una lesión macroscópica en el 44% de los casos, se obtuvo un centelleograma velado en el 30% y se observaron modificaciones morfológicas en el 29%. En dos de los 158 casos de tumores malignos, el centelleograma parecía falsamente normal, pero en el 40% de estos mismos casos los resultados obtenidos en el laboratorio fueron negativos.

Con la técnica de exploración estereoscópica en dos o tres planos se obtuvieron datos nuevos o complementarios sobre el estado del hígado en el 45% de los casos.

La centelleografía se utilizó también para el control ulterior de los resultados. Se han hecho las siguientes observaciones:

1. Después de una equinococotomía persiste una cicatriz característica en forma de lesión macroscópica.
2. Tres meses después del tratamiento de un absceso amébico, se produce una regeneración completa.
3. Después de una derivación porta-cava, la imagen del hígado es más pequeña y la del bazo más grande, incluso cuando el estado general es satisfactorio.
4. Los agentes citostáticos pueden ser momentáneamente eficaces para ciertas lesiones hepáticas difusas.
5. Ha ocurrido a veces que al explorar de nuevo una lesión dudosa ésta ha aparecido como una lesión macroscópica o ha desaparecido totalmente. Por tanto, la época en que se efectúa la exploración puede afectar al diagnóstico.

Conclusiones: 1. La exploración hepática puede considerarse como método muy útil para el diagnóstico clínico, morfológico y topográfico en hepatopatología. 2. Los resultados pueden mejorarse: a) utilizando aparatos perfeccionados o técnicas de exploración estereoscópica, y b) estableciendo una eficaz colaboración entre el clínico y el cirujano.

The hepatobiliary system was examined in 700 patients, using radioisotope [1], laboratory [2], roentgenological [3] and clinical [4] examination simultaneously. The patients were followed-up so that an objective confirmation of the diagnosis could be obtained. In most cases bioptic, operative, or post-mortem anatomo-pathological findings were collected. In some cases clinical and laboratory post-therapy follow-up examinations were performed, which enabled us to diagnose the liver condition conclusively.

The work was carried out in collaboration with neighbouring hospitals and out-patients clinics, and a clinical approach was adopted with a study of the history and a physical examination of the patients.

Morphologic and functional (biliary) aspects of the hepatobiliary pathology were studied after marking the reticuloendothelial, parenchymal and biliary systems by radioactive hepatotropic substances, namely Au^{198}, RRB (radioactive Rose Bengal), $PVPI^{131}$ (polyvinylpyrrolidone-I^{131}) [5].

Notwithstanding the facilities and the enlarged work programme, the results of the classical antero-posterior (AP) hepatoscanning were unsatisfactory, the clinical and isotope diagnoses agreeing only in 65-75% of the cases. Three additional techniques were therefore introduced: stereoscanning, evaluation of radioisotope liver coefficients, and combined use of RRB + Au^{198} + RILC (radioisotope liver coefficient).

MATERIAL AND METHODS

The livers of 317 males and 387 females, were examined according to a standard procedure [6]. The patients were aged 1 month to 84 yr, the average age being 47 yr. Half of the patients were of European origin, one third of Asiatic and African origin, 34 were Arabs and 42 Yemenites. More personal data are given in Table I.

First a short clinical history of each patient was recorded and then the costal margin and the liver limits were traced on the skin. The last detail is essential. The patient was weighed and then one of the following isotopes injected: (a) 3 to 5 μc/kg body weight of a colloidal suspension of Au^{198}, for a morphological liver study; in 12 cases $PVPI^{131}$ was used (3 μc/kg body weight). (b) I^{131}-labelled tetraiodotetrachlorofluorescein RRB: 10-15 μc for a biliary tracing study and 3-5 μc/kg body weight for a complete study, including scanning of the right hypochondrium.

In the case of Au^{198} injection scanning of the liver was started 15 min after the radiogold injection. The RRB tracing was started at the time of injection and continued for 20-30 min. In obstructive jaundice, the RRB in the stools and urine was also examined.

To the classical technique of AP hepatoscanning we added the following.

(a) Tri- or bi-plane scanning (stereoscanning) [7, 8]. The dimensions of a normal adult liver are 15×18×24 cm. The big right lobe is too large to be seen to its entire depth and lesions situated posteriorly or medially may remain undetected (Fig. 1). To avoid this we attempted to reduce the distances by placing the patient on right lateral, postero-anterior and even if necessary on left lateral positions, for the scanning. A complete stereoscanning lasts $1\frac{1}{2}$-2 h.

(b) The evaluation of two radioisotope liver coefficients (RILC). The Area Liver Coefficient (ALC) was calculated to distinguish between a physiological and pathological large liver scan. We measured the area of the scan by a ponderal method and the formula - scan area (cm^2)/body weight (kg) - gives the value of the ALC.

Livers with a high ALC may be of proliferative, or of multimicrometastatic nature. The Radiation Liver Coefficient (RLC) was investigated to facilitate differential diagnosis. We established standard conditions for the liver scanning, connected a scaler with the cliniscanner and measured the radiation emitted by the liver during the scanning. The quotient, radiation of liver (cpm)/area of liver (cm^2), gives the RLC [9].

(c) A combined liver study RRB + Au^{198} + RILC was performed in one-session examinations of the morphology, topography and biliary function of the liver [10]. A small dose of RRB was injected and its accumulation in

TABLE I

PERSONAL DATA OF 700 PATIENTS EXAMINED BY RADIOISOTOPE LIVER SCANNING

Clinical group	No. of patients	Sex		Age groups				Professions				Ethnic groups				Examined by				
		M	F	0-19	20-39	40-59	60+	Academics	Clerks	House wives	Workers	Ashkenazim	Sephardim	Yemenites	Arabs	Radioactive gold			RRB	PVP
																1	2	3+		
Infectious and parasitic disease	115	73	42	5	39	50	21	5	23	43	44	25	71	9	10	57	31	28	4	2
Hepatic tumours	158	73	85	2	6	74	76	13	20	47	78	103	43	4	8	136	18	2	8	3
Size and position changes	44	18	26	2	2	17	23	2	4	13	25	19	23	1	0	37	7	0	0	0
Cardiac livers	29	9	20	1	2	9	17	1	6	4	18	12	14	1	2	26	2	1	0	0
Cirrhosis	60	38	22	2	4	29	25	1	10	28	21	21	31	6	2	48	10	0	6	3
Diffuse condition	71	28	43	11	12	23	35	6	19	13	33	34	28	4	5	52	18	1	3	1
Biliary cases	82	27	55	1	12	27	42	8	11	15	48	48	23	8	3	66	12	1	11	0
Search for metastases	91	29	62	0	7	47	37	7	13	19	52	64	19	5	3	63	23	3	3	2
Normals (adults and infants)	50	22	28	9	17	16	8	2	7	22	19	25	20	4	1	45	4	0	7	1
Summary	700	317	383	33	101	292	274	45	113	205	337	351	272	42	34	530	125	36	42	12

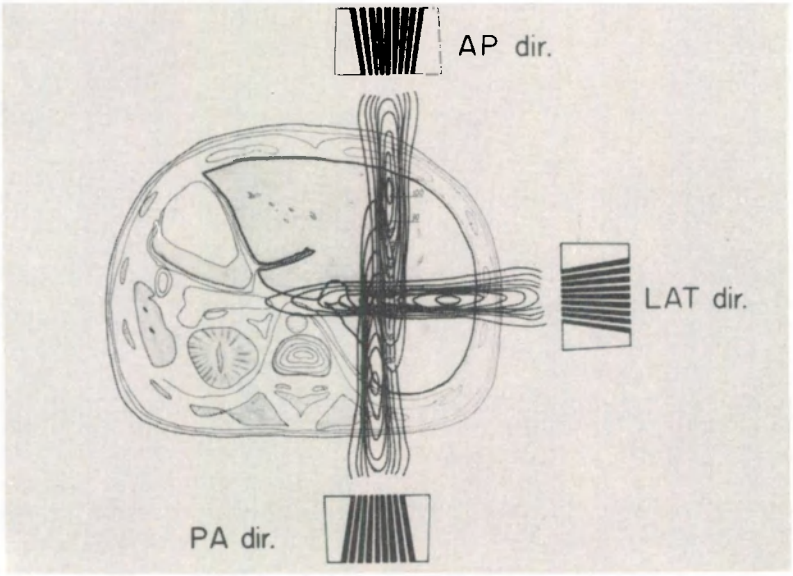

Transversal section of a man's body on the level of T 12
A multichannel focussing collimator is set in three directions (AP, LAT, PA) towards the liver. Isoresponse curves of Au^{198} radiation in water, are superposed.

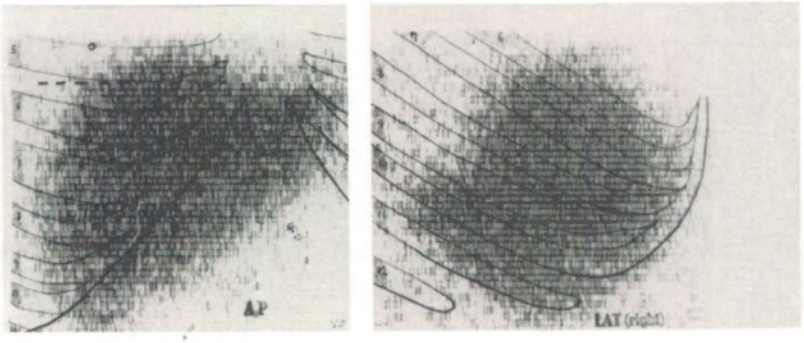

Fig. 1

Principles of the stereohepatoscanning (Normal case)

different parts of the liver was recorded, as also its passage into the intestine. Thirty minutes later Au^{198} was injected followed by stereoscanning (Fig. 2). The disappearance curve for the study of the liver circulation can also be established and the RILC calculated. This combined examination lasts about 2 h.

An autoscanner (Nuclear Chicago 1700) with a photoscanning attachment and a cliniscanner (Picker) were used. The detectors (2-in thallium-

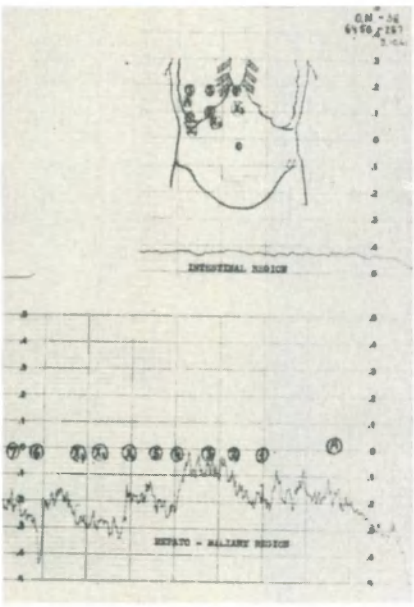

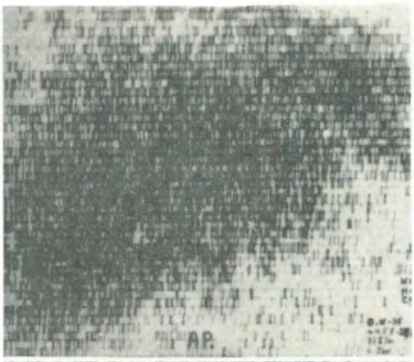

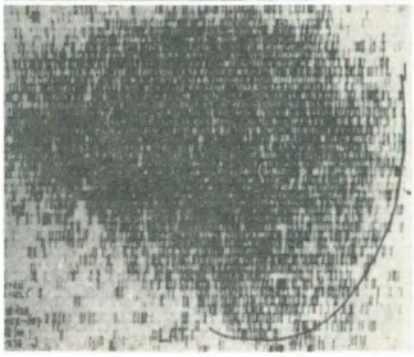

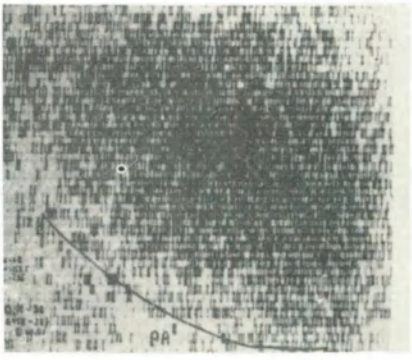

RADIOISOTOPE LIVER COEFFICIENTS (Case 287)
R. I. L. C.

Examined plane	cm^3/kg B. W.	cm^2/cm B. H.	cpm/cm^2 L. A.
A P	2, 5	1, 1	450
L A T	2, 2	0, 9	570
P A	2, 0	0, 9	510

Case 0458-287- - 40Y. Radioisotope liver study
liver cirrhosis

Fig. 2

Complete radioisotope liver study - RRB + Au^{198} + RILC (cirrhosis proved by biopsy)

activated sodium iodide crystals), multichannel collimators, and 3- to 5-cm thick lead shields were connected with rate meters and scalers.

A scheme for scannographic follow-up was established: (a) infectious and metastatic conditions were examined 2 or 4 weeks after therapy, and again 8 and 16 weeks after the therapy; (b) livers with cysts and tumours were rescanned 4-12 weeks after operation; (c) livers of cancerous patients were followed for a spray detection.

Simultaneously, laboratory examinations were performed: (a) serological: liver tests (Lugol, thymol turbidity and flocculation), BSF-test, serum bilirubin (direct and indirect), iron, cholesterol, albumin, alkali phosphatase, prothrombin time, and transaminase; the Mac Dermott's index of the hepatic function [11] was calculated. (b) Haematological examination: the erythrocyte sedimentation rate, leucocyte count and per cent of eosinophils in the smears. (c) Parasitological examination: amoeba histolytica, Casoni and Weinberg reactions. (d) Roentgenological examinations focussed to find: (i) changes in the right hypochondrium (position of the diaphragm, calcification, shadows); (ii) pressure-signs on the gastrointestinal or urological systems due to an enlarged liver, and vice versa; (iii) alterations in the biliary system.

RESULTS AND DISCUSSION

The problems will be analysed on four levels: (1) the scannography of an individual liver; (2) the scannography in groups of liver diseases; (3) the hepato-scannography for follow-up study; (4) comparison of the results from scanning and other methods.

1. *The scannography of an individual liver*

The interpretation and discussion of each individual liver scanning were carried out by two of our staff who also had additional anamnestic and physical data on the patient. The scan findings (signs) were classified as (i) normal (Fig. 1), (ii) morphologic changes (Fig. 3) or (iii) topographic changes (Fig.4), (iv) space occupying lesions (SOL) (Fig. 5), (v) fine or coarse partial or totally diffuse foggy scans with or without interpenetration (Fig. 6), (vi) hepatosplenogram (hepatosplenoosteogram) (Fig.7) and (vii) biliary or cardiac impression changes (Fig. 8).

One or more scan signs were observed on every scan. Most signs were seen in liver cirrhosis, and less in normal and tumourous livers. On the average there were 1.7 signs per scan.

Table II summarizes the percentage of each class of hepatoscanning signs in correlation with the clinical liver condition. Among 1147 signs identified on the liver scans of 650 pathological cases, we recognized: (i) 136 (or 12%) normal scans, 33% of these being in livers with hepatobiliary diseases and in cases investigated for metastatic spray; only 1% was seen in neoplastic and cirrhotic livers, and 3% each in parasitic, cardiac and diffuse liver conditions. (ii) 258 (or 23%) space occupying lesions, 44% of them in neoplastic livers, 37% in parasitic, and 7% in biliary conditions.

We can conclude that (a) none of the scan findings is pathognomonic for a hepatic lesion; there exists only a statistical prevalence; (b) the results in each case should be evaluated in conjunction with the clinical details; (c) we are able to give only a scan diagnosis but not an aetiological one.

The following new techniques were found to improve the scan diagnosis:

(a) A lateral scan provided additional information in 36% of the cases: (i) in 7%, new scan signs were detected, mostly SOL's in the posterior or

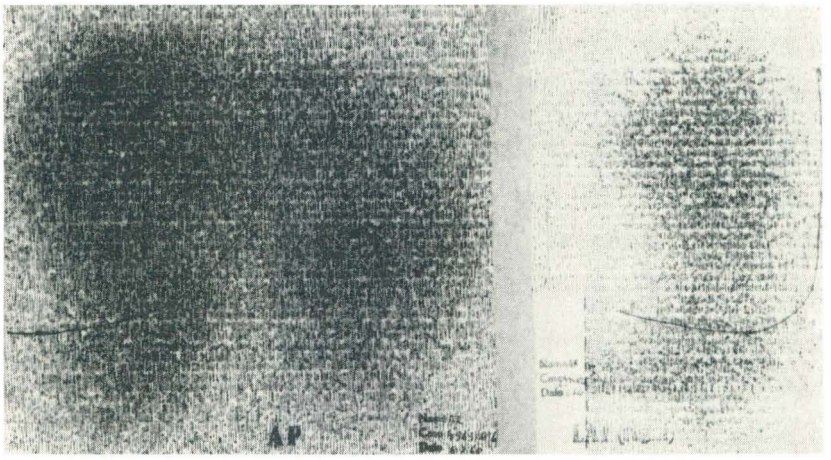

Fig. 3

Liver scan - morphologic change (A scar after hydatid operation proved by relaparatomy)

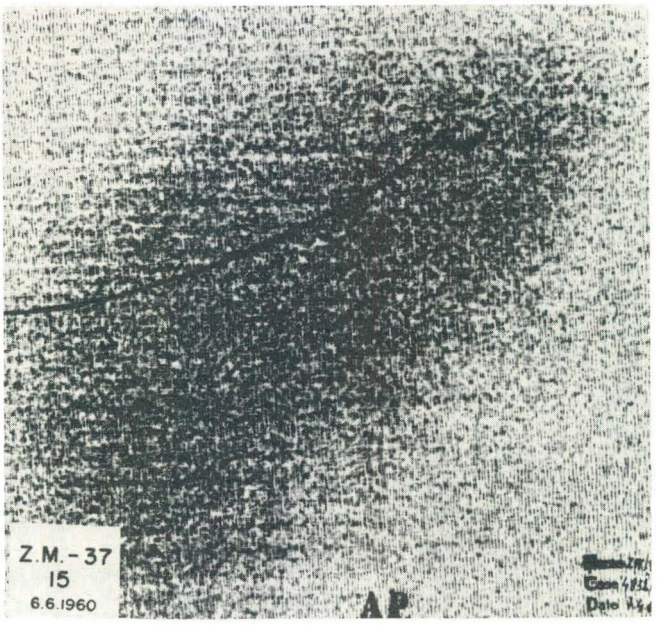

Fig. 4

Liver scan - topographic change (normal liver displaced by pleuritis carcinoma)

central part of the right lobe (metastases, echinococcus cyst, amoebic abscess, extraperitoneal tumour) (Fig. 9); (ii) 29% were of correcting value, localizing precisely the lesion seen on AP examination (important

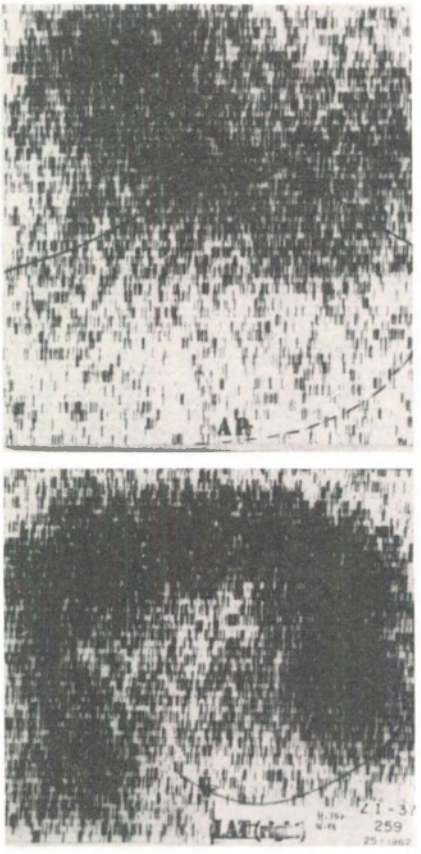

Fig. 5

Liver scan - AP+LAT - 2 space occupying lesions (on operation: 2 hydatidoses)

to establish the surgical approach) and giving information on their shape and size (important for the follow-up study of liver pathology).

(b) Postero-anterior scanning provided additional information in 9% of the cases. These were not usually new signs. (Those that were new were in the left lobe and paravertebral regions (Fig. 9)); in most cases additional information was obtained about existing lesions.

(c) Evaluation of RLC was helpful in two situations (i) in foggy micromultimacular, enlarged scans, for differential diagnosis between micrometastatic spray, and hypertrophic or hyperplastic, cardiac, cirrhotic or infiltrative livers. Normal ALC equals 2-3 cm^2/kg and RLC is 600 cpm/cm^2 in our conditions. In the metastatic livers we found an elevated ALC and a decreased RLC: the reticulo-endothelial system (RES) is partially destroyed and the infiltrating neoplastic tissue does not trap the gold particles. In the hyperplastic large livers we found an elevated ALC but a normal or even elevated RLC: The RES is conserved or hypertrophied and the Au^{198} colloid is widely taken up

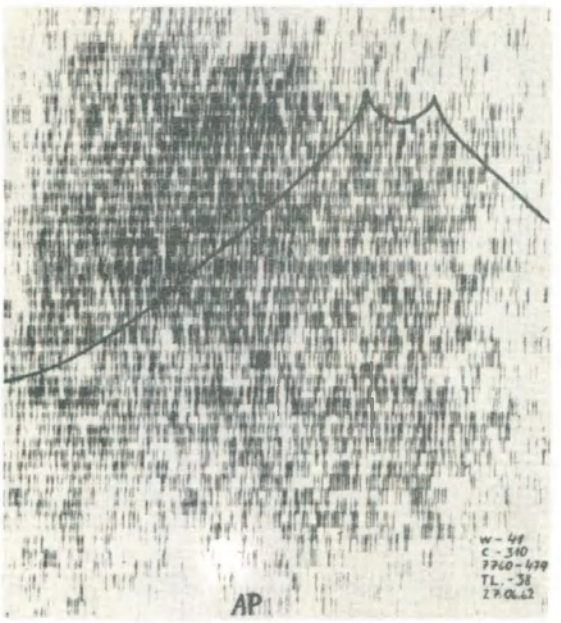

Fig. 6

Liver scan – foggy large liver (chronic leukaemia)

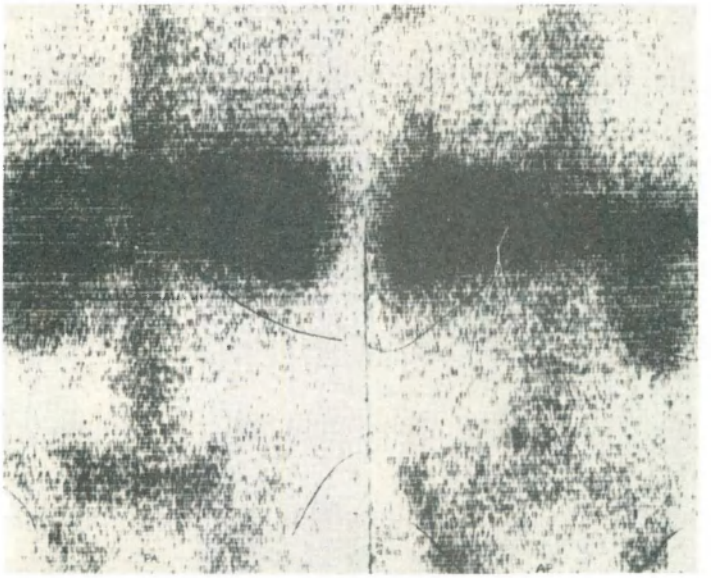

Fig. 7

Hepatosplenoosteogram (Lupoid cirrhosis)

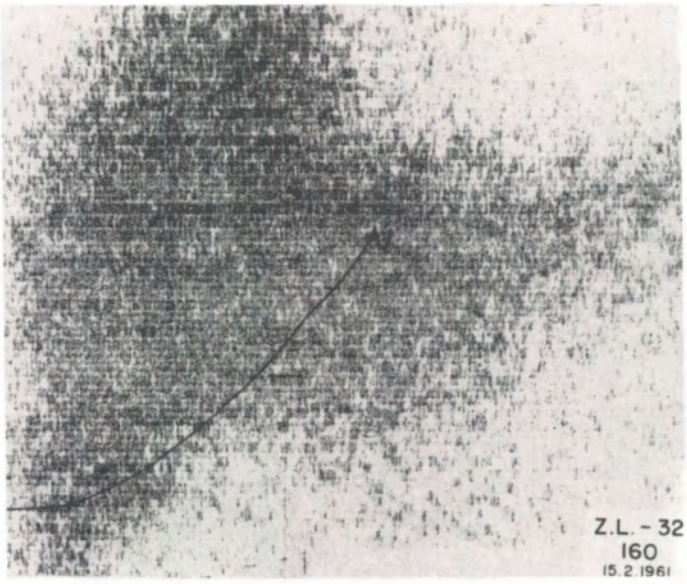

Fig. 8

Liver scan with a large cardiac impression (on X-ray: hernia diaphragmatica)

(Table III). (ii) For differential diagnosis between physiological and pathological liver enlargement. A physiological high ALC is found in normal children (Table III). It decreases with age, from 13 (at 1 month) to 2.5 (at 9 yr). The hepatoscan shows also that the infantile liver is ptotic till 9 yr when the topography becomes normal (Fig. 10).

We thus conclude that the liver coefficients may differentiate between some pathologic and physiologic liver changes, which cannot be evaluated by the simple hepatoscanning.

(d) A combined Rose Bengal-gold examination is useful for two reasons: (i) It allows a complete radioisotope examination of the hepatobiliary system to be performed at one time, for a general check-up when this system should be especially studied. (ii) It is helpful in the differential diagnosis of intrinsic or extrinsic as also congenital obstructive jaundice: The RRB examines the biliary hepatic function, the cystic accumulation and the intestinal passage; the Au^{198} bi- or tri-plane scanning detects intra- or extra-hepatic space occupying lesions (with RRB a tri-plane examination is too long and not feasible). It is also advisable to examine the urinary and faecal excretion of the RRB, especially in congenital cases.

2. The scannography in groups of liver diseases

The definite diagnosis of the 700 livers was made in 82% of the cases by histopathological examination, and in 18% by clinical and therapeutic follow-up (Table IV). The cases were classified into 9 clinical groups be-

TABLE II

THE CORRELATION BETWEEN THE SCANNOGRAPHIC AND CLINICAL DIAGNOSIS IN 650 CASES OF PATHOLOGICAL LIVERS

(Percentage evaluation)

Scannographic diagnosis		Clinical diagnosis (and number of cases)							
Scan finding	No. of scan findings	Infectious and parasitic disease (115)	Hepatic tumours (158)	Size and position changes (44)	Cardiac livers (44)	Hepatic cirrhosis (60)	Diffuse conditions (71)	Biliary cases (82)	Search for liver metastases (91)
N.L. (1)	136 (100%)	13	1	12	3	1	3	33	34
M.Ch. (2)	220	12	15	7	7	19	21	9	10
T.Ch. (3)	148	14	14	20	9	11	13	13	7
SOL (4)	258	37	44	4	0.5	2	1.5	7	4
F.L. (5)	210	5	30	1	7	17	17	10	13
L.+S. (6)	87	2	1	4	68	48	27	4	8
Ch.N. (7)	88	17	9	9	7	7	9	36	6

(1) Normal liver scan
(2) Morphologic changes
(3) Topographic changes
(4) Space occupying lesions
(5) Foggy liver scan (partial or total)
(6) Hepatosplenoscan
(7) Changed notches

Fig. 9(a)

AP and PA follow-up scan (gastric carcinoma)
A SOL appeared on PA scan only

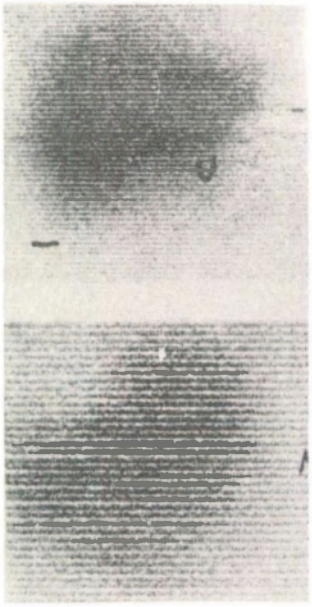

Fig. 9(b)

AP and LAT scans
A SOL visible on LAT only (recurrent hydatid cyst)

cause: (a) various pathologic, therapeutic and laboratory patterns correspond to various hepatic diseases; (b) the scanning signs for each group are also different but more selective and specific, although non-pathognomonic.

TABLE III

RADIOISOTOPE LIVER COEFFICIENTS AT DIFFERENT PATIENTS' AGES AND IN DIFFERENT LIVER CONDITIONS

Age	Diagnoses	ALC (cm^2/kg)	RLC (cpm/kg)
1 month	Normal	13.0	160
2 months	Normal	9.0	280
9 months	Normal	6.0	270
9 yr	Normal	2.5	390
9 yr	Gaucher's disease	7.5	300
Adult	Normal	2.7	640
Adult	Fatty liver	6.3	520

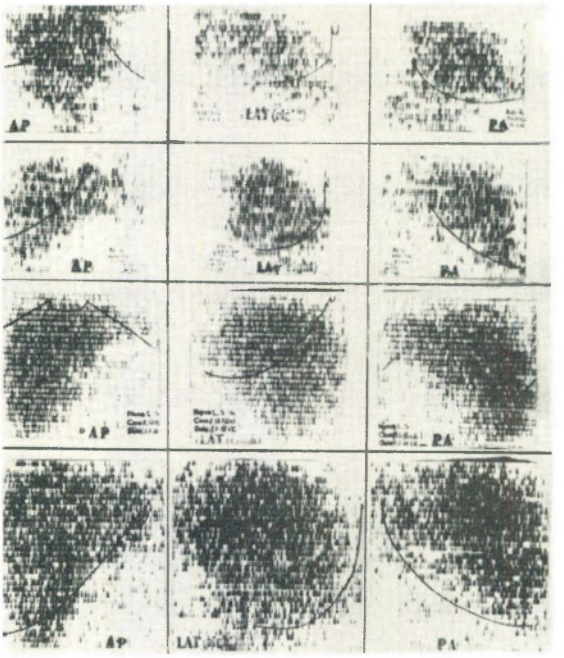

Fig. 10

Stereoscans of infantile livers
(aged 1 month, 2 months, 8 months, 9 yr)

TABLE IV

OBJECTIVE CONFIRMATIONS OF THE CLINICAL DIAGNOSES OF THE 700 EXAMINED LIVER PATIENTS

Objective examination	Clinical group								
	Infectious and parasitic disease	Hepatic tumours	Size and position changes	Cardiac livers	Cirrhosis	Diffuse conditions	Biliary cases	Search for liver metastases	Normal
Biopsy 134 (19%)	21	15	5	4	25	35	18	7	4
Operation (Expl. lap.) 298 (42%)	76	60	29	7	17	11	42	43	13
Post mortem 141 (21%)	3	75	3	6	22	11	2	19	-
Therapeutic tests and clinical appreciation 127 (18%)	15	4	7	12	0	14	20	22	33

TABLE V

THE FINDINGS ON THE LIVER SCANNINGS OF 700 PATIENTS

(Classified according to their clinical diagnosis)

Clinical diagnosis		Findings on the liver scans (their per cent in each group)								
Pathologic group	No. of cases	N. L. (1)	M. Ch. (2)	T. Ch. (3)	SOL (4)	F. L. (5)	L. +S. (6)	Ch. N. (7)	Total No. of findings	Value: findings per scan
Infectious and parasitic disease	115 (100%)	17 (14%)	27 (23%)	21 (18%)	95 (83%)	11 (10%)	2 (1%)	15 (13%)	188 (162%)	1.6
Hepatic tumours	158 (100%)	2 (1%)	32 (20%)	21 (13%)	113 (72%)	64 (40%)	1 (1%)	8 (5%)	241 (152%)	1.5
Size and position changes	44 (100%)	16 (36%)	16 (36%)	29 (66%)	10 (23%)	3 (7%)	3 (7%)	8 (18%)	85 (193%)	1.9
Cardiac livers	29 (100%)	4 (14%)	16 (55%)	13 (45%)	1 (3%)	13 (45%)	5 (17%)	6 (21%)	58 (200%)	2.0
Cirrhosis	60 (100%)	2 (3%)	41 (69%)	17 (28%)	6 (10%)	35 (58%)	42 (70%)	6 (10%)	149 (248%)	2.5
Diffuse conditions	71 (100%)	4 (5%)	47 (66%)	18 (25%)	4 (5%)	35 (49%)	24 (34%)	8 (11%)	140 (195%)	2.0
Biliary cases	82 (100%)	45 (55%)	20 (24%)	19 (23%)	18 (22%)	21 (25%)	7 (8%)	32 (39%)	162 (196%)	2.0

TABLE V (cont'd)

Clinical diagnosis		Findings on the liver scans (their per cent in each group)								
Pathologic group	No. of cases	N. L. (1)	M. Ch. (2)	T. Ch. (3)	SOL (4)	F. L. (5)	L. +S. (6)	Ch. N. (7)	Total No. of findings	Value: findings per scan
Search for liver metastases	91 (100%)	46 (51%)	21 (23%)	10 (11%)	11 (12%)	28 (31%)	3 (3%)	5 (5%)	124 (136%)	1.4
Normal	50 (100%)	49 (98%)	6 (12%)	9 (18%)	0 (0%)	4 (8%)	0 (0%)	4 (8%)	72 (144%)	1.4
Summary	700	185	226	157	258	214	87	92	1219	1.7
Percentage value		15	18	13	21	18	7	8	100%	

(1) Normal liver scan
(2) Morphologic changes
(3) Topographic changes
(4) Space occupying lesions
(5) Foggy liver scan (partial or total)
(6) Hepatosplenoscan
(7) Changed notches

The signs are classified in Table V, which shows: (a) in liver parasitoses a SOL is the predominant scan sign, and signs of morphologic and topographic changes are next in frequency; (b) a SOL is also a predominant scan sign in malignant liver but followed by foggy scans; (c) in biliary condition a normal liver scan predominates, followed by a large biliary notch. Similar observations can be made in all the other groups.

Conclusion

The study of the frequency of the scan signs correlated to the clinical group, may be of help for more correct diagnostic orientation.

3. The hepatoscannography for follow-up study

A follow-up study was carried out in five directions:

(a) Liver amoebic abscesses were followed after internal treatment [12] (Fig. 11).

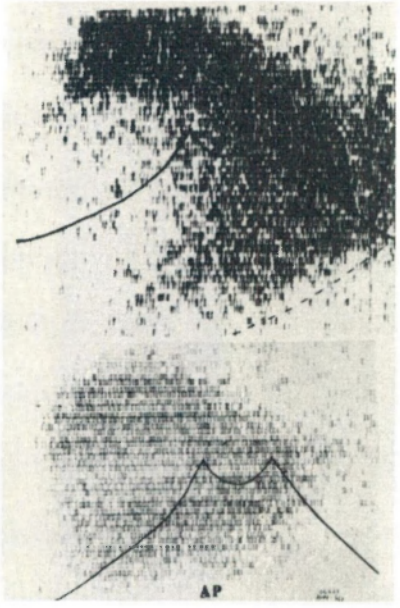

Fig. 11

Amoebic liver abscess followed 2 months after emetine treatment (regeneration)

(b) Liver echinococcuses were followed after operation [13] (Fig. 3). The results of the study of 65 hydatic cysts and 42 amoebic abscesses are summarized in Table VI.

(c) Diffuse neoplastic liver conditions were followed after cytostatic treatment. Polycythaemic enlarged livers became smaller after P^{32} treatment; diffuse livers of Hodgkin's disease became smaller after NH_2 injections (Fig. 12).

TABLE VI

SCANNOGRAPHIC FOLLOW-UP STUDY OF LIVER AMOEBIASIS AND ECHINOCOCCOSIS

	Stereo-scanning before treatment	Treatment performed	Follow-up stereoscan 2-3 months after treatment	Exceptions	Recurrence or re-infection
Amoebic abscesses	SOL	Emetine aralen (1-3 weeks)	Regeneration	Incomplete regeneration in 10% of cases	New SOL
Echinococcus	SOL	Cystectomy-marsupialization	Post-hydatid scars (SOL-morphologic change-hyperplasia)	Partial regeneration in 6% of cases (in biliary localization and in young patients)	New findings or enlargement of existing scar (difficult diagnosis)

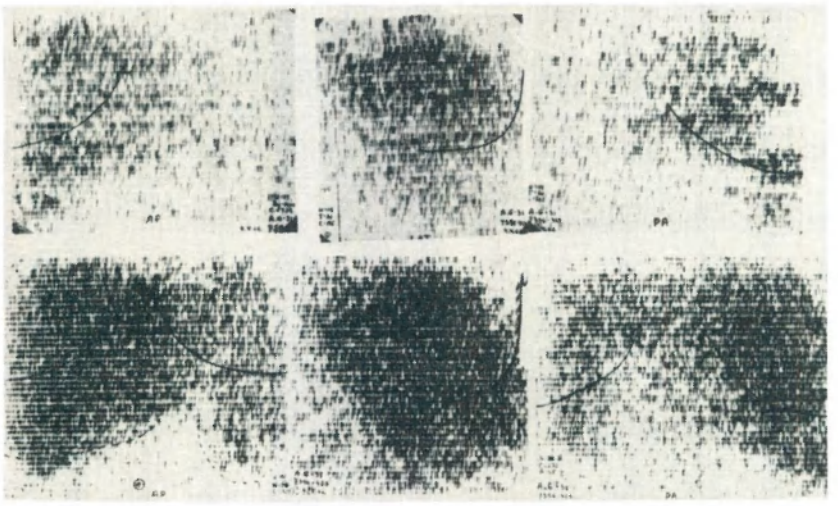

Fig. 12

Splenohepatomegaly in lymphogranulomatosis
Stereoscanning before and 1 month after NH_2 therapy.

(d) Cardiac livers were followed after cardiotonics (digoxin).
(e) The livers of cancer patients were followed-up for detection of mitotic spray (Fig. 9 (a)).

Conclusion

The follow-up rescanning is of pathologic and prognostic importance. It gives the possibility of evaluating the positive or negative changes after therapy.

4. Comparison of the results from scanning and other methods

The results of examinations other than scanning vary in different clinical groups of liver diseases. We classified these results as (i) normal, (ii) partially altered or suspected, and (iii) clearly positive. Table VII gives comparative results for four groups.

(a) In the 50 normal patients the scannings were absolutely normal in 49 cases. Displacements and enlarged notches were noted but these findings are of secondary importance. The results of X-ray and laboratory examinations are of almost similar value in these normal cases.
(b) Definitive positive scannographic results were obtained in 77% of liver tumours, but the X-ray and laboratory testings were reliable only in 7-12% of the same livers. In liver echinococcus the scannographic method is reliable in 91% of the cases and the X-ray only in 35%. The laboratory tests were 9 times less reliable than the scanning. There was more than 4% eosinophilia in 42% of the cases and more than 10% in 10% of the cases. However, this test is very non-specific. In biliary

TABLE VII

THE COMPARISON OF THE RESULTS OF HEPATOSCANNING WITH OTHER EXAMINATION METHODS

Methods of examination	Clinical groups of examined patients											
	Normal control (50 cases)			Hepatic tumour (158 cases)			Biliary diseases (82 cases)			Liver echinococcus (65 cases)		
	Percentage evaluation of the results in each group											
	Normal results	Suspected and partial	Definitive	Normal results	Suspected and partial	Definitive	Normal results	Suspected and partial	Definitive	Normal results	Suspected and partial	Definitive
Radioisotope scanning	83	17	0	1	22	77	16	53	31	5	4	91
X-ray diagnosis	78	22	0	50	43	7	31	41	28	36	29	35
Laboratory	90	10	0	40	48	12	57	29	14	62	28	10
Haematology	71	29	0	62	38	-	56	44	0	58	32	10
Parasitology	82	18	0	87	13	-	76	21	3	36	22	42

diseases the scannographic findings are clearly positive in 31% of cases, and the X-ray in 28% but the laboratory is only half as effective.

(c) False normal findings were found in similar proportions. In 1, 50, and 59% of proved hepatic tumours the results were normal in radioisotope, X-ray and laboratory testing respectively. The corresponding figures for liver echinococcus were 5, 36 and 62% and for biliary disease 16, 31 and 57%.

Conclusion

(a) In liver pathology, the radioisotope method of examination gives: (i) from 3 to 10 times more verified good results than the X-ray, and from 6 to 9 times more than the laboratory method. (ii) false normal results - from 7 to 50 times less than the X-ray, and from 12 to 60 less than the laboratory.

(b) In biliary pathology, the results of isotope and X-ray studies are almost equally positive for isotope and X-ray study, and twice as good as the laboratory. But the false normal findings are almost twice more in the X-ray and $3\frac{1}{2}$ times more in the laboratory than in the isotope study.

SUMMARY

The livers of 700 patients were examined simultaneously by radioisotope, X-ray and laboratory methods. The diseases of the same livers were diagnosed by objective methods and classified in nine clinical groups.

The results of the examinations were then correlated with the clinical diagnoses and so the reliability of each examination method was established for each of the nine clinical groups.

To improve the results of the classical AP hepatoscanning three special techniques were used in addition: *stereohepatoscanning, calculation of* radioisotope liver coefficients and combined Au^{198} + RRB + RILC liver study.

The conclusion reached is that liver scanning today may be considered a reliable method of examination of liver morphology and biliary function. It is 1-12 times more reliable than the X-ray and laboratory methods. The results can be improved by stereoscanning and some additional procedures, as also by using a clinical approach in conjunction with the radioisotope technique.

REFERENCES

[1] DONATO, L., BECCHINI, M. F. and PANICHI, S., "Liver scanning with colloidal radiogold", Medical Radioisotope Scanning, IAEA, Vienna (1959) 87-103.

[2] FRANKEL, S. and REITMAN, S., in: Gradwohl's Clinical Laboratory Methods and Diagnoses, Mosby Co., Saint Louis (1963) 94-114.

[3] ANACKER, H., MORINO, P., ROSCH, G., SCHUMACHER, W. and ZUPPINGER, A., in: Roentgendiagnostic der Leber, Springer Verlag, Berlin (1959) 1-76.

[4] POPPER, H. and SCHAFFNER, F., in: Liver: Structure and Function, The Blakiston Division, McGraw-Hill Book Co., New York, 179-613.

[5] CAROLI, J., JAMMET, H. and RENAULT, H., Semaine des Hôpitaux 34 Paris (1958) 441-442.
[6] "Liver study by radioisotopes", Research Contract IAEA No. 54, The use of radioisotope scanning in liver pathology.
[7] CZERNIAK, P. and LUBIN, E., Tijdschrift voor Gastro-Enterologie 4 (1961) 42-53.
[8] CZERNIAK, P., LUBIN, E., DJALDETTI, M. and DE VRIES, A., J. nucl. Med. 4 (1963) 35-44.
[9] CZERNIAK, P. and DEITCH, M., Harefuah 64 (1963) 353-362.
[10] CZERNIAK, P. and DEITCH, M., in: Use of Radioisotopes in Animal Biology and the Medical Sciences 2 (Proc. Conf., Mexico City, IAEA, WHO, FAO) Academic Press Inc., London (1962) 303-318.
[11] MC DERMOTT, W.V., Jr., Surg. Gynec. Obst. 110 (1960) 457-469.
[12] MARBERG, K. and CZERNIAK, P., Ann. intern. Med. 60 (1964) 66.
[13] CZERNIAK, P., BANK, H. and PAUZNER, Y., Radioisotope Scanning in Liver Echinococcosis, Radiology (accepted for publication).

DISCUSSION

(On the three foregoing papers)

E. OTERO-RUIZ: During our studies of 60 cases of hepatic lesions carried out under IAEA research contract No.159/RB, in which we used Au 198-colloid, our experience was similar to that described by the authors of the papers presented. In 45 cases (Fig.1), the anatomical data enabled

	JAN 63–JUN 63	JUL 63–MAR 64	TOTAL
NORMAL LIVER	3	–	3
CIRRHOSIS	4	1	5
POLYCYSTIC DISEASE	3	–	3
LIVER TUMOUR, PRIMARY	4	1	5
LIVER TUMOUR, METASTATIC	4	4	8
SUSPECTED AMOEBIC ABSCESS BUT NORMAL LIVER AT SCAN	3	1	4
AMOEBIC ABSCESS	12	5	17
	33	12	45

Fig.1

Results of liver scanning with Au^{198}-colloid: positive correlation

us to confirm our findings regarding the location and size of the lesions. It was established that 17 lesions were amoebic abscesses, 13 were hepatic tumours and 15 were miscellaneous in character. We ignored as "doubtful" the cases which could not be diagnosed owing to the poor resolution in the scan or the lack of anatomical confirmation of the lesions. We also think it advisable to make another scan in addition to the antero-posterior scan, since the latter (Figs. 2 and 3) may show what appears to be a normal liver, whereas the lateral scan may show a hepatic abscess in the same patient.

Recently we started using the profile technique, as suggested by Dr. MacIntyre. A characteristic metastatic lesion with its corresponding profiles can be seen in Figs. 4 and 5. We are becoming increasingly convinced of the usefulness of profiles in making a quantitative study of the filling defects observed in dot scanning.

D. IKKOS: There is no doubt that multi-plane scanning is superior to single-plane scanning in special cases, but it takes more time than we can

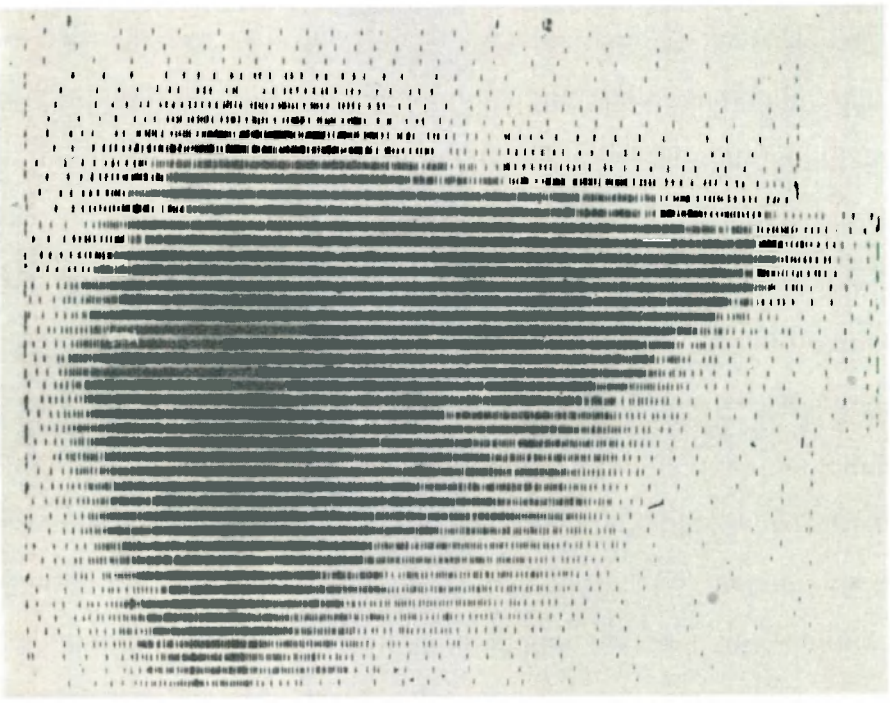

Fig. 2

Antero-posterior scan of patient with hepatic abscess

afford for routine purposes. I think that single-plane scanning is very satisfactory in detecting hydatid cysts in the liver; this is borne out, to a great extent, by our data as compared with the data presented by Dr. Czerniak. According to his data, false or doubtful results are obtained in 9% of the cases of echinococciasis of the liver – a figure very similar to our figure of 6% – although he uses a three-plane scanning technique.

A. DESGREZ: It seems to me that Dr. Gongora considers the accentuation of the interlobar notch as a pathological symptom. From earlier work, and also from the work done by Professor Caroli, I got the impression that this symptom, contrary to my former belief, had no practical significance. I should like to know if anyone has had an opportunity of studying the morphological variations which may occur in this area in a normal subject. The area concerned is particularly interesting in view of the questions asked by clinicians on the subject.

R. GONGORA: We did not observe any "isolated" accentuation of the interlobar notch. This accentuation is always accompanied by hypertrophy of the left lobe, of which it is a consequence.

P. CZERNIAK: We were unable to observe a strongly accentuated interlobar notch. The differences that we observed in the region of the boundary between the right and left lobe were as follows: (1) atrophy of the left lobe, mostly congenital; (2) compensatory hypertrophy of the left lobe resulting

Fig. 3

Lateral scan of same patient as Fig. 2

from pathological or destructive processes in the right lobe; (3) filling of the region in cases of hypertrophic Riedel's lobe. It is necessary to distinguish between the changes in this region and the changes in the biliary notch, which may be considerable.

E. LUBIN: In one of the false negative cases mentioned by Dr. Ikkos a small cyst was found on the upper border of the left lobe. I think that, for a correct evaluation of a suspected upper-border lesion, the superimposition of a conventional X-ray thorax picture of the patient on the scan would allow for a better semeiology of the liver-diaphragmatic space.

D. IKKOS: I agree. Unfortunately, we were unable to make the scan and take a conventional X-ray picture on the same X-ray film.

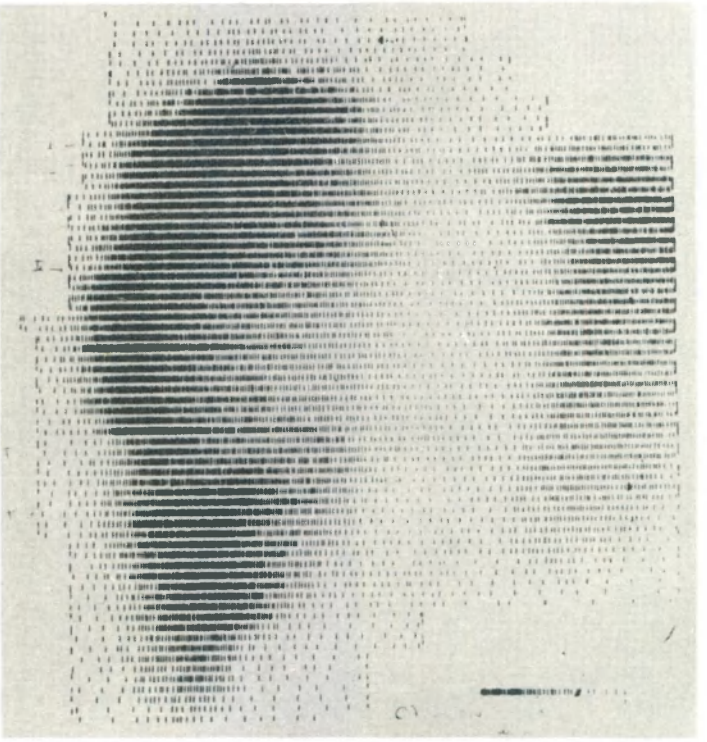

Fig. 4

Antero-posterior scan of patient with hepatic metastasis

B. BODFORSS: I should like to ask Dr. Czerniak what was the source of his I^{131}-PVP and how long after injection he performed his scans. I ask this question because we have used I^{131}-PVP from Amersham with a mean molecular weight of about 35 000. With this product the level of activity in blood is too high for liver scanning during the first 24 h.

P. CZERNIAK: We first used I^{131}-PVP produced by Gordon at the National Institutes of Health, Bethesda, Md., United States of America. We then labelled PVP ourselves, using the method developed in the National Institutes of Health, and finally we used I^{131}-PVP from the Radiochemical Centre, Amersham, England. The scanning and recording with a directional counter were performed 2 h, 24 h, and 2, 3 and 7 d after I^{131}-PVP injection. In some cases we followed the I^{131}-PVP in the liver for 10-12 d after injection.

D. IKKOS: Dr. Gongora mentioned that he uses Au^{198}-colloid because of its known advantages over I^{131}-Rose Bengal, i.e. longer biological half-life, no activity in the gut, etc. May I ask whether he has made a comparison of the value of the two substances in the same subject? Since I^{131}-Rose Bengal is taken up by parenchymal cells, while Au^{198}-colloid is taken up by the reticulo-endothelial cells, it is possible that the scans made with these two substances might differ because of specialized damage. I should also

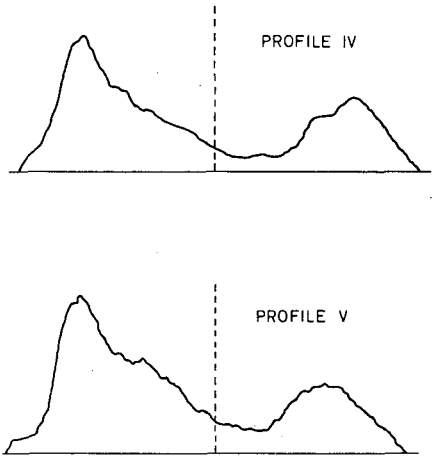

Fig. 5

Profile scan of same patient as Fig. 4

like to ask Dr. Gongora if he has any explanation for the prolongation of the clearance time in amoebiasis.

R. GONGORA: We had an opportunity to scan the same patient using, first, I^{131}-Rose Bengal and, after that, Au^{198}-colloid. It was impossible to arrive at any definite conclusion on the basis of this study. We did not find that the distributions observed in the two scintigrams differed significantly. As to your last question, an acceleration in the blood clearance time is observed in subjects with amoebiasis during the onset of the disease and seems to be due to inflammation. Prolongation of the clearance time is observed in patients who have been suffering from chronic amoebic hepatitis for a long time and can, apparently, be attributed to hepatic sclerosis.

G. GOMEZ-CRESPO: It is well known that the microscopic distributions of I^{131}-Rose Bengal and Au^{198}-colloid within the liver are not the same. However, the resolution of our collimators is not good enough to permit any differentiation.

In collaboration with Dr. MacIntyre and Dr. Christie (Highland View Hospital, Cleveland, Ohio, United States of America) I studied the distribution of I^{131}-Rose Bengal and Au^{198}-colloid in gross radioautographs of terminal patients injected with either one of these materials. For practical purposes the distribution is the same. Of course, the gall bladder will appear as a positive concentration of radioactive material in the Rose Bengal scan, whereas the same organ will appear as a void in the Au^{198} scan.

A. BAPTISTA: Two years ago, at the International Cancer Congress in Moscow, we presented the results of a comparison between Au^{198}-colloid scanning and I^{131}-Rose Bengal scanning in the same patients. The findings in patients with liver metastases can be briefly summarized as follows: (1) Defects in the liver structure were more clearly defined with Au^{198}-colloid than with I^{131}-Rose Bengal; (2) In many cases, however, no correspondence was observed between the distributions of the two radionuclides.

G. GOMEZ-CRESPO: With regard to the distribution of I^{131}-Rose Bengal and Au^{198}-colloid, I do not know of any scanner that gives better resolution than that obtained in radioautography.

A. BAPTISTA: Autoradiography with beta radiation only provides information concerning the distribution of activity in the most superficial layer of the section studied. If we require information about the distribution throughout the volume of the organ, this is much more easily obtained by using gamma radiation and scanning techniques.

I should like to draw attention to the pitfalls in studying liver blood flow in terms of the clearance of a colloidal substance from the blood, as shown in Professor Larsson's paper* and in the paper presented by Dr. Kniseley** at this Symposium. A much more reliable index of liver blood flow can be obtained from the uptake curve in the organ***. This index is much less sensitive to the influence of the reticulo-endothelial system and can, in any case, be corrected for the effect of the latter system if the form of the blood clearance curve is known.

M. BEN-PORATH: The papers under discussion show that there is a tendency to make multi-plane scans when scanning the liver. In discussions on the question of whether high-energy or low-energy isotopes should be used in liver scanning, the main point made in favour of high-energy isotopes was that they allow the detection of deep-seated lesions. If we are unable to produce a good enough collimator to achieve this by means of single-plane scanning, why should we not use low-energy isotopes, e.g. I^{125}-labelled Rose Bengal, for multi-plane liver scanning, employing an infusion technique to maintain a constant I^{125}-Rose Bengal concentration in the liver for a sufficient time to allow the scans to be made in all planes? Another possible material is Au^{195}-colloid, whose 90-keV X-rays are very convenient and whose lack of beta radiation is an advantage. In spite of its relatively long physical half-life, the dose per microcurie to the liver is similar to that from 1 μc of Au^{198}, assuming a biological half-life of infinity.

R. GONGORA: In hepatic amoebiasis the defects in the picture are not all of the same type, since some rapidly regress after medical treatment, whereas others persist. How does Dr. Czerniak interpret these facts?

P. CZERNIAK: We have not observed characteristic signs for the space-occupying lesions due to amoebic abscesses nor have we been able to give an aetiological diagnosis from the shape of any such lesions. An infected echinococcus cyst may simulate, both clinically and on the scintigram, an amoebic abscess. We have not observed different results after treatment in cases of amoebic abscess. The volume of the abscess and its location may influence the rapidity of the liver regeneration.

I should like to comment on the scanning of amoebic liver abscesses after emetine treatment. In cases of amoebic hepatitis we obtained a normal, regenerated scan two weeks after an intensive and sufficient treatment (4 d

---

* LARSSON, L.-G. and JONSSON, L., "Bone-marrow scanning after intravenous injection of colloidal Au^{198}", these Proceedings II.

** KNISELEY, R.M., ANDREWS, G.A., EDWARDS, C.L. and TANIDA, R., "Scanning of bone marrow in haematopoietic disorders", these Proceedings II.

*** See BAPTISTA, A. M. and SILVA CARVALHO, J., "Study of the liver blood flow using gamma-emitting radionuclides", Proc. 2nd. UN Int. Conf. PUAE 26 (1958) 157.

of intravenous injections of emetine followed by Arralen). In cases of amoebic abscesses we observed a regeneration of the liver 2-3 months after the same treatment. We did not observe residual space-occupying lesions after treatment of an amoebic abscess except in one out of 42 cases. The lesions observed were mostly foggy regions or morphological changes.

D. IKKOS: Our experience is similar to that of Dr. Gongora and Dr. Jammet, particularly with regard to changes in liver scans in cases of chronic amoebiasis without known liver abscesses.

I should like to ask Dr. Czerniak if he has used Au^{198} or other substances in scanning the livers of infants and older children?

P. CZERNIAK: We used I^{131}-Rose Bengal as well as Au^{198}-colloid in such cases. I^{131}-Rose Bengal was mostly used for diagnosing biliary-duct atresia in congenital jaundice. Au^{198}-colloid was used over a period of five years in selected, rare cases of children who were hospitalized suffering from malignant diseases in a terminal state. Those cases in which the liver was found at autopsy not to be involved were included in our data on liver scans of children.

LIVER SCANNING WITH RADIOMOLYBDENUM

L. B. SORENSEN
ARGONNE CANCER RESEARCH HOSPITAL, THE UNIVERSITY OF CHICAGO, CHICAGO, ILL., UNITED STATES OF AMERICA
(Presented by P. Harper)

Abstract — Résumé — Аннотация — Resumen

LIVER SCANNING WITH RADIOMOLYBDATE. Carrier-free Mo^{99} injected intravenously as molybdate concentrates rapidly and efficiently in the polygonal cells of the liver. The hepatic uptake of Mo^{99} is accompanied by a gradual build-up of the daughter Tc^{99m} whose 0.140 MeV gamma radiation is particularly suitable for scanning purposes. Good visualization of the liver is obtained when scans are done 24 h after injection of 40 to 50 μc of Mo^{99}. At this time, the maximum count-rate of Tc^{99m} is obtained over the liver, and the Tc^{99m} injected together with Mo^{99} has been almost lost, either by excretion or decay, thus securing low background count.

Metastases, abscesses and other space-occupying lesions are visible as defects. A hepatoma produced a "hot" nodule on the scan by selecting Mo^{99} to a greater extent than did the surrounding liver tissue. Decreased hepatic uptake of Mo^{99} is observed in diffuse hepatocellular diseases.

Mo^{99} has several advantages over colloidal radiogold and I^{131}-labelled Rose Bengal: (1) It accumulates in the polygonal cells and its uptake portrays effectively disease states of the parenchyma; (2) The concentration of the tracer does not change during the interval of the scan since Mo^{99} has a biological half-life of about 20 d. The scan can be repeated in case of technical failure without loss of quality; (3) The contrast ratio is superior by utilizing the low-energy gamma radiation of Tc^{99m}. A comparative evaluation of the scanning resolution obtained with Mo^{99}-Tc^{99m}, I^{131} and Au^{198} using a liver phantom is presented; and (4) the low energy of the principal radiation permits greatly reduced scintillation crystal size and greatly enhances detector and collimator efficiency.

The total radiation dose to the liver is of the order of two rad.

SCINTIGRAPHIE DU FOIE A L'AIDE D'UN RADIOMOLYBDATE. L'élément ^{99}Mo sans entraîneur, administré par injection intraveineuse sous forme de molybdate, se concentre rapidement et se fixe dans les cellules polygonales du foie. La fixation de ^{99}Mo dans le foie s'accompagne de la formation progressive d'un produit de filiation, ^{99m}Tc, dont les rayons gamma de 140 keV conviennent particulièrement bien à la scintigraphie. On obtient une bonne représentation du foie lorsque les scintigrammes sont établis 24 h après l'injection de 40 à 50 μc de ^{99}Mo. A ce moment, le taux de comptage de ^{99m}Tc a sa valeur maximum au-dessus du foie, tandis que ^{99m}Tc injecté en même temps que ^{99}Mo a virtuellement disparu, par excrétion ou par désintégration, ce qui assure un faible bruit de fond.

Les métastases, les abcès et les autres lésions en volume apparaissent sous forme d'anomalies du scintigramme. Un hépatome produisait sur le scintigramme un nodule «chaud» du fait qu'il fixait sélectivement ^{99}Mo dans une plus grande mesure que le tissu environnant du foie. On observe une diminution de la fixation de ^{99}Mo par le foie dans les affections hépatocellulaires diffuses.

L'élément ^{99}Mo présente plusieurs avantages sur l'or-198 colloïdal et le rose bengale marqué à l'iode-131: a) il s'accumule dans les cellules polygonales et sa fixation donne une idée précise de l'état pathologique du parenchyme; b) la concentration du radioindicateur ne change pas pendant le scintigramme, du fait que la période biologique de ^{99}Mo est d'une vingtaine de jours; en cas d'une défectuosité technique, il est possible de répéter le scintigramme sans perte de qualité; c) les rayons gamma de faible énergie de ^{99m}Tc permettent d'obtenir un meilleur contraste; le mémoire donne une évaluation comparée de la résolution dans des scintigrammes d'un fantôme de foie établis avec ^{99}Mo-^{99m}Tc, ^{131}I et ^{198}Au; d) la faible énergie du rayonnement principal permet de réduire considérablement la taille du cristal et d'augmenter sensiblement l'efficacité du détecteur et du collimateur.

La dose totale de rayonnement reçue par le foie est de l'ordre de 2 rad.

СКЕННИРОВАНИЕ ПЕЧЕНИ С ПОМОЩЬЮ РАДИОМОЛИБДЕНА. Молибден-99 без носителя, введенный внутривенно в виде молибдата, быстро и эффективно концентрируется в многоугольных клетках печени. Поглощение молибдена-99 печенью сопровождается постепенным образованием дочерних элементов технеция-99 m, гамма-излучение которых мощностью в 0,140 Мэв является особенно подходящим для целей скеннирования. На сканнограммах, сделанных 24 часа спустя после инъекции 40—50 мккюри молибдена-99 получается отчетливое изображение печени. В этот период максимальная степень активности технеция-99 m наблюдается над областью печени, технеций-99 m, введенный вместе с молибденом-99 почти исчезает, либо в результате выведения, либо—распада, обеспечивая, таким образом, низкий фон.

Метастазы, абсцессы и другие ограниченные участки поражения выглядят как дефекты заполнения. Гепатома выглядит на скенннограмме как "горячий" узелок, так как концентрирует молибден-99 в большей степени, чем окружающая печеночная ткань.

Пониженное поглощение молибдена-99 печенью наблюдается при диффузном поражении печеночных клеток.

Молибден-99 имеет некоторые преимущества перед коллоидальным радиоактивным золотом и меченной йодом-131 бенгальской розой: 1) он накапливается в многоугольных клетках и его поглощение эффективно отражает состояние пораженной паренхимы; 2) концентрация индикатора не изменяется во время скеннирования, поскольку период полувыведения молибдена-99 составляет примерно 20 дней; скеннирование может быть повторено в случае технических помех без ущерба для качества; 3) коэффициент контраста выше при использовании мягкого гамма-излучения технеция-99 m. Представлена сравнительная оценка разрешающей способности при скеннировании, по излучению молибдена-99—технеция-99 m, йода-131 и золота-198 с использованием фантома печени; и 4) низкая энергия основного излучения позволяет в значительной степени снизить размер сцинтилляционного кристалла и значительно повышает эффективность детектора и коллиматора.

Общая доза облучения печени составляет порядка двух рад.

CENTELLEOGRAFÍA DEL HÍGADO MEDIANTE MOLIBDATO RADIACTIVO. Inyectado por vía intravenosa en forma de molibdato y sin portador, el ^{99}Mo se concentra rápidamente y en grado apreciable en las células poligonales del hígado. La captación hepática de ^{99}Mo va acompañada de una formación gradual de su descendiente ^{99m}Tc, cuya radiación gamma de 0,140 MeV es particularmente adecuada para la centelleografía. A las 24 h de haber inyectado de 40 a 50 μc de ^{99}Mo se obtienen excelentes centelleogramas del hígado: el índice máximo de recuento del ^{99m}Tc sobre dicho órgano ha alcanzado su grado máximo y el ^{99m}Tc inyectado junto con el ^{99}Mo ha desaparecido casi completamente por excreción o por desintegración, dando un recuento de fondo muy bajo.

Las metástasis, los abscesos y otras lesiones extensas se visualizan como defectos. Un hepatoma produjo un nódulo "caliente" en el centelleograma por haber absorbido ^{99}Mo en mayor proporción que el tejido hepático circundante. En las afecciones hepatocelulares difusas se observa una captación hepática disminuida del ^{99}Mo.

El ^{99}Mo ofrece varias ventajas sobre el oro coloidal radiativo y sobre el Rosa Bengala marcado con ^{131}I: a) se acumula en las células poligonales y su captación refleja fielmente los estados patológicos del parénquima; b) la concentración del indicador no se altera mientras dura la exploración, porque el período biológico del ^{99}Mo es de unos 20 d; si resulta necesario, la exploración puede repetirse sin que empeoren las condiciones; c) como se emplea la radiación gamma de baja energía del ^{99m}Tc, el contraste es mejor; el autor presenta una evaluación comparativa del poder de resolución obtenido con ^{99}Mo-^{99m}Tc, con ^{131}I y con ^{198}Au empleando un hígado simulado; y d) la baja energía de la radiación principal permite emplear cristales centelleadores de tamaño muy reducido y aumenta notablemente la eficacia del detector y del colimador.

La dosis total de radiación recibida por el hígado es del orden de dos rad.

With the lack of a suitable radiopaque contrast material which is specifically deposited in the liver, isotope scanning is the simplest and safest method of delineating the contours and internal configuration of this organ. The clinical usefulness of this procedure is well established. It is the purpose of this report to describe the method and results of liver scanning with the use of radiomolybdate (Mo^{99}) as the tracer agent.

1. MATERIALS AND METHODS

Carrier-free Mo^{99} produced by thermal neutron fission of uranium oxide is available from Brookhaven National Laboratory as the ammonium molybdate. The radiopurity is better than 99.99% (except for the daughter Tc^{99m}). Technetium-99m was obtained by the method of milking from carrier-free parent Mo^{99} adsorbed on alumina. A special milking system and generator, from which Tc^{99m} can be milked repeatedly, is available from Brookhaven National Laboratory.

Radioassay of biologic material for Mo^{99} and Tc^{99m} was done with a 3-in by 3-in well-type sodium iodide crystal coupled to a transistorized 512-channel analyser (Nuclear Data Model ND-130). External counting over the liver and head was done in the Argonne Cancer Research Hospital whole-body counting facility with 5-in by 5-in sodium iodide crystal detectors inserted into optimum-focusing collimators.

The usual dose of radiomolybdenum for scanning of the liver is between 40 and 50 μc, which is given intravenously in a single injection. Solutions for injection are sterilized by heat. Scanning is started 24 h after injection, with the patient in the supine position. All scans were made with the commercially available Picker Magna-scanner, which uses a 3-in by 2-in thallium-activated iodide crystal, a 19-hole focusing collimator, a pulse-height selector, and two alternate data presentation systems, one of which is a background eliminating solenoid recorder, and the other a photographic recording system. In order to record the 0.140 MeV gamma radiation of Tc^{99m}, the lower and upper gates of the pulse-height analyser are set at 90 and 200 keV respectively. The scans are run at a speed of 40 cm/min, with a distance between adjacent lines of the scan of 0.3 cm. Usually 1 h is required to perform a scan. Upon completion of the scan the position of the liver edge, any palpable abdominal mass, and the costal margins are plotted on the scintigram.

2. BIOCHEMICAL AND PHYSICAL PRINCIPLES

A single tracer dose of Mo^{99} injected intravenously as sodium or ammonium molybdate disappears rapidly from the circulation of man. Six hours after injection of carrier-free material into normal subjects, the blood level has fallen to less than 1/300 of the initial concentration. Since only a minor portion of the administered molybdate is excreted during the first few hours, such rapid clearance signifies uptake of the element in one or more tissues. Secondly, the rate of clearance is dependent upon the diffusion space of molybdate, and the rate of excretion. Radioassay of tissues obtained post mortem from patients who had received carrier-free Mo^{99} from 1 to 21 d prior to death, has shown that molybdate accumulates preferentially in the liver, and to a much smaller extent in the renal cortex and adrenal gland.

The rate of accumulation of carrier-free molybdate-99 in the liver was determined by external counting with a collimated scintillation probe (Fig. 1); the hepatic uptake was virtually complete within 60 min following the intra-

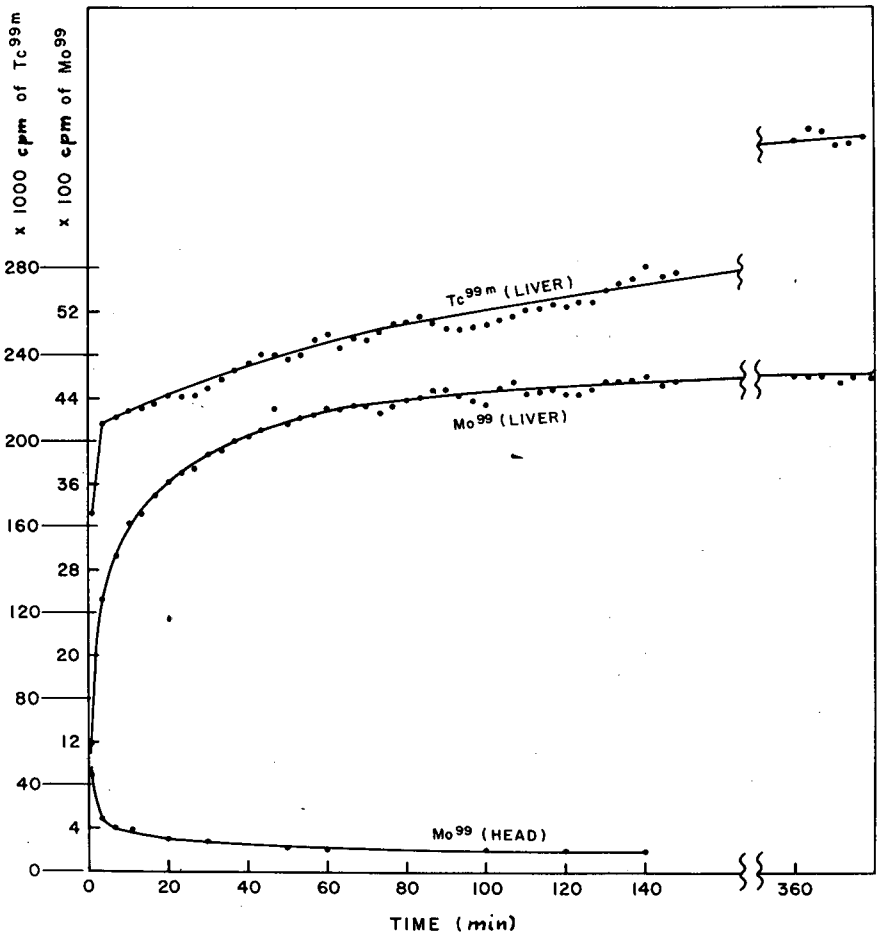

Fig. 1

Measurement with collimated scintillation probes of the rates of activity of Mo^{99} and Tc^{99m} in the liver and head following intravenous administration of 40 μc of carrier-free Mo^{99} to a normal subject (Not corrected for decay.)

venous administration. From excretion data it is estimated that the uptake of Mo^{99} by the normal liver is about 80% when carrier-free material is injected. The biological half-life of Mo^{99} determined by whole-body counting is about 20 d. Studies carried out in our laboratory have shown that labelled molybdenum is incorporated as a non-dialysable component of xanthine oxidase in the rat. In man, this enzyme is located in the liver and possibly in the small intestine [1].

Molybdenum-99 has a physical half-life of 67 h; its decay scheme is presented in Fig. 2 [2]. Eighty-five per cent of Mo^{99} decays via a 1.23-MeV beta particle to the 6-h metastable technetium-99m; the remainder decays with beta emissions of 0.45 MeV (14%) and 0.87 MeV (1%), and 6 gamma

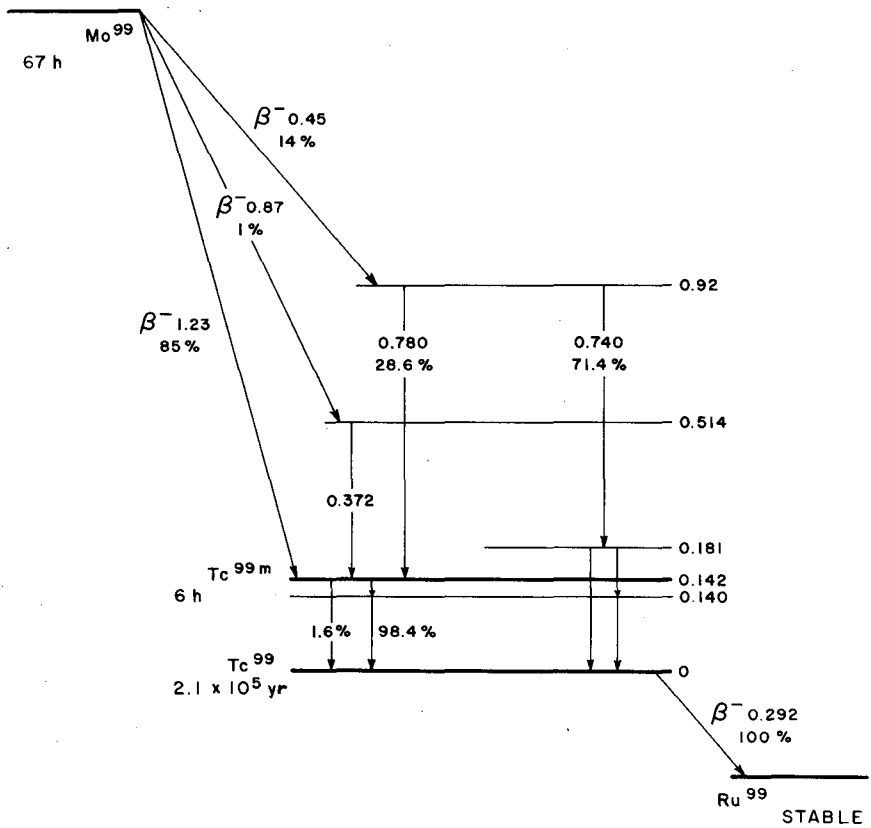

Fig. 2

Decay scheme of Mo^{99}
The radiation utilized in liver scanning is the 0.140-MeV γ-ray of Tc^{99m}

emissions of 0.780, 0.740, 0.372, 0.181, 0.140 and 0.041 MeV. Two-thirds of this remainder goes directly to Tc^{99}, while $\frac{1}{3}$ goes to Tc^{99m}. In all, 90% of Mo^{99} will pass through Tc^{99m} and thence to Tc^{99} by isomeric transmission emitting 0.142 MeV (1.6%) and 0.002 + 0.140 MeV (98.4%) γ-radiations. Technetium-99, with a half-life of 2.1×10^5 yr, decays by emission of a 0.292 MeV beta to ruthenium-99, which is stable.

The γ-radiation from Mo^{99} itself is not suitable for scanning purposes, partly because of its relatively high energy and partly because of the low emission rate. However, a considerable increase in absolute count-rate, as well as in contrast target: non-target ratio, is obtained by utilizing the low-energy radiation of the daughter Tc^{99m}.

Technetium itself does not concentrate in the liver. This can be seen from Fig. 3, which illustrates a parallel decrease in isotope concentration in the liver and head following intravenous administration of 100 μc of Tc^{99m} in the form of pertechnetate. Six hours after its administration the level of Tc^{99m} in whole blood has fallen to 10.7% of the initial value. Eighty-two per cent of the injected Tc^{99m} was recovered in urine and faeces within 72 h.

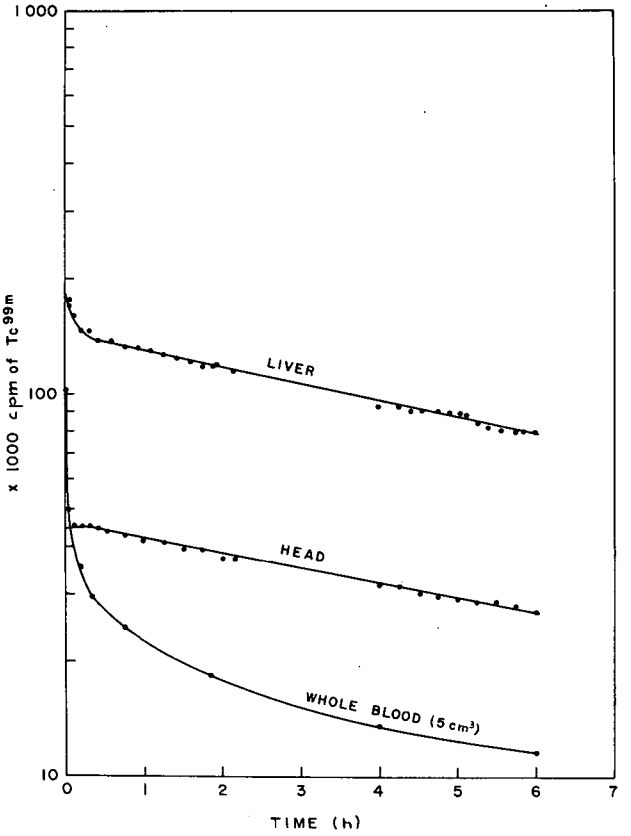

Fig. 3

Decrease in concentration of Tc^{99m} in liver, head, and whole blood following intravenous administration of 100 μc carrier-free pertechnetate at zero time (Corrected for decay.)

Radioassay of excreta beyond this time was not feasible because of the short half-life of Tc^{99m}. On succeeding days the urine contained 47, 7 and 4% of the administered technetium, and total recovery from faeces during the same interval was 24%. Whereas pertechnetate injected into the blood circulation does not concentrate in the liver, it is an interesting observation that Tc^{99m}, when produced from Mo^{99} already taken up by the liver cells, continues to stay in that organ. The liver may be likened to a column of resin which selectively retains molybdate, but not pertechnetate. The hepatic uptake of Mo^{99} is accompanied by a gradual build-up of Tc^{99m} (Fig. 1).

Figure 4 shows 5 photoscans done 3, 9, 21, 30 and 44 h after intravenous administration of 40 μc of Mo^{99} to a normal subject. The ratio between the maximum counts over the liver (counts per min), and the background counts over the left inguinal region at the same time were: at 3 h, 1500/1000; 9 h, 2400/600; 21 h, 4000/500; 30 h, 3500/500; and 44 h, 2800/400. Optimum scanning time is about 24 h after injection of molybdenum. At

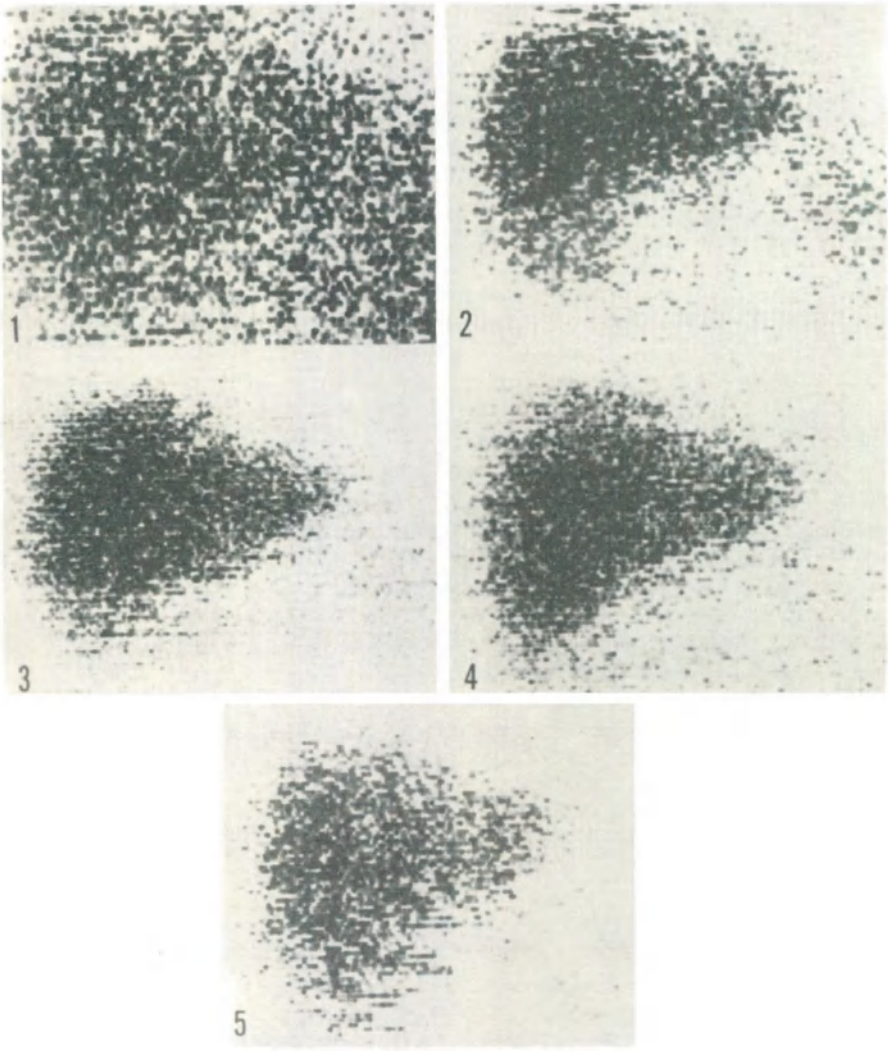

Fig. 4

Photoscans of the liver at 3, 9, 21, 30 and 44 h after intravenous administration of 40 μc of Mo^{99} to a normal subject

this time, Tc^{99m} injected together with Mo^{99} has been almost lost, either by excretion or decay, which secures low background count; at the same time maximum build-up of Tc^{99m} has taken place in the liver.

3. SCANNING RESOLUTION OBTAINED WITH Mo^{99}-Tc^{99m} AND WITH I^{131}

To compare the contrast ratio obtained when using the Mo^{99}-Tc^{99m} pair with that obtained with I^{131} a phantom was constructed to represent a liver

containing a cold lesion. The phantom consisted of 10 Lucite dishes, each having an inside diameter of 11.4 cm and an inside height of 1.0 cm. The bottom of each dish was 0.75 mm thick. The cold lesion was represented by 3 cylindrical Lucite plugs placed in the centre of 3 of the dishes. The diameter of the lesion was 3.0 cm and the total height 3.0 cm. The remaining space in the dishes was occupied by the isotope in uniform distribution in 4% agar. Count-rate profiles and photoscans were done with the lesion in 8 locations, one on the surface of the phantom and the others ranging from 1 to 7 cm beneath the surface. The equipment was the Picker Magna-scanner to which a scaler had been connected. The focal point of the 19-hole collimator traversed the centre of the lesion during the count-rate measurements. A 50-keV window was used to observe the principal photopeak of the 2 isotopes. The photoscans were done under comparable conditions, using a speed of 30 cm/min, a line spacing of 0.3 cm, and no background cut-off.

Figure 5 shows count-rate profiles over the liver phantoms. When the lesion reached the surface, the observed contrast ratio was 0.547 for Mo^{99}-Tc^{99m} and 0.545 for I^{131}. When the centre of the lesion was located 8.5 cm beneath the surface of the phantom, the contrast ratio had decreased to 0.819 and 0.809 for the 2 isotopes respectively. The two sets of photoscans are shown in Fig. 6. From the count-rate measurements as well as from the photoscans it may be seen that the scanning resolution is essentially the same for both Mo^{99}-Tc^{99m} pair and I^{131}. It should be recalled, however, that with respect to Rose Bengal-I^{131} the phantom represents a more favourable set of circumstances than does the human liver, i.e. because of the short biologic half-life of Rose Bengal, the concentration of I^{131} within the liver changes continually during the scanning procedure, which means that the initial setting of the scanning system may not be the optimal one at the end.

4. CLINICAL REPORTS

Approximately 150 liver scans using Mo^{99} as tracer have been performed in the University of Chicago hospitals. Figures 7-11 are representative hepatoscans. Figure 7 shows a huge defect along the lateral margin of the right liver lobe, with displacement of the functioning liver tissue downward and to the left. The patient was a 62-yr-old woman of Greek origin who in 1947 underwent marsupialization and cauterization of an echinococcus cyst of the liver and who complained of heaviness in the right hypochondrium and occasional pain of 2 months' duration. On the basis of the scan and the previous history, the patient was operated upon. At operation, an echinococcus cyst 7 cm in diam. and multiple daughter cysts were found involving the anterior aspect of the right lobe of the liver.

Figure 8 is a liver scan from a 52-yr-old woman who was admitted to the hospital because of pain below the right costal margin of 3 months' duration. Six months previously she had undergone radical mastectomy for carcinoma of the right breast. The liver was not palpable. The hepatoscan shows a huge central defect as well as two additional large lesions in the right liver lobe, proved at the time of adrenalectomy to be metastatic tumours.

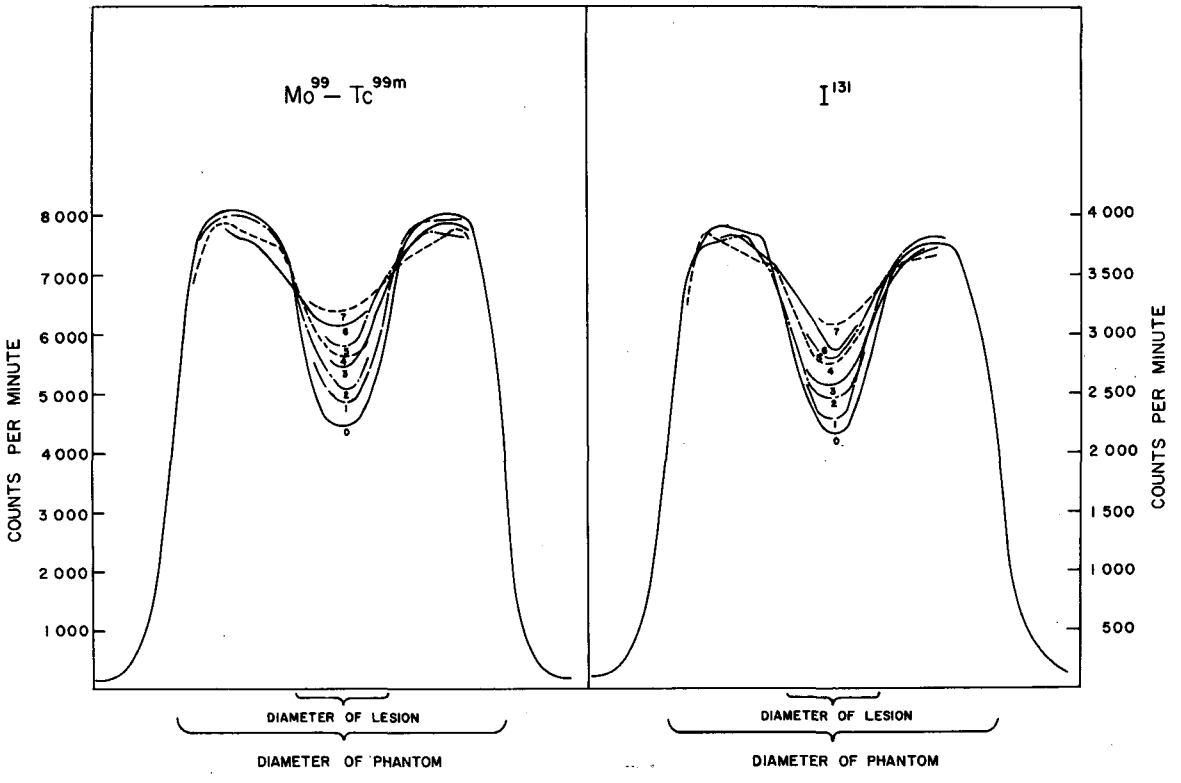

Fig. 5

Count-rate profiles across liver phantoms containing Mo^{99}-Tc^{99m} (left) and I^{131} (right)
A 3 cm × 3 cm cylindrical lesion was located
in the centre of the phantom at its surface and at different depths.

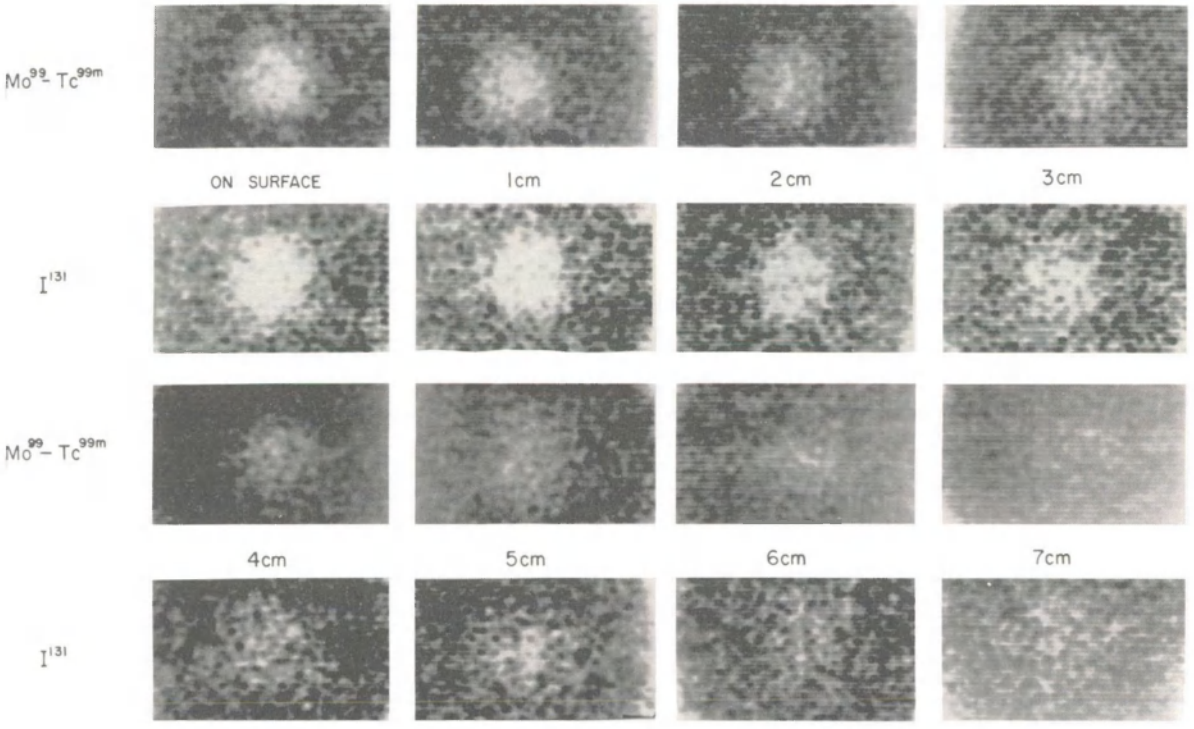

Fig. 6

Photoscans of liver phantoms containing Mo^{99}-Tc^{99m} and I^{131}
A 3 cm × 3 cm cylindrical lesion was centred in the phantom at the surface and at different depths.

Fig. 7

Photoscan showing large defect in the right upper quadrant
of the liver proved at operation to be caused by an echinococcus cyst

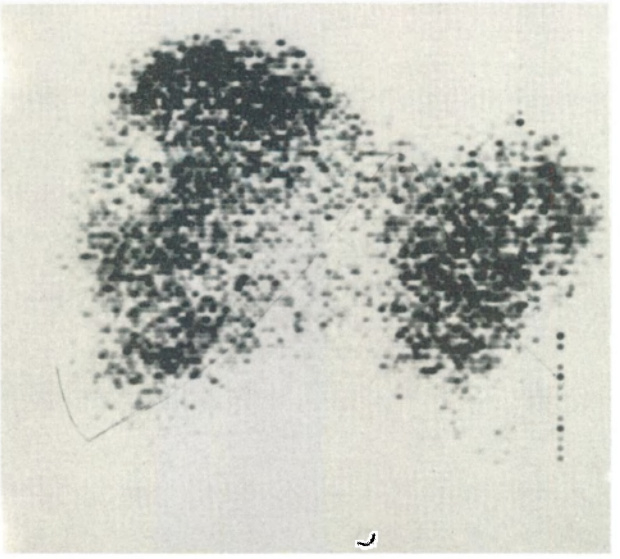

Fig. 8

Photoscan showing several large filling defects,
proved at operation to be metastatic tumours

Fig. 9

Photoscan showing several large filling defects caused by metastases from carcinoma of the lung

Figure 9 is the scan of a 47-yr-old man who entered the hospital because of progressive jaundice and epigastric distress of 2 weeks' duration. Two months before his admission, bronchial biopsy had revealed an undifferentiated small cell carcinoma as the cause of a superior vena cava syndrome. The scan shows several areas of decreased uptake indicative of metastatic disease.

Caution must be exercised in interpreting filling defects as metastatic lesions. The 63-yr-old man whose liver scan is shown in Fig. 10 was admitted to the hospital because of progressive jaundice of 5 months' duration and a 50-lb weight loss. The laboratory results were compatible with a diagnosis of obstructive biliary tract disease. At surgery, multiple stones were found to obstruct the common bile duct and it was evident that stones had perforated into the liver parenchyma causing marked scarring, visualized on the scan as an area of decreased density.

There are two primary hepatocellular carcinomas in this series, both arising in a cirrhotic liver of Laennec's type. In one case the malignant hepatic cells concentrated molybdenum to a greater extent than did the normal cells (Fig. 11). The patient, a 60-yr-old man, had been known to have cirrhosis of the liver for 2 yr. The liver was palpable 7 cm below the right costal margin. It was firm and contained large nodular masses. A diagnosis of hepatocellular carcinoma arising in a cirrhotic liver was established by biopsy. The liver scan showed increased uptake in what was believed

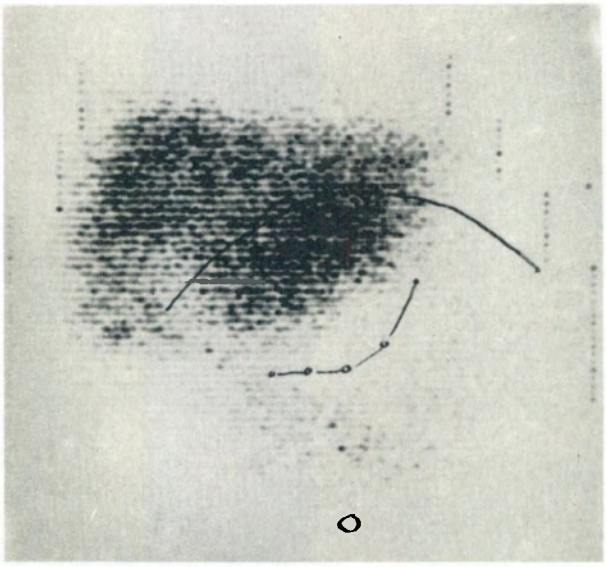

Fig.10

Filling defect in the lower part of the right lobe, confirmed at operation to be due to scarring secondary to penetration of gall-bladder stones into the liver parenchyma.

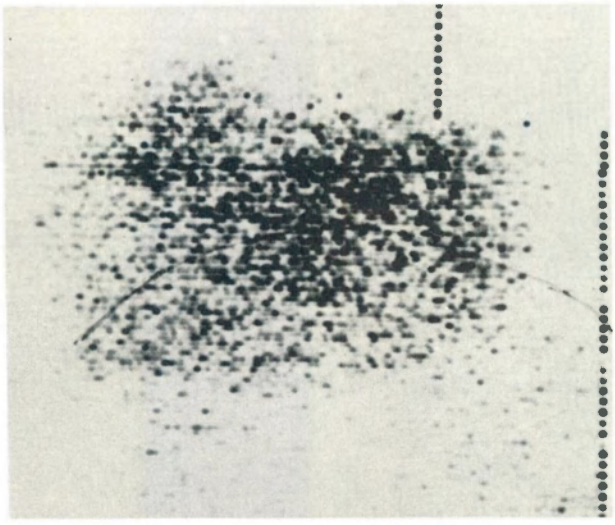

Fig. 11

Hepatocellular carcinoma, visualized as "hot" nodules in a patient with Laennec's cirrhosis.

to be a tumour and decreased uptake over the rest of the liver. This interpretation was verified by post-mortem examination which showed the upper middle portion of the liver to be studded with multiple tumours. By radioassay these nodules were found to contain up to three times as much Mo^{99} as did the surrounding cirrhotic tissue.

5. DISCUSSION

In the previous sections the principles and results of liver scanning with radiomolybdate have been presented. The basis for the method is the selective concentration in the polygonal cells of the liver of carrier-free Mo^{99}. From this procedure information can be derived about the size, shape, position and internal configuration of the liver. Metastatic tumours, abscesses and other space-occupying lesions destroy or displace the parenchyma, resulting in loci of diminished or absent radioactivity, In hepatocellular diseases, such as hepatitis and cirrhosis, the liver accumulates less of the administered dose of Mo^{99} leaving more of the isotope available for urinary excretion; on the scan, the liver image appears reduced in density with a pattern of patchy defects.

All scans presented in this report have been made with the commercially available Picker Magna-scanner. A collimated scintillation detector system [3] designed for low-to-moderate (< 200 keV) γ-energy has been

The radiation dose to the liver has been calculated using the formulae of Marinelli, Quimby and Hine [4]. Assuming (a) an uptake by the liver of 75% of an injected dose of 40 μc of Mo^{99}, (b) no biologic excretion and (c) complete physical decay, the total radiation dose to that organ would be slightly higher than 2 rad.

Mo^{99} possesses a number of advantages over tracers previously used in liver scanning: (1) Most important is the extremely favourable uptake ratio. The differential absorption ratio, i.e. the amount of radioactivity over the liver to the amount of radioactivity deposited in immediately adjacent areas is between 6 and 10. Reference has already been made to the short biological half-life of Rose Bengal and the changing concentration of I^{131} within the liver which may occur as a result. In addition, the release of Rose Bengal into the gall-bladder and intestine may obscure the inferior margin of the liver; (2) The long biological half-life of Mo^{99} within the liver is beneficial in that the interval between the injection of isotope and the beginning of the scan is not critical. The scan can be repeated in case of technical failure without loss of quality; (3) In general, the hepatic uptake of Mo^{99} has been found to be closely related to the functional state of the parenchymal cells; (4) The radiation dose to the liver is about five times smaller than when using colloidal radiogold; and (5) Carrier-free Mo^{99} is available commercially at a cost of $55.00 for 100 mc; the only preparatory measures involve dilution, sterilization, and radioassay of an aliquot of the stock solution.

tested. However, this system proved to be less sensitive than the detector of the Picker Magna-scanner because too many scattered photons originating from the high-energy parent Mo^{99} outside the geometrical field of the collimator were "seen" by the detector.

REFERENCES

[1] MORGAN, E.J., Biochem. J. 20 (1926) 1282-91.
[2] Nuclear Data Sheets, 1961, Set 1. National Academy of Sciences, National Research Council, Wash., D.C.
[3] BECK, R.N., J. nucl. Med. 2 (1961) 314-24.
[4] MARINELLI, L.D., QUIMBY, E.H. and HINE, G.J., Amer. J. Roentgenol. 59 (1948) 260-81.

DISCUSSION

W.G. MYERS: Would it not be an advantage to use a crystal about 1 cm thick, instead of 5 cm, which would absorb almost all of the 140-keV Tc^{99m} gamma rays but would not record most of the undesirable high-energy Mo^{99} gamma rays?

P. HARPER: Yes, but the thick shield must be retained. It would be even better to use a quarter-inch crystal which would still detect 80% of the 140-keV gamma rays.

R. BECK: With regard to Dr. Myers' suggestion that a thin crystal would be superior to a thick crystal for detecting 140-keV Tc^{99m} in the presence of 140-keV Mo^{99}, I should like to point out that there may be some advantage in using the thick crystal, since it would tend totally to absorb the Mo^{99} gamma rays, in which case they could be separated from the 140-keV Tc^{99m} gamma rays by pulse height analysis.

M. TER-POGOSSIAN: Did you experience any difficulties in using a relatively low-energy gamma-ray emitter in the visualization of a deep-seated organ?

P. HARPER: I can best answer your question by referring you to Fig. 5 of Dr. Sorensen's paper where the target/non-target ratios for Tc^{99m} are identical with those for I^{131}.

C. HARRIS: I do not know the half-value thickness of tissue at 140 keV, but it is a few centimetres. Dr. Harper mentioned the figure of 4.6 cm. At any rate it makes at least as much sense to scan deep-seated organs using an isotope emitting 140-keV gamma rays, as it does to scan organs at 2-cm depth using I^{125}.

PROFILE COUNTING STUDIES OF HEPATIC UPTAKE OF LABELLED MATERIALS IN MAN

E. E. POCHIN
MEDICAL RESEARCH COUNCIL, DEPARTMENT OF CLINICAL RESEARCH,
UNIVERSITY COLLEGE HOSPITAL MEDICAL SCHOOL, LONDON,
UNITED KINGDOM

Abstract — Résumé — Аннотация — Resumen

PROFILE COUNTING STUDIES OF HEPATIC UPTAKE OF LABELLED MATERIALS IN MAN. The value of a rapid and quantitative method for measuring the total radioisotope content of an organ is illustrated by profile-counting studies on the hepatic uptake of various radionuclides or labelled compounds in man. The method is likely to have wider application to the examination of uptake or turnover of materials in organs in which they are selectively concentrated.

After an intravenous injection of I^{131}-labelled thyroxine (T_4) or tri-iodothyronine (T_3) in man, serial profile or linear scans combined with blood sampling allow a determination of the distribution space of these hormones within the liver, and of the speed with which they enter and leave the organ. Concentration ratios between liver and plasma of three for T_4 and four for T_3 are observed in normal subjects and evidence is obtained that a large proportion of the circulating hormones enter and leave the liver during every hour. The rapidity with which profile scans can be obtained, and the accuracy with which hepatic contents can be estimated by these methods, facilitate such quantitative analyses.

The hepatic concentration of endogenously-produced hormone in hyper-thyroidism has been similarly examined by serial profiles in the days following test doses of radioiodine – given as iodide – and shows proportionality with levels of circulating protein-bound radioiodine. Following therapeutic doses of radioiodine to such patients, a lower proportionality is observed suggesting the liberation of metabolites from the irradiated thyroid which are less actively concentrated in the liver. Similar methods have been used to examine the hepatic uptake of circulating metabolites during radioiodine ablation of normal thyroid tissue in patients with thyroid cancer, and during the treatment of functioning thyroid cancer with radioiodine, when the detection of hepatic radioactivity at several days after a test dose of I^{131} appears to give useful evidence of the presence or persistence of iodine-concentrating tumour tissue within the body.

Estimates of hepatic content of Au^{198} or Y^{90} may be used to estimate the hepatic uptake or retention of injected particulates.

ÉTABLISSEMENT DE PROFILS SCINTIGRAPHIQUES POUR L'ÉTUDE DE LA FIXATION DE SUBSTANCES MARQUÉES PAR LE FOIE HUMAIN. La valeur d'une méthode quantitative permettant de mesurer rapidement la teneur totale d'un organe en radioisotopes est mise en évidence par l'emploi de profils scintigraphiques dans l'étude de la fixation de radionucléides ou de substances marquées par le foie humain. Il est probable que cette méthode recevra une large application dans l'étude de la fixation ou du renouvellement de certaines matières dans les organes où elles se concentrent sélectivement.

Après injection intraveineuse de thyroxine (T_4) ou de tri-iodothyronine (T_3) marquée avec ^{131}I, l'établissement d'une série de profils scintigraphiques, par balayage linéaire, associé à des analyses du sang, permet de déterminer la répartition de ces hormones dans le foie, ainsi que la vitesse à laquelle ils atteignent et quittent cet organe. Chez des sujets normaux, le rapport des concentrations dans le foie et le plasma est de 3 pour T_4 et de 4 pour T_3; on a constaté, en outre, qu'une grande partie des hormones en circulation atteignent et quittent le foie toutes les heures. Ces analyses quantitatives sont facilitées par la rapidité d'établissement des profils scintigraphiques et la précision du calcul du contenu du foie par cette méthode.

On a étudié de façon analogue la concentration hépatique des hormones endogènes chez des sujets atteints d'hyperthyroïdisme, en faisant des séries de profils scintigraphiques pendant les quelques jours suivant l'administration de doses expérimentales de radioiode sous forme d'iodure; on a constaté que cette concentration était proportionnelle à la quantité de radioiode lié aux protéines en circulation. A la suite de l'administration de doses thérapeutiques de radioiode, on a observé une diminution de la proportionnalité qui semble indiquer la libération par la thyroïde irradiée de métabolites moins activement concentrés dans le foie. On

a eu recours à des méthodes analogues pour étudier la fixation par le foie des métabolites en circulation lors de la destruction par le radioiode de tissus thyroïdiens normaux chez des malades ayant un cancer de la thyroïde, ainsi que lors du traitement par le radioiode du cancer dans une thyroïde en fonctionnement, lorsque la détection d'une radioactivité hépatique plusieurs jours après l'injection d'une dose expérimentale de ^{131}I semblait prouver la présence ou la persistance dans l'organisme de tissus néoplasiques concentrant l'iode.

Les estimations de la teneur du foie en ^{198}Au ou ^{90}Y peuvent servir à évaluer l'absorption ou la rétention hépatique des substances particulaires injectées.

ИЗУЧЕНИЯ ПРОФИЛЯ ПОГЛОЩЕНИЯ МЕЧЕНЫХ ВЕЩЕСТВ ПЕЧЕНЬЮ У ЧЕЛОВЕКА С ПОМОЩЬЮ СЧЕТА ИМПУЛЬСОВ. Ценность быстрого количественного метода измерения общего содержания радиоизотопов в каком-либо органе иллюстрируется использованием счета импульсов для изучения профиля поглощения различных радиоизотопов или меченых соединений печенью человека. Этот метод может более широко использоваться для изучения поглощения или кругооборота веществ в тех органах, где они селективно концентрируются.

После внутривенного введения меченных йодом-131, тироксина (T_4) или же трийодотиронина (T_3) у человека серийное профильное или линейное сканнирование совместно со взятием пробы крови дают возможность определения зон распределения этих гормонов в печени, а также скорости их поступления в этот орган и выхода из него. У здоровых людей коэффициент концентраций между печенью и плазмой равен 3 для T_4 и 4 для T_3, кроме того, имеются указания на то, что значительная доля циркулирующих гормонов поступает в печень и удаляется из нее каждый час. Такого рода количественный анализ может быть облегчен благодаря скорости получения профильных сканнограмм и точности, с которой эти методы позволяют определять содержание этих веществ в печени.

Концентрация эндогенных гормонов в печени при гипертиреоидизме определялась аналогичным образом путем получения серийных профильных сканнограмм в дни, следующие за введением индикаторных доз радиоактивного йода, вводимого в виде йодида, была обнаружена пропорциональность этой концентрации количеству циркулирующего связанного с белком радиоактивного йода. В результате применения терапевтических доз радиоактивного йода у таких больных наблюдается уменьшение этой пропорциональности, что позволяет думать о высвобождении метаболитов из облученной щитовидной железы, которые менее активно концентрируются в печени. Аналогичные методы были использованы для изучения поглощения печенью циркулирующих метаболитов в случае подавления функции щитовидной железы с помощью радиойода у пациентов, страдающих раком щитовидной железы, а также при лечении функционально активного рака щитовидной железы радиоактивным йодом, когда определение уровня радиоактивности печени несколько дней спустя после введения индикаторной дозы йода-131 дает, по-видимому, полезное указание на наличие или развитие концентрирующих йод опухолевых тканей в организме.

Определение содержания в печени золота-198 или иттрия-90 может быть использовано для оценки поглощения печенью или задержки в ней введенных частиц.

ESTUDIOS POR RECUENTO DE PERFILES DE LA CAPTACIÓN HEPÁTICA DE SUSTANCIAS MARCADAS. Los estudios por recuento de perfiles de la captación hepática de diversos radionúclidos o compuestos marcados demuestran el valor de un método rápido y cuantitativo para la medición del contenido total de radioisótopos de un órgano. Es probable que este método llegue a emplearse más extensamente para examinar la captación o la renovación de ciertas sustancias en aquellos órganos en que se concentran selectivamente.

Después de inyectar por vía intravenosa tiroxina (T_4) o triyodotironina (T_3) marcadas con ^{131}I, las exploraciones en serie de perfiles (o lineales) combinadas con análisis de sangre permiten determinar la distribución espacial de estas hormonas en el hígado y la velocidad con que entran y salen de dicho órgano. En individuos normales se observan entre el hígado y el plasma razones de concentración de 3 para la T_4 y de 4 para la T_3, y se comprueba que, cada hora, una proporción elevada de las hormonas en circulación entra o sale del hígado. La rapidez con que se puede obtener un perfil radiactivo y la exactitud con que esos métodos permiten estimar el contenido hepático facilitan estos análisis cuantitativos.

Se ha examinado también la concentración hepática de hormona endógena en casos de hipertiroidismo, determinando series de perfiles en los días siguientes a la administración de dosis experimentales de radioyodo (en forma de yoduro) y se ha observado una proporcionalidad con las concentraciones de radioyodo unido a las proteínas en circulación. Después de administrar dosis terapéuticas de radioyodo a esos pacientes se observa una proporción más baja, lo que sugiere que la tiroides irradiada libera metabolitos que se concentran menos

activamente en el hígado. Se han empleado métodos similares para examinar la captación hepática de metabolitos cuando el radioyodo destruye tejido tiroideo normal en enfermos de cáncer de la tiroides, y durante el tratamiento del cáncer tiroideo con yodo radiactivo cuando el tejido canceroso conserva aún la función tiroidea. En esos casos, la detección de la radiactividad hepática varios días después de la administración de una dosis experimental de ^{131}I proporciona al parecer cierta información sobre la presencia o la persistencia de tejido tumoral capaz de concentrar el yodo.

La evaluación del contenido de ^{198}Au y ^{90}Y puede servir para calcular la captación hepática o la retención de sustancias inyectadas en forma de suspensiones.

Studies of the radioisotope content of the human liver have yielded valuable information on a number of clinical and physiological problems, particularly by allowing estimates of hepatic function or blood flow to be made from determinations of the speed with which labelled materials are removed from the circulation by the liver, or by facilitating the diagnosis of space-occupying lesions of the organ by studies of the distribution of radioactive materials throughout it. It is not essential, however, for the purpose of most such types of investigation that the radioisotope content of the liver should be known at any time in absolute terms, or that the liver uptake of the nuclide should be calibrated and expressible as a percentage of the dose given.

In examining the hepatic concentration of radioiodine-labelled thyroid metabolites, it is important that the total liver content of radioiodine should be expressed in absolute terms and related, for example, either to the plasma concentration of radioiodine in organic combination or to the percentage of the administered dose of radioiodine which has passed through the thyroid at any given time. In the following investigations the hepatic content of radioiodine has been studied in subjects with or without thyroid disease by techniques of profile counting, using methods of calibration that have been described [1]. These techniques have allowed serial observations to be made under standard conditions, either during the period immediately after the intravenous injection of labelled hormone, or in the days following administration of radioiodine as iodide and during the course of discharge of naturally labelled hormone from the thyroid gland or from functioning thyroid cancers [2].

When such serial profile counts (or linear scans) are made at intervals after the administration of a radioiodine dose to a hyperthyroid subject, it is usually found that the profile peak corresponding to the thyroid content increases rapidly, while evidence of activity elsewhere in the body decreases concurrently, so that after 12-24 h a single peak at the level of the thyroid indicates the concentration in the gland of essentially all of the administered radioiodine that has not already been excreted. In the ensuing few days, however, and particularly if the discharge of radioiodine from the thyroid is rapid, the progressive fall of the thyroid peak is associated with the development of a second peak of activity at about 50 cm from the vertex of the head, which can be shown by mapping to correspond with radioactivity in the position of the liver. The height of this hepatic peak, as corrected for radioactive decay, normally reaches a maximum value after a few days, decreasing thereafter according to a curve which typically becomes parallel to that for the continuing discharge of radioiodine from the thyroid.

When the height of the hepatic peak in a particular patient is related to the plasma concentration of protein-bound radioiodine in the days follow-

ing the dose, the liver activity is found to rise and fall in proportion to the concentration during these days of organically bound radioiodine in the plasma. It appears therefore that the liver concentrates the circulating metabolites and can be described as having a constant "distribution space" for them.

The size of this distribution space can be determined if the liver content of radioiodine is calibrated and expressed in microcuries, and compared with the plasma concentration of protein-bound radioiodine as measured in microcuries per litre.

The liver content of radioiodine can be determined with moderate accuracy in those patients in whom the radioiodine is rapidly discharged from the thyroid and accumulates in large amounts in the liver, so that a considerable liver peak develops which is well separated from contributions caused by radioactivity of any other tissues. In other patients in whom the thyroid discharge is less rapid and the hepatic peak is less dominant, the calibration factor appropriate for the individual patient is determined with less accuracy and it has appeared preferable to determine a mean calibration factor for hepatic radioiodine for the counting assembly used and to apply this factor to all patients studied. Approximately the same mean value has been observed in patients with rapid discharge of naturally labelled radioiodine, in subjects after intravenous injection of I^{131}-labelled thyroxine and tri-iodothyronine, and also following the hepatic concentration of intravenously injected colloidal radiogold-198, of which the gamma energy is sufficiently similar to that of I^{131} to allow corroboration of the calibration factor appropriate to human hepatic radioisotope concentration. The results obtained by this method on individuals in whom direct calibration is not possible will clearly involve inaccuracies caused by individual variations in liver size or position. Mean values of groups of individuals should however give valid estimates of the amount of radioiodine present in the liver under different circumstances.

The proportionality between hepatic radioactivity and plasma organic radioiodine following test doses in hyperthyroid subjects can on this basis be expressed by the statement that the liver contains on average as much radioiodine as is present in protein-bound form in 8.5 l of plasma [2]. The similarity between the rise and fall with time of both hepatic and plasma contents also clearly suggests that a distribution equilibrium is established and maintained between these two compartments. No accurate information is obtainable however from these observations as to the speed with which any such distribution equilibrium is set up.

To investigate this point in more detail and to extend the information as to what compounds are concentrated in the liver, intravenous injections of radioiodine-labelled thyroxine and tri-iodothyronine were given to subjects without thyroid disease, and the course both of the hepatic radioactivity and of the plasma radioiodine content were followed during the ensuing hours. When thyroxine is given in this way, it is found that the hepatic radioactivity rises relatively rapidly to a maximum value which is usually reached by between $\frac{1}{2}$ and $1\frac{1}{2}$ h after the injection, the liver radioactivity thereafter falling in parallel with the fall of the plasma protein-bound radioiodine con-

centration. The ratio between hepatic and plasma concentrations reaches, within 2 or 3 h of the injection, a limiting value which thereafter remains constant and corresponds to a distribution space of about 5 l for this hormone in the liver.

The speed with which this ratio approaches its limiting value should indicate the rate at which thyroxine in the plasma becomes equilibrated with that in the liver. This time appears to be short, the ratio usually reaching half its limiting value within about 30 min of the injection of the labelled thyroxine, suggesting that 50% of the liver content of thyroxine is leaving the organ within $\frac{1}{2}$ h or less. This value would correspond with a clearance by the liver of 0.12 l of plasma per minute of its contained thyroxine, with redischarge of almost all of this hormone again into the circulation within a mean period of less than 1 h, since MYANT [3] has shown that the amount of thyroxine which is excreted from the liver into the gut through the bile is small in man, and since the rate of thyroxine breakdown is small compared with these rates of liver-cycling of the hormone.

Tri-iodothyronine is found to be rather more highly concentrated in the liver than is thyroxine, its distribution space having a value of about 7 l. If the mean mass of the liver is taken as 1.5 kg, this indicates a concentration ratio between hepatic tissue and plasma of about 5, as compared with one of about $3\frac{1}{2}$ for thyroxine. Moreover, the speed with which tri-iodothyronine becomes equilibrated between plasma and liver appears to be rather more rapid than for thyroxine, the maximum liver uptake being reached within a few minutes of the injection and the ratio between hepatic and plasma concentrations reaching half its final value in a mean time of 7 min in the seven subjects investigated. This value would indicate that about 10% of the hepatic tri-iodothyronine leaves the liver per minute, having about a 10-min mean stay in the organ. The hepatic clearance of plasma tri-iodothyronine is estimated as about 0.7 l of plasma per minute, which approaches the total plasma flow through the liver and implies a substantially complete removal of the hormone on every passage through the organ.

These techniques thus give evidence of a rather rapid and quite considerable but temporary concentration of each thyroid hormone in the liver. They imply that the hormone molecules are normally taken up by the liver and discharged again into the circulation many times each day. No evidence has been obtained of any factors which influence the rates of uptake or discharge of these materials or of any metabolic process that may be involved during this cycling of hormones through the liver.

It will be seen, however, that comparatively small changes of either uptake or discharge rates would rapidly alter the plasma concentration of the circulating hormones, although there is no evidence that any such control or variation of levels occurs.

It would be of interest to know whether these rates of hepatic uptake are characteristic of thyroid hormones or are common to other compounds concentrated by the liver and, in particular, whether thyroxine-binding globulin or other plasma protein fractions are taken up at similar rates, since the uptake of the thyroid hormones might simply be due to the uptake of the plasma proteins to which they were bound.

It has been stated that the liver uptake of the naturally occurring metabolites of the hyperthyroid patient is proportional to the current plasma con-

centration of organic radioiodine compounds, the distribution space of these compounds being comparable with, or a little higher than, those observed for the thyroid hormones when given intravenously. It is doubtful whether the difference in concentration observed in these situations is necessarily significant, since the hepatic uptake in the hyperthyroid patients is examined in the presence of a higher radioiodine content of surrounding tissues than when labelled hormone alone has been injected, and this may have some effect in increasing the height of the profile peak and so the estimated uptake in the liver.

In any individual patient the hepatic content can be clearly related to the amount of radioiodine which has already been discharged from the thyroid, patients with the most rapid radioiodine turnover through the gland developing the largest hepatic contents and occasionally having several times as much radioiodine in the liver as in the thyroid itself, once equilibrium is set up between the two organs. If the hepatic content at 5 d after the dose is related to the percentage of the dose which has left the thyroid between the first and fifth day, a linear regression is observed indicating that about 60% of the radioiodine which has left the thyroid in this interval is to be found in the liver at that time. Allowing for some hormone breakdown and radioiodine excretion during this period, this value is clearly consistent with the concept of the liver as containing at least half of the body thyroxine, as is suggested by a comparison between the hepatic distribution space for this hormone and conventional estimates of its total distribution space within the body.

When a therapeutic dose of iodine-131 is given to a hyperthyroid patient and profile curves are compared with those obtained following a preceding test dose in the same patient, it is observed with considerable regularity that the hepatic peak developing after the therapeutic dose is less pronounced than that after the test dose. The hepatic radioiodine content is again clearly related to the speed of radioiodine turnover through the gland but, for a given radioiodine discharge from the gland between the first and fifth days after the dose, the liver radioactivity is now seen to be considerably less than following the test dose, the regression line having a slope corresponding to only about 30% of the discharged radioiodine being present in the liver. Values are given in Fig. 1 for the hepatic contents as estimated by profile counting in about 280 patients receiving both test and therapeutic doses and indicating clearly the difference in hepatic concentration of discharged radioiodine in the two situations.

A more direct estimate of the hepatic concentration of circulating metabolites is obtained by comparing the liver radioactivity with that of the plasma protein-bound fraction observed at the same time, since the lower hepatic content of radioiodine discharged from the thyroid after therapeutic doses might merely correspond with a briefer survival in the circulation of discharged metabolites in these cases. The hepatic distribution space for circulating metabolites after therapeutic doses has had an average value of 6.5 l in 50 patients as compared with 8.5 l for test doses; and a comparison of the distribution space at 4 or 5 d after the dose in a group of patients studied after both test and therapeutic doses has shown spaces after the latter which were about 70% of the size observed after the preceding test doses in the same patients. It appears clear therefore that certain of the

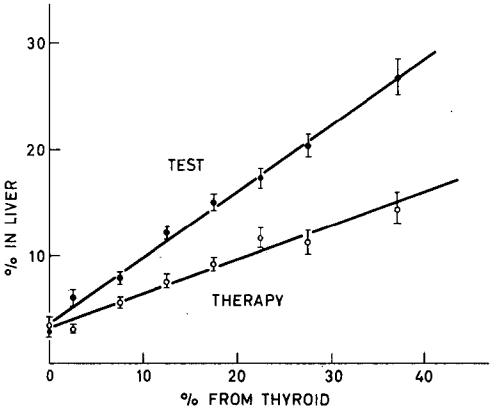

Fig. 1

Relation between height of profile peak at the position of the liver, 5 d after a radioiodine dose expressed as percentage of the dose present in the liver, and the loss of radioiodine from the thyroid, expressed as the difference between the percentage of the dose present in the gland at 1 d and at 5 d: upper graph, in 299 hyperthyroid patients following test doses; lower graph, in 278 of these patients following therapeutic doses.

metabolites discharged from the gland under the influence of the radiation received from radioiodine in this form of therapy are less highly concentrated by the liver than are the metabolites that are usually discharged from the gland, and this subject remains under investigation.

CONCLUSIONS

Techniques of profile counting appear to offer a simple and quantitative way of studying the dynamics of hepatic uptake and turnover of the thyroid hormones and metabolites, and have some diagnostic as well as considerable investigational possibilities. It is now clear on a quantitative basis why a hepatic concentration of radioiodine is not demonstrable in normal subjects or even in some hyperthyroid patients, since the relevant profile peak may be difficult to discriminate from the effects of radioiodine in surrounding tissues if the thyroid discharge of labelled hormone is not rapid. Unless about 10% of the administered dose has already been discharged from the gland within the first 5 d, the hepatic uptake can often not be clearly discriminated from radioiodine in adjacent organs with the counting arrangements used for the greater part of this work, and, although improved collimation decreases this limit somewhat, it is unlikely that the slow discharge of labelled hormone from the normal gland will often give detectable hepatic concentrations.

Correspondingly, however, a hepatic peak is likely to be demonstrable whenever the thyroid turnover is for any reason high, provided that the metabolites discharged are hormonal or in any other form which is concentrated by the liver. Such liver peaks are regularly demonstrable during the ablation of the normal thyroid gland by high doses of radioiodine, as carried

out in patients with differentiated thyroid carcinoma prior to radioiodine treatment. Moreover, following thyroid destruction and in the presence of an iodine-concentrating tumour of rapid radioiodine turnover, a hepatic peak frequently develops within a few days of the administration of a dose, and is normally attributable to a concentration of discharged metabolites in the liver. This uptake is to be distinguished from hepatic uptake of radioiodine in such patients due to the presence of a functioning metastasis in the liver, the latter usually giving a maximum uptake at a considerably earlier time (often at 6-12 h, rather than after a few days) and commonly showing a localized concentration at one site within the organ rather than an apparently uniform concentration throughout the liver substance on mapping. The detection of hepatic radioiodine uptake in such patients is, like the presence of organically bound radioiodine in the plasma, to be regarded as indicating the persistence of some remaining iodine-concentrating tumour tissue within the body if ablation of normal thyroid tissue is already complete. This finding will be of importance if radical therapy is being attempted, since any such evidence of the organic binding of iodine must in this case indicate the need for further radioiodine therapy. In patients with isolated known metastases, this guidance is seldom of importance since the persistence of the metastasis itself will readily be detectable. Where, however, multiple and disseminated metastases are present, or where iodine-concentrating deposits occur in positions which may be confused with physiological sites of iodine concentration such as the bladder, the stomach or the salivary glands, the detection of hepatic iodine concentration developing several days after a test dose may give a valuable indication of the persistence of functioning tumour tissue in the body of a patient in whom all such tumour tissue had been thought to have been destroyed by preceding radioiodine therapy. The relationship which can be established between the liver content and the amount of radioiodine already discharged from thyroid or tumour tissue may give a quantitative basis for assessing the amount of uptake in all remaining tumour tissue.

The quantitative study of the hepatic concentration and turnover of iodine metabolites by profile counting methods seems to be of interest in giving some indication of the likely applicability of such techniques to examination of the kinetics of the uptake of other compounds in organs in which they are selectively concentrated.

REFERENCES

[1] CORBETT, B. D., CUNNINGHAM, R. M., HALNAN, K. E. and POCHIN, E. E., A profile counter and its calibration, Phys. Med. Biol. 1 (1956) 37-56.

[2] POCHIN, E. E., Proc. Symp. Dynamic Clinical Studies with Radioisotopes, Oak Ridge (1963) (In press).

[3] MYANT, N. B., Clin. Sci. 15 (1956) 227.

DISCUSSION

H. A. B. SIMONS: I think that the convergent slit collimator is particularly liable to edge penetration effects and I wonder how this affects the calibration of your system in cpm/μc in the organ.

E.E. POCHIN: The counter with this collimation is, in any case, used primarily for localizing and distinguishing individual sites of uptake rather than for quantitative determinations of the amount of uptake. Since calibration is much more reliable with the wider angle collimator system, the latter is preferred for all determinations of uptake.

D. IKKOS: You mentioned that the biological half-life of thyroxine in the liver is much longer than that of tri-iodothyronine. Can you suggest the cause of this difference? Can it be caused by the binding of thyroxine to the plasma proteins?

E.E. POCHIN: That may well be the cause. It is possible, indeed, that it is really the thyroxine-binding proteins which are being concentrated rather than the thyroxine itself. This might account for the less prolonged retention of tri-iodothyronine, which is less strongly bound, although clearly it would not explain the apparently higher concentration of tri-iodothyronine than of thyroxine in the liver.

SYMPOSIUM ON MEDICAL RADIOISOTOPE SCANNING

HELD IN ATHENS, 20-24 APRIL 1964

CHAIRMEN OF SESSIONS

Session 1	B. MALAMOS	Dept. of Clinical Therapeutics, University of Athens
Session 2	L. G. LARSSON	World Health Organization, Geneva
Session 3	W. J. MacINTYRE	Highland View Hospital, Cleveland, Ohio
Session 4	E. E. POCHIN	World Health Organization, Geneva and International Commission on Radiological Protection
Session 5	G. BROWNELL	Physics Research Laboratory, Massachusetts General Hospital, Boston
Session 6	G. PANTAZIS	University of Athens
Session 7	T. SPÂRCHEZ	Faculté de Médecine, Bucarest
Session 8	L. DONATO	Centro di Medicina Nucleare, University of Pisa
Session 9	K. SCHEER	Universitäts-Strahlenklinik, Heidelberg
Session 10	M. TUBIANA	Institut Gustave Roussy, Villejuif (Seine)

SECRETARIAT OF THE SYMPOSIUM

Scientific Secretaries:	H. BELCHER	Division of Isotopes, IAEA
	G. GÓMEZ-CRESPO	Division of Isotopes, IAEA
Editor:	A. M. HAMENDE	Division of Scientific and Technical Information, IAEA
Records Officer:	N. W. A. JONES	Division of Languages, IAEA
Administrative Secretary:	H. H. STORHAUG	Division of Scientific and Technical Information, IAEA

LIST OF PARTICIPANTS

Name	Institution	Nominating State or Organization
Akerman, M.	Centre Médico-chirurgical Foch, Suresnes	France
Albarède, P.	Institut Gustave Roussy, Villejuif	France
Alevisatos, J.	Athens Polyclinic, Athens	Greece
Alevizou, V.	Department of Clinical Therapeutics, University of Athens, Alexandra Hospital, Athens	Greece
Arlman, J.	N. V. Philips-Duphar, Isotopes Commercial Dept., Amsterdam	Netherlands
Baptista, A.	Laboratorio de Isotopos Abilio Lopes do Rego, Instituto Portugues de Oncologia - Palhava, Lisbon	Portugal
Baschieri, L.	Istituto Patologia Speciale, Medical University of Rome	Italy
Becchini, F.	Medical Clinic, University of Pisa	Italy
Beck, R.	University of Chicago, Argonne Cancer Research Hospital, Chicago, Ill.	United States of America
Beckers, C.	Laboratoire de pathologie générale et Département des radioisotopes, Université de Louvain	Belgium
Bender, M.	Roswell Park Memorial Inst., Buffalo, N. Y.	United States of America
Benham, D.	Flagstaff Community Hospital, Flagstaff, Ariz.	United States of America
Ben-Porath, M	Hadassah University Hospital, Medical Physics Section, Jerusalem	Israel
Binopoulos, D.	Radioisotope Dept., Alexandra Hospital, Athens	Greece
Blanc, A.	Centre d'études nucléaires de Saclay, Gif-sur-Yvette (S et O)	France
Blau, M.	Roswell Park Memorial Inst., Buffalo, N. Y.	United States of America
Bodforss, B.	Radiophysical Dept., Gävle	Sweden
Bollini, V.	Istituto di Radilogia, University of Bologna	Italy
Brice, J.	Atkinson Merley's Hospital, London	United Kingdom

Name	Institution	Nominating State or Organization
Brownell, G.	Physics Research Lab., Massachusetts General Hospital, Boston, Mass.	United States of America
Cassen, B.	Laboratory of Nuclear Medicine and Radiation Biology, University of California, Los Angeles	United States of America
Cederlund, J.	Radiofysiska AVD, Borås	Sweden
Cheretakis, E.	Nuclear Research Centre "Democritus", Health Physics Dept., Attiki, Athens	Greece
Conrad, B.	University Clinic for Radiotherapy and Nuclear Medicine, Cantonal Hospital, Zurich	Switzerland
Courtial, J.	Fondation Curie, Paris	France
Czerniak, P.	Radium and Isotope Institute, Tel Hashomer Government Hospital	Israel
Dehshiri, K.	Tehran University, Physics Dept., Tehran	Iran
Delaloye, B.	Laboratoire des radioisotopes de la clinique médicale, University of Lausanne	Switzerland
Dermentzoglou, F.	Anticancer Hospital, Athens	Greece
Desgrez, A.	Service Hospitalier Frédéric Joliot, Orsay (S et O)	France
Domingos Filipe, A.	Hospital do Ultramar, Lisbon	Portugal
Donato, L.	Centro di Medicina Nucleare, University of Pisa	Italy
Dorta, T.	Cantonal Hospital, Chur	Switzerland
Economos, D.	Neurological Centre, Polykliniki Athinon Hospital, Piraeus	Greece
Eichhorn, O.	Neurological Department, University of Graz	Austria
Elias, C.	Alexandra Hospital, Athens	Greece
Entzian, W.	Neurochirurgische Universitätsklinik, Bonn	Federal Republic of Germany
Ephraïm, K.	Rotterdams Radiotherapeutisch Instituut	Netherlands
Erjavec, M.	Institute of Oncology, Medical School, Ljubljana	Yugoslavia

Name	Institution	Nominating State or Organization
Fedoruk, S.	Saskatchewan Cancer Commission, Saskatoon Cancer Clinic	Canada
Fischer, J.	I. Medizinische Klinik der Universität Mainz	Federal Republic of Germany
Follett, D.	Physics Dept., Bristol General Hospital, Bristol	United Kingdom
Gandy, A.	Fondation Curie, Paris	France
Gary-Bobo, J.	Centre régional anticancéreux de Montpellier, Montpellier (Hérault)	France
Gatsou, P.	Evangelismos Hospital, Athens	Greece
Gellinek, W.	Siemens-Reiniger Werke AG, Erlangen	Federal Republic of Germany
Gest, J.	Centre René Huguenin de lutte contre le cancer, Saint-Cloud	France
Gheorghescu, B.	Institut Médico-Pharmaceutique, Bucarest	Rumania
Giovannelli, G.	Centro di Medicina Nucleare, Clinica Pediatrica, University of Parma	Italy
Glass, H.	Dept. of Medical Physics, King's College Hospital, London	United Kingdom
Gongora, R.	Fondation Curie, Paris	France
Graauw, P.	N.V. Philips, Eindhoven	Netherlands
Gross, W.	Columbia University, New York, N.Y.	United States of America
Gyftaki, H.	Alexandra Hospital, Athens	Greece
Harper, P.	University of Chicago, Ill.	United States of America
Harris, C.	Oak Ridge National Laboratory, Oak Ridge, Tenn.	United States of America
Herbert, R.	Liverpool Radium Institute	United Kingdom
Héripret, G.	Institut Calot, Berck	France
Hindel, R.	Picker-Nuclear, White Plains, N.Y.	United States of America
Hine, G.J.	Veterans Administration Hospital, Boston, Mass.	United States of America
Hodes, H.	The Mount Sinai Hospital, New York, N.Y.	United States of America

Name	Institution	Nominating State or Organization
Höfer, R.	II. Medical University Clinic, Vienna	Austria
Ikkos, D.	Radioisotope Laboratory, Evangelismos Hospital, Athens	Greece
Inglessi, A.	Evangelismos Hospital, Athens	Greece
Jammet, H. P.	Fondation Curie, Paris	France
Jasinski, W.	Institute of Oncology, Warsaw	Poland
Jordan, K.	Frieseke & Höpfner GmbH., Erlangen-Brück	Federal Republic of Germany
Kakehi, H.	Dept. of Radiology, Chiba University Hospital, Chiba	Japan
Kalkman, H. J.	Gemeenteziekenhuis Zuidwal 83, The Hague	Netherlands
Kellershohn, C.	Service Hospitalier Frédéric Joliot Orsay (S et O)	France
Kenny, P.	Sloan Kettering Institute for Cancer Research, New York, N. Y.	United States of America
Khan, R. A.	Medical Radioisotope Centre, Karachi	Pakistan
Kniseley, R.	Oak Ridge Institute of Nuclear Studies, Oak Ridge, Tenn.	United States of America
Kordiolis, N.	Greek Anticancer Institute, Athens	Greece
Kostamis, P.	Dept. of Clinical Therapeutics, University of Athens, Alexandra Hospital, Athens	Greece
Krebs, A.	Federal Ministry of Health, Bad Godesberg	Federal Republic of Germany
Kuhl, D.	Dept. of Radiology, Hospital of the University of Pennsylvania, Philadelphia, Pa.	United States of America
Lansiart, A.	Centre d'études nucléaires de Saclay, Gif-sur-Yvette (S et O)	France
Larsson, L. G.	Radiotherapy Dept., University of Umeå, Sweden	World Health Organization
Laurinsich, A.	Clinica Pediatrica, University of Parma	Italy
Low, F. H.	Picker-Nuclear, White Plains, N. Y.	United States of America
Lubin, E.	Israel Atomic Energy Commission, Soreq Research Establishments, Yavne	Israel

Name	Institution	Nominating State or Organization
Maass, R.	Comision Nacional de Energia Nuclear, Mexico	Mexico
McAlister, J. M.	St. Bartholomew's Hospital, London	United Kingdom
McCusker, J.	St. Mary's Hospital, London	United Kingdom
McIntyre, W. J.	Highland View Hospital, Cleveland, Ohio	United States of America
Madsen, C. B.	Radiophysical Laboratory, Radium Centre, Aarhus	Denmark
Malamos, B.	Dept. of Clinical Therapeutics, University of Athens, Alexandra Hospital, Athens	Greece
Mallard, J.	Dept. of Medical Physics, Postgraduate Medical School, Hammersmith Hospital, London	United Kingdom
Manthopoulos, A.	First Greek Anticancer Institute, Dept. of Neurology, Athens	Greece
Marryat, J. F.	National Hospital for Nervous Diseases, Institute of Neurology, London	United Kingdom
Matthews, C. M. E.	Medical Research Council, Cyclotron Unit, Hammersmith Hospital, London	United Kingdom
Mellinck, J.	Dept. of Radiology, Academic Hospital of Leiden University	Netherlands
Mikropoulos, H.	Aghios Savvas Hospital, Athens	Greece
Morichère, J.	Centre d'études nucléaires de Saclay, Gif-sur-Yvette (S et O)	France
Morneburg, H.	Siemens-Reiniger Werke AG, Erlangen	Federal Republic of Germany
Munkner, T.	Radiological Department, University Clinic, Copenhagen	Denmark
Myers, W. G.	Ohio State University College of Medicine, Columbus, Ohio	United States of America
Nastou, A.	Evangelismos Hospital, Athens	Greece
Niklas, W.	Rauland Corporation, Chicago, Ill.	United States of America
Obara, T.	Dept. of Nuclear Medicine, Warsaw	Poland
Omsveen, P.	The Radium Station, Odense Amts og Bys Sygehus, Odense	Denmark
Oosterkamp, W. J.	Philips Research Laboratories, Eindhoven	Netherlands

Name	Institution	Nominating State or Organization
Otero-Ruiz, E.	Instituto Nacional de Cancerologia, Bogota	Colombia
Pantazis, G.	University of Athens, Athens	Greece
Papanicolaou, N.	Centre d'études nucléaires de Saclay, Gif-sur-Yvette (S et O) France	Greece
Papavasiliou, C.	Alexandra Hospital, Athens	Greece
Paraschou, E.	Anticancer Hospital, Athens	Greece
Paul, W.	Department of Pathological Chemistry, University of Toronto	Canada
Pochin, E.E.	Medical Research Council, Dept. of Clinical Research, University College Hospital Medical School, London, England	World Health Organization and International Commission on Radiological Protection
Prossalentis, A.	Athens Polyclinic, Athens	Greece
Proukakis, C.	Dept. of Clinical Therapeutics, University of Athens, Alexandra Hospital, Athens	Greece
Razis, D.	Cancer Institute of the City of Piraeus	Greece
Recht, P.	Brussels, Belgium	European Atomic Energy Community
Renda, T.	Radiobiological Institute, Ankara Medical School, Ankara	Turkey
Roberts, J.E.	Regional Adviser, U.N.T.A.B., Beirut, Lebanon	International Atomic Energy Agency
Robertson, J.S.	Brookhaven National Laboratory, Long Island, N.Y.,	United States of America
Ronen, M.	Israel Atomic Energy Commission, Tel-Aviv	Israel
Roucayrol, J.-C.	Laboratoire de biophysique, Faculté de Médecine de Paris	France
Sabsay, E., von	Bergman & Beving AB, Stockholm	Sweden
Saito, N.	Director, Division of Isotopes	International Atomic Energy Agency
Samaras, V.	Nuclear Research Centre "Democritus", Biology Dept., Athens	Greece
Savvas, C.	Nuclear Research Centre "Democritus", Biology Dept., Athens	Greece

Name	Institution	Nominating State or Organization
Scheer, K.	Universitäts-Strahlenklinik, Heidelberg	Federal Republic of Germany
Schepers, H.	Institut für Strahlen- und Kernphysik, Bonn	Federal Republic of Germany
Schoot, J., van der	Radioisotope Laboratory, University of Amsterdam	Netherlands
Scognamiglio, A.	Istituto di Patologia Medica, Reparto Medicina Nucleare, University of Rome	Italy
Scott, J.W.	Faculty of Medicine, University of Alberta, Edmonton	Canada
Seegers, G.	Ministerie van Sociale Zaken en Volksgesondheid, The Hague	Netherlands
Simons, H.A.B.	Dept. of Medical Physics, Royal Free Hospital School of Medicine, London	United Kingdom
Smejkal, W.F.	The Manitowoc Clinic, Manitowoc, Wisc.	United States of America
Sodee, D.	Doctors Hospital and Renner Clinic Foundation, Cleveland, Ohio	United States of America
Spârchez, T.	Faculté de Médecine, Bucarest	Rumania
Spinelli-Ressi, F.	Ospedale Maggiore, Milan	Italy
Spyropoulos, E.	Cancer Institute of the City of Piraeus	Greece
Stekelenburg, L., van	Radiologische Werkgroep TNO, Arnhem	Netherlands
Svedberg, J.	Radiation Physics Dept., University of Lund	Sweden
Taplin, G.V.	Laboratory of Nuclear Medicine and Radiation Biology, University of California, Los Angeles, Calif.	United States of America
Tappin, J.	Middlesex Hospital Medical School, London	United Kingdom
Taptas, J.	Saint Savvas Cancer Institute, Athens	Greece
Tarcan, Y.	Turkish Atomic Energy Commission, Ankara	Turkey
Taugner, R.	Physiologisches Institut der Universität Heidelberg	Federal Republic of Germany
Taylor, K.W.	Guy's Hospital, London	United Kingdom
Ter-Pogossian, M.	Washington University School of Medicine, St. Louis, Mo.	United States of America

Name	Institution	Nominating State or Organization
Thomopoulou, H.	Hippokrateion Hospital, Athens	Greece
Tori, G.	Istituto di Radiologia, University of Bologna	Italy
Toth, Z.	Dept. of Nuclear Medicine, Warsaw	Poland
Tubiana, M.	Institut Gustave Roussy, Villejuif	France and International Commission on Radiological Units and Measurements
Turner, P.C.R.	Medical Research Council, Cyclotron Unit, Hammersmith Hospital, London	United Kingdom
van der Schoot, J.	(see under "Schoot")	
Vandor, F.	Municipal Onkoradiological Institute, Budapest	Hungary
van Stekelenburg, L.	(see under "Stekelenburg")	
Vetter, H.	Division of Isotopes	International Atomic Energy Agency
von Sabsay, E.	(see under "Sabsay")	
Wagner, H.	Johns Hopkins University School of Medicine, Baltimore, Md.	United States of America
Wilcke, O.	Neurochirurgische Universitätsklinik, Cologne	Federal Republic of Germany
Williams, E.	Institute for Nuclear Medicine, Middlesex Hospital, London	United Kingdom
Winkler, C.	Nuclearmedizinische Abteilung, Universitäts-klinik, Bonn	Federal Republic of Germany
Wittenzellner, R.	Institut für Strahlenschutzkunde, Neuherberg n. Munich	Federal Republic of Germany
Woldring, M.	Isotopenlaboratorium, Academic Hospital, Groningen	Netherlands
Wolf, R.	Institut für Klinische Strahlenkunde der Universität Mainz	Federal Republic of Germany
Wood, R.	United States Atomic Energy Commission, Washington, D.C.	United States of America
Zanzi, I.	Hospital José Joaquin Aguirre, Universidad de Chile, Santiago	Chile
Zeifert, M.	Presbyterian Medical Center, San Francisco, Calif.	United States of America
Zwingers, W.	Tracerlab S.A., Malines	Belgium

AUTHOR INDEX

(Including Participants in Discussions)

Roman numerals are volume numbers.
Arabic numerals underlined refer to the first page of a paper by the author concerned.
Other Arabic numerals denote the page numbers of discussion comments.
Literature references have not been indexed.

Akerman, M.: II 105-06, 156
Alevizou, V.: II 325
Andrews, G.A.: II 207
Andros, G.: II 33
Arimizu, N.: I 451
Aronow, S.: II 109
Baptista, A.M.: I 191, 268-72, 329, 388, 463; II 45, 175, 191, 192, 236, 300, 369, 428, 429
Baschieri, I.: I 289, 463, 543, 545; II 300
Becchini, M.F.: II 106, 159, 171
Beck, R.N.: I 35, 56, 211, 231-32, 268, 509, 524, 525; II 445
Bell, P.R.: I 193, 529
Bender, M.A.: I 175, 189, 190-91, 391, 398, 399
Ben-Porath, M.: II 67, 68, 69, 71, 368, 429
Binopoulos, D.: II 325, 368
Blau, M.: I 55-56, 175, 268, 416, 417; II 120, 171-72, 275, 300, 301-02
Bodforss, B.: I 485; II 427
Bollini, V.: II 257
Boves, S., De: See under "De Boves"
Brice, J.: II 104-05, 107, 121, 255
Brownell, G.L.: I 3, 34, 56, 75
Burrows, B.A.: I 465
Cassen, B.: I 77, 86-87
Cederlund, J.: I 57, 75
Charleston, D.B.: I 509
Christie, J.H.: I 153
Clode, W.H.: II 175
Conrad, B.: I 491, 506-07
Corey, K.R.: I 253
Courtial, J.: I 91
Czerniak, P.: I 240, 241, 251, 289, 489; II 30, 192, 401, 425-26, 427, 429-30
De Boves, S.: I 401
Delaloye, B.: II 227, 236
Dermentzoglou, F.: II 237
Desgrez, A.: I 114, 333, 388, 542; II 222, 223-24, 271, 300, 425
Desneiges, P.: I 355
Donato, L.: I 330, 542; II 156
Dore, E.K.: II 3
Doxiades, T.: II 389
Duggan, M.H.: I 423; II 121
Economos, D.: II 107
Edwards, C.L.: II 207
Eichling, J.O.: I 411
Eidelberg, P.: I 509
Elias, C.: II 325
Entzian, W.: II 109, 255
Ephraïm, K.H.: I 291; II 368
Fischer, J.: I 141; II 337, 368-69
Follet, D.: I 241, 543; II 68
Gandy, A.: I 91, 114, 208
Gatsou, P.: II 389
Georgi, M.: II 47
Gheorghescu, B.: I 473
Glass, H.I.: I 86, 243, 251, 252, 268; II 30, 106
Gómez-Crespo, G.: II 428, 429
Gongora, R.P.: I 355; II 301, 302, 373, 425, 428, 429
Greenberg, E.I.: I 253
Gross, J.: II 71
Gross, W.: I 401, 410
Gyftaki, H.: II 325, 369
Harper, P.V.: I 190, 251, 486; II 31, 33, 45, 67, 191, 222, 271, 301, 445
Harris, C.C.: I 189, 193, 208, 329, 419, 506, 529, 542, 543; II 157, 445
Herbert, R.: I 330, 398, 419, 524
Hindel, R.: I 524
Hine, G.J.: I 465, 485-86, 487, 489

Hochman, A.: II 71
Höfer, R.: I 233, 241; II 220-21, 222
Horst, W.: I 491
Iio, M.: II 303
Ikkos, D.: II 389, 424-25, 426, 427-28, 430, 455
Jammet, H.: I 355, 388, 390; II 373
Johnson, D.E.: II 3
Jones, E.: II 121
Jonsson, L.: II 193
Jordan, J.C.: I 193, 529
Kakehi, H.: I 451, 462
Kaplan, H.S.: II 3
Kellershohn, C.: I 189, 333, 388, 398, 418-19, 484-85; II 45, 67, 156, 157, 191, 271-72
Kenny, P.J.: I 208, 253, 268, 329
Kniseley, R.M.: I 463; II 207, 221-22, 225
Kordiolis, N.: II 237
Kuhl, D.: I 190, 273, 289, 462; II 67-68, 105
Langan, J.K.: II 303
Lansiart, A.: I 333, 388, 416
Larsson, L.-G.: II 193, 221, 224, 225
Lathrop, K.A.: II 33
Laughlin, J.S.: I 253
Lubin, E.: I 268, 485; II 171, 426
McAlister, J.M.: II 68
McCardle, R.J.: II 33
MacIntyre, W.J.: I 153, 172-73
Magnenat, P.: II 227
Malamos, B.: II 106, 191, 224-25, 368, 369
Mallard, J.R.: I 190, 231, 389-90, 398, 423, 462, 463, 487; II 121, 145
Matthews, C.M.E.: I 33-34, 190, 410, 419-20; II 28, 44-45, 323
Merculiev, E.: I 473
Merikas, G.: II 389
Mikropoulos, H.: II 237, 255
Monasterio, G.: II 159
Morichère, J.: I 355, 399
Morley, T.P.: II 81
Murteira, M.A.: II 175
Myers, M.J.: I 423; II 121
Myers, W.G.: I 241, 251-52, 377, 390, 417-18, 423; II 445
Nastou, A.: II 389
Niklas, N.: I 417
Otero-Ruiz, E.: II 424
Pantazis, G.: II 237
Papavasiliou, C.: II 224
Paraschou, E.: II 237
Patten, D.H.: I 465
Paul, W.: I 86, 190, 410, 418; II 29, 81, 105, 106-07
Perez Fernandez, M.A.: II 175
Pochin, E.E.: I 462; II 447, 455
Popovici, M.: I 473
Proukakis, C.: II 325, 367, 368
Riccioni, N.: II 159
Ross, D.A.: I 193, 529
Roszuczky, A.: I 233
Roucayrol, J.-C.: II 324
Sabiston, D.C., Jr.: II 303
Sabsay, E., von: I 543
Samaras, V.: II 237
Satterfield, M.M.: I 193, 529
Savvas, C.: II 237
Scheer, K.E.: II 47, 68
Schepers, H.: I 321, 329, 330
Schlesinger, E.B.: I 401
Schuh, M.W.: I 509
Scognamiglio, A.: I 545
Simão Rodrigues, M.: II 175
Simons, H.A.B.: I 86, 115, 172, 241, 542; II 144, 454
Sodee, D.B.: II 45, 147, 156-57, 289, 300, 301
Soloway, A.H.: II 109
Sorensen, L.B.: II 431
Spârchez, T.: I 473, 489-90
Spinelli-Ressi, F.: II 355, 368, 369
Steclaci, A.: I 473
Stekelenburg, L., Van: I 398, 462
Sweet, W.H.: II 109
Tanida, R.: II 207
Taplin, G.V.: II 3, 29, 30-31, 324
Taptas, J.: II 237
Tatsuno, I.: I 153
Ter-Pogossian, M.M.: I 411, 416, 417, 418, 419, 420; II 120, 156, 445
Tori, G.: II 105, 257, 271, 301

Tubiana, M.: I 419, 487-89, 524-25; II 45, 192, 254-55
Turner, P.C.R.: I 252, 388-89, 390; II 120, 222-23
Uchiyama, G.: I 451
Van Stekelenburg, L: See under "Stekelenburg"
Vetter, H.: II 68
von Sabsay, E.: See under "Sabsay"
Wagner, H.N., Jr.: I 330, 417, 462; II 29, 303, 323, 324
Weber, D.A.: I 253
Wilcke, O.: II 95, 106, 107
Wilks, R.J.: I 423
Winkler, C.: I 321
Wolf, R.: I 141; II 156, 337, 367-68
Zum Winkel, K.: II 47

IAEA SALES AGENTS

Orders for Agency publications can be placed with your bookseller or any of our sales agents listed below:

AUSTRALIA
Hunter Publications,
23 McKillop Street
Melbourne, C.1

AUSTRIA
Georg Fromme & Co.
Spengergasse 39
Vienna V

BELGIUM
Office international de librairie
30, avenue Marnix
Brussels 5

BRAZIL
Livraria Kosmos Editora
Rua do Rosario, 135-137
Rio de Janeiro

Agencia Expoente Oscar M. Silva
Rua Xavier de Toledo, 140-1° Andar
(Caixa Postal No. 5.614)
São Paulo

BYELORUSSIAN SOVIET SOCIALIST REPUBLIC
See under USSR

CANADA
The Queen's Printer
Ottawa, Ontario

CHINA (Taiwan)
Books and Scientific Supplies Service, Ltd.,
P.O. Box 83
Taipei

DENMARK
Ejnar Munksgaard Ltd.
6 Nörregade
Copenhagen K

FINLAND
Akateeminen Kirjakauppa
Keskuskatu 2
Helsinki

FRANCE
Office international de
documentation et librairie
48, rue Gay-Lussac
Paris 5e

GERMANY, Federal Republic of
R. Oldenbourg
Rosenheimer Strasse 145
Munich 8

ISRAEL
Heiliger and Co.
3 Nathan Strauss Street
Jerusalem

ITALY
Agenzia Editoriale Internazionale
Organizzazioni Universali (A.E.I.O.U.)
Via Meravigli 16
Milan

JAPAN
Maruzen Company Ltd.
6, Tori Nichome
Nihonbashi
(P.O. Box 605)
Tokyo Central

MEXICO
Librarfa Internacional
Av. Sonora 206
Mexico 11, D.F.

NETHERLANDS
N.V. Martinus Nijhoff
Lange Voorhout 9
The Hague

NEW ZEALAND
Whitcombe & Tombs, Ltd.
G.P.O. Box 1894
Wellington, C.1

NORWAY
Johan Grundt Tanum
Karl Johans gate 43
Oslo

PAKISTAN
Karachi Education Society
Haroon Chambers
South Napier Road
(P.O. Box No. 4866)
Karachi, 2

POLAND
Ośrodek Rozpowszechniana
Wydawnictw Naukowych
Polska Akademia Nauk
Pałac Kultury i Nauki
Warsaw

SOUTH AFRICA
Van Schaik's Bookstore (Pty) Ltd.
Libri Building
Church Street
(P.O. Box 724)
Pretoria

SPAIN
Librería Bosch
Ronda de la Universidad 11
Barcelona

SWEDEN
C.E. Fritzes Kungl. Hovbokhandel
Fredsgatan 2
Stockholm 16

SWITZERLAND
Librairie Payot
40, rue du Marché
Geneva

TURKEY
Librairie Hachette
469, Istiklâl Caddesi
Beyoğlu, Istanbul

UKRAINIAN SOVIET SOCIALIST REPUBLIC
See under USSR

UNION OF SOVIET SOCIALIST REPUBLICS
Mezhdunarodnaya Kniga
Smolenskaya-Sennaya 32-34
Moscow G-200

UNITED KINGDOM OF GREAT BRITAIN AND NORTHERN IRELAND
Her Majesty's Stationery Office
P.O. Box 569
London, S.E.1

UNITED STATES OF AMERICA
National Agency for
International Publications, Inc.
317 East 34th Street
New York, N.Y. 10016

VENEZUELA
Sr. Braulio Gabriel Chacares
Gobernador a Candilito 37
Santa Rosalía
(Apartado Postal 8092)
Caracas D.F.

YUGOSLAVIA
Jugoslovenska Knjiga
Terazije 27
Belgrade

IAEA publications can also be purchased retail at the United Nations Bookshop at United Nations Headquarters, New York, at the news-stand at the Agency's Headquarters, Vienna, and at most conferences, symposia and seminars organized by the Agency.

In order to facilitate the distribution of its publications, the Agency is prepared to accept payment in UNESCO coupons or in local currencies.

Orders and inquiries from countries where sales agents have not yet been appointed may be sent to:

Publications Sales Unit, International Atomic Energy Agency,
Kärntner Ring 11, Vienna I, Austria

INTERNATIONAL
ATOMIC ENERGY AGENCY
VIENNA, 1964

PRICE: USA and Canada: US $9.50
Austria and elsewhere: S 199,50
(£2.17.0; F.Fr. 38,-; DM 33,25)